FUNDAMENTALS OF FLUID MECHANICS

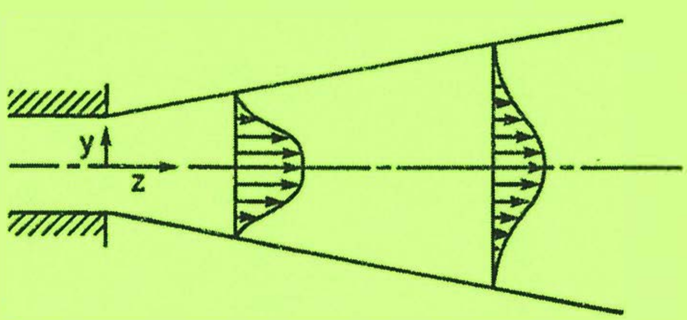

John Vlachopoulos

www.polydynamics.com

πάντα ῥεῖ

Omne influat

Everything flows

Alles fließt

Tout s’écoule

Todo fluye

Tudo flui

Tutto scorre

Всё течет

HERACLITUS (c.535 BC-c.475 BC)

FUNDAMENTALS
OF
FLUID MECHANICS

John Vlachopoulos

McMaster University

Hamilton, Ontario, Canada

WWW.POLYDYNAMICS.COM

John Vlachopoulos

Professor Emeritus

Department of Chemical Engineering

McMaster University

Hamilton, Ontario, Canada L8S4L7

John Vlachopoulos, *Fundamentals of Fluid Mechanics*
Revised internet edition (2016), www.polydynamics.com

ISBN 978-0-9952407-1-1 (Book)

ISBN 978-0-9952407-0-4 (Electronic book)

Published by:

POLYDYNAMICS INC, Dundas, ON, CANADA

www.polydynamics.com

DEDICATION

This book is dedicated to my teachers, to my students and to all people who love the beautiful science, the imaginative engineering and the powerful technology of fluid mechanics.

Following in the footsteps of my teachers, I have tried to present a unified approach to fluid mechanics in my pursuit of converting information to knowledge and knowledge to understanding for the benefit of my students.

John Vlachopoulos

About the author

John Vlachopoulos received his Dipl-Ing degree from the NATIONAL TECHNICAL UNIVERSITY of ATHENS (NTUA), GREECE and MS and DSc degrees from WASHINGTON UNIVERSITY, ST. LOUIS (WUSTL), Mo. USA. He has been teaching and doing research at McMASTER UNIVERSITY, HAMILTON, ON, CANADA since 1968. He was on sabbatical research leave at the Institut für Kunststoftechologie (IKT), University of Stuttgart, Germany (1975) and at the Centre de Mise en Forme des Materiaux (CEMEF), Ecole des Mines de Paris (now PARISTECH), Sophia Antipolis, France (1981-82 and 1988-89)

He is consultant to the polymer processing industry, member of several international professional organizations and served as President (2005-2007) of the Polymer Processing Society (PPS). He is also the recipient of the SPE Fred E. Schwab award for Outstanding Achievement in Plastics Education (Dallas, Tex., 2001), the Distinguished Achievement in Extrusion Award (Chicago, Ill., 2004) and the Bruce Maddock Award from the Extrusion Division of the Society of Plastics Engineers (SPE, Las Vegas 2014) and the Stanley G. Mason Award of the Can. Soc. of Rheology (Hamilton, ON, 2007).

He is Fellow of the Canadian Academy of Engineering (CAE), Society of Plastics Engineers (SPE) and the Chemical Institute of Canada (CIC).

Through his company POLYDYNAMICS INC he has licensed computer flow simulation software to several hundred corporations around the world.

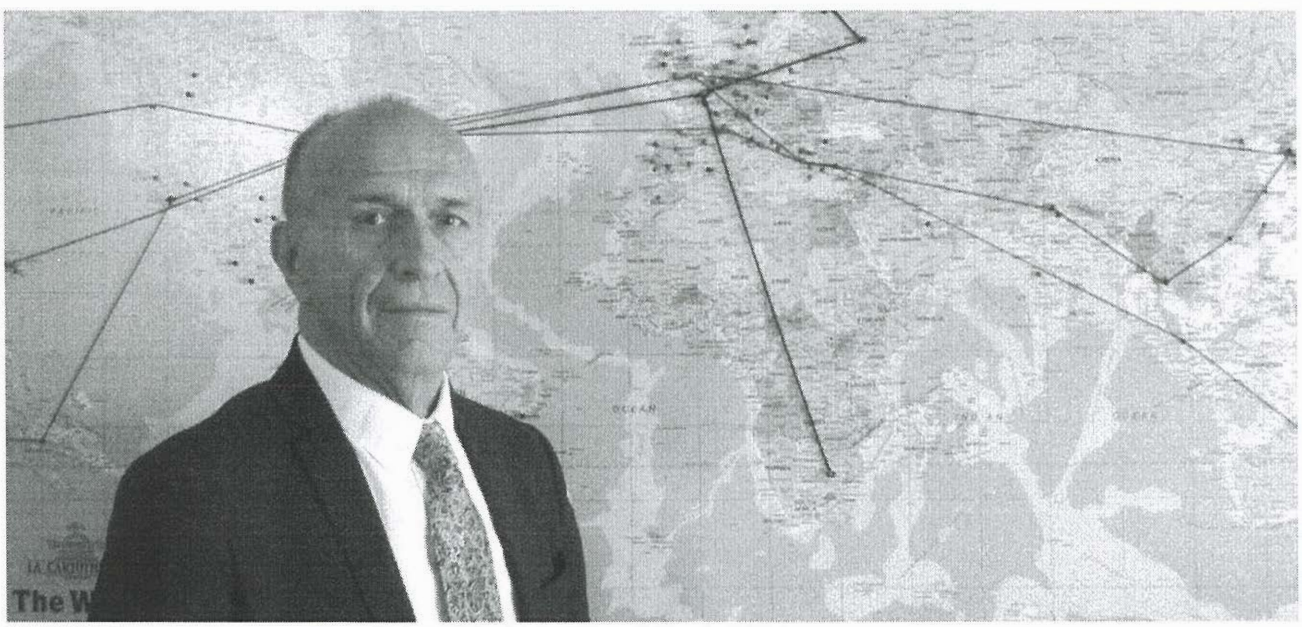

John Vlachopoulos, March 2017

PREFACE

My interest in fluid mechanics started during my high school years at the 1st Gymnasion of Volos, Greece. I was fortunate to have a brilliant physics teacher, Andreas Koukorinis, who provided me with a very firm grounding in the basic concepts and applications of the laws of physics, including an early introduction to the fundamentals of fluid flow. I applied and received a travel grant from the Ministry of Education of Greece to visit the Prespa lakes region, in the borders of Greece with Yugoslavia and Albania, and carried out a summer student project (1959, a year before my high school graduation), on the possibility of hydroelectric power generation.

My strong interest continued during my undergraduate years at the National Technical University in Athens (1960-1965) and really peaked when I arrived at Washington University in St. Louis (WUSTL), USA for my doctoral studies and research (September 1965- July1968). I was smitten by NASA's efforts for space exploration and decided to work on high temperature turbulent impinging air jets. My doctoral advisor Eric Weger gave me a wonderful research project and boundless freedom to explore my ideas. I was fortunate to continue the project that John F. Tomich was completing for his dissertation, as I was starting. I was learning fast from Eric and John and from some excellent professors at WUSTL. From W.M. Swanson I learnt a lot about compressible supersonic flows. Kurt Hohenemser (student of Prandtl) showed us with exceptional clarity, in his course on continuum mechanics, how to make complex mathematical equations easy, with the index tensor notation. My doctoral research project was related to NASA's manned space vehicles, for testing the heatshield before launching. I was obviously very thrilled when a McDonnell Douglas engineer converted, with my help, the computer program, that I had developed for temperatures reaching several hundred °F, to several thousand °F.

After starting at McMaster University as Assistant Professor in August of 1968, I focused my research mostly on computer aided mathematical modeling of molten polymer flows through process equipment. I have been, and continue to be, involved in several industrial projects as consultant. At McMaster, I was teaching fluid mechanics to undergraduate and graduate students in engineering. This book is based on my lecture notes. I was consulting numerous other monographs and publications, but overall two books had the greatest impact on my writing: H. Schlichting, *Boundary Layer Theory*, McGraw-Hill (1960) and R. B. Bird, W.E. Stewart and E.N. Lightfoot, *Transport Phenomena*, Wiley (1960) In writing this book, I decided to combine my undergraduate and graduate lecture notes in one single volume. Most of the chapters were completed by 1984. The chapter on Non-Newtonian fluid mechanics was written after I retired from active teaching and became Professor Emeritus in 2008.

How did I use this book in teaching fluid mechanics? At the post-graduate level it was easy: I would distribute the entire book to my class and then start from Appendix A on index tensor notation to make sure that everyone knew how to do tensor algebra. I would then derive the generalized constitutive equation for Newtonian fluids (Chapter 20) and subsequently work on the derivation, followed by simplifications, of the Navier-Stokes and other conservation equations. The various types of flow could easily be derived and studied, low and high Reynolds numbers, laminar and turbulent boundary layers, inviscid flows, compressible flows and all the rest. It was either a one- or a two-semester course. At the undergraduate level I was teaching a one-semester course to third year students and I would print a special abridged version for them. This usually included Chapters 1-11, 12, 14, 18, 19 plus Appendices A, C, D, E, F and the Subject Index. Although I was avoiding the use of tensors at the undergraduate level, they were there for any student who wanted a more rigorous approach. Copies of the entire book were available in the library and with my teaching assistants. If I had civil engineering students in the class, I would also include Chapter 16, on open channel flow. Of course, there was a lot of material for a one-semester course in the more than 400 pages of the abridged versions. However, the book was written with modularity in mind, so I could easily drop material that was not suitable for the class that I was teaching.

In addition to my teachers and mentors that I have already mentioned, I should also acknowledge the help from my numerous students and teaching assistants. I will only mention chronologically the names of those who, due to intensity of intellectual exchange, had the greatest impact in formulating my ideas in writing, editing and revising this book: Stamos Katotakis, C.K. John Keung, Costas Stournaras, William Garland, Costas Kiparissides, Sedky El Shammaa, Osama ElRiedy, T. W. Chan, Amir Husain, Enno Agur, Evan Mitsoulis, Peter S. Scott, Costas Tzoganakis, Harry Mavridis, Aristotle Karagiannis, Paul Behncke, Alex Zahavich, Weining Song, Agustin Torres, Alberto Rincon, Farhad Sharif, Celine Bellehumeur, Marianna Kontopoulou, Vasilis Sidiropoulos, Hector Larrazabal, Velichko Hristov and Maryam Emami. Special acknowledgements go to my former postdoctoral fellows Norberto Silvi, Mukesh Bisaria, Jian-Jun Tian, Shih-Jung Liu, to my faculty colleagues Terry Hoffman, Archie E. Hamielec, Irwin Feuerstein, Brian Latto, Farooque A. Mirza, Archie A. Harms, Andrew N. Hrymak, Michael R. Thompson, to my colleague and friend John W. Bandler, and to my long term coworkers at McMaster University, Elizabeth Takacs and at Polydynamics Inc, David Strutt and Nickolas D. Polychronopoulos (who is also my nephew).

John Vlachopoulos

Burlington, Ontario, Canada

John Vlachopoulos, *Fundamentals of Fluid Mechanics*
Chem. Eng., McMaster University, Hamilton, ON, Canada
(First Edition 1984, revised internet edition (2016), www.polydynamics.com)

CONTENTS

John Vlachopoulos, *Fundamentals of Fluid Mechanics*
Chem. Eng., McMaster University, Hamilton, ON, Canada
(First Edition 1984, revised internet edition (2016), www.polydynamics.com)

CHAPTER 1

FUNDAMENTAL CONCEPTS

1.1 INTRODUCTION

All forms of matter can be classified in terms of their physical appearance, or phase, into three classes: solids, liquids and gases. Liquids and gases are called fluids. Webster's International Dictionary defines a fluid as "a substance that alters its shape in response to any force however small, that tends to flow or to conform to the outline of its container, and that includes gases and liquids and mixtures of solids and liquids capable of flow". We will accept this elementary definition for the time being but will take up this question again.

All gases and liquids are composed of conglomerations of molecules and atoms, whose spacing depends on the strength of the intermolecular forces. In solids these forces are very strong whereas in liquids and gases they are weak. The molecular diameters are extremely small, of the order of 10^{-8} cm, so that an extremely large number of molecules and atoms are contained in volumes no larger than the tip of a needle.

In principle it is possible to study the flow of gases and liquids from the molecular point of view. The mathematical complexity, however, renders this approach impractical for most engineering problems. It is possible to treat many flow problems without a detailed knowledge of molecular motions and interactions. We introduce the continuum hypothesis according to which a fluid is considered as an infinitely divisible substance so that it's density (mass/volume) has a definite value at each point. Of course, the question might be asked as to how small a sampling volume are we allowed to consider in determining the ratio mass/volume. Fig. 1 shows the expected values of density as the sampling volume becomes gradually smaller. For volumes smaller than some critical value $Ɐ_c$ the density might be either very large or very small depending on how many, if any, molecules are present within the volume.

The density is usually denoted by the Greek symbol ρ (rho) and has units of Kg/m^3. The density of water at 15.5^oC is 1,000 Kg/m^3; and for air at 20^oC and standard pressure (101.3 kPa) the density of 1.24 kg/m^3. The density of most common fluids is given in Appendix B.

Specific weight is the weight per unit volume of a fluid and is usually denoted by the Greek symbol γ (gamma).

Specific gravity (S.G.) is defined as the ratio of the specific weight of a given liquid to the specific weight of water at a standard reference temperature usually 4^oC. The specific gravity is therefore dimensionless.

Specific volume is the volume occupied by a unit mass of fluid and is usually denoted by $\upsilon = 1/\rho$.

Specific heat of a substance is defined as the amount of heat that must be transferred to a unit mass to raise its temperature by one degree. If the specific volume of gas remains constant while the temperature changes the specific heat is denoted by C_v. If the pressure is held constant during the change the specific heat is denoted by C_p. The ratio C_p/C_v is identified by the symbol k.k = 1.666 for monatomic gases (He, Ar, Ne, Kr, etc.), k = 1.40 for diatomic gases (N_2, O_2, H_2, CO_2, NO, Air, etc.), k = 1.30 - 1.33 for polyatomic gases. Data for C_v, C_p and k are given in Appendix C.

1.2 THE EQUATION OF STATE

The equation of state determines the relationship between density and the thermodynamic pressure and temperature i.e. $\rho = \rho(p,T)$.

This relationship is extremely complicated for liquids, solids and during phase changes.

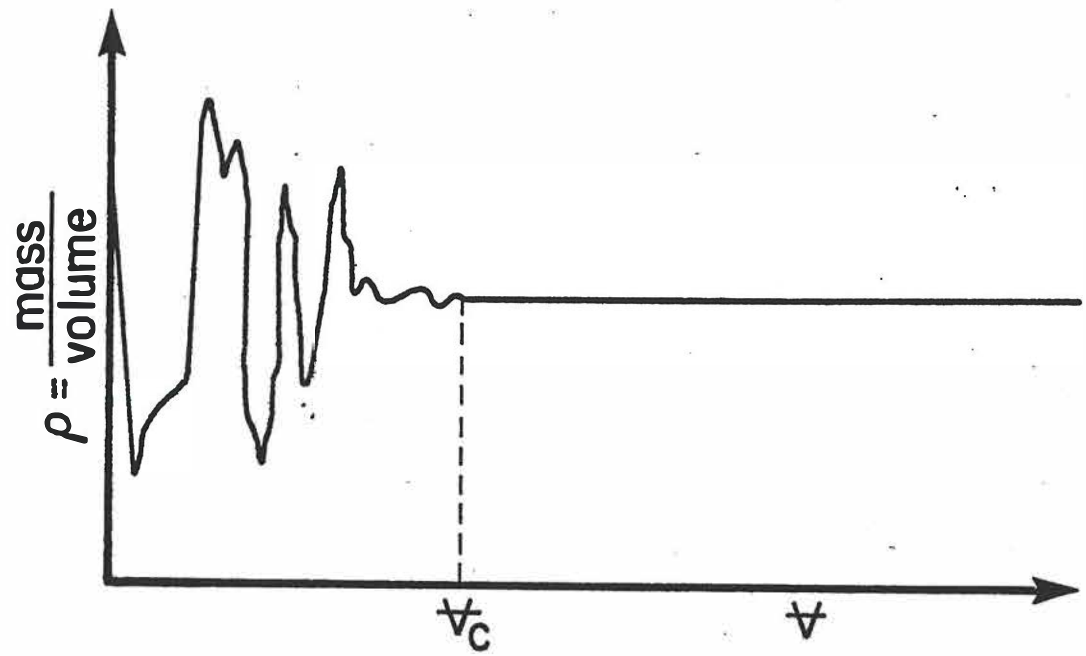

Fig. 1.1 Density as a function of sampling volume.

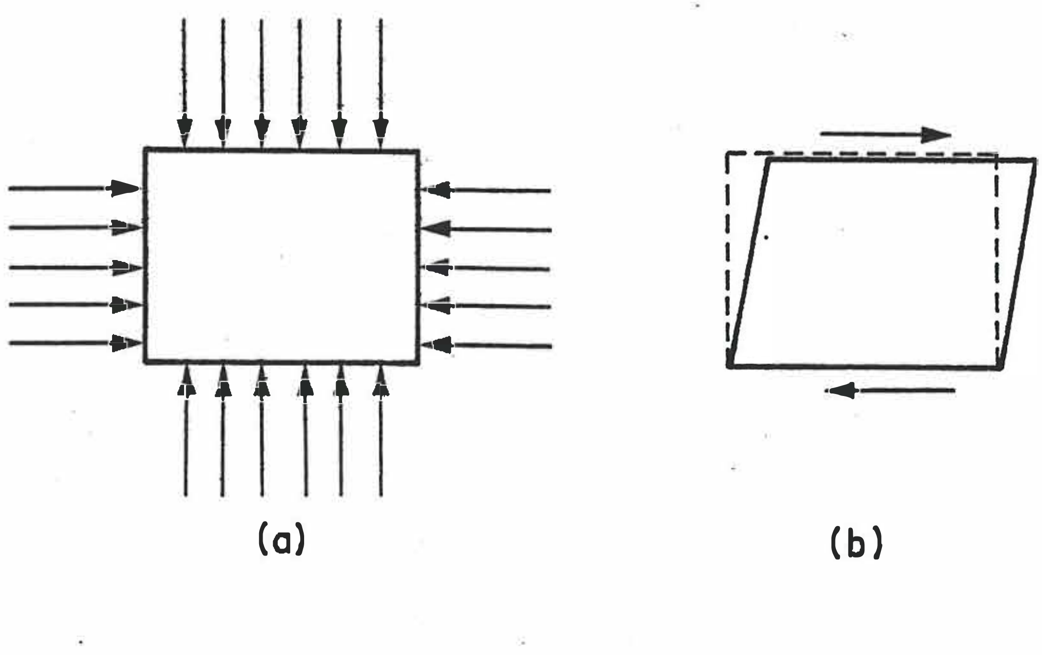

Fig. 1.2 Forces exerted on incompressible solids and fluids
(a) Normal forces
(b) Tangential (shear) forces

The equation of state for a perfect gas, as it usually appears in thermodynamics texts, is

$$pV = n\mathcal{R}T \tag{1.1}$$

where p = pressure

V = volume

T = absolute temperature

$\mathcal{R}$ = 8,314 J/kg-mol·K (universal gas constant)

n = number of moles

A more convenient form of this equation can be obtained by dividing equation (1.1) by V and the molecular weight

$$p = \rho R T \tag{1.2}$$

where ρ = density

$$R = \frac{\mathcal{R}}{\text{molecular weight}}$$

Obviously R depends on the particular gas. Values of R for some common gases are given in Appendix B.

It can be shown that for an adiabatic frictionless process (isentropic) in a perfect gas we have the relationship

$$p\,\rho^{-k} = \text{constant} \tag{1.3}$$

where $k = C_p/C_v$.

1.3 VISCOSITY

A fluid was defined as "a substance that alters its shape in response to any force however small". This elementary definition is technically correct when a tangential force is specified. We cannot distinguish between an incompressible solid and an incompressible fluid subjected to normal forces as shown in Fig. 1.2(a). However, when a tangential force is applied, as shown in Fig. 2(b), a solid material deforms but will regain its original shape upon removal of the force. On the other hand a fluid subjected to a tangential force will deform continuously.

In the study of fluid flow it turns out that it is easier to work in terms of stress rather than force. Stress is defined as the magnitude of force divided by the area of the surface upon which it is applied. When a normal force is applied, as shown in Fig. 1.2(a), we have normal stresses, whereas in Fig. 1.2(b) we have shear stresses. The most important and distinctive characteristic of a fluid is that it deforms continuously under the action of a shear stress.

Let us now consider two long parallel plates placed a small distance h apart, the space between being filled with a fluid. One of the plates is fixed and the other is moved parallel to it with a velocity U by the application of a force F, as shown in Fig. 1.3. The fluid in contact with each plate "sticks" to it and does not "slip" relative to it. Consequently the velocity of the fluid touching each plate is the same as that of the plate. Experiments have shown that for a large class of fluids the velocity profile will be a straight line as shown in Fig. 1.4. The force F is proportional to the velocity U, the area in contact with the fluid A and inversely proportional the the gap h.

$$F \propto \frac{AU}{h}$$

The quantity F/A is called shear stress and is denoted by the Greek symbol τ (tau)

$$\tau \propto \frac{U}{h}$$

In the limit of small deformations the ratio U/h can be replaced by the velocity gradient du/dy, which is often called the shear rate.

The proportionality constant between shear stress and shear rate is called viscosity and is usually denoted by the Greek symbol μ (mu).

$$\tau = \mu \frac{du}{dy} \tag{1.4}$$

Equation (1.4) is referred to as Newton's law of viscosity. μ is sometimes called the viscosity coefficient, absolute or dynamic viscosity.

The dimensions of viscosity are force per unit area divided by the velocity gradient. In SI units

$$[\mu] \rightarrow \frac{N/m^2}{\frac{m/s}{m}} = \frac{N}{m^2} \cdot s = Pa \cdot s \text{ (pascal.second)}$$

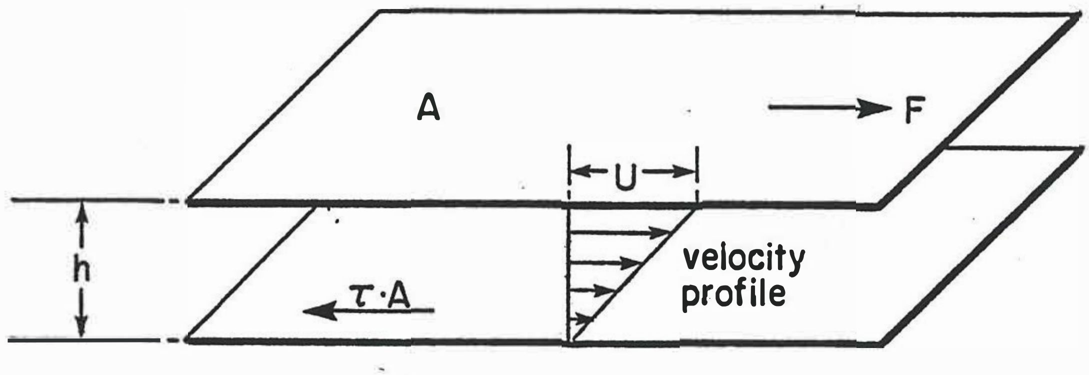

Fig. 1.3 A fluid subjected to shearing between two parallel plates.

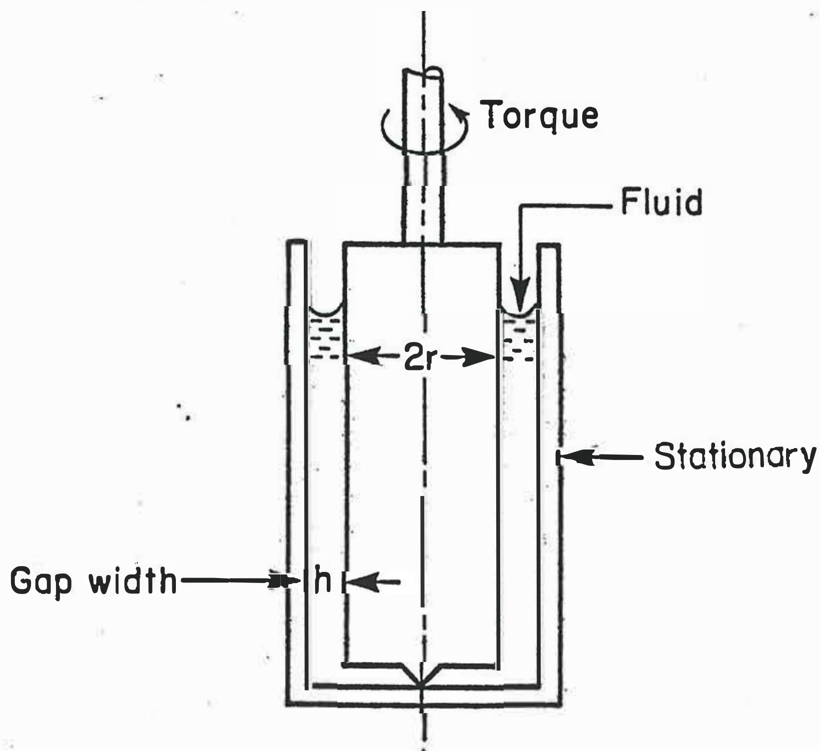

Fig. 1.4 Concentric cylinder viscometer. Torque and revolutions per minute (rpm) are directly measured.

Before the introduction of SI one of the most common viscosity units (c.g.s) was the poise (p), named after the 19th century French scientist J.L. Poiseuille. 1p = 0.10 Pa.s. The centipoise (cp) (=0.01 p) was frequently convenient because the viscosity of water at 20^{o}C is 1 c P (=10^{-3} Pa.s).

In many engineering problems the value of viscosity is divided by the fluid density. This quantity is called kinematic viscosity and it is usually denoted by the Greek symbol ν (nu).

$$\nu = \frac{\mu}{\rho} \tag{1.5}$$

The absolute viscosity of virtually all fluids is practically independent of pressure, except in the region of extremely high pressures. The kinematic viscosity of gases, however, varies with pressure because of the dependence of density on pressure.

Temperature has a strong effect on viscosity. For gases the viscosity increases with temperature. The most common approximations are the power-law and the Sutherland law:

$$\frac{\mu}{\mu_o} \simeq \left(\frac{T}{T_o}\right)^n \tag{1.6}$$

$$\frac{\mu}{\mu_o} \simeq \frac{(T/T_o)^{3/2}\,(T_o + S)}{T + S} \tag{1.7}$$

where μ_o is the viscosity at a given absolute temperature (usually T_o = 273.16 K) n and S are empirical constants (for air n=0.67 and S=110 K).

For liquids the viscosity decreases with temperature usually as an exponential function

$$\mu \simeq a\, e^{-bT}$$

where a and b are empirical constants.

Some typical values of viscosity of several common substances are given in Table 1.1. More accurate viscosity tables and graphs are provided in Appendix B.

TABLE 1.1

Order of magnitude of viscosity for various substances

Substance	
Nitrogen gas (20°C)	$\mu = 0.017 \times 10^{-3}$ Pa•s
Water (20°C)	$\mu = 10^{-3}$ Pa•s
Mercury (20°C)	$\mu = 1.5 \times 10^{-3}$ Pa•s
Crude oil	$\mu \Rightarrow 0.01 - 0.1$ Pa•s
Lubricating oil	$\mu \Rightarrow 0.1 - 1$ Pa•s
Ointments (e.g. Skin cream)	$\mu \Rightarrow 1 - 5$ Pa•s
Molten plastic	$\mu \Rightarrow 10^3 - 10^4$ Pa•s
Flour dough	$\mu \Rightarrow 10^3 - 10^5$ Pa•s
Cheddar cheese	$\mu \Rightarrow 10^7 - 10^8$ Pa•s

In the laboratory, the idealized flow configuration between the two flat plates of Fig. 1.3 is closely approximated in a concentric cylinder viscometer (cup-and-bob) which is schematically shown in Fig. 1.4. The outer cylinder is fixed and the inner cylinder rotates at a steady rate under the action of an applied torque. For such an experiment

F = (torque)/r

A = the area of the inner cylinder

U = (rpm) x $2\pi r$

The viscosity is obtained from the expression

$$\mu = \frac{F/A}{U/h} \tag{1.8}$$

and it is the slope of the line drawn through the experimental points as shown in Fig. 1.5.

From the molecular point of view viscosity represents the resistance to flow due to the random motions of molecules. It is well known that in a gas the molecules move randomly and collide with each other. As the temperature increases the molecular motions become more

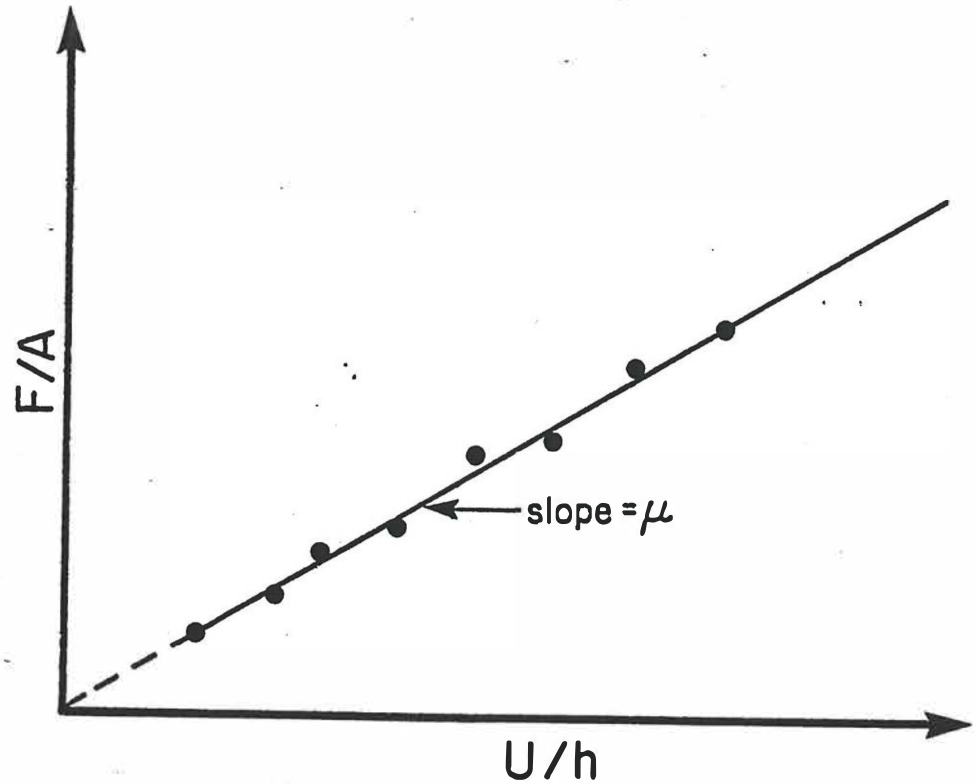

Fig. 1.5 Some typical shear stress versus shear rate results for a Newtonian fluid.

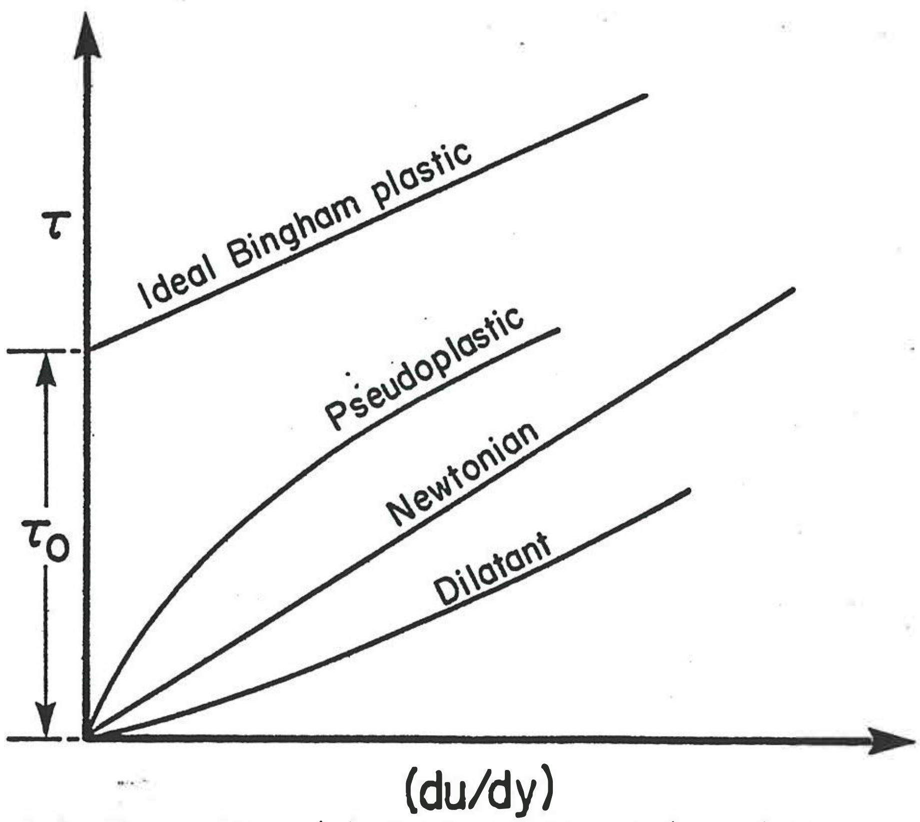

Fig. 1.6 Shear stress (τ) versus shear rate (du/dy) for various fluids.

violent and as a result the viscosity of gases increases with increasing temperature. It is possible, from the kinetic theory of gases [1,2,3], to actually estimate the viscosity as a function of temperature, molecular mass and diameter.

In liquids the random motions are primarily vibrations of molecules which are packed closely. When the temperature increases the molecular vibrations are enhanced, the overall structure weakens and as a result the viscosity decreases. The molecular theory of liquids is more complicated that the one for gases. More information may be found in Refs. [2] and [3].

Example 1.1

The space between two plates, as shown in Fig. 1.3, is filled with water. Find the shear stress and the force necessary to move the upper plate at a constant velocity of 10 m/s. The gap width is h = 0.1 mm and the area A is 0.2 m^2.

Solution: According to equation (1.4) we have

$$\tau = \mu \frac{du}{dy} = \mu \frac{U}{h} = (10^{-3}\ \text{Pa}\cdot\text{s}) \frac{(10\ \text{m/s})}{(0.1 \times 10^{-3}\ \text{m})}$$

$$= 100\ \text{Pa}$$

$$F = \tau . A = (100\ \frac{N}{m^2}) \times (0.2\ m^2) = 20\ N$$

Example 1.2

A 25 cm long shaft, 5 cm in diameter, rotates in a journal of the same length and 5.03 cm in diameter. The gap between the shaft and the journal is filled with SAE 30 Eastern lubricating oil. The gap is assumed uniform and the shaft rotates at 1800 rpm. Calculate (a) the torque (b) the power required for the rotation of the shaft.

Solution

(a) From Newton's law of viscosity

$$\tau = \mu \frac{du}{dy} = \mu \frac{U}{h}$$

at the surface of the shaft $\tau = F/A$

Then, torque $To = Fr = \tau Ar = \mu \frac{U}{h} (\pi DL) \frac{D}{2} =$

where $U = (\pi D) \times (rpm)$

$A = \pi DL \qquad L$ = length of shaft

$\mu = 4 \times 10^{-2}$ Pa•s (approximately)

$$To = 4 \times 10^{-2} \frac{(\pi\ 0.05)^2\ (1800/60) \times 0.25}{0.0003/2} \quad \frac{0.05}{2} = 1.23 \text{ N.m}$$

$$To = 1.23 \text{ N.m}$$

(b) The power required for the rotation of the shaft is

$$Po = FU = \tau AU = \mu \frac{AU^2}{h} = \mu \frac{(\pi D)[\pi D(rpm)]^2}{h} L$$

$$= \mu \frac{(\pi D)^3\ (rpm)^2}{h} L = 4 \times 10^{-2} \frac{(\pi\ 0.05)^3\ (1800/60)^2}{0.0003/2}\ 0.25 =$$

$= 232$ N•m/s

$Po = 232$ W

1.4 NON-NEWTONIAN FLUIDS

Newton's Law of viscosity (equation (1.4)) represents a linear relationship between the shear stress τ and the shear rate (du/dy). This relationship is obeyed by many fluids such as air, water, gasoline, glycerine and liquid metals to name just a few. Many other fluids exhibit a different type of behavior and are called non-Newtonian. Typical examples of non-Newtonian fluids include molten plastics, whole human blood, slurries and suspensions, pastes, etc. The study of these materials is the object of rheology [4,5]. See also Chapter 21.

Fig. 1.6 compares some of the most common types of non-Newtonian behavior with a Newtonian fluid. The ideal Bingham plastic model describes a fluid that will not flow unless the shear stress exceeds a certain value τ_o called yield stress. Mathematically this behavior is expressed by

$$\tau = \tau_o + \mu_o \frac{du}{dy} \qquad \text{if } \tau > \tau_o$$
$$\frac{du}{dy} = 0 \qquad \text{if } \tau \leq \tau_o \tag{1.9}$$

It is possible that the flow behavior after the yield may be non-linear. The ideal Bingham plastic model approximates the behavior of ordinary paints and pastes. Paints may be applied on vertical walls without a complete runoff because of their yield stress. Toothpaste will not flow out of the tube until a finite stress is applied by squeezing.

The pseudoplastic and dilatant fluids can be approximated by the power-law model

$$\tau = m \left(\frac{\partial u}{\partial y}\right)^n \tag{1.10}$$

When $n < 1$ this model describes a pseudoplastic fluid, when $n > 1$ it describes a dilatant fluid. For $n = 1$ and $m = \mu$ equation (1.10) reduces to Newton's law of viscosity. Pseudoplastic fluid behavior is exhibited by many liquids such as molten plastics, polymer solutions, dispersions of particles in water and generally liquids composed of large molecules. Dilatant fluids are not very common; for example, certain dispersions of iron oxide particles in water and some oil sands exhibit dilatant behavior.

The concept of viscosity as defined in section 1.3 is strictly valid for Newtonian fluids. μ is obtained from the slope of τ vs du/dy line. For non-Newtonian fluids we define an apparent viscosity

$$\mu_a = \frac{\tau}{(du/dy)} \tag{1.11}$$

For a Newtonian fluid $\mu_a = \mu$ (constant). For pseudoplastic and dilatant fluids the apparent viscosity is a function of shear rate as shown in Fig. 1.7. Molten plastics and polymer solutions exhibit pseudoplastic behavior. Their apparent viscosity decreases as the shear rate

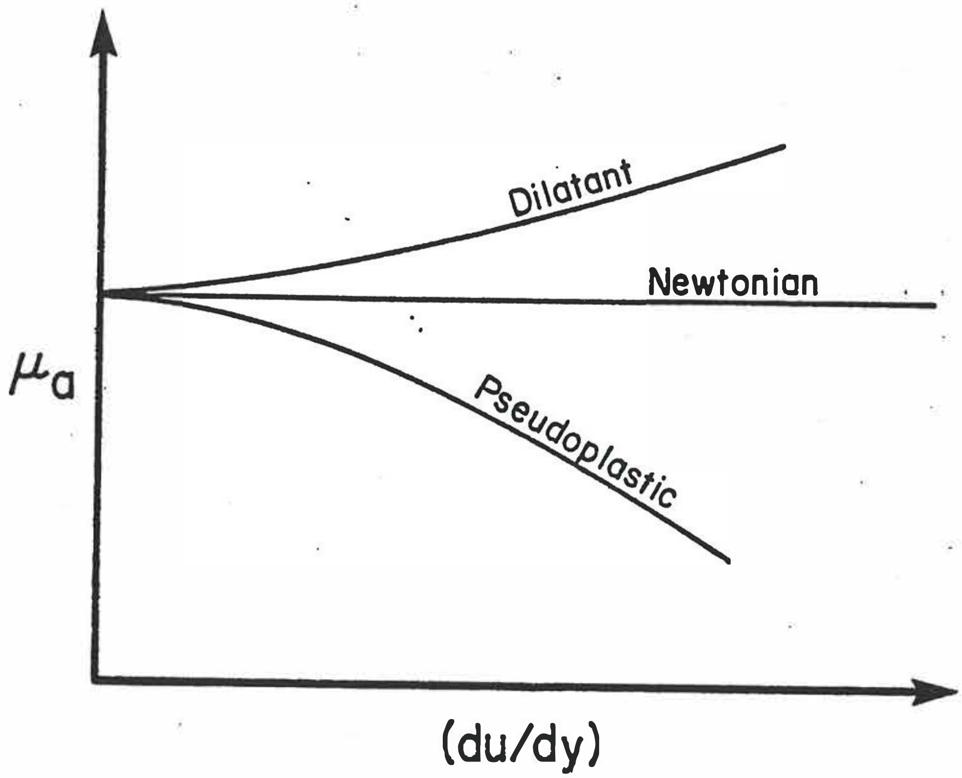

Fig. 1.7 Apparent viscosity (μ_a) versus shear rate (du/dy).

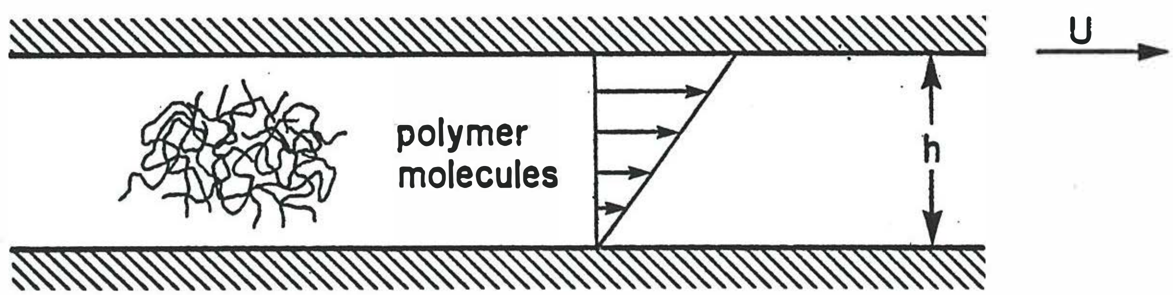

Fig. 1.8 Entangled polymer molecules subjected to shearing between two parallel plates.

increases. This can be explained in terms of Fig. 1.8 which shows some entangled polymer chains (of exaggerated size) in a shear field between two long parallel flat plates. The chains tend to align in the direction of flow and disentangle. Consequently the resistance to flow i.e. viscosity becomes smaller as the rate of shearing increases.

The power-law model (equation (1.10) with $n < 1$) describes fairly well the behavior of polymer solutions and melts except in the region of low shear rates where it gives an infinite apparent viscosity. Actually these fluids have a region of constant Newtonian viscosity as shown in Fig. 1.9.

1.5 SURFACE TENSION

The molecules at a free liquid surface are surrounded by liquid molecules on only one side, whereas those considerably below the surface are completely surrounded. Consequently the molecules near the free surface exhibit a greater attraction for each other. The free liquid surface behaves somewhat like a stretched membrane. With similar arguments we may explain an analogous behavior at an interface between a liquid and a solid and between two immiscible liquids. This "tension" is called surface tension, is denoted by σ (sigma), and has dimensions of force per length. The force necessary to hold a surface together at any line is given by

$$F = \int \sigma \, d\ell \tag{1.12}$$

This force is responsible for maintaining the height of a liquid column in a capillary tube and for keeping the two halves of a liquid bubble or drop together, as shown in Fig. 1.9.

The surface tension generally decreases with temperature and becomes zero at the critical point. Surface tension values of a given surface may change considerably in the presence of contaminants like soap or detergents. At room temperature, the surface tension for a water-air interface is $\sigma = 0.073$ N/m and for mercury-air $\sigma = 0.48$ N/m.

1.6 THE NO-SLIP CONDITION

Experiments have shown that a fluid adjacent to a solid surface cannot slip relative to the surface. This is true no matter how small the viscosity of the fluid is. In other words all fluids at a point of

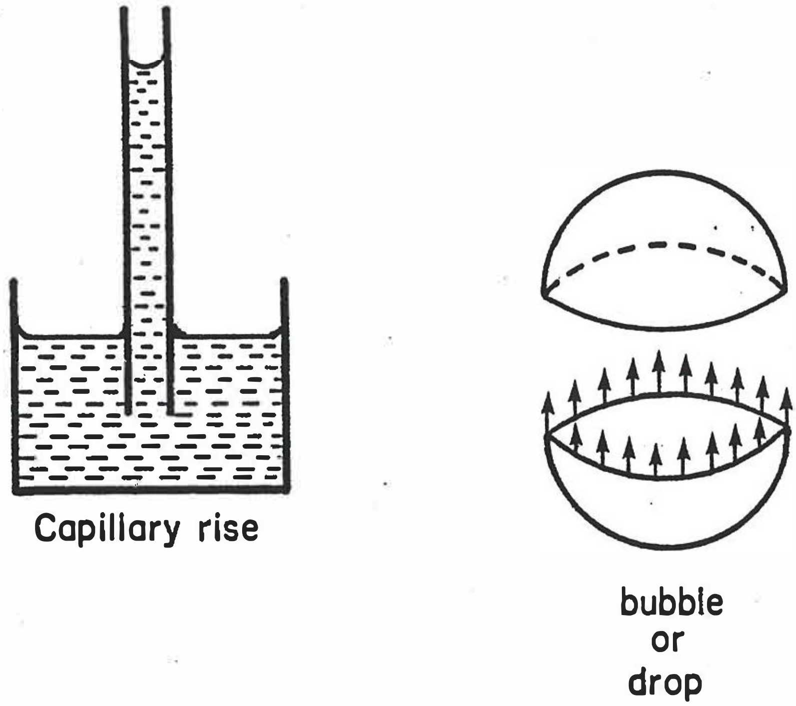

Fig. 1.9 Examples of surface tension.

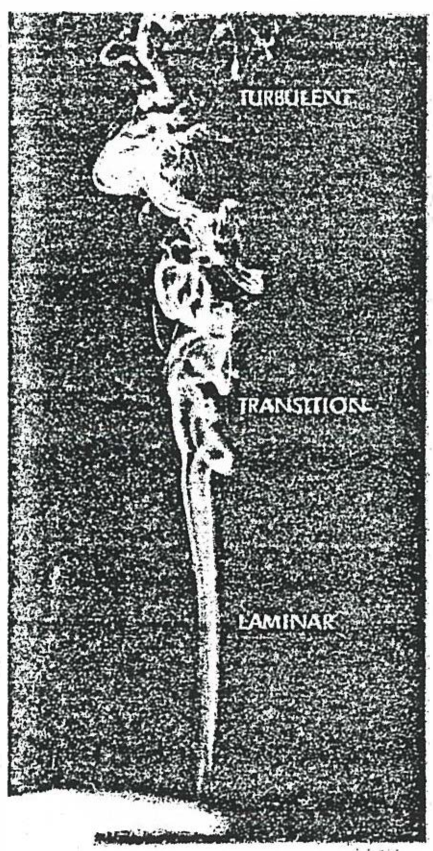

Fig. 1.10 Transition from laminar to turbulent flow in the smoke of a burning cigarette.

contact with a solid take on the velocity of the solid surface.

$$u_{fluid} = u_{wall} \tag{1.13}$$

The no-slip condition leads to the conclusion that the material of the surface has absolutely no influence on the resistance to flow. This somewhat surprising result was the subject of some controversy among nineteenth-century theoreticians. It was rather difficult to accept the no-slip condition for fluids that do not "wet" adjacent solid surfaces like water on wax. However, the "wetting" phenomenon is related to surface tension which has absolutely nothing to do with the no-slip condition.

Gases at extremely low pressures do not obey the no-slip condition and are the object of a special field of study called rarefied gas dynamics [6]. Some rheologically complex fluids exhibit a slip at the wall under certain conditions [5].

1.7 VAPOR PRESSURE OF LIQUIDS

All liquids exhibit a continuous molecular activity which at a free surface becomes evident as evaporation. Molecules escape from the liquid surface continuously and molecules from the vapor return to the liquid phase. When the net rate of exchange of molecules between a liquid and its vapor is zero the pressure is known as the saturation vapor pressure or, simply, vapor pressure and is denoted by p_v.

The vapor pressure of water at 20°C is 2.34 kPa and that of gasoline at 20°C is 55kPa. The intensity of molecular motions increases with temperature and thus the vapor pressure increases with temperature. A high rate of evaporation is known as boiling. Boiling can be brought about either by reducing the pressure in a container containing the liquid or by increasing its temperature.

1.8 COMPRESSIBILITY OF FLUIDS

All materials are to some extent compressible. It is customary, however, to divide the fluids in two broad groups, compressible and incompressible fluids, according to the sensitivity of their density to changes in pressure.

The measure of dependence of the density on pressure is provided by the bulk modulus of elasticity, E, which is defined by the relation

$$E = \rho \frac{dp}{d\rho} \tag{1.14}$$

where ρ = density and p = pressure or in terms of the specific volume, υ, by its equivalent

$$E = -\upsilon \frac{dp}{d\upsilon} \tag{1.15}$$

The compressibility of a liquid, usually denoted by β (beta), is defined by the reciprocal of the bulk modulus

$$\beta = -\frac{1}{\upsilon}\frac{d\upsilon}{dp} \tag{1.16}$$

For liquids the bulk modulus is very high (for water at 20°C and atmospheric pressure E = 2,140,000 kPa) and so the change of density with increase of pressure is very small even for extremely large pressure changes. In the analysis of most (but not all) flow problems, liquids are treated as incompressible fluids. Unlike liquids, gases are easily compressible. Whenever gases flow at velocities considerably lower than the speed of sound the density changes involved are relatively small and therefore gases are treated as incompressible fluids. Pressure (and density) disturbances propagate with the speed of sound. As a consequence, compressibility effects become dominant at velocities approaching or larger than the speed of sound.

1.9 LAMINAR VERSUS TURBULENT FLOW

In the 1840's the German engineer G. Hagen, observed that that the flow of fluids could be of two distinct types, laminar and turbulent. The structural features of these two types of flow can be observed in the smoke leaving a burning cigarette, as shown in Fig. 1.10. The smoke stream is initially smooth and straight. At a certain height above the cigarette it becomes unstable and transition from laminar to turbulent flow takes place. In the turbulent region the smoke is randomly dispersed and the flow is highly irregular.

In 1883 Osborne Reynolds [7] demonstrated clearly the essential nature of laminar and turbulent flow. Reynolds apparatus consisted of a bell-mouthed glass tube into which a dye streak was injected with the water that entered the tube from a reservoir. He observed that for low velocity flow the dye would pass down the tube without mixing with the water as shown in Fig. 1.11(a). By increasing the velocity a value was reached at which the stream began to waver and by further increases the dye became evenly mixed in the downstream portion of the tube, as shown in Fig. 1.11(b).

Reynolds also demonstrated that the transition from laminar to turbulent flow depended only on the value of the dimensionless expression

$$\frac{\rho\, V_{avg}\, D}{\mu}$$

where ρ denotes the density, V_{avg} the mean flow velocity, D the diameter of the tube and μ the viscosity of the fluid. This ratio is called the Reynolds number and it is usually denoted by Re. For smooth, straight, uniform circular pipes the critical value for transition from laminar to turbulent flow is about 2300. This value is slightly lower for pipes with the usual degree of roughness and it is usually taken as 2100. The flow becomes turbulent when the critical value of Re is reached regardless of the individual values of velocity, density, viscosity and pipe diameter, for either liquids or gases. For other flow geometries and configurations the Reynolds number is generalized as follows

$$Re_L = \frac{\rho\, V\, L}{\mu} \tag{1.17}$$

where ρ denotes the density, μ the viscosity, V a characteristic flow velocity and L a characteristic length. For pipe flow L = D, the pipe diameter. The critical value of Re depends on the flow configuration and definition of Re i.e. the choice of the characteristic velocity and length.

High speed photographs reveal that the no-slip condition is valid for laminar as well as for turbulent flow. In Fig. 1.12 the upper flow is turbulent and the lower flow is laminar. For both flows, at the surface of the plate the velocity is zero.

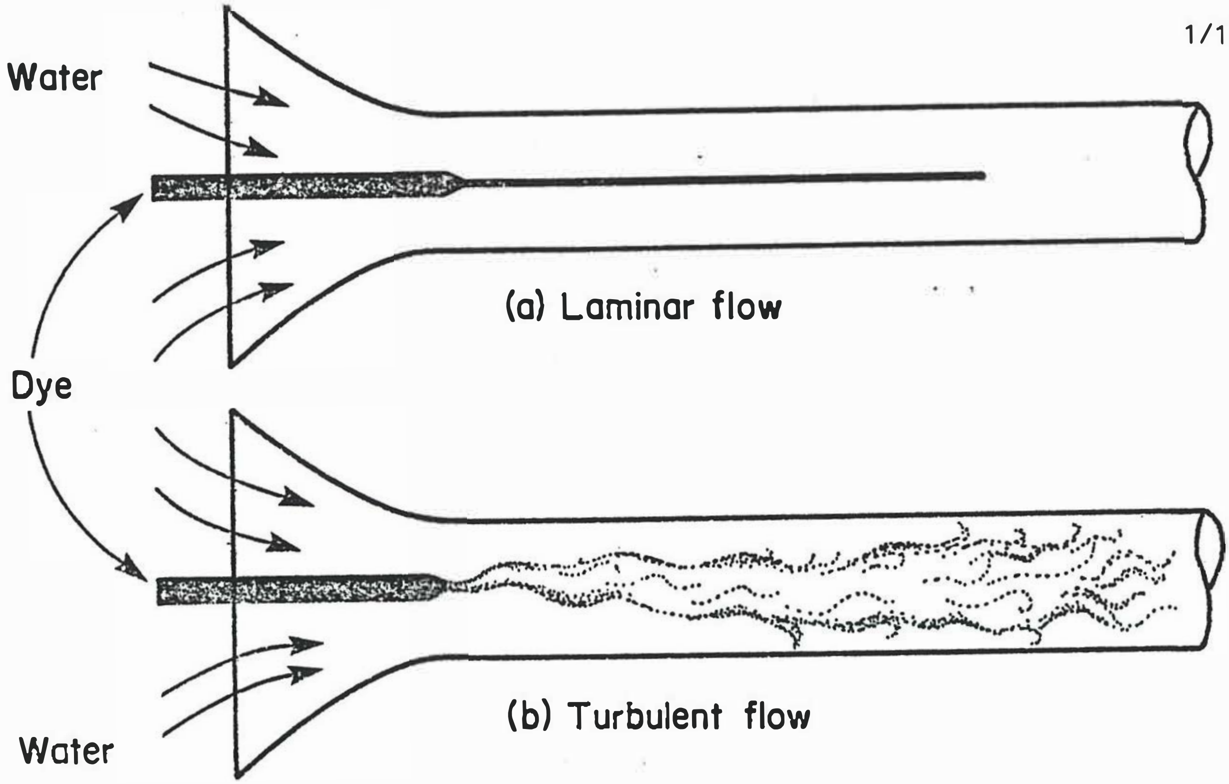

Fig. 1.11 Schematic diagram of Osborne Reynolds experiments.

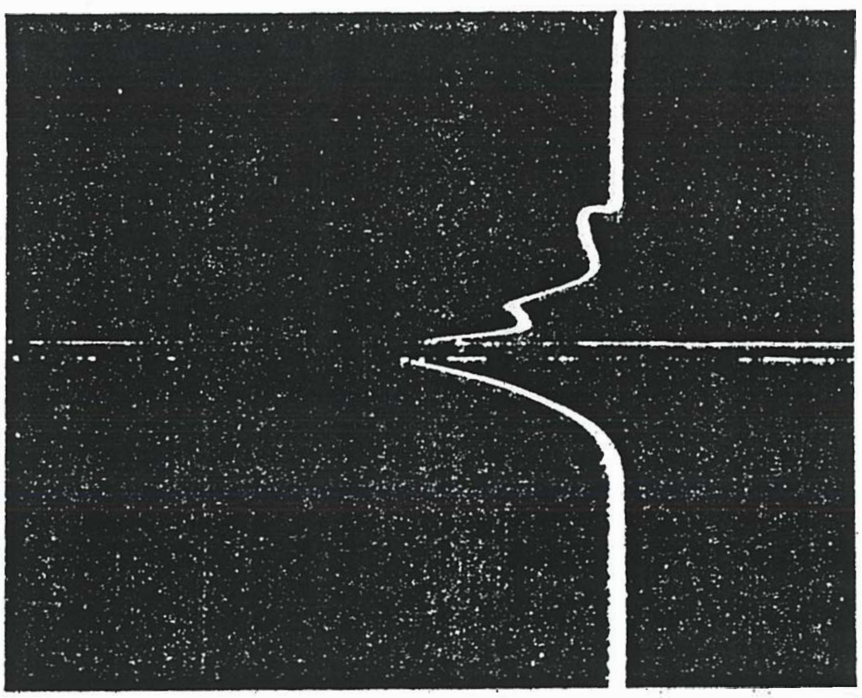

Fig. 1.12 Velocity profiles for flow past a thin flat plate visualized by a line of hydrogen bubbles discharged from a wire. The upper flow is turbulent the lower flow is laminar (reproduced with permission from "Illustrated Experiments in Fluid Mechanics" The NCFMF Book of Film Notes, The MIT Press, Cambridge, Mass., Education Development Center, Inc., copyright 1972).

REFERENCES

[1] J.H. Jeans, "An Introduction to the Kinetic Theory of Gases", Cambridge Univerity Press, Cambridge (1967).

[2] R.B. Bird, W.E. Stewart and E.N. Lightfoot, "Transport Phenomena", Wiley, New York (1960).

[3] J.O. Hirschfelder, C.F. Curtiss and R.B. Bird, "Molecular Theory of Gases and Liquids", Wiley, New York (1954).

[4] G.W. Scott Blair, "Elementary Rheology", Academic Press, London (1969).

[5] G. Astarita and G. Marrucci, "Principles of Non-Newtonian Fluid Mechanics", McGraw-Hill, New York (1974).

[6] M.N. Kogan, "Rarefied Gas Dynamics", Plenum, New York (1969).

[7] O. Reynolds, "An Experimental Investigation of the Circumstances which Determine whether the Motion of Water Shall be Direct or Sinuous and the Law of Resistance in Parallel Channels", Phil. Trans. Roy. Soc. (London) Ser. A., vol. 174, 935 (1883).

[8] C. Truesdell and R.A. Toupin: In S. Flügge (Ed.), "Handbook der Physik", Vol. 3/1, Springer-Verlag, Berlin (1960).

[9] H. Schlichting, "Boundary Layer Theory", McGraw-Hill, 6th ed., New York (1968).

[10] S. Whitaker, "Introduction to Fluid Mechanics", Prentice-Hall, Englewood Cliffs, N.J. (1968).

[11] G.K. Batchelor, "An Introduction to Fluid Dynamics", Cambridge University Press, Cambridge (1967).

[12] N. De Nevers, "Fluid Mechanics", Addison-Wesley, Reading, Mass. (1970).

[13] W.E. Langlois, "Slow Viscous Flow", Macmillan, New York (1964).

[14] S. Eskinazi, "Vector Mechanics of Fluids and Magnetofluids", Academic Press, New York (1967).

[15] M.M. Denn, "Process Fluid Mechanics", Prentice-Hall, Englewood Cliffs, N.J. (1979).

John Vlachopoulos, *Fundamentals of Fluid Mechanics*
Chem. Eng., McMaster University, Hamilton, ON, Canada
(First Edition 1984, revised internet edition (2016), www.polydynamics.com)

CHAPTER 2

FLUID STATICS

2.1 PRESSURE DISTRIBUTION IN A FLUID AT REST

The word statics is derived from the Greek word statikos, which means motionless. For a fluid at rest the three velocity components are zero by definition ($v_x = 0$, $v_y = 0$ and $v_z = 0$). Consequently there are no tangential (shearing) forces. The normal (pressure) forces must be in static equilibrium with body forces i.e. forces which depend on the amount of mass of the body, like gravitational and electromagnetic forces. We will determine the pressure distribution in a fluid at rest in which the only body force acting is due to gravity.

Consider the infinitesimal parallelpipedal volume element shown in Fig. 2.1, with gravity acting in the negative z direction. Pressure is a scalar quantity defined as the magnitude of force acting normal to a surface divided by the area of that surface. The pressure may vary from point to point and also depend on time, $p = p(x,y,z,t)$. For sufficiently small distances (infinitesimal) the pressure at a point in a continuum may be determined from its value at a neighboring point. Let p be the pressure at point O(x,y,z) of Fig. 2.1. Using Taylor's expansion formula with the higher order terms being negligible, we obtain

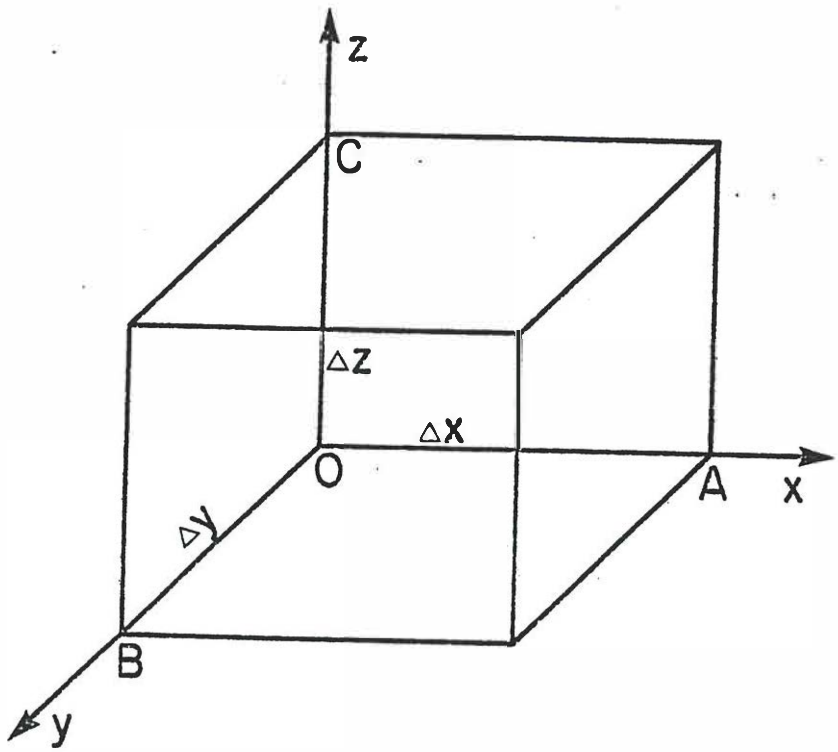

Fig. 2.1 Infinitesimal volume element Δx Δy Δz

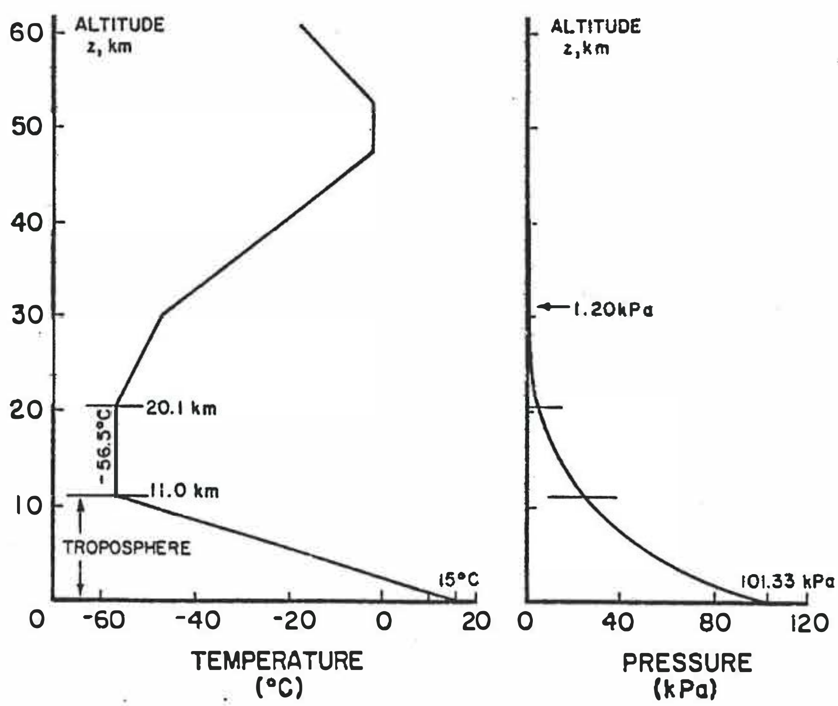

Fig. 2.2 Temperature and pressure as a function of altitude in the standard atmosphere.

$$p_A = p + \frac{\partial p}{\partial x} \Delta x \tag{2.1}$$

$$p_B = p + \frac{\partial p}{\partial y} \Delta y \tag{2.2}$$

$$p_C = p + \frac{\partial p}{\partial z} \Delta z \tag{2.3}$$

The principle of static equilibrium states that the sum of forces in any direction must be zero. Therefore

$$\Sigma F_x = 0 \tag{2.4}$$

$$\Sigma F_y = 0 \tag{2.5}$$

$$\Sigma F_z = 0 \tag{2.6}$$

Or, in terms of pressure forces, we have in the x direction

$$p \; \Delta y \; \Delta z - (p + \frac{\partial p}{\partial x} \Delta x) \; \Delta y \; \Delta z = 0$$

or

$$\frac{\partial p}{\partial x} = 0 \tag{2.7}$$

which means that the pressure cannot vary in the x direction. Similarly, in the y direction

$$p \; \Delta x \; \Delta z - (p + \frac{\partial p}{\partial y} \Delta y) \; \Delta x \; \Delta z = 0$$

or

$$\frac{\partial p}{\partial y} = 0 \tag{2.8}$$

which means that the pressure cannot vary in the y direction. Finally, in the z direction the pressure forces must be balanced by the weight of the fluid element.

$$p \; \Delta x \; \Delta y - (p + \frac{\partial p}{\partial z} \Delta z) \; \Delta x \; \Delta y - \gamma \; \Delta x \; \Delta y \; \Delta z = 0$$

or

$$\frac{\partial p}{\partial z} = -\gamma \tag{2.9}$$

where γ is the specific weight which is the product of the density (ρ) and the gravitational constant g (at sea level $g = 9.81 \text{ m/s}^2$)

$$\gamma = \rho g \tag{2.10}$$

The minus sign means that as z becomes larger (higher elevation) p be comes smaller. To find the pressure we must integrate equation (2.9) or its equivalent

$$\frac{dp}{dz} + \rho g = 0 \tag{2.11}$$

This is the basic equation of fluid statics.

Variations of the gravitational acceleration can be calculated from the relation

$$g = g_o \, (r_o/r)^2 \tag{2.12}$$

where g_o is the gravitational acceleration at the surface of the sea and r_o is the earth's radius ($r_o \simeq 6400$ Km). A simple calculation reveals that from the bottom of the deepest ocean to the maximum flight altitude of commercial aircraft the variations are less than 1%. Thus, for all practical purposes g will be taken constant.

Integration of Equation (2.11)

Case I Incompressible fluids (e.g. liquids)

$$\int_{p_1}^{p} dp = -\rho g \int_{z_1}^{z} dz \tag{2.13}$$

$$(p - p_1) = -\rho g \, (z - z_1) \tag{2.14}$$

Thus, for a point at a distance h below the surface of a liquid

$$p = \rho g h \tag{2.15}$$

where h is measured from the free liquid surface.

Case II All gases are compressible. The density is roughly proportional to pressure. Therefore, we must introduce the ideal gas law $\rho = p/RT$ or some other functional relation between density, pressure and position.

(a) isothermal conditions: $\rho = p/RT$ and $T = T_1$

$$\frac{dp}{dz} = -\frac{p}{RT} \, g \tag{2.16}$$

or by separating the variables

$$\frac{dp}{p} = -\frac{1}{RT} \, g \, dz \tag{2.17}$$

$$\int_{p_1}^{p} \frac{dp}{p} = -\frac{1}{RT_1} \int_{z_1}^{z} dz \tag{2.18}$$

and

$$p = p_1 \exp \left[-\frac{g(z-z_1)}{RT_1}\right] \tag{2.19}$$

(b) isentropic conditions: $p\,\rho^{-k} = \text{const}$

$$\frac{p}{\rho^k} = \frac{p_1}{\rho_1^k} \tag{2.20}$$

and

$$\rho = \rho_1 \left(\frac{p}{p_1}\right)^{1/k} \tag{2.21}$$

and by inserting the above expression into equation (2.11)

$$\frac{dp}{dz} = -\rho_1 \left(\frac{p}{p_1}\right)^{1/k} g \tag{2.22}$$

$$\int_{p_1}^{p} \frac{dp}{p^{1/k}} = -\frac{\rho}{p_1^{1/k}}\, g \int_{z_1}^{z} dz \tag{2.23}$$

$$\frac{p^{(1-1/k)} - p_1^{(1-1/k)}}{(1-1/k)} = -\frac{\rho}{p_1^{1/k}}\, g\,(z-z_1) \tag{2.24}$$

$$p = \left[p_1^{(k-1)/k} - \left(\frac{k-1}{k}\right) \frac{\rho}{p_1^{1/k}}\, g(z-z_1)\right]^{k/(k-1)} \tag{2.25}$$

(c) Temperature decreasing linearly with altitude. This corresponds to the standard atmosphere of Appendix B. By international agreement the temperature is assumed to vary from 288.16 K (15°C) at sea level to 216.5 K (-56.5°C) at altitude of 11,000 m. This lower portion of the atmosphere is called the troposphere. The lapse rate is

$$B = 0.00650 \text{ K/m} \tag{2.26}$$

Here, we have

$$T = T_o - Bz \tag{2.27}$$

$$dp = -\frac{p}{RT}\, g\, dz \tag{2.28}$$

$$\frac{dp}{p} = -\frac{g\,dz}{R(T_o - Bz)} \tag{2.29}$$

Then upon integrating

$$p = p_o \left(\frac{T_o - Bz}{T_o}\right)^{g/RB} \tag{2.30}$$

where $\frac{g}{RB} = 5.26$ (air)

and p_o, T_o represent the pressure and temperature respectively, at sea level.

Beyond elevation 11,000 m and up to about 20,000 m the temperature has been observed to be approximately constant at -56.5^oC. This portion of the atmosphere is called the stratosphere. The pressure and temperature variation in the standard atmosphere is schematically shown in Fig. 2.2, from refs. [1] and [2].

Example 2.1

If the air were incompressible and had a constant density $\rho = 1.24$ kg/m^3 what would be the height of air surrounding the earth to produce a pressure of 101.3 KPa at sea level?

Solution:

For this problem equation (2.14) is applicable:

$$p - p_1 = -\rho g(z - z_1)$$

$$p_1 = 101,300 \frac{N}{m^2},\ z_1 = 0,\ p = 0$$

$$z = \frac{p_1}{\rho g} = \frac{101,300\ N/m^2}{1.24\ kg/m^3 \times 9.81\ m/s^2}$$

$$= \frac{101,300\ N/m^2}{1.24 \times 9.81\ N/m} = 8328\ m$$

Example 2.2

Compute the atmospheric pressure at an altitude of 5000 m if the pressure at sea level is 101.3 kPa by the following four methods: (a) assume air of constant density $\rho = 1.24$ kg/m^3, (b) isothermal conditions, (c) isetropic conditions, and (d) temperature decreasing linearly with altitude ($B = 0.00650$ K/m).

(a)
$$p - p_1 = -\rho g(z-z_1)$$

$$p - 101.3 \text{ kPa} = -\ (1.24 \frac{Kg}{m^3}) \times (9.81 \frac{m}{s^2}) \times (5000 \text{ m})$$

$$p \simeq 40.5 \text{ kPa}$$

(b)
$$p = p_1 \exp[-\frac{g(z-z_1)}{RT_1}] = 101.3 \text{ kPa} \exp[-\frac{9.81 \text{ m/s}^2 \times 5000 \text{ m}}{287 \text{ m}^2/\text{s}^2\text{k} \times 288.16 \text{ K}}]$$

$$\simeq 56 \text{ kPa}$$

(c)
$$p = [p_1^{k-(1/k)} - (\frac{k-1}{k}) \frac{\rho}{p_1^{1/k}} g(z-z_1)]^{k/(k-1)}$$

$$= [101.3^{(1.4-1)/1.4} - (\frac{1.4-1}{1.4}) \times \frac{1.24}{(101.3)^{1/1.4}} \times 9.81 \times 5000]^{1.4/(1.4-1)}$$

$$\simeq 52 \text{ kPa}$$

(d)
$$p = p_o (\frac{T_o - Bz}{T_o})^{g/RB}$$

$$p = 101.3 (\frac{288.16 - 0.0065 \times 5000}{288.16})^{5.26} \simeq 54 \text{ kPa}$$

2.2 THE HYDROSTATIC PARADOX

From equation (2.15) we conclude that the pressure at a point in a fluid depends on density, gravity and the depth only. The shape or size of the container or the orientation of the surface have absolutely nothing to do with the pressure at the given point. The force exerted on a surface equals the product of the area of the surface and the pressure which always acts normal to it. This result is sometimes referred to as Pascal's principle. Consequently for the same area A and the same liquid elevation $(z-z_1)$ the total force on the plates at the bottom of the four vessels shown in Fig. 2.3 is the same, regardless of the total weight of liquid they support(!)

The conclusion that different quantities of fluid above a surface can produce the same force on this surface is contrary to a person's intuition and it is often referred to as the hydrostatic paradox. We

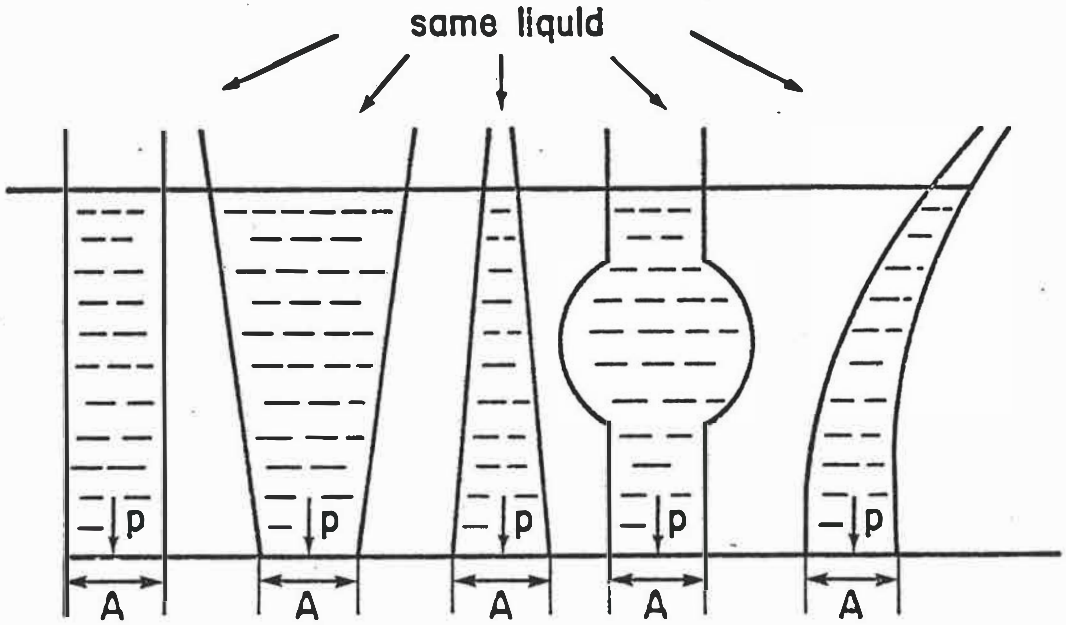

Fig. 2.3 The total force on the plates at the bottom of these four vessels is the same (hydrostatic paradox).

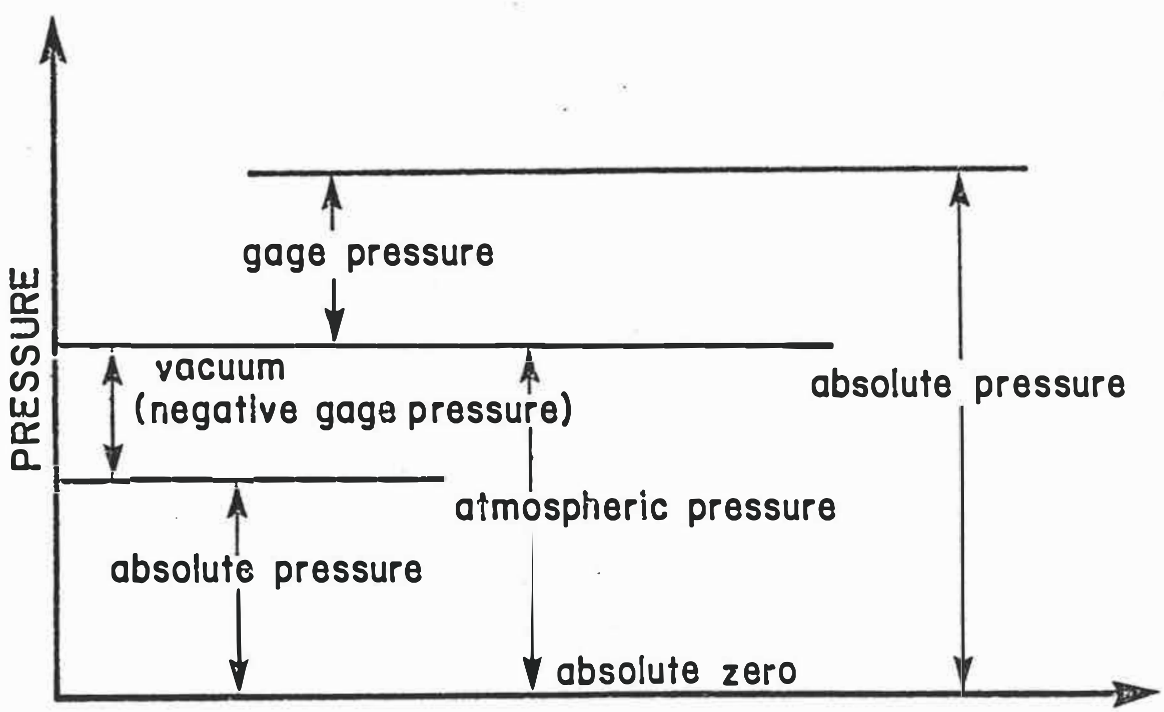

Fig. 2.4 Definition of absolute and gage pressure.

can actually explain this paradox by determining all the hydrostatic forces acting on the various surfaces and by taking into account their directions and their points of action.

2.3 ABSOLUTE AND GAGE PRESSURE

Pressure of a fluid can be expressed relative to that of vacuum (zero) and the result is known as absolute pressure. In practice, however, pressure is usually expressed as the difference between the pressure of the fluid and that of the surrounding atmosphere. This difference is recorded by the usual pressure gages and it is called gage pressure. Thus

$$p_{abs} = p_{atm} + p_{gage} \tag{2.31}$$

It is possible to have either positive or negative gage pressures as shown in Fig. 2.4. Unless otherwise specified, all numerical pressure values throughout this text refer to gage pressures.

The absolute pressure of the atmosphere is measured by the barometer. This consists of an inverted glass tube with its lower end immersed in a liquid (usually mercury) as shown in Fig. 2.5. Mercury is used in barometers because of its high density and its relatively low vapor pressure at room temperature. The pressure at A within the tube is equal to the atmospheric pressure (outside the tube). Consequently

$$p_a = \rho g h + p_v \tag{2.32}$$

where p_a is the absolute pressure of the atmosphere, ρ the density of mercury and h the height of column above A. The vapor pressure P_v is usually negligible. At sea level the atmospheric pressure is 101.33 kPa, which corresponds to h = 760 mm of Hg or h = 10.33 m of H_2O.

2.4 MANOMETERS

Manometers are devices in which one or more columns of a liquid are used to determine the pressure difference between two points. Such a manometer is shown in Fig. 2.6. The U-tube manometer measures the pressure difference between the pressure tank A and the atmosphere. To determine the pressure at A we will use equation (2.14). It is implicitly assumed that both fluids are incompressible.

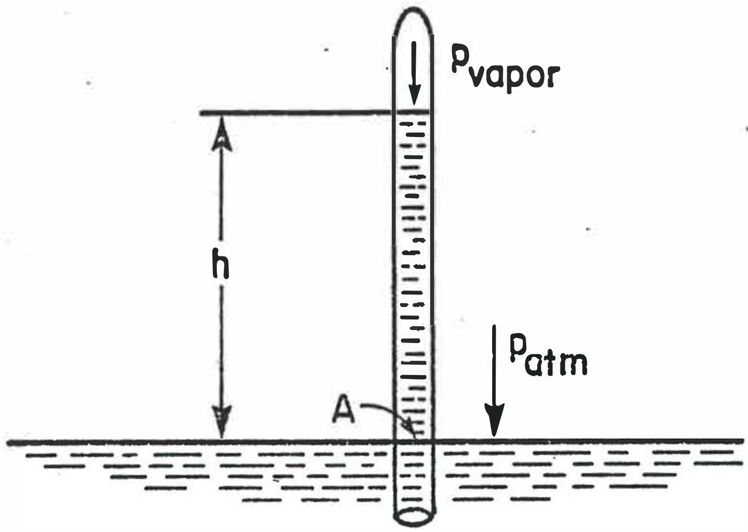

Fig. 2.5 Barometer

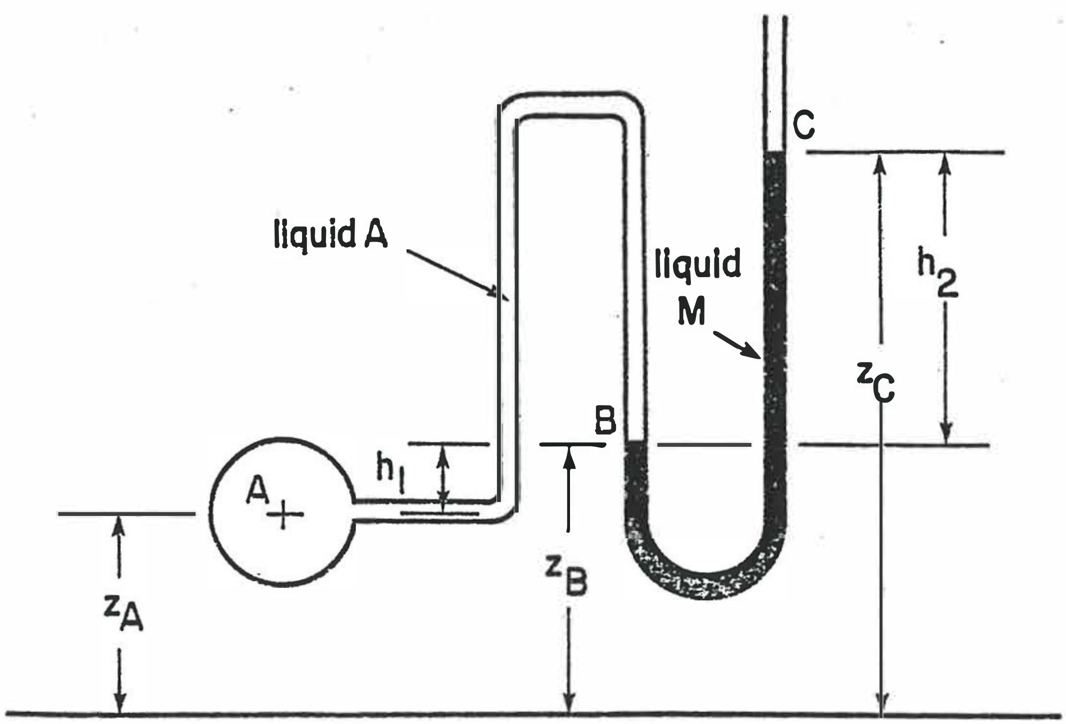

Fig. 2.6 U-tube manometer

Between A and B:

$$p_A - p_B = -\rho_A g\ (z_A - z_B)$$

Between B and C:

$$p_B - p_C = -\rho_M g\ (z_B - z_C)$$

Summing up

$$p_A - p_C = -\rho_A g\ (z_A - z_B) - \rho_M g\ (z_B - z_C)$$

But $z_A - z_B = -h_1$ and $z_B - z_C = -h_2$

$p_A - p_C$ => is the gage pressure at A

$$(p_A)_{gage} = \rho_A g h_1 + \rho_M g h_2$$

Example 2.3

Determine the gage pressure in the air tank shown in the accompanying Fig. E.2.3.

Solution

We apply equation (2.14).

between A and B:

$$p_A - p_B = -\rho_{Hg} g(z_A - z_B)$$

between B and C:

$$p_B - p_C = -\rho_{H_2O} g(z_B - z_C)$$

between C and D; $\quad p_C - p_D = -\rho_{Hg} g(z_C - z_D)$

by summing up, we obtain

$$p_A - p_D = -\rho_{Hg} g(z_A - z_B) - \rho_{H_2O} g(z_B - z_C) - \rho_{Hg} g(z_C - z_D)$$

where $z_A - z_B = 5-20 = -15\,\text{cm}$, $z_B - z_C = 20-8 = 12\,\text{cm}$, $z_C - z_D = 8-50 = -42\,\text{cm}$

$p_A - p_D$ => is the gage pressure in the tank p_T. There is no need to consider the column of air between T and A, because of its small density.

$$P_T = 1000\,\frac{kg}{m^3} \times 13.6 \times 9.81\,\frac{m^2}{s} \times 0.15\ m - 1000\,\frac{kg}{m^3} \times 9.81\,\frac{m^2}{s} \times 0.12\ m$$

$$+ 1000\,\frac{kg}{m^3} \times 13.6 \times 9.81\,\frac{m}{s^2} \times 0.42\ m$$

$$= 20012.40 - 1177.20 + 56034.72\ \text{Pa} = 74.87\ \text{kPa}$$

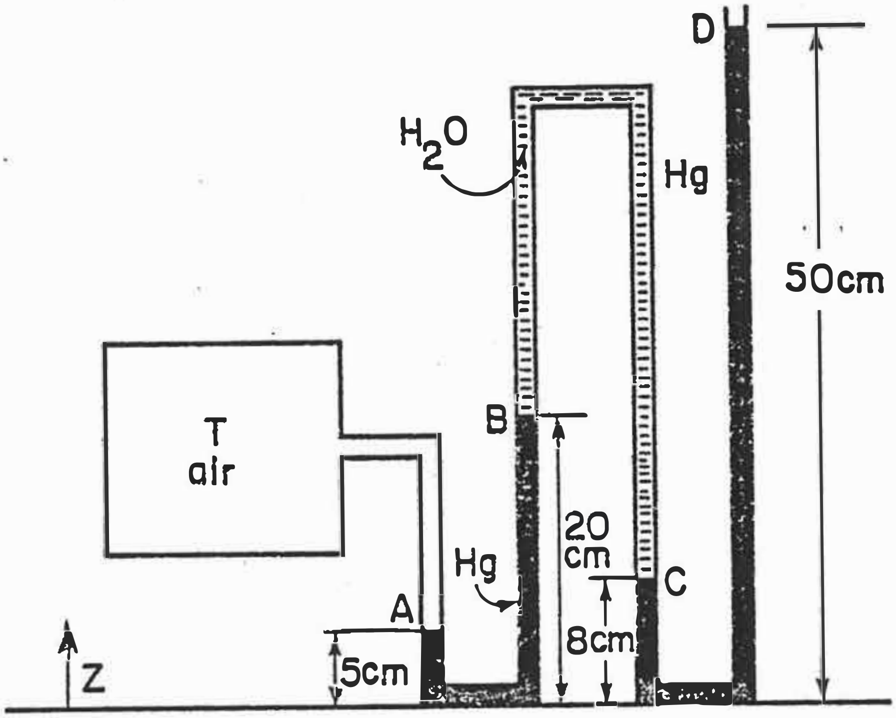

Fig. E.2.3

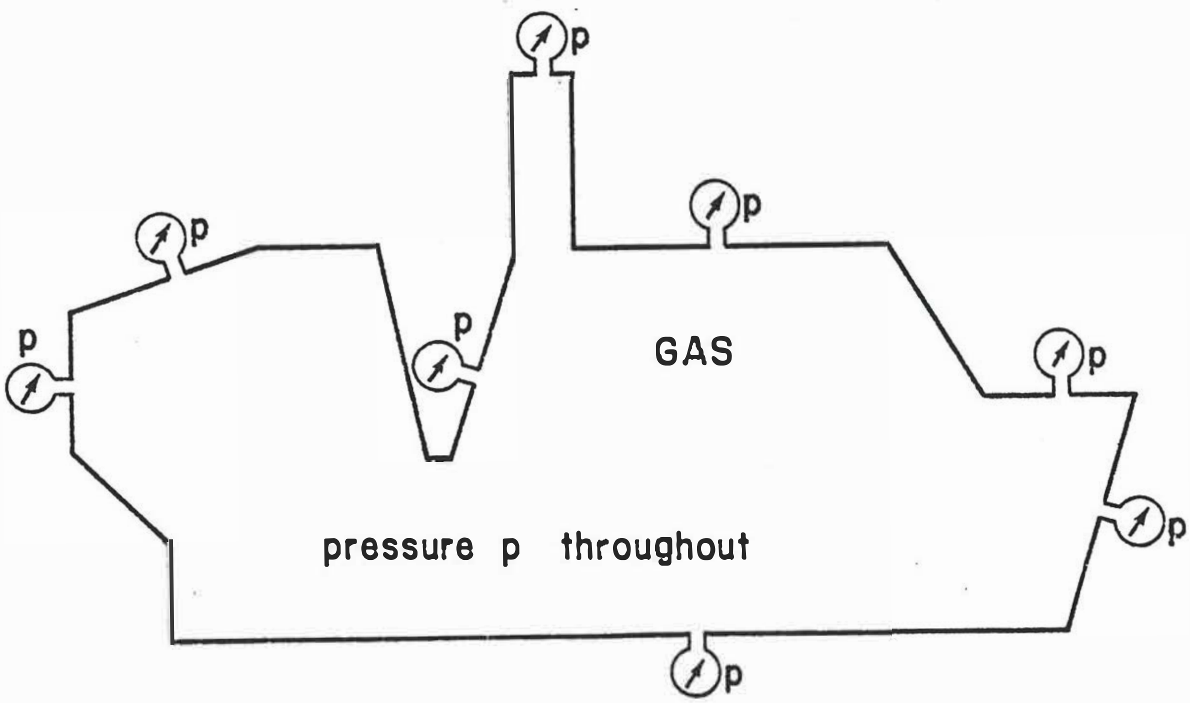

Fig. 2.7 Pressures on the walls of tank confining a gas

2.5 HYDROSTATIC FORCES ON PLANE SURFACES

Pressure always acts normal to a surface, by definition. Thus for an infinitesimal area dA the normal force due to pressure will be

$$dF = p\,dA \tag{2.33}$$

The total force acting on a finite surface can be obtained by integration

$$F = \iint_A p\,dA \tag{2.34}$$

To perform the integration shown in equation (2.34) we must know how the pressure varies over the area under consideration. When a gas is enclosed in a tank as shown in Fig. 2.7 the pressure is always constant over the walls of the tank irrespective of their orientation. The vertical variation is negligible because of the small density of gases. Therefore

$$F = pA \quad \text{(for gases)} \tag{2.35}$$

Let us now consider a plane surface of area A submerged in a liquid of constant density ρ. h is the depth measured from the free surface of the liquid as shown in Fig. 2.8. From equation (2.34) we have:

$$F = \iint_A p\,dA = \iint_A \rho g h\,dA = \iint_A \rho g y \sin\theta\,dA$$

$$= \rho g \sin\theta \iint_A y\,dA = \rho g \sin\theta\, A \frac{\iint_A y\,dA}{A} \tag{2.36}$$

The quantity $\frac{\iint_A y\,dA}{A}$ represents the distance of the centroid y_c (see Appendix C) of surface A from point O.

$$F = \rho g y_c \sin\theta\, A = \rho g h_c\, A \tag{2.37}$$

The quantity $\rho g h_c$ represents the pressure at the centroid. Consequently, the force exerted on a submerged plane surface is given by the product of the area and the pressure at the centroid.

Example 2.4

Determine the force exerted by water on the vertical, rectangular wall of width W and height H, shown in Fig. E.2.4.

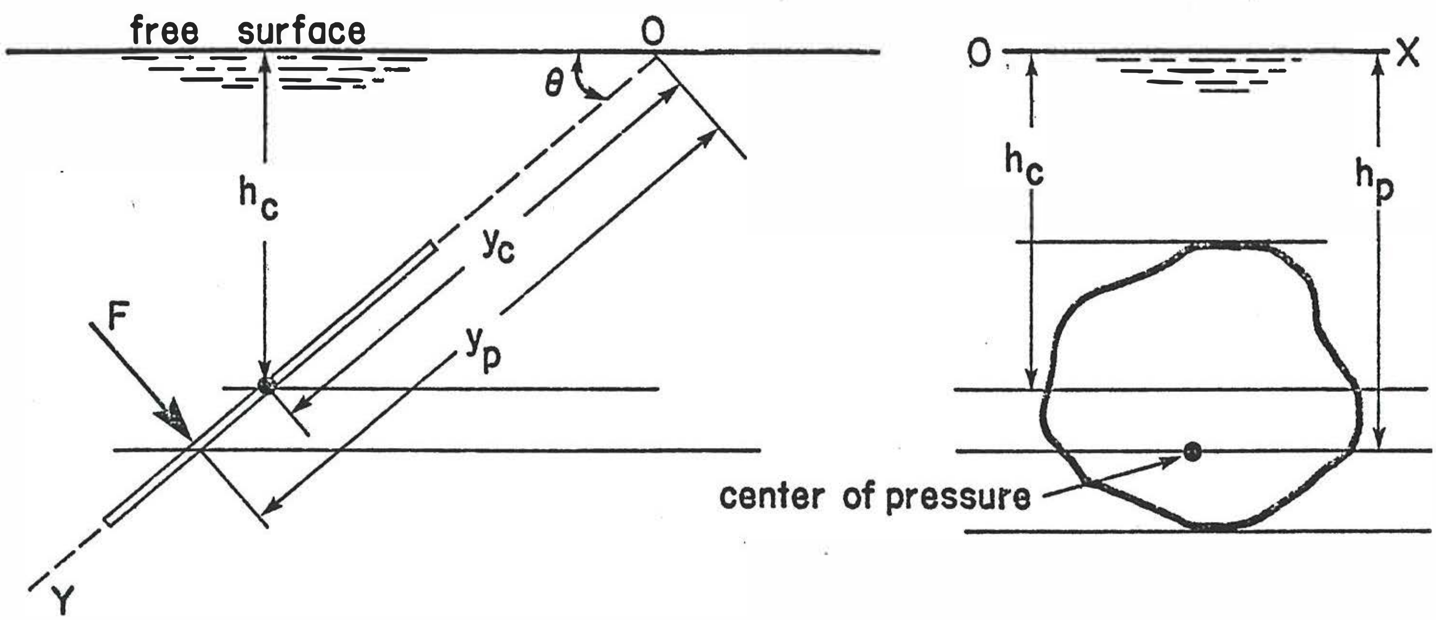

Fig. 2.8 Hydrostatic forces on a submerged plane surface.

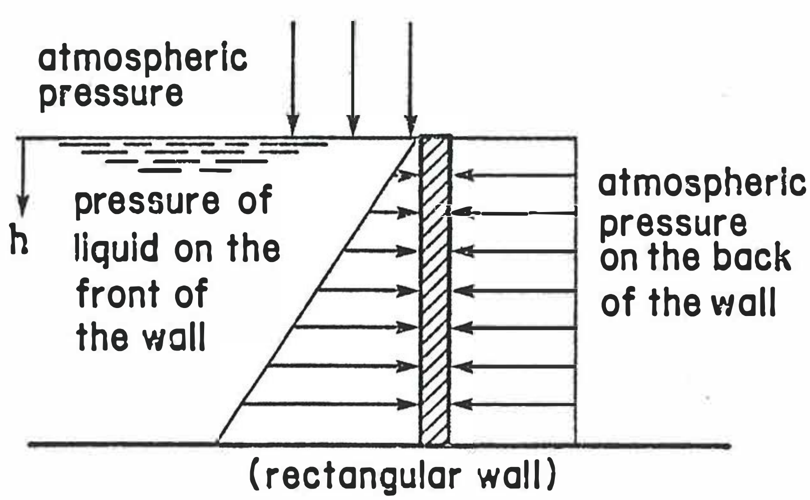

Fig. E.2.4

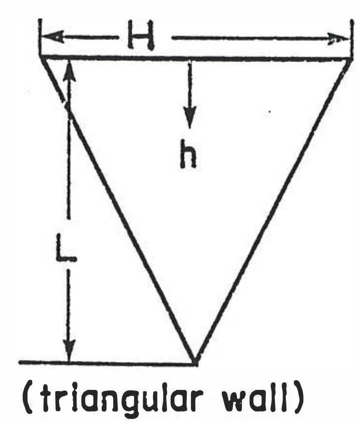

Fig. E.2.5

Solution

The centroid $H_c = H/2$

Therefore

$$F = \rho g \frac{H}{2} (HW) = \rho g W \frac{H^2}{2}$$

This result can also be obtained directly from

$$F = \iint_A p dA = \iint_A \rho g h \, dA = \rho g \int Wh \, dh = \rho g W \int h \, dh$$

$$= \rho g W \frac{H^2}{2}$$

Example 2.5

Assume that the wall in the previous example has a triangular shape. The width at the top is W and at the bottom is zero as shown in Fig. E.2.5. Determine the force.

Solution

The centroid

$$H_c = \frac{H}{3}$$

$$A = \frac{LH}{2}$$

and

$$F = \rho g \frac{LH^2}{6}$$

This result can also be obtained by direct integration

$$F = \rho g \int_o^H hW \, dh$$

$$W = L \left(1 - \frac{h}{H}\right)$$

$$F = \rho g \int_o^H L \left(1 - \frac{h}{H}\right) h \, dh$$

$$= \rho g L \left[\frac{h^2}{2} - \frac{h^3}{3H}\right]_o^H = \rho g L \frac{H^2}{6}$$

2.6 CENTER OF PRESSURE FOR PLANE SURFACES

The point where the line of action of the hydrostatic force intersects the plane surface, is called the center of pressure [2,3,4]:

The moment of the resultant force about any axis must be equal to the sum of the moments of all forces. Taking the moments about OX, in Fig. 2.8,

$$y_p F = \rho g \sin\theta \iint_A y^2 \, dA = \rho g \sin\theta \, I_o \tag{2.38}$$

where I_o is the moment of inertia of the area [5] about OX. Then, using equation (2.37),

$$y_p = \frac{I_o}{y_c A} \tag{2.39}$$

The moment of inertia about OX can be expressed as

$$I_o = y_c^2 A + I_c \tag{2.40}$$

where I_c is the moment of inertia of area A about its centroidal axis. Thus

$$y_p = \frac{A y_c^2 + I_c}{y_c A} = y_c + \frac{I_c}{y_c A} \tag{2.41}$$

From this last expression we conclude that the position of the center of pressure is independent of the angle θ, and it is always below the centroid.

The x-coordinate of the center of pressure may be determined by taking the moments about axis OY

$$x_p F = \rho g \sin\theta \iint_A xy \, dA \tag{2.42}$$

Thus, using equation (2.37),

$$x_p = \frac{\iint_A xy \, dA}{y_c A} \tag{2.43}$$

When the area has an axis of symmetry in the y direction, we can choose OY to coincide with the axis of symmetry. Then the integral $\iint_A xy \, dA$ vanishes and the center of pressure is located on the axis of symmetry.

Example 2.6:

Determine the force and the position of the center of pressure on the semicircular end of Fig. E2.6.

Solution:

From Appendix C

$$h_c = \frac{4r}{3\pi} = \frac{2D}{3\pi} \qquad I_o = \frac{\pi D^4}{128} \qquad A = \frac{\pi D^2}{8}$$

$$F = \rho g h_c A = \rho g \frac{4r}{3\pi} \frac{\pi r^2}{2} = \frac{2}{3} \rho g r^3$$

$$h_p = y_p = \frac{\pi D^4}{128} \frac{1}{\frac{2D}{3\pi} \cdot \frac{\pi D^2}{8}} = \frac{12\pi D}{128} = \frac{3}{32} \pi D$$

2.7 HYDROSTATIC FORCES ON CURVED SURFACES

On a curved surface the infinitesimal forces pdA vary in direction along the surface and thus cannot be added algebraicly as implied by the integral in equation (2.34).

We must take into account the orientation of each element and the direction of the force exerted on it. In other words we must consider the force vector. Equation (2.34) can be generalized as

$$\overline{F} = \iint p\, \overline{dA} \qquad (2.44)$$

where p represents the local pressure and $\overline{dA}$ is now a vector quantity.

This relation can be expressed with respect to a system of coordinate axis (x,y,z) having $\overline{i}$, $\overline{j}$, $\overline{k}$ as the base vectors, as

$$\overline{F} = \overline{i}F_x + \overline{j}\,F_y + \overline{k}\,\overline{F}_k = \overline{i} \iint_{A_x} pdA_x + \overline{j} \iint_{A_y} pdA_y + \overline{k} \iint_{A_z} pdA_z$$

where dA_x, dA_y, dA_z are the components of vector $\overline{dA}$ and A_x, A_y, A_z the projected areas in the y-z, x-z and x-y planes respectively as shown in Fig. 2.9.

Therefore, the three force components are

$$F_x = \iint_{A_x} pdA_x \qquad F_y = \iint_{A_y} pdA_y \qquad F_z = \iint_{A_z} pdA_z \qquad (2.45)$$

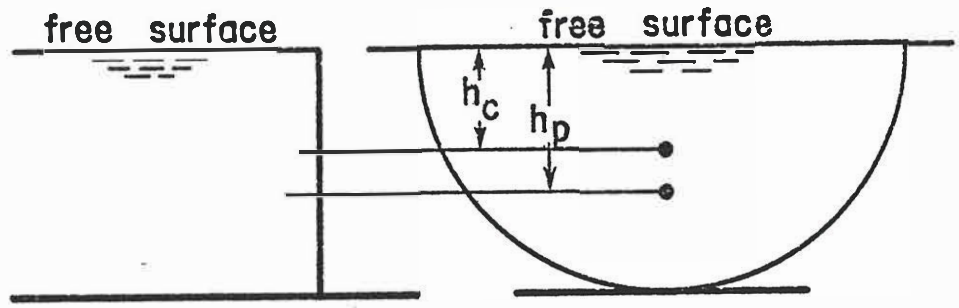

Fig. E.2.6

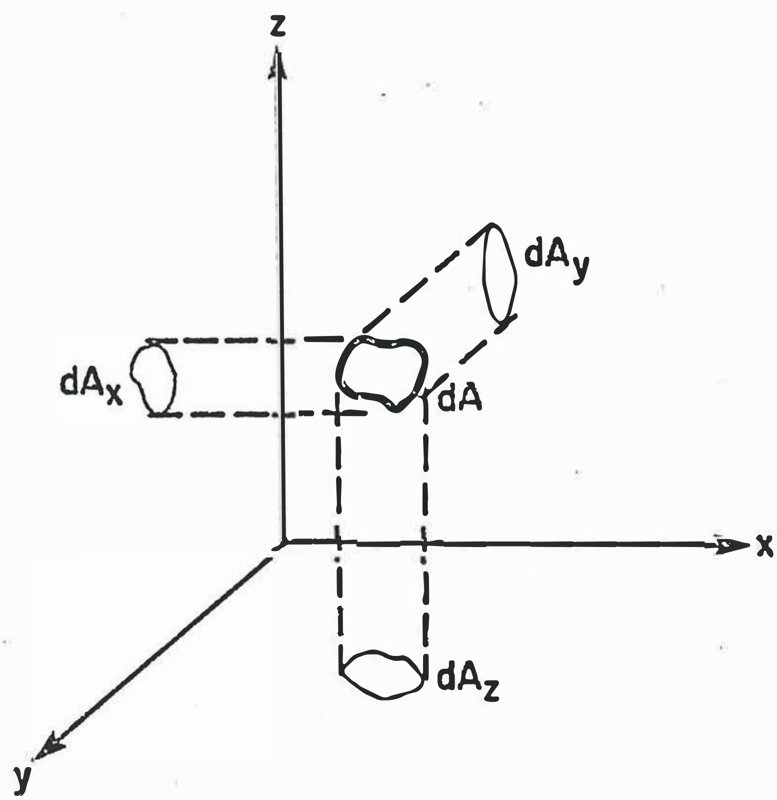

Fig. 2.9 Projections of a curved surface on planes y-z, x-z and x-y.

The horizontal component in x direction is

$$F_x = \iint_{A_x} \rho g h \, dA_x \tag{2.46}$$

where h is the depth measured from the free surface of the liquid. This is the pressure force on the plane-area projection onto the vertical y-z plane. The other horizontal component, F_y, is just the pressure force on the plane-area projection onto the vertical x-z plane. Thus we may state in general that:

> The horizontal component of force on any surface equals the force on the projection of that surface onto a vertical plane normal to the component.

The vertical component is

$$F_z = \iint_{A_z} \rho g h \, dA_z \tag{2.47}$$

which represents the weight of the fluid above the surface. Thus we may state in general that:

> The vertical component of force on any surface equals the weight of a fluid column extending from the surface up to the level of the free surface.

The three force components, two horizontal and one vertical, may not intersect at a single point. Consequently, in general, there is no single resultant force. In many practical problems, however, two forces may lie on the same plane and can be combined as vectors to give a single resultant force. In such a case the center of pressure can be located in exactly the same manner as for the plane surface.

Example 2.7

Determine the total hydrostatic force on the parabolic dam shown in Fig. E2.7, with a = 5m and b = 15m. The width of the dam is W = 50 m.

Solution

The vertical projection of this parabolic surface is a rectangle of 15 m x 50 m. The centroid is located at a depth of h = 7.5 m. Thus, the horizontal force F_x is

$$F_x = \rho g h_c A_x = (1000 \frac{Kg}{m^3})(9.81 \frac{m}{s^2})(7.5 \text{ m})(15 \text{ m})(50 \text{ m})$$

$$= 5.52 \times 10^7 \text{ N}$$

Actually this force can also be calculated by direct integration of one of equations (2.45)

$$F_x = \iint_{A_x} p dA_x = \int_o^b (\rho g h) W dz = \rho W \int_o^b (b-z) dz$$

$$= \rho g W [bz - \frac{z^2}{2}]_o^b = \rho g W \frac{b^2}{2} = (1000)(9.81)(50)(\frac{15^2}{2})$$

$$= 5.52 \times 10^7 \text{ N}$$

The vertical component equals the weight of the fluid from the parabolic surface up to the free surface of water. From Appendix C, the area is 2/3 ab and the volume of water 2/3 abW. Thus,

$$F_z = -\rho g (\frac{2}{3} abW) = -(1000 \frac{Kg}{m})(9.81 \frac{m}{s^2})(\frac{2}{3})(5)(15)(50)$$

$$= -2.45 \times 10^7 \text{ N}$$

the minus sign was introduced because the weight acts in the negative z direction. Again, this force can be determined by direct integration

$$F_z = -\iint_{A_z} p d A_z = -\int_o^a \rho g h W dx = -\rho g W \int_o^a (b-z) dx$$

$$= -\rho g W \int_o^a (b - b (\frac{x}{a})^2) dx = -\rho g W [bx - \frac{b}{a^2} \frac{x^3}{3}]_o^a$$

$$= -\rho g W [ab - \frac{ab}{3}] = -\rho g W (\frac{2}{3} ab) = -2.455 \times 10^7 \text{ N}$$

The magnitude of the total hydrostatic force is

$$F = (F_x^2 + F_z^2)^{1/2} = 6.04 \times 10^{14} \text{ N}$$

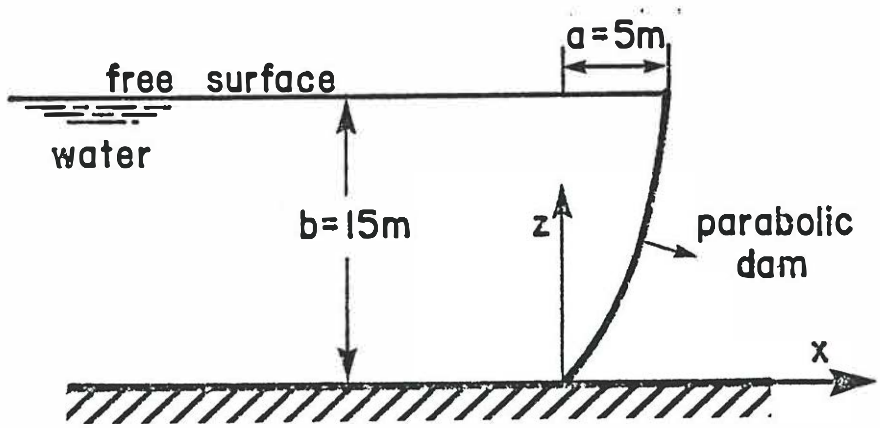

Fig. E.2.7

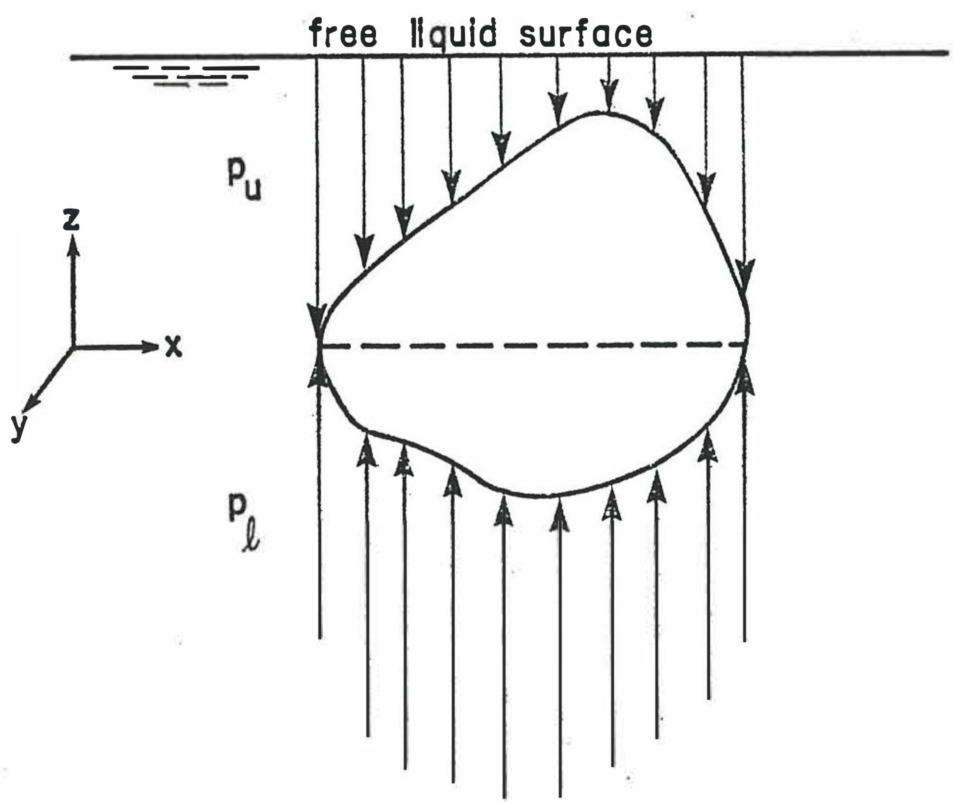

Fig. 2.10 Hydrostatic forces on a submerged body.

2.8 BUOYANCY

The hydrostatic pressure increases with depth in a fluid at rest. Therefore, a fluid exerts a resultant upward force on any body which is wholly or partially immersed in it. This force is known as buoyancy and can be determined by applying the methods used to compute hydrostatic forces on surfaces. Archimedes discovered in the third century B.C. that the buoyant force is equal to the weight of the fluid displaced.

We will prove this principle by referring to Fig. 2.10 which shows a body wholly immersed in a liquid of constant density ρ. There is obviously no net force on a horizontal direction because the forces on the vertical projections cancel each other out.

The upper surface of the body is subjected to a force which is smaller than that on the lower surface. Consequently, there is a net force upwards. For an infinitesimal element we will have a net force

$$d\,F_B = (p_\ell - p_u)\,d\,A_z$$

However, from equation (2.14)

$$p_\ell - p_u = -\rho g\,(z_\ell - z_u)$$

Thus,

$$d\,F_B = -\rho g\,(z_\ell - z_u)\,d\,A_z$$

and

$$F_B = \rho g \iint_{A_z} (z_u - z_\ell)\,d\,A_z$$

The volume of the solid body is

$$\forall_b = \iint_{A_z} (z_u - z_\ell)\,d\,A_z$$

and the buoyant force is

$$F_B = \rho g \forall_b$$

which represents the weight of fluid displaced.

This derivation can easily be generalized to include compressible fluids or buoyant forces at the interface of two immiscible fluids.

To determine the center of buoyancy we must take the moments about x, y and z. For example the moment about axis y is

$$F_B x_b = \rho g \iint_{A_z} x (z_u - z_\ell) \, d A_z$$

The volume of the infinitesimal element is $dV = (z_u - z_\ell) \, dA_z$, thus

$$x_b = \frac{\iiint_{V\!\!\!\!-} x \, dV}{V\!\!\!\!-}$$

which means that the x component of the center of buoyancy is identical to the x component of the <u>centroid</u> of the fluid volume displaced. By taking the moments about x and z we conclude that the center of buoyancy is at the centroid of the volume of fluid displaced. It should further be noted that when the density of a fluid varies with position this conclusion is not true. However, in many practical problems small density variations can be neglected.

The principle of buoyancy is used in the measurement of specific weight (or specific gravity) with a device called <u>hydrometer.</u> This consists of a glass bulb partly filled with lead shot and a graduated stem as shown in Fig. 2.11. When placed in a liquid the hydrometer floats in the vertical position and the graduated stem extends above the surface. The hydrometer will float deeper or shallower depending on the density of the liquid in which it is immersed. The graduated scale on the stem provides directly the specific weight or the specific gravity of the liquid.

<u>Example</u>

The hydrometer bulb of Fig. 2.11 has a volume of 10 cm^3 and the cylindrical glass stem has a diameter of 5 mm and a length of 20 cm. The bulb and the lead shot in it have a mass of 18 g and the glass stem 2 g. Determine at what level this device will float in liquids having specific gravities 0.8, 1.0 and 1.2.

<u>Solution</u>

The volume of the immersed part of the cylindrical stem is

$$V_s = \pi(0.5)^2 \, z \; (cm^3) = 0.7 \, z \; cm^3$$

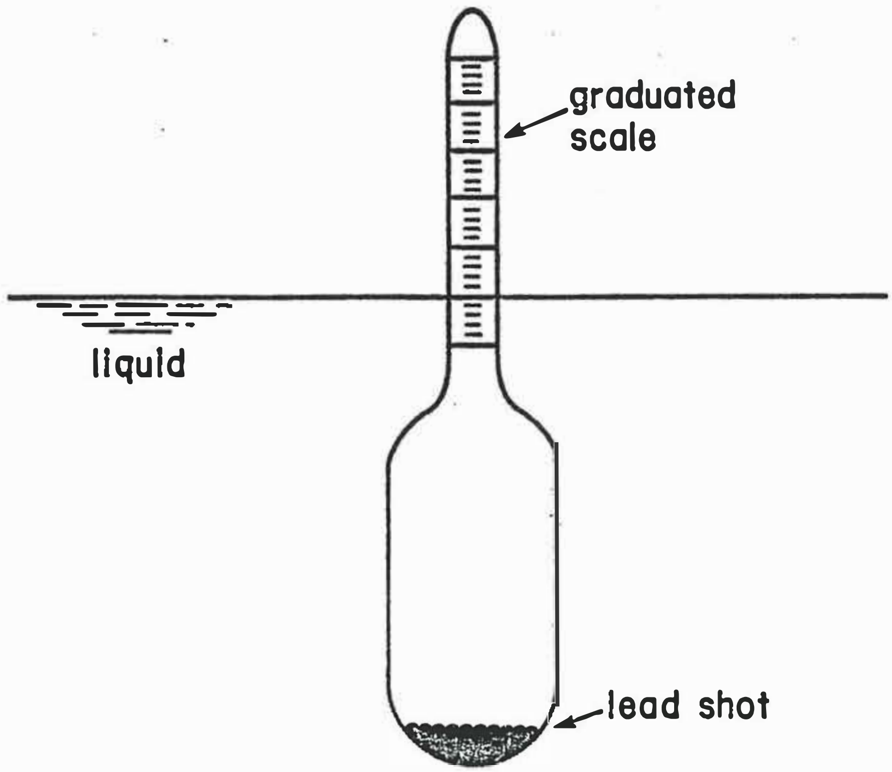

Fig. 2.11 Hydrometer

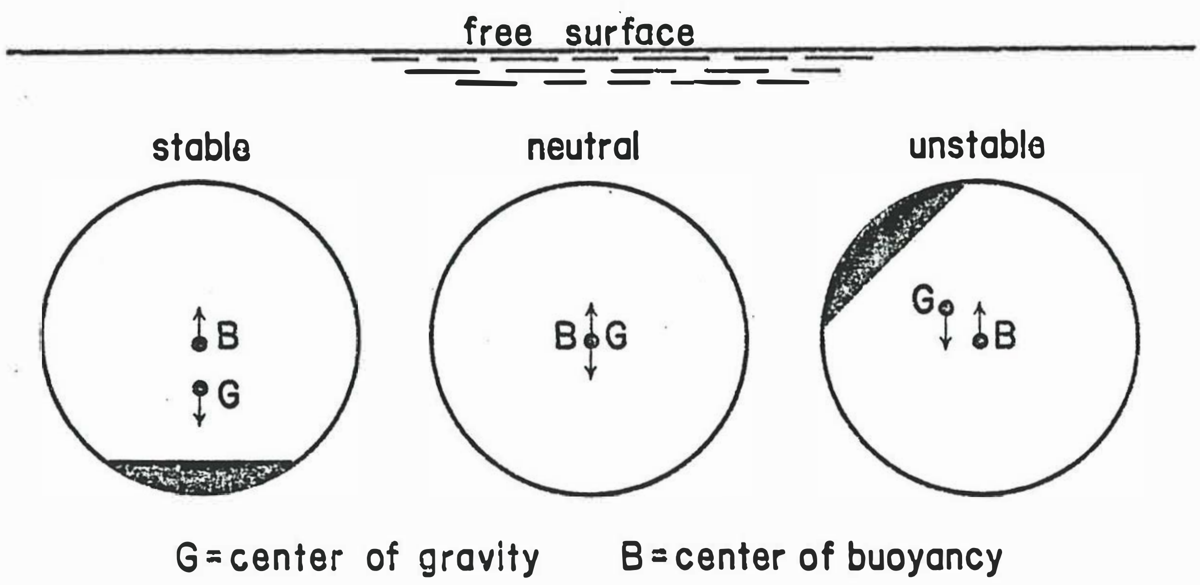

Fig. 2.12 Stability of a submerged (i.e. fully immersed) body.

where z is the immersed length of the stem in cm. The total weight of hydrometer is equal to the weight fluid displaced:

$$(18 + 2)\ g = (10 + 0.79\ z)\ \rho g$$

$$20 = (10 + 0.79\ z)\ \rho$$

Dividing by the density of water $\rho_{H_2O} = 1\ g/cm^3$

$$20 = (10 + 0.79\ z)\ \left(\frac{\rho}{\rho_{H_2O}}\right)$$

for $S.G. = \rho/\rho_{H_2O}$

for S.G. = 0.8 $\qquad$ z = 19.0 cm

for S.G. = 1.0 $\qquad$ z = 12.66

for S.G. = 1.2 $\qquad$ z = 8.44

It should be noted that the graduations are not equally spaced because the buoyancy is not directly proportional to the specific gravity.

2.9 STABILITY OF IMMERSED AND FLOATING BODIES

The stability of a body in static equilibrium can be determined by examining whether a restoring (or righting) moment is produced when a small rotation is imposed. For a fully immersed body the production of such a restoring moment depends on the relative position of the center of gravity and the center of buoyancy. By referring to Fig. 2.12, we can easily conclude that the body is

(a) stable, if the center of gravity is located below the center of buoyancy

(b) neutral, if the center of gravity coincides with the center of pressure

(c) unstable, if the center of gravity is located above the center of buoyancy.

The stability conditions are more complicated for a body floating on a free surface. Surprisingly, the center of gravity can be above the center of buoyancy and the floating body may be stable, neutral or unstable.

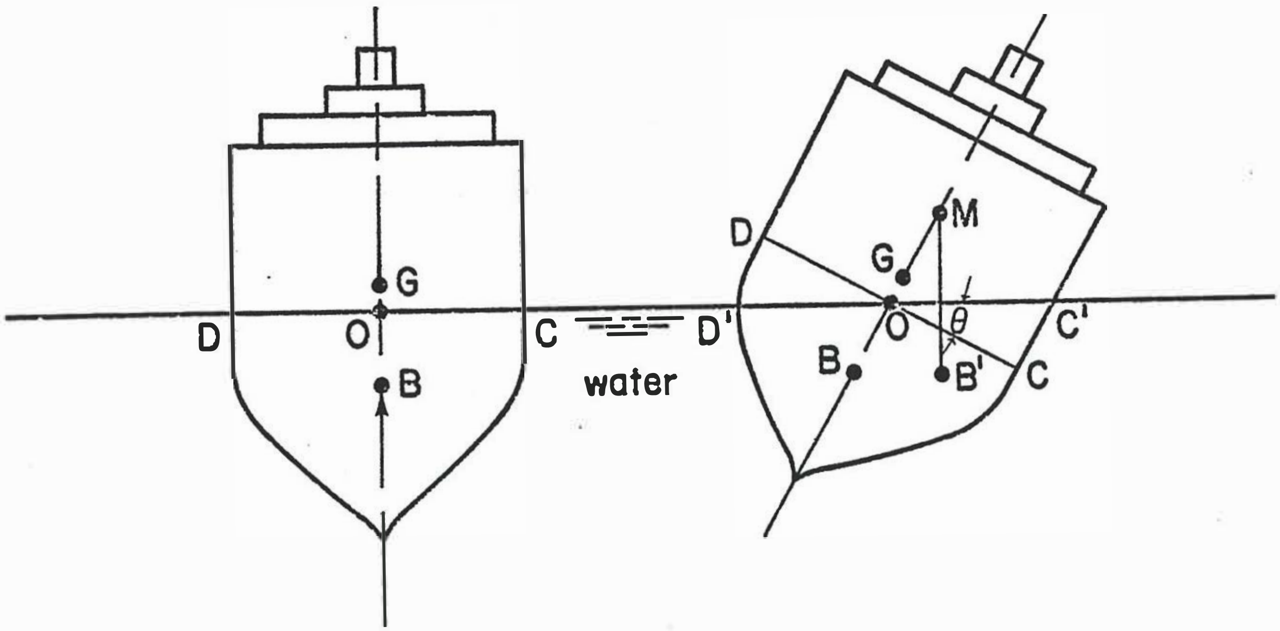

Fig. 2.13 Stability of a floating body.

Let us consider the hull section of a ship of arbitrary configuration as shown in Fig. 2.13. The center of gravity is assumed to be above the center of buoyancy. Suppose that the ship is rolled through a small angle θ. The position of the center of gravity remains unchanged. However, the position of the center of buoyancy will generally change. The point of intersection of the lines of action of the buoyant force before and after the tilt is called the metacenter M. The distance GM is called the metacentric height.

The shift of the center of buoyancy from B to B' is a result of the change in displaced volume. By taking the moments about O we can determine the length $\overline{MB}$. The stability criterion is

$$\overline{MB} - \overline{GB} > 0$$

The frequency of oscillations about O can be determined by considering the ship as a pendulum, the motion of which is governed by the relation between torque and annular acceleration [6,7]. Although the basic principles for the calculation of stability are relatively simple and straightforward [6,7,8] the application to ship design requires extensive experience [9].

REFERENCES

1. "U.S. Standard Atmosphere, 1962", U.S. Government Printing Office, Washington (1962).
2. F.M. White, "Fluid Mechanics", McGraw-Hill, New York (1979).
3. R.L. Daugherty and J.B. Franzini, "Fluid Mechanics with Engineering Applications", 7th ed., McGraw-Hill, New York (1977).
4. B.S. Massey, "Mechanics of Fluids", 4th ed., Van Nostrand Reinhold, New York (1979).
5. A. Sloane, "Mechanics of Materials", Dover, New York (1967).
6. S. Eskinazi, "Vector Mechanics of Fluids and Magnetofluids", Academic Press, New York (1967).
7. W.M. Swanson, "Fluid Mechanics", Holt, Rinehart and Winston, New York (1970).
8. A. Mironer, "Engineering Fluid Mechanics", McGraw-Hill, New York (1979).
9. T.C. Gilmer, "Modern Ship Design", United States Naval Institute, Annapolis, Md. (1970).

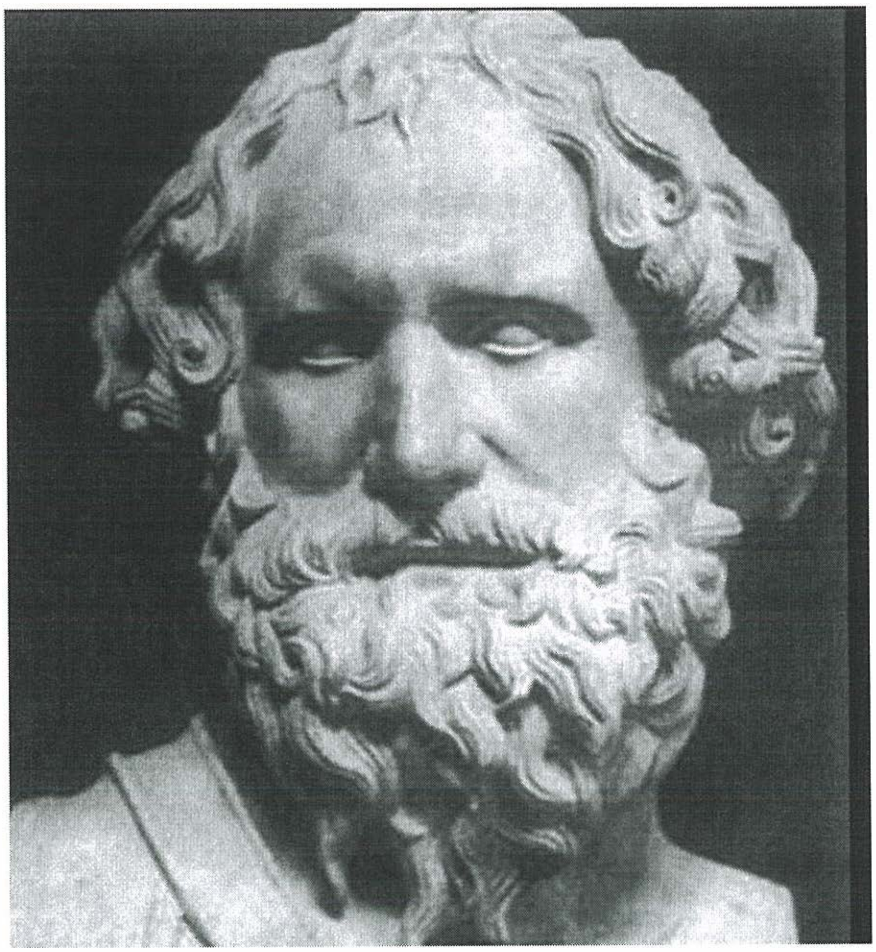

ARCHIMEDES (c.287 BC-c.212 BC)

John Vlachopoulos, *Fundamentals of Fluid Mechanics*
Chem. Eng., McMaster University, Hamilton, ON, Canada
(First Edition 1984, revised internet edition (2016), www.polydynamics.com)

CHAPTER 3

KINEMATICS OF FLOW

3.1 INTRODUCTION

The word kinematics is derived from the Greek word kinesis, which means motion. Kinematics is that part of mechanics which deals with the study of motion. In fluid mechanics we are interested in the determination of velocity, acceleration and all other quantities derivable from displacement and time.

Two points of view are possible for the study of fluid motion. In the Lagrangian approach the motion of a particle of fixed identity is followed as a function of time. If a particle is characterized by position $\bar{\xi}_o$ at time t=0 (initial position) and by position $\bar{r}$ at time t=t, the trajectory of the particle will be given by

$$\bar{r} = \bar{r}(\bar{\xi}_o, t) \tag{3.1}$$

or in terms of Cartesian components

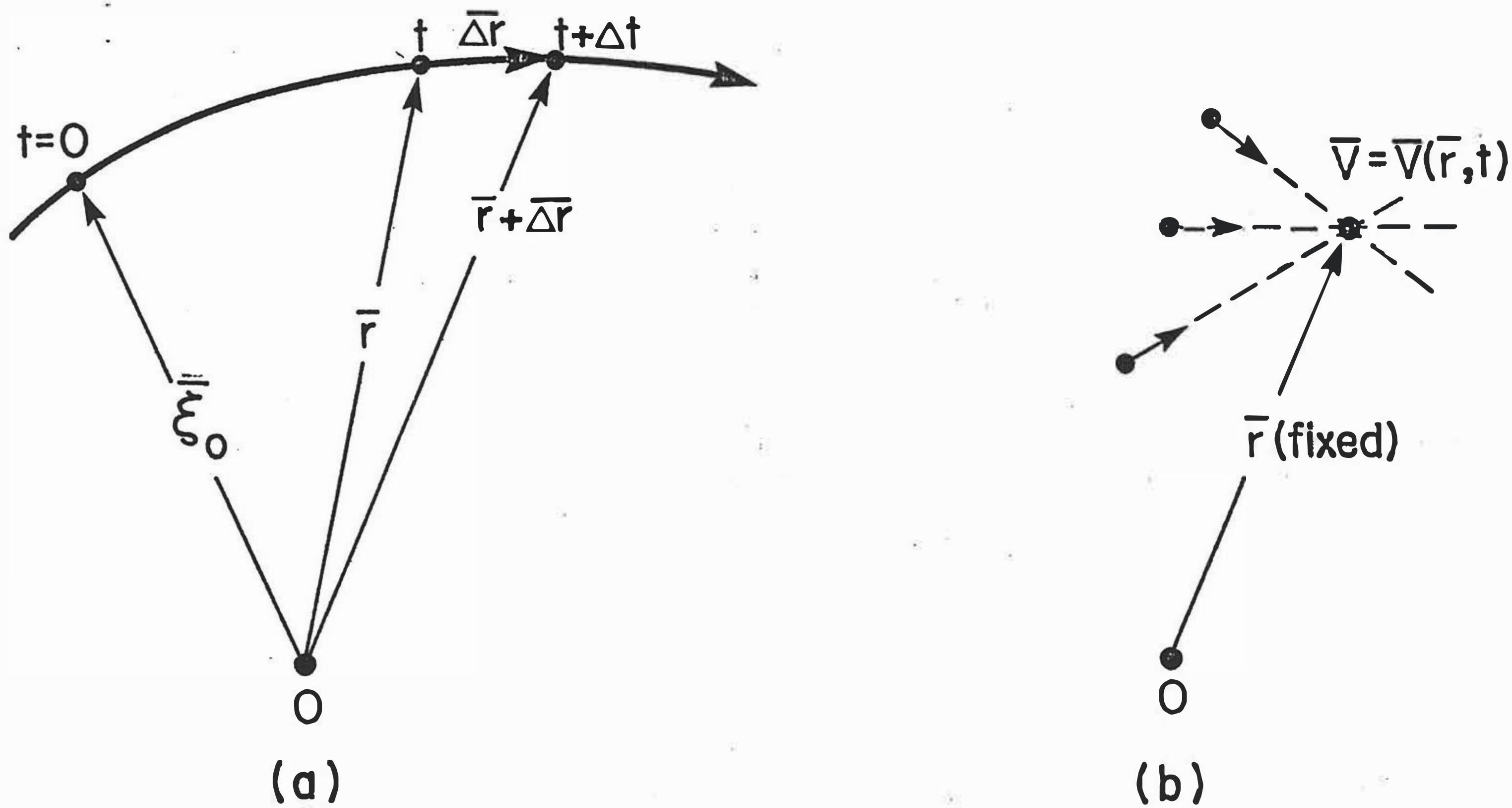

Fig. 3.1 (a) Lagrangian point of view
(b) Eulerian point of view

$$x = r_1(x_o, y_o, z_o, t)$$
$$y = r_2(x_o, y_o, z_o, t) \qquad (3.2)$$
$$z = r_3(x_o, y_o, z_o, t)$$

The velocity of the particle which at t=0 is at position ξ_o is

$$\bar{V} = \lim_{\Delta t \to 0} \frac{\Delta \bar{r}}{\Delta t} = \left(\frac{\partial \bar{r}}{\partial t}\right)_{\bar{\xi}_o} = \bar{V}(\bar{\xi}_o, t) \qquad (3.3)$$

The particle acceleration is

$$\bar{a} = \left(\frac{\partial \bar{V}}{\partial t}\right)_{\xi_o} = \left(\frac{\partial^2 \bar{r}}{\partial t}\right)_{\bar{\xi}_o} = \bar{a}(\bar{\xi}_o, t) \qquad (3.4)$$

In the <u>Eulerian</u> method a position is chosen and the velocity of the particles at this position is described as a function of time, i.e.

$$\bar{V} = \bar{V}(\bar{r}, t) \qquad (3.5)$$

or in terms of Cartesian components

$$v_x = v_1(x,y,z,t)$$
$$v_y = v_2(x,y,z,t) \qquad (3.6)$$
$$v_z = v_3(x,y,z,t)$$

The difference between the Lagrangian and Eulerian methods of description is illustrated in Figure 3.1.

The Lagrangian method is used mainly in particle mechanics. In continuum mechanics this method requires the description of motion of an infinite number of particles and thus becomes extremely cumbersome. The Eulerian method is easier to use in continuum mechanics because it is concerned with the description of motion at a fixed position.

3.2 MATERIAL OR SUBSTANTIAL DERIVATIVE

Let us consider a fluid property ϕ which is function of position and time:

$$\phi = \phi(x,y,z,t) \tag{3.7}$$

The total differential is

$$d\phi = \frac{\partial\phi}{\partial x}\,dx + \frac{\partial\phi}{\partial y}\,dy + \frac{\partial\phi}{\partial z}\,dz + \frac{\partial\phi}{\partial t}\,dt \tag{3.8}$$

and the total derivative is

$$\frac{d\phi}{dt} = \frac{\partial\phi}{\partial x}\frac{dx}{dt} + \frac{\partial\phi}{\partial y}\frac{dy}{dt} + \frac{\partial\phi}{\partial z}\frac{dz}{dt} + \frac{\partial\phi}{\partial t} \tag{3.9}$$

We note that

$$\begin{aligned} \frac{dx}{dt} &= v_x \\ \frac{dy}{dt} &= v_y \\ \frac{dz}{dt} &= v_z \end{aligned} \tag{3.10}$$

where v_x, v_y and v_z are the velocity components in x,y and z directions respectively. Thus,

$$\frac{d\phi}{dt} = v_x\frac{\partial\phi}{\partial x} + v_y\frac{\partial\phi}{\partial y} + v_z\frac{\partial\phi}{\partial z} + \frac{\partial\phi}{\partial t} \tag{3.11}$$

or in vector notation

$$\frac{d\phi}{dt} = \bar{V}\cdot\nabla\phi + \frac{\partial\phi}{\partial t} \tag{3.12}$$

In this expression the operation d/dt is the total time rate of change, $\partial/\partial t$ the time rate of change at a fixed point in space (local derivative) and $\bar{V}\cdot\nabla$ is the variation in the time it takes the fluid to move an infinitesimal distance (dx, dy, dz) (convective derivative). To distinguish the Eulerian time rate of change from the Lagrangian time rate of change, some authors use the symbol D/Dt, i.e.

$$\frac{d}{dt} = \frac{D}{Dt} = \frac{\partial}{\partial t} + \bar{V}\cdot\nabla \tag{3.13}$$

This derivative is usually called the material or substantial derivative.

If the property that changes with time is the velocity $\bar{V}$ then the acceleration in the Eulerian frame is

$$\bar{a} = \frac{d\bar{V}}{dt} = \frac{D\bar{V}}{Dt} = \frac{\partial\bar{V}}{\partial t} + \bar{V}\cdot\nabla\bar{V} \tag{3.14}$$

Thus, the relation between the particle acceleration in Lagrangian and Eulerian frames is

$$\bar{a} = \left(\frac{\partial\bar{V}}{\partial t}\right)_{\xi_o} = \frac{d\bar{V}}{dt} = \frac{D\bar{V}}{Dt} = \frac{\partial\bar{V}}{\partial t} + \bar{V}\cdot\nabla\bar{V} \tag{3.15}$$

Example 3.1

The velocity components of a fluid particle are given as $v_x = At$ and $v_y = Bt^2$ (Eulerian frame) where A and B are constants. Determine the displacement of the fluid particle and the particle acceleration.

Solution

Here, we have

$$v_x = At = \frac{dx}{dt}$$

$$v_y = Bt^2 = \frac{dy}{dt}$$

Thus

$$dx = Atdt$$

$$dy = Bt^2\, dt$$

$$\overline{ds} = dx\bar{i} + dy\bar{j}$$

and

$$ds = [(dx)^2 + (dy)^2]^{1/2} = (A^2t^2 + B^2t^4)^{1/2}\, dt$$

The length of the path (i.e. displacement) is

$$s = \int_0^t (A^2t^2 + B^2t^4)^{1/2}\,dt = \frac{1}{2}\int_0^t (A^2 + Bt^2)^{1/2}\,dt^2 =$$

$$= \left[\frac{1}{2}\,\frac{2}{3}\,\frac{1}{B^2}\,(A^2 + B^2t^2)^{3/2}\right]_o^t = \frac{1}{3B^2}\,(A^2 + B^2t^2)^{3/2}$$

The particle acceleration is given by

$$\bar{a} = \frac{\partial \bar{V}}{\partial t} + \bar{V}\cdot\nabla\bar{V}$$

$$a_x = \frac{\partial v_x}{\partial t} + v_x\,\frac{\partial v_x}{\partial x} + v_y\,\frac{\partial v_x}{\partial y}$$

$$= A + 0 + 0$$

$$a_y = \frac{\partial v_y}{\partial t} + v_x\,\frac{\partial v_y}{\partial x} + v_y\,\frac{\partial v_y}{\partial y}$$

$$= 2Bt + 0 + 0$$

Thus

$$\bar{a} = (a_x,\ a_y) = (A,\ 2Bt)\ .$$

3.3 THE SYSTEM AND CONTROL VOLUME CONCEPTS

A system is defined as an arbitrary volume of a substance across whose boundaries no mass is exchanged. The system may experience a change in its momentum and energy but no change in mass. A system can be stationary or in motion. In a moving system the boundary will move with the system so that the mass within the system remains always the same.

In contrast, a control volume is an arbitrary volume across whose boundaries not only momentum and energy, but also mass is transferred. The control volume may be stationary or in motion. Whether stationary or in motion mass is allowed to be exchanged across its boundaries.

The concept of system and control volume are related to the Lagrangian and Eulerian viewpoints. When a mathematical expression of a

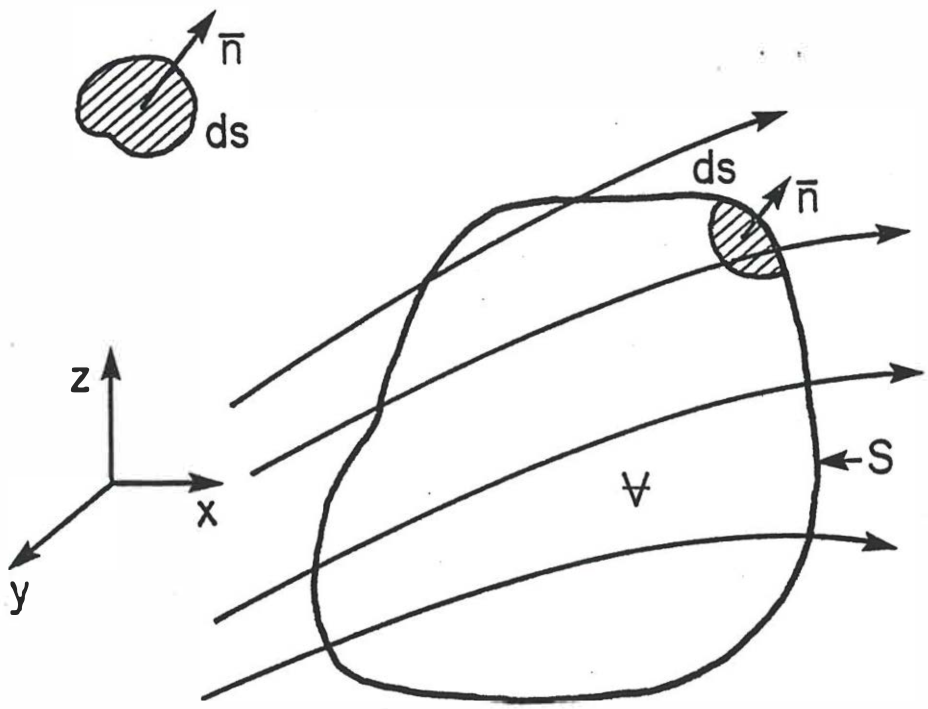

Fig. 3.2 Control volume in a flow field

physical law is attempted we may use either one of these concepts. Suppose we try to state the axiom of conservation of mass. For a system we simply state that the mass cannot be created nor destroyed, i.e.

$$\frac{d(\text{mass})}{dt} = 0 \tag{3.16}$$

Since we have fixed the identities of all particles by the fact that they exist within the system boundaries, this is a Lagrangian point of view. However, if we choose an arbitrary volume in space across whose boundaries mass is allowed to be transported, we no longer keep track of particles of certain identity. This is, therefore, an Eulerian concept. The axiom of conservation of mass should then be stated as

$$\left[\frac{d(\text{mass})}{dt}\right]_{in} - \left[\frac{d(\text{mass})}{dt}\right]_{out} = \left[\frac{d(\text{mass})}{dt}\right]_{\text{inside the C.V.}} \tag{3.17}$$

Further mathematical manipulations of the above expression are presented in Chapter 4.

3.4 REYNOLDS TRANSPORT THEOREM

We will consider the time rate of change of a fluid property ϕ integrated in an arbitrary volume $\forall$ (see Fig. 3.2), with $\forall$ being a function of time

$$\frac{d}{dt} \iiint_{\forall} \phi \, d\forall$$

Since $\forall = \forall(t)$, we have

$$\frac{d}{dt} \iiint_{\forall} \phi d\forall = \iiint_{\forall} \frac{d\phi}{dt} d\forall + \iiint_{\forall} \phi \frac{d\forall}{dt} \tag{3.18}$$

We note that if $\forall$ is expressed by $\Delta x \Delta y \Delta z$, we will have

$$\frac{d}{dt}(\forall) = \frac{d}{dt}(\Delta x \Delta y \Delta z) = \Delta y \Delta z \frac{d(\Delta x)}{dt} + \Delta x \Delta z \frac{d(\Delta y)}{dt} + \Delta x \Delta y \frac{d(\Delta z)}{dt}$$

$$= \Delta x \Delta y \Delta z \frac{1}{\Delta x} \Delta\left(\frac{dx}{dt}\right) + \Delta x \Delta y \Delta z \frac{1}{\Delta y} \Delta\left(\frac{dy}{dt}\right) + \Delta x \Delta y \Delta z \frac{1}{\Delta z} \Delta\left(\frac{dz}{dt}\right) \tag{3.19}$$

Thus

$$\frac{1}{\Delta \mathcal{V}} \frac{d\mathcal{V}}{dt} = \frac{\Delta v_x}{\Delta x} + \frac{\Delta v_y}{\Delta y} + \frac{\Delta v_z}{\Delta z} \tag{3.20}$$

In the limit as $\Delta x \to 0$, $\Delta y \to 0$ and $\Delta z \to 0$, we have

$$\frac{\Delta v_x}{\Delta x} = \frac{\partial v_x}{\partial x}, \quad \frac{\Delta v_y}{\Delta y} = \frac{\partial v_y}{\partial y}, \quad \frac{\Delta v_z}{\Delta z} = \frac{\partial v_z}{\partial z} \text{ and } \Delta\mathcal{V} = d\mathcal{V} \tag{3.21}$$

Consequently, we may write in general

$$\frac{1}{d\mathcal{V}} \frac{d\mathcal{V}}{dt} = \frac{\partial v_x}{\partial x} + \frac{\partial v_y}{\partial y} + \frac{\partial v_z}{\partial z} = \nabla\cdot\bar{V} \tag{3.22}$$

Now, equation (3.18) with the help of equation (3.22) becomes

$$\frac{d}{dt} \iiint_{\mathcal{V}} \phi d\mathcal{V} = \iiint_{\mathcal{V}} \frac{d\phi}{dt} d\mathcal{V} + \iiint_{\mathcal{V}} \phi \, (\nabla\cdot\bar{V}) d\mathcal{V} \tag{3.23}$$

or

$$\frac{d}{dt} \iiint_{\mathcal{V}} \phi d\mathcal{V} = \iiint_{\mathcal{V}} \left(\frac{d\phi}{dt} + \phi(\nabla\cdot\bar{V})\right) d\mathcal{V} \tag{3.24}$$

Using the definition of material derivative, we have

$$\frac{d\phi}{dt} = \frac{\partial\phi}{\partial t} + \bar{V}\cdot\nabla\phi \tag{3.25}$$

and

$$\frac{d}{dt} \iiint_{\mathcal{V}} \phi d\mathcal{V} = \iiint_{\mathcal{V}} \left(\frac{\partial\phi}{\partial t} + \bar{V}\cdot\nabla\bar{V} + \phi\nabla\cdot\bar{V}\right) d\mathcal{V}$$

$$= \iiint_{\mathcal{V}} \frac{\partial\phi}{\partial t} d\mathcal{V} + \iiint_{\mathcal{V}} \nabla\cdot(\phi\bar{V}) \, d\mathcal{V} \tag{3.26}$$

Finally, with the use of the Gauss divergence theorem

$$\frac{d}{dt} \iiint_{\mathcal{V}} \phi d\mathcal{V} = \iiint_{\mathcal{V}} \left(\frac{\partial\phi}{\partial t}\right) d\mathcal{V} + \oiint_{S} (\bar{V}\cdot\bar{n}) \, \phi dS \tag{3.27}$$

This relation is known as the <u>Reynolds transport theorem.</u> We note that

$\frac{d}{dt} \iiint_{V} \phi dV$ is the total rate of change of property ϕ integrated in a volume V.

$\iiint_{V} (\frac{\partial \phi}{\partial t})\ dV$ is the rate of change of property ϕ contained momentarily in volume V.

$\bar{V} \cdot \bar{n}\ dS$ is the total flux of vector $\bar{V}$ through dS and $\oiint_{S} (\bar{V} \cdot \bar{n}) \phi dS$ the net flux of property ϕ across the surface of volume V.

In the Reynolds transport theorem ϕ can be any scalar or vector property. Let us examine the case $\phi = \rho$, where ρ is the fluid density. We have

$$\frac{d}{dt} \iiint_{V} \rho dV = \iiint_{V} \frac{\partial \rho}{\partial t}\ dV + \oiint_{S} (\bar{V} \cdot \bar{n})\ \rho\ dV$$

$$= \iiint_{V} \frac{\partial \rho}{\partial t}\ dV + \iiint_{V} \nabla \cdot (\rho \bar{V})\ dV$$

$$= \iiint_{V} (\frac{\partial \rho}{\partial t} + \nabla \cdot (\rho \bar{V}))\ dV \tag{3.28}$$

In the absence of sources of sinks within volume V, the time rate of change of mass must be equal to zero, i.e.

$$\frac{d}{dt} \iiint \rho\ dV = 0 \tag{3.29}$$

and

$$\frac{\partial \rho}{\partial t} + \nabla \cdot (\rho \bar{V}) = 0 \tag{3.30}$$

This is the equation of conservation of mass which is rederived by a more straightforward method in Chapter 4.

3.5 PATHLINES, STREAMLINES AND STREAKLINES

Three generally different types of curves are considered in the study of fluid motion: Pathlines, Streamlines and Streaklines. A <u>pathline</u> is the path or trajectory traced out by a single fluid particle over some period of time. To determine a pathline we may identify a fluid with a luminous dye and then take a long exposure photograph. The curve appearing on the photograph would be a pathline. The pathline is described in the Lagrangian frame (see Fig. 3.1(a)) by

$$\bar{r} = \bar{r}\,(\bar{\xi}_o,\ t) \tag{3.31}$$

The streamline is a line which is tangent to the direction of flow at every point in the flow field. If a camera were to take a very short time exposure of a flow field, each particle would trace a short path which would indicate its velocity during that interval. A curve drawn tangent to these velocity vectors would be streamline. Since a streamline is tangent to the velocity vector there could not be any flow across a streamline.

From equation (3.3) the velocity of the fluid particle in the Lagrangian frame is

$$\bar{V} = \frac{d\bar{r}}{dt} = \bar{V}\,(\bar{\xi}_o,\ t) \tag{3.32}$$

A geometrical representation of a streamline is given in Fig. 3.3. Since $d\bar{s}$ and $\bar{V}$ are in the same direction

$$\frac{dx}{v_x} = \frac{dy}{v_y} = \frac{dz}{v_z} \tag{3.33}$$

A streakline is a line joining the temporary location of all the particles that have passed through a given point in a flow field. A plume of smoke or dye injected at one point gives a streakline. Some pathlines and streaklines for an unsteady flow field are shown in Fig. 3.4.

In steady flow, the velocity at each point in the flow field remains constant with time. Consequently, the streamlines remain unchanged as time passes. Since there is no flow across a streamline, all particles passing from a point in space will remain on a given streamline. This means that in steady flow, pathlines, streamlines and streaklines coincide. This is not true, however, for unsteady flow.

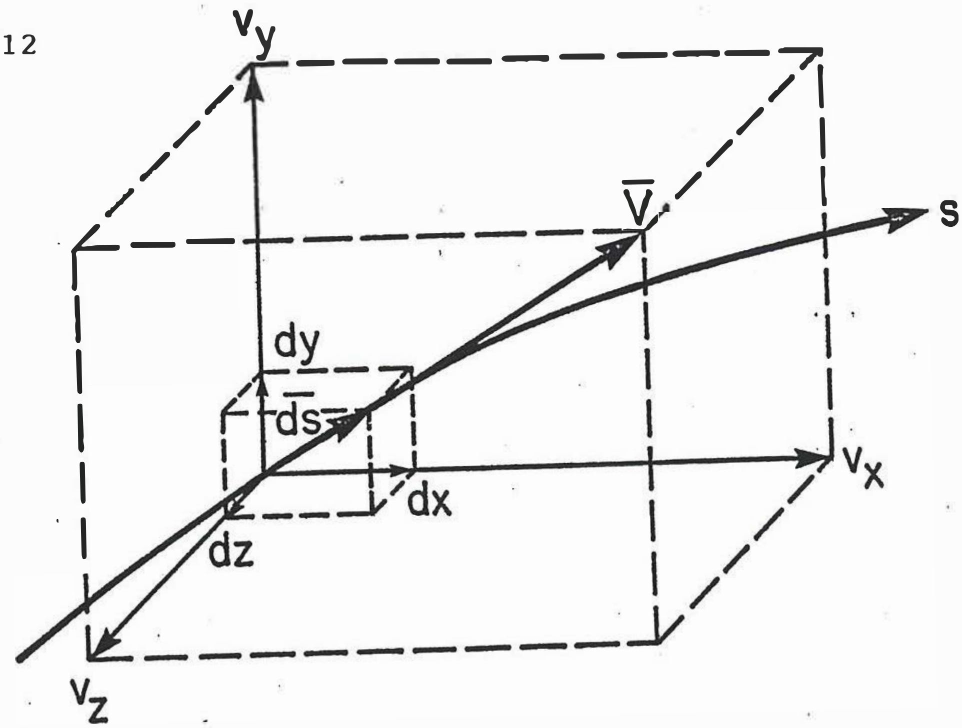

Fig. 3.3 Streamline in a flow field.

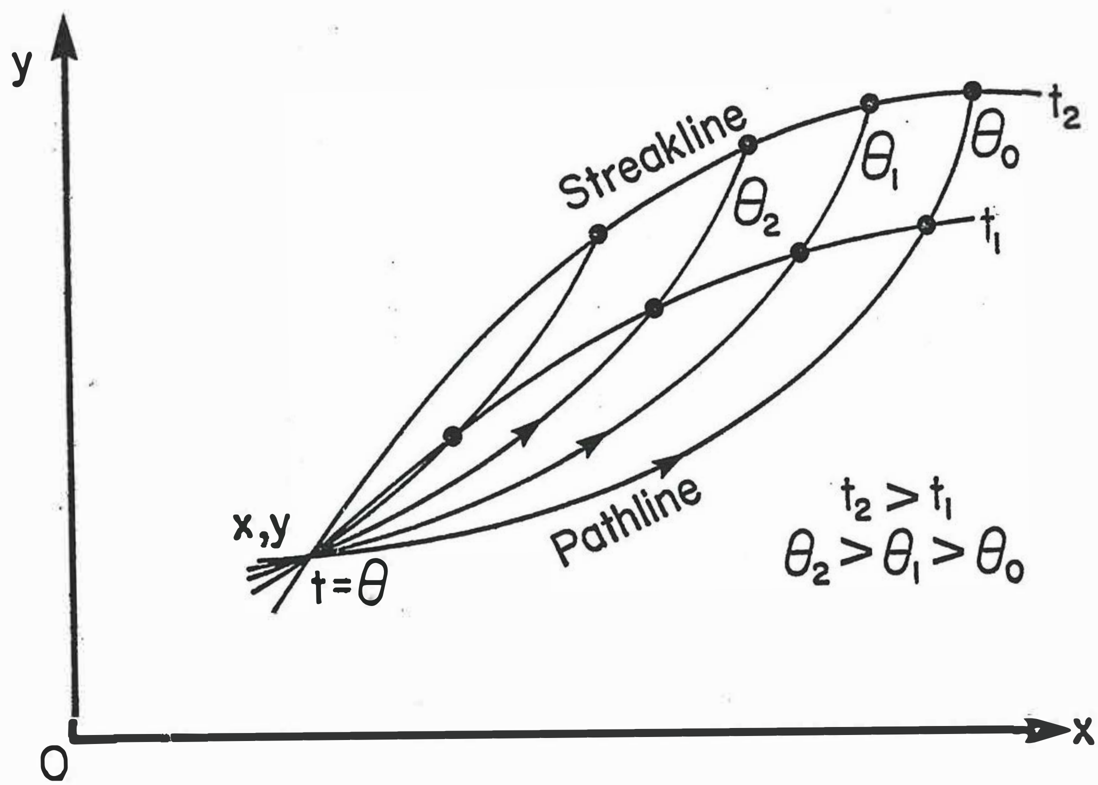

Fig. 3.4 Pathlines of particles passing through (x, y) at times θ and streaklines indicating the position of particles at times t.

3.6 ROTATION, VORTICITY AND CIRCULATION

A fluid element can be subjected to three types of flow, namely: translation, rotation and deformation. These types of elemental motions are depicted in Fig. 3.5. The concept of translational motion is self-evident. The deformational motion will be examined in greater detail in the chapter on constitutive equations. Here it suffices to say that if the relative orientation of the axis as shown in Fig. 3.5 changes the flow is said to be deformational. Deformational flow also exists if one or more axis are stretched or compressed. Here we focus our attention on rotational flow, which is depicted by the fluid element of Fig. 3.5 turning around.

Let us examine the flow in a fluid with circular streamlines as shown in Fig. 3.6. The fluid rotates like a rigid body. Each element turns around at a certain angular velocity. The arrows shown rotate at the same rate. This is unquestionably a case of rotational flow.

Now let us consider the flow between two horizontal flat plates, where the bottom plate is stationary while the top one moves at velocity V_o as shown in Fig. 3.7. We note that the horizontal arrow is simply translated, while the vertical one turns. It is not clear whether this is a case of rotational flow or not. To determine that we propose to use the average rate at rotation of the two arrows as a measure. If the average rate of rotation is zero the flow is said to be irrotational, if not the flow is rotational. For generality we refer to Fig. 3.8. We define the angular velocity ω_z about the axis z as the average rate of counterclockwise rotation of the two lines

$$\omega_z = \frac{1}{2}\left(\frac{d\alpha}{dt} - \frac{d\beta}{dt}\right) \tag{3.34}$$

In the limit of small angles we would have

$$\frac{d\alpha}{dt} = \frac{d\left(\frac{\Delta y_\alpha}{\Delta x}\right)}{dt} = \frac{d\left(\frac{\Delta y_\alpha}{\Delta t}\right)}{dx} = \frac{\partial v_y}{\partial x} \tag{3.35}$$

$$\frac{d\beta}{dt} = \frac{d\left(\frac{\Delta x_\beta}{\Delta y}\right)}{dt} = \frac{d\left(\frac{\Delta x_\beta}{\Delta t}\right)}{dy} = \frac{\partial v_x}{\partial y} \tag{3.36}$$

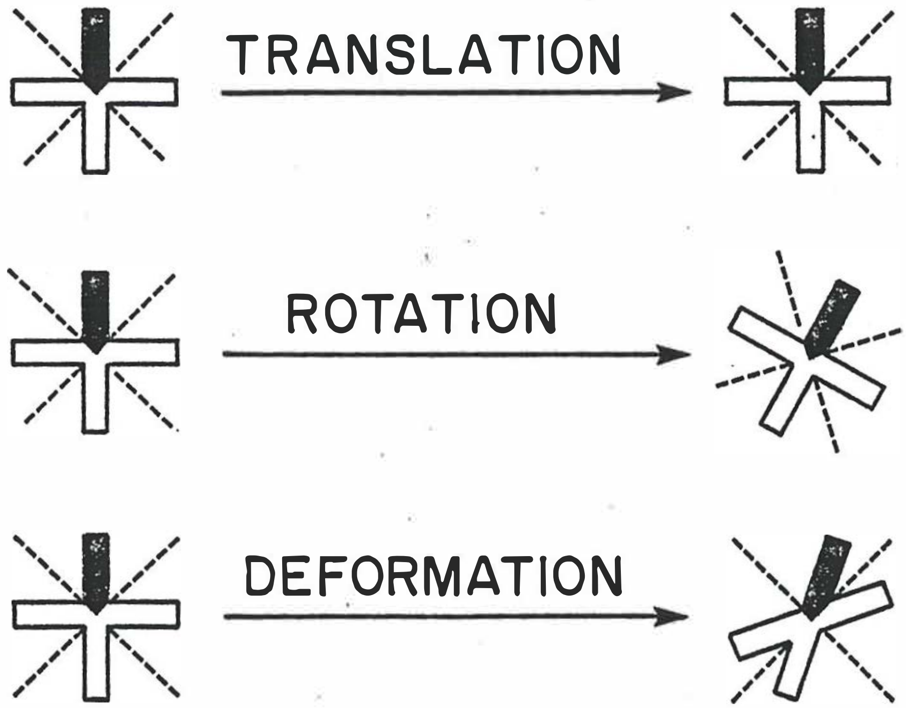

Fig. 3.5 Three types of fluid motion.

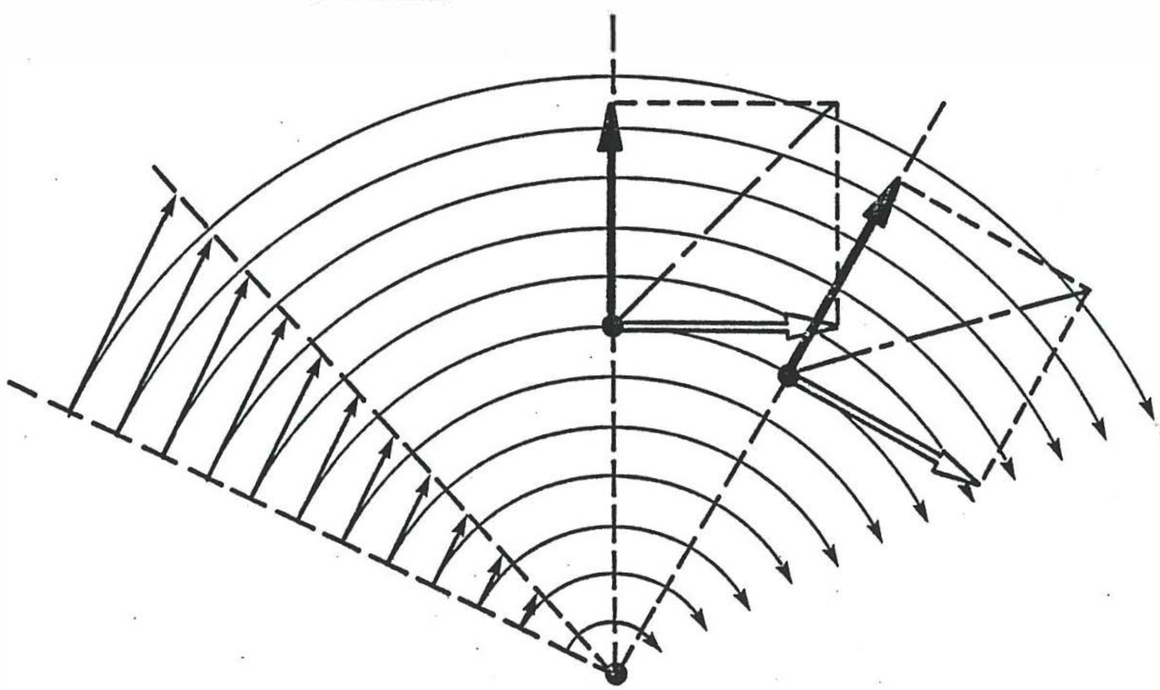

Fig. 3.6 A fluid rotating like a rigid body.

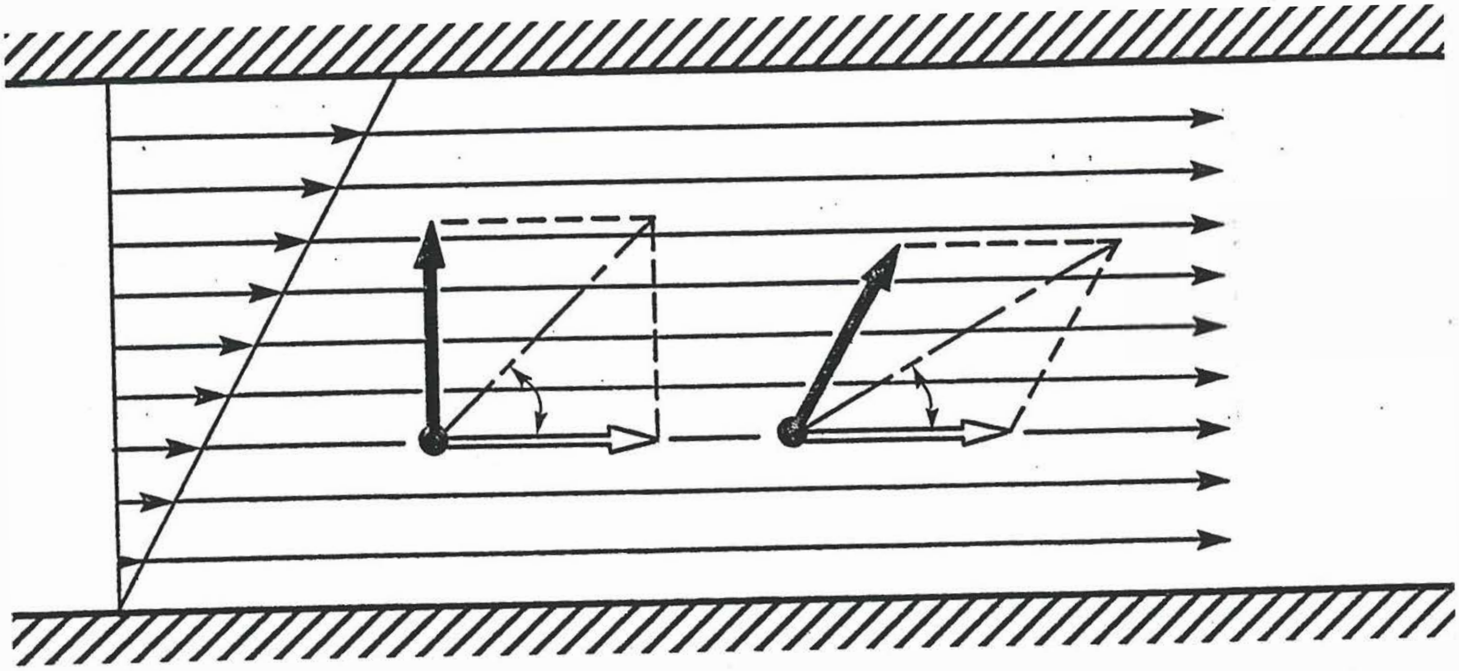

Fig. 3.7 Shearing flow between two flat plates.

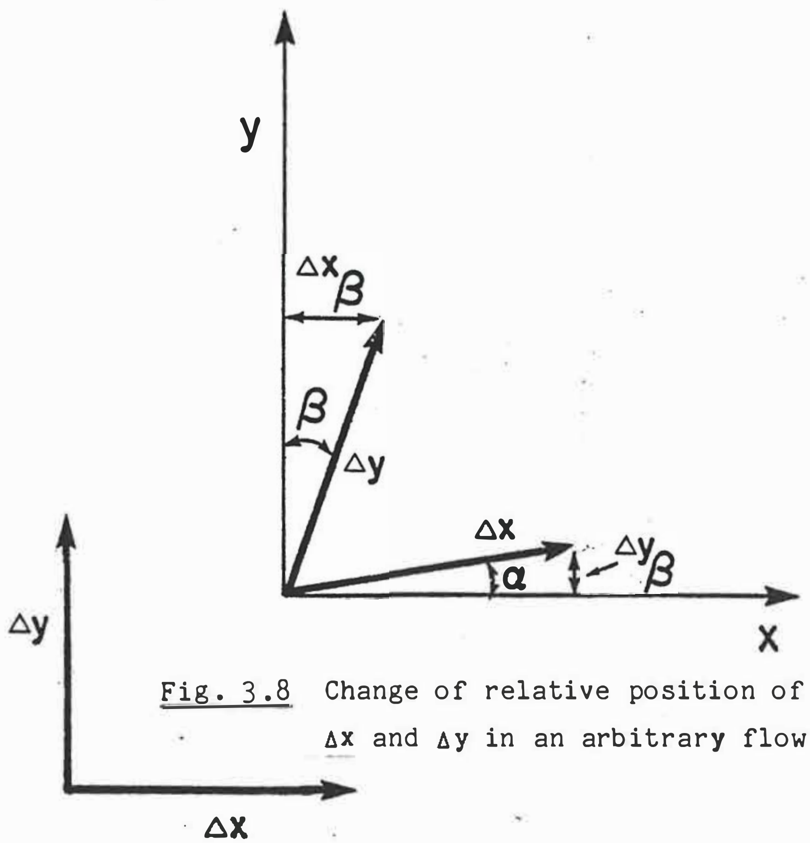

Fig. 3.8 Change of relative position of arrows Δx and Δy in an arbitrary flow field.

Thus,

$$\omega_z = \frac{1}{2}\left(\frac{\partial v_y}{\partial x} - \frac{\partial v_x}{\partial y}\right) \tag{3.37}$$

Similarly

$$\omega_x = \frac{1}{2}\left(\frac{\partial v_z}{\partial y} - \frac{\partial v_y}{\partial z}\right) \tag{3.38}$$

$$\omega_y = \frac{1}{2}\left(\frac{\partial v_x}{\partial z} - \frac{\partial v_z}{\partial x}\right) \tag{3.39}$$

The vector $\bar{\omega} = \bar{i}\omega_x + \bar{j}\omega_y + \bar{k}\,\omega_z$ is thus one-half the curl of the velocity vector

$$\bar{\omega} = \frac{1}{2}\,\nabla\times\bar{V} = \frac{1}{2}\begin{vmatrix} i & j & k \\ \frac{\partial}{\partial x} & \frac{\partial}{\partial y} & \frac{\partial}{\partial z} \\ v_x & v_y & v_z \end{vmatrix} \tag{3.40}$$

or, equivalently in index notation

$$\bar{\omega} = \frac{1}{2}\,\varepsilon_{ijk}\frac{\partial v_k}{\partial x_j} \tag{3.41}$$

Referring back to the simple flow configuration of Fig. 3.7 we note that

$$v_y = v_z = 0$$

$$v_x = V_o y$$

$$\omega_z = \frac{1}{2}(0 - V_o) = \frac{1}{2}V_o$$

The flow is rotational.

To avoid the factor 1/2 we define the vorticity ζ as equal to twice the rotation vector $\bar{\omega}$. Then

$$\zeta = 2\bar{\omega} = \nabla\times\bar{V} \tag{3.42}$$

with components

$$\zeta_x = \left(\frac{\partial v_z}{\partial y} - \frac{\partial v_y}{\partial z}\right) \tag{3.43}$$

$$\zeta_y = \left(\frac{\partial v_x}{\partial z} - \frac{\partial v_z}{\partial x}\right) \tag{3.44}$$

$$\zeta_z = \left(\frac{\partial v_y}{\partial x} - \frac{\partial v_x}{\partial y}\right) \tag{3.45}$$

The quantity $\nabla\cdot(\nabla\times\bar{V})$ is the divergence of vorticity. It can be easily shown that

$$\nabla\cdot(\nabla\times\bar{V}) = 0 \tag{3.46}$$

or

$$\nabla\cdot\bar{\zeta} = 0$$

This is known as the equation of conservation of vorticity.

In calculus books the closed line integral of a vector is given the name <u>circulation.</u> If the vector represents a force field the circulation is equal to the work done in moving a particle around the closed line. This name has a specific meaning when the vector represents the velocity and is denoted by the Greek letter Γ (gamma)

$$\Gamma = \oint \bar{V}\cdot d\bar{r} \tag{3.48}$$

From Stokes' theorem (see Appendix A) we have

$$\Gamma = \oint_C \bar{V}\cdot d\bar{r} = \iint_S (\nabla\times\bar{V}) \cdot \bar{n}dS = \iint_S \bar{\zeta}\cdot\bar{n}dS \tag{3.49}$$

This means that the circulation is equal to the total vorticity in the area S bounded by the contour C.

It is possible to have a circulatory motion and the flow to be irrotational. This is shown in Fig. 3.9. The average rotation of the arrows is zero (because the diagonals are parallel). The velocity is inversely proportional to the radius (see also Section 11.3). It is physically impossible for such a motion to exist up to the center

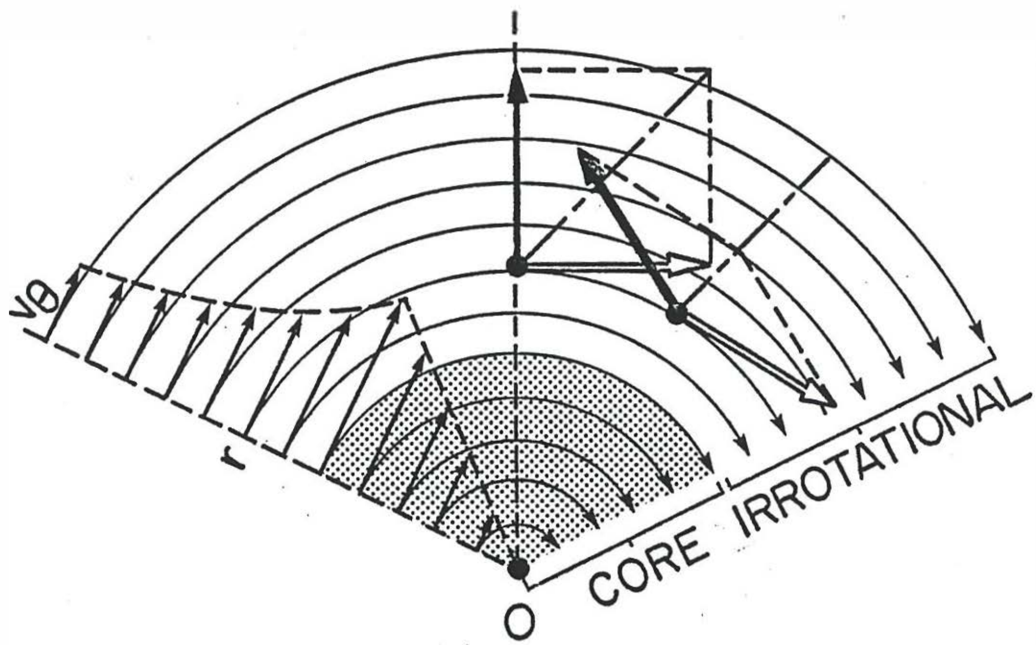

Fig. 3.9 Vortex flow

because the velocity tends to imfinity. Therefore, a reasonable assumption is that there exists a central core where the flow is that of a solid body or very nearly so. Such a combination is called a vortex or eddy.

3.7 ONE-, TWO- and THREE-DIMENSIONAL FLOW

When the flow parameters, velocity and pressure, vary in all three coordinate directions the flow is termed three-dimensional. Many problems, however, can be greatly simplified when all significant variations occur in two coordinate directions. The flow field can then be fully described in terms of

$$\begin{aligned} v_x &= v_x(x,y) \\ v_y &= v_y(x,y) \\ p &= p(x,y) \end{aligned} \tag{3.50}$$

and is termed two-dimensional. In another class of problems we may have variation of a single velocity component in one direction only, i.e. $v_x=v_x(y)$ while the pressure varies in another direction, i.e. $p=p(x)$. This is the case of unidirectional flow because the fluid flows in one direction only as shown in Fig. 3.10. The fluid flows in x-direction under the influence of a pressure gradient dp/dx.

Sometimes we use the one-dimensional flow approximation in which all flow parameters may be expressed as functions of one space coordinate only. In pipe flows we may assume that the velocity and pressure vary only in the axial direction and we may neglect any variation over the cross-sectional area. Thus the velocity profile is flat as shown in Fig. 3.11. Actually such a case is never true in the strict sense because the fluid viscosity introduces the no-slip condition at the wall and produces a velocity that decreases to zero at solid boundaries. Nevertheless, the one-dimensional assumption is very useful in the analysis of gas flows (see chapter on compressible flow).

Axisymmetric flow can be analyzed in the two-dimensional sense because all flow parameters can be expressed as functions at two space coordinates (x and r).

If one or more flow parameters vary with time the flow is said to be unsteady. If there is no variation with time the flow is said to be steady.

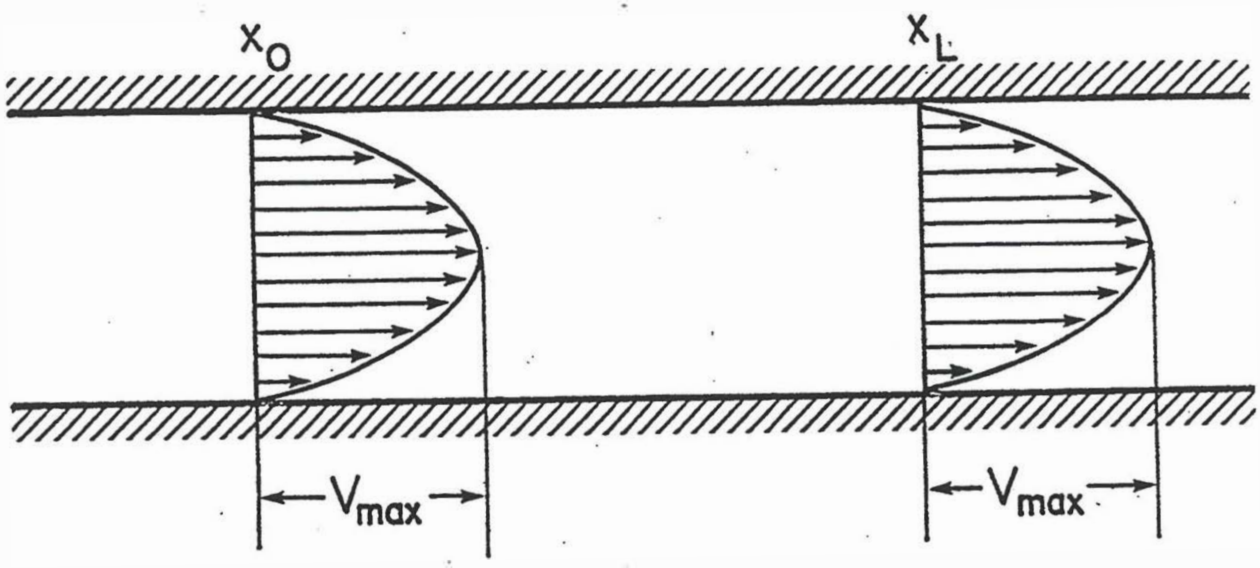

Fig. 3.10 Unidirectional flow

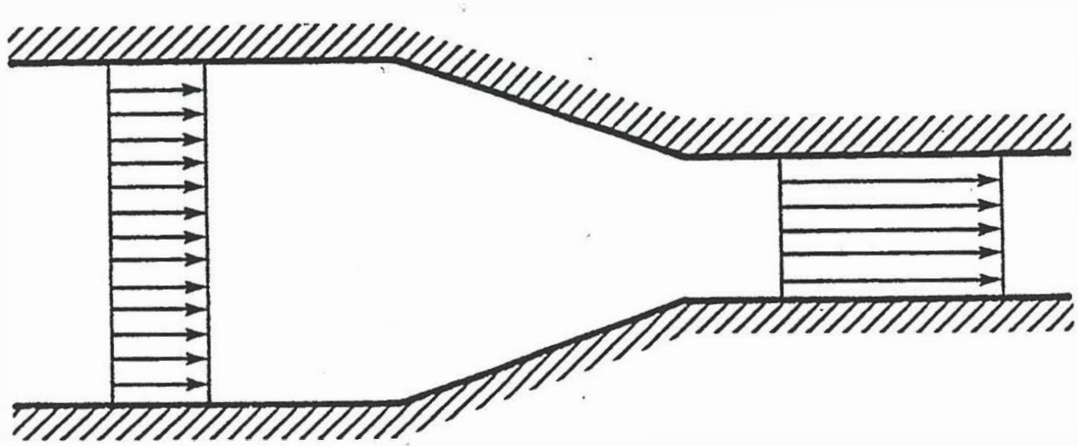

Fig. 3.11 One-dimensional flow.

John Vlachopoulos, *Fundamentals of Fluid Mechanics*
Chem. Eng., McMaster University, Hamilton, ON, Canada
(First Edition 1984, revised internet edition (2016), www.polydynamics.com)

CHAPTER 4

CONSERVATION OF MASS

4.1 THE DIFFERENTIAL CONTINUITY EQUATION

The philosophical recognition that matter cannot be created nor destroyed was first clearly stated by the Greek philosopher Anaxagoras in the 5th century B.C. This principle was reiterated by such natural philosophers as Sir Francis Bacon (16th century), but the first experimental proof was made, on the basis of precise weight measurements involving chemical reactions, by the French chemist Antoine Lavoisier (18th century). In the light of modern physics this principle was extended to include the sum of mass and energy, because mass can be converted to energy and vice-versa. We will use this principle in the classical sense, that is by neglecting any mass generation from or conversion to energy, thereby disregarding Einstein's equation $E = mc^2$.

Let us consider a control volume $\forall$ having a surface S with its boundaries fixed in space as shown in Fig. 4.1. A fluid is assumed to flow through this volume in arbitrary directions. The principle of conservation of mass for this control volume can be stated as

$$\begin{matrix}\text{rate of} \\ \text{mass} \\ \text{in}\end{matrix} - \begin{matrix}\text{rate of} \\ \text{mass} \\ \text{out}\end{matrix} = \begin{matrix}\text{rate of} \\ \text{mass} \\ \text{accumulation}\end{matrix} \qquad (4.1)$$

The rate of mass flow is generally denoted by $\dot{m}$ (i.e. kg/s). We will

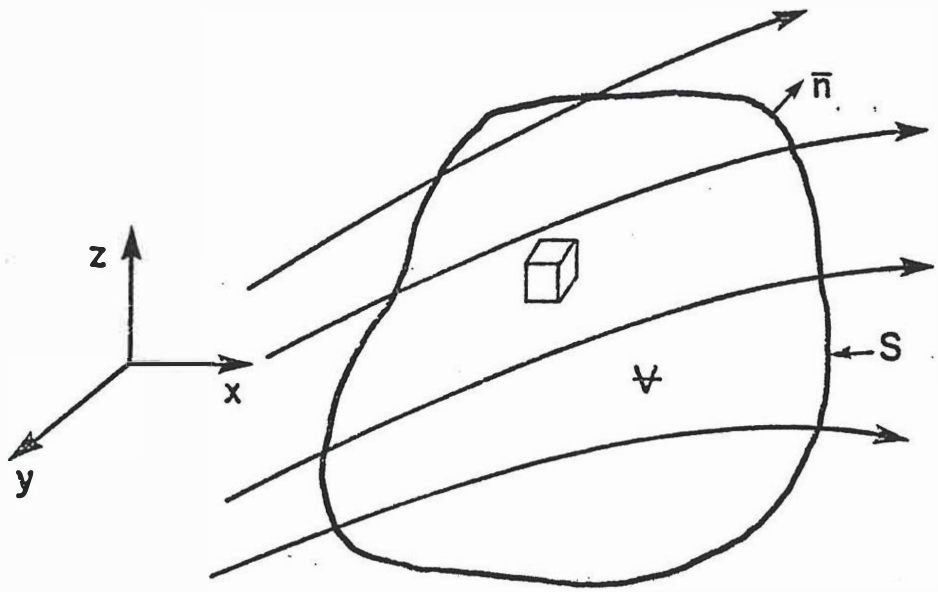

Fig. 4.1 A control volume in a flow field

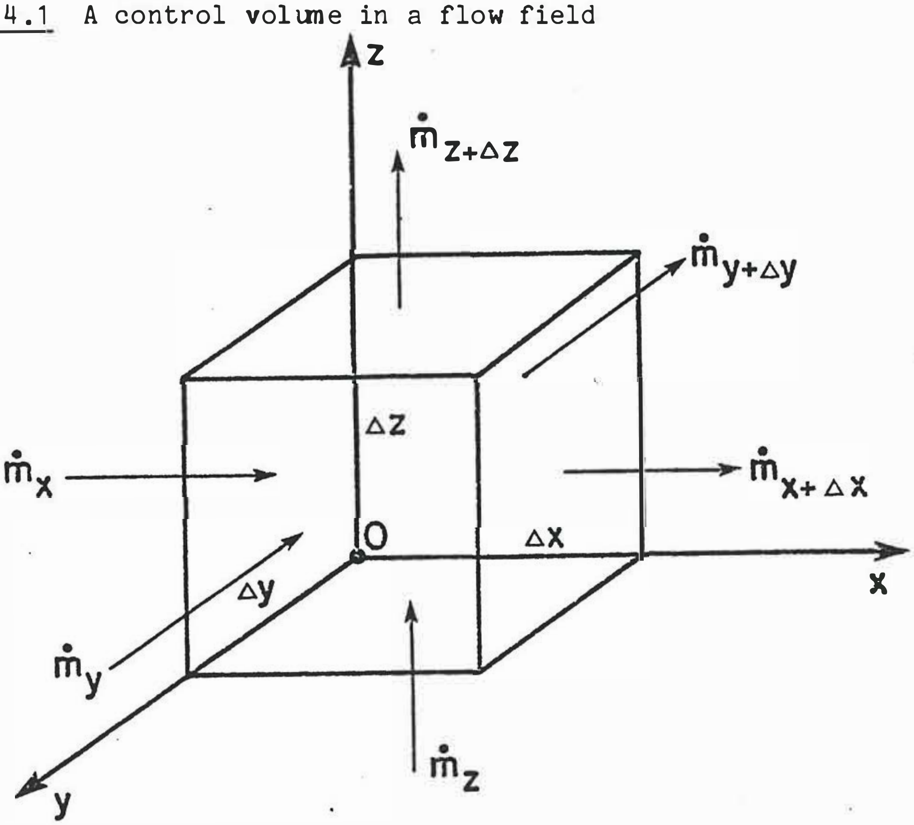

Fig. 4.2 Infinitesimal volume element $\Delta x \Delta y \Delta z$

derive the differential equation for the conservation of mass by applying the above principle for a volume element $\Delta x\Delta y\Delta z$ within the control volume $\forall$, which is also fixed in space as shown in Fig. 4.2. In this figure $\dot{m}_x$ is the rate of mass in, in the x direction crossing the volume face perpendicular to x and passing through O(x,y,z). $\dot{m}_{x+\Delta x}$ is the rate of mass out through the face which is perpendicular to x at $x+\Delta x$. The quantity $\dot{m}_{x+\Delta x}$ may be related to $\dot{m}_x$ with the help of the Taylor series

$$\dot{m}_{x+\Delta x} = \dot{m}_x + \frac{\partial}{\partial x}(\dot{m}_x)\,\Delta x + \frac{\partial}{\partial x^2}(\dot{m}_x)\frac{(\Delta x)^2}{2!} + \frac{\partial}{\partial x^3}(\dot{m}\ )\frac{(\Delta x)^3}{3!} + \ldots \tag{4.2}$$

Because Δx is an infinitesimal the higher powers are negligible with respect to the term containing Δx. Thus, we may write

$$\dot{m}_{x+\Delta x} = \dot{m}_x + \frac{\partial}{\partial x}(\dot{m}_x)\,\Delta x \tag{4.3}$$

By analogy, we may write for the rate of mass flow in the other two directions

$$\dot{m}_{y+\Delta y} = \dot{m}_y + \frac{\partial}{\partial y}(\dot{m}_y)\,\Delta y \tag{4.4}$$

$$\dot{m}_{z+\Delta z} = \dot{m}_z + \frac{\partial}{\partial z}(\dot{m}_z)\,\Delta z \tag{4.5}$$

By summing up equations (4.3), (4.4) and (4.5) and rearranging, we yet

$$(\dot{m}_x+\dot{m}_y+\dot{m}_z) - (\dot{m}_{x+\Delta x}+\dot{m}_{y+\Delta y}+\dot{m}_{z+\Delta z}) = -[\frac{\partial}{\partial x}(\dot{m}_x)\Delta x + \frac{\partial}{\partial y}(\dot{m}_y)\Delta y + \frac{\partial}{\partial z}(\dot{m}_z)\,\Delta z] \tag{4.6}$$

The first sum of terms on the left hand side of equation (4.6), represents the rate of mass in and the second sum of terms the rate of mass out of the volume element $\Delta x\Delta y\Delta z$. The rate of mass flow $\dot{m}$ is the product (density)×(velocity)×(area). Thus by denoting v_x, v_y and v_z the velocities in the x, y and z directions respectively we may write

$$\begin{aligned} \dot{m}_x &= \rho\, v_x\, \Delta y\, \Delta z \\ \dot{m}_y &= \rho\, v_y\, \Delta x\, \Delta z \\ \dot{m}_z &= \rho\, v_z\, \Delta y\, \Delta x \end{aligned} \tag{4.7}$$

Then, by introducing these relations in the right hand side of equation (4.6), we get

$$\begin{matrix}\text{rate of} \\ \text{mass} \\ \text{in}\end{matrix} - \begin{matrix}\text{rate of} \\ \text{mass} \\ \text{out}\end{matrix} = -\left[\frac{\partial}{\partial x}(\rho\ v_x) + \frac{\partial}{\partial y}(\rho\ v_y) + \frac{\partial}{\partial z}(\rho\ v_z)\right] \Delta x\ \Delta y\ \Delta z \tag{4.8}$$

The rate of mass accumulation within the volume element is

$$\frac{\partial}{\partial t}(\rho\ \Delta x\ \Delta y\ \Delta z)$$

Because the volume is fixed in space (constant), we may write

$$\begin{matrix}\text{rate of} \\ \text{mass} \\ \text{accumulation}\end{matrix} = \Delta x\ \Delta y\ \Delta z\ \frac{\partial \rho}{\partial t} \tag{4.9}$$

Thus the conservation principle for the volume element becomes

$$-\left[\frac{\partial(\rho v_x)}{\partial x} + \frac{\partial(\rho v_y)}{\partial y} + \frac{\partial(\rho v_z)}{\partial z}\right] \Delta x\ \Delta y\ \Delta z = \frac{\partial \rho}{\partial t}\ \Delta x\ \Delta y\ \Delta z \tag{4.10}$$

or, by eliminating the volume $\Delta x \Delta y \Delta z$ (= constant)

$$\frac{\partial \rho}{\partial t} + \frac{\partial}{\partial x}(\rho\ v_x) + \frac{\partial}{\partial y}(\rho\ v_y) + \frac{\partial}{\partial z}(\rho\ v_z) = 0 \tag{4.11}$$

This is the differential equation for the conservation of mass, which is often called the <u>equation of continuity.</u> In symbolic vector notation we may write equation (4.11) as

$$\frac{\partial \rho}{\partial t} + \nabla \cdot (\rho\ \overline{V}) = 0 \tag{4.12}$$

where ρ is the density (scalar), $\overline{V}$ is the velocity vector and t denotes time. $\nabla \cdot (\rho\ \overline{V})$ is the divergence of the vector $\rho\ \overline{V}$.

In cartesian index notation this equation may be written as

$$\frac{\partial \rho}{\partial t} + \partial_i\ (\rho\ v_i) = 0 \tag{4.13}$$

Obviously, equation (4.13) can be expressed in the form of equation (4.11) by applying the range and summation conventions of Appendix A.

The continuity equation in cylindrical and spherical coordinates is given in Appendix D.

For a fluid of constant density the continuity equation reduces to

$$(\text{incompressible fluid})\quad \nabla \cdot \bar{V} = \frac{\partial v_x}{\partial x} + \frac{\partial v_y}{\partial y} + \frac{\partial v_z}{\partial z} = 0 \tag{4.14}$$

This equation is used frequently not only for liquids which are nearly incompressible, but also for gases at relatively low flow velocities. As it is shown in the chapter on compressible flow a gas may be considered incompressible for speeds up to about 30% of the speed of sound.

4.2 THE INTEGRATED CONTINUITY EQUATION

We will integrate the continuity equation over the volume $\forall$ of Fig. 4.1. Thus

$$\iiint_{\forall} \left(\frac{\partial \rho}{\partial t} + \nabla \cdot (\rho \bar{V})\right) d\forall = 0 \tag{4.15}$$

or

$$\iiint_{\forall} \left(\frac{\partial \rho}{\partial t}\right) d\forall = - \iiint_{\forall} \nabla \cdot (\rho \bar{V})\ d\forall \tag{4.16}$$

Let $\bar{n}$ be a unit vector normal to the surface S enclosing the volume $\forall$. By applying Gauss' divergence theorem for the vector field $\rho\bar{V}$, we get

$$\iiint_{\forall} \nabla \cdot (\rho \bar{V})\ d\forall = \oiint_{S} \rho \bar{V} \cdot \bar{n}\ dS \tag{4.17}$$

Thus,

$$\iiint_{\forall} \left(\frac{\partial \rho}{\partial t}\right) d\forall = - \oiint_{S} (\rho \bar{V} \cdot \bar{n})\ dS \tag{4.18}$$

Equation (4.18) is the integral continuity equation. The left hand side of this equation is the accumulation term for the whole volume $\forall$ of fluid. Obviously if the fluid is incompressible $\partial\rho/\partial t = 0$ and this term drops out. The dot product $\bar{V} \cdot \bar{n}$ can be interpreted as the projection of vector $\bar{V}$ in the direction of $\bar{n}$ which is normal to the surface dS. Then, the product $(\rho\bar{V} \cdot \bar{n})dS$ is the rate of mass flow through the surface S. The integral

$$\oiint_{S} \rho\ \bar{V} \cdot \bar{n}\ dS$$

represents the total rate of mass out of volume $\forall$ (because $\bar{n}$ points outwards) which is completely enclosed by surface S. Thus equation (4.18) simply states that the rate of mass accumulation within the volume is equal to the negative mass rate of flow out of this volume.

We will now apply the integral continuity equation to the branching flow problem illustrated in Fig. 4.3. It is assumed that the fluid density does not vary with time but may vary with position (i.e. $\partial\rho/\partial t=0$, $\rho_1 \neq \rho_2 \neq \rho_3$). Therefore, equation (4.18) becomes

$$\oiint \rho \, \bar{V} \cdot \bar{n} \, dS = 0 \tag{4.19}$$

$\bar{V}_1$, $\bar{V}_2$ and $\bar{V}_3$ represent the velocity vectors at positions "1", "2" and "3" and $\bar{n}_1$, $\bar{n}_2$ and $\bar{n}_3$ the corresponding unit vectors normal to surfaces A_1, A_2 and A_3. Note that $\bar{V}_1$ is in opposite direction to $\bar{n}_1$. A_1, A_2, A_3 are the areas and ρ_1, ρ_2, ρ_3 the densities at positions "1", "2" and "3" respectively. Thus, we may write

$$\iint_{A_1} \rho_1 \bar{V}_1 \cdot \bar{n}_1 \, dS + \iint_{A_2} \rho_2 \bar{V}_2 \cdot \bar{n}_2 \, dS + \iint_{A_3} \rho_3 \bar{V}_3 \cdot \bar{n}_3 \, dS = 0$$

The dot product between a vector $\bar{V}$ and the unit vector $\bar{n}$ is the projection of $\bar{V}$ onto $\bar{n}$ and it is equal to the magnitude of $\bar{V}$, which is here denoted simply as V, because $\bar{V}$ and $\bar{n}$ are parallel vectors.

$$\bar{V}_1 \cdot \bar{n}_1 = -V_1$$

$$\bar{V}_2 \cdot \bar{n}_2 = V_2$$

$$\bar{V}_3 \cdot \bar{n}_3 = V_3$$

$$-\iint_{A_1} \rho_1 V_1 \, dS + \iint_{A_2} \rho_2 V_2 \, dS + \iint_{A_3} \rho_3 V_3 \, dS = 0$$

Further assuming that neither densities nor velocities vary over their respective areas, we get

$$-\rho_1 V_1 A_1 + \rho_2 V_2 A_2 + \rho_3 V_3 A_3 = 0$$

for a single pipe this equation becomes

$$\rho_1 V_1 A_1 = \rho_2 V_2 A_2$$

Example 4.1

The velocity field in an incompressible fluid is given by

$$\bar{V} = x^4 y z^2 \bar{i} + (x^3 y^2 z^2 - 1/2 \, y^2) \bar{j} - (2 x^3 y z^3 - yz) \bar{k}.$$

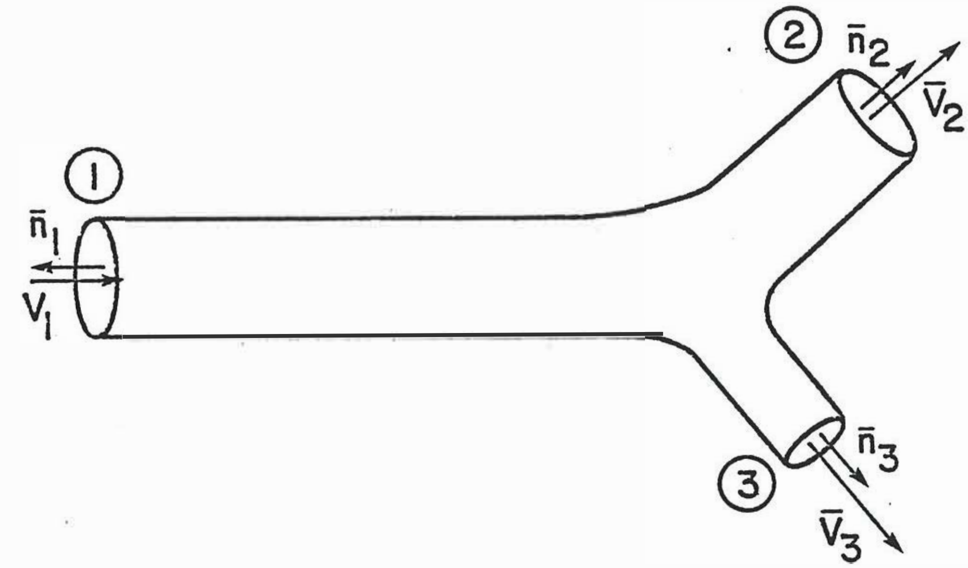

Fig. 4.3 Branching flow

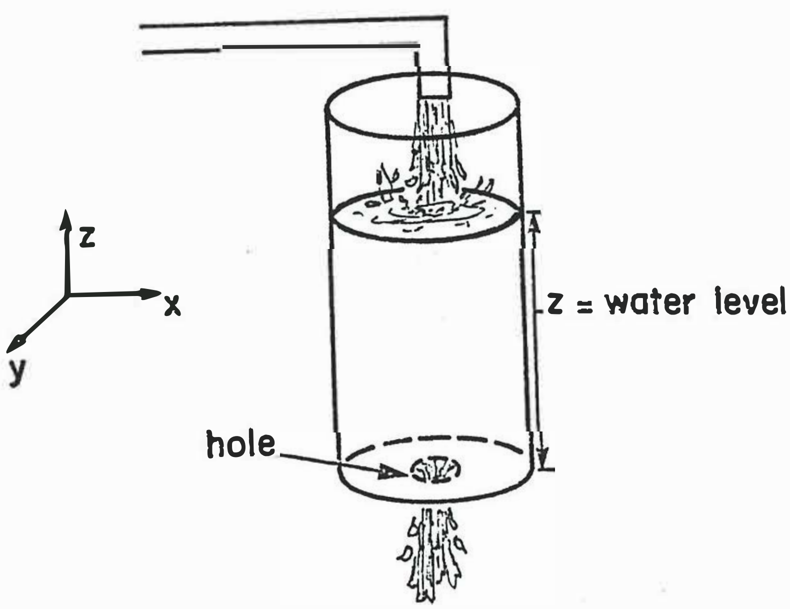

Fig. E.4.2

Show that this velocity field satisfies the continuity equation.

Solution

For an incompressible fluid

$$\nabla \cdot \vec{V} = \frac{\partial v_x}{\partial x} + \frac{\partial v_y}{\partial y} + \frac{\partial v_z}{\partial z} = 0$$

Here, we have

$$4\, x^3\, y\, z^2 + (2\, x^3\, y\, z^2 - y) - (6\, x^3\, y\, z^2 - y) = 0$$

This is identical to zero for all values of x, y, z.

Example 4.2

A vertical cylindrical tank of 1 m in diameter is being filled with water at a rate of 11 kg per minute. Water also escapes from a hole of 5 cm diameter at a velocity of 10 cm/s. Determine the rate at which the water level in the tank is rising or falling.

Solution

A simple mass balance, by taking the cylindrical tank as our control volume, gives

$$(\dot{m})_{in} - (\dot{m})_{out} = \frac{dm}{dt}$$

$$(\dot{m})_{in} = 11 \text{ kg/min} = 183.33 \text{ g/s}$$

$$(\dot{m})_{out} = \rho\, AV = 1\, \frac{g}{cm^3} \times (\frac{\pi\, 5^2}{4}\, cm^2) \times 10\, \frac{cm}{s} = 196.25 \text{ g/s}$$

Therefore

$$\frac{dm}{dt} = 183.33 - 196.25 = -12.92 \text{ g/s}$$

Which means that the water level in the tank is falling

$$\frac{dm}{dt} = \rho\, A\, V_{tank} = \rho\, A\, \frac{dz}{dt}$$

$$-12.92\, \frac{g}{s} = 1\, \frac{g}{cm^3} \times (\frac{\pi\, 100^2}{4}\, cm^2) \times \frac{dz}{dt}$$

$$\frac{dz}{dt} = -0.0052 \text{ cm/s}$$

which means that the water level is falling at a rate of 0.0052 cm/s.

Example 4.3

A piston moves with a constant velocity V inside a cylinder of diameter D, which is filled with a liquid. The liquid leaving the open end of the cylinder is assumed to have a conical velocity profile as shown in Fig. E.4.3. Determine the volume rate of flow leaving through the two exhaust holes.

Solution

From equation (4.18)

$$\iiint_{V} \left(\frac{\partial \rho}{\partial t}\right) dV = -\oint\!\!\oint_{S} (\rho\, \bar{V} \cdot \bar{n})\, dS$$

The fluid density does not change with time: $\partial\rho/\partial t = 0$. Therefore

$$\oint\!\!\oint_{S} (\rho\, \bar{V} \cdot \bar{n})\, dS = 0$$

or

$$\iint_{A} (\rho\, \bar{V}_p \cdot \bar{n})\, dS + \iint_{holes} (\rho\, V_h \cdot \bar{n})\, dS + \iint_{A} (\rho\, \bar{V} \cdot \bar{n})\, dS = 0$$

where

A = the cross-sectional area of the cylinder

V_p = the velocity of the piston

V = the velocity of the liquid leaving through the open end: $V = V_{max}\,(1 - 2(r/D))$

$\iint_{holes} (\rho\, \bar{V}_h \cdot \bar{n})\, dS$ = the mass flow rate leaving through the exhaust holes, $\rho\, \dot{Q}$ = (density) × (volume flow rate).

Therefore

$$-\rho\, V_p \frac{\pi D^2}{4} + \rho\, \dot{Q} + \int_0^{D/2} \rho\, V\, 2\pi r dr = 0$$

$$-V_p \frac{\pi D^2}{4} + \dot{Q} + 2\pi \int_0^{D/2} V_{max}\, (1 - 2\, (\frac{r}{D}))\, rdr = 0$$

$$\dot{Q} = V_p \frac{\pi D^2}{4} - 2\pi D^2 V_{max} \left[(\frac{1}{2}\, (\frac{r}{D})^2 - \frac{2}{3}\, (\frac{r}{D})^3\right]_0^{1/2}$$

$$= V_p \frac{\pi D^2}{4} - 2\pi D^2 V_{max} \left[\frac{1}{8} - \frac{2}{24}\right]$$

$$= \frac{\pi D^2}{4} (V_p - \frac{1}{3} V_{max})$$

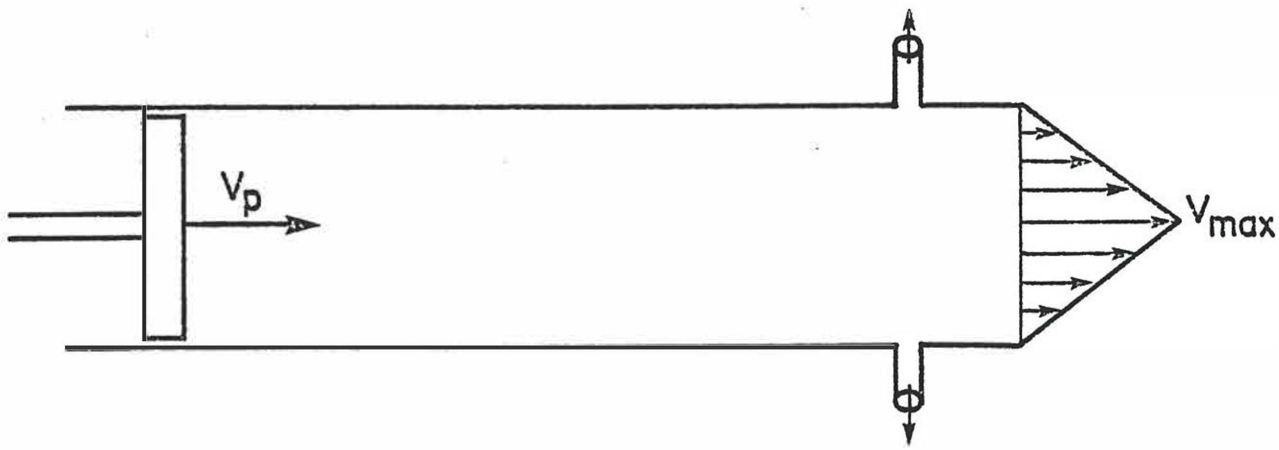

Fig. E.4.3

John Vlachopoulos, *Fundamentals of Fluid Mechanics*
Chem. Eng., McMaster University, Hamilton, ON, Canada
(First Edition 1984, revised internet edition (2016), www.polydynamics.com)

CHAPTER 5

BASIC CONCEPTS OF FLUID DYNAMICS

5.1 INTRODUCTION

The word dynamics is derived from the Greek word dynamis, which means force. Dynamics is the branch of mechanics which is devoted to the study of the relationships between forces and the motions that they cause.

The forces acting on a fluid are generally characterized either as body forces or surface forces. Body forces act on every mass element of the body and are proportional to the total mass of the body. The gravitational force, electromagnetic or centrifugal forces are body forces. These forces are exerted on an arbitrary body without the necessity of physical contact between the body and the surroundings where such a force is present.

On the contrary surface forces, as the name implies, require a surface contact with the surroundings causing these forces. Pressure and the viscous resistance forces, which are described in Chapter 1, are surface forces.

In the case of static equilibrium (Fluid Statics) the body and surface forces cancel each other. When motion is involved the algebraic sum of body and surface forces must be proportional to the mass times the acceleration of the body (Newton's second law of motion).

5.2 DEFINITION AND NOTATION OF STRESS

It is easier to illustrate the concept of stress for a solid body rather than a fluid. Of course, both solids and fluids, whether liquids or gases, are continua and the various definitions are applicable irrespective of the physical state.

Let us consider a body subjected to forces as shown in Fig. 5.1(a). We pass a cutting plane through the body and draw a sketch of the lower half as shown in Fig. 5.1(b). Assume that a distributed load acts over the entire cross section and consider a concentrated force F acting on a small area A. Resolving $\bar{F}$ into $\bar{F}_n$, a normal component, and $\bar{F}_s$, a tangential component, as shown in Fig. 5.1(b), we can define the normal stress as

$$N = \lim_{A \to 0} \frac{|F_n|}{A} \qquad (5.1)$$

and the shear stress as

$$S = \lim_{A \to 0} \frac{|F_s|}{A} \qquad (5.2)$$

where $|F_n|$ and $|F_s|$ are the magnitudes of the force vectors $\bar{F}_n$ and $\bar{F}_s$, respectively.

It should be noted here that while forces are vectors, the corresponding stresses are scalars, and have units of force divided by area (N/m^2 = Pa).

It is customary to choose a system of coordinates with x and y parallel to the cutting plane and further resolve the tangential force into a component in the x direction and another in the y direction. Thus, the force vector acting on it is resolved into one normal and two tangential components. The corresponding stresses are defined by dividing the magnitudes of the force components by the area.

Let us now consider an infinetisimal volume element formed by six

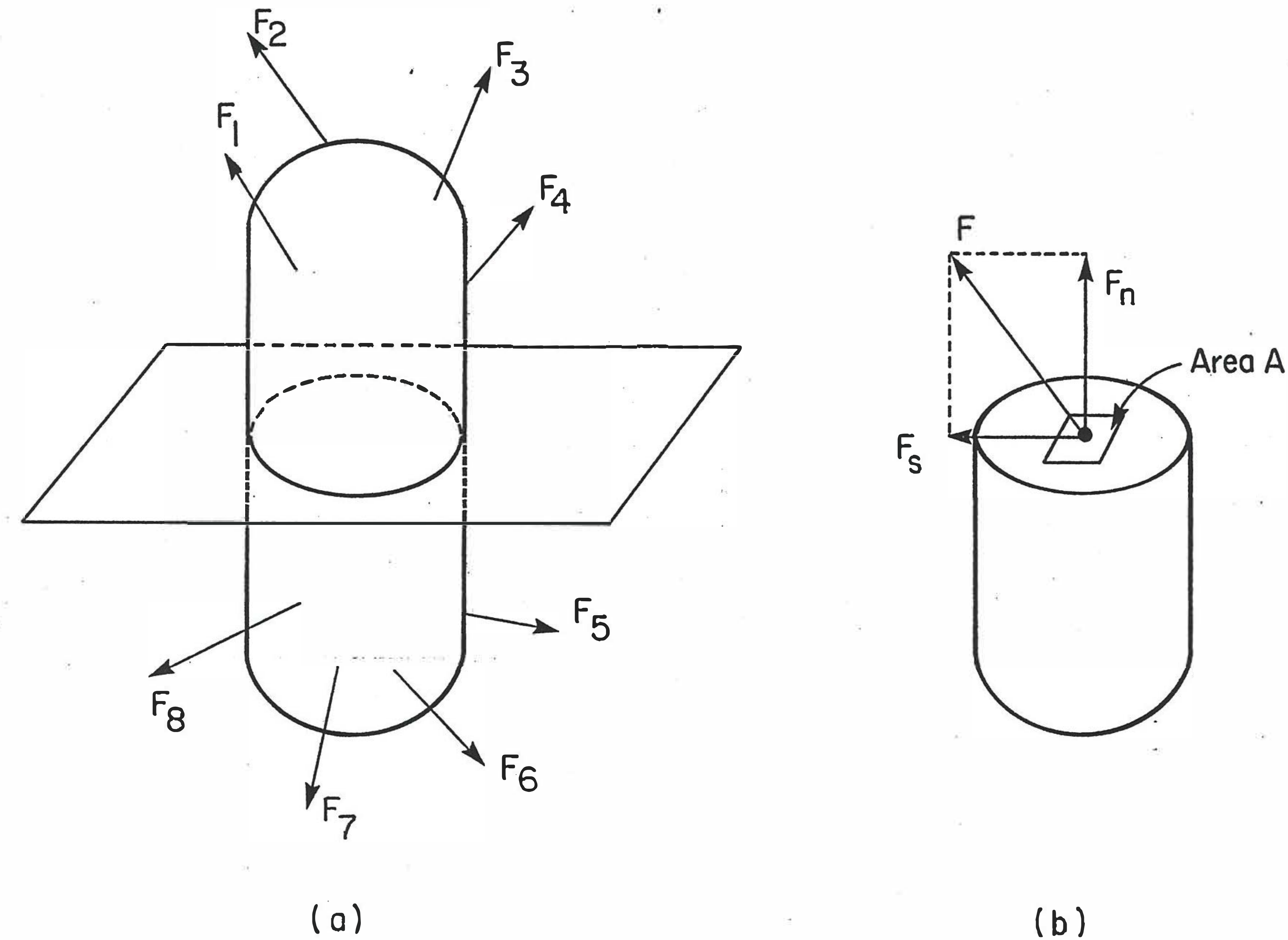

Fig. 5.1 Body subjected to arbitrary forces

cutting planes as shown in Fig. 5.2. There will be one normal stress and two shear stresses for each of the three pairs of planes as shown in the figure. Thus, to define the state of stress at a point in a continuum, we need nine stress components. These stress components form an array of nine scalar quantities which can be written as

$$\begin{matrix} \tau_{xx} & \tau_{xy} & \tau_{xz} \\ \tau_{yx} & \tau_{yy} & \tau_{yz} \\ \tau_{zx} & \tau_{zy} & \tau_{zz} \end{matrix}$$

or equivalently

$$\begin{matrix} \tau_{11} & \tau_{12} & \tau_{13} \\ \tau_{21} & \tau_{22} & \tau_{23} \\ \tau_{31} & \tau_{32} & \tau_{33} \end{matrix}$$

It can be shown rigorously (see Appendix A) that the stress array obeys a linear transformation law and is therefore a tensor. This tensor is denoted in symbolic form as

$$\overset{=}{\tau}$$

or in Cartesian index notation as

$$\tau_{ij}$$

The stress is a symmetric tensor, therefore $\tau_{ij} = \tau_{ji}$ which means $\tau_{xy} = \tau_{yx}$, $\tau_{xz} = \tau_{zx}$ etc.

To denote the various stress components we use certain conventions which are followed by most authors in North America. Namely

(i) the first subscript i refers to the plane which is normal to the i axis and on which the stress acts (indicates the rows in matrix notation)

(ii) the second subscript j refers to the coordinate direction j of the stress (indicates columns in matrix notation).

Thus, τ_{xy} is a shear stress which acts on a plane normal to the x-axis and in the y-direction. τ_{xx} is a normal stress which acts on a plane normal to the x-axis and in the x-direction.

When making force balances a sign convention is also necessary: Stresses are positive if tensile and negative if compressive.

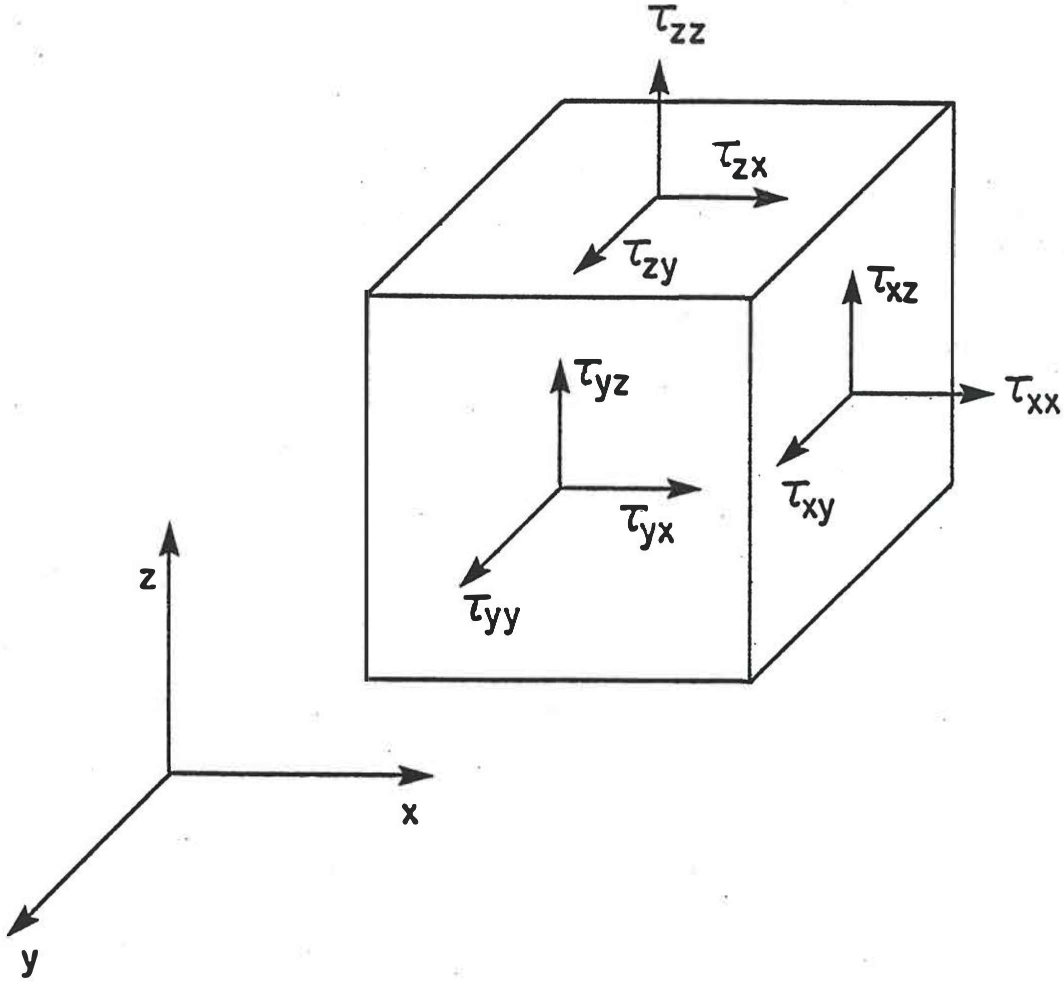

Fig. 5.2 Stresses exerted on three planes of an elemental parallelepiped.

Pressure is a normal stress and compressive, therefore, it is negative according to our convention. Thus, we may write the total stress tensor as

$$\bar{\bar{\sigma}} = -p\bar{\bar{\delta}} + \bar{\bar{\tau}} = -p\delta_{ij} + \tau_{ij} \Rightarrow \begin{matrix} -p+\tau_{11} & \tau_{12} & \tau_{13} \\ \tau_{21} & -p+\tau_{22} & \tau_{23} \\ \tau_{31} & \tau_{32} & -p+\tau_{33} \end{matrix} \tag{5.3}$$

$\bar{\bar{\tau}}$ is often called the deviatoric stress tensor. The deviatoric stress tensor is related to the deformation (for solids) or the rate of deformation (for fluids). In the simple shearing flow of a Newtonian fluid between two flat plates of Chapter 1, we had

$$\tau_{yx} = \tau_{xy} = \mu \left(\frac{dv_x}{dy}\right) \tag{5.4}$$

We may write in general

$$\tau_{ij} = \text{function of } \left(\frac{\partial v_j}{\partial x_i}\right)$$

Such relations are called constitutive equations (see Chapter 16).

4.3 PROBLEM SOLVING IN FLUID DYNAMICS

A flow field can be fully described in terms of the three velocity components (v_x, v_y, v_z), the pressure p, the density ρ, and the temperature T. To determine these quantities we must first express mathematically the conservation principles of mechanics [1]. These are the conservation of mass, conservation of momentum and conservation of energy. Momentum is a vector quantity and thus the principle of conservation yields three scalar equations. In addition, a thermodynamic equation of state relating ρ, p and T is needed. To summarize we may write

UNKNOWNS	
v_x, v_y, v_z, p, ρ, T	6
EQUATIONS	
conservation of mass	1
conservation of momentum	3
conservation of energy	1
equation of state $\rho = \rho(p,T)$	1
	6

Thus, we have 6 equations and 6 unknowns and in principle we can obtain solutions to all flow problems if we can come up with the appropriate methods and techniques. However, such general solutions are extremely complicated and often virtually impossible. Actually most problems (but not all) can be reasonably well approximated by determining two or three of the above variables. For example, the unidirectional flow problems require only the determination of one velocity component and pressure (v_x,p). Two-dimensional problems require v_x, v_y and p.

Thus to obtain solutions to flow problems we will invoke some classical approximations, such as unidirectional flow (Chapter 7), creeping flow (Chapter 8), boundary layer flow (Chapter 9), inviscid flow (Chapter 11), and one-dimensional flow (Chapter 15).

In problems involving turbomachines we use, in addition, the principle of conservation of angular momentum (see section 6.7).

In Magnetohydrodynamics we need also the equation of conservation of charges and Maxwell's equations of electromagnetism (see Chapter 17).

5.4 SIMILARITY AND MODELLING

Two flow fields are said to be similar if all their corresponding important parameters are one by one proportional. These parameters can be geometric, kinematic or dynamic.

Geometric similarity means that all geometrical boundaries and the corresponding interior points between two flow fields are different by a constant scale. Kinematic similarity implies that the velocity ratios at corressponding points between two flow fields are constant. Dynamic similarity means that all ratios of the corresponding forces in two flow fields are constant. The forces that control the motion of fluids are usually inertia, pressure, viscous (stress) forces, gravity, and surface tension and electromagnetic forces for conducting fluids. The various force ratios are dimensionless numbers and are given specific names. The Reynolds number, which was introduced in Chapter 1, represents the ratio of inertia to viscous forces. The ratio of inertia to gravity forces is called the Froude number (see section 6.8). We have

$$Re = \frac{\rho VL}{\mu} \text{ (Reynolds number)} \qquad (5.5)$$

$$Fr = \frac{V^2}{gL} \quad \text{(Froude number)} \tag{5.6}$$

In the above expressions ρ is the fluid density, μ the viscosity, V a characteristic velocity and L a characteristic length.

Let us consider the flow of fluids in two long horizontal pipes of different diameters. It is well known that the flow in such pipes is governed by the inertia and viscous forces. Consequently, the Reynolds number in the two pipes must be the same, i.e.

$$(Re)_1 = (Re)_2 \tag{5.7}$$

in order for the two flow fields to be completely similar. By taking the average velocity as the characteristic velocity and the diameter as the characteristic length, we have

$$\frac{\rho_1 V_1 D_1}{\mu_1} = \frac{\rho_2 V_2 D_2}{\mu_2} \tag{5.8}$$

This means that the two flow systems might have totally different ρ,V,D or μ but they will behave in the same manner if the above relation is satisfied. This in turn implies that we can use small scale models in order to determine the flow behavior of larger prototypes. Such small scale models are commonly used to predict the performance not only of pipelines but also of aircraft, ships, fluid machinery, bridges and other structures. The models are vastly less expensive and can be well instrumented for testing in wind tunnels, water tunnels or towing tanks.

The Reynolds number is just one of many parameters used in similarity analysis and modelling. For free surface flows the gravity forces are also important in addition to the inertia and viscous forces. Thus, both the Reynolds number and the Froude number must be matched between model and prototype, i.e.

$$\frac{\rho_m V_m L_m}{\mu_m} = \frac{\rho_p V_p L_p}{\mu_p} \tag{5.9}$$

and

$$\frac{V_m^2}{g_m L_m} = \frac{V_p^2}{g L_p} \tag{5.10}$$

In other flow problems the behavior may also be governed by such forces as pressure and surface tension and may involve energy and mass transfer phenomena. For such problems the proper dimensionless groups (numbers) must be considered which express the ratio of the forces involved. These groups appear in the appropriate sections of this book.

The analysis of flow problems in terms of dimensional groups is called dimensional analysis. In this method the objective is the determination of the functional relationship between certain flow quantities and the appropriate dimensionless groups. For example for flow through pipes it has been found that the flow resistance which is expressed by the pressure drop between two locations in the pipe is a function of the Reynolds number. This is usually written in the form of the so-called friction coefficient as

$$f = \frac{2\Delta p}{\rho V_{avg}^2} \Big/ \frac{L}{D} = F(Re) = F\left(\frac{\rho V_{avg} D}{\mu}\right) \tag{5.11}$$

where Δp is the pressure drop between two points L distance apart in a pipe of diameter D and with average velocity of V_{avg}.

For laminar flow ($Re \leq 2100$) it has been found that

$$f = \frac{64}{Re} \tag{5.12}$$

for turbulent flow in smooth pipes ($Re > 2100$)

$$f = \frac{0.316}{(Re)^{1/4}} \tag{5.13}$$

A formalized procedure for the identification of the proper grouping of dimensionless terms has been developed which is based on the so-called Buckingham's pi theorem. According to this theorem a function of n independent physical variables $x_1, x_2, \ldots, x_n$

$$f(x_1, x_2, \ldots, x_n) = 0 \tag{5.14}$$

can be expressed as a function of n-m dimensionless groups of the original n variables.

$$F(\pi_1, \pi_2, \ldots \pi_{n-m}) = 0 \tag{5.15}$$

Each group is called a pi group and may contain any number of the independent variables $x_1, x_2, \ldots, x_n$. m is the number of the primary units, which in fluid mechanics are usually three (length, time and mass). Detailed description of this method can be found elsewhere [2-4]. Nowadays, this procedure is seldom used. Instead, it is preferable to work with the dimensionless forms of the conservation equations and thus identify directly the important dimensional groups (see Chapters 13 and 14).

REFERENCES

1. S. Eskinazi, "Vector Mechanics of Fluids and Magnetofluids", Academic Press, New York (1967).

2. L. Brand, "The Pi Theorem of Dimensional Analysis", Arch. Ration. Mech. Anal., 1, 35 (1957).

3. T. Allen and R.L. Ditsworth, "Fluid Mechanics", McGraw-Hill, New York (1972).

4. A. Mironer, "Engineering Fluid Mechanics", McGraw-Hill, New York (1979).

John Vlachopoulos, *Fundamentals of Fluid Mechanics*
Chem. Eng., McMaster University, Hamilton, ON, Canada
(First Edition 1984, revised internet edition (2016), www.polydynamics.com)

CHAPTER 6

CONSERVATION OF MOMENTUM

6.1 THE LINEAR MOMENTUM BALANCE

The first significant advance in understanding motion was made by the Italian astronomer and physicist Galileo who discovered the principle of inertia: if a body is at rest or moving at a constant speed in a straight line, it will remain at rest or keep moving in a straight line at constant speed unless it is acted upon by a force. Newton restated the Galilean principle of inertia which is usually called Newton's first law of motion. Newton's second law is a quantitative description of the changes that a force can produce in the motion of a body and can be stated as: the time-rate-of-change of momentum (mass × velocity) of a body is equal to the sum of forces acting upon it, or mathematically

$$\Sigma \bar{F} = \frac{d}{dt}(m\bar{V}) \tag{6.1}$$

This law as stated here applies to an identified particle moving in space, that is in the Lagrangian sense. In the study of fluid motion, however, it is difficult to identify a "fluid body" and apply Newton's second law. It is therefore appropriate to reformulate the momentum principle in the Eulerian sense. We choose a volume of fixed size and position in space (control volume) as shown in Fig. 6.1 and write a

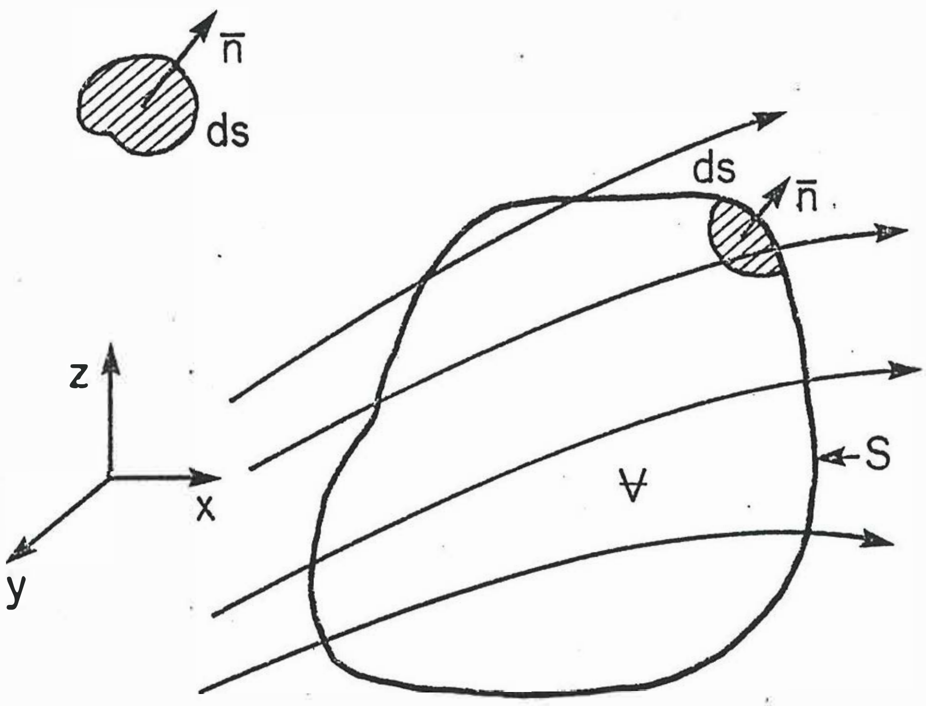

Fig. 6.1 A control volume in a flow field

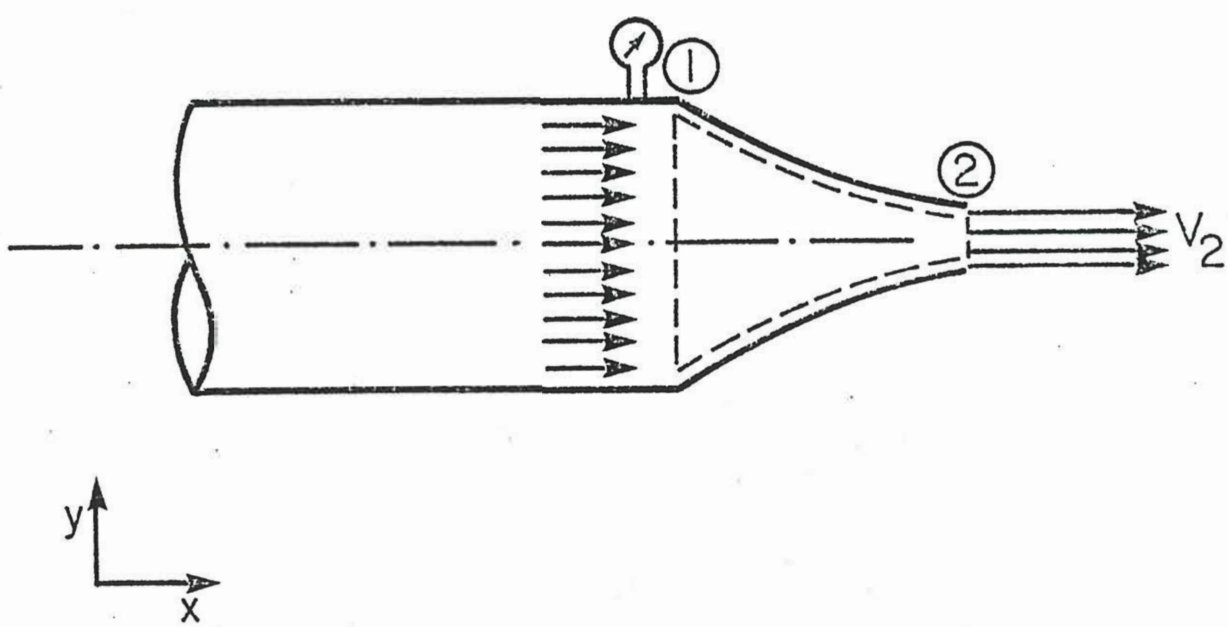

Fig. 6.2 Uniform flow through a converging nozzle

momentum balance in the form

$$\begin{matrix}\text{RATE OF} \\ \text{MOMENTUM} \\ \text{ACCUMULATION}\end{matrix} = \begin{matrix}\text{RATE OF} \\ \text{MOMENTUM} \\ \text{IN}\end{matrix} - \begin{matrix}\text{RATE OF} \\ \text{MOMENTUM} \\ \text{OUT}\end{matrix} + \begin{matrix}\text{SUM OF FORCES} \\ \text{ACTING ON} \\ \text{CONTROL VOLUME}\end{matrix} \tag{6.2}$$

or mathematically

$$\frac{d}{dt}(m\overline{V}) = (\overline{V}_{in}\,\dot{m}_{in} - \overline{V}_{out}\,\dot{m}_{out}) + \Sigma\,\overline{F} \tag{6.3}$$

where $\dot{m}$ represents the mass rate of flow.

Equation (6.3) is a vector equation and can be represented by three scalar equations i.e. for a rectangular system of coordinates

$$\frac{d}{dt}(m\,v_x) = (v_x)_{in}\,\dot{m}_{in} - (v_x)_{out}\,\dot{m}_{out} + \Sigma\,F_x \tag{6.4}$$

$$\frac{d}{dt}(m\,v_y) = (v_y)_{in}\,\dot{m}_{in} - (v_y)_{out}\,\dot{m}_{out} + \Sigma\,F_y \tag{6.5}$$

$$\frac{d}{dt}(m\,v_z) = (v_z)_{in}\,\dot{m}_{in} - (v_z)_{out}\,\dot{m}_{out} + \Sigma\,F_z \tag{6.6}$$

The above forms of Newton's second law are valid for a coordinate system fixed in space or any coordinate system translating with a constant velocity. These types of coordinate systems are usually referred to as <u>inertial frames of reference</u> [1,2].

6.2 APPLICATIONS OF THE LINEAR MOMENTUM BALANCE

6.2.1 FORCE ON A NOZZLE

We will determine the force exerted by the fluid on the walls of the horizontal nozzle shown in Fig. 6.2. The fluid is assumed to have uniform densities ρ_1, ρ_2 and velocities V_1, V_2 at boundaries 1 and 2 respectively. The flow is steady so that there is no variation of momentum with time. The momentum balance in the x-direction (equation (6.4)), for a control volume indicated by the broken line, gives:

$$0 = (v_{x1})\,\dot{m}_1 - (v_{x2})\,\dot{m}_2 + \Sigma\,F_x \tag{6.7}$$

The forces acting on the control volume in the x direction are

$$\Sigma F_x = p_1 A_1 - p_2 A_2 + F_{wx} \tag{6.8}$$

where A represents the cross-sectional area, p the pressure and F_{wx} the force exerted by the nozzle wall <u>on the fluid</u> in the control volume. The principle of conservation of mass gives $\dot{m}_1 = \dot{m}_2$ where $\dot{m}_1 = \rho_1 A_1 V_1$ and $\dot{m}_2 = \rho_2 A_2 V_2$. Thus, the momentum balance becomes

$$(v_{x1}) \rho_1 A_1 V_1 - (v_{x2}) \rho_2 A_2 V_2 + p_1 A_1 - p_2 A_2 + F_{wx} = 0 \tag{6.9}$$

and, since $v_{x1} = V_1$ and $v_{x2} = V_2$

$$F_{wx} = -p_1 A_1 + p_2 A_2 - \rho_1 A_1 V_1^2 + \rho_2 A_2 V_2^2 \tag{6.10}$$

is the force exerted by the nozzle wall on the fluid in the control volume. Consequently the force exerted by the fluid on the nozzle wall should be opposite.

The only forces acting on the fluid in the y direction are the weight W of the fluid and the force exerted by the nozzle wall on the fluid in the control volume F_{wy}. Thus the momentum balance in the y-direction (equation (6.5)) simplifies to

$$0 = -W + F_{wy} \tag{6.11}$$

and

$$F_{wy} = W \tag{6.12}$$

<u>Example 6.1</u>

The fluid flowing through the nozzle of Fig. 6.2 is water (ρ = 1000 kg/ms) and p_1 = 1000 kPa gage, $p_2 = p_{atm}$ = 101.33 kPa, D_1 = 25 cm, D_2 = 5 cm, V_2 = 50 m/s.

<u>Solution</u>

Water is virtually incompressible under these conditions $\rho_1 = \rho_2$ = 1000 kg/m^3.

The principle of conservation of mass gives

$$V_1 = \frac{A_2}{A_1} V_2 = \left(\frac{5}{25}\right)^2 (50) = 2 \ \frac{m}{s}$$

Then, introducing the numerical values in equation (6.10), we obtain

$$F_{wx} = -(1000 \frac{N}{m^2} + 101.33 \frac{N}{m^2}) \times 10^3 \times \frac{\pi}{4} (.25m)^2 + 101.33 \times 10^3 \frac{N}{m^2} \frac{\pi}{4} (.05m)^2$$

$$+ 1000 \frac{kg}{m^3} \frac{\pi}{4} [-(0.25m)^2 (2 \frac{m}{s})^2 + (0.05m)^2 (50 \frac{m}{s})^2]$$

$$= -54030 + 199 N + 4710 N = -49121 N$$

$$= -49.12 kN$$

The negative sign means that the force exerted by the nozzle on the fluid (F_{wx}) acts in the negative x direction. Therefore the force exerted by the fluid on the nozzle is 49.12 N acting in the positive x direction.

The question of a positive or negative sign in front of the external force term is often confusing. For this problem one might be tempted to introduce the negative sign in front of F_{wx} in equation (6.8), because one would expect F_{wx} to act in the negative x direction. Such practice, however, is not recommended. Very often the direction of an external force is not known beforehand and intuition might be misleading. It is preferable to introduce the force exerted by the surroundings on the fluid as a positive quantity in equation (6.8). The correct direction of the force would thus be determined after the introduction of the numerical values.

6.2.2 FORCE ON A PIPE BEND

We will determine the force exerted by the fluid on the pipe bend shown in Fig. 6.3. The control volume is shown by the dotted line.

We apply the momentum balance for steady flow in the x and y directions (equations (6.4) and (6.5) respectively).

x direction:

$$0 = (v_{x1}) \dot{m}_1 - (v_{x2}) \dot{m}_2 + \Sigma F_x \qquad (6.13)$$

where

$$\Sigma F_x = p_1 A_1 - p_2 A_2 \cos \theta + F_{wx} \qquad (6.14)$$

A represents the cross sectional areas, p the pressures and F_{wx} the force exerted by the pipe wall on the fluid in the control volume.

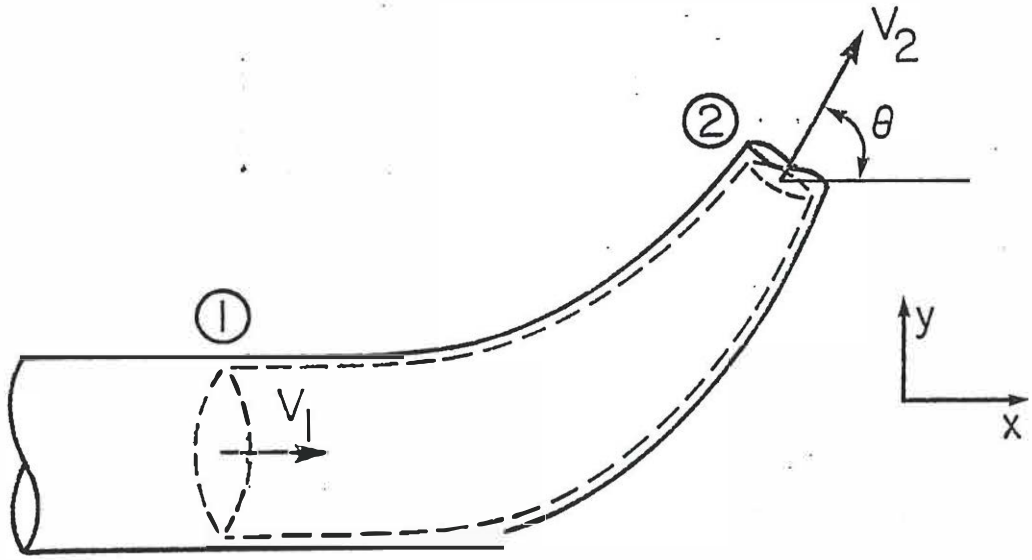

Fig. 6.3 Uniform flow through a pipe bend

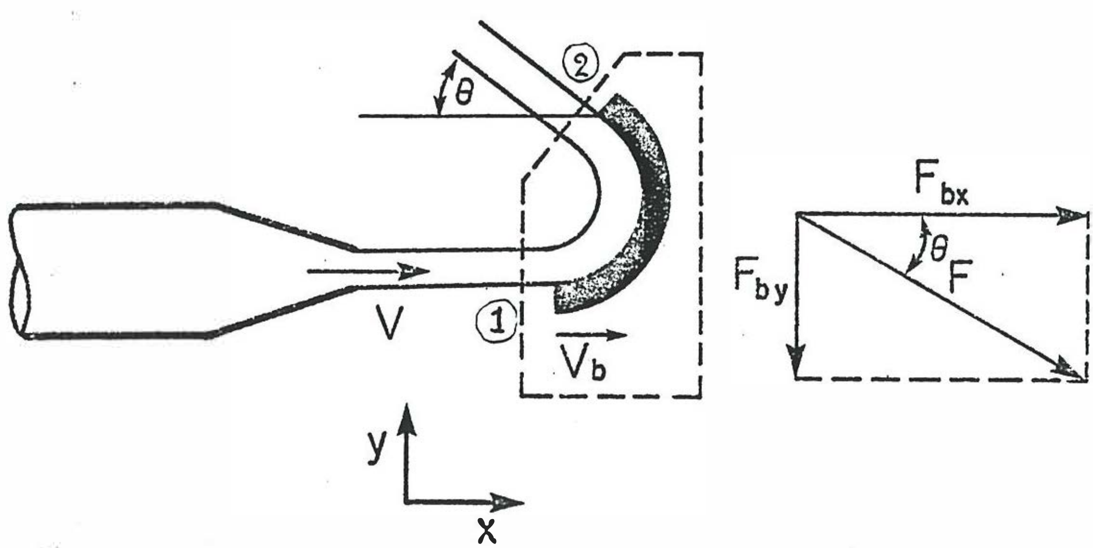

Fig. 6.4 Liquid jet impinging on a moving blade

y direction:

$$0 = (v_{y1})\,\dot{m}_1 - (v_{y2})\,\dot{m}_2 + \Sigma F_y \tag{6.15}$$

where

$$\Sigma F_y = -p_2 A_2 \sin\theta + F_{wy} - W \tag{6.16}$$

F_{wy} represents the force exerted by the pipe wall on the fluid in the control volume in the y direction, and W the weight of the fluid.

The principle of conservation of mass gives $\dot{m}_1 = \dot{m}_2$, where

$$\dot{m}_1 = \rho_1 A_1 V_1 \quad \text{and} \quad \dot{m}_2 = \rho_2 A_2 V_2$$

We note that

$$v_{x1} = V_1$$

$$v_{x2} = V_2 \cos\theta$$

$$v_{y1} = 0$$

$$v_{y2} = v_2 \sin\theta$$

Thus, we have in the x direction

$$\rho_1 A_1 V_1^2 - \rho_2 A_2 V_2^2 \cos\theta + p_1 A_1 - p_2 A_2 \cos\theta + F_{wx} = 0 \tag{6.17}$$

or

$$F_{wx} = p_2 A_2 \cos\theta - p_1 A_1 + \rho_2 A_2 V_2^2 \cos\theta - \rho_1 A_1 V_1^2 \tag{6.18}$$

and in the y direction

$$-\rho_2 A_2 V_2^2 \sin\theta - p_2 A_2 \sin\theta + F_{wy} - W = 0 \tag{6.19}$$

or

$$F_{wy} = W + p_2 A_2 \sin\theta + \rho_2 A_2 V_2^2 \sin\theta \tag{6.20}$$

It is repeated here that F_{wx} and F_{wy} represent the forces in the x and y directions exerted by the pipe walls on the fluid. Consequently the forces exerted by the fluid on the pipe bend should be opposite. It should also be noted that in setting up the linear momentum balance (equations (6.13) through (6.16)), F_{wx} and F_{wy} were assumed to be positive i.e. acting in the positive x and y direction respectively. Whether this is the case in a particular problem it would depend on the numerical values of velocities, pressures, angle of bend, areas etc.

6.2.3 FORCE EXERTED BY A JET ON A MOVING BLADE

The blade shown in Fig. 6.4 moves at a constant velocity V_b and receives a liquid jet which leaves the nozzle at a velocity V. We will determine the forces in the x and y directions and the total force of the blade.

We choose a control volume as shown in Fig. 6.4, which moves with a constant velocity equal to the blade velocity for steady flow. For steady flow the momentum balance in the x direction gives

$$(v_{x1})\,\dot{m}_1 - (v_{x2})\,\dot{m}_2 + F_{bx} = 0 \tag{6.21}$$

where F_{bx} is the force exerted by the blade on the fluid. v_{x1} and v_{x2} are the velocities entering and leaving relative to the moving control volume. We note that

$$v_{x1} = (V-V_b)$$

$$v_{x2} = -\,(V-V_b)\cos\theta$$

$$\dot{m}_1 = \dot{m}_2 = \rho\,A(V-V_b)$$

Thus,

$$F_{bx} = \rho A(V-V_b)\,[-(V-V_b)\cos\theta - (V-V_b)]$$

$$= -\rho A(V-V_b)^2\,[\cos\theta + 1] \tag{6.22}$$

The x direction force on the blade should have the opposite sign.

The momentum balance in the y direction gives

$$(v_{y1})\,\dot{m}_1 - (v_{y2})\,\dot{m}_2 + F_{by} = 0 \tag{6.23}$$

Obviously,

$$v_{y1} = 0$$

$$v_{y2} = (V-V_b)\sin\theta$$

Thus,

$$F_{by} = \rho A(V-V_b)\,[(V-V_b)\sin\theta - 0]$$

$$= \rho A(V-V_b)^2\sin\theta \tag{6.24}$$

This expression gives the force exerted by the blade on the fluid in the y direction. The force exerted by the fluid on the blade should be opposite.

The magnitude of the total force on the blade can be calculated from

$$|F| = [F_{bx}^2 + F_{by}^2]^{1/2} \tag{6.25}$$

and the direction from

$$\tan\theta = \frac{F_{by}}{F_{bx}} \tag{6.26}$$

It should be noted that the weight of the fluid jet was not taken into consideration.

Example 6.2

Consider a blade moving with $V_b = 10$ m/s. A water jet leaves the nozzle at 50 m/s and has a diameter D = 5 cm. Determine the total force exerted on the blade if $\theta = 60^\circ$.

Solution

Introducing the numerical values into the equations of Section 6.2.3.we obtain

$$F_{bx} = -(1000\ \frac{kg}{m^3})\ (\pi\ \frac{0.05^2}{4}\ m^2)\ (50\ \frac{m}{s} - 10\ \frac{m}{s})^2\ [\cos 60^\circ + 1]$$

$$= -4710\ N = -4.71\ kN$$

which means that the force on the blade would be $F_x = 4.71$ kN
Similarly

$$F_{by} = (1000\ \frac{kg}{m^3})\ (\pi\ \frac{0.05^2}{4}\ m^2)\ (50\ \frac{m}{s} - 10\ \frac{m}{s})^2\ \sin 60^\circ$$

$$= 2719\ N \simeq 2.72\ kN$$

or $F_{by} = -2.72$ on the blade

The magnitude of the total force is

$$|F| = \{4.71^2 + (-2.72)^2\}^{1/2} = 5.44\ kN$$

The direction is determined from

$$\tan\theta = -\frac{2.72}{4.71} = -0.5775$$

$$\theta = 30^\circ$$

The negative sign indicates that the force acts downward as shown in Fig. 6.4.

6.2.4 MOMENTUM BALANCE IN ROCKET PROPULSION

A rocket is driven forward by the reaction of an exhaust gas jet which is produced by a combustion of an appropriate fuel and oxidizer. We will apply the linear momentum balance for two problems: (a) Stationary rocket on a test stand (b) Rocket travelling in space.

(a) Stationary rocket on a test stand

A schematic diagram is shown in Fig. 6.5(a). We apply the momentum balance, for the control volume indicated by the broken line, in the vertical z direction

$$\frac{d}{dt}(m V_z) = -(v_z)_{out}\, \dot{m}_{out} + \Sigma F_z \tag{6.27}$$

where

$$\Sigma F_z = -p_{atm} A_e + p_e A_e + F_{TS} \tag{6.28}$$

p_{atm} is the atmospheric pressure, p_e the pressure of the exhaust gas jet assumed uniform over the cross-sectional area of the exhaust A_e, and F_{TS} is the force exerted by the test stand on the fluid in the rocket.

For a stationary rocket we may assume d/dt $(m\ v_z) = 0$. This is not strictly correct because of the internal fuel motions. However if the amount of fluid which participates in these motions is small, it may be a reasonable approximation. Thus,

$$0 = -(v_z)_{out}\, \dot{m}_{out} - p_{atm} A_e + p_e A_e + F_{TS} \tag{6.29}$$

or

$$-F_{TS} = -(v_z)_{out}\, \dot{m}_{out} + (p_e - p_{atm}) A_e \tag{6.30}$$

Obviously F_{TS} and $(v_z)_{out}$ are directed in the negative z direction. The force exerted by the rocket on the test stand is usually referred to as thrust

$$\text{Thrust} = F_R = -F_{TS}$$

Thus, for a uniform exhaust velocity $V_e = -(v_z)_{out}$ we have

$$\text{Thrust} = F_R = V_e\, \dot{m}_{out} + (p_e - p_{atm}) A_e \tag{6.31}$$

where

$$\dot{m}_{out} = \rho_e A_e V_e$$

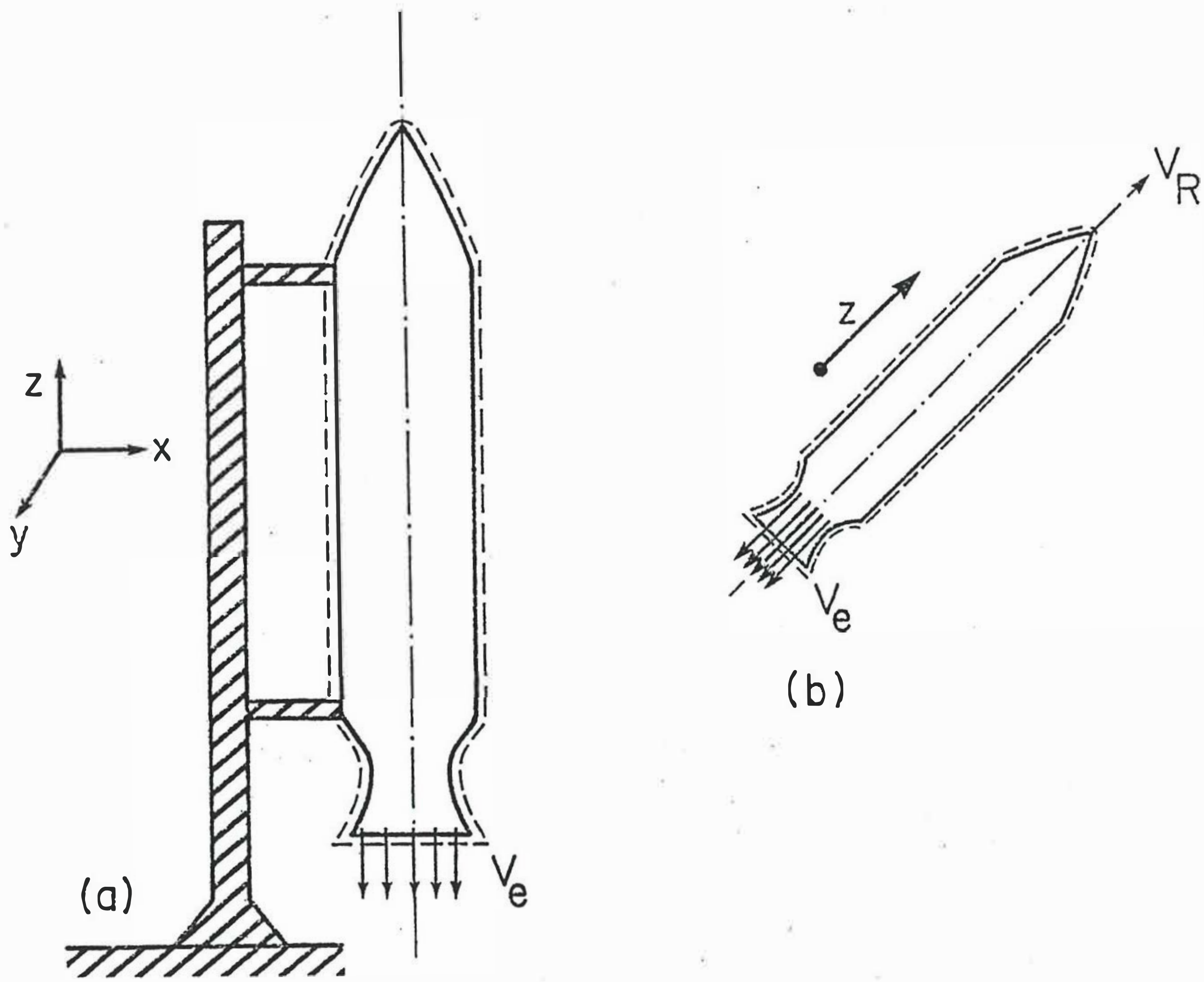

Fig. 6.5 (a) Stationary rocket on a test stand
(b) Rocket travelling in outer space

Example 6.3

Determine the rocket thrust for a ground test if the velocity of the exhaust gases is 2000 m/s and their pressure p = 150 kPa absolute. Both velocity and pressure are assumed uniform over the exhaust area of 500 cm^2. The mass rate of flow is assumed constant at 10 kg/s.

Solution

$$\text{Thrust} = F_R = V_e \dot{m}_{out} + (p_e - p_{atm}) A_e$$

$$= (2000 \frac{m}{s}) \times (10 \frac{kg}{s}) + (150 \frac{N}{m^2} - 101.33 \frac{N}{m^2}) \times 10^3 \times 500 \times 10^{-4} m^2$$

$$= 20000 \frac{kgm}{s^2} + 2433 N = 22433 N$$

$$= 22.43 kN$$

It should be noted that $p_e > p_{atm}$ because the exhaust gas jet is supersonic (see chapter on compressible flow). For a subsonic jet (uncommon for rockets) we would simply have $p_e = p_{atm}$. The exhaust pressure p_e for supersonic jets is determined from the geometrical characteristics of the nozzle and the gas pressure inside the rocket.

(b) Rocket travelling in space

It is assumed that the rocket moves in a straight line in outer space (p_{atm} = 0), where we can neglect the air resistance and gravitational force. The rocket burns α kg/s of fuel. Thus, if the initial mass of rocket and fuel is M for any subsequent instant of time we would have $m = M - \alpha t$. The exhaust gas jet velocity relative to the rocket is V_e and pressure p_e. The velocity of the rocket relative to a system of coordinates fixed in space is V_R. We will determine V_R as a function of time.

We choose a control volume moving with the rocket which is indicated by a broken line in Fig. 6.5(b). The rocket is accelerating and this problem, therefore, should involve a noninertial frame of reference [1,2]. We will use a simplified approach which provides a reasonable approximation. We write a linear momentum balance for an inertial control volume moving with the rocket in the positive z direction

$$\frac{d}{dt}(m\,V_r) = -(V_r)_{out}\,\dot{m}_{out} + \Sigma\,F_z \qquad (6.32)$$

where the subscript r denotes the velocities relative to the control volume which moves at velocity V_R with respect to a fixed system of coordinates. The only external force acting on the fluid in the control volume is $p_e\,A_e$ $(= \Sigma\,F_z)$ which is obviously directed in the positive z direction.

The mass balance for this control volume gives

$$\frac{dm}{dt} = -\,\dot{m}_{out} \qquad (6.33)$$

by multiplying the above expression by V_R and adding equation (6.32), we obtain

$$\frac{d}{dt}[m(V_r+V_R)] = -[(V_r)_{out} + V_R]\,\dot{m}_{out} + p_e\,A_e \qquad (6.34)$$

We now assume that the internal velocities are small as compared to the rocket velocity V_R (i.e. $V_r << V_R$). Thus, we may write

$$\frac{d}{dt}(m\,V_R) = -[(V_r)_{out} + V_R]\,\dot{m}_{out} + p_e\,A_e \qquad (6.35)$$

We note that

$$\dot{m}_{out} = \alpha$$

$$m = M - \alpha t$$

therefore

$$\frac{d}{dt}[(M-\alpha t)\,V_R] = -\,[(V_r)_{out} + V_R]\,\alpha + p_e\,A_e \qquad (6.36)$$

$$(M-\alpha t)\,\frac{dV_R}{dt} + V_R\,\frac{d}{dt}(M-\alpha t) = -\alpha(V_r)_{out} - \alpha V_R + p_e\,A_e \qquad (6.37)$$

$$(M-\alpha t)\,\frac{dV_R}{dt} + \alpha V_R = -\alpha(V_r)_{out} - \alpha V_R + p_e\,A_e \qquad (6.38)$$

$$(M-\alpha t)\,\frac{dV_R}{dt} = -\alpha(V_r)_{out} + p_e\,A_e \qquad (6.39)$$

Assuming $-(V_r)_{out} = V_e$ is a uniform exhaust gas velocity relative to the rocket, we have

$$(M-\alpha t)\frac{dV_R}{dt} = \alpha V_e + p_e A_e \tag{6.40}$$

$$dV_R = (\alpha V_e + p_e A_e)\frac{dt}{M-\alpha t} \tag{6.41}$$

which integrates to

$$V_R = -\left(\frac{\alpha V_e + p_e A_e}{\alpha}\right) \ln (M-\alpha t) + C_1 \tag{6.42}$$

here we assume $V_R = 0$ at $t = 0$ and we obtain

$$V_R = \left(V_e + \frac{p_e A_e}{\alpha}\right) \ln \left(\frac{M}{M-\alpha t}\right) \tag{6.43}$$

In this expression all the quantities (including V_e) should have positive numerical values. We note that the negative sign in the exhaust gas velocity was introduced in equation (6.40).

6.3 GENERALIZATION OF THE LINEAR MOMENTUM BALANCE

Newton's second law of motion was formulated in section 6.1 in the Eulerian sense, that is for a control volume of fixed position and size as shown in Fig. 6.1, and was written in the form

$$\frac{d}{dt}(m\bar{V}) = (\bar{V}_{in}\,\dot{m}_{in} - \bar{V}_{out}\,\dot{m}_{out}) + \Sigma\bar{F} \tag{6.3}$$

The left-hand side represents the rate of accumulation of momentum within the control volume. The term $(\bar{V}_{in}\,\dot{m}_{in} - \bar{V}_{out}\,\dot{m}_{out})$ expresses the net rate of momentum (momentum flux) into the control. The term $\Sigma\bar{F}$ represents the sum of forces acting on the control volume boundaries. Let us now generalize this expression using integrals.

The momentum of the fluid within the control volume $\forall$ may be expressed as

$$m\bar{V} \Rightarrow \iiint_{\forall} \rho\bar{V}\, d\forall$$

where ρ represents the fluid density.

We note the volume is fixed in space, and the derivative d()/dt expresses a local change with respect to time. Therefore the left-hand side of equation (6.3) should be written as

$$\frac{d}{dt}(m\bar{V}) \Rightarrow \frac{\partial}{\partial t} \iiint_{\forall} \rho\bar{V}\, d\forall$$

Now, let us consider an infinitesimal surface area dS on the control volume $\forall$ and $\bar{n}$ a unit vector normal to it. The dot product $\bar{V} \cdot \bar{n}$ is the projection of $\bar{V}$ onto an axis normal to dS. Therefore the mass rate through dS would be

$$\rho\bar{V} \cdot \bar{n}\, dS \quad \text{(scalar)}$$

and the momentum rate of flow

$$\bar{V}\,(\rho\bar{V} \cdot \bar{n})\, dS \quad \text{(vector)}$$

Thus, the net momentum rate of flow out of the control volume $\forall$ which is completely enclosed by surface S would be

$$\oiint_{S} \bar{V}\,(\rho\bar{V} \cdot \bar{n})\, dS$$

Then by referring to equation (6.3), we note that the first term (in parentheses) of the right-hand side represents the net momentum rate of flow into the control volume and can be expressed as

$$(\bar{V}_{in}\,\dot{m}_{in} - \bar{V}_{out}\,\dot{m}_{out}) \Rightarrow -\oiint \bar{V}\,(\rho\bar{V} \cdot \bar{n})\, dS$$

Thus the linear momentum balance represented by (6.3) can be rewritten as

$$\frac{\partial}{\partial t} \iiint_{\forall} \rho\bar{V}\, d\forall = -\oiint_{S} \bar{V}\,(\rho\bar{V} \cdot \bar{n})\, dS + \Sigma\, \bar{F} \qquad (6.44)$$

Since the volume $\forall$ is independent of time the order of differentiation and integration are interchangeable. Thus

$$\iiint_{\forall} \frac{\partial}{\partial t}(\rho\bar{V})\, d\forall + \oiint_{S} \bar{V}\,(\rho\bar{V} \cdot \bar{n})\, dS = \Sigma\, \bar{F} \qquad (6.45)$$

Then using Gauss' divergence theorem

$$\oiint_{S} \bar{V}\,(\rho\bar{V} \cdot \bar{n})\, dS = \iiint_{\forall} \nabla \cdot (\bar{V}\,\rho\bar{V})\, d\forall \qquad (6.46)$$

and

$$\iiint_{\forall} \left(\frac{\partial}{\partial t}(\rho\bar{V}) + \nabla \cdot (\bar{V}\,\rho\bar{V})\right) d\forall = \Sigma\, \bar{F} \qquad (6.47)$$

Note that

$$\nabla \cdot (\bar{V}\ \rho\bar{V}) = \bar{V}\ \nabla \cdot (\rho\bar{V}) + (\rho\bar{V}) \cdot \nabla\bar{V} \qquad (6.48)$$

Thus

$$\iiint_{V} \left(\frac{\partial}{\partial t} (\rho\bar{V}) + \bar{V}\ \nabla \cdot (\rho\bar{V}) + (\rho\bar{V}) \cdot \nabla\ \bar{V}\right) dV = \Sigma\ \bar{F} \qquad (6.49)$$

$$\iiint_{V} \left(\rho \frac{\partial\bar{V}}{\partial t} + \bar{V} \frac{\partial\rho}{\partial t} + \bar{V}\ \nabla \cdot (\rho\bar{V}) + (\rho\bar{V}) \cdot \nabla\ \bar{V}\right) dV = \Sigma\ \bar{F} \qquad (6.50)$$

or, by regrouping

$$\iiint_{V} \left[\rho \frac{\partial\bar{V}}{\partial t} + \rho\bar{V} \cdot \nabla\ \bar{V} + \bar{V} \left(\frac{\partial\rho}{\partial t} + \nabla \cdot (\rho\bar{V})\right)\right] dV = \Sigma\ \bar{F} \qquad (6.51)$$

Then, using the equation of conservation of mass

$$\frac{\partial\rho}{\partial t} + \nabla \cdot (\rho\bar{V}) = 0 \qquad (6.52)$$

we obtain

$$\iiint_{V} \left(\rho \frac{\partial\bar{V}}{\partial t} + \rho\bar{V} \cdot \nabla\ \bar{V}\right) dV = \Sigma\ \bar{F} \qquad (6.53)$$

There are two types of forces acting on the fluid in the control volume: Surface forces and body forces. The surface forces (or stress forces) are normal and tangential (shear) forces acting on surface S which encloses volume V. Let $\bar{n}$ be a unit vector normal to an infinitesimal area dS in a stress field $\bar{\bar{\sigma}}$. The quantity

$$\bar{\bar{\sigma}} \cdot \bar{n}\ dS$$

represents the stress force acting on this surface. Thus, the sum of surface (stress) forces acting on surface S which encloses volume V would be

$$\oiint_{S} \bar{\bar{\sigma}} \cdot \bar{n}\ dS$$

Body forces act on the whole mass of fluid. These are either gravitational or electromagnetic forces (for conducting fluids). In this section we will consider only gravity i.e. the weight of the fluid in the control volume, which is

$$\iiint_{V} \rho\bar{g}\, dV$$

Therefore, equation (6.53) becomes

$$\iiint_{V} \left(\rho \frac{\partial\bar{V}}{\partial t} + \rho\bar{V} \cdot \nabla\bar{V}\right) dV = \iint_{S} \bar{\bar{\sigma}} \cdot \bar{n}\, dS + \iiint_{V} \rho\bar{g}\, dV \tag{6.54}$$

Using Gauss' divergence theorem

$$\iint_{S} \bar{\bar{\sigma}} \cdot \bar{n}\, dS = \iiint_{V} \nabla \cdot \bar{\bar{\sigma}}\, dV \tag{6.55}$$

Thus

$$\iiint_{V} \left(\rho \frac{\partial\bar{V}}{\partial t} + \rho\bar{V} \cdot \nabla\bar{V}\right) dV = \iiint_{V} \nabla \cdot \bar{\bar{\sigma}} dV + \iiint \rho\bar{g}\, dS \tag{6.56}$$

which yields the stress form of the differential equation of momentum

$$\rho \frac{\partial\bar{V}}{\partial t} + \rho\bar{V} \cdot \nabla\bar{V} = \nabla \cdot \bar{\bar{\sigma}} + \rho\bar{g} \tag{6.57}$$

The stress tensor $\bar{\bar{\sigma}}$ represents an array of nine stress components

$$\bar{\bar{\sigma}} = \sigma_{ij} \Rightarrow \begin{matrix} \sigma_{11} & \sigma_{12} & \sigma_{13} \\ \sigma_{21} & \sigma_{22} & \sigma_{23} \\ \sigma_{31} & \sigma_{32} & \sigma_{33} \end{matrix} \tag{6.58}$$

It includes the stresses due to viscosity of the fluid and pressure. Since pressure forces are normal to surfaces and compressive (i.e. act in a direction opposite to unit vector $\bar{n}$) we may write

$$\bar{\bar{\sigma}} = -p\bar{\bar{\delta}} + \bar{\bar{\tau}} = -p\ \delta_{ij} + \tau_{ij} \Rightarrow \begin{matrix} -p+\tau_{11} & \tau_{12} & \tau_{13} \\ \tau_{21} & -p+\tau_{22} & \tau_{23} \\ \tau_{31} & \tau_{32} & -p+\tau_{33} \end{matrix} \tag{6.59}$$

where p denotes pressure and $\bar{\bar{\tau}}$ the so-called deviatoric stress tensor. Noting that

$$\nabla \cdot \bar{\bar{\sigma}} = \nabla \cdot (-p\bar{\bar{\delta}} + \bar{\bar{\tau}}) = -\nabla p + \nabla \cdot \bar{\bar{\tau}} \quad (6.60)$$

We obtain

$$\rho \frac{\partial \bar{V}}{\partial t} + \rho \bar{V} \cdot \nabla \bar{V} = -\nabla p + \nabla \cdot \bar{\bar{\tau}} + \rho \bar{g} \quad (6.61)$$

This equation can be written in Cartesian index notation as

$$\rho \frac{\partial}{\partial t} v_j + \rho v_i \frac{\partial v_j}{\partial x_i} = -\frac{\partial p}{\partial x_j} + \frac{\partial \tau_{ij}}{\partial x_i} + \rho g_j \quad (6.62)$$

or, in terms of three Cartesian components

$$\rho \left(\frac{\partial v_x}{\partial t} + v_x \frac{\partial v_x}{\partial x} + v_y \frac{\partial v_x}{\partial y} + v_z \frac{\partial v_x}{\partial z}\right) = -\frac{\partial p}{\partial x} + \left(\frac{\partial \tau_{xx}}{\partial x} + \frac{\partial \tau_{yx}}{\partial y} + \frac{\partial \tau_{zx}}{\partial z}\right) + \rho g_x \quad (6.63)$$

$$\rho \left(\frac{\partial v_y}{\partial t} + v_x \frac{\partial v_y}{\partial x} + v_y \frac{\partial v_y}{\partial y} + v_z \frac{\partial v_y}{\partial z}\right) = -\frac{\partial p}{\partial y} + \left(\frac{\partial \tau_{xy}}{\partial x} + \frac{\partial \tau_{yy}}{\partial y} + \frac{\partial \tau_{zy}}{\partial z}\right) + \rho g_y \quad (6.64)$$

$$\rho \left(\frac{\partial v_z}{\partial t} + v_x \frac{\partial v_z}{\partial x} + v_y \frac{\partial v_z}{\partial y} + v_z \frac{\partial v_z}{\partial z}\right) = -\frac{\partial p}{\partial z} + \left(\frac{\partial \tau_{xz}}{\partial x} + \frac{\partial \tau_{yz}}{\partial y} + \frac{\partial \tau_{zz}}{\partial z}\right) + \rho g_z \quad (6.65)$$

6.4 AN ALTERNATIVE DERIVATION OF THE DIFFERENTIAL EQUATION OF MOMENTUM

In this section we will derive the differential equation for the conservation of linear momentum by referring to a volume element $\Delta x \Delta y \Delta z$ which is fixed in space with respect to the system of coordinate x, y and z as shown in Fig. 6.6. Again, we start from Newton's second law for a control volume

RATE OF MOMENTUM ACCUMULATION	=	RATE OF MOMENTUM IN	−	RATE OF MOMENTUM OUT	+	SUM OF FORCES ACTING ON SYSTEM	(6.2)

Let us now consider this momentum balance in the x-direction. The rate of momentum accumulation is

rate: $$(\text{ACCUM})_x = \frac{\partial}{\partial t}(m\, v_x) \quad (6.66)$$

where m is the mass within the volume element, $m = \rho\, \Delta x\, \Delta y\, \Delta z$ and the rate of momentum accumulation becomes

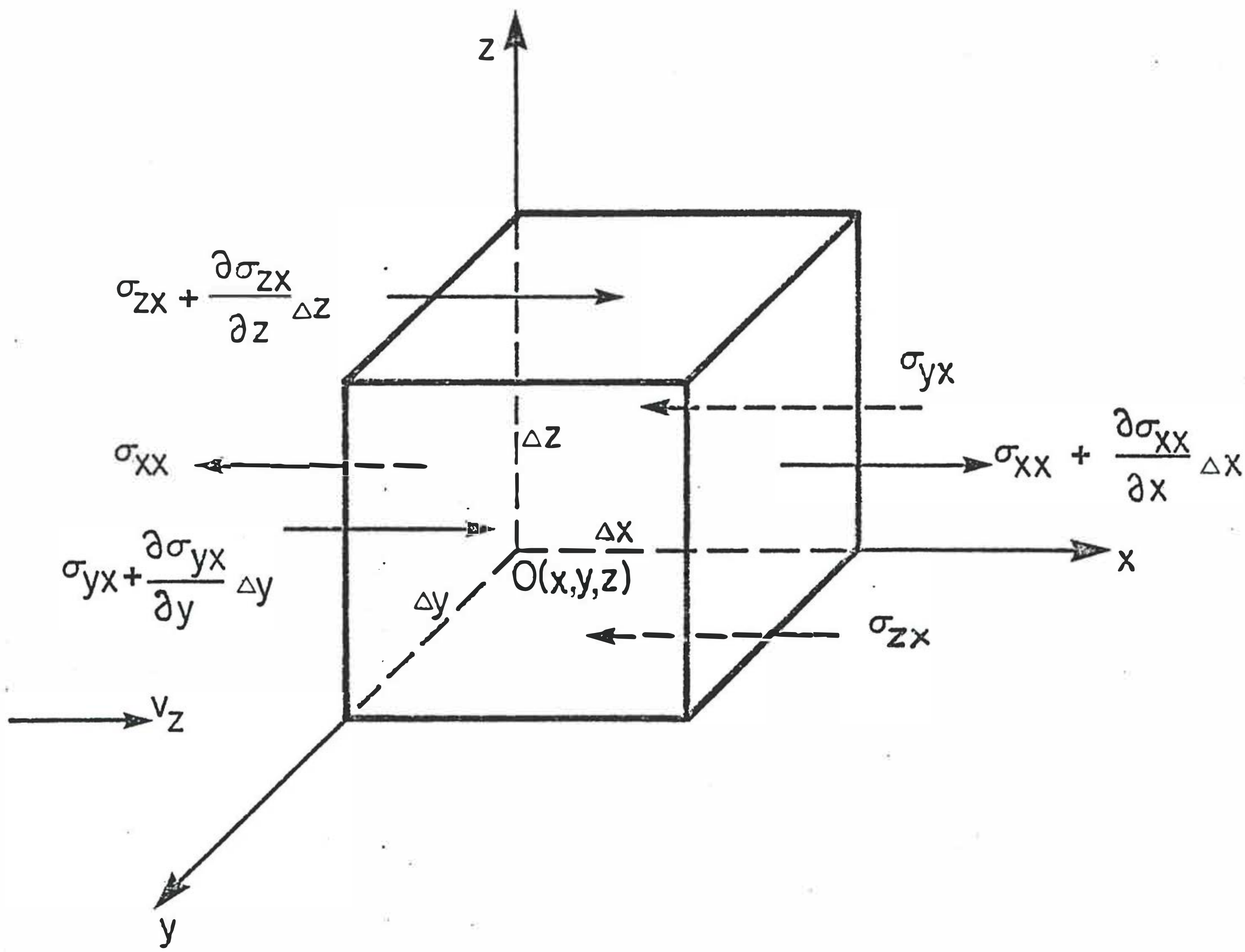

Fig. 6.6 Total stress components acting in the x direction

$$(ACCUM)_x = \Delta x\ \Delta y\ \Delta z \frac{\partial (\rho\ v_x)}{\partial t} \tag{6.67}$$

The rate at which the x component of momentum enters the volume through the plane area perpendicular to coordinate x at point x, y z is

$$(x\text{-MOM})_x = (\dot{m}_x\ v_x) \tag{6.68}$$

where $\dot{m}_x$ is the rate of mass entering this area, $\dot{m}_x = \rho v_x\ \Delta y\ \Delta z$, thus

$$(x\text{-MOM})_x = (\rho v_x\ v_x)\ \Delta y\ \Delta z \tag{6.69}$$

The rate of which the x component of momentum leaves the volume through the plane area perpendicular to x at point x + Δx, y, z is

$$(x\text{-MOM})_{x+\Delta x} = (\rho v_x\ v_x)_{x+\Delta x}\ \Delta y\ \Delta z \tag{6.70}$$

Thus, using Taylor's expansion formula, we get

$$(x\text{-MOM})_x - (x\text{-MOM})_{x+\Delta x} = -\frac{\partial}{\partial x}(\rho v_x\ v_x)\ \Delta x\ \Delta y\ \Delta z \tag{6.71}$$

The rate at which the x component of momentum enters the volume through the plane area perpendicular to coordinate y at point x, y, z is

$$(x\text{-MOM})_y = (\dot{m}_y\ v_x) = (\rho v_y\ \Delta x\ \Delta z\ v_x) \tag{6.72}$$

The rate at which it leaves the plane area perpendicular to coordinate y at point x, y+Δy, z is

$$(x\text{-MOM})_{y+\Delta y} = (\rho v_y\ \Delta x\ \Delta z\ v_x)_{y+\Delta y} \tag{6.73}$$

Thus

rate: $$(x\text{-MOM})_y - (x\text{-MOM})_{y+\Delta y} = -\frac{\partial}{\partial y}(\rho v_y\ v_x)\ \Delta x\ \Delta y\ \Delta z \tag{6.74}$$

Similarly

rate: $$(x\text{-MOM})_z - (x\text{-MOM})_{z+\Delta z} = -\frac{\partial}{\partial z}(\rho v_z\ v_x)\ \Delta x\ \Delta y\ \Delta z \tag{6.75}$$

Consequently the rate of momentum <u>in</u> minus the rate of momentum <u>out</u> in the x direction is

rate: $$(x\text{-MOM})_{in} - (x\text{-MOM})_{out} = -\left[\frac{\partial}{\partial x}(\rho v_x v_x) + \frac{\partial}{\partial y}(\rho v_y v_x) + \frac{\partial}{\partial z}(\rho v_z v_x)\right]\Delta x \Delta y \Delta z \tag{6.76}$$

The net normal force on the fluid in the control volume can be obtained by referring to Fig. 6.6.

$$(\text{Net normal force in x direction}) = (\sigma_{xx} + \frac{\partial \sigma_{xx}}{\partial x} \Delta x)\, \Delta y\, \Delta z - \sigma_{xx}\, \Delta y\, \Delta z$$

$$= \frac{\partial \sigma_{xx}}{\partial x} \Delta x\, \Delta y\, \Delta z \qquad (6.77)$$

The net shear force on the fluid in the control volume is

$$(\text{Net shear force in the x direction}) = (\sigma_{yx} + \frac{\partial \sigma_{yx}}{\partial y} \Delta y)\, \Delta x\, \Delta z - \sigma_{yx}\, \Delta x\, \Delta z$$

$$+ (\sigma_{zx} + \frac{\partial \sigma_{zx}}{\partial z} \Delta z)\, \Delta x\, \Delta y - \sigma_{zx}\, \Delta x\, \Delta y$$

$$= \frac{\partial \sigma_{yx}}{\partial y} \Delta x\, \Delta y\, \Delta z + \frac{\partial \sigma_{zx}}{\partial z} \Delta x\, \Delta y\, \Delta z \qquad (6.78)$$

Thus, the sum of surface forces on the fluid is

$$(\text{Sum of surface forces in x direction}) = (\frac{\partial \sigma_{xx}}{\partial x} + \frac{\partial \sigma_{yx}}{\partial y} + \frac{\partial \sigma_{zx}}{\partial z})\, \Delta x\, \Delta y\, \Delta z \qquad (6.79)$$

The gravitational force exerted on the fluid in the x direction is

$$(\text{gravitational force in x direction}) = \rho g_x\, \Delta x\, \Delta y\, \Delta z \qquad (6.80)$$

Finally, by substituting the various terms in the verbal statement of momentum balance (equation (6.2)) in the x direction, and by eliminating $\Delta x\ \Delta y\ \Delta z$, we have

$$\frac{\partial(\rho v_x)}{\partial t} = -\left[\frac{\partial}{\partial x}(\rho v_x v_x) + \frac{\partial}{\partial y}(\rho v_y v_x) + \frac{\partial}{\partial z}(\rho v_z v_x)\right]$$

$$+ (\frac{\partial \sigma_{xx}}{\partial x} + \frac{\partial \sigma_{yx}}{\partial y} + \frac{\partial \sigma_{zx}}{\partial z}) + \rho g_x \qquad (6.81)$$

or

$$\rho \frac{\partial v_x}{\partial t} + v_x \frac{\partial \rho}{\partial t} + v_x \frac{\partial}{\partial x}(\rho v_x) + \rho v_x \frac{\partial v_x}{\partial x} + v_x \frac{\partial}{\partial y}(\rho v_y) + \rho v_y \frac{\partial v_x}{\partial y}$$

$$+ v_x \frac{\partial}{\partial z}(\rho v_z) + \rho v_z \frac{\partial v_x}{\partial z}$$

$$= (\frac{\partial \sigma_{xx}}{\partial x} + \frac{\partial \sigma_{yx}}{\partial y} + \frac{\partial \sigma_{zx}}{\partial z}) + \rho g_x \qquad (6.82)$$

by grouping various terms we obtain

$$\rho\left(\frac{\partial v_x}{\partial t} + v_x \frac{\partial v_x}{\partial x} + v_y \frac{\partial v_x}{\partial y} + v_z \frac{\partial v_z}{\partial z}\right) + v_x \left[\frac{\partial \rho}{\partial t} + \frac{\partial}{\partial x}(\rho v_x) + \frac{\partial}{\partial y}(\rho v_y) + \frac{\partial}{\partial z}(\rho v_z)\right]$$

$$= \left(\frac{\partial \sigma_{xx}}{\partial x} + \frac{\partial \sigma_{yx}}{\partial y} + \frac{\partial \sigma_{zx}}{\partial z}\right) + \rho g_x \qquad (6.83)$$

The second term on the left-hand side (in brackets) represents the continuity equation (multiplied by v_x)

$$\frac{\partial \rho}{\partial t} + \frac{\partial}{\partial x}(\rho v_x) + \frac{\partial}{\partial y}(\rho v_y) + \frac{\partial}{\partial z}(\rho v_z) = 0 \qquad (6.84)$$

Thus, the x component of the momentum equation becomes

$$\rho\left(\frac{\partial v_x}{\partial t} + v_x \frac{\partial v_x}{\partial x} + v_y \frac{\partial v_x}{\partial y} + v_z \frac{\partial v_x}{\partial z}\right) = \left(\frac{\partial \sigma_{xx}}{\partial x} + \frac{\partial \sigma_{yx}}{\partial y} + \frac{\partial \sigma_{zx}}{\partial z}\right) + \rho g_x \qquad (6.85)$$

Similarly, we may derive the corresponding differential momentum equations in the y and z directions. Further, by introducing the relation between the total stress and pressure

$$\bar{\bar{\sigma}} = -p\bar{\bar{\delta}} + \bar{\bar{\tau}} \qquad (6.86)$$

We can obtain the three components of the stress form of the equation of momentum of the previous section (i.e. equations (6.63), (6.64), and (6.65)).

6.5 NAVIER-STOKES EQUATIONS

The stress form of the differential momentum equation contains the stress tensor σ. As shown in the chapter on constitutive equations for a Newtonian fluid we have

$$\bar{\bar{\sigma}} = -p\bar{\bar{\delta}} + \bar{\bar{\tau}}$$

$$= -p\delta_{ij} + \tau_{ij} \qquad (6.87)$$

where

$$\tau_{ij} = \mu\left[\left(\frac{\partial v_i}{\partial x_j}\right) + \left(\frac{\partial v_j}{\partial x_i}\right) - \frac{2}{3}\delta_{ij}\left(\frac{\partial v_k}{\partial x_k}\right)\right] \qquad (6.88)$$

or in Cartesian components

$$\tau_{xx} = \mu\ [2\ \frac{\partial v_x}{\partial x} - \frac{2}{3}\ (\nabla \cdot \bar{V})]$$

$$\tau_{yy} = \mu\ [2\ \frac{\partial v_y}{\partial y} - \frac{2}{3}\ (\nabla \cdot \bar{V})]$$

$$\tau_{zz} = \mu\ [2\ \frac{\partial v_z}{\partial z} - \frac{2}{3}\ (\nabla \cdot \bar{V})] \tag{6.89}$$

$$\tau_{xy} = \tau_{yx} = \mu\ [\frac{\partial v_x}{\partial y} + \frac{\partial v_y}{\partial x}]$$

$$\tau_{yz} = \tau_{zy} = \mu\ [\frac{\partial v_y}{\partial z} + \frac{\partial v_z}{\partial y}]$$

$$\tau_{xz} = \tau_{zx} = \mu\ [\frac{\partial v_x}{\partial z} + \frac{\partial v_z}{\partial x}]$$

where

$$\nabla \cdot \bar{V} = \frac{\partial v_x}{\partial x} + \frac{\partial v_y}{\partial y} + \frac{\partial v_z}{\partial z}$$

Substitution of the Cartesian components of the deviatoric stress tensor into equations (6.63), (6.64) and (6.65) gives

$$\rho(\frac{\partial v_x}{\partial t} + v_x\ \frac{\partial v_x}{\partial x} + v_y\ \frac{\partial v_x}{\partial y} + v_z\ \frac{\partial v_x}{\partial z}) = -\ \frac{\partial p}{\partial x} + \mu\ (\frac{\partial^2 v_x}{\partial x^2} + \frac{\partial^2 v_x}{\partial y^2} + \frac{\partial^2 v_x}{\partial z^2})$$

$$+ \frac{1}{3}\ \mu\ \frac{\partial}{\partial x}\ (\nabla \cdot \bar{V}) + \rho g_x \tag{6.90}$$

$$\rho(\frac{\partial v_y}{\partial t} + v_x\ \frac{\partial v_y}{\partial x} + v_y\ \frac{\partial v_y}{\partial y} + v_z\ \frac{\partial v_y}{\partial z}) = -\ \frac{\partial p}{\partial y} + \mu\ (\frac{\partial^2 v_y}{\partial x^2} + \frac{\partial^2 v_y}{\partial y^2} + \frac{\partial^2 v_y}{\partial z^2})$$

$$+ \frac{1}{3}\ \mu\ \frac{\partial}{\partial y}\ (\nabla \cdot \bar{V}) + \rho g_y \tag{6.91}$$

$$\rho(\frac{\partial v_z}{\partial t} + v_x\ \frac{\partial v_z}{\partial x} + v_y\ \frac{\partial v_z}{\partial y} + v_z\ \frac{\partial v_z}{\partial z}) = -\ \frac{\partial p}{\partial z} + \mu\ (\frac{\partial^2 v_z}{\partial x^2} + \frac{\partial^2 v_z}{\partial y^2} + \frac{\partial^2 v_z}{\partial z^2})$$

$$+ \frac{1}{3}\ \mu\ \frac{\partial}{\partial z}\ (\nabla \cdot \bar{V}) + \rho g_z \tag{6.92}$$

These equations can be written in Cartesian index notation as

$$\rho\left(\frac{\partial v_j}{\partial t} + v_i \frac{\partial v_j}{\partial x_i}\right) = -\frac{\partial p}{\partial x_j} + \mu \frac{\partial^2 v_j}{\partial x_i^2} + \frac{1}{3}\mu \frac{\partial}{\partial x_j}\left(\frac{\partial v_k}{\partial x_k}\right) + \rho g_j \qquad (6.93)$$

or in symbolic vector notation as

$$\rho\left(\frac{\partial \bar{V}}{\partial t} + \bar{V} \cdot \nabla\bar{V}\right) = -\nabla p + \mu \nabla^2 \bar{V} + \frac{1}{3}\mu \nabla(\nabla \cdot \bar{V}) + \rho\bar{g} \qquad (6.94)$$

Equations (6.90), (6.91) and (6.92) or their equivalent shorthand forms (6.93) and (6.94) are known as the Navier-Stokes equations [3,4]. They were first derived for incompressible fluids (i.e. $\nabla \cdot \bar{V} = 0$) by the French engineer Navier in 1822 using molecular arguments and generalized by the British physicist and mathematician Stokes in 1845.

A restricted form of the Navier-Stokes equation for $\mu = 0$ is the Euler equation

$$\rho\left(\frac{\partial \bar{V}}{\partial t} + \bar{V} \cdot \nabla\bar{V}\right) = -\nabla p + \rho\bar{g} \qquad (6.95)$$

which was derived by the German mathematician Euler in 1755.

In the absence of fluid motion $\bar{V} = 0$, this equation further reduces to

$$0 = -\nabla p + \rho\bar{g} \qquad (6.96)$$

or in Cartesian component form

$$\frac{\partial p}{\partial x} = \rho g_x$$

$$\frac{\partial p}{\partial y} = \rho g_y \qquad (6.97)$$

$$\frac{\partial p}{\partial z} = \rho g_z$$

For z pointing in the vertical direction (upward)

$$g_x = g_y = 0 \quad g_z = -g \text{ (earth's gravitational constant)}$$

Thus

$$\frac{\partial p}{\partial x} = 0$$

$$\frac{\partial p}{\partial y} = 0 \qquad (6.98)$$

$$\frac{\partial p}{\partial z} + \rho g = 0$$

These are the equations of fluid statics which were derived by applying the principle at static equilibrium in Chapter 2.

The Navier-Stokes equations in cylindrical and spherical coordinates are given in Appendix D.

6.6 FLUID STATICS REVISITED—UNIFORM LINEAR ACCELERATION

In the absence of relative fluid motion there are no stresses in a fluid. Therefore, Euler's equation applies

$$\rho\left(\frac{\partial \bar{V}}{\partial t} + \bar{V} \cdot \nabla \bar{V}\right) = -\nabla p + \rho \bar{g} \tag{6.99}$$

As discussed in Chapter 3 the linear acceleration of a fluid particle is given by

$$\bar{a} = \frac{\partial \bar{V}}{\partial t} + \bar{V} \cdot \nabla \bar{V} \tag{6.100}$$

Thus

$$\rho \bar{a} = -\nabla p + \rho \bar{g} \tag{6.101}$$

and

$$\nabla p = \rho(\bar{g} - \bar{a}) \tag{6.102}$$

Let z be the vertical axis and assume that the fluid mass is accelerated uniformly (constant magnitude and direction) in the z-x plane as shown in Fig. 6.7. We would have $g_z = -g$, $g_x = g_y = 0$ and $a_y = 0$.

Thus, the pressure gradient components in x and z directions are

$$\frac{\partial p}{\partial x} = -\rho a_x \tag{6.103}$$

$$\frac{\partial p}{\partial z} = -\rho (g + a_z) \tag{6.104}$$

The total differential of the pressure is

$$dp = \frac{\partial p}{\partial x} dx + \frac{\partial p}{\partial z} dz \tag{6.105}$$

or

$$dp = -\rho a_x dx - \rho (g + a_z) dz \tag{6.106}$$

Integrating, we get

$$p(x,z) = -\rho a_x x - \rho (g + a_z) z + \text{const.} \tag{6.107}$$

If $p = p_o$ at (x_o, z_o)

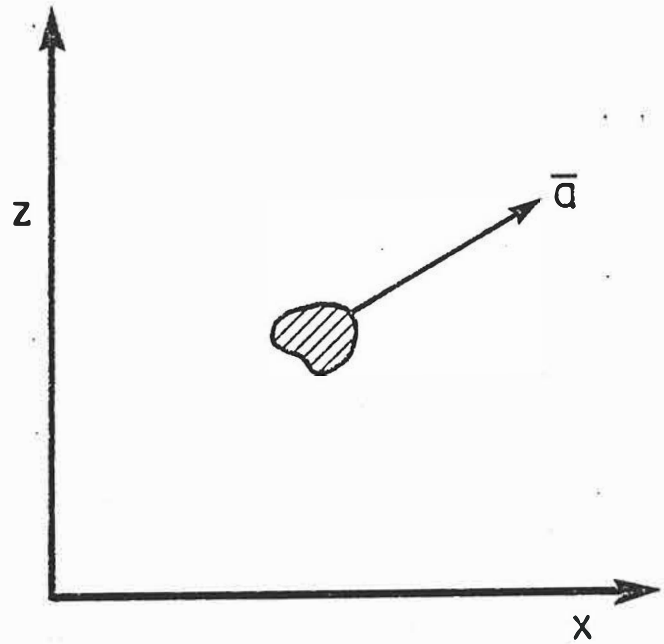

Fig. 6.7 Uniformly accelerated fluid mass

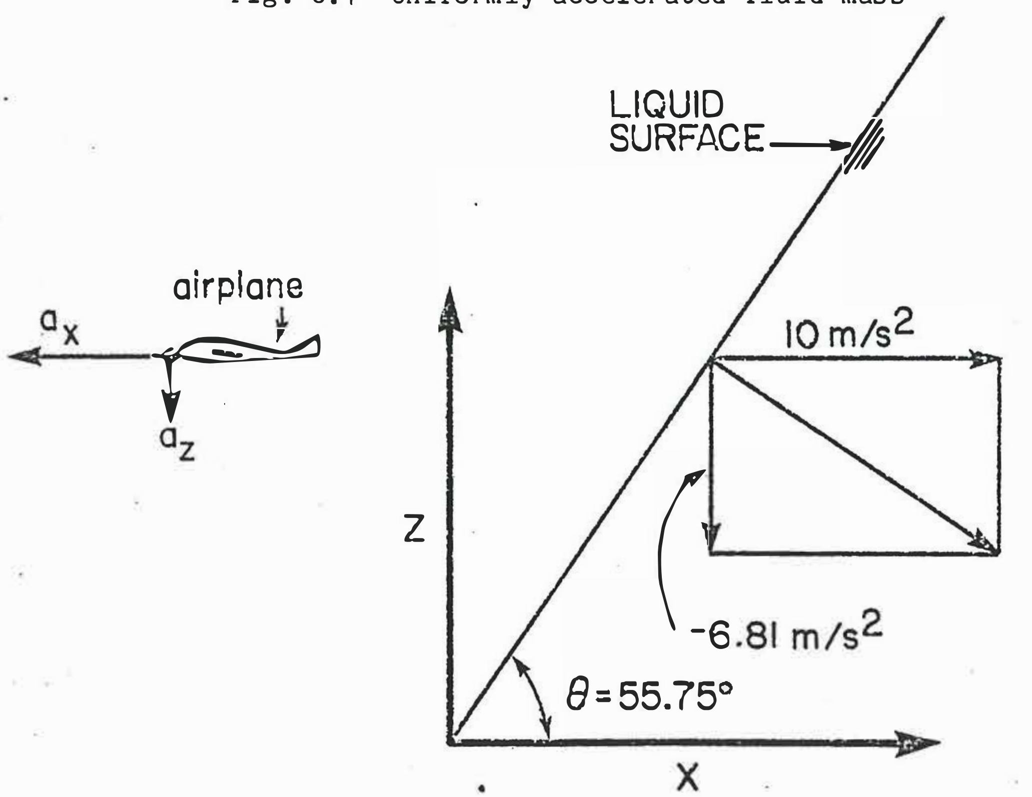

Fig. 6.8

$$p = p_o - \rho\, a_x\,(x - x_o) - \rho\,(g + a_z)\,(z - z_o) \qquad (6.108)$$

Surfaces of contant pressure (e.g. the free surface) are determined by setting p = const. or dp = 0

$$- \rho\, a_x\, dx - \rho\,(g + a_z)\, dz = 0 \qquad (6.109)$$

Solving for the slope

$$\left(\frac{dz}{dx}\right)_{p=const} = - \frac{a_x}{a_z+g} \qquad (6.110)$$

where x is horizontal, z vertically upward and $g = +9.81\ m/s^2$.

Example 6.4

An airplane is travelling downward with acceleration components $a_x = -10\ m/s^2$ and $a_z = -3\ m/s^2$. The fuel tank is partly filled with gasoline S.G. = 0.75 to a height of 20 cm. (a) Determine the pressure at the bottom of the fuel tank before and during the downward travel; (b) Determine the slope of the free surface of gasoline in the tank.

(a) The pressure on the bottom of the fuel tank before the downward travel is

$$p = \rho g h = 0.75 \times 1000\ \frac{kg}{m^3} \times 9.81\ \frac{m}{s^2} \times 0.20\ m = 1471.50\ N/m^2$$

During the downward travel it is

$$p = - \rho\,(a_z+g)\,(0-h) = 0.75 \times 1000\ \frac{kg}{m^2} \times (-3\ \frac{m}{s^2} + 9.81\ \frac{m}{s^2}) \times 0.20\ m$$

$$= 1021.50\ N/m^2$$

(b) The slope of the free surface is

$$\frac{dz}{dx} = - \frac{-10}{-3 + 9.81} = + \frac{10}{6.81}$$

$$\theta = 55.75^o$$

The results are shown schematically in Fig. 6.8. Note that the body force from the acceleration acts in a direction opposite to the acceleration. The free liquid surface is perpendicular to the effective body force.

6.7 THE ANGULAR MOMENTUM BALANCE

Newton's second law for a particle of infinesimal mass m can be written as

$$\Sigma \bar{F} = \frac{d}{dt} (m\bar{V}) \tag{6.111}$$

We take the cross product of $\bar{r}$ on each side of the above equation, where $\bar{r}$ is the position vector to the particle as shown in Fig. 6.9. We have

$$\bar{r} \times (\Sigma \bar{F}) = r \times \frac{d}{dt} (m\bar{V}) \tag{6.112}$$

Using the product rule of vector analysis

$$\frac{d}{dt} (\bar{r} \times m\bar{V}) = \frac{d\bar{r}}{dt} \times (m\bar{V}) + \bar{r} \times \frac{d}{dt} (m\bar{V}) \tag{6.113}$$

where $d\bar{r}/dt = \bar{V}$ and therefore the first term on the right hand side is zero (since $\bar{V} \times \bar{V} = 0$).

Thus, equation (6.113) may be written as

$$\bar{r} \times (\Sigma \bar{F}) = \frac{d}{dt} (\bar{r} \times m\bar{V}) \tag{6.114}$$

The left-hand side is the moment of the sum of forces acting on the particle about the origin (i.e. torques). Thus, this equation states that the moment of the sum of forces on the system is equal to the time-rate-of-change of moment of momentum.

The moment of momentum balance for a control volume may be written in the form

$$\begin{matrix} \text{RATE OF MOMENT} & & \text{RATE OF MOMENT} & & \text{RATE OF MOMENT} & & \text{SUM OF TORQUES} \\ \text{OF MOMENTUM} & = & \text{OF MOMENTUM} & - & \text{OF MOMENTUM} & + & \text{ON CONTROL} \\ \text{ACCUMULATION} & & \text{IN} & & \text{OUT} & & \text{VOLUME} \end{matrix} \tag{6.115}$$

or mathematically

$$\frac{d}{dt} (\bar{r} \times m\bar{V}) = (r \times \bar{V})_{in} \dot{m}_{in} - (\bar{r} \times \bar{V})_{out} \dot{m}_{out} + \Sigma \bar{T}_o \tag{6.116}$$

This equation can then be easily generalized (in a manner analogous to the one for momentum in section 6.3) as

$$\frac{\partial}{\partial t} \iiint_{\forall} \rho (\bar{r} \times \bar{V}) \, d\forall + \iint_{S} (\bar{r} \times \bar{V}) (\rho\bar{V} \cdot \bar{n}) \, dS = \Sigma \bar{T}_o \tag{6.117}$$

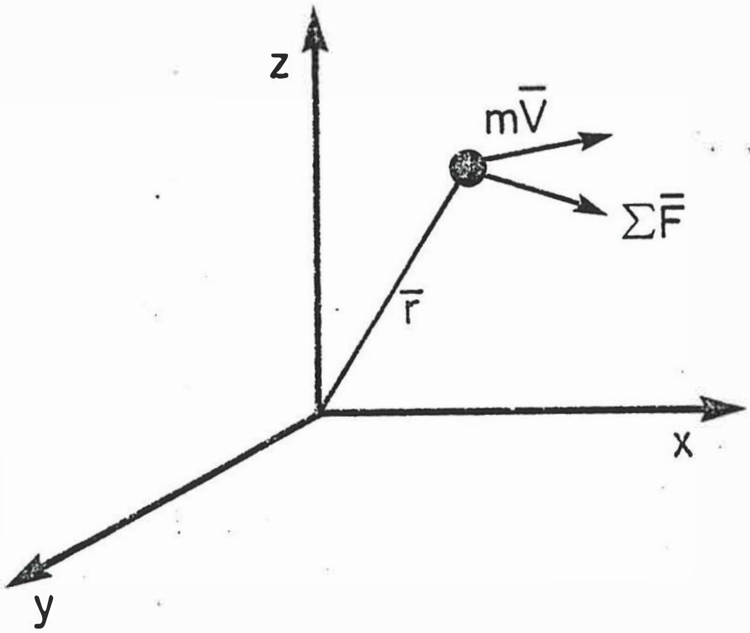

Fig. 6.9 Fluid particle in motion

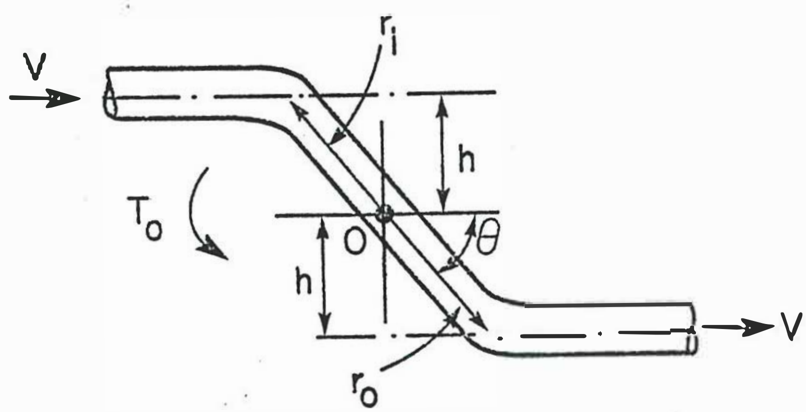

Fig. 6.10

This equation is often referred to as the moment of momentum equation or angular momentum equation. It is used extensively in the analysis of rotating fluid machines, such as turbines and pumps [5,6].

In most applications the moment is taken about an axis rather than a point. If this axis is the z-axis in cylindrical coordinates then the magnitude of the cross product $\bar{r} \times \bar{V}$ is equal to $r\ v_\theta$ where r is the distance from the z-axis to the fluid particle and v_θ its tangential component of velocity. In steady flow through turbomachines the left hand side of equation (6.116) is zero, therefore the magnitude of the torque is given by

$$T_o = |\bar{T}_o| = \dot{m}\,[(r\ v_\theta)_{out} - (r\ v_\theta)_{in}] \tag{6.118}$$

This expression is known as Euler's turbine equation.

Example 6.5

A pipe bend connects two straight pipe sections as shown in Fig. 6.10 V is the steady flow velocity which is assumed uniform over the cross-sectional area $A = \pi D^2/4$ and ρ the fluid density. Determine the torque which must be applied by a support at point O to prevent rotation.

Solution

We choose a control volume as shown by the broken line. Applying equation (6.116) for steady flow, we have

$$\bar{T}_o = (\bar{r} \times \bar{V})_{out}\ \dot{m}_{out} - (\bar{r} \times \bar{V})_{in}\ \dot{m}_{in}$$

$$\dot{m}_{in} = \dot{m}_{out} = \rho\ AV = \rho V\ \frac{\pi D^2}{4}$$

Since $\bar{r}_i = -\bar{r}_o$

$$(\bar{r} \times \bar{V})_{out} = (\bar{r}_o \times \bar{V})$$

and $(\bar{r} \times \bar{V})_{in} = (\bar{r}_i \times \bar{V}) = -(\bar{r}_o \times \bar{V})$

Thus $\bar{T}_o = 2\ \rho\ A\ V\ (\bar{r}_o \times \bar{V})$

where

$$|\bar{r}_o \times \bar{V}| = (r_o \sin \theta) V = hV$$

Therefore, the magnitude of the torque which must be applied (counter-clockwise) to prevent rotation is

$$T_o = 2 \rho A h V^2 = 2\rho (\frac{\pi D^2}{4}) h V^2$$

Example 6.6

The impeller of a centrifugal water pump rotates at 1800 rpm (revolutions per minute). The water flows into the central inlet as shown in Fig. 6.11, is spun outward and flows out at the periphery of the blades. The inlet pipe has a diameter of 5 cm and the blades a diameter of 50 cm. The water rate of flow is 1 m^3/min. Determine the torque exerted by the rotating shaft.

Solution

It is reasonable to assume that the tangential velocity of the water as it enters and leaves the pump are equal to the tangential velocity of the impeller at the corresponding radii. Therefore, we have:

$$(V_\theta)_{in} = r_{in} \omega = r_{in} (2\pi r) N$$

$$(V_\theta)_{out} = r_{out} \omega = r_{out} (2\pi r) N$$

$\dot{m} = \dot{m}_{in} = \dot{m}_{out} = 1000$ kg/min

$$T_o = \dot{m} [(r V_\theta)_{out} - (r V_\theta)_{in}]$$

$$= \dot{m} (2\pi N) [r^2_{out} - r^2_{in}]$$

$$= \frac{1000 \text{ kg}}{60 \text{ s}} \times (2\pi \times \frac{1800}{60} \frac{1}{s}) \times [0.25^2 \text{ m}^2 - 0.025 \text{ m}^2]$$

$$= 194.29 \text{ N·m}$$

This is the net torque exerted by the impeller shaft on the water flowing through the pump.

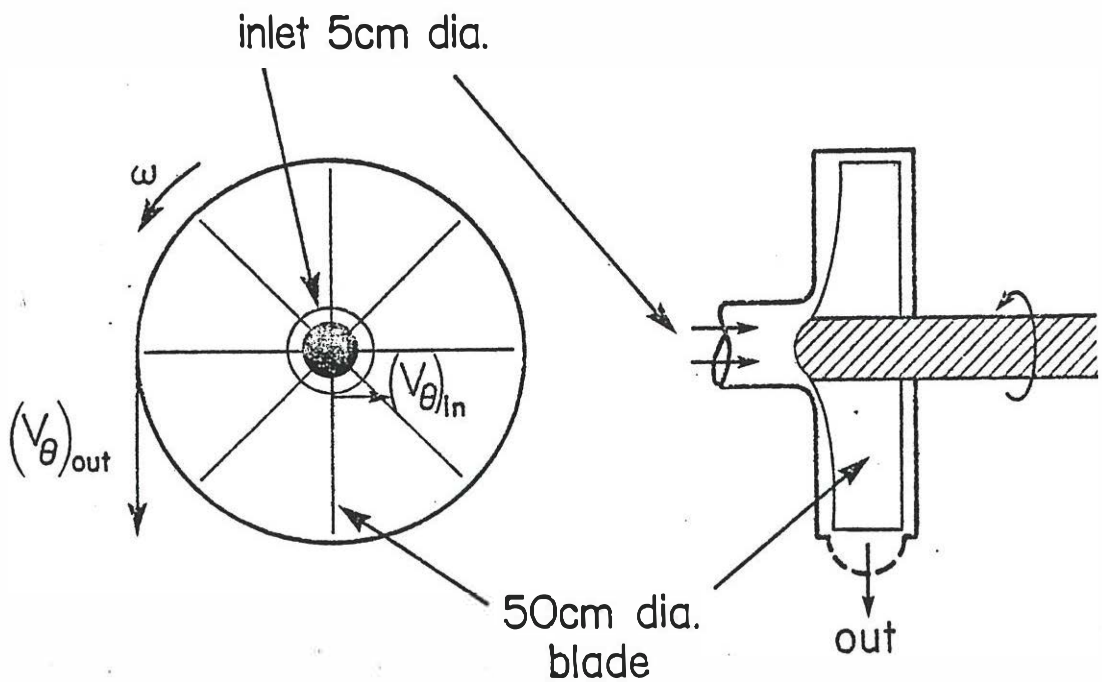

Fig. 6.11

6.8 DIMENSIONLESS GROUPS

The principle of conservation of momentum led to the development of the Navier-Stokes equations for Newtonian fluids. It is helpful in the study of fluid motion to explain the physical significance of the various terms as they appear in these equations. To simplify the discussion we will use the steady state form of the x component of the equation of conservation of momentum for an incompressible Newtonian fluid:

$$v_x \frac{\partial v_x}{\partial x} + v_y \frac{\partial v_x}{\partial y} + v_z \frac{\partial v_x}{\partial z} = -\frac{1}{\rho}\frac{\partial p}{\partial x} + \frac{\mu}{\rho}\left(\frac{\partial^2 v_x}{\partial x^2} + \frac{\partial^2 v_x}{\partial y^2} + \frac{\partial^2 v_x}{\partial z^2}\right) + g_x$$

Let us now introduce the following notation: [M] = Mass, [L] = Length [T] = Time. Therefore, we will have Force F = $[MLT^{-2}]$, Velocity V = $[LT^{-1}]$, Area = $[L^2]$, Volume = $[L^3]$, Pressure p = $[FL^{-2}]$. We note that:

(a) The left-hand side term $v_x\, \partial v_x/\partial x + v_y\, \partial v_x/\partial y + v_z\, \partial v_x/\partial z$ has dimensions $[L^2T^{-2}]/L = [LT^{-2}]$ which can be interpreted as force/mass = $[LT^{-2}]$ and can be approximated by V^2/L where V is a characteristic velocity and L is a characteristic length. This term represents the forces (per unit mass) due to the velocity of the fluid i.e. the inertia forces.

(b) The term $1/\rho\, \partial p/\partial x$ has dimensions $1/[ML^{-3}] \cdot [FL^{-2}]/[L] = [F]/[M] = [LT^{-2}]$ and can be approximated by $p/\rho L$. It expresses the force (per unit mass) due to the pressure.

(c) from the definition of viscosity (Chapter 1) we have $\tau = \mu\, \partial v_x/\partial y$ which means that the viscosity has dimensions $\mu \Rightarrow [FL^{-2}/T^{-1}] = [FL^{-2}T]$. The term $\mu/\rho\, (\partial^2 u_x/\partial x^2 + \partial^2 u_x/\partial y^2 + \partial^2 u_x/\partial z^2)$ has dimensions $[FL^{-2}T]/[ML^{-3}] \cdot [LT^{-1}]/[L^2] = [F]/[M] = [LT^{-2}]$, and represents the force (per unit mass) due to the viscosity of the fluid. An approximate estimate will be $\mu V/\rho L^2$.

(d) The term g_x has dimensions $[LT^{-2}]$ and represents the force (per unit mass) due to gravity ($g_x = g \cos\theta$, where θ is the angle between x and the vertical).

We now establish the following force ratios:

$$\frac{\text{INERTIA FORCES}}{\text{VISCOUS FORCES}} = \frac{V^2/L}{\mu V/\rho L^2} = \frac{\rho V L}{\mu} = \text{Re} \quad \text{(Reynolds Number)}$$

$$\frac{\text{INERTIA FORCES}}{\text{GRAVITY FORCES}} = \frac{V^2/L}{g} = \frac{V^2}{gL} = \text{Fr} \quad \text{(Froude Number)}$$

$$\frac{\text{PRESSURE FORCES}}{\text{INERTIA FORCES}} = \frac{p/\rho L}{V^2/L} = \frac{p}{\rho V^2} = \text{Eu} \quad \text{(Euler Number)}$$

Of these three dimensionless groups the Reynolds number is the most significant because it is involved in virtually all types of flow problems. We noted in Chapter 1 that for flow inside a tube the Reynolds number (with $L = D$ tube diameter, $V = V_{avg}$) $Re = \rho\, V_{avg}\, D/\mu$ is used as the criterion for the transition from laminar to turbulent flow ($Re > 2100$). An elementary explanation of this flow instability can be given in terms of force ratio established above. When the inertia forces (which tend to disperse the fluid) become 2100 times larger than the viscous forces (which are cohesive) the flow becomes highly irregular and it is called turbulent. The Froude number is important in gravity driven flows especially those in open channels. The Euler number merely represents a dimensionless form of pressure. It is rarely important except for flow problems involving pressure drops low enough to cause vapor formation in liquids (see Cavitation, Chapter 12). We will see some more dimensionless groups in other parts at this book.

We now define the following dimensionless variables

$$\begin{aligned} x^* &= x/L \\ y^* &= y/L \\ z^* &= z/L \\ v^* &= v/V \\ p^* &= \text{Eu} = p/\rho V^2 \\ g_x^* &= \frac{g_x}{V^2/L} = \frac{g}{V^2/L}\cos\theta = \frac{1}{\text{Fr}}\cos\theta \\ t^* &= tV/L \end{aligned} \tag{6.120}$$

The x-component of the equation of conservation of momentum becomes

$$\frac{\partial v_x^*}{\partial t^*} + v_x^* \frac{\partial v_x^*}{\partial x^*} + v_y \frac{\partial v_x^*}{\partial y^*} + v_z^* \frac{\partial v_x^*}{\partial z} = - \frac{\partial p^*}{\partial x^*} + \frac{1}{Re} \left(\frac{\partial^2 v_x^*}{\partial x^{*2}} + \frac{\partial^2 v_x^*}{\partial y^{*2}} + \frac{\partial^2 v_x^*}{\partial z^2} \right) + g_x^* \quad (6.121)$$

This dimensionless form is often useful in assessing the relative magnitude of the various terms. For example when $Re << 1$ the flow is dominated by viscous effects whereas the inertia effects are negligible. When $Re >> 1$ the visous effects are not important except in the immediate vicinity of solid surfaces where large velocity gradients are present.

6.9 FLOW PROBLEMS AND THEIR SOLUTION

Generally speaking there are two types of flow problems: (a) Macroscopic and (b) Microscopic. The distinction is, to some extent, arbitrary, but it is helpful as a problem solving tool. In macroscopic problems we are mainly interested in overall effects, whereas in microscopic problems we are interested in the detailed structure of the flow field. To illustrate the difference we refer back to section 6.2.5 (stationary rocket on a test stand). The method of approach and the results as presented suggest a macroscopic problem. We simply determined the overall thrust produced by the exhaust gas jet. However, one might also wish to determine the velocity and pressure distribution in the jet itself and the structure at turbulence (if the jet happens to be turbulent). This is, then, a microscopic problem.

As pointed out by Denn [7] macroscopic problems generally require a great deal of intuition but the resulting mathematical models are simple. Somehow, we must identify the physical principles involved (continuity, momentum, etc.) and express them in the proper mathematical form. Such a procedure varies widely from one problem to another and does not always follow an identified rational approach.

The determination of the appropriate mathematical models (differential equations) for microscopic problems is usually accomplished by the systematic elimination of terms from the general conservation equations. For example, in analyzing a certain problem we may realize that the velocity does not vary in, say, the z direction and remains constant with time. Consequently, the corresponding terms may be eliminated from the general differential equations for conservation of mass and momentum. Even after the simplifications many of the resulting differential equations require the application of elaborate analytical and numerical methods. The limitations in problem solving are very often due to limitations in mathematical techniques rather than lack of mathematical models. However, it should not be misunderstood that problem solving is mainly mathematics with a little physics. On the contrary, it is the understanding of the physical principles and their application that leads to simplified mathematical equations which can be solved and which provide the required information.

The differential continuity equation (derived in Chapter 3) and the Navier-Stokes equations together represent a system of four, coupled, non-linear equations with four unknowns [the three velocity components (v_x, v_y, v_z) and either pressure (p) or density (ρ)]. Exact analytical solutions of the general equations are possible in a very limited number of cases. With the use of modern high speed computers solutions can be obtained for many practical problems. Very often, however, the computational cost is prohibitive or possibly the numerical procedure introduces artifacts that mask the essential features of the problem itself. It is nearly always necessary to introduce a number of approximations which will lead to acceptable solutions. It is often helpful to anticipate the form of "a reasonable solution" and then introduce the appropriate approximations to obtain the exact expressions. Anticipation in this context should always be based on sound physical reasoning. The student of fluid mechanics soon realizes that the setting up of the appropriate mathematical model and the solution itself are intertwined.

REFERENCES

[1] I.H. Shames, "Mechanics of Fluids", McGraw-Hill, New York (1962).

[2] W.M. Swanson, "Fluid Mechanics", Holt, Rinehart and Winston, New York (1970).

[3] J. Serrin, "Mathematical Principles of Classical Fluid Mechanics", Encyclopedia of Physics (Handbuch der Physik), Vol. 8, No. 1, Springer-Verlag, Berlin (1959).

[4] R.B. Bird, W.E. Stewart and E.N. Lightfoot, "Transport Phenomena", Wiley, New York (1960).

[5] D.G. Shepherd, "Principles of Turbomachinery", MacMillan, New York (1956).

[6] S.L. Dixon, "Fluid Mechanics of Turbomachinery", 2nd Ed., Pergamon, Oxford (1975).

[7] M.M. Denn, "Process Fluid Mechanics", Prentice-Hall, Englewood Cliffs, N.J. (1980).

CLAUDE-LOUIS NAVIER (1785-1836)

John Vlachopoulos, *Fundamentals of Fluid Mechanics*
Chem. Eng., McMaster University, Hamilton, ON, Canada
(First Edition 1984, revised internet edition (2016), www.polydynamics.com)

CHAPTER 7

UNIDIRECTIONAL LAMINAR VISCOUS FLOW

7.1 INTRODUCTION

All viscous flows are necessarily two- or three-dimensional because of the no-slip condition on solid boundaries. However, there is a large class of laminar flows which were called unidirectional in Chapter 3. In this class of flows, the fluid moves in one direction only, e.g. in the x-direction in rectangular coordinates or perhaps in the r- or θ-directions in curvilinear coordinates. The velocity varies as a function of one space coordinate only. The pressure may also vary as a function of one space coordinate (which may be the same or, more commonly, different than that of the velocity variation). This class of flows includes both steady and unsteady problems.

Most of the problems examined in this chapter can be termed as "classical" because they were the first ones historically to be solved exactly and now appear in nearly every textbook on fluid mechanics. Schlichting [1] and Bird et al [2] present several other problems of this type.

7.2 PRESSURE-DRIVEN FLOW BETWEEN TWO FLAT PLATES

We will consider steady laminar flow of an incompressible, Newtonian fluid between two horizontal parallel plates under the influence of a pressure gradient as shown in Fig. 7.1. The plates are

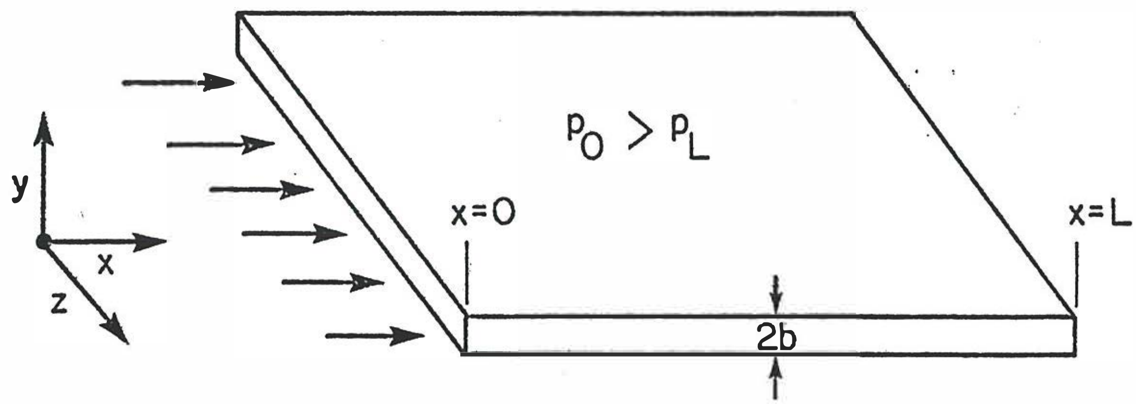

Fig. 7.1 Flow between two parallel plates. The width (in the z direction) is practically infinite and the gap (2b) is small.

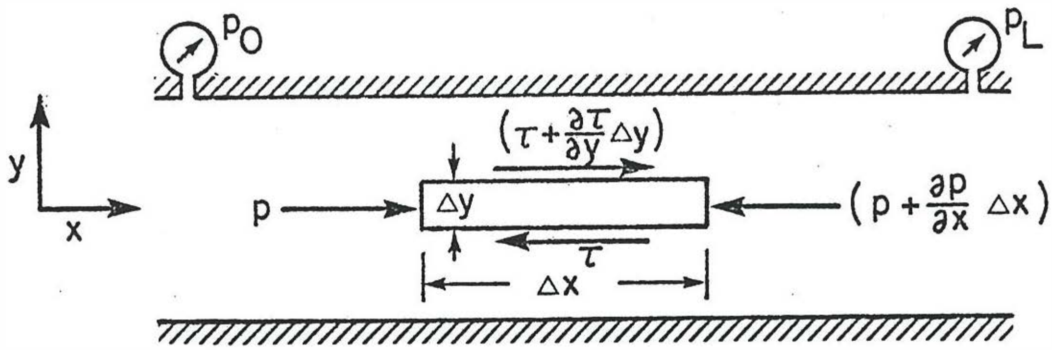

Fig. 7.2 Force balance for a differential volume element

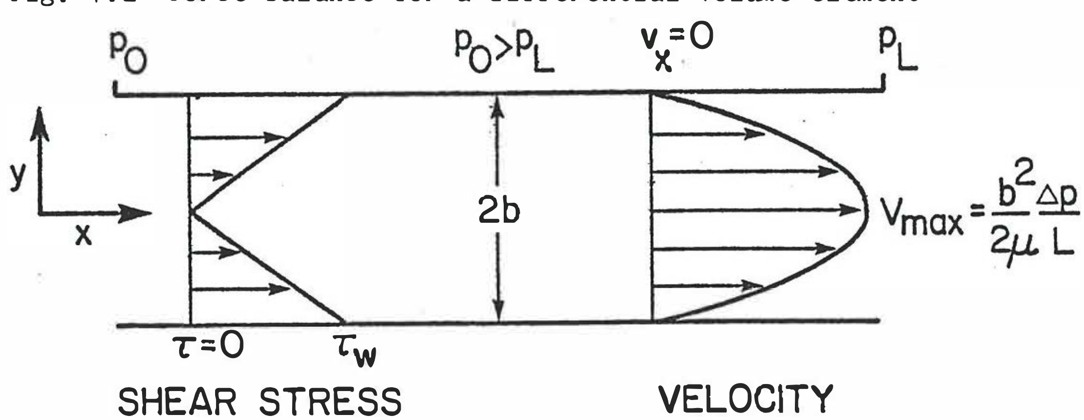

Fig. 7.3 Velocity and stress profiles for pressure-driven flow between two parallel plates.

sufficiently long so that the flow is fully developed which means that there are no velocity variations in the x direction. To derive the appropriate differential equation we may either perform a simple momentum balance for a differential element between the plates or simplify the general conservation equations (i.e. continuity and Navier-Stokes).

(a) Momentum balance for a volume element

From the description of the problem it is apparent that the pressure gradient causes the fluid to flow from left to right. The viscosity of the fluid exhibits resistance to flow which is manifested as a shear stress. There is no change of momentum in the x direction. Consequently, we must balance pressure forces against shear stress forces.

We have

$F_{Pressure}$ = [Pressure] × [Area (normal)]

F_{Shear} = [Shear stress] × [Area (tangential)]

For the differential element shown in Fig. 7.2 we note that

(a) The pressure is p on the left-hand side and by using Taylor's expansion we get $p + \frac{\partial p}{\partial x} \Delta x$ on the right-hand side.

(b) The stress is τ on the lower side and by using Taylor's expansion we get $\tau + \frac{\partial \tau}{\partial y} \Delta y$ on the upper side.

It is intuitively obvious that pressure forces and stress forces acting on opposite sides of the volume element should act in opposite directions.

We used a very definite sign convention in choosing the direction of the arrows. A positive stress acts in the positive x direction and on a surface facing the direction of increase of y. The pressure is a compressive normal stress and according to the sign convention of Chapter 5 it is negative.

A simple force balance gives

$$p\Delta y\Delta z - (p + \frac{\partial p}{\partial x}\Delta x)\,\Delta y\Delta z + (\tau + \frac{\partial \tau}{\partial y}\Delta y)\,\Delta x\Delta z - \tau\Delta x\Delta z = 0 \tag{7.1}$$

After eliminating certain terms and dividing by $\Delta x\Delta y\Delta z$, we get the differential equation

$$-\frac{\partial p}{\partial x} + \frac{\partial \tau}{\partial y} = 0 \tag{7.2}$$

For a Newtonian fluid

$$\tau = \mu \frac{\partial v_x}{\partial y} \tag{7.3}$$

Thus

$$-\frac{\partial p}{\partial x} + \frac{\partial}{\partial y}\left(\mu \frac{\partial v_x}{\partial y}\right) = 0 \tag{7.4}$$

or

$$\frac{\partial p}{\partial x} = \mu \frac{\partial^2 v_x}{\partial y^2} \tag{7.5}$$

We note that the left-hand side of the above equation is a function of x only. The right hand side is a function of y only. Since x and y are independent variables, we conclude that both sides must be equal to a constant, say K_1.

Thus we have

$$\frac{dp}{dx} = K_1 \quad \text{and} \quad \mu \frac{d^2 v_x}{dy^2} = K_1 \tag{7.6}$$

The boundary conditions for pressure are

$$\begin{aligned} x &= 0 \qquad p = p_o \\ x &= L \qquad p = p_L \end{aligned} \tag{7.7}$$

The general solution for pressure is

$$p = K_1x + K_2 \tag{7.8}$$

and

$$K_1 = \frac{dp}{dx} = -\frac{p_o - p_L}{L} = -\frac{\Delta p}{L} \tag{7.9}$$

where Δp represents the pressure drop ($p_o > p_L$)
The velocity profile will be determined from

$$\mu \frac{d^2 v_x}{dy^2} = \left(-\frac{\Delta p}{L}\right) \tag{7.10}$$

with the boundary conditions (no-slip at the walls)

$$\begin{array}{llll} \text{B.C.1} & v_x = 0 & \text{at} & y=b \\ \text{B.C.2} & v_x = 0 & \text{at} & y=-b \end{array} \tag{7.11}$$

A first integration gives

$$\frac{dv_x}{dy} = \frac{1}{\mu}\left(-\frac{\Delta p}{L}\right) y + C_1 \tag{7.12}$$

and a second integration

$$v_x = \frac{1}{2\mu}\left(-\frac{\Delta p}{L}\right) y^2 + C_1 y + C_2 \tag{7.13}$$

The constants of integration can be determined by applying the boundary conditions B.C.1 and B.C.2

$$\text{B.C.1: } 0 = \frac{1}{2\mu}\left(-\frac{\Delta p}{L}\right) b^2 + C_1 b + C_2 \tag{7.14}$$

$$\text{B.C.2: } 0 = \frac{1}{2\mu}\left(-\frac{\Delta p}{L}\right) b^2 - C_1 b + C_2 \tag{7.15}$$

Solving these two simultaneous equations for C_1 and C_2 we get

$$C_1 = 0 \tag{7.16}$$

$$C_2 = \frac{1}{2\mu} \left(\frac{\Delta p}{L}\right) b^2 \tag{7.17}$$

and the solution is expressed as

$$v_x = \frac{1}{2\mu} \left(\frac{\Delta p}{L}\right) (b^2 - y^2) \tag{7.18}$$

or

$$v_x = \frac{b^2}{2\mu} \left(\frac{\Delta p}{L}\right) \left[1 - \left(\frac{y}{b}\right)^2\right] \tag{7.19}$$

Thus, the velocity profile is parabolic with a maximum at the centerplane (y=0) as shown in Fig. 7.3. The maximum velocity is

$$V_{max} = \frac{b^2}{2\mu} \frac{\Delta p}{L} \tag{7.20}$$

and the velocity profile can be expressed as

$$v_x = V_{max} \left[1 - \left(\frac{y}{b}\right)^2\right] \tag{7.21}$$

The average velocity can be obtained by integrating the velocity over a cross-section (infinite in the z direction) and dividing by the cross-sectional area

$$V_{avg} = \frac{\iint v_x dA}{\iint dA} = \frac{\iint v_x dz dy}{\iint dz dy} = \frac{\int_{-b}^{b} v_x dy}{\int_{-b}^{b} dy} = \frac{2}{3} V_{max} \tag{7.22}$$

Note that the average velocity is equal to two-thirds the maximum velocity.

The shear stress profile can be calculated from the definition of shear stress $\tau = \mu \ (\partial v_x/\partial y)$ (i.e. by differentiating the velocity profile) or preferably from equation 7.2 which is written as

$$\frac{dp}{dx} = \frac{d\tau}{dy} \tag{7.23}$$

The pressure gradient was $\frac{dp}{dx} = -\frac{\Delta p}{L}$, thus

$$\frac{d\tau}{dy} = -\frac{\Delta p}{L} \tag{7.24}$$

$$\tau = -\frac{\Delta p}{L} y + C_1 \tag{7.25}$$

$$\text{Since } \tau = \mu \frac{\partial v_x}{\partial y} = 0 \text{ at } y = 0 \text{ (symmetry)} \tag{7.26}$$

$$C_1 = 0 \tag{7.27}$$

and

$$\tau = -\frac{\Delta p}{L} y \tag{7.28}$$

at $y = b$ $\quad \tau_w = -\frac{\Delta p}{L} b$. The negative sign indicates that this quantity when multiplied by the surface area gives the force exerted by the plate on the fluid which is, of course, directed in the negative x direction. The force exerted by the fluid on the wetted plate should, therefore, be positive. The linear variation of shear stress in the fluid is usually expressed as

$$\frac{\tau}{\tau_w} = \frac{y}{b} \tag{7.29}$$

where τ_w is taken as a positive quantity by convention.

The shear stress profile is shown together with the velocity profile in Fig. 7.3.

It is interesting to note that instead of using the no-slip condition on both plates (equation 7.11) we could have used the no-slip condition on one plate and a symmetry boundary condition at $y=0$, i.e.

$$u = 0 \qquad y = b$$

$$\frac{\partial u}{\partial y} = 0 \qquad y = 0 \tag{7.30}$$

Obviously, $C_1=0$ could be easily obtained from equation 7.12. The rest of the results are, of course, identical to those determined earlier.

(b) Simplification of the general conservation equations:

We will establish the differential equation for the pressure-driven flow by simplifying the equation of conservation of mass (eq. 4.11) and the Navier-Stokes equations (eqs. 6.90, 6.91 and 6.92).

From the statement of the problem it is apparent that $\frac{\partial p}{\partial x} \neq 0$ and $v_x \neq 0$. There is no motion in either the y or z direction, thus $v_y=v_z=0$. The plates are horizontal thus $g_x=g_z=0$ and $g_y = -g$.

The continuity equation for an incompressible fluid is

$$\frac{\partial v_x}{\partial x} + \underbrace{\cancel{\frac{\partial v_y}{\partial y}}}_{0} + \underbrace{\cancel{\frac{\partial v_z}{\partial z}}}_{0} = 0 \tag{7.31}$$

Thus

$$\frac{\partial v_x}{\partial x} = 0 \tag{7.32}$$

which means that the velocity does not vary in the x direction (fully developed flow). The plates are infinite in the z direction thus we may assume $(\partial v_x/\partial z) = 0$. However, we note that the velocity becomes zero at the two plates, thus $v_x = v_x(y)$.

The x component of the equation of conservation at momentum (eq. 6.90) simplifies to the form

$$\rho\, v_x \frac{\partial v_x}{\partial x} = -\frac{\partial p}{\partial x} + \mu \frac{\partial^2 v_x}{\partial y^2} \tag{7.33}$$

Using equation 7.32, we get

$$0 = -\frac{\partial p}{\partial x} + \mu \frac{\partial^2 v_x}{\partial y^2} \qquad (7.34)$$

which is identical to the differential equation established by a direct differential momentum balance.

The y component of the equation of conservation of momentum (eq. 6.91) reduces to

$$0 = -\frac{\partial p}{\partial y} + \rho g_y \qquad (g_y = -g) \qquad (7.35)$$

The z component of the equation of conservation of momentum (eq. 6.92) reduces to

$$0 = -\frac{\partial p}{\partial z} \qquad (7.36)$$

Thus, the pressure-driven flow problem between two flat places is described by the following equations

$$0 = -\frac{\partial p}{\partial x} + \mu \frac{\partial^2 v_x}{\partial y^2} \qquad (7.37)$$

$$0 = -\frac{\partial p}{\partial y} - \rho g \qquad (7.38)$$

$$0 = -\frac{\partial p}{\partial z} \qquad (7.39$$

Integrating equations (7.38) and (7.39) we get

$$p = -\rho g y + C_1(x,z) \qquad (7.40)$$

and

$$p = C_2(x,y) \qquad (7.41)$$

Differentiating equations (7.40) and (7.41) with respect to x and equating the results, we get

$$\frac{\partial C_1(x,z)}{\partial x} = \frac{\partial C_2(x,y)}{\partial x} \tag{7.42}$$

The left-hand side of the above equation is not a function of y and the right-hand side is not a function of z. Consequently, we conclude that the derivatives of C_1 and C_2 can only be functions of x, i, e.

$$\frac{\partial p}{\partial x} = \frac{\partial C_1(x)}{\partial x} = \frac{\partial C_2(x)}{\partial x} \tag{7.43}$$

Now, that we have shown that the pressure gradient $\frac{\partial p}{\partial x}$ is a function of x only, we can solve equation (7.37) as presented in section 7.2(a).

7.3 PRESSURE-DRIVEN FLOW IN A TUBE

We will consider steady laminar flow of an incompressible fluid in a horizontal, smooth, round tube under the influence of a pressure gradient as shown in Fig. 7.4. The tube is sufficiently long so that the flow is fully developed, which means that the velocity does not vary in the axial direction. Again, we will use both the direct momentum balance and the simplification of the Navier-Stokes equations in order to derive the appropriate differential equations. Pressure-driven flows are often called Poiseuille flows in honor of the French physician J.L.M. Poiseuille who performed a long and accurate series of experiments in the 1840's with the object of studying blood flow through veins.

(a) Momentum balance for a volume element

We choose an annular fluid element as shown in Fig. 7.5. The momentum principle, for the conditions of this problem, reduces to a simple force balance

$$F_{pressure} + F_{stress} = 0 \tag{7.44}$$

where

$$F_{pressure} = p\ 2\pi r\Delta r - (p + \frac{\partial p}{\partial z}\Delta z)\ 2\pi r\Delta r = -\frac{\partial p}{\partial z}\ 2\pi r\Delta z\Delta r \tag{7.45}$$

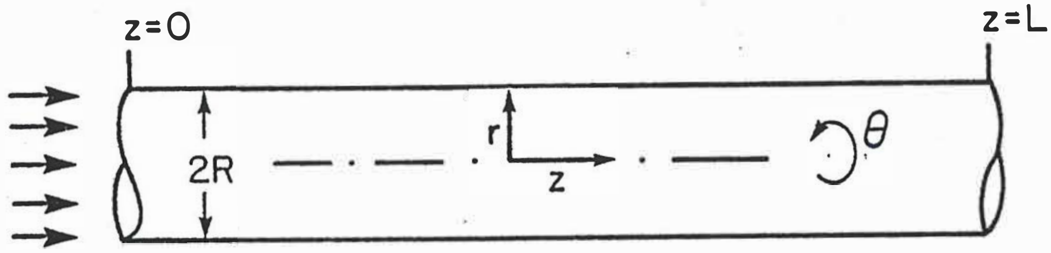

Fig. 7.4 Axial flow in a long tube

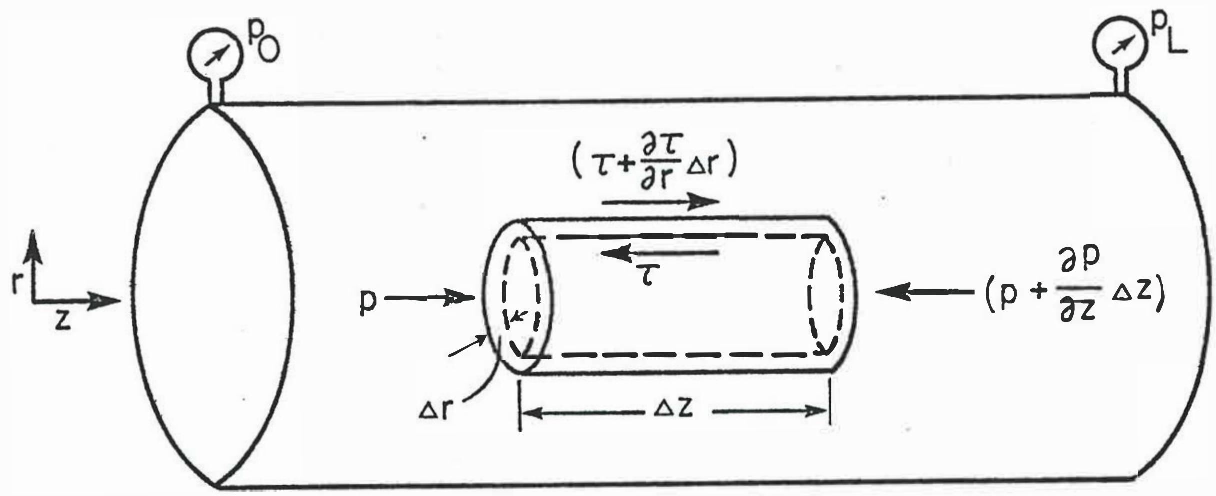

Fig. 7.5 Force balance for an annular volume element

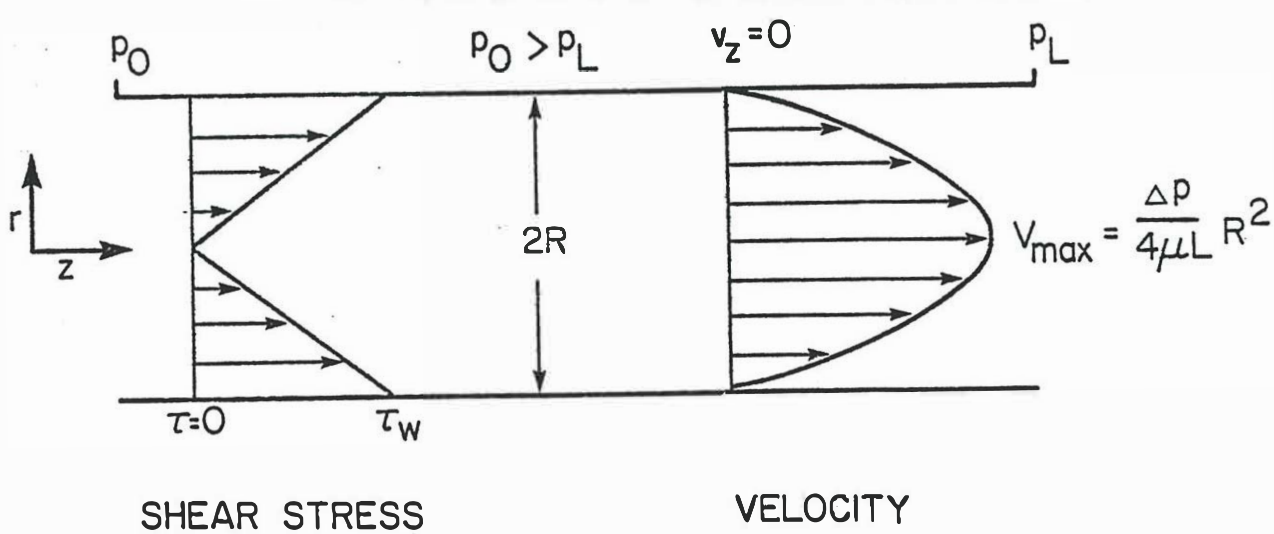

Fig. 7.6 Velocity and stress profiles for pressure-driven flow in a tube

and

$$F_{stress} = -\tau 2\pi r\Delta z + (\tau + \frac{\partial\tau}{\partial r}\Delta r)\, 2\pi(r+\Delta r)\,\Delta z$$

$$= -\tau 2\pi r\Delta z + \tau 2\pi r\Delta z + \frac{\partial\tau}{\partial r} 2\pi r\Delta r\Delta z + \tau 2\pi\Delta r\Delta z$$

$$+ \frac{\partial\tau}{\partial r} 2\pi(\Delta r)^2\Delta z \qquad (7.46)$$

The term having $(\Delta r)^2$ is negligible as compared to the rest of the terms, thus

$$F_{stress} = (\frac{\partial\tau}{\partial r} r + \tau)\, 2\pi\Delta r\Delta z = \frac{\partial}{\partial r}(r\tau) 2\pi\Delta r\Delta z$$

$$= \frac{1}{r}\frac{\partial}{\partial r}(r\tau)\, 2\pi r\Delta r\Delta z \qquad (7.47)$$

After substituting in equation (7.44) and dividing by $2\pi r\,\Delta r\Delta z$, we get

$$-\frac{\partial p}{\partial z} + \frac{1}{r}\frac{\partial}{\partial r}(r\,\tau) = 0 \qquad (7.48)$$

For a Newtonian fluid $\tau = \mu\,\dfrac{\partial v_z}{\partial r}$

thus

$$\frac{\partial p}{\partial z} = \frac{1}{r}\frac{\partial}{\partial r}(r\,\mu\,\frac{\partial v_z}{\partial r}) \qquad (7.49)$$

or

$$\frac{\partial p}{\partial z} = \mu\,\frac{1}{r}\frac{\partial}{\partial r}(r\,\frac{\partial v_z}{\partial r}) \qquad (7.50)$$

The left-hand side of equation (7.50) is a function of z only and the right-hand side is a function of r only. Since z and r are independent variables both sides of equation (7.50) must be equal to a constant, say K_1. Thus, we have

$$\frac{dp}{dz} = K_1 \text{ and } \mu \frac{1}{r}\frac{d}{dr}\left(r\frac{dv_z}{dr}\right) = K_1 \qquad (7.51)$$

The first equation (7.51) can be easily solved to give a linear pressure drop with pressure gradient

$$\frac{dp}{dz} = -\frac{p_o - p_L}{L} = -\frac{\Delta p}{L} \qquad (7.52)$$

The second equation (7.51) can be integrated once to give

$$r\frac{dv_z}{dr} = -\frac{1}{2\mu}\frac{\Delta p}{L}r^2 + C_1 \qquad (7.53)$$

then dividing by r

$$\frac{dv_z}{dr} = -\frac{1}{2\mu}\frac{\Delta p}{L}r + \frac{C_1}{r} \qquad (7.54)$$

A second integration gives

$$v_z = -\frac{1}{4\mu}\frac{\Delta p}{L}r^2 + C_1 \ln r + C_2 \qquad (7.55)$$

The boundary conditions are

B.C.1	$v_z = 0$	$r = R$	(no-slip at the wall)	(7.56)
B.C.2	$\frac{\partial v_z}{\partial r} = 0$	$r = 0$	(symmetry)	

The integration constants can be easily determined

$$C_1 = 0$$

$$C_2 = \frac{\Delta p}{4\mu L}R^2 \qquad (7.57)$$

Note that $C_1 = 0$ also follows directly from equation (7.55). The logarithmic term would give an infinite velocity for r=0 if C_1 were not zero (physically impossible).

Thus, the velocity profile takes the parabolic form (shown in Fig. 7.6).

$$v_z = \frac{\Delta p}{4\mu L} R^2 \left[1 - \left(\frac{r}{R}\right)^2\right] \tag{7.58}$$

The maximum velocity occurs along the axis (r=0)

$$V_{max} = \frac{\Delta p}{4\mu L} R^2 \tag{7.59}$$

The average velocity is determined by integrating the velocity over a cross-section and then dividing by the cross-sectional area

$$V_{avg} = \frac{\int_0^{2\pi} \int_0^{R} v_z \, r dr d\theta}{\int_0^{2\pi} \int_0^{R} r dr d\theta} = \frac{\Delta p}{8\mu L} R^2 \tag{7.60}$$

Note that $V_{avg} = \frac{1}{2} V_{max}$

The volume rate of flow is equal to the product of the cross-sectional area and the average velocity

$$Q = \frac{\pi(\Delta P)}{8\mu L} R^4 \tag{7.61}$$

This result is known as the Hagen-Poiseuille formula in honor of the two scientists who did extensive work on fluid flow through tubes, and established an empirical relation between ΔP, Q, L and R^4. However, neither Hagen nor Poiseuille ever derived such an expression. When using the Hagen-Poiseuille formula one must remember that it is valid for steady, laminar flow of a Newtonian, incompressible fluid in a long tube.

The shear stress profile can be obtained by either differentiating equation (7.58) and using the definition $\tau = \mu \, (\partial v_z/\partial r)$ or preferably from equation (7.48) as follows

$$\frac{dp}{dz} = \frac{1}{r} \frac{d}{dr} (r \, \tau) \tag{7.62}$$

The pressure gradient is

$$\frac{dp}{dz} = -\frac{\Delta p}{L} \tag{7.63}$$

and

$$-\frac{\Delta p}{L} = \frac{1}{r}\frac{\partial}{\partial r}(r\tau) \tag{7.64}$$

Integrating, we get

$$r\tau = -\frac{\Delta p}{L}\frac{r^2}{2} + C_1 \tag{7.65}$$

Since $\tau = \mu \frac{\partial v_z}{\partial r} = 0$ at $r = 0$ (7.66)

$$C_1 = 0 \tag{7.67}$$

and

$$\tau = -\frac{\Delta p}{2L} r \tag{7.68}$$

At the tube wall r=R we have $\tau_w = -\frac{\Delta p}{2L} R$. The frictional force exerted by the tube wall on the fluid is

$$F_f = -\frac{\Delta p}{2L} R\ (2\pi RL) = -\pi R^2 \Delta P \tag{7.69}$$

The force exerted by the fluid on the wetted tube wall should be opposite

$$F_f = \pi R^2 \Delta p \tag{7.70}$$

The linear shear stress variation in the fluid is expressed as

$$\frac{\tau}{\tau_w} = \frac{r}{R} \tag{7.71}$$

where τ_w is taken by convention a positive quantity (shown in Fig. 7.6).

(b) Simplification of the general equations

In this problem it is obvious that there is no swirling motion i.e. $v_\theta = 0$ and no flow in the r direction i.e. $v_r = 0$. The pressure varies in the x direction and the axial velocity component varies as a function of r. The tube is horizontal so that $g_z = 0$.

The continuity equation for an incompressible fluid in cylindrical coordinates (from Appendix D) is:

$$\frac{1}{r}\frac{\partial}{\partial r}(r \cancelto{0}{v_r}) + \frac{1}{r}\frac{\partial \cancelto{0}{v_\theta}}{\partial \theta} + \frac{\partial v_z}{\partial z} = 0 \tag{7.72}$$

Thus

$$\frac{\partial v_z}{\partial z} = 0 \tag{7.73}$$

This means that the axial velocity does not vary in the axial direction. This result was expected from the fully developed flow assumption.

The equations of conservation of momentum (from Appendix D) simplify to the forms

r component
$$0 = -\frac{\partial p}{\partial r} + \rho g_r \tag{7.74}$$

θ component
$$0 = -\frac{1}{r}\frac{\partial p}{\partial \theta} + \rho g_\theta \tag{7.75}$$

z component
$$0 = -\frac{\partial p}{\partial z} + \mu \frac{1}{r}\frac{\partial}{\partial r}\left(r \frac{\partial v_z}{\partial r}\right) \tag{7.76}$$

Integrating equations (7.74) and (7.75), we get

$$p = \rho \int g_r \, dr + C_1(\theta, z) \tag{7.77}$$

and

$$p = \rho r \int g_\theta \, d\theta + C_2(r, z) \tag{7.78}$$

Differentiating equations (7.77) and (7.78) with respect to z and equating the results, we get

$$\frac{\partial C_1(\theta, z)}{\partial z} = \frac{\partial C_2(r, z)}{\partial z} \tag{7.79}$$

The left-hand side of the above equation is a function of θ and the right-hand side is a function of r. Consequently, we conclude that the derivatives of C_1 and C_2 can only be functions of z, i.e.

$$\frac{\partial p}{\partial z} = \frac{\partial C_1(z)}{\partial z} = \frac{\partial C_2(z)}{\partial z} \tag{7.80}$$

Now, that we have shown that the pressure gradient is a function of z only, we can solve equation (7.76) as presented in section 7.3(b).

7.4 THE DIRECT DIFFERENTIAL MOMENTUM BALANCE VERSUS THE SIMPLIFICATION OF THE NAVIER-STOKES EQUATIONS

We have used two methods in solving the pressure-driven flow problems of sections 7.2 and 7.3. The direct differential momentum balance method requires more intuition, because the various force terms must be identified and properly expressed. With every new problem a new balance is required and all expressions must be established anew. It is possible that some terms might be entirely neglected without a clear reasoning as to their relative importance or simply forgotten. On the other hand, the simplification of the general conservation equations (continuity and Navier-Stokes) is fairly straightforward. We have all the possible terms in front of us (Appendix D) and we must exercise our judgement in eliminating those that are not important. As it will be shown in the chapter on boundary layer flow we may also assess the order of magnitude of each term. Clearly then, starting from the general conservation equations and eliminating the appropriate terms is a far better method. This method will therefore be used almost entirely for the rest of the book in setting up the appropriate equations for microscopic flow problems.

Referring back to sections 7.3 and 7.4 we note that in simplifying the components of the momentum equation we ended up with three equations two of which contained very little information (variation of pressure as expected from hydrostatics). The component of the equation of momentum in the direction of the flow had all the essential parameters of the problems. To avoid repetition in subsequent problems we will refer to the simplified equation of momentum in the direction of flow as the governing equation of motion for flow problems with parallel streamlines.

7.5 DRAG FLOW BETWEEN PARALLEL PLATES

We consider two flat parallel plates separated by a distance b as shown in Fig. 7.7(a). The top plate moves in the x direction at a constant speed V while the botton plate remains stationary. The fluid between the plates is assumed incompressible and Newtonian. As the top plate moves the fluid is dragged along. This type of flow is often referred to as Couette flow [after M.F.A. Couette (1858-1943)].

The governing equation for this problem can be easily obtained after simplifying the Navier-Stokes equations in the form

$$\frac{d^2 v_x}{dy^2} = 0 \tag{7.81}$$

Integrating this equation twice, we get

$$v_x = C_1 y + C_2 \tag{7.82}$$

The integration constants can be determined from the boundary conditions

$$\begin{array}{lll} \text{B.C. 1} & y = 0 & v_x = 0 \\ \text{B.C. 2} & y = b & v_x = V \end{array} \tag{7.83}$$

We get $C_1 = V/b$ and $C_2 = 0$

Thus

$$v_x = \frac{V}{b} y \tag{7.84}$$

This linear velocity profile is shown in Fig. 7.7(b).

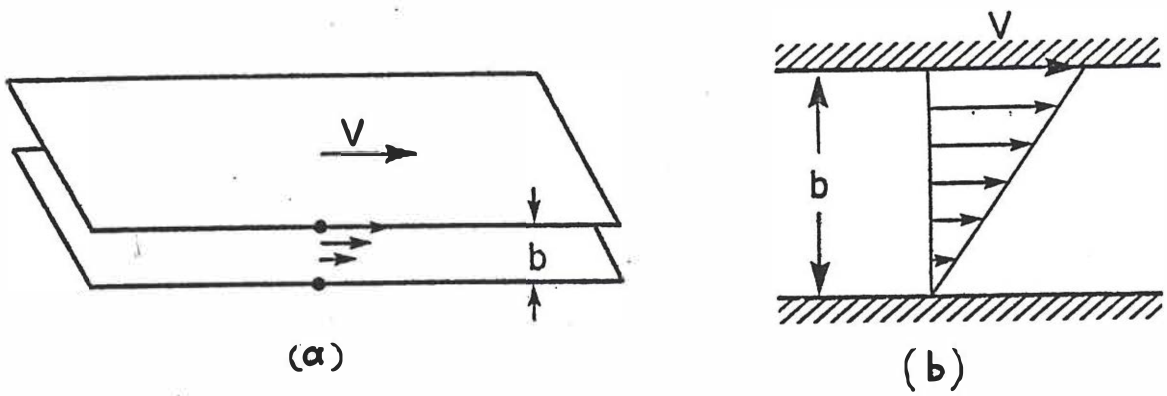

Fig. 7.7 (a) Drag (also called Couette) flow.
(b) The velocity profile in drag flow.

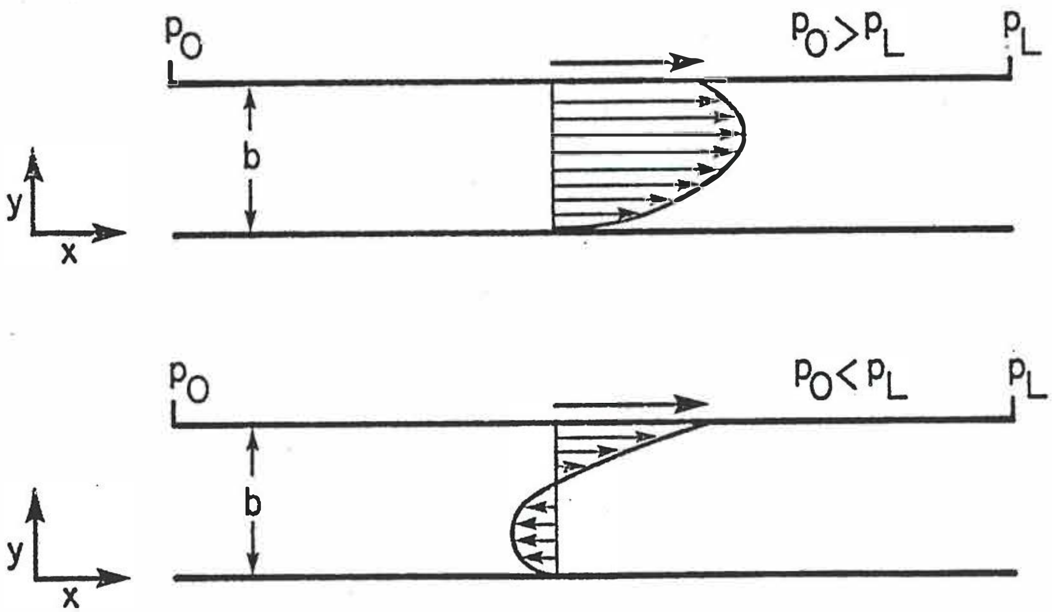

Fig. 7.8 Typical velocity profiles for combined pressure and drag flow.

7.6 COMBINED PRESSURE AND DRAG FLOW BETWEEN PARALLEL PLATES

We now consider the previous problem with an imposed pressure gradient. The governing equation is

$$0 = -\frac{\partial p}{\partial x} + \mu \frac{\partial^2 v_x}{\partial y^2} \tag{7.85}$$

The boundary conditions for pressure are

$$\begin{array}{lll} \text{B.C.1} & x = 0 & p = p_o \\ \text{B.C.2} & x = L & p = p_L \end{array} \tag{7.86}$$

The boundary conditions for velocity are

$$\begin{array}{lll} \text{B.C.1} & y = 0 & v_x = 0 \\ \text{B.C.2} & y = b & v_x = V \end{array} \tag{7.87}$$

If $p_o > p_L$ the pressure gradient is aiding the drag flow. If $p_o < p_L$ the pressure gradient is opposing the drag flow. Again, the pressure is a function of x only whereas the velocity is a function of y only. Thus, we may write

$$\frac{dp}{dx} = \mu \frac{d^2 v_x}{dy^2} \tag{7.88}$$

where

$$\frac{dp}{dx} = -\frac{p_o - p_L}{L} = -\frac{\Delta p}{L}$$

and

$$-\frac{\Delta p}{L} = \mu \frac{d^2 v_x}{dy^2} \tag{7.89}$$

After integrating twice and determining the integration constants, we get

$$v_x = \frac{V}{b} y + \frac{1}{2\mu} \frac{\Delta p}{L} y(b-y) \tag{7.90}$$

where $\Delta p = p_o - p_L$.

The velocity profiles are sketched in Fig. 7.8 for both aiding and opposing pressure gradients. It is obvious that if the pressure gradient is zero we get the linear velocity profile of section 7.5.

The volume rate of flow for two plates each of width W may be expressed as

$$Q = W \int_o^b v_x \, dy \tag{7.91}$$

and after performing the integration we get

$$\frac{Q}{W} = \frac{Vb}{2} \left(1 + \frac{b^2}{6\mu V} \frac{\Delta p}{L}\right) \tag{7.92}$$

or in terms of the pressure gradient

$$\frac{Q}{W} = \frac{Vb}{2} \left(1 - \frac{b^2}{6\mu V} \frac{dp}{dx}\right) \tag{7.93}$$

This may be integrated to give the pressure as a linear function of x

$$p - p_o = \frac{12\mu}{b^3} \left(\frac{Vb}{2} - \frac{Q}{W}\right) (x - x_o) \tag{7.94}$$

where $p = p_o$ at $x = x_o$.

7.7 PRESSURE-DRIVEN FLOW IN AN ANNULUS

We consider flow in the annular space between two tubes as shown in Fig. 7.9. The flow is steady and the fluid is incompressible and Newtonian.

The governing equation is

$$\frac{dp}{dz} = \mu \frac{1}{r} \frac{d}{dr} \left(r \frac{\partial v_z}{\partial r}\right) \tag{7.95}$$

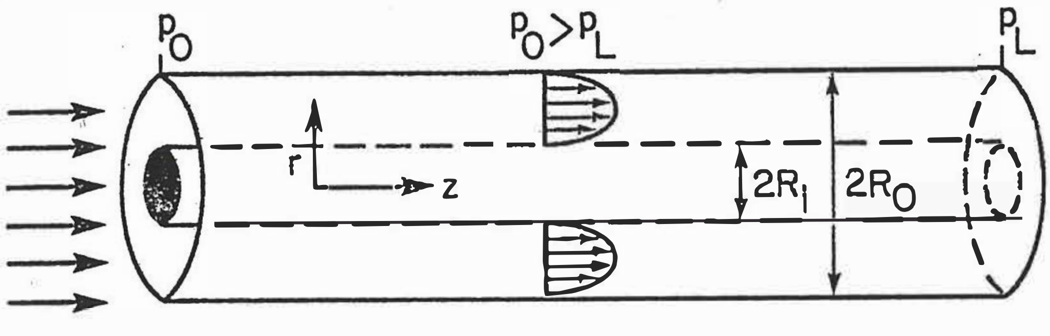

Fig. 7.9 Pressure-driven flow in an annulus

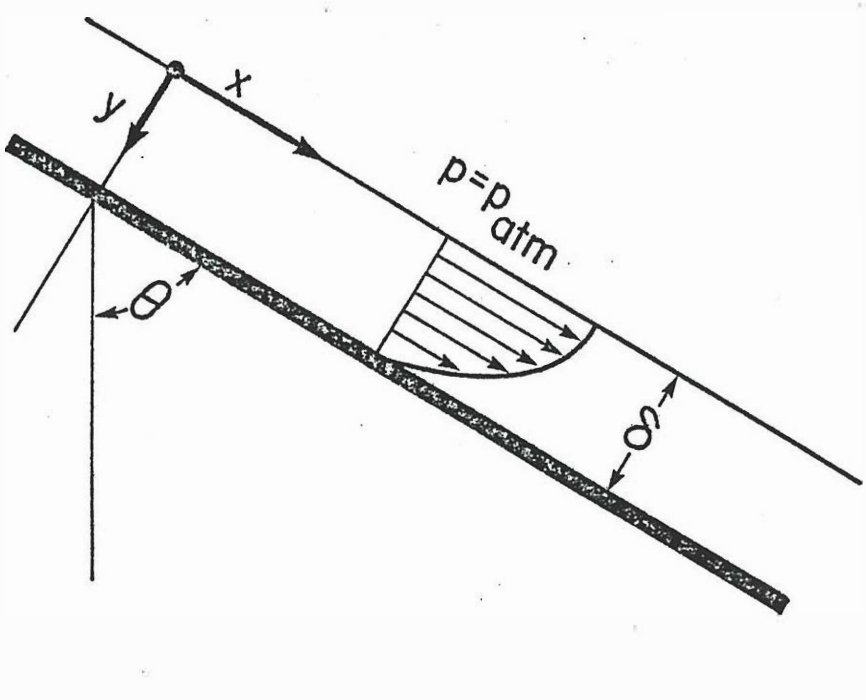

Fig. 7.10 Flow of a liquid film over an inclined plate

The boundary conditions are

$$v_z = 0 \qquad r = R_i$$
$$v_z = 0 \qquad r = R_o \tag{7.96}$$

The general solution may be written as

$$v_z = \frac{1}{4\mu}\frac{dp}{dz} r^2 + \frac{C_1}{\mu} \ln r + C_2 \tag{7.97}$$

After determining C_1 and C_2 we get

$$v_z = -\frac{1}{4\mu}\frac{dp}{dz}\left[R_o^2 - r^2 + \frac{R_o^2 - R_i^2}{\ln (R_o/R_i)} \ln \frac{r}{R_o}\right] \tag{7.98}$$

where $\quad \frac{dp}{dz} = -\frac{\Delta p}{L} \qquad \Delta p = p_o - p_L$

The volume rate of flow is

$$Q = \frac{\pi \Delta P R_o^4}{8\mu L}\left[1 - \left(\frac{R_i}{R_o}\right)^4 - \frac{\left[1 - \left(\frac{R_i}{R_o}\right)^2\right]^2}{\ln\left(\frac{R_o}{R_i}\right)}\right] \tag{7.99}$$

7.8 FLOW OF A FALLING LIQUID FILM

The flow of a liquid film over a flat plate is schematically shown in Fig. 7.10. The plate is sufficiently long so that entry and exit disturbances may be neglected. Again, fully developed flow is assumed in this case, which means that the velocity does not vary in the direction of flow. For steady flow of an incompressible, Newtonian fluid the governing differential equation can be easily obtained by simplifying the x component of the equation of momentum. In this case there is no pressure gradient because everywhere above the film the pressure is equal to atmospheric pressure. We note that $g_x = g \cos \theta$, thus, we have

$$0 = \mu \frac{d^2 v_x}{dy^2} + \rho g_x \tag{7.100}$$

or

$$0 = \mu \frac{d^2 v_x}{dy^2} + \rho g \cos \theta \tag{7.101}$$

At the plate surface the no-slip condition applies, i.e. B.C.1: $v_x=0$ at $y = \delta$. At the air-liquid interface the air is dragged downwards by the flowing liquid. At the interface the shear stress on the liquid side must be equal to the shear stress on the air side. We have

$$\tau = \tau_{air} \tag{7.102}$$

or

$$\mu \frac{dv_x}{dy} = \mu_{air} \left(\frac{dv_x}{dy}\right)_{air} \tag{7.103}$$

The viscosity of air is significantly smaller than that of liquids. Thus, the right-hand side of the above expression is practically equal to zero, which leads to a boundary condition

B.C.2: $$\frac{dv_x}{dy} = 0 \quad \text{at} \quad y = 0 \tag{7.104}$$

Integrating equation (7.101) twice and determining the integration constants with the help of the boundary conditions, we get

$$v_x = \frac{\rho g \delta^2 \cos \theta}{2\mu} \left[1 - \left(\frac{y}{\delta}\right)^2\right] \tag{7.105}$$

This is a parabolic velocity profile as sketched in Fig. 7.10. The maximum velocity occurs at y=0, which is

$$V_{max} = \frac{\rho g \delta^2 \cos \theta}{2\mu} \tag{7.106}$$

The average velocity can be easily obtained by carrying out the integrations shown in the expression

$$V_{avg} = \frac{\int_0^W \int_0^\delta v_x dzdy}{\int_0^W \int_0^\delta dzdy}$$

$$= \frac{1}{\delta} \int_0^\delta v_x dy$$

$$= \frac{\rho g \delta^2 \cos\theta}{3\mu} \tag{7.107}$$

The volume rate of flow is equal to the product of the average velocity and the cross-sectional area:

$$Q = \frac{\rho g W \delta^3 \cos\theta}{3\mu} \tag{7.108}$$

where W is the film width.

The film thickness δ may be expressed in terms of the average velocity, the volume rate of flow or the mass rate of flow ($\dot{m} = \rho Q$)

$$\delta = \left(\frac{3\mu V_{avg}}{\rho g \cos\theta}\right)^{1/2} = \left(\frac{3\mu Q}{\rho g W \cos\theta}\right)^{1/3} = \left(\frac{3\mu \dot{m}}{\rho^2 W g \cos\theta}\right)^{1/3} \tag{7.109}$$

7.9 PRESSURE-DRIVEN FLOW OF TWO IMMISCIBLE FLUIDS BETWEEN PARALLEL PLATES

Now, we will consider the steady flow of two incompressible Newtonian fluids between two long parallel plates under the influence of a pressure gradient, as shown in Fig. 7.11.

The governing equations of motion are

$$0 = -\frac{\partial p}{\partial x} + \mu^A \left(\frac{\partial^2 v_x^A}{\partial y^2}\right) \quad \text{(for fluid A)} \tag{7.110}$$

$$0 = -\frac{\partial p}{\partial x} + \mu^B \left(\frac{\partial^2 v_x^B}{\partial y^2}\right) \quad \text{(for fluid B)} \tag{7.111}$$

The pressure is a function of x only and the velocities are functions of y only. Thus, we may write

$$\frac{dp}{dx} = \mu^A \left(\frac{d^2 v_x^A}{dy^2}\right) \tag{7.112}$$

$$\frac{dp}{dx} = \mu^B \left(\frac{d^2 v_x^B}{dy^2}\right) \tag{7.113}$$

Integrating each equation twice, we get

$$v_x^A = \left(\frac{dp}{dx}\right) \frac{y^2}{2\mu^A} + C_1 y + C_2 \tag{7.114}$$

$$v_x^B = \left(\frac{dp}{dx}\right) \frac{y^2}{2\mu^B} + C_3 y + C_4 \tag{7.115}$$

Now, we must determine the four integration constants by using the boundary conditions. At the upper and lower plates the velocity is zero (no-slip condition). At the interface the velocities must be equal (i.e. $v_x^A = v_x^B$) as well as the shear stresses (i.e. $\tau^A = \tau^B$). Thus, the four boundary conditions may be written as

B.C.1	$v_x^A = 0$	$y = -b$	
B.C.2	$v_x^B = 0$	$y = b$	
B.C.3	$v_x^A = v_x^B$	$y = 0$	(7.116)
B.C.4	$\tau^A = \tau^B$	$y = 0$	
or	$\mu^A \left(\frac{\partial v_x^A}{\partial y}\right) = \mu^B \left(\frac{\partial v_x^B}{\partial y}\right)$	$y = 0$	

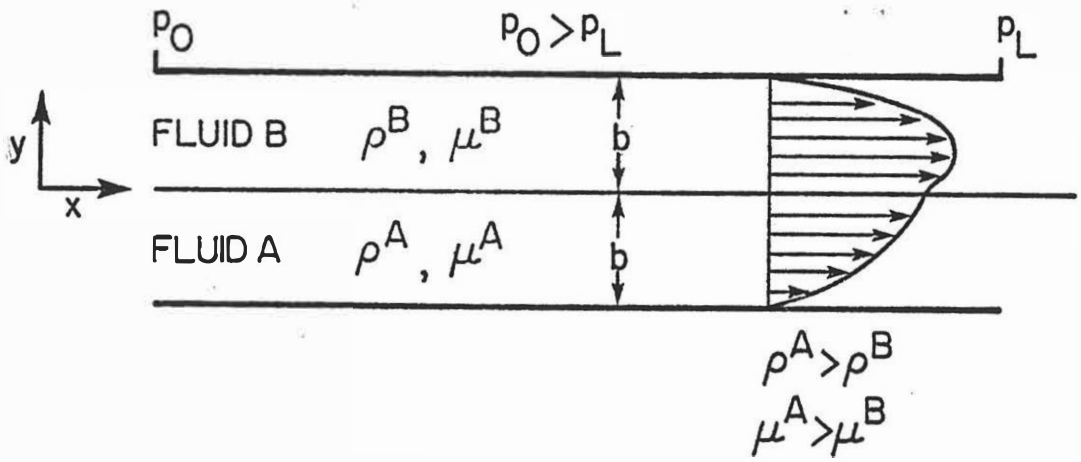

Fig. 7.11 Pressure-driven flow of two immiscible fluids between two parallel plates

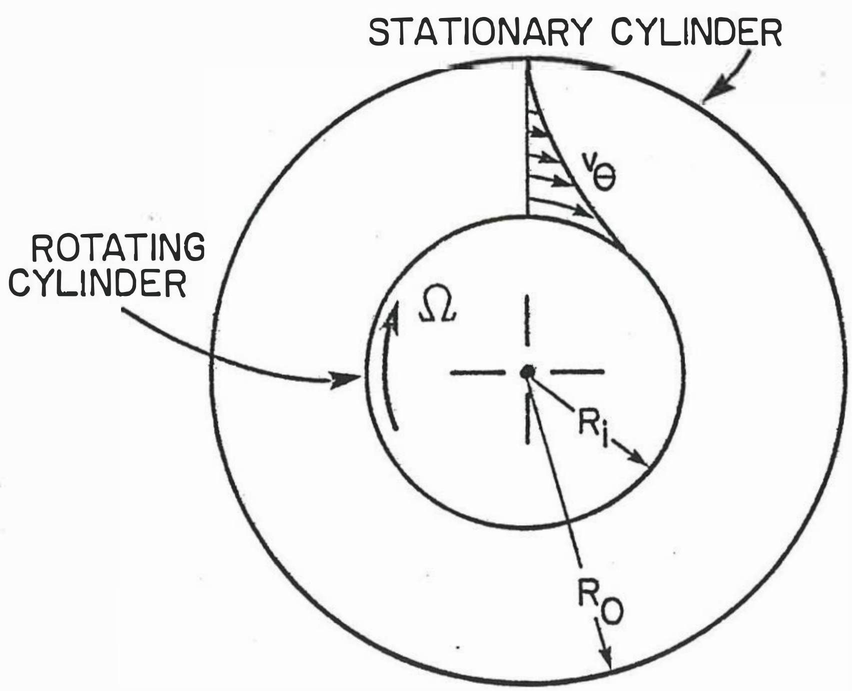

Fig. 7.12 Tangential drag flow between two concentric cylinders

From B.C.3, we have

$$C_2 = C_4 \tag{7.117}$$

From B.C.4, we have

$$\mu^A C_1 = \mu^B C_3 \tag{7.118}$$

Further, using B.C.1 and B.C.2 we get

$$C_1 = \left(\frac{dp}{dx}\right) \frac{b}{2} \left(\frac{\mu^A - \mu^B}{\mu^A + \mu^B}\right) \tag{7.119}$$

$$C_2 = - \left(\frac{dp}{dx}\right) \frac{b^2}{2\mu^A} \left(\frac{2\mu^A}{\mu^A + \mu^B}\right) \tag{7.120}$$

Thus, the velocity profiles are

$$v_x^A = - \left(\frac{dp}{dx}\right) \frac{b^2}{2\mu^A} \left[\left(\frac{2\mu^A}{\mu^A + \mu^B}\right) + \left(\frac{\mu^A - \mu^B}{\mu^A + \mu^B}\right) \left(\frac{y}{b}\right) - \left(\frac{y}{b}\right)^2 \right] \tag{7.121}$$

$$v_x^B = - \left(\frac{dp}{dx}\right) \frac{b^2}{2\mu^B} \left[\left(\frac{2\mu^B}{\mu^A + \mu^B}\right) + \left(\frac{\mu^A - \mu^B}{\mu^A + \mu^B}\right) \left(\frac{y}{b}\right) - \left(\frac{y}{b}\right)^2 \right] \tag{7.122}$$

where $\quad - \dfrac{dp}{dx} = \dfrac{\Delta p}{L} = \dfrac{P_o - P_L}{L}$

These velocity profiles are sketched in Fig. 7.11. We note that if $\mu^A = \mu^B$ the velocity profiles for both fluids are identical and equations (7.121) and (7.122) reduce to the single parabolic expression of section 7.2.

7.10 TANGENTIAL DRAG FLOW IN AN ANNULUS

In this section we will examine the flow in the annular gap between two concentric cylinders as shown in Fig. 7.12. The outer cylinder is stationary and the inner cylinder rotates with a constant angular velocity Ω and the fluid in the gap is incompressible and Newtonian. The cylinders are assumed to be sufficiently long so that end disturbances may be neglected.

As the inner cylinder rotates it drags along the fluid in the gap. Obviously then $v_z=0$, $v_r=0$ and $v_\theta = v_\theta(r)$.

The Navier-Stokes equations in cylindrical coordinates (from Appendix D) may be simplified to

r component
$$-\rho\left(\frac{v_\theta^2}{r}\right) = -\frac{\partial p}{\partial r} \tag{7.123}$$

θ component
$$0 = \mu\left[\frac{\partial}{\partial r}\left(\frac{1}{r}\frac{\partial}{\partial r}(r\,v_\theta)\right)\right] \tag{7.124}$$

z component
$$0 = -\left(\frac{\partial p}{\partial z}\right) + \rho g \tag{7.125}$$

Equation (7.124) may be integrated once to give

$$\frac{1}{r}\frac{\partial}{\partial r}(rv_\theta) = C_1 \tag{7.126}$$

A second integration yields

$$v_\theta = \frac{C_1 r}{2} + \frac{C_2}{r} \tag{7.127}$$

The boundary conditions are

$$\begin{aligned} v_\theta &= R_i\Omega & r &= R_i \\ v_\theta &= 0 & r &= R_o \end{aligned} \tag{7.128}$$

Determination of the integration constants C_1 and C_2 gives

$$v_\theta = R_i\,\Omega\,\frac{\left[\left(\frac{R_i}{r}\right) - \left(\frac{R_i r}{R_o^2}\right)\right]}{\left[1 - \left(\frac{R_i}{R_o}\right)^2\right]} \tag{7.129}$$

To determine the torque exerted by the rotating cylinder of length L on the fluid we must multiply the shear stress on the inner cylinder $(\tau_{r\theta})_{r=Ri}$ by the surface area of the cylinder and the radius R_i. From appendix D we find that

$$\tau_{r\theta} = \mu \left[r \frac{\partial}{\partial r} \left(\frac{v_\theta}{r}\right) + \frac{1}{r} \frac{\partial v_r}{\partial \theta}\right] \tag{7.130}$$

$$(\tau_{r\theta})_{r=R_i} = \mu \left[r \frac{d}{dr} \left(\frac{v_\theta}{r}\right)\right]_{r=R_i} = - \frac{2\mu \Omega}{1 - \left(\frac{R_i}{R_o}\right)^2} \tag{7.131}$$

Thus

$$T_o = (\tau_{r\theta})_{r=R_i} (2\pi R_i L) R_i$$

$$= - \frac{4\pi\mu L R_i^2 \Omega}{1 - \left(\frac{R_i}{R_o}\right)^2} \tag{7.132}$$

The negative sign indicates that T_o is the torque exerted by the fluid on the cylinder. The torque required to turn the cylinder would be equal in magnitude and positive.

7.11 SHAPE OF LIQUID SURFACE IN A ROTATING VESSEL

A vertical cylindrical vessel partly filled with an incompressible Newtonian liquid rotates about its axis at a constant angular velocity Ω. We will determine the shape of the liquid surface in the vessel.

We note that for a vertical vessel as shown in Fig. 7.13 we have $g_r = g_\theta = 0$ and $g_z = -g$. It is obvious that $v_r = 0$, $v_z = 0$ and $v_\theta = v_\theta(r)$.

The Navier-Stokes equations in cylindrical coordinates (from Appendix D) reduce to

r component
$$\rho \frac{v_\theta^2}{r} = \frac{\partial p}{\partial r} \tag{7.133}$$

θ component
$$0 = \mu \frac{\partial}{\partial r}\left(\frac{1}{r} \frac{\partial}{\partial r} (r\, v_\theta)\right) \tag{7.134}$$

z component $$0 = -\frac{\partial p}{\partial z} + \rho g_z \qquad (g_z = -g) \tag{7.135}$$

The velocity distribution $v_\theta = v_\theta(r)$ may be obtained from equation (7.134). The pressure distribution $p = p(r,z)$ is due to centrifugal and gravitational forces and may be obtained from equations (7.133) and (7.135).

Integration of equation (7.134) gives

$$v_\theta = \frac{C_1 r}{2} + \frac{C_2}{r} \tag{7.136}$$

Since $v_\theta = \Omega R$ at $r=R$ and $v_\theta = 0$ at $r=0$, we get

$$v_\theta = \Omega r \tag{7.137}$$

Substituting this result into equation (7.133) we have

$$\frac{\partial p}{\partial r} = \rho\Omega^2 r \tag{7.138}$$

Equation (7.135) may be written as

$$\frac{\partial p}{\partial z} = -\rho g \tag{7.139}$$

The total pressure differential is

$$dp = \frac{\partial p}{\partial r}dr + \frac{\partial p}{\partial z}dz$$

$$= \rho\Omega^2 r dr - \rho g dz \tag{7.140}$$

Integrating, we get

$$p = \frac{1}{2}\rho\Omega^2 r^2 - \rho g z + C \tag{7.141}$$

Since $p = p_{atm}$ at $z=z_o$ and $r=0$

$$C = \rho g z_o + p_{atm} \tag{7.142}$$

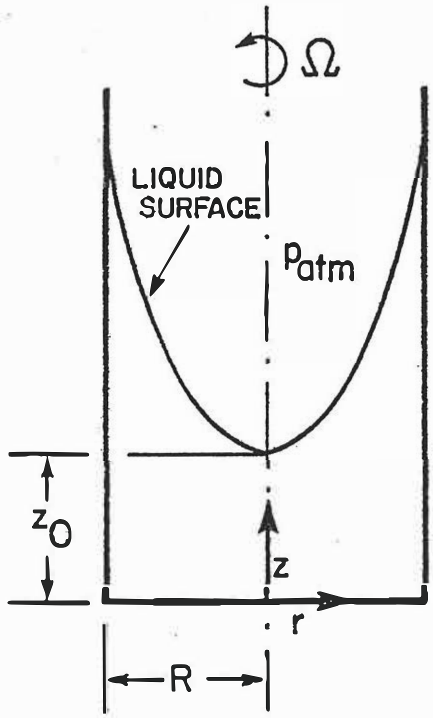

Fig. 7.13 Free liquid surface of a rotating liquid

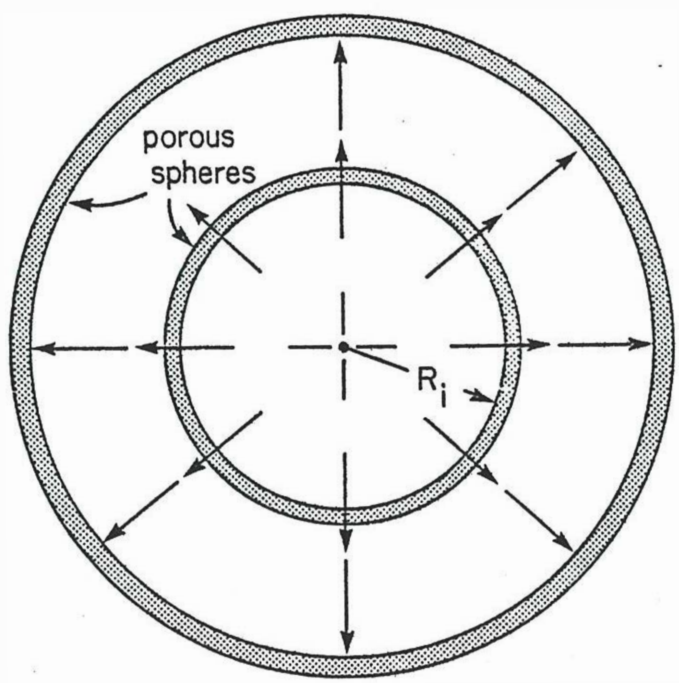

Fig. 7.14 The fluid flows radially from the inner sphere towards the outer sphere.

Thus

$$p-p_{atm} = \frac{1}{2}\rho\Omega^2 r^2 - \rho g(z-z_o) \tag{7.143}$$

The pressure on all points of the free liquid surface must be atmospheric i.e. $p = p_{atm}$. Thus, the shape of the surface is given by

$$0 = \frac{1}{2}\rho\Omega^2 r^2 - \rho g\,(z-z_o) \tag{7.144}$$

or

$$z - z_o = \left(\frac{\Omega^2}{2g}\right) r^2 \tag{7.145}$$

which means that it is a paraboloid of revolution as shown in Fig. 7.13.

7.12 RADIAL FLOW BETWEEN CONCENTRIC SPHERES

We now consider steady flow of an incompressible, Newtonian fluid in the space between two porous spherical shells as shown in Fig. 7.14. The fluid is somehow generated in the inner sphere and flows through the porous surface radially towards the outer sphere surface. The volumetric rate of flow is Q.

The continuity equation in spherical coordinates (from Appendix D) reduces to

$$\frac{1}{r^2}\frac{\partial}{\partial r}(\rho r^2 v_r) = 0 \tag{7.146}$$

and further simplifies to

$$\frac{d}{dr}(r^2\, v_r) = 0 \tag{7.147}$$

Integration gives

$$v_r = \frac{C}{r^2} \tag{7.148}$$

Since $Q = 4\pi R_i^2 (v_r)_{r=R_i}$, we have

$$\frac{Q}{4\pi R_i^2} = (v_r)_{r=R_i} = \frac{C}{R_i^2} \tag{7.149}$$

Therefore
$$C = \frac{Q}{4\pi} \tag{7.150}$$

and
$$v_r = \frac{Q}{4\pi r^2} \tag{7.151}$$

The Navier-Stokes equations in sperical coordinates reduce to

r component
$$\rho v_r \frac{\partial v_r}{\partial r} = -\frac{\partial p}{\partial r} + \frac{1}{r^2}\frac{\partial}{\partial r}\left(r^2 \frac{\partial v_r}{\partial r}\right) - \frac{2}{r^2} v_r + \rho g_r \tag{7.152}$$

θ component
$$0 = -\frac{1}{r}\frac{\partial p}{\partial \theta} + \rho g_\theta \tag{7.153}$$

φ component
$$0 = -\frac{1}{r\sin\theta}\frac{\partial p}{\partial \phi} + \rho g_\phi \tag{7.154}$$

Substituting $v_r = Q/4\pi r^2$ into equation (7.152) we get

$$\rho\left(\frac{Q}{4\pi}\right)\frac{1}{r^2}\left(-\frac{Q}{4\pi}\frac{2}{r^3}\right) = -\frac{\partial p}{\partial r} + \frac{1}{r^2}\frac{\partial}{\partial r}\left[r^2\left(-\frac{Q}{4\pi}\frac{2}{r^3}\right)\right] - \frac{2}{r^2}\frac{Q}{4\pi}\frac{1}{r^2} + \rho g_r \tag{7.155}$$

or

$$\frac{\partial p}{\partial r} = \rho\left(\frac{Q}{4\pi}\right)^2 \frac{2}{r^5} + \left(\frac{Q}{4\pi}\right)\frac{2}{r^4} - \left(\frac{Q}{4\pi}\right)\frac{2}{r^4} + \rho g_r \tag{7.156}$$

or

$$\frac{\partial p}{\partial r} = \rho\left(\frac{Q}{4\pi}\right)^2 \frac{2}{r^5} + \rho g_r \tag{7.157}$$

Integrating, we get

$$p = -\frac{1}{2}\rho\left(\frac{Q}{4\pi}\right)^2 \frac{1}{r^4} + \rho g_r r + C \tag{7.158}$$

Let $p = p_{R_i}$ at $r=R_i$, thus

$$p - p_{R_i} = \frac{1}{2}\rho\left(\frac{Q}{4\pi R^2}\right)^2 \left[1 - \left(\frac{R}{r}\right)^4\right] + \frac{\rho g_r}{R}\left(\frac{r}{R} - 1\right) \tag{7.159}$$

This is the equation for the pressure distribution in the gap between the two porous spherical shells.

7.13 SOME PRESSURE AND GRAVITY DRIVEN FLOWS

It is not always obvious how to differentiate between the pressure term $\frac{\partial p}{\partial x}$ and the gravity term ρg_x (where x is the flow direction). To do just that it is best to think of the pressure gradient $\frac{\partial p}{\partial x}$ as being somehow "externally imposed on the flow" whereas the gravity term "is due to the flow region itself". The three examples described below will help illustrate this point. For all three cases the flow is steady and laminar and the fluid is incompressible and Newtonian. Also, the flow is assumed to be one-dimensional and fully developed in the region AB of Figs. 7.15, 7.16 and 7.17. This means that any disturbances at the tube entry or exit are neglected and the velocity varies only in a direction perpendicular to the flow direction.

(a) Tube flow due to an imposed pressure gradient

The pressure gradient is due to the large reservoir shown in Fig. 7.15. It remains practically constant. The outflow tube is horizontal which means $g_z = 0$. The governing equation is

$$\text{z component} \qquad 0 = -\frac{\partial p}{\partial z} + \mu\left[\frac{1}{r}\frac{\partial}{\partial r}\left(r\frac{\partial v_z}{\partial r}\right)\right] \tag{7.160}$$

We note that

$$\begin{aligned} z = 0 \qquad & p = p_A = \rho g H + p_{atm} \\ z = L \qquad & p = p_B = p_{atm} \end{aligned} \tag{7.161}$$

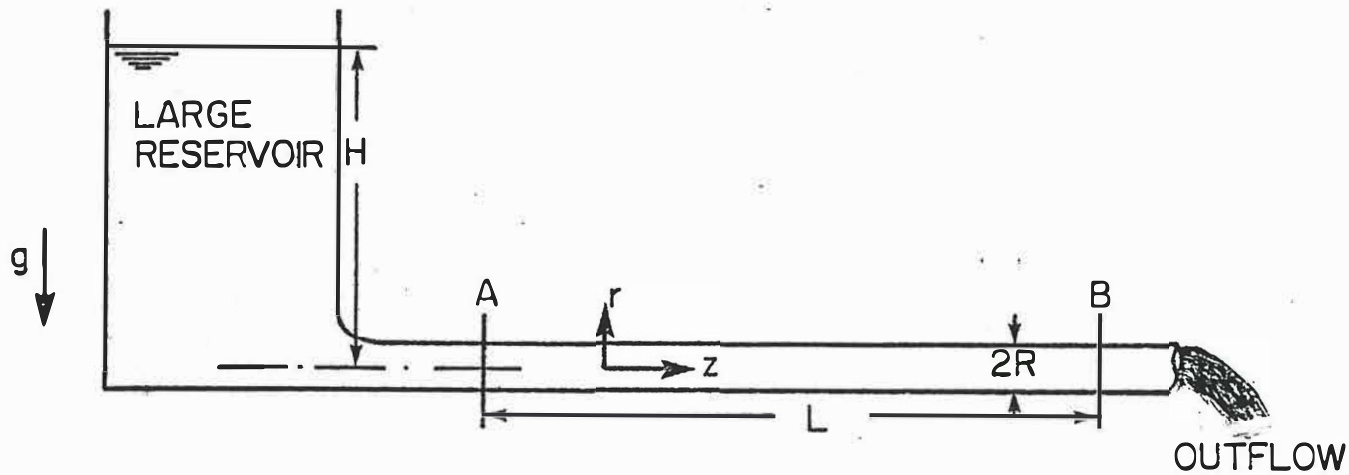

Fig. 7.15 Pressure-driven flow in a horizontal tube

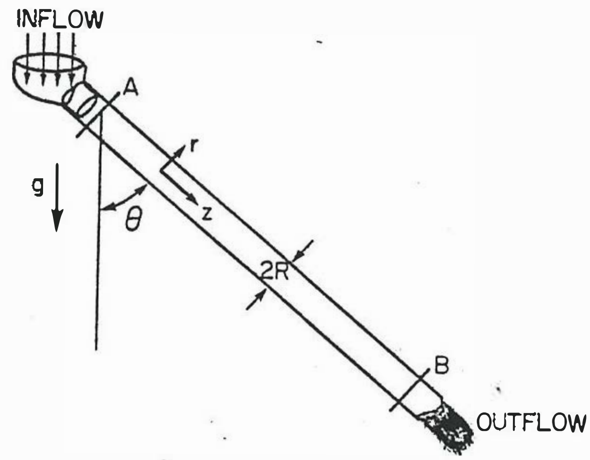

Fig. 7.16 Flow in a tube under the influence of gravity

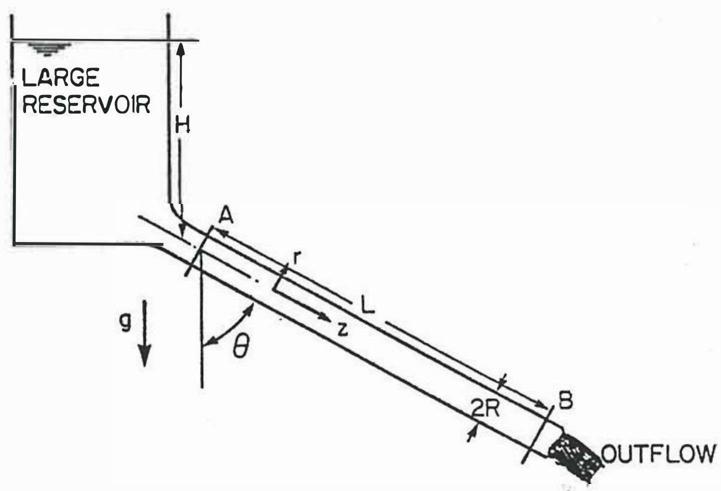

Fig. 7.17 Flow in an inclined tube under the influence of a pressure gradient

Since

$$\frac{\partial p}{\partial z} = \text{const} = \mu \left[\frac{1}{r}\frac{\partial}{\partial r}\left(r\frac{\partial v_z}{\partial r}\right)\right] \tag{7.162}$$

We have

$$\frac{\partial p}{\partial z} = \frac{dp}{dz} = -\frac{\rho gH}{L} \tag{7.163}$$

The velocity boundary conditions are

$$\begin{aligned} r &= 0 \qquad \frac{\partial v_z}{\partial r} = 0 \\ r &= R \qquad v_z = 0 \end{aligned} \tag{7.164}$$

The velocity profile can be expressed by the equation of a parabola (see section 7.3).

(b) Tube flow due to gravity

There is no externally imposed pressure gradient in this case, if we neglect the liquid in the funnel shown in Fig. 7.16. The fluid flows under the influence of gravity. The pressure difference (hydrostatic) between A and B is accounted for by the gravity term ρg_z.

The z component of momentum reduces to

$$0 = \mu \left[\frac{1}{r}\frac{\partial}{\partial r}\left(r\frac{\partial v_z}{\partial r}\right)\right] + \rho g_z \qquad (g_z = g\cos\theta) \tag{7.165}$$

The boundary conditions are

$$\begin{aligned} r &= 0 \qquad \frac{\partial v_z}{\partial r} = 0 \\ r &= R \qquad v_z = 0 \end{aligned} \tag{7.166}$$

The velocity profile can be easily determined (parabolic).

(c) Combined pressure and gravity flow in a tube

This is a mere combination of the previous two problems as shown in

Fig. 7.17. The flow in the tube is due to the (hydrostatic) pressure gradient imposed by the reservoir and to gravity.

The z component of momentum reduces to

$$0 = -\frac{\partial p}{\partial z} + \mu\left[\frac{1}{r}\frac{\partial}{\partial r}\left(r\frac{\partial v_z}{\partial r}\right)\right] + \rho g_z \quad (g_z = g\cos\theta) \qquad (7.167)$$

We note that

$$\begin{aligned} z &= 0 \qquad p = p_A = \rho g H + p_{atm} \\ z &= L \qquad p = p_B = p_{atm} \end{aligned} \qquad (7.168)$$

Since

$$\frac{\partial p}{\partial z} = \text{const} = \mu\left[\frac{1}{r}\frac{\partial}{\partial r}\left(r\frac{\partial v_z}{\partial r}\right)\right] + \rho g\cos\theta \qquad (7.169)$$

We have

$$\frac{\partial p}{\partial z} = \frac{dp}{dz} = -\frac{\rho g H}{L} \qquad (7.170)$$

The velocity boundary conditions are

$$\begin{aligned} r &= 0 \qquad \frac{\partial v_z}{\partial r} = 0 \\ r &= R \qquad v_z = 0 \end{aligned} \qquad (7.171)$$

Integration of equation (7.169) yields a parabolic velocity profile.

7.14 DIAMETER OF A FREE LIQUID JET

Whenever a liquid jet emerges from a tube into air its diameter (d) is generally not equal to the tube diameter (D). For low Reynolds number flows (Re<10) the jet swells and the diameter ratio d/D may reach a value of 1.13 for Newtonian fluids. For non-Newtonian fluids the observed swelling is much larger with d/D values between 1.5 and 3.0 being common for molten polymers (see extrudate swell in the chapter on non-Newtonian flow). For a larger Reynolds number the diameter of the jet becomes smaller than that of the tube. We will now use the one-dimensional approach to determine the reduction in the diameter of the jet. We note that we are interested in the overall diameter change and not in the detailed flow structure. This problem can therefore be classified as a macroscopic one.

We consider a liquid emerging from a long horizontal tube as shown in Fig. 7.18. The liquid has a parabolic velocity profile inside the tube. In the free jet the velocity profile is practically flat because the resistance to flow at the liquid-air interface is negligible.

The principle of conservation of mass gives

$$\iint_{tube} \rho \, v_z dA = \iint_{jet} \rho \, v_z dA \tag{7.172}$$

or

$$V_{avg} \frac{\pi D^2}{4} = V_j \frac{\pi d^2}{4} \tag{7.173}$$

which reduces to

$$V_{avg} \, D^2 = V_j d^2 \tag{7.174}$$

The principle of conservation of momentum (for steady flow and in the absense of external forces) gives

$$\iint_{tube} \rho \, v_z^2 dA = \iint_{jet} \rho \, v_z^2 dA \tag{7.175}$$

or

$$\int_o^{2\pi} \int_o^R v_z^2 \, r dr d\theta = V_j^2 \frac{\pi d^2}{4} \tag{7.176}$$

Since $v_z = 2V_{avg} \, [1 - (\frac{r}{R})^2]$ we get

$$\frac{4}{3} V_{avg}^2 \, D^2 = V_j^2 d^2 \tag{7.177}$$

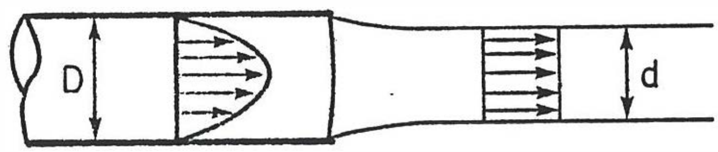

Fig. 7.18 . Liquid jet emerging from a tube

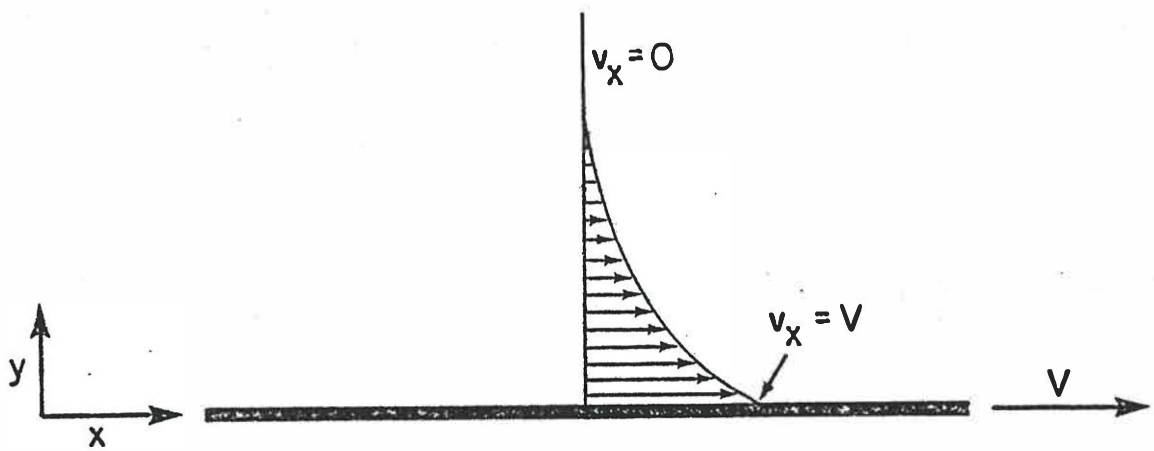

Fig. 7.19 Flow near a plate suddenly set in motion at velocity V

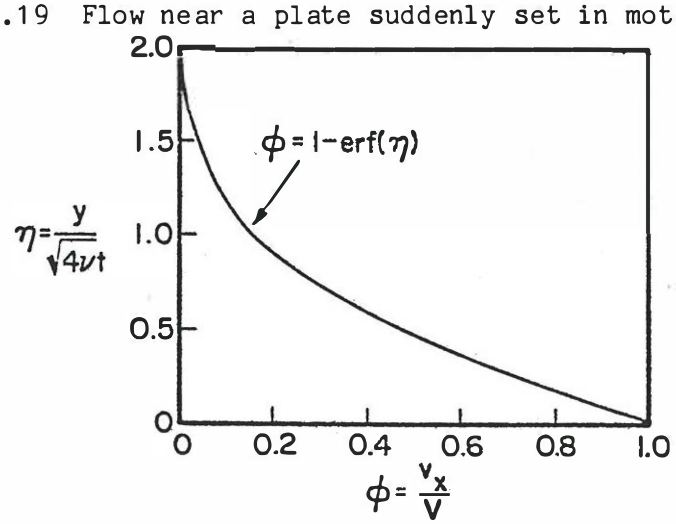

Fig. 7.20 Dimensionless velocity profile near a plate suddenly set in motion

Using equation (7.174) to eliminate the velocities we obtain a diameter ratio

$$\frac{d}{D} = \frac{\sqrt{3}}{2} = 0.87 \qquad (7.178)$$

This result is close to experimental observations for Reynolds numbers in the neighborhood of 100. For smaller Reynolds numbers the approach followed in this section is not valid because the velocity profile changes substantially before the end of the tube. Note also that under certain conditions surface tension becomes important.

7.15 FLOW NEAR A PLATE SUDDENLY SET IN MOTION

We consider the flow in the immediate vicinity of a plate which is adjacent to a large body of a fluid. For all time $t \leq 0$ the plate is stationary. At time $t=0^+$ the plate is set in motion at velocity V in the positive x direction. Because of the no-slip condition the plate drags along part of the fluid as shown in Fig. 7.19.
In this case the flow is one-dimensional and unsteady, that is

$$v_x = v_x\,(y,t) \text{ and } v_y = v_z = 0$$

It is clearly a drag flow situation without an external pressure gradient. For an incompressible, Newtonian fluid the Navier-Stokes equations reduce to

x component $$\rho \frac{\partial v_x}{\partial t} = \mu \frac{\partial^2 v_x}{\partial y^2} \qquad (g_x = 0) \qquad (7.179)$$

y component $$0 = -\frac{\partial p}{\partial y} + \rho g_y \qquad (g_y = -g) \qquad (7.180)$$

z component $$0 = -\frac{\partial p}{\partial z} \qquad (g_z = 0) \qquad (7.181)$$

Equations (7.180) and (7.181) describe merely the static equilibrium in y and z directions respectively. Equation (7.179) is a partial differential equation which may be solved to give the velocity v_x as a function of position y and time t.

The initial and boundary conditions are

$$\begin{aligned}
&\text{I.C.:} && v_x = 0 \text{ at } t = 0 \text{ for } y \geq 0 \\
&\text{B.C.1:} && v_x = V \text{ at } y = 0 \text{ for } t > 0 \\
&\text{B.C.2:} && v_x = 0 \text{ at } y = \infty
\end{aligned} \tag{7.182}$$

To solve equation (7.179) we will introduce a <u>similarity transformation</u> (for more on similarity see Chapter 8, Laminar Boundary Layers).

The kinematic viscosity is defined as $\nu = \mu/\rho$, thus equation (7.179) may be written as

$$\frac{\partial v_x}{\partial t} = \nu \frac{\partial^2 v_x}{\partial y^2} \tag{7.183}$$

Let us now define a relative distance $\eta = \dfrac{y}{\sqrt{4\nu t}}$

We assume that a solution can be found in the form

$$\frac{v_x}{V} = \phi(\eta) \tag{7.184}$$

Thus, we have

$$\frac{\partial v_x}{\partial t} = \frac{dv_x}{d\eta}\frac{d\eta}{dt} = -V\phi' \frac{y}{2t\sqrt{4\nu t}} \tag{7.185}$$

$$\frac{\partial v_x}{\partial y} = \frac{dv_x}{d\eta}\frac{d\eta}{dy} = V\phi' \frac{1}{\sqrt{4\nu t}} \tag{7.186}$$

$$\frac{\partial^2 v_x}{\partial y^2} = \frac{d}{dy}\left(\frac{\partial v_x}{\partial y}\right)\frac{d\eta}{dy} = V\phi'' \frac{1}{4\nu t} \tag{7.187}$$

Substituting these expressions into equation (7.183) we get

$$- V\phi' \frac{y}{2t\sqrt{4\nu t}} = \nu V\phi'' \frac{1}{4\nu t} \tag{7.188}$$

which simplifies to the ordinary differential equation

$$\phi'' + 2\eta\phi' = 0 \tag{7.189}$$

The initial and boundary conditions in terms of the new variable η are

$$\begin{array}{lll} \text{B.C.1:} & \text{at } \eta = 0 & \phi = 1 \\ \text{I.C.+B.C.2:} & \text{at } \eta = \infty & \phi = 0 \end{array} \tag{7.190}$$

A first integration of equation (7.189) gives

$$\phi' = C_1 e^{-\eta^2} \tag{7.191}$$

and a second integration yields a general solution in the form

$$\phi = C_1 \int_o^\eta e^{-\eta^2} d\eta + C_2 \tag{7.192}$$

Using the boundary condition $\eta = 0$ $\phi = 1$, we obtain

$$C_2 = 1 \tag{7.193}$$

Thus

$$\phi = C_1 \int_o^\eta e^{-\eta^2} d\eta + 1 \tag{7.194}$$

From boundary condition $\eta = \infty$ $\phi = 0$, we obtain

$$\phi = C_1 \int_o^\infty e^{-\eta^2} d\eta + 1 \tag{7.195}$$

The value of the definite integral $\int_o^\infty e^{-\eta^2} d\eta = (\sqrt{\pi}/2)$ can be found in standard tables of integrals (e.g. reference [3]).

Thus, we have

$$C_1 = -\frac{2}{\sqrt{\pi}} \tag{7.196}$$

and the solution can be expressed as

$$\phi = 1 - \frac{2}{\sqrt{\pi}} \int_0^{\eta} e^{-\eta^2}\, d\eta \tag{7.197}$$

The quantity $\frac{2}{\sqrt{\pi}} \int_0^{\eta} e^{-\eta^2}\, d\eta$ is the so-called "error function" and is denoted by $erf(\eta)$. The error function is tabulated in standard mathematical tables (e.g. reference [3]). A plot of the dimensionless velocity profile

$$\frac{v_x}{V} = 1 - erf\left(\frac{y}{\sqrt{4\nu t}}\right) \tag{7.198}$$

is given in Fig. 7.20.

7.16 UNSTEADY FLOW BETWEEN PARALLEL PLATES

An incompressible, Newtonian fluid is flowing between two long, horizontal, parallel plates separated by a distance 2b. This is again a pressure-driven flow (see section 7.2) with the additional assumption that the pressure gradient changes which means that the flow is unsteady. We wish to determine the velocity profiles as a function of time i.e. $v_x=v_x(y,t)$. To do that we must know the initial velocity profile and how the pressure changes as a function of time. Two problems will be examined: (a) Sudden removal of a pressure gradient and (b) Sudden imposition of a pressure gradient.

(a) Sudden removal of a pressure gradiennt

The flow is initially steady and fully developed under the influence of a constant pressure gradient. The velocity profile (from section 7.2) can be expressed as

$$v_x = \frac{3}{2} V_{avg} \left[1 - \left(\frac{y}{b}\right)^2\right] \tag{7.199}$$

At time $t = 0^+$ the pressure gradient is removed. The governing equation of motion is

$$\frac{\partial v_x}{\partial t} = \nu \frac{\partial^2 v_x}{\partial y^2} \tag{7.200}$$

The initial and boundary conditions are

$$\text{I.C.} \qquad v_x = \frac{3}{2} V_{avg} \left[1 - \left(\frac{y}{b}\right)^2\right] \quad \text{at } t=0 \tag{7.201}$$

$$\text{B.C.1} \qquad v_x = 0 \qquad \text{at } y=b \text{ for all } t\geq 0$$

$$\text{B.C.2} \qquad v_x = 0 \qquad \text{at } y=-b \text{ for all } t\geq 0$$

The solution to this problem can be obtained by the method of <u>separation of variables</u> [4]. The result is

$$\frac{v_x}{V_{avg}} = \frac{48}{\pi^3} \sum_{n=0}^{\infty} \frac{(-1)^n}{(2n+1)^3} \cos \frac{(2n+1)\pi}{2} \frac{y}{b} \exp\left[-\frac{(2n+1)^2 \pi^2 \nu}{4b^2} t\right] \tag{7.202}$$

Several velocity profiles are given in Fig. 7.21 for different values of $\nu t/b^2$. Initially the velocity profile is parabolic and becomes more "flat" as time progresses. For $t\to\infty$ there will be no flow and $v_x=0$ throughout.

(b) <u>Sudden imposition of a pressure gradient</u>

Here the fluid is initially at rest and at time $t=0^+$ a constant pressure gradient is imposed. The governing equation of motion is

$$\frac{\partial v_x}{\partial t} = -\frac{1}{\rho} \frac{\partial p}{\partial x} + \nu \frac{\partial^2 v_x}{\partial y^2} \tag{7.203}$$

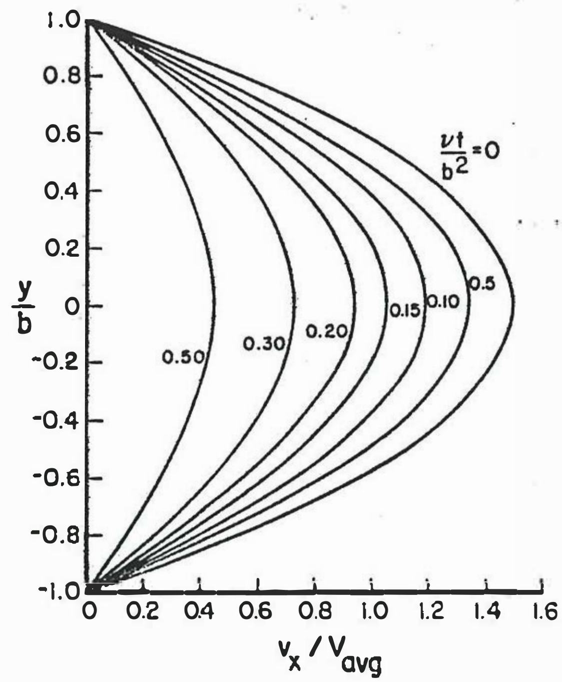

Fig. 7.21 Dimensionless velocity profiles for unsteady flow between two parallel plates with sudden removal of the pressure gradient.

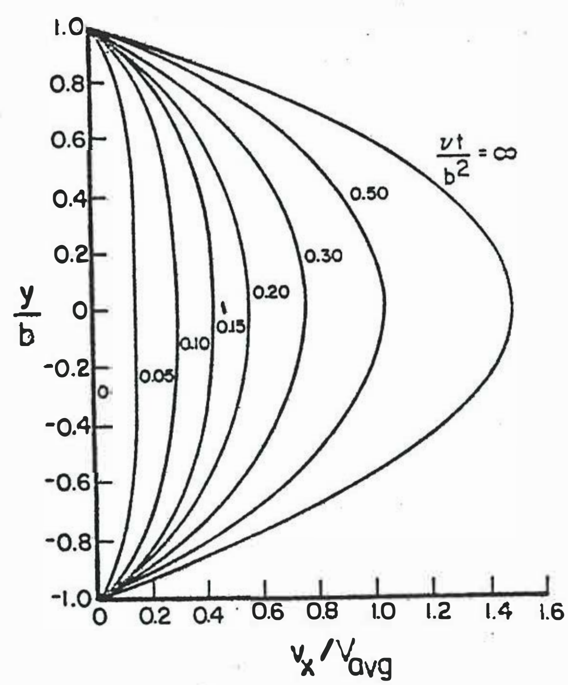

Fig. 7.22 Dimensionless velocity profiles for unsteady flow between two parallel plates with sudden imposition of a pressure gradient.

The initial and boundary conditions are

$$
\begin{array}{llll}
\text{I.C.} & v_x = 0 & \text{at } t=0 & \text{for } -b \le y \le b \\
\text{B.C.1} & v_x=0 & \text{at } y=b & \text{for all } t \ge 0 \\
\text{B.C.2} & v_x=0 & \text{at } y=-b & \text{for all } t \ge 0
\end{array}
\tag{7.204}
$$

Again the method of separation of variables can be used. The velocity profiles are expressed, in terms of V_{avg} for steady flow, in the form

$$
\frac{v_x}{V_{avg}} = \frac{3}{2}\left[1 - \left(\frac{y}{b}\right)^2\right] - \frac{48}{\pi^3}\sum_{n=0}^{\infty} \frac{(-1)^n}{(2n+1)^3} \cos\left[\frac{(2n+1)\pi}{2}\,\frac{y}{b}\right] \exp\left[-\frac{(2n+1)\pi^2 \nu}{4b^2} t\right]
\tag{7.205}
$$

Several velocity profiles are given in Fig. 7.22 for different values of $\nu t/b^2$. Initially the velocity is zero everywhere. As time progresses a profile develops which looks more and more like a parabola. For $t \to \infty$ the steady-state parabolic profile is obtained.

The unsteady one-dimensional flow problems, like those of sections 7.15 and 7.16, are governed by exactly the same equations that describe one-dimensional unsteady heat conduction in solids. Generally the method of separation of variables is used to obtain solutions. A book by Carslaw and Jaeger [5] contains a very large number of solutions of such problems. Many heat conduction solutions can be applied directly to flow problems by noting that velocity (v_x) corresponds to temperature (T), kinematic viscosity (ν) corresponds to thermal diffusivity (α) and the pressure gradient corresponds to heat generation.

7.17 THE USUAL TYPES OF BOUNDARY CONDITIONS

In this section we summarize the various types of boundary conditions which were used in the determination of the solutions for the problems examined in this chapter. u denotes the velocity component in the direction of flow and y is perpendicular to the direction of flow.

(a) FLUID-SOLID INTERFACE

The fluid takes the velocity of the solid wall (no-slip condition). This velocity will be either zero or will have a certain value V (constant or varying with time).

B.C.(a): $$u = 0 \quad \text{or} \quad u = V \tag{7.206}$$

(b) LIQUID-LIQUID INTERFACE

At the interface of two immiscible liquids A and B the velocities and shear stresses from both sides must be respectively identical.

B.C.(b1): $$u_A = u_B \tag{7.207}$$

B.C.(b2): $$\tau_A = \tau_B \tag{7.208}$$

The equality of shear stress (B.C.(b2)) implies the following relation in terms of the velocity gradients:

B.C.(b2): $$\mu_A \left(\frac{du_A}{dy}\right) = \mu_B \left(\frac{du_B}{dy}\right) \tag{7.209}$$

(c) LIQUID-GAS INTERFACE

The velocity of the liquid at the interface must be equal to the velocity of the gas $u_L = u_G$ and the shear stress from the liquid phase must be equal to the shear stress from the gas phase, $\tau_L = \tau_G$. We would normally be interested in determining the velocity profile in the liquid. Since the gas velocity will generally be unknown, the boundary condition $u_L = u_G$ provides no information. The equality of shear stresses may be rewritten as

B.C.(c): $$\mu_L \left(\frac{\partial u_L}{\partial y}\right) = \mu_G \left(\frac{\partial u_G}{\partial y}\right) \tag{7.210}$$

For many practical problems $\mu_L >> \mu_G$ and the above expression simply reduces to

B.C.(c): $$\frac{\partial u_L}{\partial y} = 0 \tag{7.211}$$

Note that in the study of wind driven currents in lakes and oceans equation (7.210) rather than (7.211) is used (see chapter on open channel flows).

(d) AXIS OR PLANE OF SYMMETRY

For symmetrical flows, at the axis (or plane) of symmetry the derivative must be zero.

B.C.(d): $$\frac{\partial u_x}{\partial y} = 0 \tag{7.212}$$

(e) FAR FROM THE SOURCE OF MOTION IN INFINITE FLUID

In section 7.15 (plate suddenly set in motion), we noted that at large distances from the plate the velocity is zero.

B.C.(e): $$y \to \infty \quad u = 0 \tag{7.213}$$

It is possible, however, that the outside fluid has a velocity of its own (free stream velocity V_∞) not connected with the impulsive plate motion. Thus, we may generalize to

B.C.(e): $$y \to \infty \quad u = V_\infty \tag{7.214}$$

This type of boundary condition is particularly common in boundary layer flows which are discussed in Chapter 9.

7.18 SOME NUMERICAL EXAMPLES

Example 7.18.1

Determine the pressure drop for each 100m of length for flow of an oil (μ=0.1 Pa•s, S.G.=0.9) through a pipe having a diameter of 5 cm, when the volume rate of flow is 200 liters per minute.

Solution

We must first examine whether the flow is laminar

$$Re = \frac{\rho \, V_{avg} \, D}{\mu}$$

$$V_{avg} = \frac{Q}{A} = \frac{(0.2 m^3)/(60 \ s)}{\pi(5x10^{-2})^2 \ m^2/4} = 1.70 \ m/s$$

and

$$Re = \frac{(900 \ kg/m^3) \times (1.70 \ m/s) \times (5 \times 10^{-2} m)}{0.1 \ N \cdot s/m^2} = 765$$

Since Re < 2100 the flow in the pipe is indeed laminar. We can therefore use the Hagen-Poiseuille formula (eq. 7.61) which gives

$$\Delta p = Q \frac{8 \mu L}{\pi R^4}$$

Introducing the numerical values, we get

$$\Delta p = (\frac{0.2 \ m^3}{60 \ \ s}) \frac{8 \times (0.1 \ N \cdot s/m^2) \times (100m)}{\pi \times (\frac{5}{2} \times 10^{-2} \ m)^4}$$

$$= 217409 \ N/m^2 = 217.4 \ kPa$$

Example 7.18.2

A common method for measuring viscosity (particularly of oils and polymer solutions) requires the determination of the time needed for a certain quantity of the fluid to flow through a capillary tube under the influence of a pressure gradient which is held nearly constant. If the flow in the tube is laminar and the tube is relatively long the Hagen-Poiseuille formula (eq. 7.61) applies. To illustrate this method let us consider a large reservoir and a capillary outlet tube having a diameter of 2mm, as shown in Fig. E.18.2. We will determine the absolute (μ) and kinematic viscosity ($\nu = \mu/\rho$) if 7.5 cm^3 of the fluid flow through the tube per minute and the density is $\rho = 0.9 \ g/cm^3$.

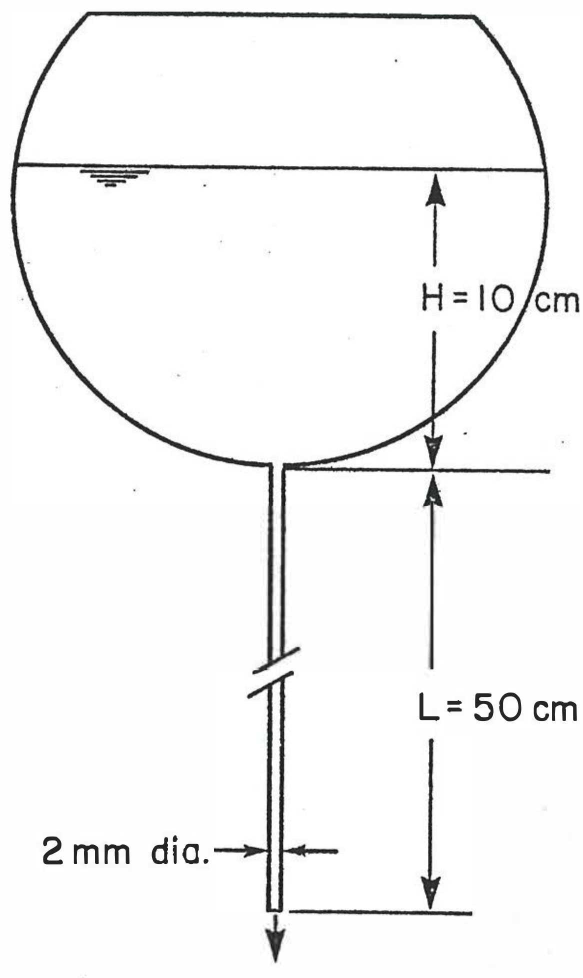

Fig. E.18.2

Solution

The Hagen-Poiseuille formula is

$$Q = \frac{\pi(\Delta p)}{8\mu L} R^4$$

Here, the pressure drop Δp consists of two parts: the externally imposed pressure $\Delta p_1 = \rho g H$ and the hydrostatic pressure in the tube $\Delta p_2 = \rho g L$. This result can be easily obtained by working out the solution for the case of combined pressure and gravity flow of section 7.13(c).

Thus, we have

$$Q = \frac{\pi(\rho g H + \rho g L)}{8\mu L} R^4$$

or

$$Q = \frac{\rho g \pi}{8\mu} \left(\frac{H}{L} + 1\right) R^4$$

The kinematic viscosity can be determined from

$$\nu = \frac{g\pi}{8Q} \left(\frac{H}{L} + 1\right) R^4$$

and the absolute viscosity from

$$\mu = \nu\rho$$

Introducing the numerical values, we have

$$\nu = \frac{9.81 \ (m/s^2)\pi}{8 \times \frac{7.5\times 10^{-6}}{60} \ m^3/s} \times \left(\frac{0.10}{0.50} + 1\right) \times (10^{-3} m)^4$$

$$= 36.96 \times 10^{-6} \ m^2/s = 3.69 \times 10^{-5} \ m^2/s$$

$$\mu = (36.96 \times 10^{-6} \ m^2/s) \times (900 \ kg/m^3)$$

$$= 0.033 \ N\cdot s/m^2 = 0.033 \ Pa\cdot s$$

Example 7.18.3

Oil having an absolute viscosity $\mu = 0.1$ Pa•s, ρ=0.9 g/cm^3 flows over a flat plate inclined at an angle $\theta = 30^o$ to the vertical. The thickness of the film formed is 5mm. Determine the maximum velocity and the Reynolds number.

Solution

We use equation (7.106)

$$V_{max} = \frac{\rho g\ \delta^2 \cos\theta}{2\mu}$$

$$= \frac{(900\ kg/m^3) \times (9.81\ m/s^2) \times (5\times10^{-3} m)^2\ \cos 60^o}{2 \times 0.1\ N\bullet 3/m^2}$$

$$= 0.55\ m/s$$

The Reynolds number is

$$Re = \frac{\rho\ V_{avg}\ \delta}{\mu}$$

Using equation (7.107) we have

$$V_{avg} = \frac{\rho g\ \delta^2 \cos\theta}{3\mu}$$

which means that $V_{avg} = \frac{2}{3} V_{max} = 0.37$ m/s

Thus, the Reynolds number is

$$Re = \frac{(900\ kg/m^3) \times (0.37\ m/s) \times (5\times10^{-3} m)}{10^{-2}\ N\bullet s/m^2} = 166$$

Note that the flow is laminar for falling liquid films when the Reynolds number is less than about 500.

Example 7.18.4

We will now re-examine example 1.2 without using the flat plate approximation for the 25 cm long shaft, D_i = 5cm, which rotates in a journal, D_o = 5.03 cm (μ = 4 x 10^{-2} Pa•s and N = 1800 rpm).

Solution

The torque exerted by the rotating shaft is given by equation (7.132)

$$T_o = \frac{4\pi\mu L R_i^2 \Omega}{1 - (\frac{R_i}{R_o})^2}$$

where R_i = 2.5 cm, R_o = 2.515 cm, $\Omega = 2\pi N$

Thus,

$$T_o = \frac{4\pi \times (4\times10^{-2} N\cdot s/m^2) \times (0.25 m) \times (2.5\times10^{-2} m)^2 \times 2\pi(1800/60s)}{1 - (\frac{2.50}{2.515})^2}$$

$$= 1.244 \text{ N}\cdot\text{m}$$

This result is very close to the value obtained (1.232 N•m) by making use of the two flat plates approximation because the gap is very narrow.

REFERENCES

[1] H. Schlichting, "Boundary Layer Theory", McGraw-Hill, 6th ed., New York (1968).

[2] R.B. Bird, W.E. Stewart and E.N. Lightfoot, "Transport Phenomena", Wiley, New York (1960).

[3] R.V. Churchill, "Fourier Series and Boundary Value Problems", McGraw-Hill, ed., (19).

[4] W.H. Beyer (Ed.), "Standard Mathematical Tables", The Chemical Rubber Co., 25th ed., (1978).

[5] H.S. Carslaw and J.C. Jaeger, "Conduction of Heat in Solids", Oxford University Press, 2nd ed., (1959).

John Vlachopoulos, *Fundamentals of Fluid Mechanics*
Chem. Eng., McMaster University, Hamilton, ON, Canada
(First Edition 1984, revised internet edition (2016), www.polydynamics.com)

CHAPTER 8

LOW REYNOLDS NUMBER FLOW

8.1 INTRODUCTION

It is evident from Chapter 7 that the Navier-Stokes equations must be simplified before solution of certain simple flow problems is attempted. In this chapter, we consider a special class of viscous flow problems having low Reynolds number ($Re = \rho VL/\mu$). We have noted that the Reynolds number expresses the relative magnitude of inertia to viscous forces. Consequently, for $Re \ll 1$ the inertia terms can be eliminated from the Navier-Stokes equations (6.90, 6.91 and 6.92). For incompressible steady flow of a Newtonian fluid, we have

continuity
$$\frac{\partial v_x}{\partial x} + \frac{\partial v_y}{\partial y} + \frac{\partial v_z}{\partial z} = 0 \tag{8.1}$$

momentum
$$0 = -\frac{\partial p}{\partial x} + \mu\left(\frac{\partial^2 v_x}{\partial x^2} + \frac{\partial^2 v_x}{\partial y^2} + \frac{\partial^2 v_x}{\partial z^2}\right) + \rho g_x \tag{8.2}$$

$$0 = -\frac{\partial p}{\partial y} + \mu\left(\frac{\partial^2 v_y}{\partial x^2} + \frac{\partial^2 v_y}{\partial y^2} + \frac{\partial^2 v_y}{\partial z^2}\right) + \rho g_y \tag{8.3}$$

$$0 = -\frac{\partial p}{\partial z} + \mu\left(\frac{\partial^2 v_z}{\partial x^2} + \frac{\partial^2 v_z}{\partial y^2} + \frac{\partial^2 v_z}{\partial z^2}\right) + \rho g_z \qquad (8.4)$$

or in Cartesian index notation

continuity $$\frac{\partial v_i}{\partial x_i} = 0 \qquad (8.5)$$

momentum $$0 = -\frac{\partial p}{\partial x_j} + \mu \frac{\partial^2 v_j}{\partial x_i^2} + \rho g_j \qquad (8.6)$$

and in vector notation

$$\nabla \cdot \bar{V} = 0 \qquad (8.7)$$

$$0 = -\nabla P + \mu \nabla^2 \bar{V} + \rho \bar{g} \qquad (8.8)$$

The gravity force term can be absorbed into the pressure term by introducing an equivalent pressure $P = p + \rho g h$ where h is measured upwards while the gravity acts downward i.e.

$$g_x = -g \frac{\partial h}{\partial x}, \quad g_y = -g \frac{\partial h}{\partial y}, \quad g_z = -g \frac{\partial h}{\partial z},$$

thus

$$0 = -\nabla P + \mu \nabla^2 \bar{V} \qquad (8.9)$$

This is the so-called creeping motion or Stokes flow equation. It is important to note the significant simplifications achieved by imposing the restriction $Re \ll 1$. The creeping motion equations represented by (8.9) are linear partial differential equations, whereas the Navier-Stokes equations are non-linear, because they contain the quadratic inertia terms. The restrictive condition $Re = \rho VL/\mu \ll 1$ implies that creeping motion does not necessarily require extremely small characteristic velocities. For highly viscous fluids like polymer melts we have $Re \ll 1$ even for relatively high velocities. Generally speaking low Reynolds number flows are encountered in several important technological applications. These include: processing of plastics and rubbers, processing of suspensions, emulsions, foam and powders, flotation and settling operations in mining engineering, flows of water or oil through porous soils and many others. There are two excellent books by Happel and Brenner [1] and Langlois [2] which are devoted exclusively to low Reynolds number flows.

Taking the divergence of equation (8.9), we have

$$0 = -\nabla \cdot \nabla P + \nabla \cdot (\nabla^2 \overline{V}) \tag{8.10}$$

or

$$0 = -\nabla^2 P + \nabla^2 (\nabla \cdot \overline{V}) \tag{8.11}$$

Since the fluid is assumed incompressible $\nabla \cdot \overline{V} = 0$, equation (8.11) becomes

$$\nabla^2 P = 0 \tag{8.12}$$

Thus, the pressure field $P(x,y,z)$ satisfies the Laplace equation and is, therefore, a harmonic function.

For <u>two-dimensional</u> creeping flows the equations of motion can be expressed in a particularly simple form by the introduction of the stream function Ψ, which is defined by

$$v_x = \frac{\partial \Psi}{\partial y} \qquad v_y = -\frac{\partial \Psi}{\partial x} \tag{8.13}$$

The two-dimensional continuity equation is automatically satisfied, because

$$\frac{\partial^2 \Psi}{\partial x \partial y} - \frac{\partial^2 \Psi}{\partial x \partial y} = 0 \tag{8.14}$$

The equations of motion are

$$0 = -\frac{\partial P}{\partial x} + \mu\left(\frac{\partial^2 v_x}{\partial x^2} + \frac{\partial^2 v_x}{\partial y^2}\right) \tag{8.15}$$

$$0 = -\frac{\partial P}{\partial y} + \mu\left(\frac{\partial^2 v_y}{\partial x^2} + \frac{\partial^2 v_y}{\partial y^2}\right) \tag{8.16}$$

By differentiating equation (8.15) with respect to y and equation (8.16) with respect to x and then subtracting, we find

$$\frac{\partial}{\partial y}\left(\frac{\partial^2 v_x}{\partial x^2}+\frac{\partial^2 v_x}{\partial y^2}\right)+\frac{\partial}{\partial x}\left(\frac{\partial^2 v_y}{\partial x^2}+\frac{\partial^2 v_y}{\partial y^2}\right)=0 \tag{8.17}$$

which, by the introduction of definitions (8.13), becomes

$$\frac{\partial^4 \Psi}{\partial x^4}+2\frac{\partial^4 \Psi}{\partial x^2\,\partial y^2}+\frac{\partial^4 \Psi}{\partial y^4}=0 \tag{8.18}$$

or, equivalently

$$\nabla^4 \Psi = 0 \tag{8.19}$$

Because of equation (8.19) the stream function Ψ is said to be biharmonic.

There are at least four different types of flow problems which are described by the creeping motion equations:

(a) Fully developed laminar flows. These problems were dealt with in Chapter 7, in the framework of what was referred to as unidirectional

(b) Laminar flows through narrow but variable width passages. (Sections 8.2 and 8.3). This class of problems comprise the so-called hydrodynamic lubrication theory, because it was first developed for the study of the lubrication mechanism of thin fluid films. Detailed expositions can be found in the books by Pinkus and Sternlicht [3] and Walowit and Anno [4].

(c) Creeping flows about immersed bodies. Starting with Stokes solution for flow around a sphere (see Sec. 8.4), many other problems have been treated in the relevant literature. A thorough treatment is presented in Happel and Brenner's book [1].

(d) Flow through porous media. (Sec. 8.5) These problems are important in the study of water or oil flow through porous soils and in fluid flow through process equipment like filters and catalyst beds. Specialized texts by Muskat [5], Scheidegger [6] and Dullien [7] cover most theoretical and practical aspects of this type of flow.

In the following sections of this chapter we present a detailed analysis of some classical low Reynolds number flow problems.

8.2 SQUEEZE FILM FLOW

A fluid of constant density ρ and viscosity μ is contained in the gap between two disks of radii R. The lower disk is stationary and the upper one is forced down slowly at a constant velocity V. As the gap between the disks decreases the fluid is squeezed out radially as shown in Fig. 8.1. We will determine the force F required to sustain disk velocity V and the time required for the disks to reach a distance h.

We assume that the flow is sufficiently slow so that fluid inertia effects can be neglected. Since there is no rotation, $v_\theta = 0$ and $\partial/\partial\theta = 0$. If Q is the volume rate of flow, the principle of conservation of mass gives

$$\pi r^2 V = Q = 2\pi r \int_o^h v_r \, dz \tag{8.20}$$

where V is the velocity of the upper disk and h is a function of time t.

For a sufficiently small gap h the main fluid motion is in the r direction. The flow field can, therefore, be determined by the r component of the equation of conservation of momentum for creeping motion, which is

$$0 = -\frac{\partial p}{\partial r} + \mu \left[\frac{\partial}{\partial r}\left(\frac{1}{r}(rv_r)\right) + \frac{\partial^2 v_r}{\partial z^2}\right] \tag{8.21}$$

We note that the pressure varies from a finite value at r = 0, to p = 0 at the edge of the disks (r = R). Thus, the flow occurs under the influence of a non-zero pressure gradient $\partial p/\partial r$. The first viscous term can be eliminated from equation (8.21) because the velocity change in the z direction is much larger than the change in the r direction. Thus, we have

$$0 = -\frac{\partial p}{\partial r} + \mu \frac{\partial^2 v_r}{\partial z^2} \tag{8.22}$$

The no-slip condition at lower and upper plates gives

$$\begin{aligned} v_r &= 0 \quad \text{at} \quad z = 0 \\ v_r &= 0 \quad \text{at} \quad z = h \end{aligned} \tag{8.23}$$

This problem is, therefore, mathematically identical to the pressure flow problem between two flat plates of Section 7.2. (Note that the horizontal axis, here, lies on the lower plate rather than on the midplane). Thus, the velocity profile is of the form

$$v_r = -\frac{1}{2\mu}\left(\frac{\partial p}{\partial r}\right)(zh - z^2) \tag{8.24}$$

By introducing v_r into equation (8.20) and performing the integration we find

$$\frac{\partial p}{\partial r} = -\frac{6\mu V r}{h^3} \tag{8.25}$$

By integrating this first-order differential equation with p = 0 at r = R, we get

$$p = \frac{3\mu V(R^2 - r^2)}{h^3} \tag{8.26}$$

We note that the pressure distribution is parabolic having a maximum at the center (r = 0).

The total force required to sustain the upper disk velocity V is

$$F = \int_o^{2\pi}\int_o^R p r dr d\theta = 2\pi \int_o^R \frac{3\mu V(R^2 - r^2)}{h^3} r dr$$

which gives

$$F = \frac{3\pi\mu V R^4}{2h^3} \tag{8.27}$$

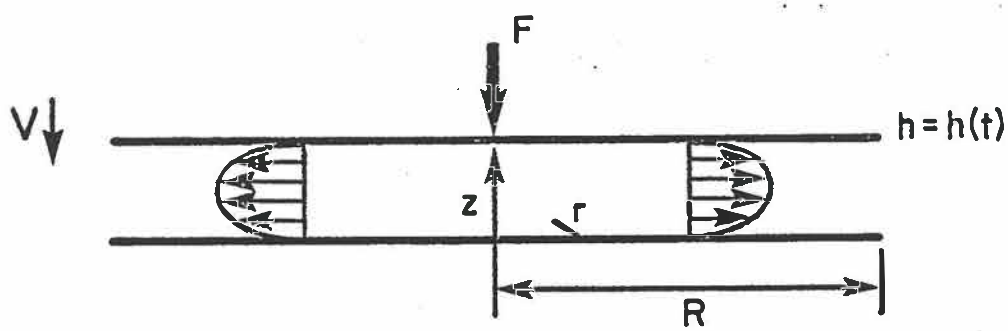

Fig. 8.1: Squeeze film flow between two parallel disks.

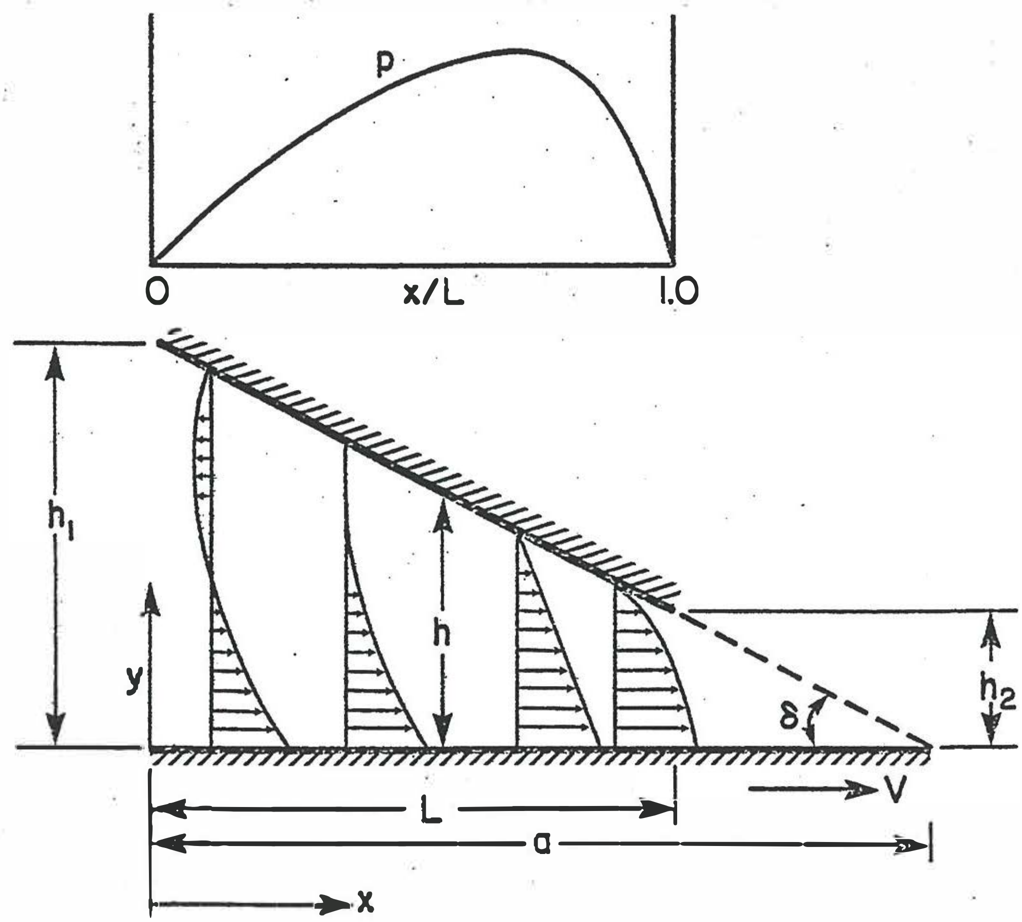

Fig. 8.2: Velocity and pressure distributions in the slider bearing problem.

The disk velocity can be expressed as

$$V = -\frac{dh}{dt} \tag{8.28}$$

where the minus sign is needed because the plate moves downwards, while the positive z direction is upwards. Thus, we may write

$$\frac{dh}{dt} = -\frac{2F}{3\pi\mu R^4} h^3 \tag{8.29}$$

and integrating by assuming h = H at t = 0, we get

$$h = \left(\frac{1}{H^2} + \frac{4Ft}{3\pi\mu R^4}\right)^{-1/2} \tag{8.30}$$

This equation is known as the Stefan equation. More details on the squeeze film flow problem can be found elsewhere [8,9].

8.3 THE SLIDER BEARING PROBLEM

Films of lubricants are usually found between two solid objects which are supposed to stay apart. The most common application is in lubricated bearings. To keep the bearing surfaces apart the film must be capable of sustaining forces normal to these surfaces. Imposition of a high pressure from an external source can generate the normal forces required. This is known as hydrostatic lubrication. More often, however, the load carrying capacity is generated by the lateral motion at the two surfaces (slider bearings). It should also be noted that the squeeze film flow has a load carrying capacity as shown in Section 8.2, because of the relative surface motion. These types of lubrication are known as hydrodynamic lubrication. Here, we focus our attention to load carrying capacity due to lateral motion of the bearing surfaces.

If the two surfaces are parallel and one is stationary while the other moves, we have the classical drag flow problem (Sec. 7.5). In such a case the same pressure acts uniformly over the entire surfaces. Consequently, such a configuration has no load carrying capacity. To generate a pressure between the two surfaces the width must be variable. Figure 8.2 shows a greatly exaggerated angle between the two slider bearing surfaces. The upper surface is stationary while the lower one moves at a constant velocity V.

For slightly inclined surfaces the equation of momentum in x direction should be identical to that describing combined pressure and drag flow between parallel surfaces (Sec. 7.6). In this case, however, the pressure gradient is no longer constant. In the film between the two surfaces the pressure must reach a maximum and drop to the ambient value, say p_o, at the two edges. The flow rate between the surfaces must be the same at all x positions. Thus, we have

$$q = \int_0^{h(x)} v_x dy = \text{const} \tag{8.31}$$

where q = Q/W is the flow rate per unit width. The momentum equation for creeping motion in the x direction simplifies to

$$\frac{\partial p}{\partial x} = \mu \frac{\partial^2 v_x}{\partial y^2} \tag{8.32}$$

The boundary conditions are

$$\begin{aligned} y &= 0 \quad & v_x &= V \\ y &= h \quad & v_x &= 0 \\ x &= 0 \quad & p &= p_o \\ x &= L \quad & p &= p_o \end{aligned} \tag{8.33}$$

The velocity profile must, therefore, be identical to that of Section 7.6.

$$v_x = \frac{V}{h}(h-y) - \frac{1}{2\mu}\frac{dp}{dx}y(h-y) \tag{8.34}$$

and

$$q = \frac{Vh}{2} - \frac{h^3}{12\mu}\frac{dp}{dx} \tag{8.35}$$

Solving for dp/dx, we have

$$\frac{dp}{dx} = 12\,\mu\left(\frac{V}{2h^2} - \frac{q}{h^3}\right) \tag{8.36}$$

and integrating

$$p(x) = p_o + 6\mu V \int_o^x \frac{dx}{h^2} - 12\mu q \int_o^x \frac{dx}{h^3} \tag{8.37}$$

Introducing the boundary condition $p = p_o$ at $x = L$, we get an expression for the volume rate of flow per unit width

$$q = \frac{\int_o^L \frac{dx}{h^2}}{2 \int_o^L \frac{dx}{h^3}} \tag{8.38}$$

This means that q can be determined if the shape of the gap as expressed by $h = h(x)$ is known. For a wedge having two flat surfaces $h(x) = \delta(a-x)$ where a and δ are geometrical constants as shown in Fig. 8.2, we have

$$q = V\delta \frac{a(a-L)}{2a-L} \tag{8.39}$$

and

$$p(x) = p_o + 6\mu V \frac{x(L-x)}{\delta^2(a-x)^2(2a-L)} \tag{8.40}$$

Alternatively, introducing the two gap widths h_1 and h_2 and using the geometrical relations

$$\delta = (h_1 - h_2)/L \tag{8.41}$$

and

$$\frac{a}{L} = \frac{h_1}{h_1 - h_2} \tag{8.42}$$

we get

$$p(x) - p_o = \frac{6\mu VL}{h_1^2 - h_2^2} \frac{(h_1 - h)(h - h_2)}{h^2} \tag{8.43}$$

Thus, the net normal force acting on the upper surface for plate width W is

$$F_N = W \int_o^L (p(x) - p_o)\, dx$$

$$= \frac{6\mu VL^2}{(h_1-h_2)^2} W \left[\ln \left(\frac{h_1}{h_2}\right) - \frac{2(h_1 - h_2)}{h_1 + h_2}\right] \quad (8.44)$$

The force F_N has a maximum for $h_1/h_2 = 2.189$. Thus,

$$F_{N,max} = 0.1602 \frac{\mu VL^2}{h_2^2} W \quad (8.45)$$

The force required to pull the lower plate is

$$F_S = - W \int_o^L \mu\left(\frac{\partial v_x}{\partial y}\right)_{y=0} dx \quad (8.46)$$

The negative sign is needed because

$$\tau_{xy} = \mu\left(\frac{\partial v_x}{\partial y}\right)_{y=0}$$

is the stress exerted by the fluid on the plate. Introducing the previous geometrical relations, we get

$$F_S = \frac{\mu VLW}{(h_1 - h_2)} \left[4 \ln\left(\frac{h_1}{h_2}\right) - \frac{6(h_1 - h_2)}{h_1 + h_2}\right] \quad (8.47)$$

Then, for $h_1/h_2 = 2.189$, which corresponds to maximum upward force ($F_{N,max}$), we have

$$F_{S,max} = 0.754 \frac{\mu VL}{h_2} W \quad (8.48)$$

The ratio $F_{S,max}/F_{N,max}$ is a measure of the coefficient of friction of the bearing and is equal to $4.702\ h_2/L$. This can be made very small for sufficiently small h_2 values. Sketches of the pressure and velocity distributions are shown in Fig. 8.2.

Here are some typical numerical calculations per unit width W = 1m. For V = 10 m/s, L = 10 cm, $\mu = 10^{-1}$ Pa•s and h_2 = 0.1 mm, we get

$$F_{N,max} = 160{,}200 \text{ N}$$

$$F_{S,max} = 754 \text{ N}$$

and the coefficient of friction is

$$F_{S,max}/F_{N,max} = 0.0047$$

It is interesting to note for comparison that in the absence of a lubricant the coefficient of friction for two clean metal surfaces is of the order of 0.3 to 0.4.

For a slider bearing of finite width we must also consider the flow in the z direction where z is perpendicular to the plane of Fig. 8.2. Thus, the equation of continuity is

$$\frac{\partial v_x}{\partial x} + \frac{\partial v_z}{\partial z} = 0 \tag{8.49}$$

Integrating from y = 0 to y = h, we have

$$\frac{\partial}{\partial x} \int_0^h v_x dy + \frac{\partial}{\partial z} \int_0^h v_z dy = 0 \tag{8.50}$$

If U is the velocity of the boundary in the z direction, we would have an expression for the flow rate in the z direction analogous to that given by equation (8.35).

$$Q_z = \int_0^h v_z dy = \frac{Uh}{2} - \frac{h^3}{12\mu} \frac{\partial p}{\partial z} \tag{8.51}$$

By introducing equations (8.35) and (8.51) into equation (8.50) we get

$$\frac{\partial}{\partial x} (h^3 \frac{\partial p}{\partial x}) + \frac{\partial}{\partial z} (h^3 \frac{\partial p}{\partial z}) = 6\mu \left[\frac{\partial}{\partial z} (hV) + \frac{\partial}{\partial z} (hU)\right] \tag{8.52}$$

This is the so-called Reynolds lubrication equation. It is often the starting point for the study of lubrication in journal bearings of finite width and other configurations. For more information the reader is referred to Langlois [2], Massey [10] and Schlichting [11]. The more practical aspects of lubrication, in addition to the theoretical developments, may be found in the books by Pinkus and Sternlicht [3], Walowit and Anno [4] and Gross [12].

8.4 SLOW VISCOUS FLOW AROUND A SPHERE

We now consider the case of steady and slow viscous flow of an incompressible Newtonian fluid around a sphere as shown in Fig. 8.3. For this case the Reynolds number is defined by

$$Re = \frac{\rho\, V_\infty\, D}{\mu} \tag{8.53}$$

where D is the diameter of the sphere. When Re << 1 equation (8.19) is applicable, i.e.

$$\nabla^4 \Psi = 0 \tag{8.54}$$

In sperical coordinates r, θ, ϕ the stream function Ψ can be defined from the continuity equation, with ϕ-direction symmetry, which is

$$\frac{1}{r^2}\frac{\partial}{\partial r}(r^2\, v_r) + \frac{1}{r\sin\theta}\frac{\partial}{\partial\theta}(v_\theta \sin\theta) = 0 \tag{8.55}$$

This is satisfied automatically by setting

$$v_r = \frac{1}{r^2\sin\theta}\frac{\partial\Psi}{\partial\theta} \tag{8.56}$$

$$v_\theta = -\frac{1}{r\sin\theta}\frac{\partial\Psi}{\theta r} \tag{8.57}$$

It can be shown that in spherical coordinates, with ϕ-symmetry, equation (8.54) becomes

$$\left[\frac{\partial}{\partial r^2} + \frac{\sin\theta}{r^2}\frac{\partial}{\partial\theta}\left(\frac{1}{\sin\theta}\frac{\partial}{\partial\theta}\right)\right]^2 \Psi = 0 \tag{8.58}$$

The no-slip boundary conditions at the sphere surface are

$$r = R \qquad v_r = 0 = \frac{1}{r^2\sin\theta}\frac{\partial\Psi}{\partial\theta} \tag{8.59}$$

$$r = R \qquad v_\theta = 0 = -\frac{1}{r\sin\theta}\frac{\partial\Psi}{\partial r} \tag{8.60}$$

Far from the sphere, the velocity in the direction of the polar axis z, v_z, must approach the uniform velocity V_∞. Thus, by referring to Fig.

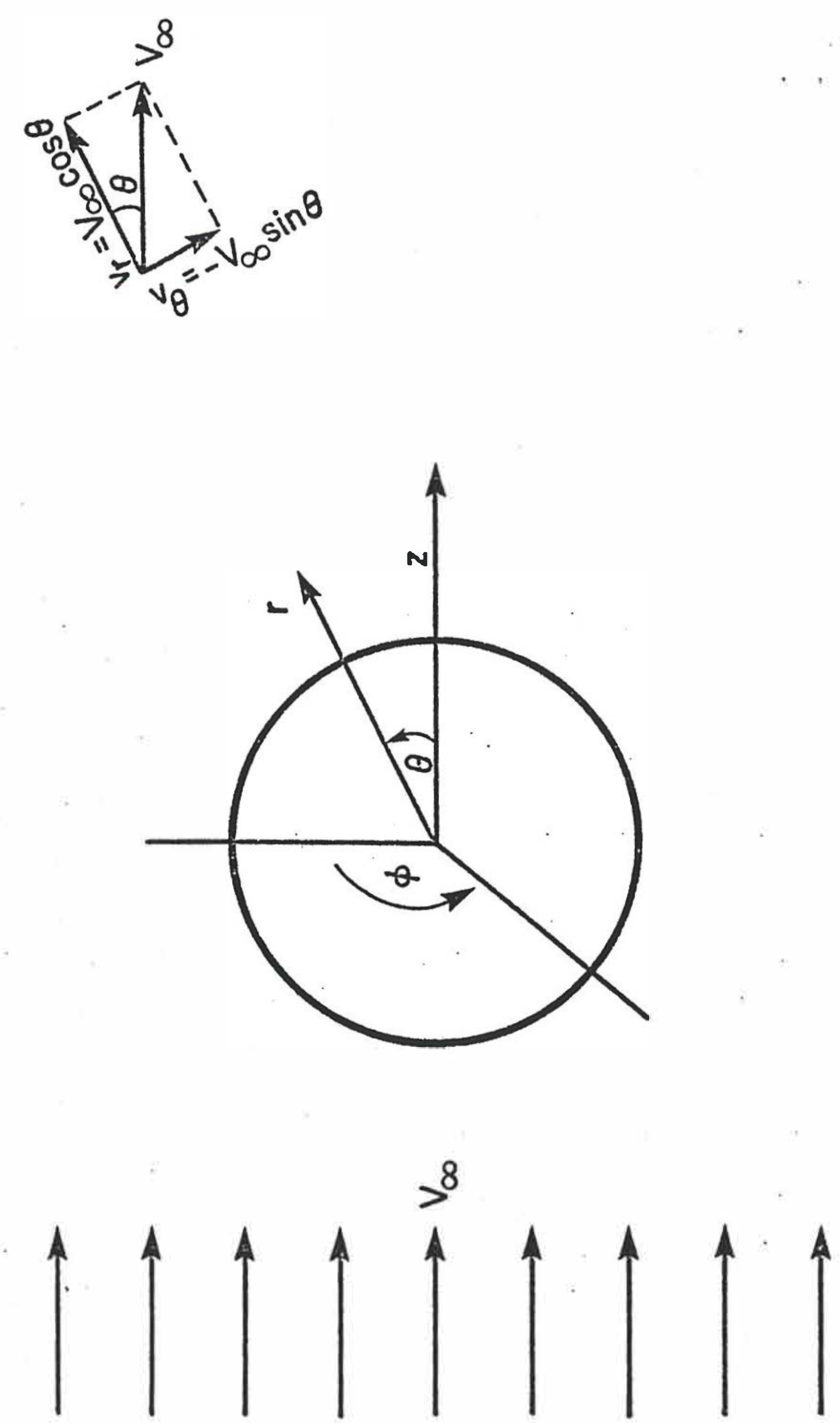

Fig. 8.3: Uniform flow past a sphere.

8.3, we have

$$r \to \infty \qquad v_r = V_\infty \cos\theta \quad \text{and} \quad v_\theta = -V_\infty \sin\theta \tag{8.61a}$$

or in terms of the stream function Ψ

$$\frac{1}{r^2 \sin\theta} \frac{\partial \Psi}{\partial \theta} = V_\infty \cos\theta \quad \text{and} \quad -\frac{1}{r\sin\theta} \frac{\partial \Psi}{\partial r} = -V_\infty \sin\theta \tag{8.61b}$$

and

$$\frac{\partial \Psi}{\partial \theta} = r^2 V_\infty \cos\theta \sin\theta \quad \text{and} \quad \frac{\partial \Psi}{\partial r} = r V_\infty \sin^2\theta \tag{8.62}$$

Integration yields

$$\Psi = \frac{r^2}{2} V_\infty \sin^2\theta + K(r) \quad \text{and} \quad \Psi = \frac{r^2}{2} V_\infty \sin^2\theta + K(\theta) \tag{8.63}$$

Thus,

$$\Psi = \frac{r^2}{2} V_\infty \sin^2\theta + \text{constant} \tag{8.64}$$

The arbitrary constant can be set equal to zero, and equation (8.58) can now be solved with boundary conditions (8.59), (8.60) and (8.64).

The condition (8.64) suggests a trial solution of the form

$$\psi = f(r) \sin^2\theta \tag{8.65}$$

which, when substituted into equation (8.58), yields

$$\left(\frac{d^2}{dr^2} - \frac{2}{r^2}\right)\left(\frac{d^2}{dr^2} - \frac{2}{r^2}\right) f(r) = 0 \tag{8.66}$$

This is a linear, homogeneous equation that can be satisfied by a sum of terms at the form cr^n, where each n satisfies the algebraic equation

$$[(n-2)(n-3) - 2][n(n-1) - 2] = 0 \tag{8.67}$$

The roots are n = -1, 1, 2, 4, so that

$$f(r) = \frac{A}{r} + Br + Cr^2 + Dr^4 \tag{8.68}$$

The third boundary condition (Eq. 8.64) requires that

$$C = \frac{1}{2} V_\infty \quad \text{and} \quad D = 0 \tag{8.69}$$

The no-slip boundary conditions (eqs. 8.59 and 8.60) give:

$$\frac{1}{r^2 \sin\theta} \frac{\partial \Psi}{\partial \theta} = \frac{2}{r^2} f(r) \cos\theta = 0 \quad \text{at} \quad r = R \tag{8.70}$$

$$- \frac{1}{r\sin\theta} \frac{\partial \Psi}{\partial r} = - \frac{\partial f(r)}{\partial r} \frac{\sin\theta}{r} = 0 \quad \text{at } r = R \tag{8.71}$$

Introducing equation (8.68) into (8.70) and (8.71), we have

$$\frac{A}{R^3} + \frac{B}{R} + \frac{V_\infty}{2} = 0 \tag{8.72}$$

$$- \frac{A}{R^3} + \frac{B}{R} + V_\infty = 0 \tag{8.73}$$

Thus

$$A = \frac{1}{4} V_\infty R^3 \quad \text{and} \quad B = - \frac{3}{4} V_\infty R \tag{8.74}$$

Hence, the stream function is

$$\Psi = \frac{1}{2} V_\infty \left(\frac{R^3}{2r} - \frac{3R}{2} r + r^2\right) \sin^2\theta \tag{8.75}$$

and the velocity components take the form

$$v_r = \frac{1}{r^2 \sin\theta} \frac{\partial \Psi}{\partial \theta} = V_\infty \left[1 - \frac{3}{2} \left(\frac{R}{r}\right) + \frac{1}{2} \left(\frac{R}{r}\right)^3\right] \cos\theta \tag{8.76}$$

$$v_\theta = - \frac{1}{r\sin\theta} \frac{\partial \Psi}{\partial r} = V_\infty \left[-1 + \frac{3}{4} \left(\frac{R}{r}\right) + \frac{1}{4} \left(\frac{R}{r}\right)^3\right] \sin\theta \tag{8.77}$$

Streamlines (i.e. lines of constant Ψ) and velocity profiles computed from equations (8.75), (8.76) and (8.77) are shown in Fig. 8.4. It is interesting to subtract the free stream velocity V_∞ from equations (8.75), (8.76) and (8.77) and plot the corresponding streamlines and velocity profiles for a sphere moving at a constant velocity V_∞ in an infinite otherwise undisturbed fluid, as shown in Fig. 8.5. It should be noted that in both Figs. (8.4) and (8.5) the streamlines are the same ahead of and behind the sphere, a preculiarity which will not hold when inertia effects become important.

To determine the pressure distribution we must go back to the original creeping flow equation of Section 8.1 (neglecting gravitational forces):

$$0 = -\nabla p + \mu \nabla^2 \mathbf{V} \tag{8.79}$$

which in spherical coordinates, with ϕ-symmetry (see Appendix) can be written as

$$\frac{1}{\mu}\frac{\partial p}{\partial r} = \frac{1}{r^2}\frac{\partial}{\partial r}\left(r^2 \frac{\partial v_r}{\partial r}\right) + \frac{1}{r^2 \sin\theta}\frac{\partial}{\partial \theta}\left(\sin\theta \frac{\partial v_r}{\partial \theta}\right) - \frac{2v_r}{r^2} - \frac{2}{r^2}\frac{\partial v_\theta}{\partial \theta} - \frac{2v_\theta \cot\theta}{r^2} \tag{8.80}$$

$$\frac{1}{\mu r}\frac{\partial p}{\partial \theta} = \frac{1}{r^2}\frac{\partial}{\partial r}\left(r^2 \frac{\partial v_\theta}{\partial r}\right) + \frac{1}{r^2 \sin\theta}\frac{\partial}{\partial \theta}\left(\sin\theta \frac{\partial v_\theta}{\partial \theta}\right) + \frac{2}{r^2}\frac{\partial v_r}{\partial \theta} - \frac{v_\theta}{r^2 \sin^2\theta} \tag{8.81}$$

Introducing equations (8.76) and (8.77) into the above expressions, we get

$$\frac{\partial p}{\partial r} = \left(\frac{3\mu R V_\infty}{r^3}\right)\cos\theta \tag{8.82}$$

$$\frac{\partial p}{\partial \theta} = \left(\frac{3\mu R V_\infty}{2r^2}\right)\sin\theta \tag{8.83}$$

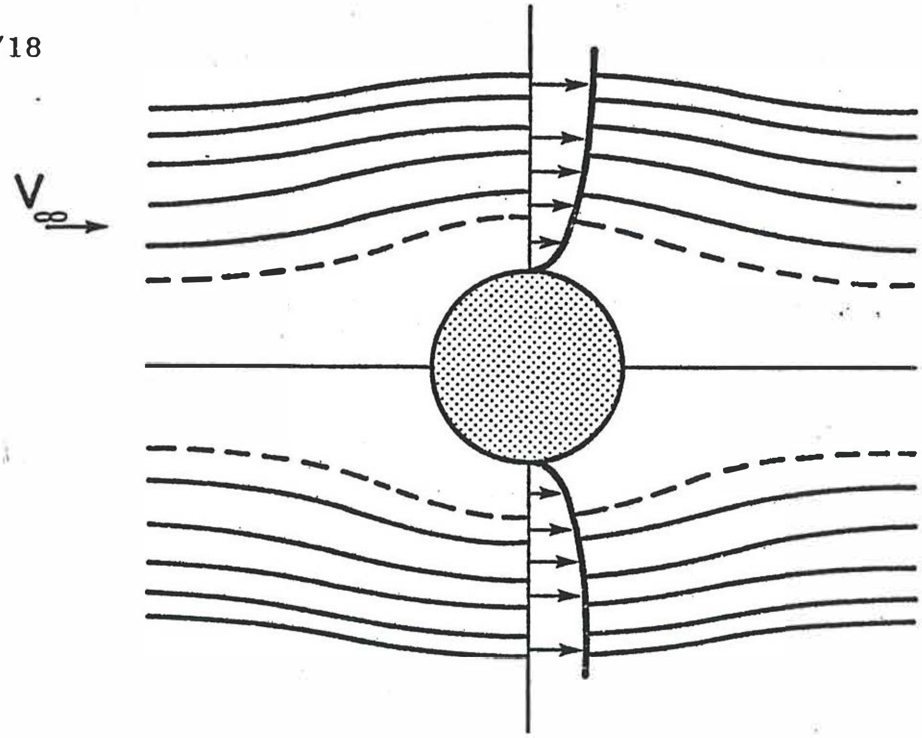

Fig. 8.4: Streamlines and velocity profile for creeping flow past fixed sphere.

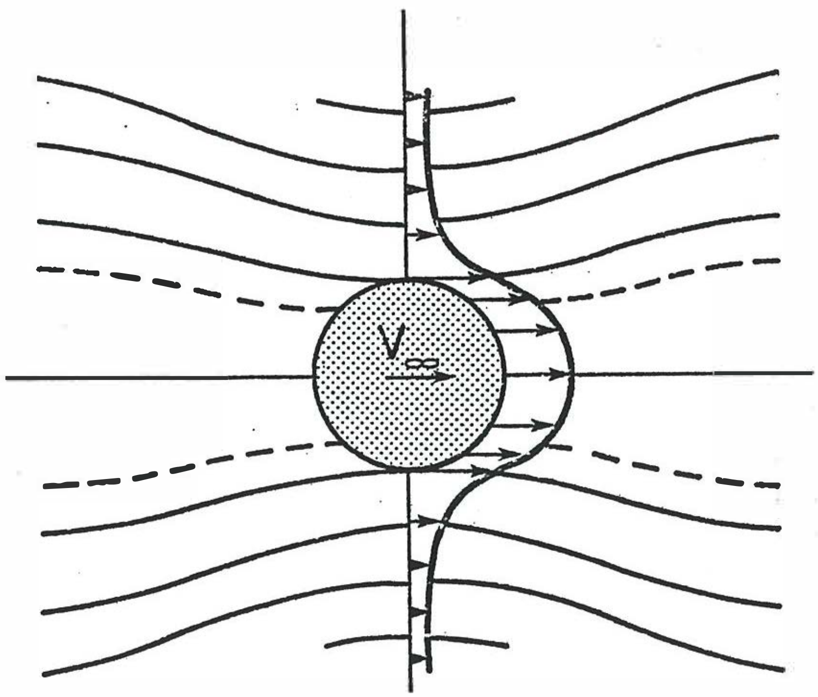

Fig. 8.5: Streamlines and velocity profile caused by a slowly moving sphere in a fluid.

so that

$$p = p_\infty - \left(\frac{3\mu R V_\infty}{2r^2}\right) \cos\theta \tag{8.84}$$

where p_∞ denotes the pressure far from the sphere. The pressure on the sphere surface can be obtained from equation (8.84) by setting $r = R$ and $p_\infty = 0$):

$$p_{r=R} = -\frac{3}{2}\frac{\mu V_\infty}{R}\cos\theta \tag{8.85}$$

The maximum value occurs at the upstream stagnation point ($\theta=\pi$)

$$(p_{r=R})_{max} = +\frac{3}{2}\frac{\mu V_\infty}{R} \tag{8.86}$$

and the minimum value occurs at the downstream stagnation point ($\theta=0$)

$$(p_{r=R})_{min} = -\frac{3}{2}\frac{\mu V_\infty}{R} \tag{8.87}$$

The pressure distribution around a sphere is shown in Fig. 8.6.

The total drag exerted on the sphere is the sum of the pressure drag or form drag F_{DP} and friction drag F_{DF}. The pressure drag is the resistance to flow due to the pressure p (i.e. z component of pressure force). Referring to Fig. 8.7, we have

$$F_{DP} = -\iint_S (p_{r=R}) \cos\theta \, dS \tag{8.88}$$

where $dS = R^2 \sin\theta d\theta d\phi$ and

$$F_{DP} = -\int_0^{2\pi}\int_0^{\pi} (p_{r=R}) R^2 \cos\theta \sin\theta \, d\theta d\phi \tag{8.89}$$

Using equation (8.85), we get the magnitude of the pressure drag

$$F_{DP} = 2\pi\mu R V_\infty \tag{8.90}$$

The friction drag is due to the resistance to flow caused by the shear stress on the sphere surface. The shear stress on the $r\theta$-plane

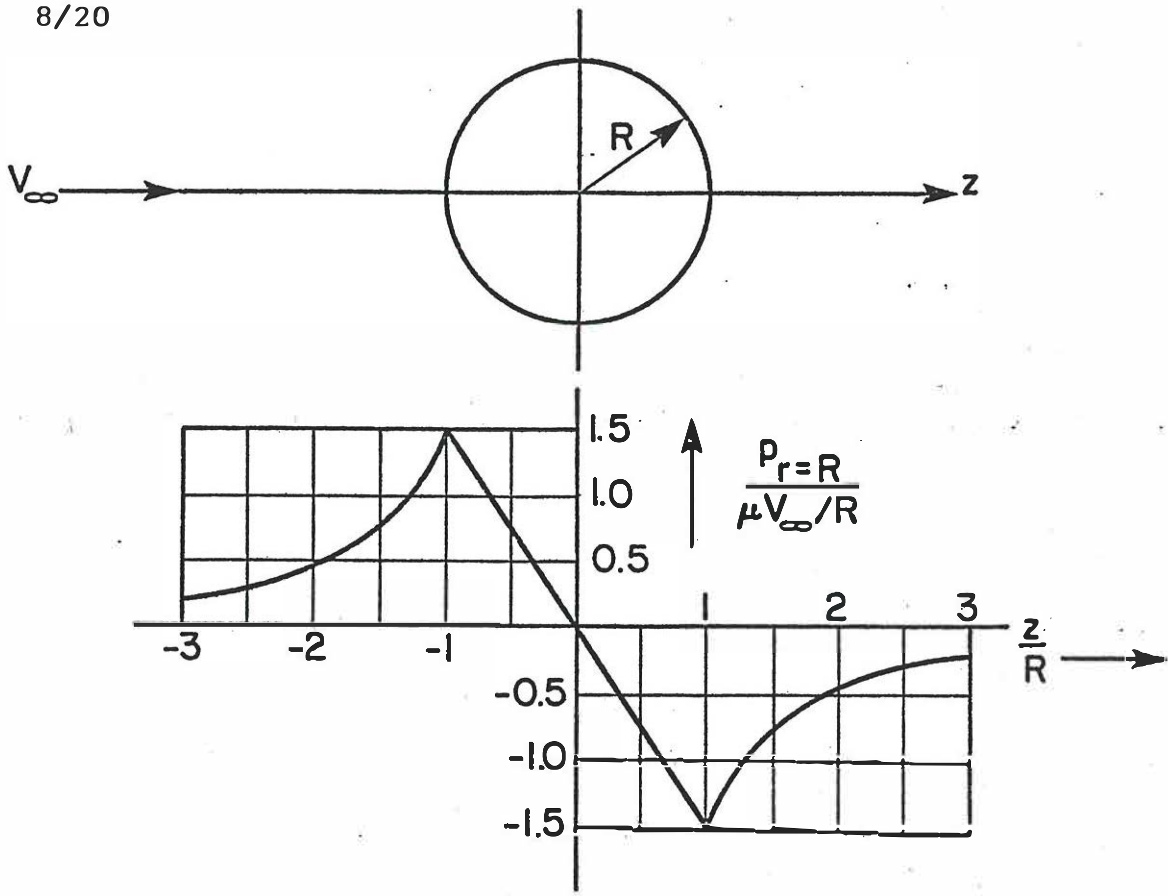

Fig. 8.6: Surface pressure distribution for creeping flow around a sphere.

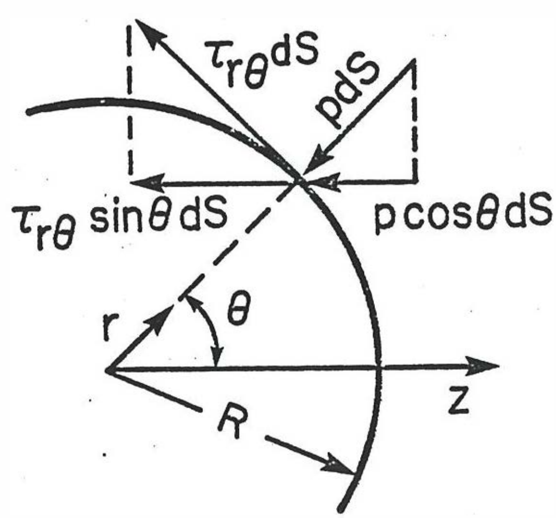

Fig. 8.7: Shear stress and pressure forces acting on the surface of a sphere.

is

$$\tau_{r\theta} = \mu \left[r \frac{\partial}{\partial r}\left(\frac{v_\theta}{r}\right) + \frac{1}{r}\frac{\partial v_r}{\partial \theta}\right] \tag{8.91}$$

Using Equation (8.76) and (8.77), we get

$$(\tau_{r\theta})_{r=R} = -\frac{3}{2}\frac{\mu V_\infty}{R}\sin\theta \tag{8.92}$$

The friction drag is the z component of the tangential stress force (see Fig. 8.7)

$$F_{DF} = -\iint_S (\tau_{r\theta})_{r=R} \sin\theta dS$$

$$= -\int_0^{2\pi}\int_0^{\pi} (\tau_{r\theta})_{r=R} R^2 \sin\theta^2 d\theta d\phi$$

$$= 4\pi\mu R V_\infty \tag{8.93}$$

Thus, the magnitude of the total drag is

$$F_D = F_{DP} + F_{DF} = 2\pi\mu R V_\infty + 4\pi\mu R V_\infty = 6\pi\mu R V_\infty \tag{8.94}$$

This expression is known as Stokes´ law (13). It is interesting to note that for a solid sphere of density ρ_s falling with terminal velocity V_t under the influence of gravity in a fluid of density ρ and viscosity μ, we have

weight of sphere = drag + buoyant force

or

$$\frac{4}{3}\pi R^3 \rho_s g = 6\pi\mu R V_t + \frac{4}{3}\pi R^3 \rho g \tag{8.95}$$

The above equation can be used to calculate either the terminal velocity (steady state) V_t or the viscosity of the fluid (see example 8.1). It should be noted, however, that the expression for total drag (Eq. (8.94)) is valid for small Reynolds number values (typically Re < 0.5).

For larger Reynolds numbers the inertia effects cannot be neglected. Oseen [14] suggested that the inertia term in the Navier-Stokes equations, $\rho\bar{V} \cdot \nabla\bar{V}$, can be reasonably approximated by

$\rho\bar{V}_\infty \cdot \nabla\bar{V}$ and equations (8.7) and (8.8) can now be simplified to read

$$\nabla \cdot \bar{V} = 0 \tag{8.96}$$

$$\rho\bar{V}_\infty \cdot \nabla\bar{V} = -\nabla p + \mu\nabla^2 \bar{V} + \rho\bar{g} \tag{8.97}$$

We note that by replacing $\rho\bar{V}\cdot\nabla\bar{V}$ by $\rho\bar{V}_\infty\cdot\nabla\bar{V}$, Oseen linearized the Navier-Stokes equations (since V_∞ = constant) and simplified the solution. The results of this analysis show that the streamlines are no longer the same in front of and behind the sphere. The total drag has been found to be

$$F_D = 6\pi\mu\, RV_\infty \left(1 + \frac{3}{16}\, Re\right) \tag{8.98}$$

An improvement of Stokes' and Oseen's solution has been suggested by Proudman and Pearson [15] which leads to

$$F_D = 6\pi\mu RV_\infty \left[1 + \frac{3}{8}\, Re_R + \frac{9}{40}\, Re_R^2\, \ell n Re_R + 0\, (Re_R^2)\right. \tag{8.99}$$

where $Re_R = Re/2$.

Some questions have been raised in connection with the range validity of the above equations (see for example refs. [1,2]). However, these methods of treatment also give solutions for the two-dimensional problem (i.e. flow around a cylinder) whereas Stokes' equations (8.7) and (8.8) do not possess a solution (Whitehead's paradox). Some experimental results and Stokes' and Oseen's solutions are given in Fig. 8.8 in terms of a drag coefficient which is defined by

$$C_D = \frac{F_D}{\frac{\rho V_\infty^2}{2} A} = \frac{F_D}{\frac{\rho V_\infty^2}{2} \pi R^2} \tag{8.100}$$

Using equation (8.94), we get

$$C_D = \frac{24}{Re} \tag{8.101}$$

and using equation (8.98) we get

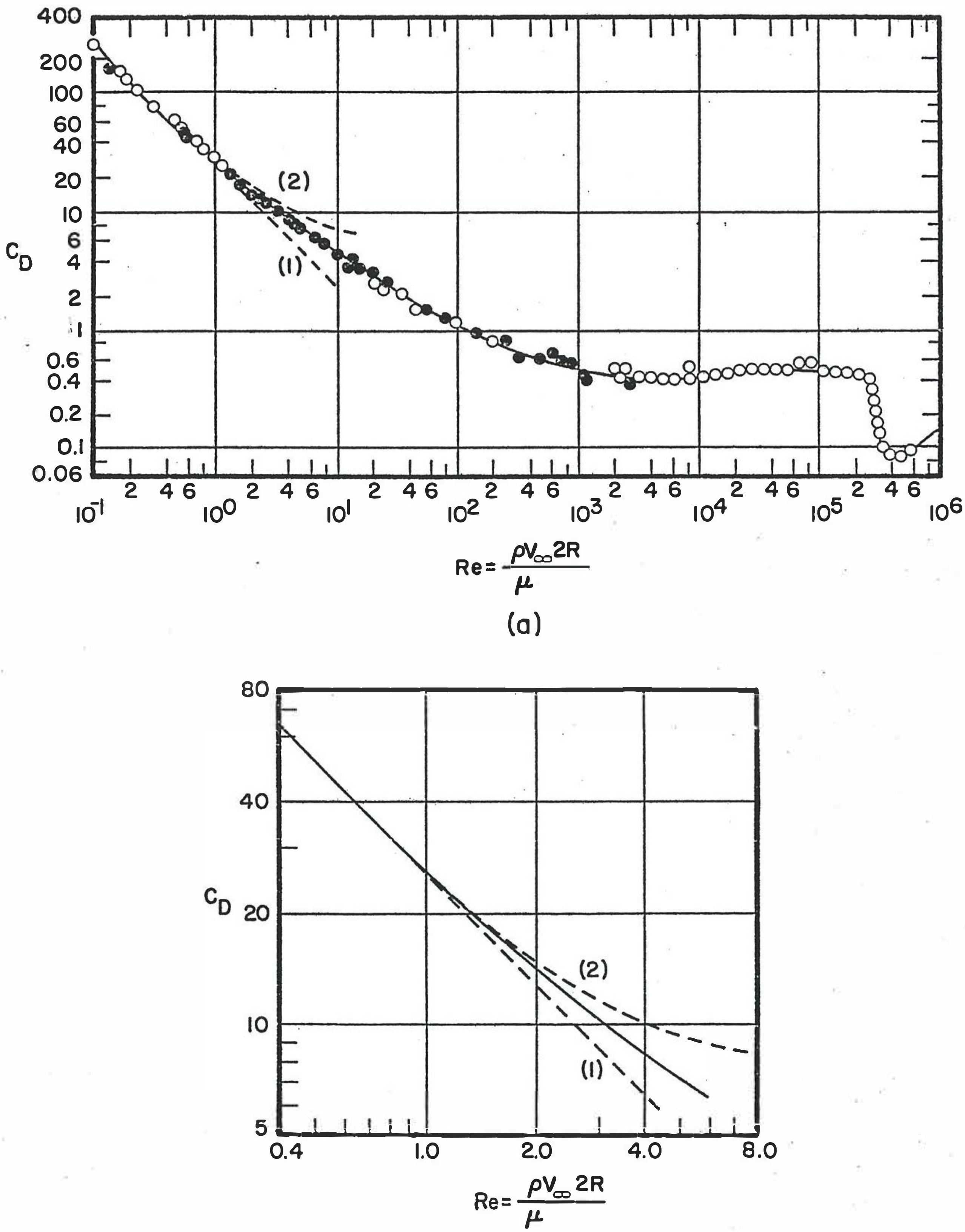

Fig. 8.8: Drag coefficient for flow around a sphere as a function of Reynolds number. The solid line represents the best fit for the experimental data. Dashed line (1) is Stokes' law (Eq. 8.101) and (2) Oseen's equation (8.102).

$$C_D = \frac{24}{Re}\left(1 + \frac{3}{16} Re\right) \qquad (8.102)$$

The figure shows that equation (8.101) gives good agreement with experiments up to Re $\simeq$ 1 whereas equation (8.102) up to Re $\simeq$ 1 whereas equally (8.102) up to Re $\simeq$ 2. For higher Reynolds number flows the reader is referred to the book by Cliff et al [16].

Example 8.1 The Falling Sphere Viscometer

A small steel ball of 5 mm diameter (ρ_s = 7800 k_g/m^3) is allowed to fall vertically down the center of a glass cylinder containing a fluid of density 1100 kg/m^3 as shown in Fig. 8.9. The terminal velocity is determined by measuring the time required for the steel ball to travel between the two lines shown and is found to be 4.2 cm/s. Determine the viscosity at the fluid.

Solution

Solving equation (8.95) for μ we get

$$\mu = \frac{2R^2(\rho_s - \rho)g}{9\ V_t}$$

$$= \frac{2(2.5 \times 10^{-3}\ m)^2(7800\ kg/m^3 - 1100\ kg/m^3)(9.81\ m/s^2)}{9(4.2 \times 10^{-2}\ m/s)}$$

$$= 2.17\ N{\bullet}s/m^2 = 2.17\ Pa{\bullet}s$$

We now check the Reynold's number to see whether it is within the region of applicability of Stokes' law.

$$Re = \frac{\rho\ V_t\ D}{\mu} = \frac{(1100\ kg/m^3)(4.2{\times}10^{-2}\ m/s)(5{\times}10^{-3}\ m)}{2.17\ N{\bullet}s/m^2} = 0.106$$

For such a Reynolds number Stokes' law is valid.

It should be noted that falling sphere viscometers are useful only for highly viscous fluids (low Re). The viscosity measurement, however,

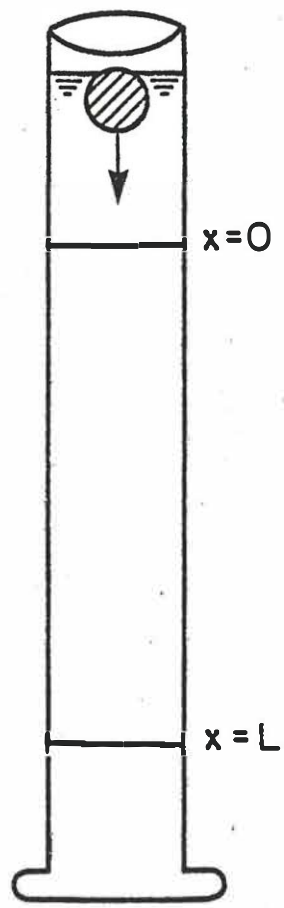

Fig. E.8.1

might not be terribly accurate because Stokes´ law was based on flow around a sphere in an infinite fluid. In the falling sphere viscometer the cylinder walls will influence the flow pattern and consequently the velocity of fall.

8.5 FLOW THROUGH POROUS MEDIA

The flow of fluids through porous media occurs in many technologically important processes (see references [5], [6] and [7]). Common examples include flow of water or oil through porous rocks and flow of various fluids through filters and packed bed reactors for the production of chemicals. For most common applications the flow is slow enough so that the simplications carried out in section 8.1 are valid. The pressure field is described by the Laplace equation for an incompressible fluid.

$$\nabla^2 P = 0 \tag{8.103}$$

or, equivalently

$$\nabla^2 (p + \rho g h) = 0 \tag{8.104}$$

If we consider variation in the z direction only, we have

$$\frac{\partial^2 (p + \rho g h)}{\partial z} = 0 \tag{8.105}$$

and

$$\frac{\partial (p + \rho g h)}{\partial z} = \text{const} \tag{8.106}$$

Assuming that the porous medium can be described as an assemblage of small conduits in the z-direction, we would expect that the volume rate of flow be expressed by a Hagen-Poiseuille type expression (see Sec. 7.3), i.e.

$$Q = - \frac{\text{const}}{\mu} \frac{\partial P}{\partial z} \tag{8.107}$$

or by defining a superficial velocity

$$u = \frac{Q}{A} = \frac{\text{volume of fluid}}{\text{cross-sectional area of porous medium}} \tag{8.108}$$

we get

$$u = -\frac{\kappa}{\mu}\frac{\partial P}{\partial z} = -\frac{\kappa}{\mu}\frac{\partial}{\partial z}(p + \rho g h) \tag{8.109}$$

This is known as Darcy's law after the French engineer who established the above expression by performing experiments of water percolation through sand filters [17]. The constant κ is usually called permeability, and it has dimensions of length squared. Measurement of the permeability constant can be simply performed by determining the flow rate through a cylindrical porous sample confined in a tube at a given pressure gradient. Some typical values are given in table 1. For a porous medium having the same permeability in all directions (i.e. isotropic), we may write

$$u_x = -\frac{\kappa}{\mu}\frac{\partial(p + \rho g h)}{\partial x} \tag{8.110}$$

$$u_y = -\frac{\kappa}{\mu}\frac{\partial(p + \rho g h)}{\partial y} \tag{8.111}$$

$$u_z = -\frac{\kappa}{\mu}\frac{\partial(p + \rho g h)}{\partial z} \tag{8.112}$$

or in vector notation

$$\overline{U} = -\frac{\kappa}{\mu}\nabla(p + \rho g h) \tag{8.113}$$

It should be noted that Darcy's law is valid only for laminar flow conditions with inertial effects being negligible.

For a porous medium having porosity or voidage fraction ε (where ε is the ratio of pore volume to total volume) we can write the continuity equation in terms of the suferficial velocity $\overline{U}$. This can be done by referring to the derivation of Chapter 4 and noting that the mass rate of flow per unit area is now $\rho\overline{U}$ rather than $\rho\overline{V}$ and the fluid mass per unit volume is $\varepsilon\rho$ rather than ρ. Thus, we can easily end up with an equation of continuity analogous to (4.12), which reads

TABLE 1

TYPICAL VALUES OF POROSITY AND PERMEABILITY FOR POROUS MATERIALS

Material	Porosity or Voidage Fraction ϵ	Permeability $\kappa(m^2)$
Silica powder	0.37 - 0.49	$1.3 \times 10^{-14} - 5.1 \times 10^{-14}$
Loose sand	0.37 - 0.50	$2 \times 10^{-11} - 1.8 \times 10^{-10}$
Soils	0.43 - 0.54	$2.9 \times 10^{-11} - 1.4 \times 10^{-10}$
Sandstone	0.08 - 0.38	$5 \times 10^{-16} - 3 \times 10^{-12}$
Limestone	0.04 - 0.10	$2 \times 10^{-16} - 4.5 \times 10^{-14}$
Brick	0.12 - 0.34	$4.8 \times 10^{-15} - 2.2 \times 10^{-13}$
Leather	0.56 - 0.59	$9.5 \times 10^{-14} - 1.2 \times 10^{-13}$
Fiber glass	0.88 - 0.93	$2.4 \times 10^{-11} - 5.1 \times 10^{-11}$

Reproduced from R.E. Collins, "Flow of Fluids through Porous Materials", Van Nostrand Reinhold, New York (1961).

$$\varepsilon \frac{\partial \rho}{\partial t} + \nabla \cdot (\rho \overline{U}) = 0 \tag{8.114}$$

Introducing Darcy's law (Equ. 8.113) into the above equation, we have

$$\varepsilon \frac{\partial \rho}{\partial t} - \nabla \cdot [\frac{\rho \kappa}{\mu} \nabla (p + \rho g h) = 0 \tag{8.115}$$

For a fluid of constant viscosity μ and constant permeability κ, we have

$$\frac{\mu \varepsilon}{\kappa} \frac{\partial \rho}{\partial t} - \nabla \cdot [\rho \nabla (p + \rho g h)] = 0 \tag{8.116}$$

For an incompressible fluid ρ = const. Thus, the pressure field is described by the Laplace equation

$$\nabla^2 (p + \rho g h) = 0 \tag{8.117}$$

In many cases, however, we may write an equation of state for the fluid, in the form

$$\rho = \rho_o \, p^m \exp(\beta p) \tag{8.118}$$

Liquids under certain conditions can be considered slightly compressible, with $m = 0$ and $\beta \neq 0$. Gases are compressible with $\beta = 0$ and $m = 1$ (for isothermal flow) or $m = C_v/C_p$ (for adiabatic flow). Introducing the appropriate form of the equation of state we can easily obtain various simplified forms of equation (8.116) (see for example, Longwell [18]). The solution of these equations yields the pressure as a function of position. The superficial velocity can then be obtained from Darcy's law.

Several attempts have been made to determine Darcy's constant theoretically. Kozeny's approach [19], which was further elaborated by Carman [20], is based on the assumption that a porous medium consists of a bundle of parallel capillaries, as shown in Fig. 8.9(a). The superficial velocity can be expressed as $u = (V_{avg})\,\varepsilon$ where V_{avg} is the average velocity through each capillary and ε the porosity or voidage fraction (volume of voids/total volume porous medium). We can define a mean hydraulic radius as the ratio of the cross-sectional area and the wetted perimeter. Here, we have

$$R_H = \frac{\text{cross section of flow area}}{\text{wetted perimeter}}$$

$$= \frac{\text{total volume of voids}}{\text{total area of particles}}$$

$$= \frac{(\text{total volume of voids})/(\text{total volume of porous medium})}{(\text{total area of particles})/(\text{total volume of porous medium})}$$

$$= \frac{\text{porosity}}{(\text{total area of particles})/(\text{total volume of porous medium})} \tag{8.119}$$

The porosity is ε and thus the (total volume of the particles) should be equal to $(1-\varepsilon)$ (total volume of porous medium). Consequently,

$$R_H = \frac{\varepsilon}{(1-\varepsilon)\dfrac{\text{total area of particles}}{\text{total volume of particles}}} = \frac{\varepsilon}{(1-\varepsilon)S_p} \tag{8.120}$$

where S_p is the specific area of particles. For an assemblage of spherical particles of diameter D_p, we have

$$S_p = \frac{\pi D_p^2}{\pi D_p^3/6} = \frac{6}{D_p} \tag{8.121}$$

For laminar flow through a tube of radius R the average velocity (see Sec. 7.3) is given by

$$V_{avg} = \frac{\Delta p}{8\mu L} R^2 = \frac{\Delta p}{2\mu L} R_H^2 \tag{8.122}$$

(Note that for a single tube of radius R, $R_H = \frac{1}{2} R$ as defined by equation 8.119). Introducing the superficial velocity into the above expression, we get

$$u = \frac{\Delta p}{2\mu L} R_H^2 \varepsilon = \frac{\Delta p}{2\mu L} \frac{\varepsilon^3}{(1-\varepsilon)^2 S_p^2} = \frac{\Delta p}{L} \frac{D_p^2}{72\mu} \frac{\varepsilon^3}{(1-\varepsilon)^2} \tag{2.123}$$

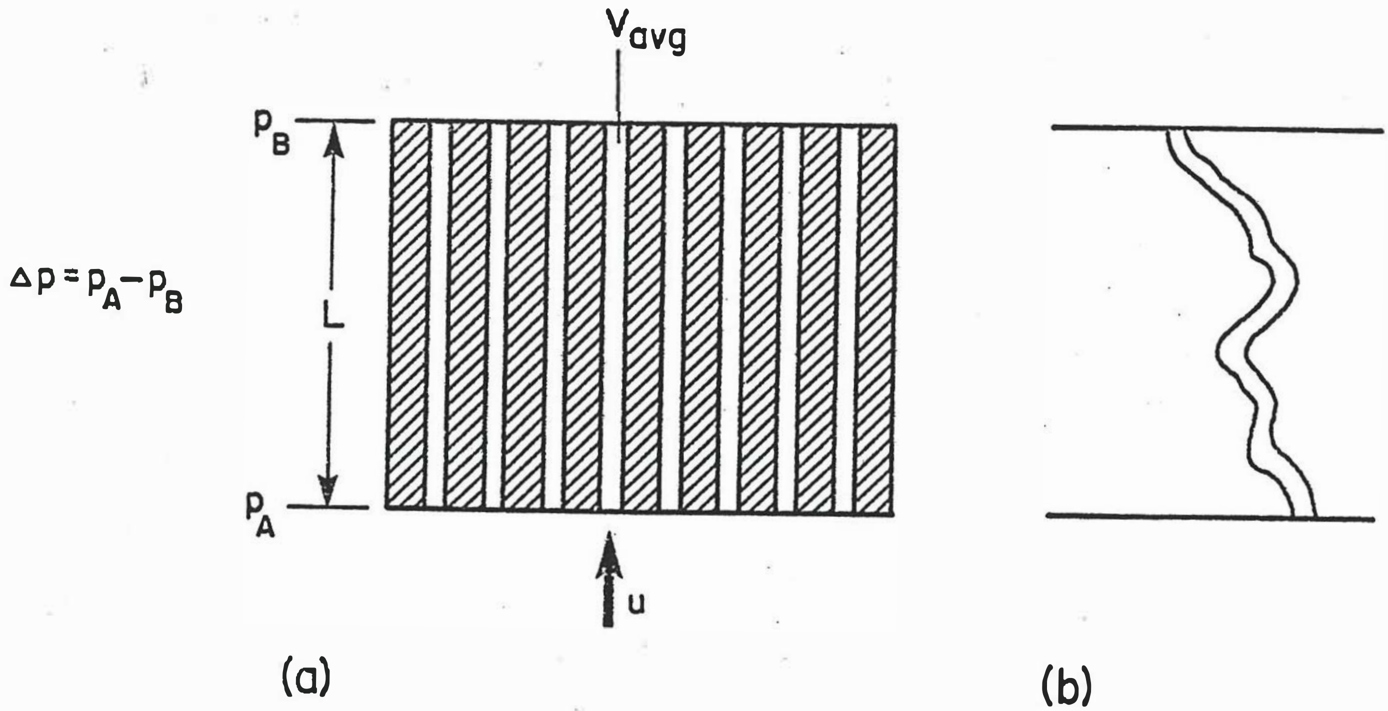

Fig. 8.9: (a) Kozeny's hydraulic model for a porous medium consisting of an assemblage of parallel capillaries.
(b) A likely tortuous flow path through a porous medium.

The length L in Kozeny's hydraulic model of Fig. 8.9(a) is shown to be equal to the height of the porous medium. It is reasonable, however, to anticipate that the fluid through the capillaries should follow a tortuous path as shown in Fig. 8.9(b). Thus, the effective length is longer than L. Large number of experimental data suggest that the numerical factor 72 should be changed to 150, to give the so-called Blake-Kozeny equation [24]

$$u = \frac{\Delta p}{L} \frac{D_p^2}{150\mu} \frac{\varepsilon^3}{(1-\varepsilon)^2} \tag{8.124}$$

which can be solved for $\Delta p/L$ to give:

$$\frac{\Delta p}{L} = u \frac{150\mu}{D_p^2} \frac{(1-\varepsilon)^2}{\varepsilon^3} \tag{8.125}$$

This equation is valid for laminar flow with negligible inertia forces.

It is customary to define a Reynolds number as

$$Re_H = \frac{\rho V_{avg} (4R_H)}{\mu} \tag{8.126}$$

Since $v_{avg} = u/\varepsilon$ and $R_H = \varepsilon/(1-\varepsilon)S_p$ we get

$$Re_H = \frac{4\rho u}{(1-\varepsilon)S_p} = \frac{4\rho D_p u}{6\ (1-\varepsilon)} \tag{8.127}$$

Most authors, however, prefer a definition of Reynolds number without the numerical factor 4/6, i.e.

$$Re_p = \frac{\rho\ D_p\ u}{(1-\varepsilon)\mu} \tag{8.128}$$

Comparison with experiments shows that the Blake-Kozeny equation is valid up to about $Re_p \simeq 10$. A large number of experimental data in the range of Re_p from about 1 to about 2500, as shown in Fig. 8.10, obey the Ergun equation [22], which is

$$\frac{\Delta p}{L} = u \frac{150\mu}{D_p^2} \frac{(1-\varepsilon)^2}{\varepsilon^3} + \frac{1.75\ \rho u^2}{D_p} \frac{(1-\varepsilon)}{\varepsilon^3} \tag{8.129}$$

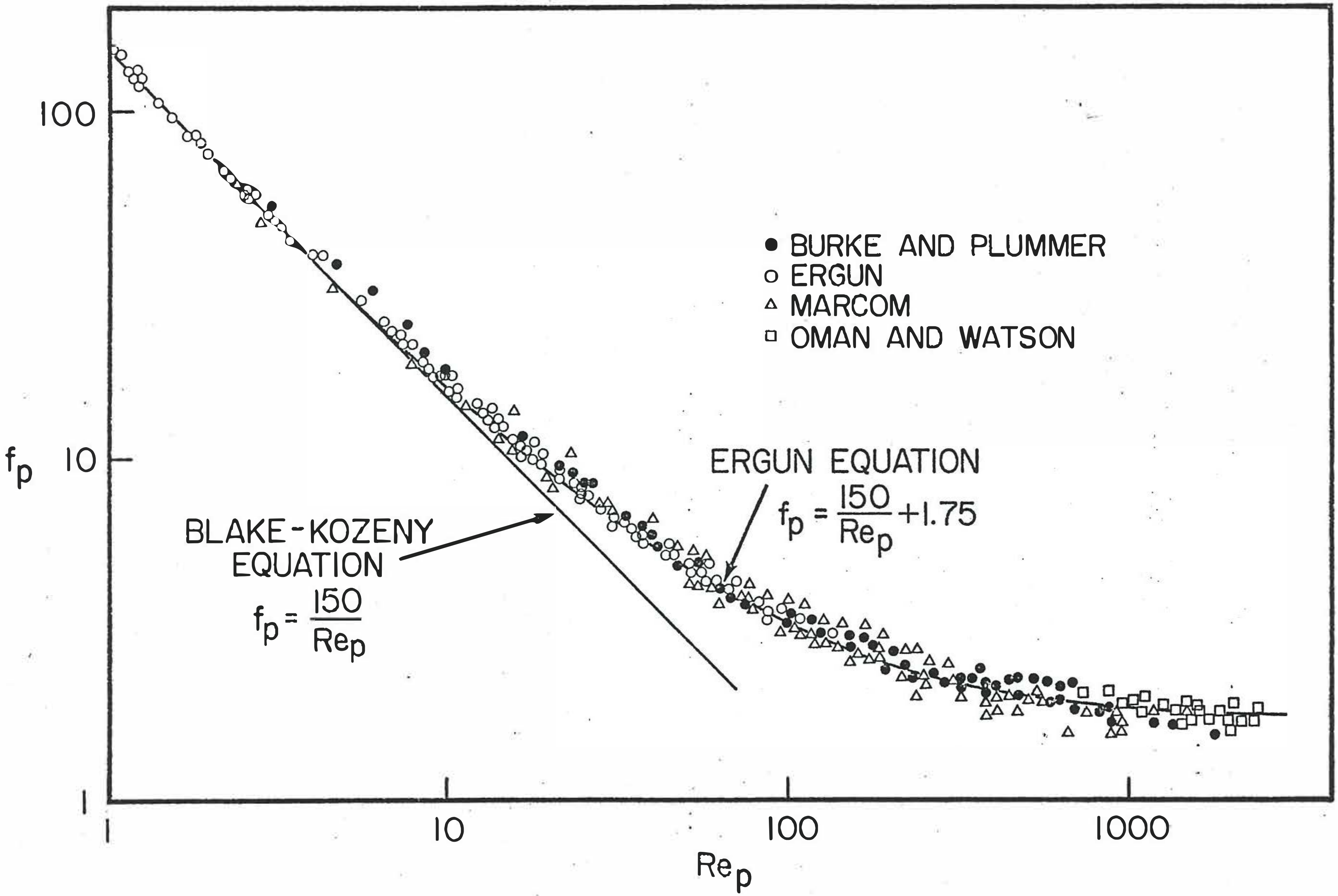

Fig. 8.10: Friction factor for flow through a packed bed of particles [reproduced from S. Ergun, Chem. Eng. Progr., 48, 93 (1952)].

This equation is often written in dimensionless form as

$$f_p = \frac{D_p \varepsilon^3}{\rho u^2 (1-\varepsilon)} \frac{\Delta p}{L} = \frac{150}{Re_p} + 1.75 \tag{8.130}$$

where f_p is the packed-bed friction factor. For more on packed beds and industrial filtration processes the reader is referred to the books by Bennet and Myers [23] and Orr [24].

When a fixed bed of particles is subjected to upward flow, depending on the superficial velocity, the bed may remain fixed, loosen up as to attain maximum voidage or may become fluidized as shown in Fig. 8.11. At the point of incipient fluidization the weight of the particles minus buoyancy must be equal to the pressure drop multiplied by the cross-sectional area. Thus, we have

$$(\rho_p - \rho)\, gAL = (\Delta p)\, A \tag{8.131}$$

Assuming that the Blake-Kozeny equation is valid we can combine equations (8.125) and (8.131) and then solve for the superficial velocity to obtain the fluidization velocity

$$u_f = \frac{(\rho_p - \rho)\, g\, D_p^2\, \varepsilon^3}{150\, \mu\, (1-\varepsilon)^2} \tag{8.132}$$

Detailed expositions on theoretical as well as practical aspects of fluidization can be found in the books by Zenz and Othmer [25], Kunii and Levenspiel [26] and Davidson and Harrison [27].

Example 8.2

An incompressible liquid flows radially through a porous cylindrical shell as shown in Fig. E.8.2. Determine: (a) the pressure distribution, (b) superficial velocity, and (c) the volume rate of flow.

Solution

The Laplace equation is applicable in this case

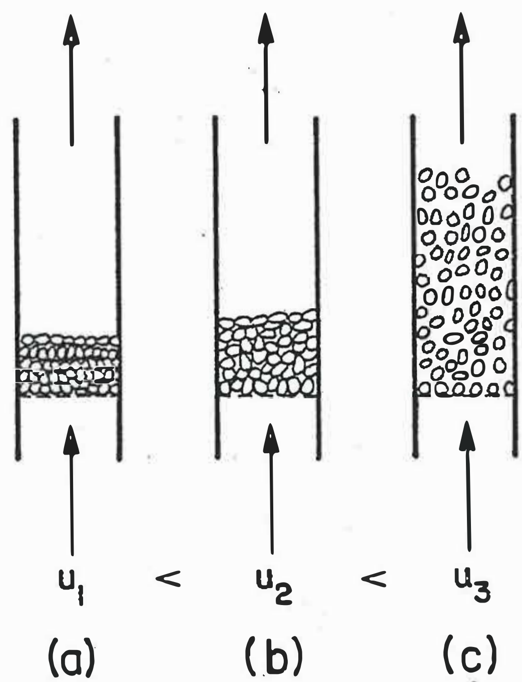

Fig. 8.11: Schematic representation of a packed bed of particles (a), which attains maximum voidage (b), and eventually becomes fluidized (c), as the velocity u increases.

$$\nabla^2(p + \rho gh) = 0$$

Neglecting gravitational effects and writing the Laplace equation in cylindrical coordinates, we have

$$\frac{1}{r}\frac{\partial}{\partial r}\left(r\frac{\partial p}{\partial r}\right) + \frac{1}{r^2}\frac{\partial p}{\partial \theta^2} + \frac{\partial^2 p}{\partial z^2} = 0$$

There is no pressure variation in either θ or z directions, thus

$$\frac{1}{r}\frac{\partial}{\partial r}\left(r\frac{\partial p}{\partial r}\right) = 0$$

The boundary conditions are

$$r = r_i \qquad p = p_o$$

$$r = r_o \qquad p = p_o$$

The solution of the differential equation is

$$p = C_1\, \ell n r + C_2$$

After determining the coefficients C_1 and C_2 and rearranging, we get

$$\frac{p - p_i}{p_o - p_i} = \frac{\ell n(r/r_i)}{\ell n(r_o/r_i)}$$

The superficial velocity can be obtained from Darcy's law

$$u = -\frac{\kappa}{\mu}\frac{\partial p}{\partial r} = -\frac{\kappa}{\mu r}\frac{p_o - p_i}{\ell n(r_o/r_i)}$$

The volume rate of flow is

$$Q = |u|\ A(r) = |u|\ 2\pi rL = \frac{2\pi\kappa L}{\mu}\frac{p_o - p_i}{\ell n(r_o/r_i)}$$

Example 8.3

A bed of graded sand of 10 m^2 cross-sectional area and 1.5 m deep, is used for clarification of water. The sand particles are assumed to be spherical of 1.2 mm diameter. The bed porosity is ϵ = 0.2. The

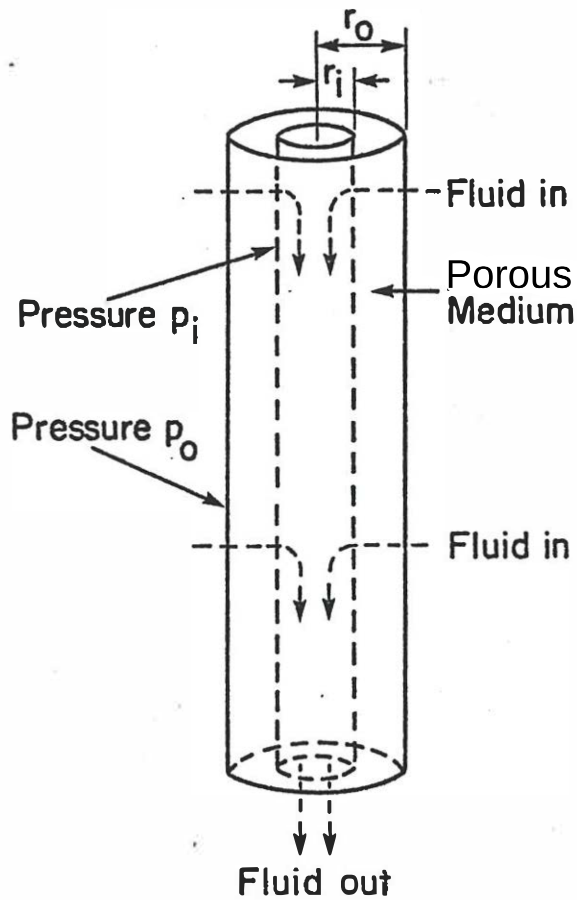

r_o
r_i
Fluid in
Porous Medium
Pressure p_i
Pressure p_o
Fluid in
Fluid out

E.8.2

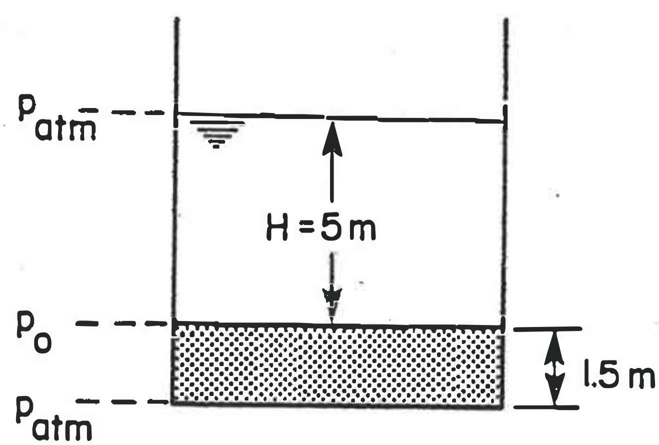

p_{atm}
H = 5 m
p_o
1.5 m
p_{atm}

E.8.3

water surface is maintained at a level of 5 m above the top surface of the sand as shown in Figure E.8.3. Determine the volume rate of flow.

Solution

We start from the Blake-Kozeny equation

$$u = \frac{\Delta p}{L} \frac{D_p^2}{150\mu} \frac{\varepsilon^3}{(1-\varepsilon)^2}$$

Here, we have

$$p_o - p_{atm} = \Delta p = \rho g H$$

$$u = \frac{\rho g H}{L} \frac{D_p^2}{150\mu} \frac{\varepsilon^3}{(1-\varepsilon)^2} =$$

$$= \frac{(1000\ kg/m^3)(9.81\ m/s^2)(5m)}{1.5\ m} \frac{(1.2 \times 10^{-3}\ m)^2}{150\times10^{-3}\ N\ m^{-2} s} \frac{0.2^3}{(1-0.2)^2}$$

$$= 0.00392\ m/s$$

$$Q = (0.00392\ m/s)(10\ m^2) = 0.0392\ m^3/s$$

We will now check the Reynolds number

$$Re = \frac{\rho D_p u}{(1-\varepsilon)\mu} = \frac{(1000\ kg/m\ )(1.2 \times 10^{-3}\ m)(0.00392\ m/s)}{(1-0.2)\ 10^{-3}\ Nm^{-2}\ s} = 5.8$$

Since the Reynolds number is less than 10 the Blake-Kozeny equation used above is valid.

Example 8.4

Determine the minimum fluidization velocity for a bed of mineral particles 100 μm in diameter in air having viscosity of 0.02×10^{-3} Pa•s. The particle density is 5.25×10^3 kg/m^3 and air density 1.24

kg/m^3. Assume $\varepsilon^3/(1-\varepsilon) = 0.091$.

Solution

The air density can be neglected. Thus, we have

$$u_f = \frac{(5.25 \times 10^3 \ \ kg/m^3)(9.81\ m/s)(100 \times 10^{-6}\ m)^2}{150 \times 0.02 \times 10^{-3}\ Nm^{-2}s} \ 0.091$$

$$= 0.0156\ m/s$$

The corresponding particle Reynolds number is

$$Re_p = \frac{\rho\ D_p\ u_f}{(1-\varepsilon)\mu} = \frac{(1.24\ kg/m^3)(100 \times 10^{-6}\ m)(0.0156\ m/s)}{(1-\varepsilon)(0.02 \times 10^{-3}\ Nm^{-2}s)}$$

$$= \frac{0.0967}{(1-\varepsilon)}$$

Since $(1-\varepsilon)$ is less than 1, Re_p is well within the range of validity of the Blake-Kozeny equation, on which we based the calculation of u_f.

REFERENCES

1. J. Happel and H. Brenner, "Low Reynolds Number Hydrodynamics", Noordhoff International Publishing, Leyden, The Netherlands (1973).

2. W.E. Langlois, "Slow Viscous Flow", MacMillan, New York, (1964).

3. O. Pinkus and B. Sternlicht, "Theory of Hydrodynamic Lubrication", McGraw-Hill Book Co., New York (1961).

4. J.A. Walowit and J.N. Anno, "Modern Developments in Lubrication Mechanics" Wiley, New York (1975).

5. M. Muskat, "The Flow of Homogeneous Fluids through Porous Media", McGraw-Hill, New York, (1937).

6. A.E. Scheidegger, "The Physics of Flow Through Porous Media", University of Toronto Press, 3rd Edition, Toronto, (1974).

7. F.A.L. Dullien, "Porous Media Fluid Transport and Pore Structure", Academic Press, New York, (1979).

8. M.M. Denn, "Process Fluid Mechanics", Prentice-Hall, Englewood Cliffs, New Jersey (1980).

9. P.J. Leider and R.B. Bird, "Squeezing Flow between Parallel Disks I. Theoretical Analysis", Ind. Eng. Chem. Fund., 13, 336 (1974).

10. B.S. Massey, "Mechanics of Fluids", Van Nostrand Reinhold, 4th Edition, New York (1979).

11. H. Schlichting, "Boundary-Layer Theory", McGraw-Hill, 7th Edition, New York (1979).

12. W. Gross, "Gas Lubrication", Wiley, New York (1962).

13. G.G. Stokes, "On the Effect of the Internal Friction of Fluids on the Motion of Pendulums", Trans. Cambridge Phil. Soc., 9, (1851).

14. C.W. Oseen, "Über die Stokes´ sche Formel and über eine verwandte Aufgabe in der Hydrodynamik", Ark. f. Math. Astron. och Fys., 6, No. 29 (1910).

15. I. Proudman and J.R.A. Pearson, "Expansions at Small Reynolds Number for the Flow Past a Sphere and a Circular Cylinder", J. Fluid Mech., 2, 237 (1957).

16. R. Cliff, J.R. Grace and W.E. Weber, "Bubbles, Drops and Particles", Academic Press, New York (1978).

17. H. Darcy, "Les Fontaines Publiques de la Ville de Dijon", Victor Dalmond, Paris (1856).

18. P.A. Longwell, "Mechanics of Fluid Flow", McGraw-Hill, New York (1966).

19. J. Kozeny, Sitz.-Ber. Wiener Akad., Abt. IIa, 136, 271 (1927), also Hydraulik, Springer-Verlag, Wien (1953).

20. P.C. Carman, "Flow of Gases through Porous Media", Academic Press, New York (1956).

21. R.B. Bird, W.E. Stewart and E.N. Lightfoot, "Transport Phenomena", Wiley, New York (1960).

22. S. Ergun, "Fluid Flow through Packed Columns", Chem. Eng. Progr., 48, 89 (1952).

23. C.O. Bennett and J.E. Myers, "Momentum, Heat, and Mass Transfer", McGraw-Hill, 2nd Edition, New York (1974).

24. C. Orr (Ed.), "Filtration: Principles and Practices", Marcel Dekker, Inc., New York (Part I, 1977 and Part II, 1979).

25. F.A. Zenz and D.F. Othmer, "Fluidization and Fluid-Particle Systems", Van Nostrand Reinhold, New York (1960).

26. D. Kunii and O. Levenspiel, "Fluidization Engineering", Wiley, New York (1969).

27. J.F. Davidson and D. Harrison, "Fluidization", Elsevier, Amsterdam (1973).

GEORGE GABRIEL STOKES (1819-1903)

John Vlachopoulos, *Fundamentals of Fluid Mechanics*
Chem. Eng., McMaster University, Hamilton, ON, Canada
(First Edition 1984, revised internet edition (2016), www.polydynamics.com)

CHAPTER 9

LAMINAR BOUNDARY LAYERS

9.1 INTRODUCTION

In this chapter we consider the flow of fluids at high Reynolds numbers (Re>>1). With this assumption we will simplify the general Navier-Stokes equations. When the Reynolds number is very high the flow is dominated by inertia forces. It is tempting to try to eliminate the term

$$\frac{1}{Re}\left(\frac{\partial^2 v_x^*}{\partial x^{*2}} + \frac{\partial^2 v_x^*}{\partial y^{*2}} + \frac{\partial^2 v_x^*}{\partial z^{*2}}\right)$$

which represents the viscous forces, from equation (6.121). However, the no-slip condition suggests the possibility of large velocity gradients near solid boundaries, which might be of the same order of magnitude as the Reynolds number, Re. In order to be able to simplify the Navier-Stokes equations we must assess the relative magnitude of the various terms.

In 1904 Ludwig Prandtl [1] introduced the concept of boundary layer and showed how the Navier-Stokes equations could be simplified. This concept literally revolutionized the science of fluid mechanics. The most comprehensive and authoritative reference on the subject is a text by Schlichting [2]. More recently other scientists succeeded in deriving the boundary layer equations in the framework of perturbation theory [3]. In this chapter we will essentially follow Prandtl's approach because of its simplicity.

According to Prandtl's boundary layer concept viscous effects at high Reynolds numbers are confined in thin fluid layers adjacent to solid boundaries. Outside these thin boundary layers the flow may be considered inviscid ($\mu = 0$) and can, thus, be described by the Euler equation (6.95). Within a boundary layer the velocity component in the main flow direction (x) changes from $v_x = 0$ (at the solid boundary) to $v_x \approx V\infty$ (the free stream velocity at the "edge" of the boundary layer). An exaggerated sketch of the boundary layer formed around a body is shown in Fig. 9.1. To make the simplifications we must introduce the assumption that the boundary layer thickness δ is small relative to any other significant dimension L of the flow field (e.g. body size, radius of curvature, channel width etc.):

$$\delta << L$$

Let us now write the equation of conservation of mass and momentum for steady two-dimensional flow of an incompressible, Newtonian fluid (where $\nu = \mu/\rho$):

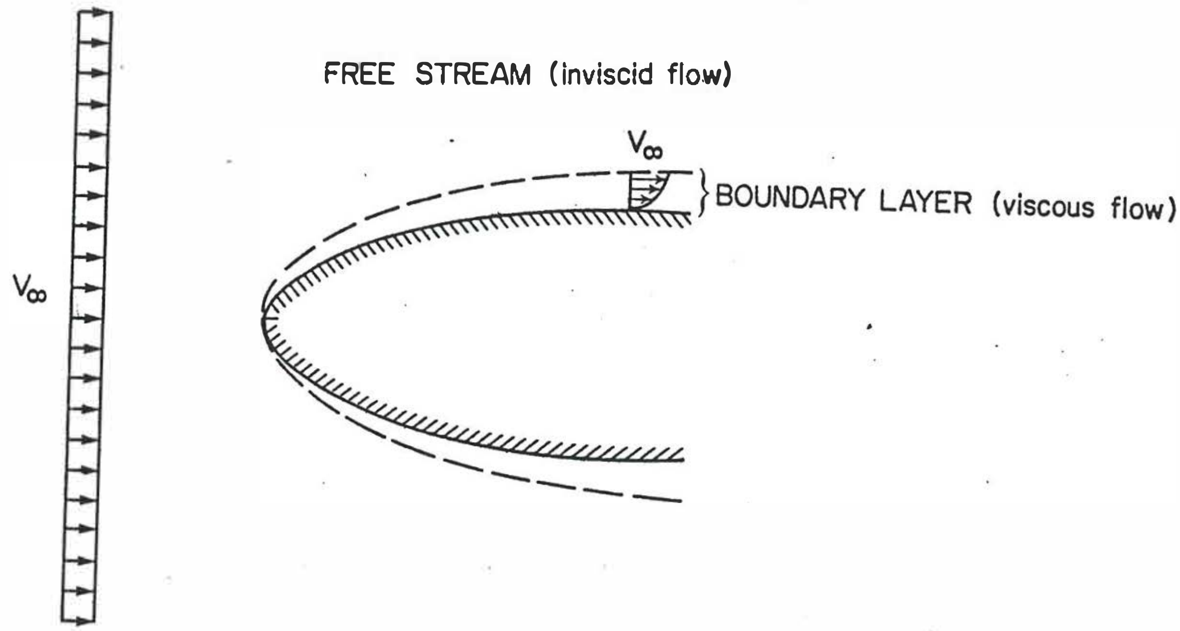

Fig. 9.1 Boundary layer formation around a blunt body.

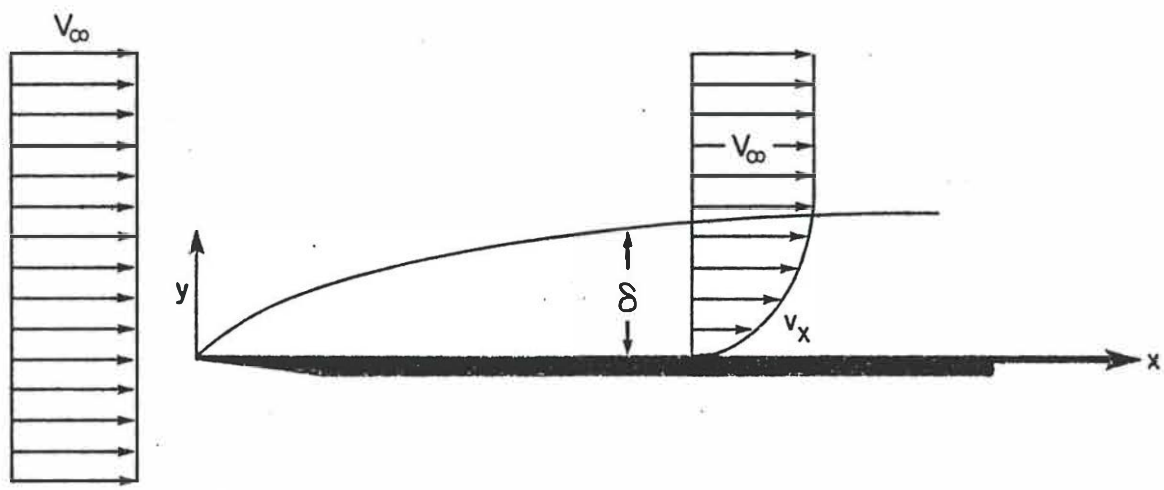

Fig. 9.2 Boundary layer flow over a flat plate

continuity $$\frac{\partial v_x}{\partial x} + \frac{\partial v_y}{\partial y} = 0 \qquad (9.1)$$

x momentum $$v_x \frac{\partial v_x}{\partial x} + v_y \frac{\partial v_x}{\partial y} = - \frac{1}{\rho}\frac{\partial p}{\partial x} + \nu\left(\frac{\partial^2 v_x}{\partial x^2} + \frac{\partial^2 v_x}{\partial y^2}\right) + g_x \qquad (9.2)$$

y momentum $$v_x \frac{\partial v_y}{\partial x} + v_y \frac{\partial v_y}{\partial y} = - \frac{1}{\rho}\frac{\partial p}{\partial y} + \nu\left(\frac{\partial^2 v_y}{\partial x^2} + \frac{\partial^2 v_y}{\partial y^2}\right) + g_y \qquad (9.3)$$

We now convert these equations to their dimensionless forms by introducing the following dimensionless variables

$$v_x^* = v_x/V_\infty$$
$$v_y^* = v_y/V_\infty$$

$$x^* = x/L$$
$$y^* = y/L \qquad (9.4)$$

$$p^* = p/\rho V_\infty^{\ 2}$$
$$g_x^* = g_x/(V_\infty^{\ 2}/L)$$

$$Re = \frac{\rho\, V_\infty L}{\mu} = \frac{V_\infty L}{\nu}$$

Equations (9.1), (9.2) and (9.3) take the form

continuity $$\frac{\partial v_x^*}{\partial x^*} + \frac{\partial v_y^*}{\partial y^*} = 0 \qquad (9.5)$$

x component $$v_x^* \frac{\partial v_x^*}{\partial x} + v_y \frac{\partial v_x^*}{\partial y^*} = - \frac{\partial p^*}{\partial x^*} + \frac{1}{Re}\left(\frac{\partial^2 v_x^*}{\partial x^{*2}} + \frac{\partial^2 v_x^*}{\partial y^{*2}}\right) + \frac{g_x}{V_\infty^2/L} \qquad (9.6)$$

y component $$v_x^* \frac{\partial v_x^*}{\partial x^*} + v_y^* \frac{\partial v_x^*}{\partial y^*} = - \frac{\partial p^*}{\partial y^*} + \frac{1}{Re} \left(\frac{\partial^2 v_y^*}{\partial x^{*2}} + \frac{\partial^2 v_y^*}{\partial y^{*2}}\right) + \frac{g_y}{V_\infty^2/L} \qquad (9.7)$$

These equations may describe the flow over a flat plate as shown in Fig. 9.2. The plate is in an infinite fluid which has a flat velocity profile (V_∞) as it approaches the leading edge. At the leading edge the velocity becomes zero and a velocity profile (v_x) develops as shown in Fig. 9.2. The "edge" of the boundary layer is defined by the approximation $v_x \simeq 0.99\ V_\infty$. Because of the boundary layer growth the fluid is "pushed" away from the plate, which means that the velocity has also a component in the y direction, v_y. We would expect that $v_y << v_x$. The dimensionless velocity $v_x^* = v_x/V_\infty$ is of order 1. The characteristic length L is chosen so that $x^* = x/L$ is also of order 1. Thus the derivative $\partial v_x^*/\partial x^*$ is of order 1. The dimensionless velocity $v_y^* = v_y/V_\infty$ should be of order Δ, where $\Delta << 1$. Because the boundary layer thickness δ is small compared to any significant body dimension ($\delta << L$), we would expect $y^* = y/L$ to be of order Δ. We can summarize these approximations in the form

$$\begin{aligned} v_x^* &\rightarrow [1] \\ v_y^* &\rightarrow [\Delta] \\ x^* &\rightarrow [1] \\ y^* &\rightarrow [\Delta] \end{aligned} \qquad (9.8)$$

Introducing the order of magnitude approximations into the continuity equation, we have

$$\frac{\partial v_x^*}{\partial x^*} + \frac{\partial v_y^*}{\partial y^*} = 0 \tag{9.9}$$

$$[\frac{1}{1}] \quad [\frac{\Delta}{\Delta}]$$

$$[1] \quad [1]$$

This means that both terms in the continuity equation are of order of magnitude 1. The x component of the equation of conservation of momentum gives

$$v_x^* \frac{\partial v_x^*}{\partial x^*} + v_y^* \frac{\partial v_x^*}{\partial y^*} = - \frac{\partial p^*}{\partial x^*} + \frac{1}{Re} \left(\frac{\partial^2 v_x^*}{\partial x^{*2}} + \frac{\partial^2 v_x^*}{\partial y^{*2}}\right) + g_x^* \tag{9.10}$$

$$[1 \; \frac{1}{1}] \quad [\Delta \; \frac{1}{\Delta}] \qquad [?] \qquad \frac{1}{Re} \; [\; \frac{1}{1^2} \qquad \frac{1}{\Delta^2}] \qquad [?]$$

$$[1] \qquad [1] \qquad [?] \qquad \frac{1}{Re} \; [\; 1 \qquad \frac{1}{\Delta^2}] \qquad [?]$$

We note that the term $(\partial^2 v_x^*/\partial x^{*2})$ is much smaller than $(\partial^2 v_x^*/\partial y^{*2})$ $(1 << (1/\Delta^2))$ and can be eliminated from the above expression. The viscous term is, therefore, of order $[1/Re]$ $[1/\Delta^2]$. Our original boundary layer hypothesis was that viscous effects are important, which means that the viscous term should be of order 1 or Re of order $[1/\Delta^2]$. This result implies that for boundary layer flow the Reynolds number must be large or alternatively we may conclude that the fluid viscosity must be small, because

$$Re = \frac{V_\infty L}{\nu}$$

$$[\frac{1}{\Delta^2}] = \frac{[1]}{[\nu]} \tag{9.11}$$

We also note that for g_x^* to be order 1 we must have g_x of order V_∞^2/L. A typical value of L might be of the order of 1m. Since g_x can be at most equal to 9.81 m/s^2 we must have V_∞ less than about 3m/s. In most (but not all) engineering applications of boundary layer theory the gravitational term can be eliminated from equation (9.10) because the velocities are generally larger. The y component of the equation of conservation of momentum is

$$v_x^* \frac{\partial v_y^*}{\partial x^*} + v_y^* \frac{\partial v_y^*}{\partial y^*} = - \frac{\partial p^*}{\partial y^*} + \frac{1}{Re} \left(\frac{\partial^2 v_y^*}{\partial x^{*2}} + \frac{\partial^2 v_y^*}{\partial y^{*2}}\right) + g_y^* \tag{9.12}$$

$$[\,1\ \frac{\Delta}{1}\,] \quad [\,\Delta\ \frac{\Delta}{\Delta}\,] \quad [?] \quad \Delta^2\ [\,\frac{\Delta}{1^2} \quad \frac{\Delta}{\Delta^2}\,] \quad [?]$$

The gravitational term will be of order 1 only if g_y is of order V_∞^2/L. All the other terms shown are of order Δ or less, thus the pressure gradient can be estimated from

$$0 = - \frac{\partial p^*}{\partial y^*} + g_y^* \tag{9.13}$$

This is the equation of static equilibrium in the y direction (see Section 2.1). Thus, for a thin boundary layer (with g_y^* generally a small number) it is reasonable to conclude that the pressure will be constant in the y direction. The pressure gradient $\partial p^*/\partial x^*$ in equation (9.10) can be determined from the inviscid flow (μ = 0) analysis of the flow region outside the boundary layer (see Chapter 11).

We now summarize the most important conclusions of the order of magnitude analysis:

(a) Both terms in the continuity equation are of the same order

(b) $\dfrac{\partial^2 v_x^*}{\partial x^{*2}} << \dfrac{\partial^2 v_x^*}{\partial y^{*2}}$

(c) The pressure across the boundary layer is constant

(d) The pressure gradient $(\partial p^*/\partial x^*)$ is prescribed by the inviscid flow outside the boundary layer.

(e) For most boundary layer flow problems gravitational effects will be unimportant.

Thus, reverting to dimensional quantities we can write the simplified form of equations (9.1), (9.2) and (9.3) as

continuity $$\frac{\partial v_x}{\partial x} + \frac{\partial v_y}{\partial y} = 0 \tag{9.14}$$

x momentum $$v_x \frac{\partial v_x}{\partial x} + v_y \frac{\partial v_x}{\partial y} = - \frac{1}{\rho} \frac{\partial p}{\partial x} + \nu \frac{\partial^2 v_x}{\partial y^2} \tag{9.15}$$

y momentum $$\frac{\partial p}{\partial y} = 0 \tag{9.16}$$

These are the boundary layer equations for steady flow with boundary conditions usually in the form

$$\begin{aligned} y &= 0 \qquad & v_x &= 0, \quad v_y = 0 \\ y &= \infty \qquad & v_x &= V_\infty(x) \end{aligned} \tag{9.17}$$

Note that the y component does not contain any information except that p = const across the boundary layer.

To determine the velocities at any point (x,y) we must, in addition, specify a velocity profile at a starting position $x = x_o$ where $v_x = v_x\,(x_o,y)$.

For unsteady flow problems the boundary layer equations are

$$\frac{\partial v_x}{\partial x} + \frac{\partial v_y}{\partial y} = 0 \tag{9.18}$$

x momentum $$\frac{\partial v_x}{\partial t} + v_x \frac{\partial v_x}{\partial x} + v_y \frac{\partial v_x}{\partial y} = -\frac{1}{\rho}\frac{\partial p}{\partial x} + \nu \frac{\partial^2 v_x}{\partial y^2} \tag{9.19}$$

with boundary conditions

$$y = 0 \qquad v_x = 0 \quad v_y = 0$$

$$y = \infty \qquad v_x = V_\infty(x,t) \tag{9.20}$$

Comparison of equations (9.2) and (9.3) with equations (9.15) and (9.16) shows the significant simplifications achieved. The y component has been completely dropped. The three unknowns v_x, v_y and p have been reduced to two, v_x and v_y, because the pressure gradient is prescribed by the inviscid flow outside the boundary layer (see Chapter 11, Inviscid Flow). Also, one of the two viscous terms has been dropped from the x component. The boundary layer equations are parabolic whereas the general Navier-Stokes equations are elliptic (for such classifications see for example reference [4]). Consequently, the boundary layer development and the velocity profiles at any station x are independent of further developments downstream. It should be noted, however, that downstream developments may affect upstream conditions in flows involving wake formation. The boundary layer approximation is indeed powerful but it has its limitations.

9.2 BOUNDARY LAYER ON A FLAT PLATE

We will now present a solution for the boundary layer flow on a flat plate, as shown in Fig. 9.2, in the absence of a pressure gradient. The governing equations are

$$\frac{\partial v_x}{\partial x} + \frac{\partial v_y}{\partial y} = 0 \tag{9.21}$$

$$v_x \frac{\partial v_x}{\partial x} + v_y \frac{\partial v_x}{\partial y} = \nu \frac{\partial^2 v_x}{\partial y^2} \tag{9.22}$$

The boundary conditions are

$$v_x = 0, \; v_y = 0 \qquad \text{at } y = 0 \tag{9.23}$$

$$v_x = V_\infty \qquad \text{at } y = \infty$$

This problem was first solved by Blasius [5] with the introduction of a similarity transformation.

Blasius assumed that the solution can be expressed in the form

$$\frac{v_x}{V_\infty} = \phi \left(\frac{y}{\delta}\right) \tag{9.24}$$

This means that the normalized (v_x/V_∞) velocity varies as a function of the normalized distance (y/δ). Such a transformation was used for the flow near a flat plate suddenly set in motion (section 7.15). In that problem the thickness δ was proportional to $\sqrt{\nu t}$. For a particle at the edge of the boundary layer $t = x/V_\infty$, so that δ will be proportional to $\sqrt{\nu x/V_\infty}$. The proportionality factor may be incorporated into the function ϕ. Thus, we may write in general

$$\frac{v_x}{V_\infty} = \phi\,(\eta) \text{ where } \eta = \frac{y}{\sqrt{\nu x/V_\infty}} = y\sqrt{V_\infty/\nu x} \tag{9.25}$$

It is convenient to introduce a stream function $\psi(x,y)$ which automatically satisfies the continuity equation (9.21). Let the stream function be defined by

$$v_x = \frac{\partial\psi}{\partial y} \qquad v_y = -\frac{\partial\psi}{\partial x} \tag{9.26}$$

The continuity equation becomes

$$\frac{\partial^2\psi}{\partial x\,\partial y} - \frac{\partial^2\psi}{\partial x\,\partial y} = 0 \tag{9.27}$$

We can further introduce a dimensionless function $f(\eta)$ and let

$$\psi = \sqrt{\nu x\, V_\infty}\, f(\eta) \tag{9.28}$$

Thus, the velocity components in terms of $f(\eta)$ are

$$v_x = \frac{\partial\psi}{\partial y} = \frac{\partial\psi}{\partial\eta}\frac{\partial\eta}{\partial y} = V_\infty f' \tag{9.29}$$

$$v_y = -\frac{\partial\psi}{\partial x} = -f(\eta)\frac{\partial}{\partial x}(\sqrt{\nu x V_\infty}) - \sqrt{\nu x V_\infty}\,\frac{df}{d\eta}\frac{\partial\eta}{\partial x}$$

$$= \frac{1}{2}\sqrt{\frac{\nu\, V_\infty}{x}}\,(\eta f' - f) \tag{9.30}$$

Expressing $\partial v_x/\partial x$, $\partial v_x/\partial y$ and $\partial^2 u_x/\partial y^2$ in terms of $f(\eta)$ and substituting the resulting expressions in equation (9.22) we get

$$-\frac{V_\infty^2}{2x}\,\eta\, f'\, f'' + \frac{V_\infty^2}{2x}(\eta\, f' - f)f'' = \nu\,\frac{V_\infty^2}{x\nu}\, f''' \tag{9.31}$$

which simplifies to the ordinary, nonlinear, third-order differential equation

$$f\, f'' + 2\, f''' = 0 \tag{9.32}$$

The boundary conditions (eqs. 9.23) in terms of the new variable η are

$$f = 0 \quad f' = 0 \quad \text{at } \eta = 0$$

$$f' = 1 \qquad\qquad \text{at } \eta = \infty \tag{9.33}$$

These three boundary conditions are sufficient for the determination of the solution of the third order ordinary differential equation (9.32).

However, the solution of this equation cannot be given in closed form. Blasius [5] obtained a power series solution. Howarth [6] obtained a more accurate solution and recently purely numerical methods have been used. The results given on table 9.1 are taken from Howarth's paper [6]. The velocity profile v_x is in excellent agreement with experiments by Nikuradse [7] as shown in Fig. 9.3. The variation of the velocity component v_y with dimensionless distance η is shown in Fig. 9.4. It is interesting to note that v_y is not zero at the outer edge of the boundary layer ($\eta \to \infty$). Finite difference solutions of equations (9.21) and (9.22) have also been presented (e.g. reference [8]).

The boundary layer thickness, that is the value of y for which $v_x = 0.99\ V_\infty$, can be obtained from Table 9.1 ($\eta \simeq 5$)

$$\delta \simeq 5.0 \sqrt{\frac{\nu x}{V_\infty}} = \frac{5x}{\sqrt{Re_x}} \tag{9.34}$$

where
$$Re_x = \frac{\rho\ V_\infty x}{\mu} = \frac{V_\infty x}{\nu} \tag{9.35}$$

The experimental determination of the boundary layer thickness is very difficult because the velocity approaches asymptotically the free stream value V_∞. The "edge" of the boundary layer is poorly defined. For this reason alternative thicknesses which can be measured more accurately are often used. The displacement thickness δ^* is obtained by equating the volume rate of flow which is "missing" because of the boundary layer $\int_0^\infty (V_\infty - u_x)dy$ to that for a fictitious layer having a flat profile ($V_\infty\ \delta^*$). Thus

$$\delta^* = \int_0^\infty (1 - \frac{v_x}{V_\infty})dy \tag{9.36}$$

Table 9.1

Howarth's [6] results for laminar boundary layer flow on a flat plate.

$\eta = y\sqrt{\dfrac{V_\infty}{\nu x}}$	f	$f' = \dfrac{v_x}{V_\infty}$	f''
0	0	0	0·33206
0·2	0·00664	0·06641	0·33199
0·4	0·02656	0·13277	0·33147
0·6	0·05974	0·19894	0·33008
0·8	0·10611	0·26471	0·32739
1·0	0·16557	0·32979	0·32301
1·2	0·23795	0·39378	0·31659
1·4	0·32298	0·45627	0·30787
1·6	0·42032	0·51676	0·29667
1·8	0·52952	0·57477	0·28293
2·0	0·65003	0·62977	0·26675
2·2	0·78120	0·68132	0·24835
2·4	0·92230	0·72899	0·22809
2·6	1·07252	0·77246	0·20646
2·8	1·23099	0·81152	0·18401
3·0	1·39682	0·84605	0·16136
3·2	1·56911	0·87609	0·13913
3·4	1·74696	0·90177	0·11788
3·6	1·92954	0·92333	0·09809
3·8	2·11605	0·94112	0·08013
4·0	2·30576	0·95552	0·06424
4·2	2·49806	0·96696	0·05052
4·4	2·69238	0·97587	0·03897
4·6	2·88826	0·98269	0·02948
4·8	3·08534	0·98779	0·02187
5·0	3·28329	0·99155	0·01591
5·2	3·48189	0·99425	0·01134
5·4	3·68094	0·99616	0·00793
5·6	3·88031	0·99748	0·00543
5·8	4·07990	0·99838	0·00365
6·0	4·27964	0·99898	0·00240
6·2	4·47948	0·99937	0·00155
6·4	4·67938	0·99961	0·00098
6·6	4·87931	0·99977	0·00061
6·8	5·07928	0·99987	0·00037
7·0	5·27926	0·99992	0·00022
7·2	5·47925	0·99996	0·00013
7·4	5·67924	0·99998	0·00007
7·6	5·87924	0·99999	0·00004
7·8	6·07923	1·00000	0·00002
8·0	6·27923	1·00000	0·00001
8·2	6·47923	1·00000	0·00001
8·4	6·67923	1·00000	0·00000
8·6	6·87923	1·00000	0·00000
8·8	7·07923	1·00000	0·00000

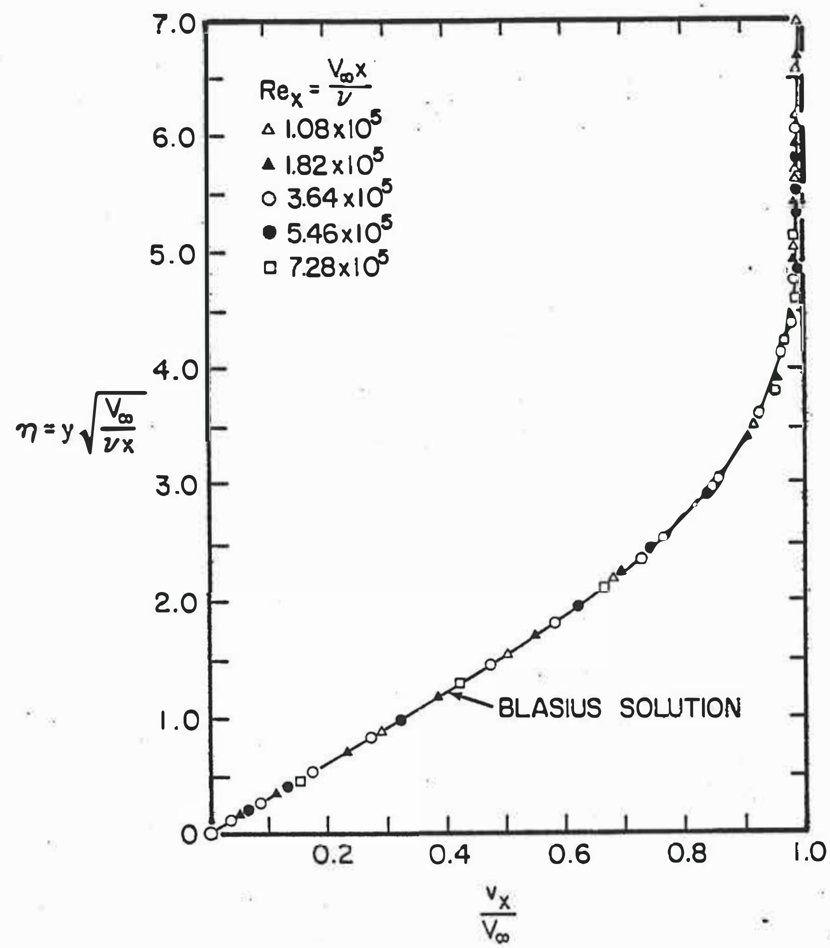

Fig. 9.3 Comparison of Blasius similarity solution and Nikuradse's experimental data for the longitudinal velocity v_x.

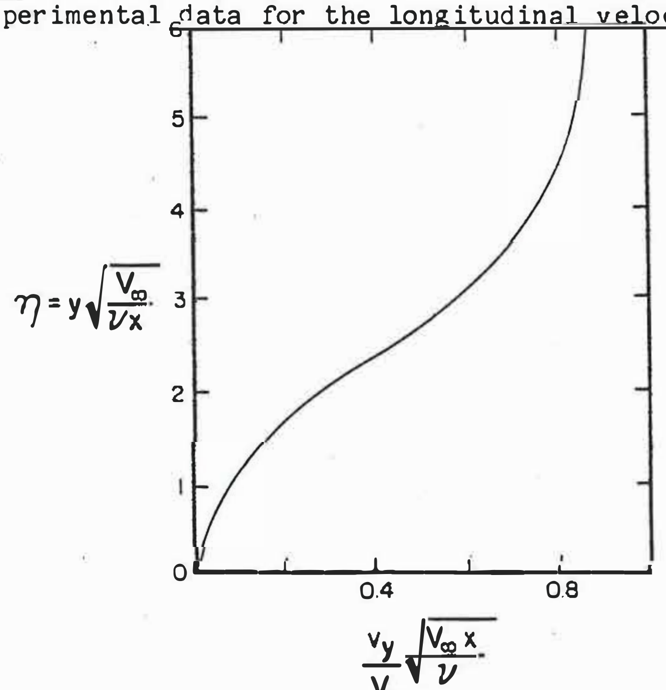

Fig. 9.4 The transverse velocity component v_y, in laminar boundary layer on a flat plate, as a function of distance from the plate surface according to Blasius solution.

Similarly, the <u>momentum thickness</u> θ is defined by equating the rate of momentum "missing" because of the boundary layer $\int_0^\infty \rho\, v_x(V_\infty - v_x)dy$ to the rate of momentum of a fictitious boundary layer having a flat profile $\rho\, V_\infty^2\, \theta$. Thus

$$\theta = \int_0^\infty \frac{v_x}{V_\infty}\left(1 - \frac{v_x}{V_\infty}\right)dy \tag{9.37}$$

A rough comparison between the various thicknesses gives

$$\delta^* \simeq \delta/3 \quad \text{and} \quad \theta \simeq \delta/8 \tag{9.38}$$

The displacement and momentum thicknesses appear in the integral methods analysis (Section 9.6).

The <u>shear stress at the wall</u> (or skin friction) can be determined from the expression

$$\tau_w = \mu\left(\frac{\partial v_x}{\partial y}\right)_{y=0} \tag{9.39}$$

The slope of the dimensionless velocity profile at the wall (y = 0) is 0.332, that is

$$\left.\frac{\partial\,(v_x/V_\infty)}{\partial\left(y\sqrt{\frac{V_\infty}{\nu x}}\right)}\right|_{y=0} = 0.332 \tag{9.40}$$

or

$$\left(\frac{\partial\, v_x}{\partial y}\right)_{y=0} = 0.332\, V_\infty \sqrt{\frac{V_\infty}{\nu x}} = 0.332\,\frac{V_\infty}{x}\sqrt{Re_x} \tag{9.41}$$

which gives

$$\tau_w = 0.332\,\frac{\mu\, V_\infty}{x}\sqrt{Re_x} \tag{9.42}$$

or

$$\tau_w = 0.332 \frac{\rho V_\infty^2}{\sqrt{Re_x}} \tag{9.43}$$

For generality we introduce a dimensionless <u>local friction coefficient</u> which is defined by

$$C_f = \frac{\tau_w}{\frac{\rho V_\infty^2}{2}} \tag{9.44}$$

Inserting the expression for τ_w from equation (9.43) we get

$$C_f = \frac{0.664}{\sqrt{Re_x}} \tag{9.45}$$

The local skin friction coefficient is plotted as a function of Re_x in Fig. 9.5.

In many practical problems the average friction coefficient for a plate of finite length L is useful. It can be easily obtained by integrating the expression for the local friction coefficient from x = 0 to x = L and dividing by L:

$$\bar{C}_f = \frac{1}{L} \int_o^L C_f \, dx = \frac{1}{L} \int_o^L \frac{0.664}{\sqrt{\frac{\rho V_\infty x}{\mu}}} dx = \frac{1.33}{\sqrt{\frac{\rho V_\infty L}{\mu}}} \tag{9.46}$$

or

$$\bar{C}_f = \frac{1.33}{\sqrt{Re_L}} \tag{9.47}$$

<u>Comments</u>

(a) From the expression for the boundary layer thickness (eq. 9.34) we note that $\delta = 0$ at the leading edge (x = 0). Downstream the boundary layer grows and $\delta \propto x^{1/2}$. For a given x station the boundary layer thickness decreases as the velocity V_∞ increases.

(b) From the expression for shear stress at the wall (eq. 9.43) we note that τ_w is very large near the leading edge (infinite at $x = 0$) and decreases with increasing distance.

(c) The boundary layer approximation is not valid in the immediate vicinity of the leading edge because the assumption $\partial^2 v_x/\partial x^2 \ll \partial^2 v_x/\partial y^2$ cannot be satisfied. This region however is insignificant for engineering problems.

(d) For large distances from the leading edge the Reynolds number is large and the inertia forces are much larger than the viscous forces. Transition from laminar to turbulent flow usually takes place at $Re_x \approx 500{,}000$.

Example 9.1

A flat plate of practically infinitesimal thickness is towed behind a boat travelling at 12 km/hr. The plate has dimensions 25 cm x 25 cm and the temperature of the water is 15°C. We will determine the boundary layer thickness at the trailing edge and the total force required to tow the plate.

Solution

We must first calculate the Reynolds number at the trailing edge to see whether the flow is laminar

$$Re_x = \frac{\rho\, V_\infty x}{\mu} = \frac{(1000\ \mathrm{kg/m^3})(\frac{12000}{3600}\ \mathrm{m/s})\quad(0.25\ \mathrm{cm})}{0.0012\ \mathrm{N \cdot s/m^2}} = 694444$$

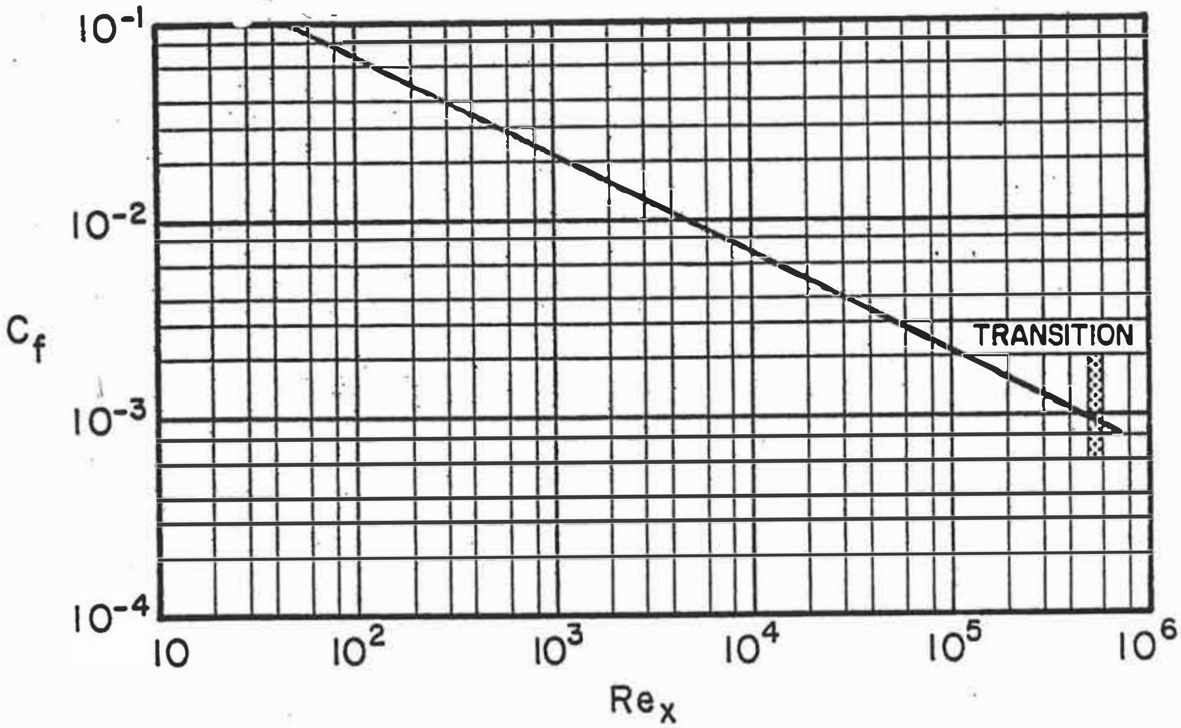

Fig. 9.5 The local skin friction coefficient C_f as a function of the Reynolds number Re_x for a laminar boundary layer on a flat plate.

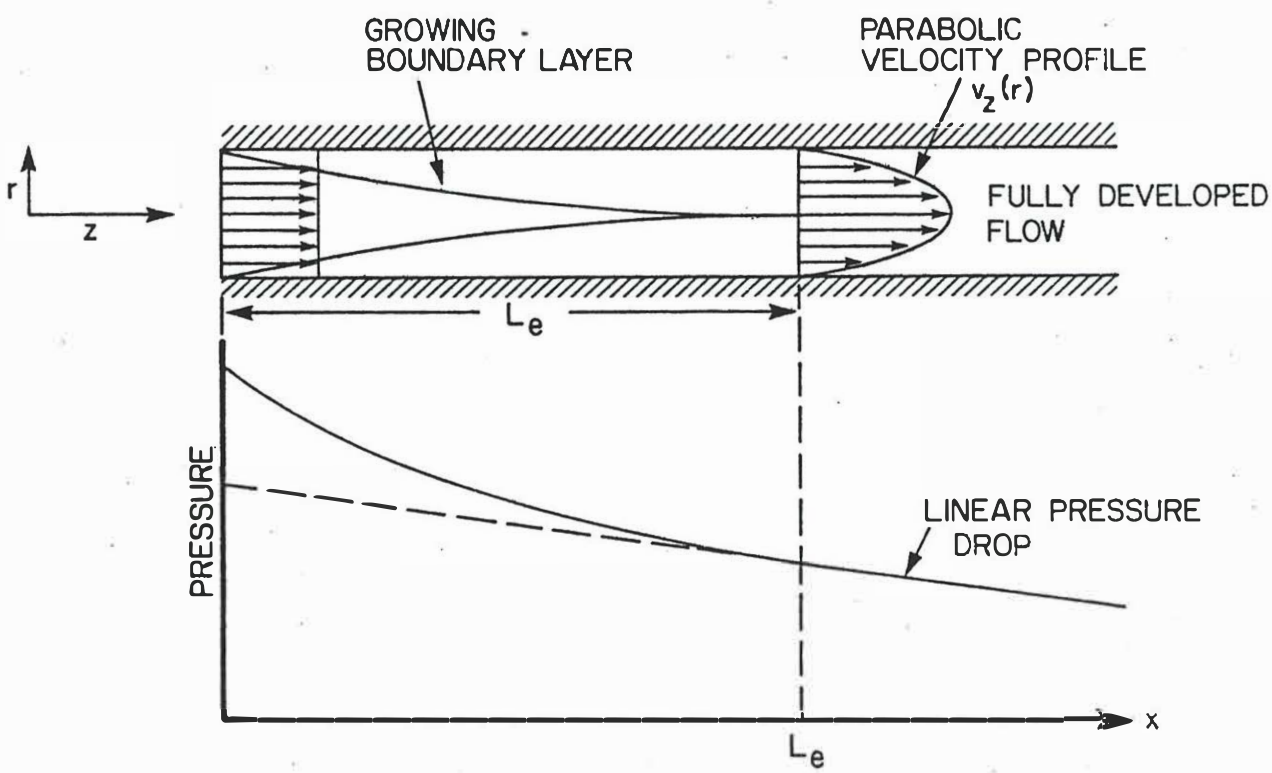

Fig. 9.6 Velocity profile development and pressure drop in the entry region in a tube.

This value is above the usually accepted critical value of 500,000. However, if the external flow is undisturbed and the plate is smooth it is possible to have laminar flow up to Re = 1,000,000. Thus, assuming the boundary layer to be laminar over the whole plate, we have

$$\delta = \frac{5x}{\sqrt{Re_x}} = \frac{5 \times 0.25\text{m}}{\sqrt{694444}} = 0.0015\text{m} = 1.5\text{mm}$$

$$\bar{C}_f = \frac{1.33}{\sqrt{Re_x}} = \frac{1.33}{\sqrt{694444}} = 1.6 \times 10^{-3}$$

$$\tau_w = \frac{1}{2}\bar{C}_f\,\rho\,V_\infty^2 = \frac{1}{2} \times 1.6 \times 10^{-3}\ (1000\ \text{kg/m}^3)\left(\frac{12000}{3600}\text{m/s}\right)^2 = 8.87\ \frac{\text{N}}{\text{m}^2}$$

Thus, the force required (for two sides) is

$$F = 2\,\tau_w\,A = 2\left(8.87\ \frac{\text{N}}{\text{m}^2}\right)(0.25 \times 0.25\ \text{m}^2) = 1.11\ \text{N}$$

9.3 Laminar Entry Flow

In Chapter 7 we examined laminar flow in long tubes and obtained the well known parabolic velocity profile. In the entry region, however, we have the development of a boundary layer just as in the case of flow over a flat plate. For the tubular geometry, the boundary layer develops around the inside cylindrical surface, grows downstream and at some distance its thickness becomes equal to the tube radius. From this distance downstream the streamlines are parallel, the velocity profile is parabolic and the pressure drop is linear as we have seen in Section 7.3. This is the region of fully developed flow. The development of the boundary layer, the velocity profiles and the pressure drop for entry flow is shown in Fig. 9.6.

In the entry region of a tube the boundary layer equations, for steady flow of an incompressible Newtonian fluid, are:

continuity $$\frac{1}{r}\frac{\partial}{\partial r}(r\ v_r) + \frac{\partial}{\partial z}(v_z) = 0 \tag{9.48}$$

z momentum $$\rho(v_r \frac{\partial v_z}{\partial r} + v_z \frac{\partial v_z}{\partial z}) = -\frac{\partial p}{\partial z} + \mu[\frac{1}{r}\frac{\partial}{\partial r}\ (r\frac{\partial v_z}{\partial r})] \tag{9.49}$$

The integral continuity equation for this type of flow may be written as

$$V_o\ 2\pi R^2 = \int_o^{2\pi}\int_o^R v_z\ rdrd\theta \tag{9.50}$$

or $$V_o\ R^2 = \int_o^R v_z\ rdr \tag{9.51}$$

The boundary conditions are

$$\begin{aligned} &x = 0 && v_z = V_o \\ &r = 0 && \frac{\partial\ v_z}{\partial r} = 0 \\ &r = R && v_z = 0\ ,\ v_r = 0 \end{aligned} \tag{9.52}$$

The unknown variables are three v_z, v_r and p. The three equations (9.48), (9.49) and (9.51) can be solved simultaneously by the method of finite differences following Hwang and Fan's [9] approach or by approximate analytical methods [2], [10]. Both methods of solution are rather involved and they are beyond the scope of this book. An interesting result of the analysis is the entry length L_e. The entry length is usually defined as the distance from the plane of entry at which the centerline velocity is within 1% of its final value. Downstream from $z = L_e$ the flow is fully developed and the velocity profile is parabolic as shown in Fig. 9.6. The solutions of the differential equations yield an estimate for the entry length in tubes which is in good agreement with experimental data. An approximate value is given by

$$\frac{L_e}{D} \approx 0.056 \, Re_D \tag{9.53}$$

For entry flow in the gap between two flat plates separated by a distance H, the entry length is [11]:

$$\frac{L_e}{H} \approx 0.044 \, Re_H \tag{9.54}$$

The above expressions are often used in design considerations. For example if we were asked to design an experiment to demonstrate the parabolic velocity profile and the linear pressure drop in tubes we could determine the shortest possible length required. Assuming Re_D = 1000 and D = 5 cm we would need at least 5 × 56 = 280 cm of pipe length for the flow to become fully developed.

9.4 LAMINAR JETS

Whenever a fluid is issuing from an opening into a large body of the same fluid we observe the formation of a jet which spreads downstream as shown in Fig. 9.7. If the opening is an orifice the velocity profile will be nearly flat at the exit. If the opening is the end of a long tube the velocity profile will be parabolic at the exit. In either case the jet will spread and the velocity profile at a certain distance will look like a bell-shaped curve. Because of the jet spreading there is also a velocity component in a direction perpendicular to the main flow direction. It is reasonable to assume that this type of flow is described by the boundary layer equations of section 9.1. We note, however, that there will not be a pressure gradient because the pressure in the boundary layer (the jet in this

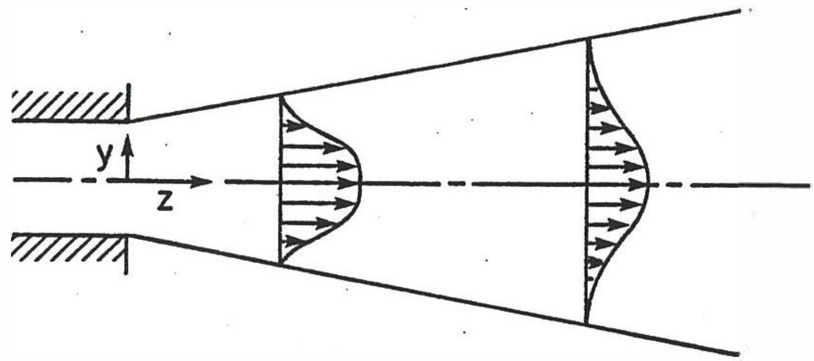

Fig. 9.7 Schematic of jet spreading and velocity profile development.

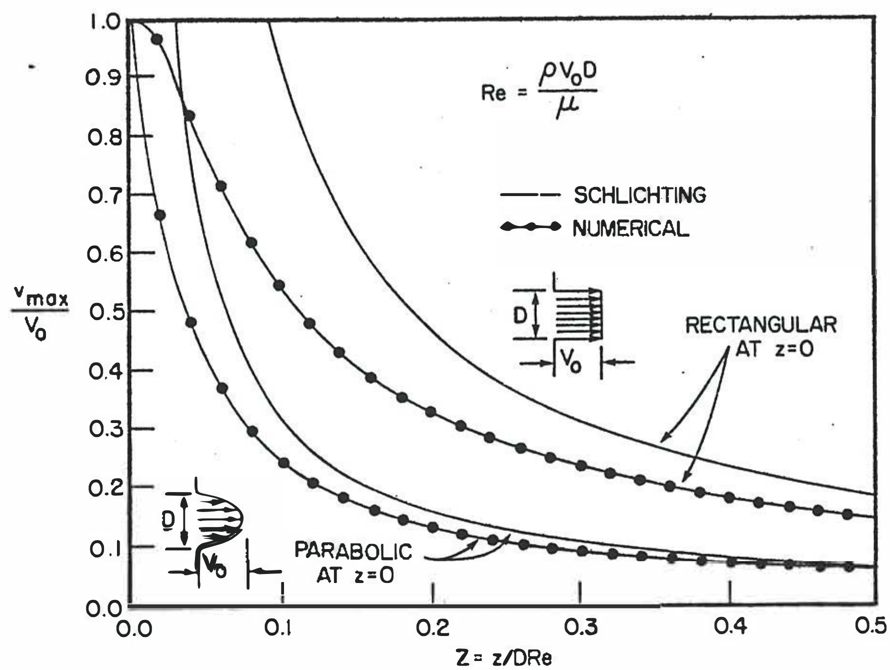

Fig. 9.8 Comparison of centerline velocity drop between Schlichting's [2] similarity solution and Vlachopoulos [13] finite difference calculations for an axisymmetric jet.

case) is prescribed by conditions outside. For an air jet issuing into air the outside pressure is p_{atm}, throughout, therefore the pressure gradient is zero.

For a two-dimensional jet of an incompressible and Newtonian fluid under steady state conditions we have the boundary layer equations

$$\frac{\partial v_y}{\partial y} + \frac{\partial v_z}{\partial z} = 0 \qquad (9.55)$$

$$v_y \frac{\partial v_z}{\partial y} + v_z \frac{\partial v_z}{\partial z} = \nu \frac{\partial^2 v_z}{\partial y^2} \qquad (9.56)$$

The boundary conditions are

$$z = 0 \qquad v_z = V_o(y) \text{ (must be known)}$$

$$y = 0 \qquad \frac{\partial v_z}{\partial y} = 0 \quad v_y = 0 \qquad (9.57)$$

$$y = \infty \qquad v_z = 0$$

Schlichting [2] developed a similarity solution for equations (9.55) and (9.56). Finite difference solutions have also been presented [12, 13]. Schlichting'g solution predicts a midplane (maximum) velocity drop in the form

$$v_{max} = 0.4543 \left(\frac{J^2}{\rho\mu z}\right)^{1/3} \qquad (9.58)$$

where $J = \left[\rho \int_{-H/2}^{H/2} v_z^2 \, dy\right]_{z = 0}$ and H = orifice width

if $v_z = V_o$ (flat velocity profile) at $z = 0$ we get

$$J^2 = \rho^2 V_o^4 H^2 \qquad (9.59)$$

Then, by substituting into equation (9.58) and rearranging we can express the velocity drop at the centerplane in dimensionless form as

$$\frac{v_{max}}{V_o} = 0.4543 \left(\frac{C^2}{\frac{z}{H\ Re}}\right)^{1/3} \tag{9.60}$$

where $\qquad C^2 = 1 \quad$ for $v_z = V_o$ at $z = 0$.

Similarly, we can obtain equation (9.60) with

$$C^2 = \frac{8}{15} \quad \text{for } v_z = V_o \left(1 - \left(\frac{y}{H}\right)^2\right) \text{ at } z = 0$$

In equation (9.60) $Re = \rho V_o H/\mu$. The jet width b is defined as twice the distance y where $v_z \simeq 0.01\ v_{max}$ and it is given by the following expression:

$$b = 2y|_{0.01} = 21.8 \left(\frac{\mu^2}{J\rho}\right)^{1/3} z^{2/3} \tag{9.61}$$

It should be noted that Schlichting's analysis is valid for a jet issuing from a point source at x = 0 where the predicted maximum velocity becomes infinite. Therefore the results are not valid in the immediate vicinity of an opening of width H.

For an <u>axisymmetric jet</u> (also called round jet) the boundary layer equations are

continuity $\qquad \frac{1}{r}\frac{\partial}{\partial r}(r\ v_r) + \frac{\partial}{\partial z}(v_z) = 0 \qquad (9.62)$

z momentum $\qquad v_r \frac{\partial v_z}{\partial r} + v_z \frac{\partial v_z}{\partial z} = \nu \frac{1}{r}\frac{\partial}{\partial r}\left(r \frac{\partial v_z}{\partial r}\right) \qquad (9.63)$

and the boundary conditions

$$z = 0 \qquad v_z = V_o(r) \quad \text{(must be known)}$$

$$y = 0 \qquad \frac{\partial v_z}{\partial r} = 0 \qquad v_y = 0 \tag{9.64}$$

$$y = \infty \qquad v_z = 0$$

Schlichting's [2] similarity solution for an axisymmetric jet gives

$$v_{max} = \frac{3}{8\pi}\frac{J}{\mu z} \tag{9.65}$$

where $$J = 2\pi\rho \int_0^D v_z^2 \, r dr$$

In dimensionless form we have

$$\frac{v_{max}}{V_o} = \frac{3}{32}\frac{C}{\frac{z}{D\,Re}} \tag{9.66}$$

where $$Re = \frac{\rho V_o D}{\mu}$$

$$C = 1 \qquad \text{for } v_z = V_o \qquad \text{at } z = 0$$

$$C = 1/3 \qquad \text{for } v_z = V_o\,(1 - (\frac{r}{D})^2) \text{ at } z = 0$$

The jet width increases linearly with axial position, i.e

$$b = 2r|_{0.01} = 49.10\,(\frac{\mu^2}{J\rho})^{1/2}\, z \tag{9.67}$$

A comparison of v_{max} from Schlichting's similarity solution and numerical calculations [13] is given in Fig. 9.8. We note that the similarity solution is not valid in the neighborhood of the jet origin. The dimensionless velocity profiles v_z and v_r as obtained by the finite difference method [13] are shown in Figs 9.9 and 9.10. The axial velocity component v_z tends to flatten out as the dimensionless distance $Z = z/DRe$ increases. It is interesting to note that at short distances from the centerline the radial velocity v_r is positive whereas at large distances it is negative. This means that near the centerline the jet

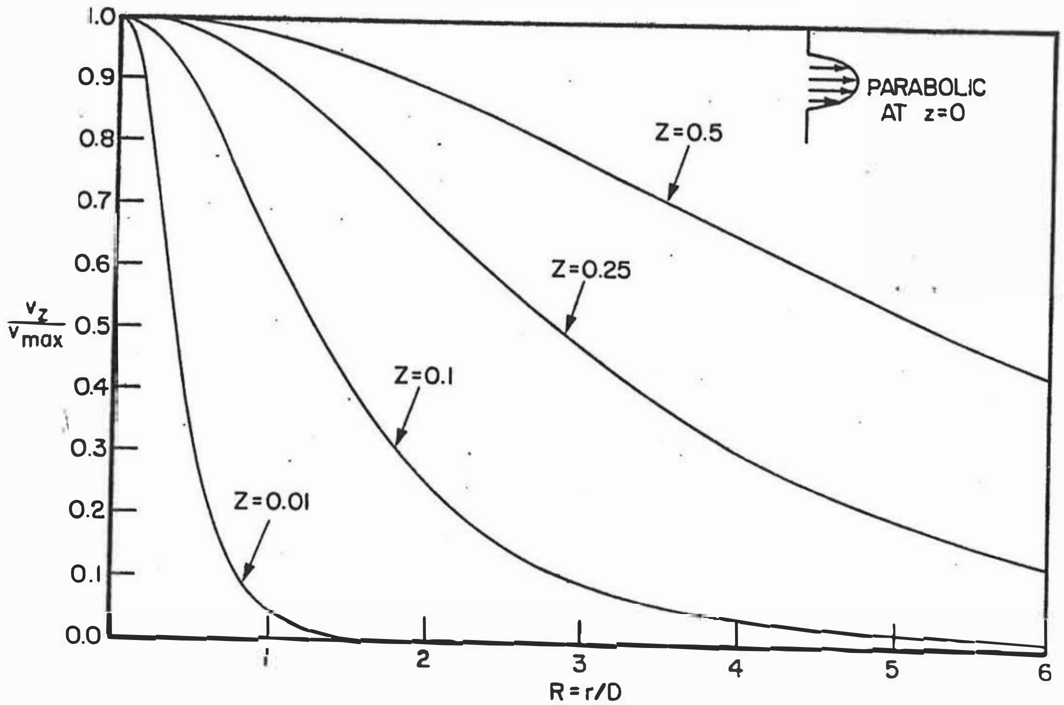

Fig. 9.9 Longitudinal velocity profiles v_z in a axisymmetric jet from reference [13].

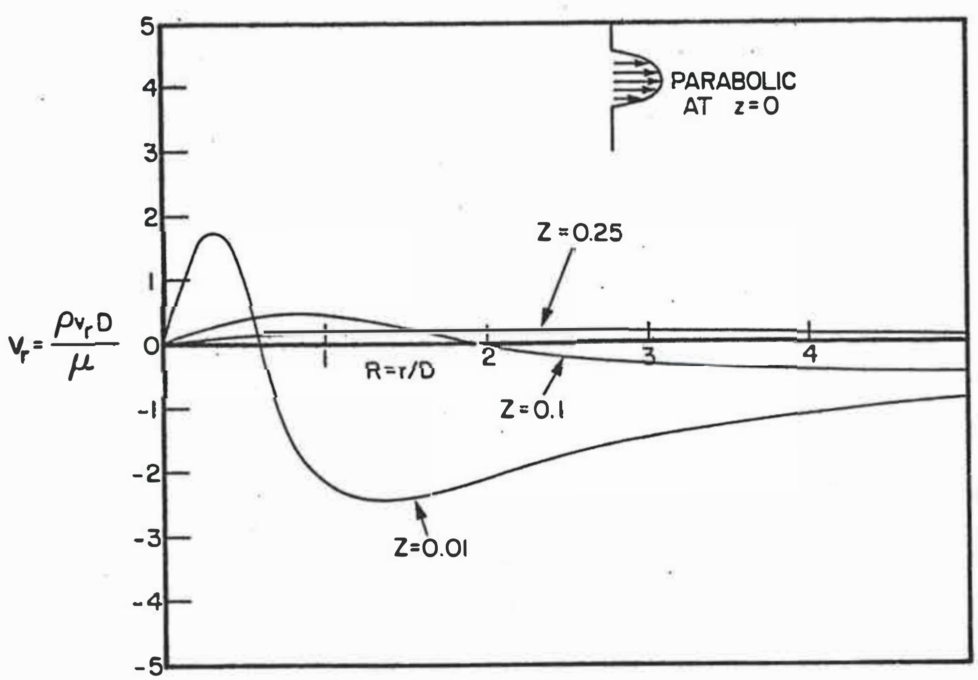

Fig. 9.10 Transverse velocity profiles v_r in an axisymmetric jet from reference [13].

spreads towards the outside whereas near the jet boundaries fluid is entrained from the surroundings. The fluid entrainment in a jet explains physically the diminution of its velocity. The total momentum must be the same at any cross-section at the jet. At larger distances from the exit more and more fluid mass participates with a corresponding reduction in jet velocity.

Measurements of Andrade [14] on two-dimensional jets confirmed the boundary layer theory as presented above. It should be noted, however, that jets tend to become turbulent at a surprisingly low Reynolds number ($Re = \rho V_{avg} H/\mu$ of about 30). Experimental velocity profiles in the exit region of a laminar jet have been obtained by Samuels and Wenzel (15).

The boundary layer equations for two-dimensional and axisymmetric jets describe also the flow field in a wake (shown in Fig. 9.11) or the mixing layer between two uniform streams (shown in Fig. 9.12). The boundary conditions are of course, different in each case. Again, similarity type solutions can be obtained [2, 16]. The main features of these flow fields, which are usually called free shear flows, are summarized in Table 9.2.

Example 9.2

In a fluidic valve an air jet is issuing from a long 0.2 mm diameter tube at an average velocity of 10 m/s. Determine the centerline velocity in the jet at a distance of 1 cm from the tube exit.

Solution

The Reynolds number with respect to average velocity ($V_{avg} = {}^1/_2\, V_o$) is

$$Re_a = \frac{V_{avg}\, D}{\nu} = \frac{(10\ \mathrm{m/s})(2 \times 10^{-4}\ \mathrm{m})}{1.3 \times 10^{-5}} \approx 154$$

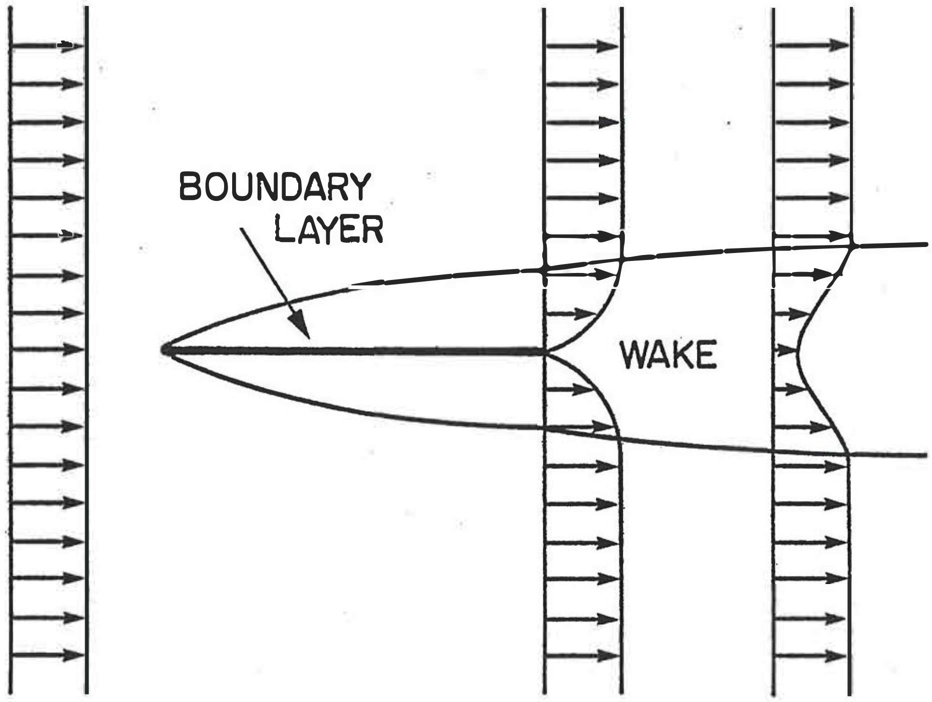

Fig. 9.11 Schematic of a wake formed behind a thin flat plate

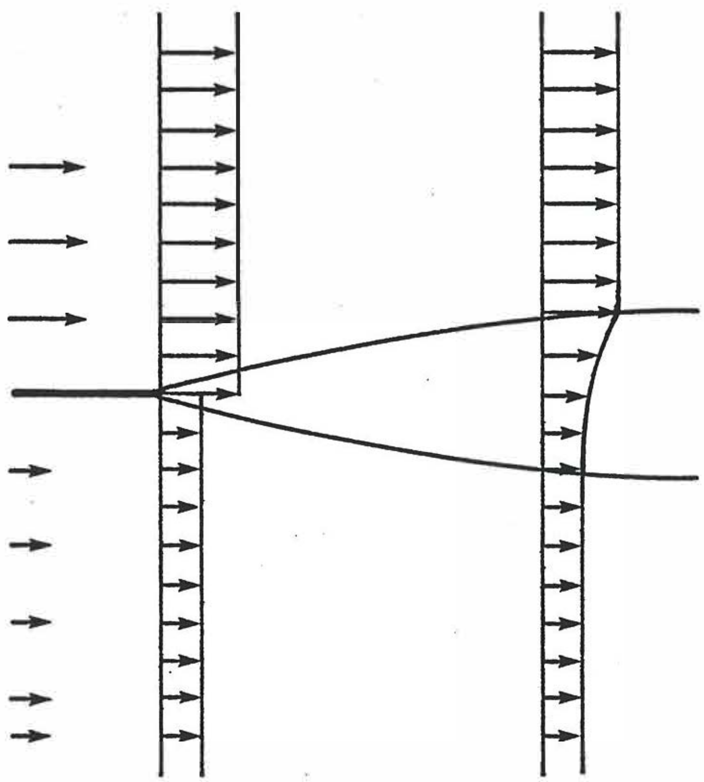

Fig. 9.12 Schematic of the mixing zone of two uniform streams having different velocities.

<u>Table 9.2</u>

Layer width and centerline velocity decay as
a function of position for free shear flows
(LAMINAR)

FLOW	SKETCH	WIDTH	CENTERLINE VELOCITY
TWO-DIMENSIONAL JET	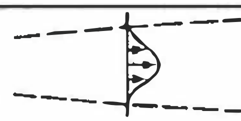	$z^{2/3}$	$z^{-1/3}$
AXISYMMETRIC JET	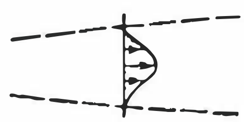	z	z^{-1}
TWO-DIMENSIONAL WAKE	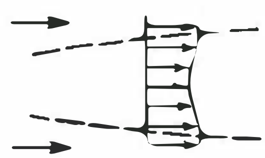	$z^{1/2}$	$z^{-1/2}$
AXISYMMETRIC WAKE	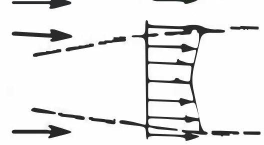	$z^{1/2}$	z^{-1}
TWO UNIFORM STREAMS	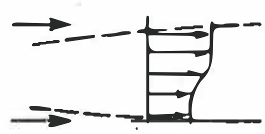	$z^{1/2}$	z^{0}

Although the Reybolds number is larger than 30 it is possible that the jet will be laminar at a distance 1 cm from the tube exit. We will therefore, use the laminar theory to determine the centerline velocity.

The dimensionless axial distance is

$$\frac{z}{D\ Re} = \frac{10^{-2} m}{(2\times10^{-4}\ m)\ 308} = 0.162$$

The velocity at the end of a long tube is nearly parabolic. Thus, referring to Fig. 9.8 we note that the numerical and analytical solutions are very close at z/D Re ≃ 0.326. We will use equation (9.66):

$$\frac{v_{max}}{V_o} = \frac{3}{32}\frac{C}{\frac{z}{D\ Re}} = \frac{3}{32}\frac{1}{3\times0.162} = 0.192$$

and

$$v_{max} = 3.85\ m/s$$

9.5 FURTHER COMMENTS ON SIMILARITY SOLUTIONS

The success of the similarity transformation is due to the fact that many boundary layer flows exhibit geometrically similar velocity profiles. This means that the velocity profiles at all x positions differ only by scale factors in v_x and y, or mathematically

$$\frac{v_x}{V(x)} = \phi\left(\frac{y}{h(x)}\right) \tag{9.68}$$

For boundary layer flow over a flat plate (sec. 9.2) we used $V(x) = V_\infty$ and $h(x) = \delta(x)$ (see eq. 9.24). It is not possible, however, to state a priori whether a particular problem will have similar solutions. We can only anticipate such solutions either by comparison to other problems of the same type or by "guessing" the probable development of the velocity profiles. By introducing a similarity transformation we may reduce the partial differential equations to an ordinary differential equation which is then solved. Numerous solutions of this type have been developed before the advent of the modern high speed computers. Besides Schlichting [2] and Cebeci and Bradshaw [16], Dorrance [17] presents a most general approach to similarity in boundary layer flows.

The rapid development of numerical techniques like finite differences, has limited the usefulness of similarity transformations. However, the study of similarity solutions is still very important not only because of their historical significance but also because they provide more physical insight to flow problems than computer solutions.

9.6 THE INTEGRAL MOMENTUM APPROXIMATION

The introduction of the boundary layer concept led to the simplication of the general conservation equations for "thin" flow regions to the form

$$\frac{\partial v_x}{\partial x} + \frac{\partial v_y}{\partial y} = 0 \tag{9.69}$$

$$\rho \left(v_x \frac{\partial v_x}{\partial x} + v_y \frac{\partial v_x}{\partial y}\right) = - \frac{\partial p}{\partial x} + \mu \frac{\partial^2 v_x}{\partial y^2} \tag{9.70}$$

The pressure gradient is prescribed by the flow outside the boundary layer where the inviscid flow approximation ($\mu = 0$) is valid. For inviscid flow Euler's equation (6.95) can be used. When the flow is steady and the gravitational effects negligible we have

$$\rho \bar{V} \cdot \nabla \bar{V} = - \nabla p \tag{9.71}$$

since $v_x = V_\infty$, $v_z = 0$, $\frac{\partial v_x}{\partial y} = 0$ and $v_y \simeq 0$, we can write

$$\rho V_\infty \frac{d V_\infty}{dx} = - \frac{dp}{dx} \tag{9.72}$$

Introducing equation (9.72) into (9.70), we obtain

$$\rho \left(v_x \frac{\partial v_x}{\partial x} + v_y \frac{\partial v_x}{\partial y} - V_\infty \frac{d V_\infty}{dx}\right) = \mu \frac{\partial^2 v_x}{\partial y^2} \tag{9.73}$$

We now integrate over y from y = 0 to y = ∞, thus

$$\rho \int_0^\infty \left(v_x \frac{\partial v_x}{\partial x} + v_y \frac{\partial v_x}{\partial y} - V_\infty \frac{d V_\infty}{dx}\right) = - \mu \left.\frac{\partial v_x}{\partial y}\right|_{y = 0} = - \tau_w \tag{9.74}$$

where τ_w is the shear stress at the wall.

The second term can be integrated by parts to give

$$\int_0^\infty v_y \frac{\partial v_x}{\partial y} = v_y \left. v_x \right|_0^\infty - \int_0^\infty v_x \frac{\partial v_y}{\partial y} dy = V_\infty \left. V_y \right|_\infty + \int_0^\infty v_x \frac{\partial v_x}{\partial x} dy \tag{9.75}$$

Integrating the continuity equation, we obtain

$$v_y \left.\right|_\infty = - \int_0^\infty \frac{\partial v_x}{\partial x} dy \tag{9.76}$$

Substitution of equations (9.75) and (9.76) into equation (9.74) gives

$$\int_0^\infty \left(2 v_x \frac{\partial v_x}{\partial x} - V_\infty \frac{\partial v_x}{\partial y} - V_\infty \frac{d V_\infty}{dx}\right) dy = - \frac{\tau_w}{\rho} \tag{9.77}$$

which can be further rearranged to the form

$$\int_0^\infty \frac{\partial}{\partial x} [v_x (V_\infty - v_x)] \, dy + \frac{d V_\infty}{dx} \int_0^\infty (V_\infty - v_x) \, dy = \frac{\tau_w}{\rho} \tag{9.78}$$

Introducing the definitions for displacement and momentum thicknesses (δ^* and θ from eqs (9.36) and (9.37)) we have

$$\frac{\tau_w}{\rho} = \frac{d}{dx}(V_\infty^2 \theta) + \delta^* V_\infty \frac{d V_\infty}{dx} \tag{9.79}$$

This equation is usually referred to as the integral momentum equation for two-dimensional boundary layer flow.

In the absense of a pressure gradient $(d V_\infty/dx) = 0$ and equation (9.79) reduces to

$$\frac{d\theta}{dx} = \frac{\tau_w}{\rho V_\infty^2} \tag{9.80}$$

$$\theta = \int_o^\delta \frac{v_x}{V_\infty}\left(1 - \frac{v_x}{V_\infty}\right) dy \tag{9.81}$$

It is possible to solve equation (9.80) by introducing probable forms of the velocity profile $v_x/V_\infty = \phi\ (y/\delta)$.

Assuming that the velocity profile can be represented by the cubic polymomial

$$\frac{v_x}{V_\infty} = a + b\left(\frac{y}{\delta}\right) + C\left(\frac{y}{\delta}\right)^3 \tag{9.82}$$

we can determine the coefficients by applying the usual boundary conditions

$$\begin{aligned} v_x &= 0 \quad \text{at } y = 0 \\ v_x &= V_\infty \quad \text{at } y = \delta \end{aligned} \tag{9.83}$$

and in addition the condition

$$\frac{\partial v_x}{\partial y} = 0 \quad \text{at } y = \delta \tag{9.84}$$

We have

$$a = 0$$
$$b = {}^{3}/_{2} \tag{9.85}$$
$$C = -\,{}^{1}/_{2}$$

Thus

$$\frac{v_x}{V_\infty} = \frac{3}{2}\left(\frac{y}{\delta}\right) - \frac{1}{2}\left(\frac{y}{\delta}\right)^3 \tag{9.86}$$

Therefore, equation (9.80) becomes

$$\frac{d}{dx}\left\{\delta \int_0^1 \left[\frac{3}{2}\left(\frac{y}{\delta}\right) - \frac{1}{2}\left(\frac{y}{\delta}\right)^3\right]\left[1 - \frac{3}{2}\left(\frac{y}{\delta}\right) + \frac{1}{2}\left(\frac{y}{\delta}\right)^3\right] d\left(\frac{y}{\delta}\right)\right\}$$

$$= \frac{\tau_w}{\rho\, V_\infty^2} = \frac{1}{\rho V_\infty^2}\, \mu \left(\frac{\partial\, v_x}{\partial y}\right)_{y\,=\,0} = \frac{1}{\rho V_\infty^2}\,\frac{3}{2}\,\mu\,\frac{V_\infty}{\delta} \tag{9.87}$$

After performing the integrations we get

$$\delta\,\frac{d\delta}{dx} = \frac{140}{13}\,\frac{\nu}{V_\infty} \tag{9.88}$$

which further gives

$$\delta = \frac{4.64\ x}{\sqrt{\dfrac{V_\infty x}{\nu}}} \tag{9.89}$$

The local friction coefficient is

$$C_f = \frac{\tau_w}{\rho\,\dfrac{V_\infty^2}{2}} = \frac{3\mu}{\rho V_\infty \delta} = \frac{0.646}{\sqrt{\dfrac{V_\infty x}{\nu}}} \tag{9.90}$$

We note that the numerical coefficients of δ and C_f are very close to those obtained by Blasius exact solution of section 9.2. Actually these numerical coefficients are relatively insensitive to the form of function used. This is shown in Table 9.3 where A and B are defined by

$$A = \frac{\delta}{x}\sqrt{\frac{V_\infty x}{\nu}} \tag{9.91}$$

$$B = C_f\sqrt{\frac{V_\infty x}{\nu}} \tag{9.92}$$

TABLE 9.3

Coefficients of δ and C_f for various approximations of the velocity profile

Assumed function	A	B
Blasius exact solution (Sec. 9.2)	5 (asymptotic)	0.664
$\frac{v_x}{V_\infty} = \frac{y}{\delta}$	3.5	0.577
$\frac{v_x}{V_\infty} = \frac{3}{2}(\frac{y}{\delta}) - \frac{1}{2}(\frac{y}{\delta})^3$	4.6	0.646
$\frac{v_x}{V_\infty} = \sin(\frac{\pi}{2}\frac{y}{\delta})$	4.8	0.654

For laminar boundary layer flows with pressure gradients the most widely known approximate method is that of Pohlhausen [18]. In this method the velocity is approximated by an expression of the form

$$\frac{v_x}{V_\infty} = a\,(\frac{y}{\delta}) + b\,(\frac{y}{\delta})^2 + C\,(\frac{y}{\delta})^3 + d\,(\frac{y}{\delta})^4 \tag{9.93}$$

The coefficients are determined by using the usual boundary conditions

$$v_x = 0 \qquad \text{at } y = 0$$

$$v_x = V_\infty \qquad \text{at } y = \delta \tag{9.94}$$

and in addition the conditions

$$\frac{\partial\ v_x}{\partial y} = 0 \quad \text{and} \quad \frac{\partial^2 v_x}{\partial y^2} = 0 \quad \text{at } y = \delta \tag{9.95}$$

The whole procedure is rather tedious. More details are given in Schlichting's book [2].

Although the approximate integral momentum methods have now been superseded by the modern numerical techniques they still merit some study mainly for historical and educational purposes.

9.7 FURTHER REMARKS ON LAMINAR BOUNDARY LAYER FLOW

We have seen that the boundary layer equations describe the flow field not only in thin layers adjacent to solid boundaries but also in jets, wakes and mixing zones. The term boundary layer has been translated from the german "grenzschicht" and it is to some extent a misnomer. Perhaps it is more appropriate to speak of "shear layers" than just boundary layers. It is the assumption of a slender flow region in which viscous effects are important that leads to the simplification of the general conservation equations. The existence of a solid boundary for some problems is merely incidental.

In this chapter we presented solutions to some classical boundary layer flow problems. Numerous other problems are dealt with in the literature. A large number of similarity and approximate solutions can be found in references [2], [16], [17] and [19]. Numerical solutions of the finite difference type have also been developed. Some fairly general computer programs are now available in references [16], [20] and [21].

Most of the problems studied in the literature are either for two-dimensional or axisymmetric boundary layers. We note that the boundary layer equations can be generally written in the form

$$\frac{\partial u}{\partial x} + \frac{\partial v}{\partial y} + \frac{\varepsilon v}{y} = 0 \qquad (9.96)$$

$$\rho u \frac{\partial u}{\partial x} + \rho\, v \frac{\partial u}{\partial y} = - \frac{\partial p}{\partial x} + \frac{\mu}{y^{\varepsilon}} \frac{\partial}{\partial y} (y^{\varepsilon} \frac{\partial u}{\partial y}) \qquad (9.97)$$

where u is velocity component the direction of flow (x) and v is the velocity component in a direction perpendicular to flow direction (y), $\varepsilon = 0$ for the two-dimensional case and $\varepsilon = 1$ for the axisymmetric case. The above formulation is particularly useful whenever a general computer solution for both two-dimensional and axisymmetric problems is attempted. Three-dimensional flow problems are considerably more difficult and require large computational times.

Some unsteady boundary layer flows are discussed by Schlichting [2]. However, before proceeding with the unsteady momentum equation (9.19) one must assess the relative magnitude of the term $\partial v_x/\partial t$. If this term is to be retained in equation (9.19) it must be of the same order of magnitude as $v_x\,(\partial v_x/\partial x)$. This means that

$$\frac{V_\infty}{t_o} \approx \frac{V_\infty^2}{L}$$

and

$$t_o = \frac{L}{V_\infty}$$

Assuming L = 1 m and V_∞ = 100 m/s we have

$$t_o = \frac{1\ \text{m}}{100\ \text{m/s}} = \frac{1}{100}\ \text{s}$$

In certain cases it is likely that changes in such short times (0.01s) will not be present. Thus, for many engineering problems a quasi-steady state approximation might be appropriate. By "quasi-steady" we mean that although a particular problem might be unsteady in a strict sense the main features of the flow can be described reasonably well by the steady state equations at any instant of time.

REFERENCES

1. L. Prandtl, "Uber Flussigkeifsbewegung bei sehr Kleiner Reibung" Proc. 3rd Intern. Math. Congr., Heidelberg (1904). Also see NACA Tech. Memo 452 (1928).

2. H. Schlichting, "Boundary Layer Theory", McGraw-Hill, 6th ed., New York (1968).

3. M. van Dyke, "Perturbation Methods in Fluid Mechanics", The Parabolic Press, Stanford, California (1975).

4. G.D. Smith, "Numerical Solution of Partial Differential Equations: Finite Difference Methods", Oxford Univ. Pres, 2nd. ed., Oxford (1978).

5. H. Blasius, "Grenzschichten in Flussigkeiten mit Kleiner Reibung" Z. Math. u. Phys., 56, 1 (1908). Engl. Trans. in NACA Tech. Memo No. 1256.

6. L. Howarth, "On the solution of the laminar boundary layer equations" Proc. Roy. Soc., London, A 164, 547 (1938).

7. J. Nikuradse, "Laminare reibungsschichten an der Langsangestromten Platte" Monograph, Zentrale f. wiss. Berichtswesen, Berlin (1942).

8. S.D. Katotakis and J. Vlachopoulos "Application of a general finite-difference method to boundary layer flows" Trans. CSME, 1, 146 (1978).

9. C-L. Hwang and L-T. Fan, "Finite difference analysis of forced-convection heat transfer in entrance region of a flat rectangular duct", Appl. Sci. Res., B13, 401 (1964).

10. H.L. Langhaar, "Steady flow in the transition length of a straight tube", J. Appl. Mech, 9, A 55 (1942).

11. J.R. Bodoia and J.F. Osterle "Finite Difference Analysis of Plane Poiseuille and Couette Flow Developments" Appl. Sci. Res., A10, 265 (1961).

12. S.I. Pai and T. Hsieh, "Numerical solution of laminar jet mixing with and without free stream", Appl. Sci. Res., 27, 39 (1972).

13. J. Vlachopoulos, "A numerical study of laminar magnetohydrodynamic free jets" Comp. Fluids, 2, 261 (1974).

14. E.N. Andrade, "The velocity distribution in a liquid-into-liquid jet. The plane jet" Proc. Phys. Soc., London, 51, 784 (1939).

15. M.R. Samuels and D.M. Wetzel "Velocity profiles in the exit region of a submerged laminar jet" Chem. Eng. J., 4, 41 (1972).

16. T. Cebeci and P. Bradshaw "Momentum transfer in Boundary layers" McGraw-Hill, New York (1977).

17. W.H. Dorrance "Viscous Hypersonic Flow" McGraw-Hill, New York (1962).

18. K. Pohlhausen, "Zur näherungsweisen integration der differentialgleichung der laminaren reibungsschicht" ZAMM, 1, 255-268 (1921).

19. L.G. Loitsianski, "Laminare Grenzschichten" Akademie-Verlag, Berlin (1967) [Trans. from Russian].

20. S.V. Patankar and D.B. Spalding, "Heat and Mass Transfer in Boundary Layers", International Textbook Co., London (1970).

21. D.B. Spalding "GENMIX. A General Computer Program for Two-Dimensional Parabolic Phenomena" Pergamon Press, Oxford (1977).

LUDWIG PRANDTL (1875-1953)

John Vlachopoulos, *Fundamentals of Fluid Mechanics*
Chem. Eng., McMaster University, Hamilton, ON, Canada
(First Edition 1984, revised internet edition (2016), www.polydynamics.com)

CHAPTER 10

TURBULENT FLOW

10.1 INTRODUCTION

In chapter 1 it was explained that in laminar flow fluid particles move in straight lines whereas in turbulent flow they follow random paths. Reynolds experiment (Sec.1.9) offers an excellent visualization of the phenomenon of transition from laminar to turbulent flow. The complete dispersion of the dye injected in a tube, as shown in Fig. 1.11 for high rates of water flow, illustrates the chaotic character of turbulent flow. At a given point in a turbulent flow field neither the velocity nor the pressure are constant. They exhibit incessantly highly irregular, high-frequency fluctuations. It is impossible to have the complete description of a turbulent flow field as a function of position and time. It is possible, however, to distinguish an average velocity and pressure over a short time interval. Hinze [1] gives the following definition for turbulent fluid motion: "An irregular condition of flow in which the various quantities show a random variation with time and space coordinates, so that statistically distinct average values can be discerned."

It was stated in Chapter 1 that experiments involving flow in tubes with circular cross-section have shown that on slowly increasing the velocity the streamlines remain smooth and straight up to about Re_D = 2300. For higher Re_D transition from laminar to turbulent flow takes place. Some investigators managed to reach $Re_D \approx 40{,}000$ while maintaining laminar flow in carefully controlled experiments. In a vibration-free environment and virtual elimination of disturbances at the tube inlet it is possible to raise further this "upper bound" of the critical Reynolds number. The reverse experiment, that is, starting from turbulent flow and slowly decreasing the velocity, shows that the "lower bound" for the critical Reynolds number where the flow ceases to be turbulent is about 2000. Below this value the flow is always laminar even with the presence of strong disturbances. For practical applications, engineers usually assume a critical value of Re_D = 2100.

For flow over a flat plate the first part of the boundary layer (Sec. 9.2), near the leading edge, is always laminar. Further downstream the Reynolds number $Re_D = V_\infty x/\mu$ increases and transition to turbulent flow occurs at about Re_x = 300,000. For jets and wakes transition occurs at surprisingly low Reynolds number e.g. for the two-dimensional jet (Sec. 9.4) the critical Reynolds number is $Re_H = \rho V_{avg}/\mu = 30$ where H is the diameter of the jet at the orifice exit. When specifying a critical Reynolds number we must clearly identify the characteristic length (also called hydrodynamic length) D or x or H or whatever else happens to be the appropriate one.

The transition from laminar to turbulent flow is due to the amplification of certain small disturbances which are always present in laminar flow no matter how carefully an experiment is conducted. When the Reynolds number is low the disturbances which are superimposed on the main flow decrease and die out with time. At high Reynolds numbers some disturbances are amplified and eventually the resulting irregularity of motion dominates the flow field, which is then called turbulent. The prediction of the critical parameters for the onset of turbulence is the object of the theory of hydrodynamic stability.

The description of growth or diminution of certain forms of disturbances is a formidable mathematical task. An elementary explanation as to the reason for having the Reynolds number as the critical parameter was given in section 6.8. Re represents the ratio (inertia forces/viscous forces). When the inertia forces are much larger than the viscous forces (i.e. for flow in tubes $Re_D>2100$) the main flow has enough kinetic energy to provide for the amplification and maintenance of the disturbances. However, at low Reynolds numbers the cohesive viscous forces tend to diminish and eventually eliminate all disturbances.

When the flow is turbulent the velocity and pressure fluctuate very rapidly. To measure the turbulent fluctuations we use probes with fast response (see chapter on flow measurements). The results of some actual measurements [2] with fast response probes are shown in Fig. 10.1. The velocity components at a point in a turbulent flow field fluctuate about a mean value as shown. A probe with sufficiently slow response would be

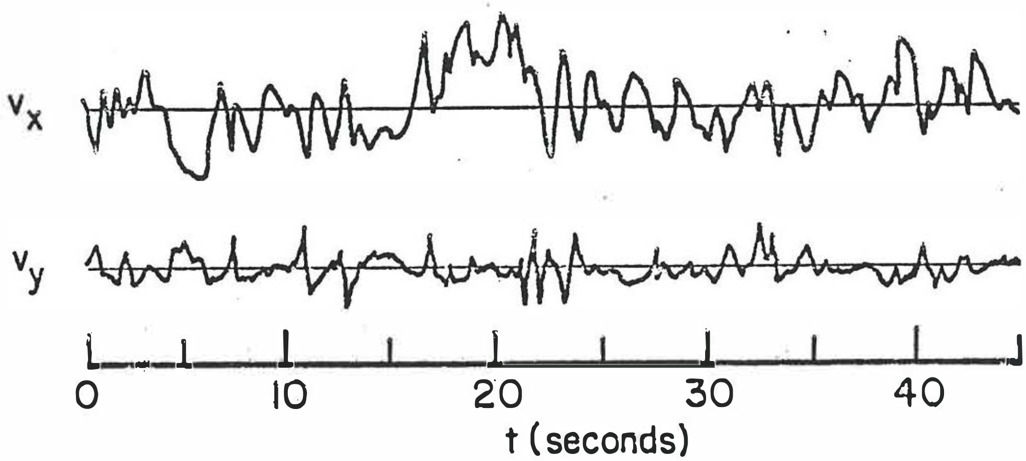

Fig. 10.1 Local velocity components in turbulent flow in an oil channel, Re = 7000 (x is the main flow direction and y is normal to the wall). Reproduced from reference [2].

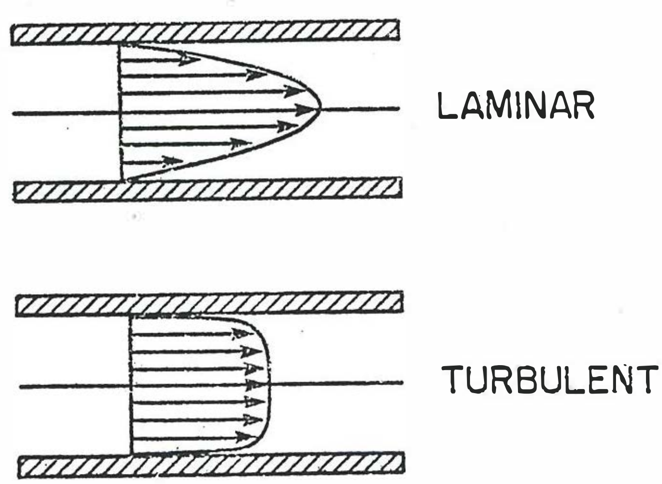

Fig. 10.2 Velocity profiles for laminar and turbulent flow in tubes having approximately equal flow rates.

unable to follow these rapid fluctuations and would simply record the velocity components averaged over a period of time. Since the complete description of a flow field is impossible we will focus our efforts to the determination of the time-averaged velocity components and time-averaged pressure.

For laminar flow in tubes with circular cross-section the velocity profile was found to obey the parabolic equation (Sec.7.3).

$$\frac{v_z}{V_{z,max}} = [1 - (\frac{r}{R})^2] \tag{10.1}$$

and the average velocity (over the cross-section) was found to be one-half of the maximum:

$$\frac{V_{avg}}{V_{z,max}} = \frac{1}{2} \tag{10.2}$$

These classical results have been fully verified by experimental measurements by numerous investigators.

As it will be shown in subsequent section the determination of velocity profiles for turbulent flow is not easy and in most cases it requires direct experimental measurements. The experimental data are usually interpreted and expressed in terms of certain mathematical models. The resulting expressions can, thus, be termed semi-empirical.

For turbulent flow in tubes the time-averaged velocity profile can be expressed in terms of the 1/7- power law equation

$$\frac{\bar{v}_z}{\bar{V}_{z,max}} = (1 - \frac{r}{R})^{1/7} \tag{10.3}$$

for Re_D of the order of 10^5.

We introduced the quantities with bars $\bar{v}_z$ and $\bar{V}_{z,max}$ to indicate the mean values (over a period of time), whereas the quantities without bars v_z and $V_{z,max}$ would represent fluctuating values, when the flow is turbulent. The (area) average velocity can be obtained by integrating the time-averaged velocity over the cross-section and dividing by the cross-sectional area.

$$\bar{V}_{avg} = \frac{\int_0^{2\pi}\int_0^{R} \bar{v}_z \, r dr d\theta}{\int_0^{2\pi}\int_0^{R} r dr d\theta} \approx \frac{4}{5}\,\bar{V}_{z,max} \approx 0.807\,\bar{V}_{z,max} \quad (10.4)$$

We note that the velocity profile for turbulent flow is more flat than that for laminar flow, as shown in Fig. 10.2.

The Hagen-Poiseuille formula of Section 7.3 shows that for laminar flow in a pipe the pressure drop is proportional to the volume rate of flow. It has been established experimentally that for turbulent flow the pressure drop is approximately proportional to the 1.75 power of the volume rate of flow (for smooth pipes). These conclusions are schematically shown in Fig. 10.3.

A closer examination of turbulent flow reveals that the fluid motion is not entirely random throughout the tube. At the center of the tube the velocity fluctuations are completely irregular. Near the immediate vicinity of the wall the fluctuations virtually disappear. It is often assumed that there exists a <u>laminar sublayer</u> near the tube wall in which the flow is smooth and dominated by the viscosity of the fluid. This is followed by the <u>buffer zone</u> which is dominated by both viscosity and turbulent fluctuations, and the <u>turbulent core</u> where the flow is almost completely random, as shown in Fig. 10.4.

An analogous situation may be assumed to exist in a turbulent

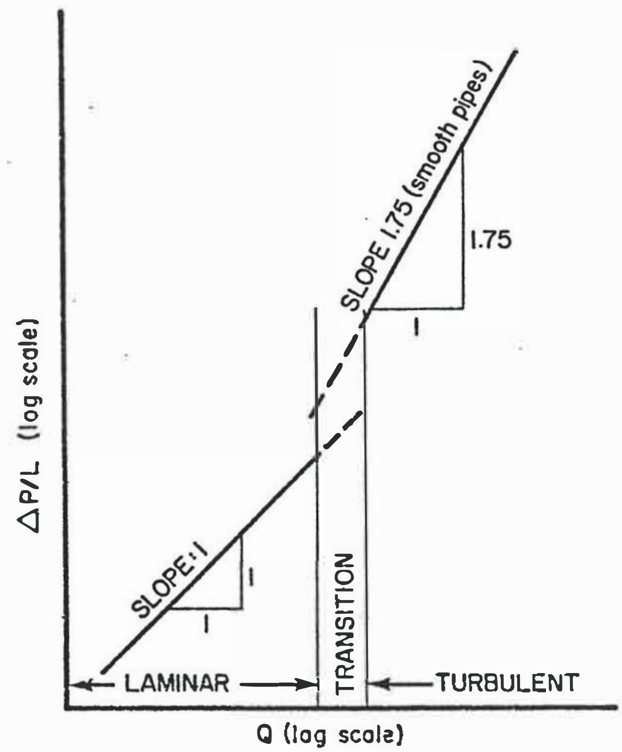

Fig. 10.3 Pressure drop as a function of the volume rate of flow.

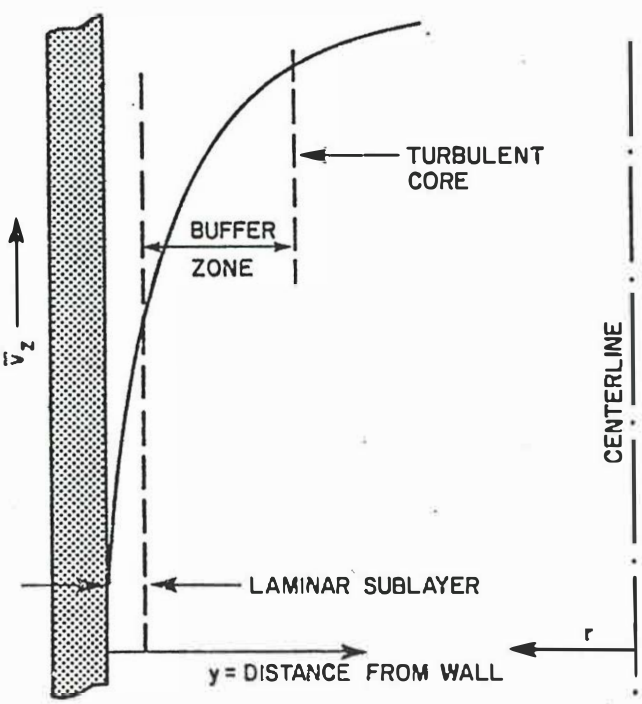

Fig. 10.4 A sketch of the velocity profile and the various flow regions for turbulent flow in a tube.

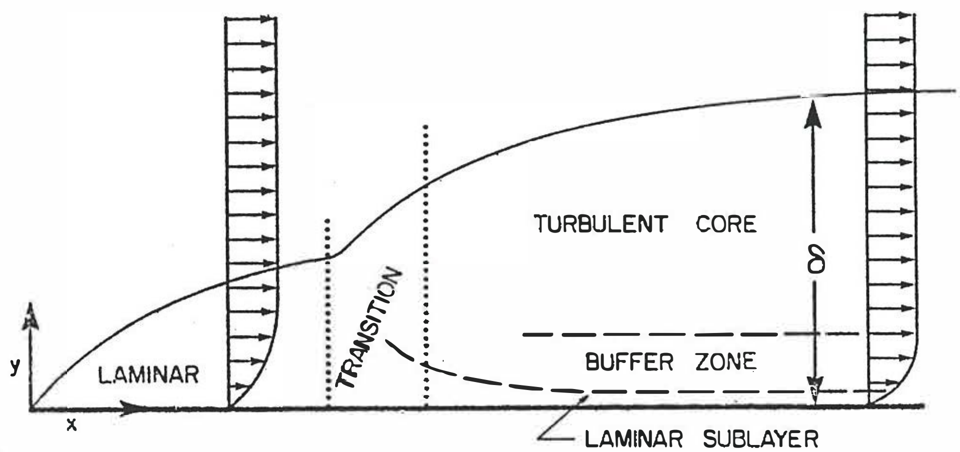

Fig. 10.5 Sketch of flow regions in a boundary layer formed over a flat plate.

boundary layer formed over a flat plate as shown in Fig. 10.5. It should be understood that there are no sharp boundaries between the various flow regions and their existence, in either tube or flat plate flow, should not be interpreted too rigidly.

The velocity profile in the turbulent boundary layer on a flat plate can be approximated fairly well by the 1/7 - power law expression

$$\frac{\bar{v}_x}{\bar{V}_\infty} = \left(\frac{y}{\delta}\right)^{1/7} \tag{10.5}$$

It will be shown that the boundary layer thickness varies with $x^{4/5}$ for turbulent flow, whereas, $\delta \propto x^{1/2}$ for laminar flow.

10.2 FLUCTUATIONS, EDDIES AND TIME-AVERAGING

The velocity at a point inside a tube having a constant flow rate remains constant with time when the flow is laminar (see Fig. 10.6(a)). For turbulent flow with a constant flow rate the local velocity fluctuates around a mean value as shown in Fig. 10.6(b)). In other words, in turbulent flow the velocity is always locally unsteady. The time-averaged local velocity $\bar{v}_z$ is defined by

$$\bar{v}_z = \frac{1}{T} \int_o^T v_z dt \tag{10.6}$$

This definition also holds for unsteady turbulent flow. Fig. 10.7 shows the irregular oscillations of local velocity about a mean value in a turbulent flow field with varying flow rate. The time interval T, over which the velocity is averaged, should be large with respect to turbulent fluctuations but small with respect to changes in the overall flow rate.

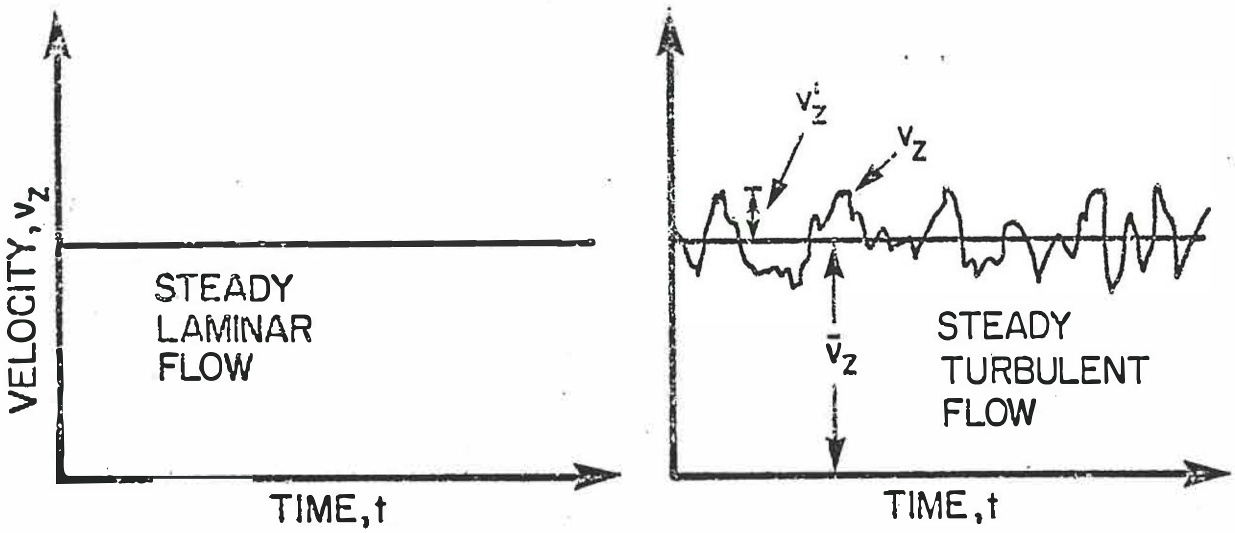

Fig. 10.6 Local velocity in (a) steady laminar flow and (b) steady turbulent flow.

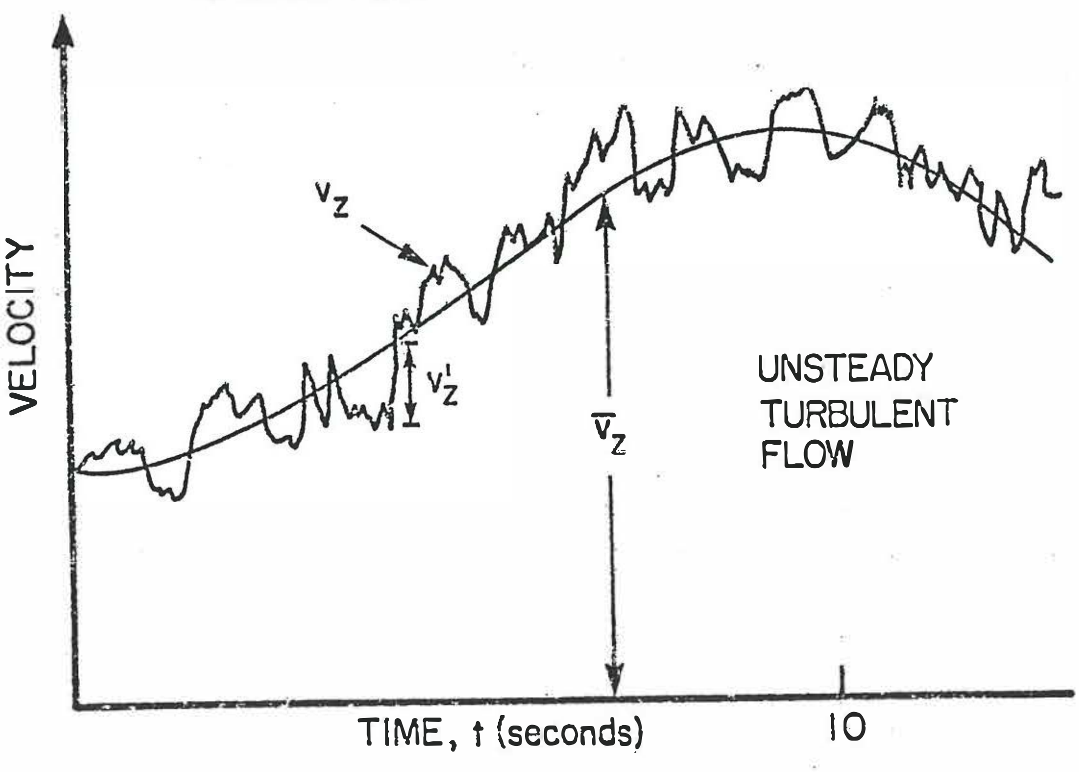

Fig. 10.7 Local velocity in unsteady turbulent flow.

The instantaneous local velocity v_z may be written as the sum of the time-averaged velocity $\bar{v}_z$ and a velocity fluctuation v_z':

$$v_z = \bar{v}_z + v_z' \tag{10.7}$$

Similar expressions may be written for the other velocity components and the pressure, i.e.

$$v_x = \bar{v}_x + v_x' \tag{10.8}$$

$$v_y = \bar{v}_y + v_y' \tag{10.9}$$

$$p = \bar{p} + p' \tag{10.10}$$

From the foregoing discussion it is clear that the time-averaged values of the fluctuations are identical to zero

$$\overline{v_z'} = \overline{v_y'} = \overline{v_x'} = 0 \qquad \overline{p'} = 0 \tag{10.11}$$

However, the roots of the time-averaged squares (root mean squares) of the fluctuations will not be zero. The quantities

$$\frac{\left(\overline{v_z'^2}\right)^{1/2}}{\bar{V}_{ref}}, \quad \frac{\left(\overline{v_y'^2}\right)^{1/2}}{\bar{V}_{ref}} \quad \text{and} \quad \frac{\left(\overline{v_x'^2}\right)^{1/2}}{\bar{V}_{ref}} \tag{10.12}$$

where $\bar{V}_{ref}$ is a suitable reference velocity (usually the maximum velocity) are used as measures of the magnitude of turbulent fluctuations and are referred to as turbulence intensities or turbulence levels. The variation of turbulence intensities as measured by Reichardt [3] in a wind tunnel is shown in Fig. 10.8. We note that the intensities in the immediate vicinity of the wall are very small, they increase with distance, reach their maximum values and drop in the central portion of the wind tunnel. The existence of maximum values of intensity at relatively short distances from the wall is due to the fact that many flow disturbances have their origin at the surface. Towards

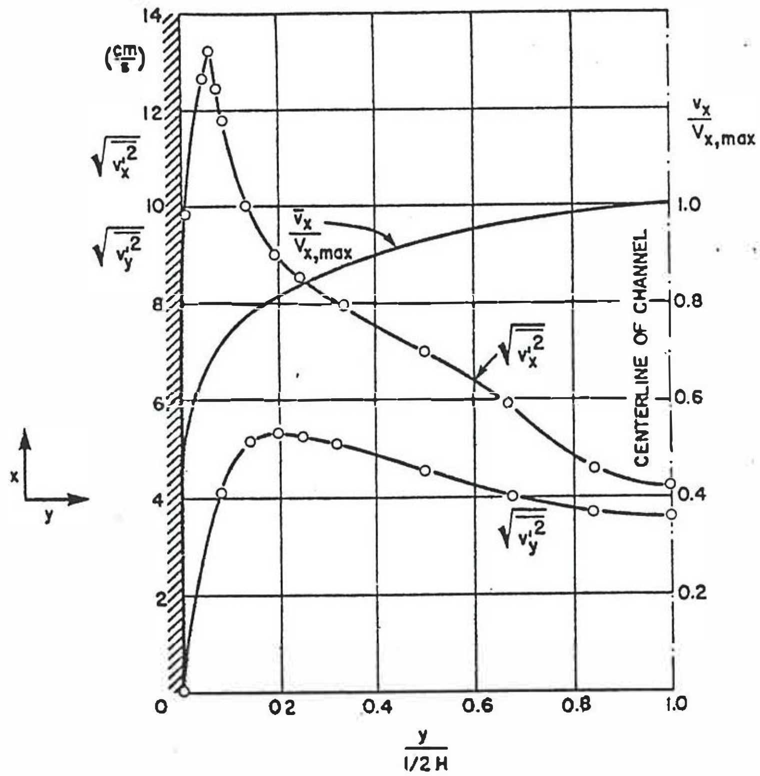

Fig. 10.8 Variation of turbulence intensities and the time-averaged velocity profile as measured in a wind tunnel by Reichardt[3].

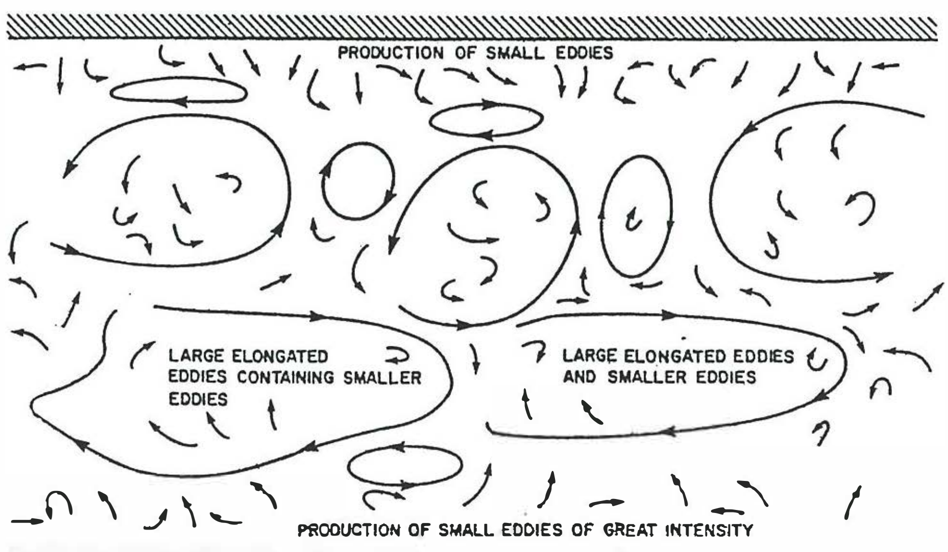

Fig. 10.9 Schematic representation of eddy structure in pipe flow, according to Davies [4].

the center of the conduit, however, the influence of the wall is diminished and the turbulence intensities drop. For internal channel flows, the maximum turbulence intensity is usually less than 15%. In free jets turbulence intensities may reach maximum values of up to 30% near the outer edges because of fluid entrainment from the surroundings and violent mixing motions.

In discussing turbulent flow we emphasized the irregularity of motion and the appearance of random fluctuations. Locally the velocity field exhibits gradients which correspond to recirculating flow and formation of eddies of various sizes. The upper size of these eddies is limited by the size of the equipment. The lower size is determined by the viscosity of the fluid and generally decreases as the mean flow velocity increases. The smallest eddies can be very small and the corresponding frequency of the fluctuations very high. Davies [4] gives an excellent schematic representation of eddy structure in a pipe as shown in Fig. 10.9. Because of the large velocity gradients near the wall the large eddies are broken up into small ones which dissipate the kinetic energy by the action of the fluid viscosity.

The turbulent effects are far removed from molecular scale as pointed in a simple example by Hinze [1]: For mean air flow of 100 m/s the smallest eddy will be about 1 mm, large compared to mean free path which is of the order of 10^{-4} mm. 1 mm^3 of air contains roughly 1.7×10^{16} molecules under atmospheric conditions. The turbulent fluctuations will be at most of the order of 10 m/s whereas the mean velocity of molecules is of the order of 500 m/s. The turbulence frequencies will be less than 10,000 s^{-1} whereas molecular collision frequencies for air are about 5×10^9 s^{-1}.

Since the scale of turbulent motions is sufficiently different from the scale of molecular motions it is reasonable to apply the principles of conservation of mass and momentum as developed for a continuum in Chapters 4 and 6.

Example 10.1

At a given point in a flow field the instantaneous velocity is given by $v_x = 10 + 2\sin\pi t$ and $v_y = \sin\pi t$. We will evaluate the following quantities:

(a) $\bar{v}_x$, $\bar{v}_y$

(b) $\overline{v_x' v_y'}$

(c) $\overline{v_x v_y}$

Solution

A sketch of the velocity components is shown in Fig. E10.1 obviously the minimum time interval for averaging is T=2

(a) we have

$$\bar{v}_x = \frac{1}{T}\int_o^T v_x dt = \frac{1}{T}\int_o^T (10+2\sin\pi t)dt = \frac{1}{2}(10t - \frac{2}{\pi}\cos\pi t)\Big|_o^2 = 10$$

$$\bar{v}_y = \frac{1}{T}\int_o^T v_y dt = \frac{1}{2}\int_o^2 \sin\pi t = -\frac{1}{2\pi}\cos\pi t\Big|_o^2 = 0$$

(b) $$\overline{v_x' v_y'} = \frac{1}{T}\int_o^T v_x' v_y' dt = \frac{1}{2}\int_o^2 (2\sin\pi t)\cos\pi t dt = \frac{1}{2}[2(\frac{t}{2}-\frac{1}{4\pi}\sin 2\pi t)]_o^2 = 1$$

(c) $$\overline{v_x v_y} = \frac{1}{T}\int_o^T v_x v_y dt = \frac{1}{2}\int_o^T (10+2\sin\pi t)\sin\pi t =$$

$$\frac{1}{2}[-\frac{10}{\pi}\cos\pi t + 2(\frac{t}{2} - \frac{1}{4\pi}\sin 2\pi t)]_o^2 = 1$$

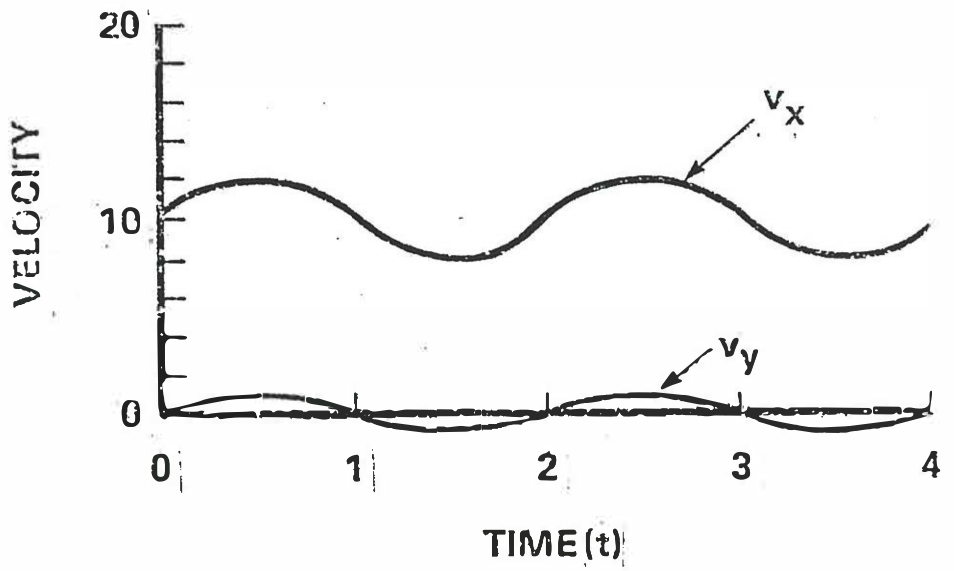

Fig. E.10.1

10.3 THE TIME-AVERAGED CONSERVATION EQUATIONS FOR AN INCOMPRESSIBLE FLUID

The equation of conservation of mass (continuity) for an incompressible fluid (Sec. 4.1) is:

$$\frac{\partial v_x}{\partial x} + \frac{\partial v_y}{\partial y} + \frac{\partial v_z}{\partial z} = 0 \tag{10.13}$$

Introducing $v_x = \bar{v}_x + v_x'$, $v_y = \bar{v}_y + v_y'$ and $v_z = \bar{v}_z + v_z'$, we get

$$\frac{\partial(\bar{v}_x + v_x')}{\partial x} + \frac{\partial(\bar{v}_y + v_y')}{\partial y} + \frac{\partial(\bar{v}_z + v_z')}{\partial z} = 0 \tag{10.14}$$

or

$$\frac{\partial \bar{v}_x}{\partial x} + \frac{\partial \bar{v}_y}{\partial y} + \frac{\partial \bar{v}_z}{\partial z} + \frac{\partial v_x'}{\partial x} + \frac{\partial v_y'}{\partial y} + \frac{\partial v_z'}{\partial z} = 0 \tag{10.15}$$

We will now take the time-average of this equation by using the definition

$$\overline{(\quad)} = \frac{1}{T}\int_o^T (\quad)dt \tag{10.16}$$

where T is a suitable time constant. With this definition of time-average the following rules can be easily established for quantities $A = \bar{A} + A'$ and $B = \bar{B} + B'$:

$$\begin{aligned}
&\bar{A} = \overline{\bar{A} + A'} = \bar{\bar{A}} + \overline{A'} = \bar{A} + \overline{A'} \quad \text{thus } \overline{A'} = 0 \\
&\overline{\bar{A}\,\bar{B}} = \bar{\bar{A}}\,\bar{\bar{B}} = \bar{A}\,\bar{B} \\
&\overline{\bar{A}\,B'} = \bar{\bar{A}}\,\overline{B'} = \bar{A}\,\overline{B'} = 0 \quad \text{since } \overline{B'} = 0 \\
&\overline{\bar{B}\,A'} = \bar{\bar{B}}\,\overline{A'} = \bar{B}\,\overline{A'} = 0 \quad \text{since } \overline{A'} = 0
\end{aligned} \tag{10.17}$$

$$\overline{A\,B} = \overline{(\bar{A} + A')\,(\bar{B} + B')} = \overline{\bar{A}\,\bar{B}} + \overline{\bar{A}\,B'} + \overline{\bar{B}\,A'} + \overline{A'B'}$$

$$= \bar{A}\,\bar{B} + \overline{A'B'}$$

$$\overline{\frac{\partial A}{\partial x}} = \frac{\partial \bar{A}}{\partial x}$$

$$\overline{B\frac{\partial A}{\partial x}} = \overline{(\bar{B} + B')\,\frac{\partial(\bar{A} + A')}{\partial x}} = \overline{\bar{B}\frac{\partial \bar{A}}{\partial x}} + \overline{B'\frac{\partial \bar{A}}{\partial x}} + \overline{\bar{B}\frac{\partial A'}{\partial x}} + \overline{B'\frac{\partial A'}{\partial x}} =$$

$$= \bar{B}\frac{\partial \bar{A}}{\partial x} + \overline{B'\frac{\partial A'}{\partial x}}$$

Thus, the time-average form of equation (10.15) may be written as

$$\overline{\frac{\partial v_x}{\partial x}} + \overline{\frac{\partial v_y}{\partial y}} + \overline{\frac{\partial v_z}{\partial z}} + \overline{\frac{\partial v_x'}{\partial x}} + \overline{\frac{\partial v_y'}{\partial y}} + \overline{\frac{\partial v_z'}{\partial z}} = 0 \tag{10.18}$$

Since $\overline{v_x'} = \overline{v_y'} = \overline{v_z'} = 0$, we get

$$\frac{\partial \bar{v}_x}{\partial x} + \frac{\partial \bar{v}_y}{\partial y} + \frac{\partial \bar{v}_z}{\partial z} = 0 \tag{10.19}$$

This means that the time-averaged continuity equation for an incompressible fluid is identical to the continuity equation for laminar flow with the velocity components replaced by their time-averages.

Let us now apply this time-averaging procedure to the x-component of the equation of conservation of momentum (Sec.6.5) starting from

$$\rho\left(\frac{\partial v_x}{\partial t} + v_x\frac{\partial v_x}{\partial x} + v_y\frac{\partial v_x}{\partial y} + v_z\frac{\partial v_x}{\partial z}\right) = -\frac{\partial p}{\partial x} + \mu\nabla^2 v_x + \rho g_z \tag{10.20}$$

Introducing $v_x = \bar{v}_x + v_x'$, $v_y = \bar{v}_y + v_y'$, $v_z = \bar{v}_z + v_z'$ and $p=\bar{p}+p'$, we get

$$\rho[\frac{\partial}{\partial t}(\bar{v}_x + v_x') + (\bar{v}_x + v_x')\frac{\partial}{\partial x}(\bar{v}_x + v_x') +$$

$$(\bar{v}_y + v_y')\frac{\partial}{\partial y}(\bar{v}_x + v_x') + (\bar{v}_z + v_z')\frac{\partial}{\partial z}(\bar{v}_x + v_x')]$$

$$= -\frac{\partial}{\partial x}(\bar{p} + p') + \mu\nabla^2(\bar{v}_x + v_x') + \rho g_x \tag{10.21}$$

Thus, taking the time average according to the definition given by equation (10.16) and observing the rules established above (Eqs. 10.17) we have

$$\rho(\frac{\partial \bar{v}_x}{\partial t} + \bar{v}_x\frac{\partial \bar{v}_x}{\partial x} + \bar{v}_y\frac{\partial \bar{v}_x}{\partial y} + \bar{v}_z\frac{\partial \bar{v}_x}{\partial z}) = -\frac{\partial \bar{p}}{\partial x} + \mu\nabla^2\bar{v}_x + \rho g_x$$

$$-\rho[\overline{v_x'\frac{\partial v_x'}{\partial x} + v_y'\frac{\partial v_x'}{\partial y} + v_z'\frac{\partial v_z'}{\partial z}}] \tag{10.22}$$

We note that

$$v_x'\frac{\partial v_x'}{\partial x} = \frac{\partial}{\partial x}(v_x' v_x') - v_x'\frac{\partial v_x'}{\partial x}$$

$$v_y'\frac{\partial v_x'}{\partial y} = \frac{\partial}{\partial y}(v_x' v_y') - v_x'\frac{\partial v_y'}{\partial y} \tag{10.23}$$

$$v_z'\frac{\partial v_x'}{\partial z} = \frac{\partial}{\partial z}(v_x' v_z') - v_x'\frac{\partial v_z'}{\partial z}$$

Thus, the last group of terms in equation (10.22) becomes

$$\overline{v_x'\frac{\partial v_x'}{\partial x} + v_y'\frac{\partial v_x'}{\partial y} + v_z'\frac{\partial v_x'}{\partial z}} = \overline{\frac{\partial}{\partial x}(v_x' v_x') + \frac{\partial}{\partial y}(v_x' v_y') + \frac{\partial}{\partial z}(v_x' v_z')}$$

$$\overline{- v_x'(\frac{\partial v_x'}{\partial x} + \frac{\partial v_y'}{\partial y} + \frac{\partial v_z'}{\partial z})} \tag{10.24}$$

With the help of the continuity equation we can eliminate the second group of terms of equation (10.24) and thus rewrite equation (10.22) as

$$\rho\left(\frac{\partial \bar{v}_x}{\partial t} + \bar{v}_x \frac{\partial \bar{v}_x}{\partial x} + \bar{v}_y \frac{\partial \bar{v}_x}{\partial y} + \bar{v}_z \frac{\partial \bar{v}_x}{\partial z}\right) = -\frac{\partial \bar{p}}{\partial x} + \mu \nabla^2 \bar{v}_x + \rho g_x$$

$$+\left[\frac{\partial}{\partial x}(-\rho \overline{v_x' v_x'}) + \frac{\partial}{\partial y}(-\rho \overline{v_x' v_y'}) + \frac{\partial}{\partial z}(-\rho \overline{v_x' v_z'})\right] \qquad (10.25)$$

By a similar procedure we can obtain the time-averaged y and z components of the equation of conservation of momentum:

$$\rho\left(\frac{\partial \bar{v}_y}{\partial t} + \bar{v}_x \frac{\partial \bar{v}_y}{\partial x} + \bar{v}_y \frac{\partial \bar{v}_y}{\partial y} + \bar{v}_z \frac{\partial \bar{v}_y}{\partial z}\right) = -\frac{\partial \bar{p}}{\partial y} + \mu \nabla^2 \bar{v}_y + \rho g_y$$

$$+\left[\frac{\partial}{\partial x}(-\rho \overline{v_y' v_x'}) + \frac{\partial}{\partial y}(-\rho \overline{v_y' v_y'}) + \frac{\partial}{\partial z}(-\rho \overline{v_y' v_z'})\right] \qquad (10.26)$$

$$\rho\left(\frac{\partial \bar{v}_z}{\partial t} + \bar{v}_x \frac{\partial \bar{v}_z}{\partial x} + v_y \frac{\partial v_z}{\partial y} + v_z \frac{\partial v_z}{\partial z}\right) = -\frac{\partial \bar{p}}{\partial z} + \mu \nabla^2 \bar{v}_z + \rho g_z$$

$$+\left[\frac{\partial}{\partial x}(-\rho \overline{v_z' v_x'}) + \frac{\partial}{\partial y}(-\rho \overline{v_z' v_y'}) + \frac{\partial}{\partial z}(-\rho \overline{v_z' v_z'})\right] \qquad (10.27)$$

10.4 REYNOLDS STRESSES AND EDDY VISCOSITY

In the formulation of laminar flow problems we ended up with four equations (continuity and three components of the equation of conservation of momentum) and four unknnowns (v_x, v_y, v_z and p). By time-averaging the various terms for turbulent flow we still have four equations, but the number of unknowns is now seven namely $\bar{v}_x$, $\bar{v}_y$, $\bar{v}_z$, $\bar{p}$ and v_x', v_y', v_z'. To solve turbulent flow problems we must reduce the number of unknowns to four ($\bar{v}_x$, $\bar{v}_y$, $\bar{v}_z$ and $\bar{p}$). By referring to equations (6.93), (6.64) and (6.65) we note that the viscous terms $\mu\nabla^2 v_x$, $\mu\nabla^2 v_y$ and $\mu\nabla^2 v_z$ have been derived from the deviatoric stress tensor τ_{ij} i.e for an incompressible Newtonian fluid in laminar flow

$$\mu \nabla^2 v_x = \frac{\partial \tau_{xx}}{\partial x} + \frac{\partial \tau_{yx}}{\partial y} + \frac{\partial \tau_{zx}}{\partial z} \tag{10.28}$$

These stresses represent the resistance to flow which at the microscopic level is due to random molecular motions. The random eddy motions also exhibit resistance to flow. Thus, it is reasonable to assume that the term involving the velocity fluctuations in equation (10.25) can be expressed in terms of the components of the so-called turbulent stress tensor $\bar{\tau}_{ij}^{(t)}$ i.e

$$\frac{\partial}{\partial x}(-\rho \overline{v_x' v_x'}) + \frac{\partial}{\partial y}(-\rho \overline{v_x' v_y'}) + \frac{\partial}{\partial z}(-\rho \overline{v_x' v_z'}) = \frac{\partial \bar{\tau}_{xx}^{(t)}}{\partial x} + \frac{\partial \bar{\tau}_{yx}^{(t)}}{\partial y} + \frac{\partial \bar{\tau}_{zx}^{(t)}}{\partial z} \tag{10.29}$$

Similar expressions may be written for the groups of terms containing the velocity fluctuations in equations (10.27) and (10.28) with

$$\bar{\tau}_{xx}^{(t)} = -\rho \overline{v_x' v_x'} \qquad \bar{\tau}_{xy}^{(t)} = \bar{\tau}_{yx}^{(t)} = -\rho \overline{v_x' v_y'} \qquad \bar{\tau}_{xz}^{(t)} = \bar{\tau}_{zx}^{(t)} = -\rho \overline{v_z' v_x'}$$

$$\bar{\tau}_{yy}^{(t)} = -\rho \overline{v_y' v_y'} \qquad \bar{\tau}_{yz}^{(t)} = \bar{\tau}_{zy}^{(t)} = -\rho \overline{v_y' v_z'} \qquad \bar{\tau}_{zz}^{(t)} = -\rho \overline{v_z' v_z'}$$

The turbulent stress tensor may, therefore, be written as

$$\overline{\overline{\tau}}^{(t)} = - \begin{pmatrix} \overline{\rho v'_x v'_x} & \overline{\rho v'_x v'_y} & \overline{\rho v'_x v'_z} \\ \overline{\rho v'_x v'_y} & \overline{\rho v'_y v'_y} & \overline{\rho v'_y v'_z} \\ \overline{\rho v'_x v'_z} & \overline{\rho v'_y v'_z} & \overline{\rho v'_z v'_z} \end{pmatrix} \qquad (10.30)$$

These are called the Reynolds stresses. In analogy to viscous stresses the Reynolds stresses may be expressed by relations of the form

$$\overline{\tau}_{yx}^{(t)} = \mu^{(t)} \frac{d\overline{v}_x}{dy} \qquad (10.31)$$

where $\mu^{(t)}$ is the so-called turbulent or eddy viscosity. We may also define a kinematic eddy viscosity as

$$\nu^{(t)} = \frac{\mu^{(t)}}{\rho} \qquad (10.32)$$

Many problems involving the Reynolds stresses will be of boundary layer nature. The time-averaged form of the unsteady boundary layer equations (9.18) and (9.19) may be written as

$$\frac{\partial \overline{v}_x}{\partial x} + \frac{\partial \overline{v}_y}{\partial y} = 0 \qquad (10.33)$$

$$\rho\left(\frac{\partial \overline{v}_x}{\partial t} + \overline{v}_x \frac{\partial \overline{v}_x}{\partial x} + \overline{v}_y \frac{\partial \overline{v}_x}{\partial y}\right) = - \frac{\partial \overline{p}}{\partial x} + (\mu + \mu^{(t)}) \frac{\partial^2 \overline{v}_x}{\partial y^2} \qquad (10.34)$$

We note that the viscous term has two coefficients of viscosity, μ and $\mu^{(t)}$. The viscosity μ is due to the random motions of molecules. The eddy viscosity $\mu^{(t)}$ is due to random motions of lumps of fluid. Because of the relatively large size of fluid lumps we may conclude that

$$\mu^{(t)} \gg \mu$$

except in the immediate vicinity of walls where $\mu^{(t)} \to 0$.

The viscosity μ is a fundamental property of the fluid and for certain simple fluids it can be determined entirely from kinetic arguments (see Chapter , Molecular Hydrodynamics). On the other hand the concept of eddy viscosity $\mu^{(t)}$ is based on conjectures rather than a fundamental theory and can only be determined by direct measurement of the fluctuating velocity components and the definition

$$\tau^{(t)} = \mu^{(t)} \frac{d\bar{v}_x}{dy} = -\rho \overline{v_x' v_y'} \qquad (10.35)$$

Since $\mu^{(t)}$ depends on the magnitude of the velocity fluctuations it should vary from point to point within a flow field. It should also be different for different flow configurations and vary with the size of experimental equipment. The variation of $\mu^{(t)}$ with position in pipe flow is shown in Fig. 10.10 from reference [1]. Usually for pipe flows $\mu^{(t)}$ is about 100 or 200 times larger than μ. For jets and wakes $\mu^{(t)}$ is usually more than 1000 times larger than μ, because of the highly irregular and strong mixing motions involved.

10.5 PROBLEM SOLVING IN TURBULENT FLOW

Basically the same approach as in laminar flows can be followed for the solution of turbulent flow problems. We start from the time-averaged conservation equations and eliminate the appropriate terms. <u>The resulting equations are identical to those for the corresponding laminar flow problems with velocities replaced by their time-averages and viscosity replaced by the effective viscosity</u> (<u>i.e.</u>

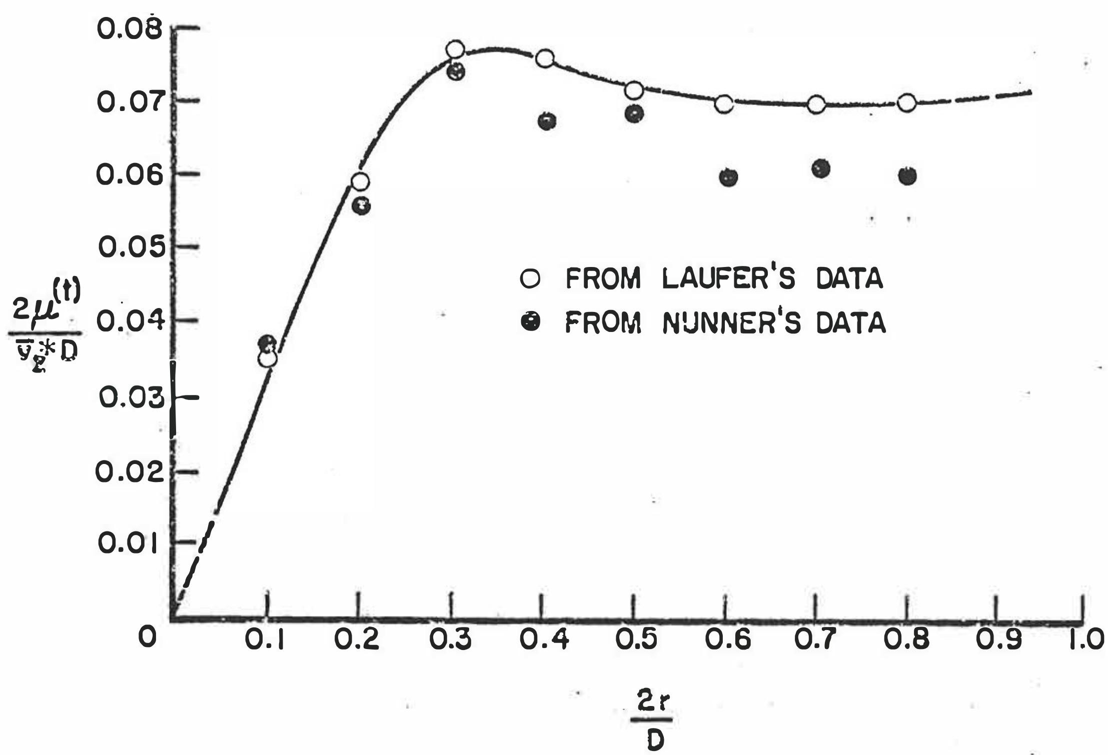

Fig. 10.10 The eddy viscosity coefficient as a function of radial position in pipe flow (from Hinze [1]).

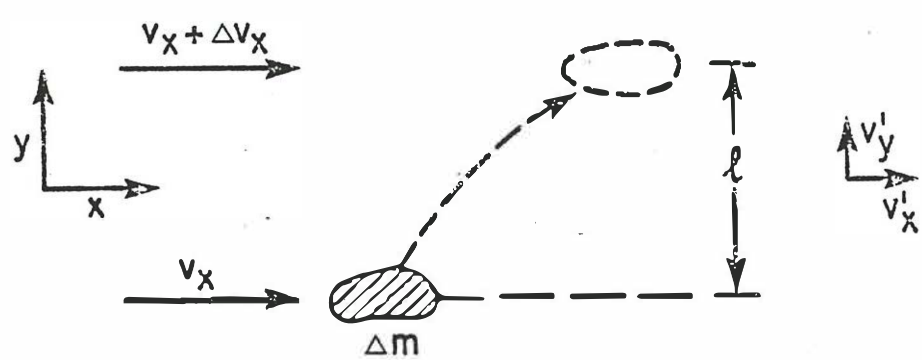

Fig. 10.11 Schematic representation of the mixing length concept.

laminar plus turbulent contribution

$$\mu^{(T)} = \mu + \mu^{(t)} \tag{10.36}$$

The difficulty lies in the fact that $\mu^{(t)}$ is a very complicated function of many parameters. Generally we may state symbolically that

$$\mu^{(t)} = f\text{ (position, velocity, flow configuration, size, roughness)}$$

It is of course impossible to take all those factors into consideration and present general solutions. We must apply this methodology to each problem and in addition exploit the special features that each problem may have. In following this approach it is essential to have an expression for $\mu^{(t)}$. The literature of fluid mechanics abounds with such expressions, most of them for specific problems. Here, we present some of the more popular ones.

10.5.1 Prandtl's mixing length model

This model attempts to describe in a crude manner what actually happens in turbulent flow [5], [6]. The turbulent exchange mechanism is assumed to be described by the motion of lumps of fluid transverse to the velocity field. Let us focus our attention to one such a fluid lump of mass Δm and velocity v_x which is moved in the y direction at a distance ℓ, under the influence of the fluctuating velocity component v_y', as shown in Fig. 10.11. Obviously, in order to satisfy continuity another fluid lump of equal mass must move in the opposite direction. It is assumed that these lumps retain their momentum while they travel through the fluid. The complete exchange is accomplished (through the viscosity) after they travel the distance ℓ, which is thus called mixing length.

The x-momentum transported by Δm is $\Delta m \Delta v_x$. The shear force acting between the two fluid layers will be

$$F = \frac{(\Delta m)(\Delta v_x)}{(\Delta t)} \tag{10.37}$$

where Δt is the time required for the travel of mass Δm. Thus, we can define an apparent (turbulent) shear stress

$$\tau^{(t)} = \frac{F}{A} = \frac{1}{A}\frac{(\Delta m)(\Delta v_x)}{(\Delta t)} \tag{10.38}$$

where A is the area over which force F acts.

Using the Taylor series expansion one may write approximately

$$v_x + \Delta v_x \simeq v_x + \ell \frac{dv_x}{dy} \tag{10.39}$$

$$\Delta v_x \simeq \ell \frac{dv_x}{dy} \tag{10.40}$$

Further, we note that $\frac{(\Delta m)}{(\Delta t)}$ is the mass rate of flow and according to continuity

$$\frac{(\Delta m)}{(\Delta t)} = \rho \, |v_y'| A \tag{10.41}$$

Introducing equations (10.40) and (10.41) into equation (10.38) we get

$$\tau^{(t)} = \rho \, \ell |v_y'| \frac{dv_x}{dy} \tag{10.42}$$

To determine $\tau^{(t)}$ we must know ℓ and v_y'. Prandtl assumed that

$$|v_y'| = \text{const}|(\Delta v_x)| = \text{const} \; \ell \left|\frac{dv_x}{dy}\right| \tag{10.43}$$

Thus, incorporating the constant into ℓ we may write

$$\tau^{(t)} = \rho\, \ell^2 \left|\frac{dv_x}{dy}\right| \left(\frac{dv_x}{dy}\right) \qquad (10.44)$$

Prandtl also assumed that the mixing length is proportional to the distance from the wall i.e.

$$\ell = \kappa y \qquad (10.45)$$

and wrote equation (10.44) as

$$\tau^{(t)} = \rho\, \kappa^2 y^2 \left|\frac{dv_x}{dy}\right| \left(\frac{dv_x}{dy}\right) \qquad (10.46)$$

where κ is an experimentally determined constant.

Von Karman's similarity model

Von Karman [7] made the assumption of geometrical similarity (see Sec. 9.5) and deduced an expression for the mixing length. He expressed the turbulent stress as

$$\bar{\tau}_{yx}^{(t)} = -\rho\, \kappa_1^2 \left| \frac{\left(\frac{dv_x}{dy}\right)^3}{\left(\frac{d^2 v_x}{dy^2}\right)^2} \right| \frac{dv_x}{dy} \qquad (10.47)$$

where κ is known as von Karman's universal constant (approximately κ=0.4)

Deissler's empirical formula

Deissler [8] proposed an empirical expression for eddy viscosity, which is applicable in the immediate neighborhood of solid surfaces, in the form

$$\mu^{(t)} = -\rho\, m\, \bar{v}_x y\, [1 - \exp(-m\, \bar{v}_x y/\nu)] \qquad m=0.0154 \qquad (10.48)$$

Prandtl's formula for free shear flows

For jets, wakes and mixing zones, Prandtl's mixing length model leads to the following formula

$$\mu^{(t)} = \kappa \rho b (\bar{V}_{max} - \bar{V}_{min}) \qquad (10.49)$$

where b is the width of the shear layer at a given cross-section $\bar{V}_{max}$ and $\bar{V}_{min}$ are the maximum and minimum velocity respectively across the layer and κ an experimentally determined constant.

10.6 TURBULENT FLOW IN A TUBE. THE LAW OF THE WALL

We now consider the steady turbulent flow of an incompressible fluid in a horizontal, round tube under the influence of a pressure gradient as shown in Fig. 7.4. The tube is assumed to be sufficiently long so that the flow is fully developed (i.e. no variation in $\bar{v}_z$). The time-averaged equation of momentum in the z direction reduces to

$$\frac{\partial \bar{p}}{\partial z} = \frac{1}{r}\frac{\partial}{\partial r}(r\bar{\tau}_{rz}^{(T)}) \qquad (10.50)$$

where $$\bar{\tau}_{rz}^{(T)} = \bar{\tau}_{rz} + \bar{\tau}_{rz}^{(t)}$$

Following the arguments used in the laminar flow analysis (Sec. 7.3) we conclude that the left-hand side is a function z only and the right-hand side is a function of r only. Thus, we may write

$$-\frac{\Delta\bar{p}}{L} = \frac{1}{r}\frac{d}{dr}(r\bar{\tau}_{rz}^{(T)}) \qquad (10.51)$$

Integrating with $\bar{\tau}_{rz} = (\mu+\mu^{(t)})\frac{d\bar{v}_z}{dr} = 0$ at r=0 we get

$$\tau^{(T)} = \bar{\tau}_{rz} + \bar{\tau}_{rz}^{(t)} = -\frac{\Delta p}{2L} r$$

$$(10.52)$$

where $$\bar{\tau}_{rz} = \mu\frac{d\bar{v}_z}{dr} \quad \text{and} \quad \bar{\tau}^{(t)} = \mu^{(t)}\frac{d\bar{v}_z}{dr}$$

In Fig. 10.12 the total shear stress $\bar{\tau}^{(T)}$ and some typical experimental results for $\tau^{(t)} = -\rho\, \overline{v_z'\, v_r'}$ are shown as a function of r. We note that the maximum value of $\tau_{rz}^{(t)}$ is near $r/R = 0.9$ where the velocity fluctuations are also very large.

To obtain the velocity profile we must introduce into equation (10.51) an expression which describes $\mu^{(t)}$ over the entire domain $0 \le r \le R$. The eddy viscosity $\mu^{(t)}$ is a complicated function of r (see Fig. 10.10) and thus the velocity profile can be obtained only with numerical methods. It is important, however, to present the classical semi-empirical analysis which leads to the so-called "law of the wall"

From equation (10.52) we have

at $r = R$
$$\bar{\tau}_{rz}^{(T)} = -\frac{\Delta\bar{p}}{2L}R \tag{10.53}$$

Let $\frac{\Delta p}{2L}R = \bar{\tau}_w$ thus

$$\bar{\tau}_{rz}^{(T)} = -\frac{r}{R}\,\bar{\tau}_w \tag{10.54}$$

Note that it is merely a convention whether a minus or a plus sign in equation (10.54) should be used (see also section 7.3).

We will now assume that the total shear stress will be approximately constant and equal to $(-\tau_w)$ in the immediate vicinity of the wall ($r \simeq R$)

$$\bar{\tau}_{rz}^{(T)} = -\bar{\tau}_w \tag{10.55}$$

or

$$\bar{\tau}_{rz} + \bar{\tau}_{rz}^{(t)} = -\bar{\tau}_w \tag{10.56}$$

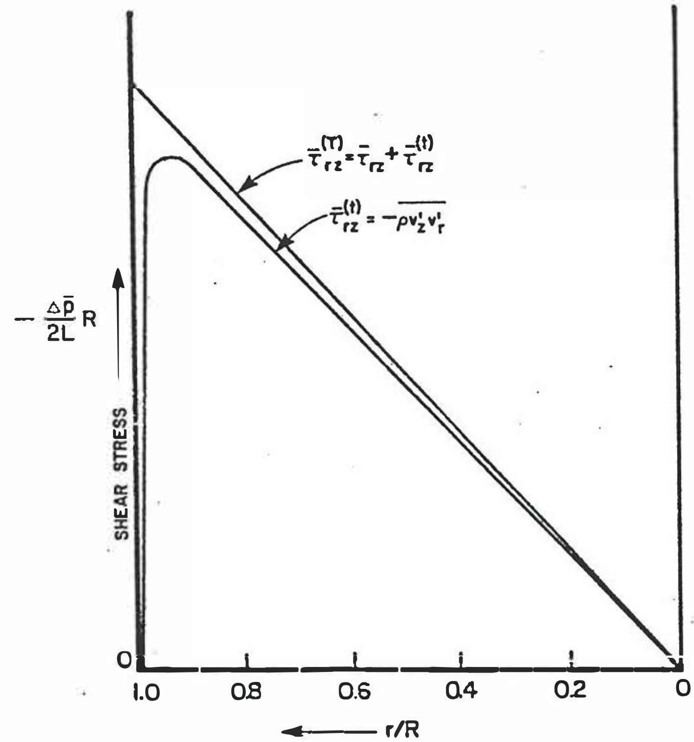

Fig. 10.12 Variation of shear stress for turbulent flow in a tube.

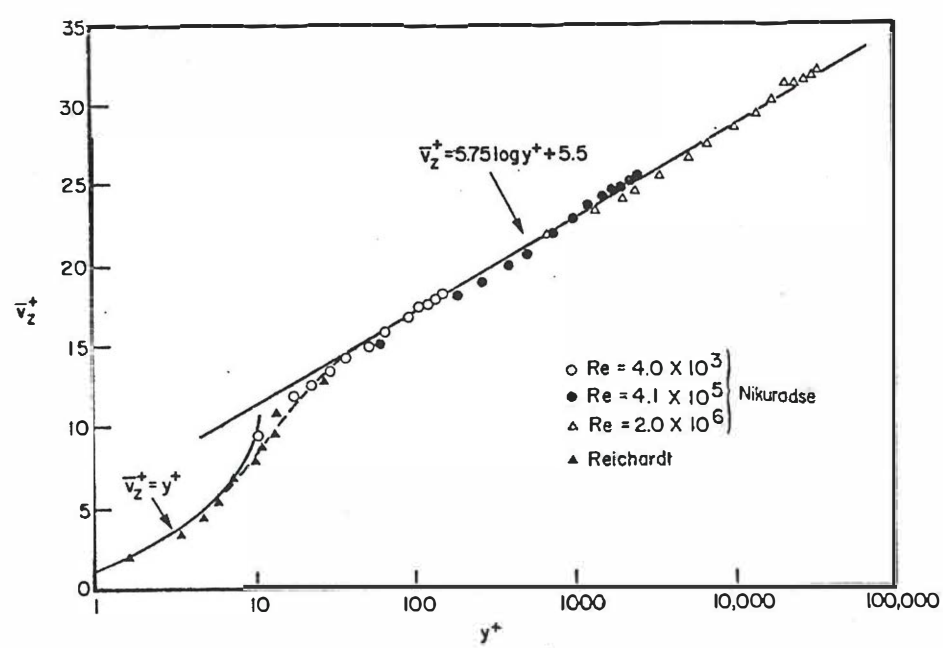

Fig. 10.13 The universal turbulent velocity profile.

or

$$\mu\left(\frac{d\bar{v}_z}{dr}\right) + \mu^{(t)}\left(\frac{d\bar{v}_z}{dr}\right) = -\bar{\tau}_w \qquad (10.57)$$

For the region where $\mu^{(t)} \approx 0$ we can simply write

$$\mu\left(\frac{d\bar{v}_z}{dr}\right) = -\bar{\tau}_w \qquad (10.58)$$

Let $r = R - y$ and $\frac{d}{dr} = -\frac{d}{dy}$

Thus

$$\mu\frac{d\bar{v}_z}{dy} = \bar{\tau}_w \qquad (10.59)$$

Solving we get

$$\bar{v}_z = \frac{\bar{\tau}_w}{\mu} y + C_1 \qquad (10.60)$$

$C_1 = 0$ because $\bar{v}_z = 0$ at $y = 0$

Thus the velocity profile very close to the wall where the viscous effects dominate (i.e. in the laminar sublayer) is

$$\bar{v}_z = \frac{\bar{\tau}_w}{\mu} y = \frac{1}{\rho}\frac{\bar{\tau}_w}{\nu} y \qquad (10.61)$$

It is customary to rewrite this equation in dimensionless form as

$$\frac{\bar{v}_z}{\sqrt{\frac{\tau_w}{\rho}}} = \frac{y\sqrt{\frac{\tau_w}{\rho}}}{\nu} \qquad (10.62)$$

where the quantity $\sqrt{\tau_w/\rho}$ has dimensions of velocity and is it called shear velocity v_z^* or by letting

$$\bar{v}_z^+ = \frac{\bar{v}_z}{\sqrt{\frac{\tau_w}{\rho}}} \text{ and } y^+ = \frac{y\sqrt{\frac{\bar{\tau}_w}{\rho}}}{\nu}$$

we have

$$v^+ = y^+ \tag{10.63}$$

Just outside the region of the laminar sublayer we assume that $\mu^{(t)} >> \mu$ and introduce Prandtl's mixing length model

$$\mu^{(t)} \frac{d\bar{v}_z}{dr} = - \bar{\tau}_w \tag{10.64}$$

or

$$\mu^{(t)} \frac{d\bar{v}_z}{dy} = \bar{\tau}_w \tag{10.65}$$

and

$$\rho\, \kappa^2 y^2 \left(\frac{d\bar{v}_z}{dy}\right)^2 = \bar{\tau}_w \tag{10.66}$$

$$\frac{d\bar{v}_z}{dy} = \frac{1}{\kappa} \sqrt{\frac{\bar{\tau}_w}{\rho}}\, \frac{1}{y} \tag{10.67}$$

or in terms of the dimensionless variables v_z^+ and y^+

$$\frac{d\bar{v}_z^+}{dy^+} = \frac{1}{\kappa} \frac{1}{y^+} \tag{10.68}$$

Integrating we get the velocity distribution as

$$\bar{v}_z^+ = \frac{1}{\kappa} \ln y^+ + C \tag{10.69}$$

Although several assumptions of questionable validity were made [e.g. $\bar{\tau}^{(T)} = \tau_w(\text{const.})$ rather than $\bar{\tau}^{(T)} = (y/R)\tau_w$ and discontinuity in $\mu^{(T)}$ from μ to $\mu^{(t)}$] experimental turbulent profile measurements yield a logarithmic relationship between $\bar{v}_z^+$ and y^+. In fact this relationship is obeyed over a large part of the cross-sectional area except in the immediate vicinity of the wall where the linear relation (Eq. 10.63) applies. Equations (10.63) and (10.69) involve only the distance from the wall and compare well with turbulent velocity profile measurements in other flows, not just for flow through tubes. Thus, the relations between v_z^+ and y^+ constitute a <u>universal turbulent velocity profile,</u> which is also called the <u>law of the wall.</u>

The universal turbulent velocity profile is usually described in terms of one, two or three separate algebraic equations. Perhaps the most often quoted profile is the one used for the interpretation of Nikuradse's extensive data [9]. It consists of three distinct equations the first for $y^+<5$, which is interpreted as the region of laminar sublayer, the second for $5<y^+<30$, the buffer layer, and the third one for $y^+>30$, the turbulent core. These are

$$y^+<5 \qquad \bar{v}_z^+ = y^+ \tag{10.70}$$

$$5<y^+<30 \qquad \bar{v}_z = 5.00\ln y^+ - 3.05 \tag{10.71}$$

$$(\text{or } \bar{v}_z = 11.50\log y^+ - 3.05)$$

$$y^+>30 \qquad \bar{v}_z = 2.5\ln y^+ + 5.5 \tag{10.72}$$

$$(\text{or } \bar{v}_z = 5.75\log y^+ + 5.5)$$

where log is the logarithm to base 10. Fig. 10.13 shows the excellent agreement between Nikuradse's data (for water) and equations 10.70, 10.71 and 10.72. The above equations are also in good agreement with Laufer's data [10] (for air) and measurements by other investigators [11,12]. Note that from equations (10.69) and (10.72) we have for Prandtl's mixing length constant $\kappa=0.4$ (since $\frac{1}{\kappa} = \frac{1}{0.4} = 2.5$). Another commonly used value is $\kappa=0.36$ which also fits the data as a two equation velocity profile

$$y^+<10 \qquad \bar{v}_z^+ = y^+ \tag{10.73}$$

$$y^+>10 \qquad \bar{v}_z^+ = 3.8 + 2.78\ \ln y \tag{10.74}$$

The agreement, however, is not good in the region from about $y^+ = 5$ to about $y^+ = 20$. Using Deissler's [8] empirical formula it is easy to show that

$$\bar{v}_z^+ = \int_0^{y^+} \frac{dy^+}{1+m\,\bar{v}_z^+\,y^+\,[1 - \exp(-m\,\bar{v}_z^+\,y^+)} \tag{10.75}$$

which fits a large body of literature data (m=0.0154) in the region $0 \le y^+ \le 26$ with equation (10.74) being used for $y^+ > 26$.

Very often, however, the empirical power-law equation

$$\frac{\bar{v}_z}{\bar{V}_{z,max}} = (1 - \frac{r}{R})^{1/n} \tag{10.76}$$

is used instead of the universal velocity profiles. The above equation fits the literature data very well with $1/10 < n < 1/6$ for a large range of Reynolds numbers ($4 \times 10^3 < Re_D < 3.24 \times 10^6$) according to Schlichting [6].

Care must be taken when using the previous equations to perform further calculations. An illustration of the possible pitfalls can be given by trying to determine the shear stress at the wall using the usual relation

$$\bar{\tau}_w = \mu(\frac{\partial v_z}{\partial r})_w \tag{10.77}$$

Both the logarithmic velocity profile (Eq. 10.69) and the power-law equation (10.76) give infinite wall stress, which is unrealistic.

It is possible, however, to obtain expressions for τ_w in terms of the friction factor f which is defined by

$$f = 4\,\frac{\bar{\tau}_w}{\frac{\rho \bar{V}^2_{avg}}{2}} \tag{10.78}$$

By determining $\bar{V}_{avg}$ for the logarithmic profile and after some adjustments in the coefficients (see for example reference [12]) we get the von Karman-Nikuradse equation, which fits the experimental data very well over a large Re range:

$$\frac{1}{\sqrt{f}} = 2.0 \log (Re_D \sqrt{f}) - 0.8 \qquad (10.79)$$

This equation, however, is somewhat inconvenient because it cannot be solved explicitly for f.

A simpler expression is often used which approximates the data very well for turbulent flow in smooth pipes up to $Re_D = 10^5$

$$f = \frac{0.316}{(Re)^{1/4}} \text{ (turbulent)} \qquad (10.80)$$

This is known as the Blasius equation and it is based on direct pressure drop measurements in pipes. The friction factor in laminar flow can be easily obtained from the results of Sec. 7.3:

For $\tau_w = (\Delta p/2L)R$ and $V_{avg} = (\Delta p/8\mu L)R^2$ we get

$$\tau_w = \frac{4V_{avg}\,\mu}{R} = \frac{8\,V_{avg}\mu}{D} \qquad (10.81)$$

Thus

$$f = 4\,\frac{\tau_w}{\frac{\rho V_{avg}^2}{2}} = 4\,\frac{\frac{8\,V_{avg}\,\mu}{D}}{\frac{\rho V_{avg}^2}{2}} = \frac{64}{\frac{\rho\,V_{avg} D}{\mu}} \qquad (10.82)$$

or

$$f = \frac{64}{Re} \quad \text{(laminar)} \qquad (10.83)$$

Note that some authors prefer a definition of the friction factor f without the numerical factor 4 in the right-hand side of equation (10.78).

The pressure drop Δp as a function of the volume rate of flow can be determined easily by combining the definition for the friction factor (Eq. 10.78) with the expression for the shear stress at the wall. We have

$$f = 4 \frac{\overline{\tau}_w}{\frac{\rho \overline{V}_{avg}^2}{2}} = 4 \frac{\frac{\Delta p}{2L} R}{\frac{\rho \overline{V}_{avg}^2}{2}} = \frac{2(\Delta p)D}{\rho L \overline{V}_{avg}^2} \tag{10.84}$$

Using Blasius empirical equation for <u>turbulent flow in smooth tubes,</u> we get

$$\frac{0.316}{\left(\frac{\rho \overline{V}_{avg} D}{\mu}\right)^{1/4}} = \frac{2(\Delta p)D}{\rho L \overline{V}_{avg}^2} \tag{10.85}$$

and solving for Δp

$$(\Delta p) = 0.158 \frac{\rho^{3/4} \mu^{1/4} L}{D^{5/4}} \overline{V}^{7/4} \tag{10.86}$$

Since $\overline{V} = Q/(\pi D^2/4)$

we have

$$(\Delta p) = 0.241 \frac{\rho^{0.75} \mu^{0.25} L}{D^{4.75}} Q^{1.75} \tag{10.87}$$

More pressure drop calculations for smooth and rough tubes are presented in Chapter 13 as applications of the Bernoulli equation. It is interesting to compare the above equation to the Hagen-Poiseuille formula (Equ. 7.61) which is valid for laminar flow. A log-log plot of Δp vs. Q for laminar and turbulent flow has already been given in section 10.1 (Fig. 10.3).

Example 10.2

Air flows through a smooth 20 cm diameter pipe at an average velocity of 10 m/s. We will determine the total stress $\tau_{xy}^{(T)}$, the Reynolds stress $\tau_{xy}^{(t)}$ and the viscous stress τ_{xy} at r/R = 0.9.

Solution

From equations (10.78) and (10.80) we have

$$f = 4 \frac{\tau_w}{\frac{\rho \overline{V}_{avg}}{2}}$$

$$f = \frac{0.316}{(Re)^{1/4}}$$

Thus

$$[\tau_{rz}^{(T)}]_{r=R} = \tau_w = 0.0395 \frac{\rho \overline{V}^2_{avg}}{(Re)^{1/4}}$$

$$Re = \frac{\overline{V}_{avg} D}{\nu} = \frac{(10 m/s)(0.2 m)}{1.5\times10^{-5} m^2/s} = 1.33\times10^5$$

and $\tau_w = 0.0395 \times \frac{(1.24\ kg/m^3)(10\ m/s)^2}{(1.33\times10^5)^{1/4}} = 0.256\ N/m^2 = 0.256\ Pa$

Since $\frac{\tau}{\tau_w} = \frac{r}{R}$ we have $\tau_{0.9} = 0.9\times0.256 = 0.23$ Pa

The stress due to viscosity is

$$\tau = \mu \frac{\partial \overline{v}_z}{\partial r} = \mu \frac{\partial}{\partial r} (\overline{V}_{max} (1 - \frac{r}{R})) = \mu V_{max} \frac{1}{7R} (1 - \frac{r}{R})^{-6/7}$$

$$\tau_{0.9} = (1.5\times10^{-5}\ m^2/s)\times(\tfrac{5}{4}\times10\ m/s) \frac{1}{7\times0.1} (1 - 0.9)^{-6/7} = 0.0019\ Pa$$

We note that the total stress is $\frac{0.256}{0.0019} \simeq 135$ times larger than the viscous one.

Since $\tau = \mu\left(\frac{\partial \bar{v}_z}{\partial r}\right)_{r/R=0.9}$ $\quad \tau^{(t)} = \mu^{(t)}\left(\frac{\partial \bar{v}_z}{\partial r}\right)_{r/R=0.9}$ and $\tau^{(T)}=\tau+\tau^{(t)}$

$$\frac{\mu^{(t)}}{\mu} = \frac{0.256-0.0019}{0.0019} \simeq 134$$

10.7 TURBULENT BOUNDARY LAYER ON A FLAT PLATE

For turbulent boundary layer flow on a flat plate the equations of conservation of mass and momentum are identical to those of Section 9.2, with viscosity replaced by the effective or total viscosity $\mu^{(T)}=\mu+\mu^{(t)}$. Thus, we have

$$\frac{\partial \bar{v}_x}{\partial x} + \frac{\partial \bar{v}_y}{\partial y} = 0 \tag{10.88}$$

$$\rho\left(\bar{v}_x \frac{\partial \bar{v}_x}{\partial x} + \bar{v}_y \frac{\partial \bar{v}_x}{\partial y}\right)=(\mu + \mu^{(t)}) \frac{\partial^2 \bar{v}_x}{\partial y^2} \tag{10.89}$$

Because $\mu^{(t)}$ varies widely over the boundary layer thickness it is very difficult to obtain analytical solutions. Finite difference solutions have been used to obtain the velocity profiles by several investigators. Detailed discussions and results can be found in the monographs by Patankar and Spalding [13] and Cebeci and Bradshaw[14].

In this section, we use the approximate integral momentum method and confine our efforts to the determination of shear stress at the wall and boundary layer thickness.

Equation (9.79) of Section 9.6 applies readily to turbulent boundary layers by substituting the instantaneous velocities by their time averages. In the absence of a pressure gradient, we have

$$\frac{d\theta}{dx} = \frac{\bar{\tau}_w}{\rho \vec{V}_\infty^2} \tag{10.90}$$

$$\text{where} \quad \theta = \int_0^\delta \frac{\bar{v}_x}{V_\infty} \left(1 - \frac{\bar{v}_x}{V_\infty}\right) dy \tag{10.91}$$

After some rearrangements, we get

$$\rho \frac{d}{dx} \int_0^\delta \bar{v}_x (V_\infty - \bar{v}_x) dy = \bar{\tau}_w \tag{10.92}$$

Note that the above equation can also be derived directly by performing an overall momentum balance to the boundary layer. The left-hand side represents the rate of change of momentum and the right-hand side the shear stress at the wall.

Introducing the 1/7 power-law expression

$$\frac{\bar{v}_x}{V_\infty} = \left(\frac{y}{\delta}\right)^{1/7} \tag{10.93}$$

into equation (10.92), we have

$$\bar{\tau}_w = \rho \frac{d}{dx} \int_0^\delta [V_\infty^2 \left(\frac{y}{\delta}\right)^{1/7} - V_\infty^2 \left(\frac{y}{\delta}\right)^{2/7}] dy =$$

$$= \rho V_\infty^2 \frac{d}{dx} \left(\frac{7}{72} \delta\right) \tag{10.94}$$

and

$$\frac{\bar{\tau}_w}{\rho V_\infty^2} = \frac{7}{72} \frac{d\delta}{dx} \tag{10.95}$$

We will now use Blasius equation (10.80) for pipe flow and the definition of the friction factor. We have

$$\frac{\overline{\tau}_w}{\rho V_{avg}^2} = \frac{1}{8} f = \frac{1}{8} \left[0.316 \left(\frac{\rho \overline{V}_{avg} D}{\mu}\right)^{-1/4}\right] \qquad (10.96)$$

For the boundary layer it is reasonable to replace D by 2δ. The average velocity can be determined by the general expression for the 1/n - power law profile

$$\overline{V}_{avg} = \frac{1}{\pi R^2} \int_o^{2\pi} \int_o^{R} \overline{V}_{max} \left(\frac{y}{R}\right)^{1/n} r dr d\theta$$

$$= \frac{2 \overline{V}_{max}}{R^2} \int_o^{R} \left(\frac{R-r}{R}\right)^{1/n} r dr \qquad (10.97)$$

which gives

$$\frac{\overline{V}_{avg}}{\overline{V}_{max}} = \frac{2n^2}{(n+1)(2n+1)} \qquad (10.98)$$

and for $n = 7$

$$\overline{V}_{avg} = 0.817 \ \overline{V}_{max} = 0.817 \ V_\infty \qquad (10.99)$$

Thus, equation (10.96) becomes

$$\frac{\overline{\tau}_w}{\rho V_\infty^2} = \frac{1}{8} \left[0.316 \left(\frac{\rho V_\infty \delta}{\mu} \times 2 \times 0.817\right)^{-1/4} (0.817)^2 \qquad (10.100)$$

and after performing the numerical calculations

$$\frac{\bar{\tau}_w}{\rho V_\infty^2} = 0.023 \left(\frac{\rho V_\infty \delta}{\mu}\right)^{-1/4} \tag{10.101}$$

Combining equation (10.95) and (10.101) we have

$$0.023 \left(\frac{\rho V_\infty \delta}{\mu}\right)^{-1/4} = \frac{7}{72} \frac{d\delta}{dx} \tag{10.106}$$

or

$$\frac{7}{72} \delta^{1/4} d\delta = 0.023 \left(\frac{\rho V_\infty}{\mu}\right)^{-1/4} dx \tag{10.107}$$

Integrating

$$\frac{7}{90} \delta^{5/4} = 0.023 \left(\frac{\rho V_\infty}{\nu}\right) x + C \tag{10.108}$$

Assuming a boundary condition $\delta=0$ at $x=0$ we get $C=0$, and

$$\delta = \frac{0.38x}{\left(\frac{\rho V_\infty x}{\mu}\right)^{1/5}} = \frac{0.38x}{(Re_x)^{1/5}} \tag{10.109}$$

Note that the turbulent boundary layer thickness increases with the 4/5-power of distance from the leading edge x. Actually near the leading edge the boundary layer is laminar and equation (10.108) is not valid. However, it seems like a reasonable approximation to extend the turbulent boundary layer up to $x=0$ where $\delta=0$.

For flow over a flat plate the local friction coefficient is defined by

$$C_f = \frac{\bar{\tau}_w}{\frac{\rho \bar{V}_\infty^2}{2}} \tag{10.110}$$

Introducing equation (10.101), we get

$$C_f = 0.046 \left(\frac{\rho V_\infty \delta}{\mu}\right)^{-1/4} \tag{10.111}$$

Further by inserting the value of δ into the above equation

$$C_f = \frac{0.058}{(Re_x)^{1/5}} \tag{10.112}$$

The average friction coefficient for a plate of length L is obtained from

$$\overline{C}_f = \frac{1}{L}\int_0^L C_f \, dx = \frac{1}{L}\int_0^L \frac{0.058}{\left(\frac{\rho V_\infty x}{\mu}\right)^{1/5}} dx$$

$$= \frac{0.072}{\left(\frac{\rho V_\infty x}{\mu}\right)^{1/5}} \tag{10.113}$$

or

$$\overline{C}_f = \frac{0.072}{(Re)^{1/5}} \tag{10.114}$$

According to Schlichting [6] the experimental results are apparently in better agreement if the numerical coefficient 0.072 is replaced by 0.074. For somewhat more accurate formulas see White [15].

The main results of the analysis for a turbulent boundary layer over a flat plate are summarized in Table 10.1 together with those of the laminar boundary layer. For the transition region empirical expressions are used [6] e.g.

$$\overline{C}_f = \frac{0.074}{(Re)^{1.5}} - \frac{A}{Re} \tag{10.115}$$

where A=1050 for $(Re)_{crit}=3\times10^5$, A=1700 for $(Re)_{crit}=5\times10^5$, A=3300 for $(Re)_{crit}=10^6$ and A=8700 for $(Re)_{crit}=3\times10^6$. A plot of $\bar{C}_f$ for smooth plates is given in Fig. 10.14.

All of the above equations are valid for smooth surfaces where the Reynolds number is the only parameter that determines the velocity profile and friction. For rough surfaces the magnitude of roughness ϵ, form and distribution also become important parameters. For artificially roughened surfaces the magnitude ϵ can be established from the geometrical characteristics, as shown in Fig. 10.15. For naturally rough surfaces the magnitude ϵ is expressed by an equivalent sand grain roughness. This is established experimentally by comparing the hydrodynamic behavior of a given rough surface to that of a smooth surface having uniform sand grains cemented on it. The form and distribution of roughness are also relevant parameters. However, there is not any generally accepted method of characterization.

The surface irregularities (natural or artificial) disrupt the laminar sublayer and may disturb the whole flow field in amounts depending on the magnitude of roughness ϵ. Let δ' be the thickness of the laminar sublayer. If $\epsilon/\delta' < 1$ the roughness has a negligible effect on the friction coefficient, and such surfaces are considered hydrodynamically smooth. For $\epsilon/\delta' > 1$ the roughness effects become important and the formulas developed for the velocity distribution and wall stress for smooth surfaces no longer apply. When ϵ/δ' exceeds 15 to 25 the velocity distribution and wall stress depend only on ϵ and are independent of the Reynolds number. Empirical correlations for rough surfaces are presented by Schlichting [6]. The effect of

Table 10.1

Comparative results for
flow over a flat plate

Laminar	Turbulent
$\frac{U}{V_\infty} \simeq \frac{3}{2}\left(\frac{y}{\delta}\right) - \frac{1}{2}\left(\frac{y}{\delta}\right)^3$	$\frac{U}{V_\infty} \simeq \left(\frac{y}{\delta}\right)^{1/7}$
$C_f = \frac{0.664}{\sqrt{Re_x}}$	$C_f = \frac{0.058}{(Re_x)^{1/5}}$
$\bar{C}_f = \frac{1.33}{\sqrt{Re_L}}$	$\bar{C}_f = \frac{0.074}{(Re_L)^{1/5}}$
$\tau_w = \frac{\rho V_\infty^2}{2} C_f$	$\tau_w = \frac{\rho V_\infty^2}{2} C_f$
$\frac{\delta}{x} = \frac{5}{\sqrt{Re_x}}$	$\frac{\delta}{x} = \frac{0.38}{(Re_x)^{1/5}}$

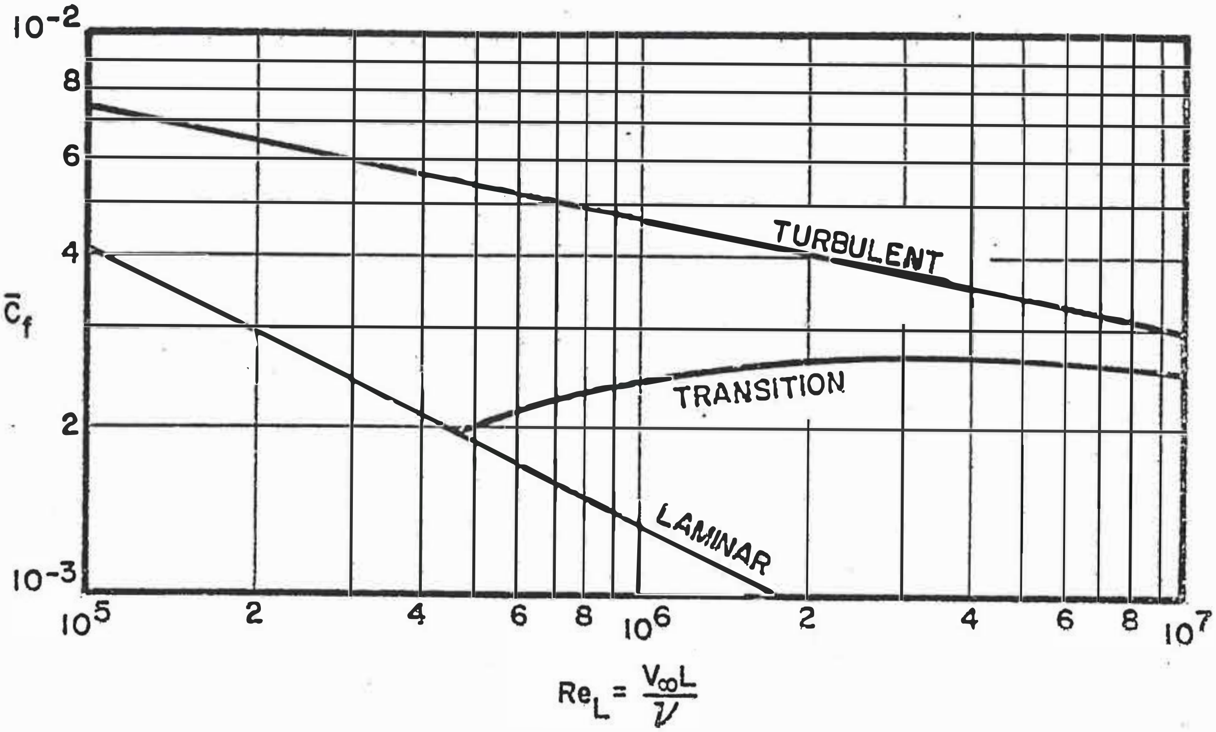

LAMINAR $\bar{C}_f = \frac{1.33}{\sqrt{Re}}$, TRANSITION $\bar{C}_f = \frac{0.074}{Re^{1/5}} - \frac{1700}{Re}$, TURBULENT $\bar{C}_f = \frac{0.074}{Re^{1/5}}$

Fig. 10.14 The average friction coefficient for boundary layer flow over a flat plate

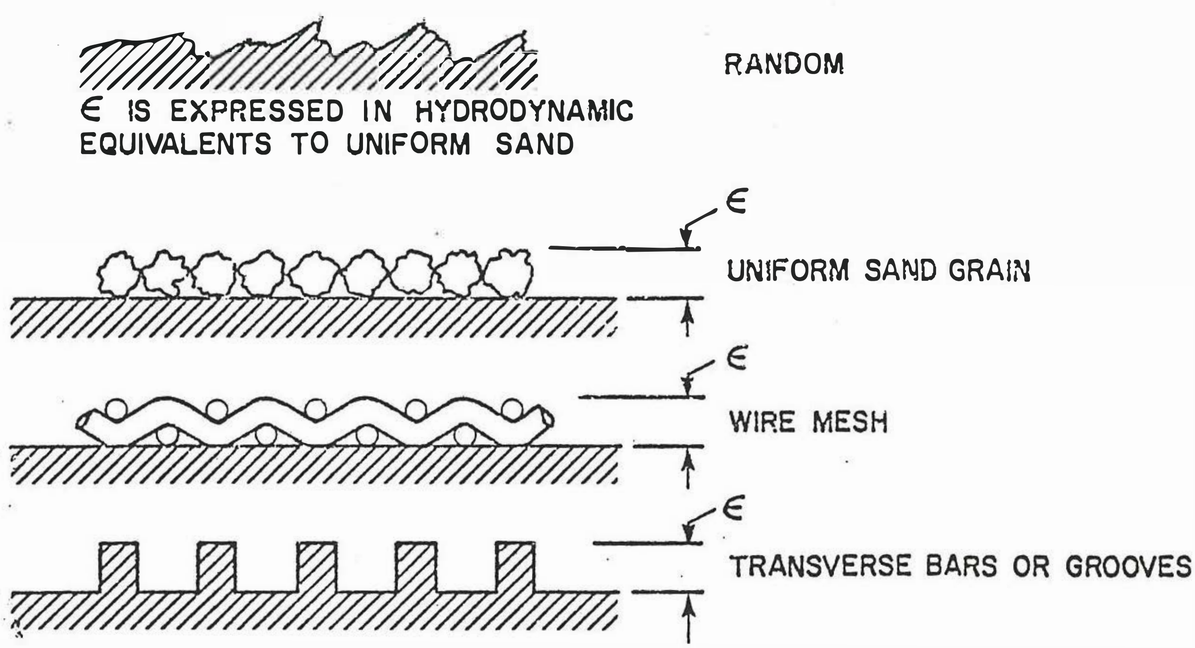

Fig. 10.15 Definition of roughness ε for naturally and artificially rough surfaces.

roughness on the local skin friction coefficient is illustrated in Fig. 10.16 (from White [15]). Note that at long distances x from the leading edge the effect decreases because δ' increases.

Example 10.3

We will repeat the calculations for the data given in example 9.1 assuming that the boundary layer is turbulent throughout the whole plate surface.

Solution

We found $Re_x = 694444$

Thus, $\delta = \dfrac{0.38x}{(Re_x)^{1/5}} = \dfrac{0.38 \times 0.25\text{m}}{(694444)^{1/5}} = 0.0065\text{m} = 6.5 \text{ mm}$

we note that the turbulent boundary layer is much thicker than the laminar one (from example 9.1, $\delta = 1.5$ mm)

$$\overline{C}_f = \frac{0.074}{(Re_x)^{1/5}} = \frac{0.074}{(694444)^{1/5}} = 0.005$$

$$\tau_w = \frac{1}{2}\overline{C}_f \; \rho \; V_\infty^2 = \frac{1}{2}\times 0.005\times(1000 \text{ kg/m}^3)\left(\frac{12000}{3600} \text{ m/s}\right)^2 = 27.78\frac{\text{N}}{\text{m}^2}$$

and the force required to tow the plate is (for two sides)

$$F = 2 \; \tau_w A = 2(27.78 \; \frac{\text{N}}{\text{m}^2})(0.25 \times 0.25 \text{ m}^2) = 3.47 \text{ N}$$

Perhaps a somewhat more accurate calculation would be to assume a laminar boundary layer up to distance x where $Re_x = 300{,}000$ and turbulent thereafter. For most practical problems, however, the laminar portion would probably be insignificant.

Example 10.4.

Determine the thickness of the laminar sublayer and the thickness of the buffer zone for the data used in example 10.3.

Solution

In developing the universal logarithmic profile we assumed that the laminar sublayer extends up to

$$y^+ = 5$$

Thus,

$$\frac{y\sqrt{\tau_w/\rho}}{\nu} = 5$$

at the trailing edge of the plate $\tau_w = 27.78\ N/m^2$ and

$$y = 5\nu \frac{1}{\sqrt{\tau_w/\rho}} = 5(1.2{\times}10^{-6} N{\cdot}s/m^2)\frac{1}{\sqrt{\dfrac{27.78\ N/m^2}{1000\ kg/m^3}}} \simeq 3.6{\times}10^{-5} m \simeq 3.6{\times}10^{-2} mm$$

The buffer zone extends up to $y^+ = 30$

Thus $$y = \frac{30}{5} \times 3.6{\times}10^{-2} mm = 2.16{\times}10^{-1} mm$$

It is interesting to compare the various thicknesses: In problem 9.1 we found that if the boundary layer is laminar δ=1.5 mm. For turbulent flow throughout the plate we found that at the trailing edge the laminar sublayer is only 0.036 mm thick. The buffer zone occupies the region from 0.036 mm to 0.216 mm and the turbulent core from 0.216 mm to 6.5 mm.

10.8 ENTRY LENGTH FOR TURBULENT PIPE FLOW

The entry region problem for laminar flow was examined in Sec. 9.3. For turbulent flow the analysis is considerably more difficult because of the uncertainty in the value of the eddy viscosity $\mu^{(t)}$ and the associated mathematical complexities. However, we can get a rough estimate by using the results of the boundary layer analysis for flow

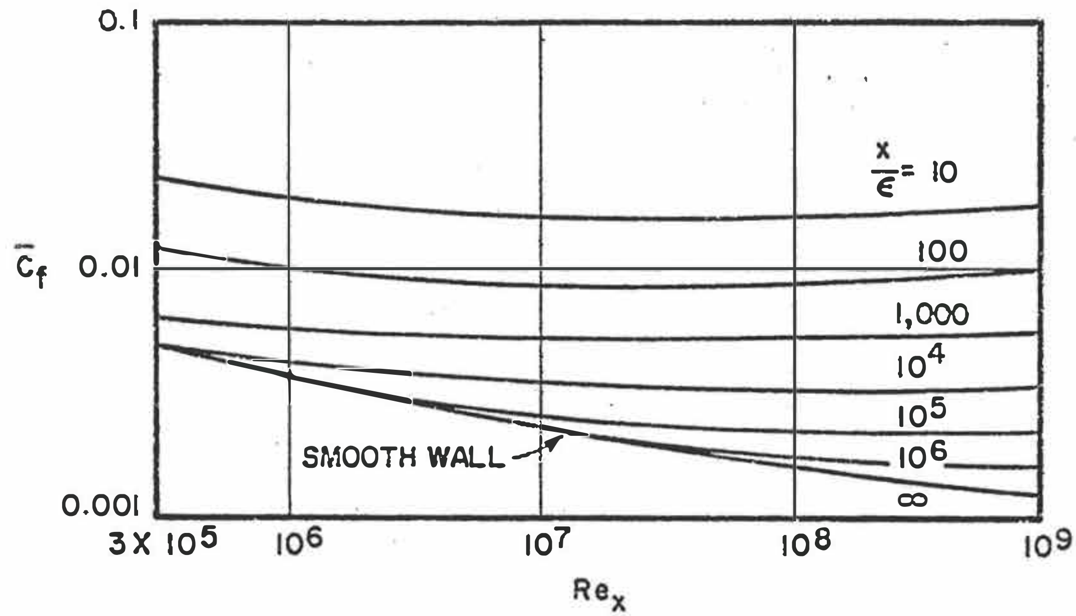

Fig. 10.16 The influence of roughness on the local friction coefficient

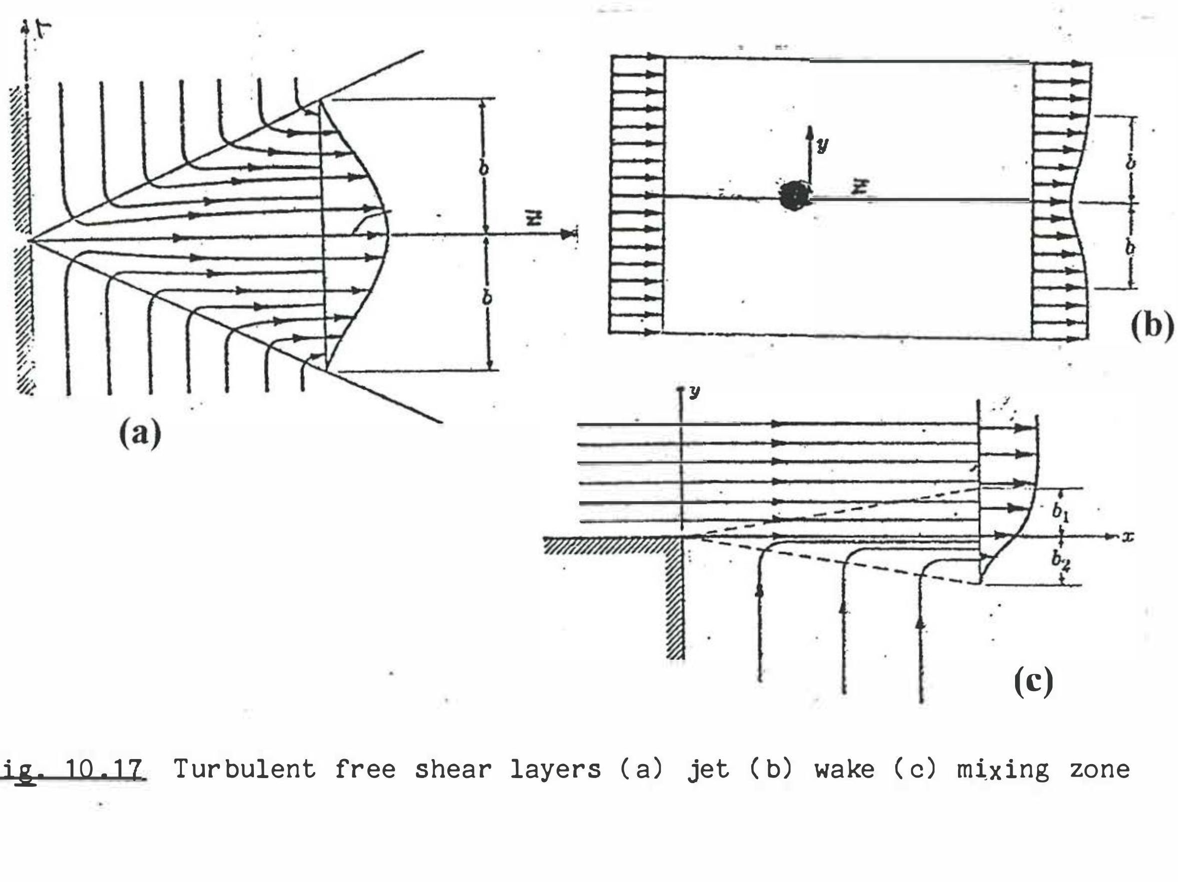

Fig. 10.17 Turbulent free shear layers (a) jet (b) wake (c) mixing zone

over a flat plate.

As the fluid enters the pipe it has a nearly flat velocity profile. Downstream from the entry a boundary layer grows in the inside tube surface. At some distance the boundary layer "fills" the tube, thus, $\delta=R=D/2$. From this distance downstream the velocity profile can be approximated fairly well by the 1/7-power law expression.

We can rewrite equation (10.109) as

$$x \simeq \frac{\delta}{0.38}\left(\frac{\rho V_\infty x}{\partial}\right)^{1/5} \tag{10.116}$$

Since at $x=L_e$ $\delta=D/2$ and from equation (10.99) $V_\infty=\bar{V}_{avg}/0.817$ we have

$$L_e^{4/5} \simeq \frac{D}{2\times0.38} \times \frac{1}{(0.817)^{1/5}} \left(\frac{\rho \bar{V}_{avg}}{\mu}\right)^{1/5}$$

or

$$\frac{L_e}{D} \simeq 1.48 \left(\frac{\rho V_{avg} D}{\mu}\right)^{1/4} \simeq 1.48\ Re^{1/4} \tag{10.117}$$

Kirsten [16] made entry length measurements in the range of 50 to 100 pipe diameters and Nikuradse [9] in the range of 25 to 40 pipe diameters. Nikuradse's 40-diameter value was for $Re_D = 9\times10^5$ whereas the equation developed above gives $L_e/D = 45$. The agreement is actually better than one might anticipate and must be regarded as fortuitous. For most practical problems the 40-diameter value is recommended as a minimum length for turbulent flow to become fully developed.

10.9 TURBULENT JETS, WAKES AND MIXING ZONES

Turbulent jets, wakes and mixing zones between two uniform streams, are called free shear flows because of the absence of solid boundaries. These types of flow are schematically shown in Fig. 10.17. We note that the fluid in the shear layer itself is the same as the surrounding fluid i.e. a jet of air in air or a jet of water in water. These types of flow can be treated with the turbulent boundary layer equations. Since $\mu \ll \mu^{(t)}$ throughout a free shear layer, we may eliminate the viscosity μ. The eddy (or turbulent) viscosity can be usually expressed (sec. 10.5) as

$$\mu^{(t)} = \kappa \rho b(\bar{V}_{max} - \bar{V}_{min}) \tag{10.118}$$

Thus by substituting expressions of the above type into the boundary layer equations we may solve these equations to obtain the longitudinal and transverse velocity distributions. Detailed discussions on theoretical developments as well as experimental data may be found in the monographs of Pai [17], Abramovich [18] and Rajaratnam [12]. The classical solutions for jets, wakes and mixing zones are also presented by Schlichting [6]. In this section we will summarize some of the main results following closely Schlichting's presentation.

10.9.1 Axisymmetric turbulent jet

For the axisymmetric turbulent jet of an incompressible fluid the time-averaged boundary layer equations are

$$\frac{1}{r}\frac{\partial (r\bar{v}_r)}{\partial r} + \frac{\partial \bar{v}_z}{\partial z} = 0 \tag{10.119}$$

$$\rho\left(\bar{v}_r \frac{\partial \bar{v}_z}{\partial r} + \bar{v}_z \frac{\partial \bar{v}_z}{\partial z}\right) = \mu^{(t)} \frac{1}{r}\frac{\partial}{\partial r}\left(r \frac{\partial \bar{v}_z}{\partial r}\right) \tag{10.120}$$

The boundary conditions are

$$z = 0 \qquad \bar{v}_z = V_o(r) \quad \text{(must be known)}$$

$$r = 0 \qquad \frac{\partial \bar{v}_z}{\partial r} = 0 \qquad \bar{v}_r = 0 \tag{10.121}$$

$$r = \infty \qquad \bar{v}_z = 0$$

It turns out that the increase of jet width is $b = Bz$ the velocity decay $\bar{V}_{max} \propto z^{-1}$ and equation (10.118) with $\bar{V}_{min} = 0$ gives

$$\mu^{(t)} = \rho\kappa b\, \bar{V}_{max} = \rho\kappa B = \text{const} \tag{10.122}$$

Thus, from the mathematical point of view the equations describing the turbulent free jet are identical to those for the laminar jet (Sec. 9.4). However, the viscous term is now due to random eddy motions rather than molecular movements. Tollmien [20] obtained a similarity type solution which gives the axial velocity component as

$$\frac{\bar{v}_z}{\bar{V}_{z,max}} = \frac{1}{1 + \frac{\eta^2}{4}} \qquad \eta = \frac{\sigma r}{z} \tag{10.123}$$

where $\sigma \simeq 15.18$

or

$$\bar{V}_{z,max} = 7.41 \left(\frac{J}{\rho}\right)^{1/2} \frac{1}{z} \text{ and } J = \left[2\pi\rho \int_0^{D/2} \bar{v}_z^2\, r\,dr\right]_{z=0} \tag{10.124}$$

Thus, for a flat velocity profile $v_z = V_o$ at $z = 0$, we get

$$\frac{\bar{v}_{z,max}}{\bar{V}_o} = \frac{6.56}{\left(\frac{z}{D}\right)} \tag{10.125}$$

The radial velocity component v_r is

$$\bar{v}_r = \left(\frac{3J}{\pi\rho}\right)^{1/2} \frac{\eta - \frac{1}{4}\eta^2}{z(1+\frac{1}{4}\eta^2)^2} \tag{10.126}$$

The volume rate of flow at a position z is given by

$$Q = 2\pi \int_0^\infty v_z r dr \tag{10.127}$$

Then, by introducing the axial velocity component into the above equation, we get

$$Q = 8\pi\, \mu^{(t)}\, z = 0.404\, (J\rho)^{1/2}\, z \tag{10.128}$$

This means that the volume rate of flow increases linearly with distance, because of fluid entrainment from the surroundings. Note that the numerical constants appearing in Equations (10.123) - (10.128) have been determined by Schlichting [5] by fitting the theory to Reichard's [21] experiments. Other investigators suggest somewhat different numerical values (see Rajaratnam [19]).

Because the outer "edges" of the jet are poorly defined it is customary to define the <u>half-velocity width</u> ($r_{1/2}$) which is a line along which $\bar{v}_z/\bar{V}_{max} = 1/2$. From Tollmien's solution [20] and Reichart's results [21],[6], we get

$$(r_{1/2}) = 0.0848z \tag{10.129}$$

$$\nu^{(t)} = \frac{\mu^{(t)}}{\rho} = 0.0256\, (r_{1/2})\, \bar{v}_{z,max} \tag{10.130}$$

and

$$\nu^{(t)} = 0.00217\, z\, \bar{v}_{z,max} \tag{10.131}$$

Since $r_{1/2}/z \simeq 0.0848 \simeq \tan 5^{\circ}$ the axisymmetric jet is a cone with half angle of 5°. It is important to note that this angle is independent of the mass rate of flow. On the contrary, the rate of spreading of a laminar jet as given by equation (9.67) depends on the mass rate of flow J. The difference in spreading behavior is due to the fact that the viscosity is a property of the fluid whereas the eddy viscosity is a property of the flow field itself.

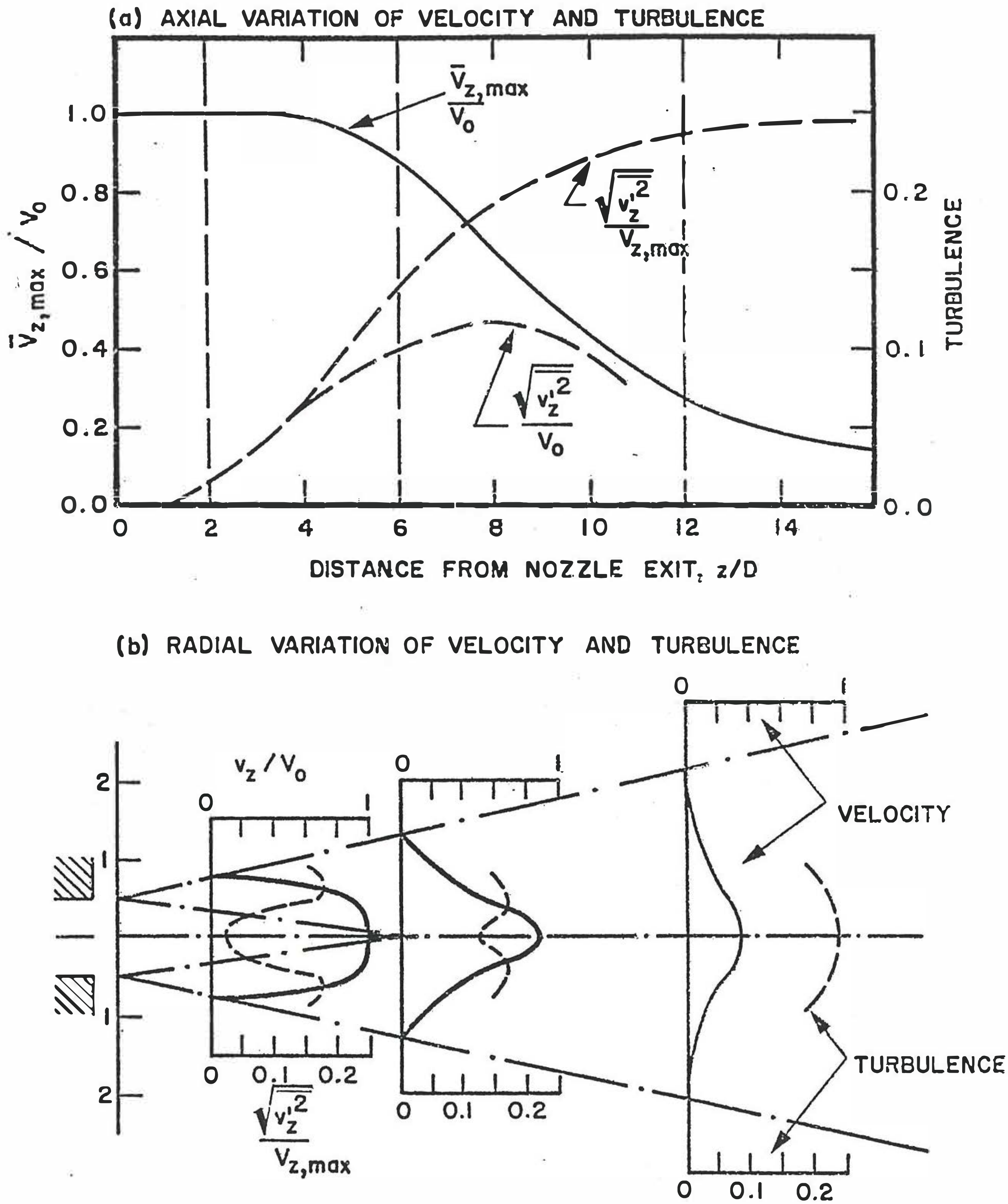

Fig. 10.18 Schematic representation of velocity and turbulence variation in a round jet, according to Corrsin [22].

The results of the above similarity analysis have been found in relatively good agreement with experimental data for distances usually larger than 8 nozzle diameters from the plane of exit. In the exit region these solutions do not apply because of flow development in the exit region [22], [23], as shown in Fig. 10.18. In this figure the corresponding turbulence levels are also shown for the various regions of the jet.

10.9.2 Two-dimensional wake

The wake formed behind a circular cylinder in cross-flow as shown in Fig. 10.17 (b) is a two-dimensional one. It looks like a jet drawn backward, however, its hydrodynamic characteristics are quite different. It represents a "defect" in a flow field of relatively high velocity. Consequently the inertia forces in a wake are much larger than those in a jet.

The time-averaged boundary layer equations which apply in this case are

$$\frac{\partial \bar{v}_y}{\partial y} + \frac{\partial \bar{v}_z}{\partial z} = 0 \tag{10.132}$$

$$\rho\left(\bar{v}_y \frac{\partial \bar{v}_z}{\partial y} + \bar{v}_z \frac{\partial \bar{v}_z}{\partial z}\right) = \mu^{(t)} \frac{\partial^2 \bar{v}_z}{\partial y^2} \tag{10.133}$$

We may assume that the term $\bar{v}_y \frac{\partial \bar{v}_z}{\partial y}$ is small compared to $\bar{v}_z \frac{\partial \bar{v}_z}{\partial z}$.

Moreover, since a wake is a "defect" in a flow field we may also assume that

$\bar{v}_z \frac{\partial \bar{v}_z}{\partial z} \simeq V_\infty \frac{\partial \bar{v}_z}{\partial z}$. Thus, the momentum equation becomes

$$\rho V_\infty \frac{\partial \bar{v}_z}{\partial z} = \mu^{(t)} \frac{\partial^2 \bar{v}_z}{\partial y^2} \tag{10.34}$$

We now introduce the velocity difference

$$\bar{v}_1 = V_\infty - \bar{v}_z \tag{10.135}$$

and rewrite the momentum equation as

$$\rho V_\infty \frac{\partial \bar{v}_1}{\partial z} = \mu^{(t)} \frac{\partial^2 \bar{v}_1}{\partial y^2} \tag{10.136}$$

The boundary conditions are

$$\begin{aligned} y = 0 \quad & \frac{\partial \bar{v}_1}{\partial y} = 0 \\ y = \infty \quad & \bar{v}_1 = 0 \end{aligned} \tag{10.137}$$

Schlichting [6] used Prandtl's mixing length model (Eq. 10.118) and obtained a similarity solution in the form

$$\frac{\bar{v}_1}{\bar{v}_{1,max}} = [1 - (\frac{y}{b})^{3/2}]^2 \tag{10.138}$$

where b represents the wake width which is related to the drag coefficient (see Chapter 12) of the upstream cylindrical body causing the wake. By matching theory and experiment Schlichting [6] gives

$$b \simeq 0.57 \, (z \, C_D D)^{1/2} \tag{10.139}$$

where C_D is the drag coefficient of a cylinder of diameter D.

Table 10.2

Layer width and centerline velocity decay as a function of position for free shear flows

(Turbulent Flow)

FLOW	SKETCH	WIDTH	CENTERLINE VELOCITY
TWO-DIMENSIONAL JET	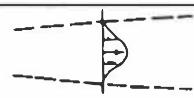	z	$z^{-1/2}$
AXISYMMETRIC JET	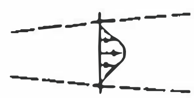	z	z^{-1}
TWO-DIMENSIONAL WAKE	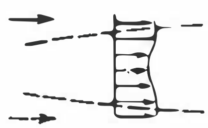	$z^{1/2}$	$z^{-1/2}$
AXISYMMETRIC WAKE	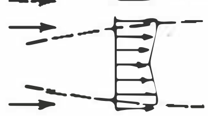	$z^{1/3}$	$z^{-2/3}$
TWO UNIFORM STREAMS	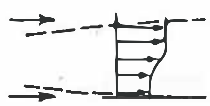	z	z^{0}

Equation (10.139) is in good agreement with experiments for $z>10C_D D$. The velocity difference at the midplane of a wake decays according to the relation

$$\frac{\overline{V}_{1,max}}{V_\infty} \simeq 0.98 \left(\frac{C_D D}{z}\right)^{1/2} \qquad (10.140)$$

This relation is accurate for distances of $z>50C_D D$.

The time-averaged boundary layer equations also describe the flow field in mixing zones. Again similarity solutions have been developed [6], [19]. The width and midplane velocity variation as a function of position of a mixing zone between two uniform streams are given in table 10.2. The corresponding results for jets and wakes are also shown for comparison. Note that Table 9.2 (in Sec. 9.4) provides the same kind of information for laminar jets, wakes and mixing zones.

Example 10.5

We will repeat the maximum velocity calculation for the data of example 9.2 assuming turbulent flow.

Solution

$$\overline{V}_{z,max} = 7.41 \left(\frac{J}{\rho}\right)^{1/2} \frac{1}{z}$$

$$\text{where } J = 2\pi\rho \int_0^{D/2} \overline{v}_z^2 r dr = 2\pi\rho \int_0^{D/2} V_o^2 \left(1 - \left(\frac{2r}{D}\right)^2\right)^2 r dr$$

$$= 2\pi\rho\ V_o^2 \left[\frac{r^2}{2} - \frac{8r^4}{4D^2} + \frac{16r^6}{6D^4}\right]_o^{D/2} = 2\pi\rho\ V_o^2 \frac{D^2}{24} = \frac{\pi\rho V_o^2 D^2}{12}$$

Thus,

$$\bar{V}_{z,max} = 7.41\left(\frac{\pi V_o^2 D^2}{12}\right)\frac{1}{z} = 7.41\, V_o D\left(\frac{\pi}{12}\right)\frac{1}{z} = 3.79\, V_o D\,\frac{1}{z}$$

$$= 3.79 \times (20\text{m/s}) \times (0.2\times10^{-3}\text{m}) \times \frac{1}{0.01\,\text{m}} \simeq 1.52\text{m/s}$$

The change of velocity as a laminar jet becomes turbulent is used in certain devices to cause pressure differences large enough to drive mechanical switches (known as fluidics).

Example 10.6

A cross-flow heat exchanger consists of a parallel row of tubes 2.5 cm in diameter, spaced at 25 cm apart. Determine the distance downstream at which the wakes formed behind the tubes will meet and find the maximum velocity difference at this point assuming no interactions. The cross-flow velocity V_∞ is 100 m/s and kinematic viscosity of the fluid (air) is $\nu = 1.3\times10^{-5}\ m^2/s$

Solution

$$Re_D = \frac{V_\infty D}{\nu} = \frac{(100\ m/s) \times (0.025\ m)}{1.3\times10^{-5}\ m^2/s} = 1.92\times10^5$$

From Chapter 12 we choose an approximate value of the drag coefficient $C_D = 0.9$. Thus, we have:

$$b \simeq 0.57\,(z\, C_D D)^{1/2}$$

for b = 12.5 cm, we get

$$z = \left(\frac{0.125}{0.57}\right)^2 \frac{1}{0.025} = 1.92\ m$$

The maximum velocity difference in the absence of interactions is

$$\bar{V}_{1,max} = 0.98\left(\frac{0.9\times0.025\,m}{1.92\ m}\right)^{1/2} \times (100\ m/s) = 10.6\ m/s$$

Although $z>50\ C_D D$ (1.92>1.13) the maximum velocity difference estimate might not be terribly accurate.

10.10 STATISTICAL THEORIES OF TURBULENCE

The first step in the solution of the time-averaged conservation equations is the introduction of an appropriate eddy viscosity coefficient $\mu^{(t)}$. We discussed several models for $\mu^{(t)}$ which contain one or more adjustable parameters. We noted that, unlike μ, $\mu^{(t)}$ is not a property of the fluid but a property of the flow field. The eddy viscosity increases with the size of the flow field and its overall velocity. The fluid flow in a large pipe appears to be dominated by an eddy viscosity larger than the same fluid in a small pipe. Also, at high flow rates the effective viscosity is larger than at low flow rates. $\mu^{(t)}$ is usually several hundred or thousand times larger than μ depending on flow configuration and velocity, but it does not bear any definite relation to them. Virtually for every new experiment a set of parameters must be adjusted in the theoretical models. Consequently, this is not a fundamental theory on which to base a thorough study of turbulent fluid flow. It is usually referred to as the <u>phenomenological theory of turbulence</u>

Statistical approaches to the study of turbulent flow have been developed by such distinguished scientists like G.I. Taylor, Von Karman, Kolmogoroff and Heisenberg (see references [24] and [25]). Most of the classical papers have been compiled in a single volume edited by Friedlander and Topper [25]. More recent advances can be found in books by C.C. Lin [27], Monin and Yaglom [28], Orszag [29] and Tennekes and Lumley [30].

For most of the statistical theories the basic step is the definition of correlations of velocity fluctuations at two or three points. Actually the Reynolds stresses (Sec. 10.4) are statistical correlations of the velocity fluctuations at one point. The correlation concept can be simply explained by the pictorial representation (Fig. 10.19) taken from Brodkey [31].

Most of the statistical theories have been developed for homogeneous and isotropic fields of turbulence in the absence of mean motion ($\bar{v}_x = \bar{v}_y = \bar{v}_z = 0$). Homogeneity implies that the various turbulence quantities are independent of position i.e. for two points A and B $v'^2_{Ax} = v'^2_{Bx}$, $v'^2_{Ay} = v'^2_{By}$ etc. Isotropy means that the various measures of turbulence at a particular point are equal irrespective of their direction in space i.e. $v'^2_x = v'^2_y = v'^2_z = u'^2$. An approximately homogeneous and isotropic turbulent flow field can be realized behind a grid in a wind tunnel. The eddies generated must be relatively small otherwise there might be preferred directions in space i.e. anisotropy. To facilitate the presentation we will alter our notation. The symbols, u', v', w' will be representing the velocity fluctuations in the x, y and z directions respectively. For the two points A and B, shown in Fig. 10.20, we define a longitudinal correlation coefficient f(r) by

$$\frac{\overline{u'_A u'_B}}{\overline{u'^2}} = f(r) \qquad (10.141)$$

Similarly we define a transverse correlation coefficient g(r) by

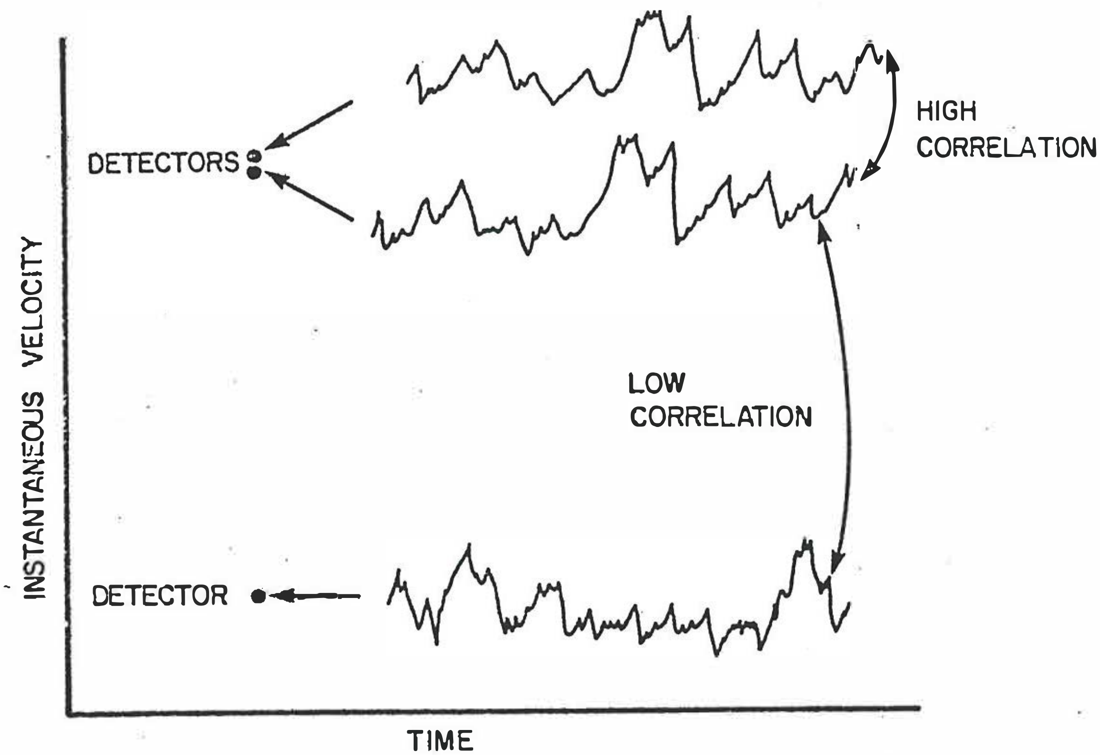

Fig. 10.19 Sketch illustrating the correlation of velocity fluctuations in turbulent flow.

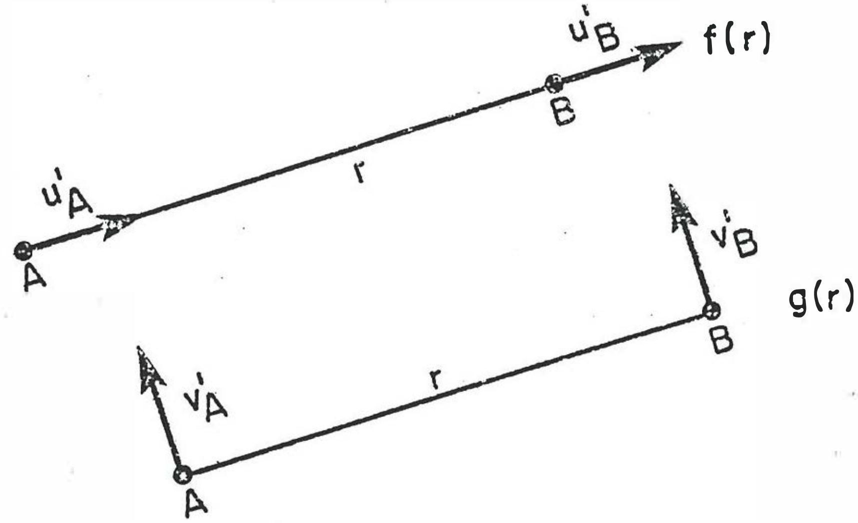

Fig. 10.20 Longitudinal and transverse velocity correlations in a turbulent flow field.

$$\frac{\overline{v'_A v'_B}}{\overline{u'^2}} = g(r) \tag{10.142}$$

Because of isotropy we may also write

$$\frac{\overline{w'_A w'_B}}{\overline{u'^2}} = g(r) \tag{10.143}$$

All the other possible correlations between u'_A, v'_A, w'_A and u'_B, v'_B, w'_b will be zero i.e. $u'_A\ v'_B = 0$, $u'_B\ w'_B = 0$ etc. because of isotropy.

Thus, we may define a correlation tensor for the two points A and B with all its elements zero except those on the diagonal i.e.

$$\begin{matrix} f(r) & 0 & 0 \\ 0 & g(r) & 0 \\ 0 & 0 & g(r) \end{matrix}$$

The above tensor can be decomposed to

$$(f(r) - g(r))\begin{pmatrix} 1 & 0 & 0 \\ 0 & 0 & 0 \\ 0 & 0 & 0 \end{pmatrix} + g(r)\begin{pmatrix} 1 & 0 & 0 \\ 0 & 1 & 0 \\ 0 & 0 & 1 \end{pmatrix}$$

In a new coordinate system defined by $\zeta_1 = x_B - x_A$, $\zeta_2 = y_B - y_A$ $\zeta_3 = z_B - z_A$ we will have a general correlation tensor in the form

$$R_{ij} = (f(r) - g(r))\,\frac{\zeta_i \zeta_j}{r^2} + g(r)\ \delta_{ij} \tag{10.144}$$

where $r^2 = \zeta_i \zeta_i = \zeta_1^2 + \zeta_2^2 + \zeta_3^2$ and $\delta_{ij} \Rightarrow \begin{pmatrix} 1 & 0 & 0 \\ 0 & 1 & 0 \\ 0 & 0 & 1 \end{pmatrix}$

The continuity equation at point B is

$$\frac{\partial u'_B}{\partial x_B} + \frac{\partial v'_B}{\partial y_B} + \frac{\partial w'_B}{\partial z_B} = 0 \tag{10.145}$$

Multiplying by $\frac{u'_A}{\overline{u'^2}}$ which is independent of x_B, y_B and z_B, and time-averaging

$$\frac{\partial}{\partial x_B} \frac{\overline{u'_A u'_B}}{\overline{u'^2}} + \frac{\partial}{\partial y_B} \frac{\overline{u'_A v'_B}}{\overline{u'^2}} + \frac{\partial}{\partial z_B} \frac{\overline{u'_A w'_B}}{\overline{u'^2}} = 0 \tag{10.146}$$

or

$$\frac{\partial}{\partial \zeta_1} (R_{11}) + \frac{\partial}{\partial \zeta_2} (R_{12}) + \frac{\partial}{\partial \zeta_3} (R_{13}) = 0 \tag{10.147}$$

From equation (10.144) we have

$$R_{11} = (f(r) - g(r)) \frac{\zeta_1^2}{r^2} + g(r) \tag{10.148}$$

$$R_{12} = (f(r) - g(r)) \frac{\zeta_1 \zeta_2}{r^2} \tag{10.149}$$

$$R_{13} = (f(r) - g(r)) \frac{\zeta_1 \zeta_3}{r^2} \tag{10.150}$$

Substituting the expressions for R_{11}, R_{12} and R_{13} into equation (10.147), performing the differentiations and rearranging we get

$$\zeta_1 \, [2(f - g) + r(\frac{\partial f}{\partial r})] = 0 \tag{10.151}$$

This relation must be true for any ζ_1 thus

$$g = f + \frac{r}{2}\frac{\partial f}{\partial r} \tag{10.152}$$

This means that in homogeneous isotropic turbulence the correlations can be expressed in terms at a single function, say f(r). The above relation was first derived by von Karman [32]. Experimental verifications have been performed by a number of investigators using hot wire anemometry (see Chapter Flow Measurements). Fig. 10.21 shows such a verification (from Hinze [1]). We note from the definition of f(r) and g(r) (Eqs. 10.141 and 10.142), that the correlation functions would become equal to unity if the separation r were reduced to zero. Similarly, f(r) and g(r) would reduce to zero if the separation were large enough so that no correlation occurred. Fig. 10.22(a) shows f(r) as a function of position r [33]. While f(r) is always positive g(r) may become negative for certain values of r because a negative correlation is expected between the velocities on opposite sides of an eddy.

The <u>triple velocity correlation</u> for two points A and B can be defined in general tensorial form by

$$T_{ij,k} = \frac{1}{u'^3}\ \overline{(v_i'(A)\ v_j'(A)\ v_k'(B))} \tag{10.153}$$

This tensor has 27 components. It turns out, because of the condition of isotropy, that the only non-zero terms are $\overline{u_A^2\ u_B}$, $\overline{u_A\ v_B\ v_B}$, $\overline{u_A\ w_A\ w_B}$, $\overline{v_A^2\ u_B}$ and $\overline{w_A^2\ u_B}$. From these five terms the second and third represent the same configuration. The fourth and fifth terms also represent an identical configuration. Thus, the three distinct components of the third order tensor are

$$K(r) = T_{11,1} = \frac{\overline{u'_A u'_A u'_B}}{\overline{u'^3}} \tag{10.154}$$

$$h(r) = T_{22,1} = \frac{\overline{v'_A v'_A u'_B}}{\overline{u'^3}} \tag{10.155}$$

$$g(r) = T_{21,1} = \frac{\overline{v'_A u'_A v'_B}}{\overline{u'^3}} \tag{10.156}$$

Using the continuity equation it is possible to show that

$$k = -2h \tag{10.157}$$

$$g = -h - \frac{r}{2}\frac{\partial h}{\partial r} \tag{10.158}$$

This means that the triple correlation tensor for a homogeneous and isotropic field of turbulence can be represented by a single function, say k or h. Fig. 10.22 (b) shows the triple correlation k(r) as a function of position (after Kistler et al [33]).

To determine theoretically the statistical properties of turbulence, such as the turbulence intensity and the correlation functions we must start from the Navier-Stokes equations which are (in tensorial form):

$$\frac{\partial v_i}{\partial t} + v_j \frac{\partial v_i}{\partial x_j} = -\frac{1}{\rho}\frac{\partial p}{\partial x_j} + \nu \nabla^2 v_i \tag{10.159}$$

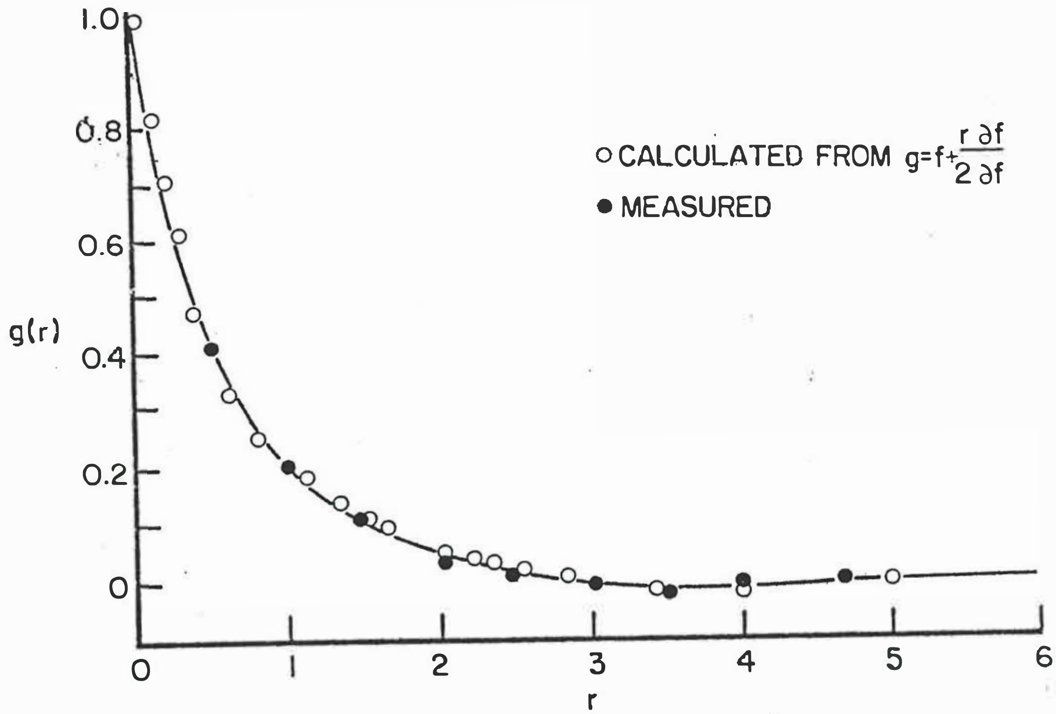

Fig. 10.21 Verification of relation between g(r) and f(r) (from Hinze [1])

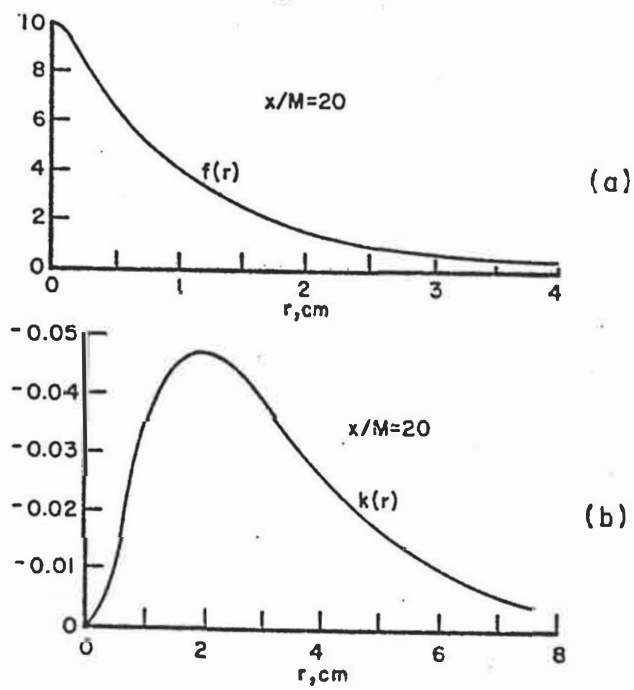

Fig. 10.22(a) Double velocity correlation f(r) and (b) Triple velocity correlation k(r) as functions of distance (from reference [33])

In the absence of mean flow we can write the x component for the fluctuations at point A as

$$\frac{\partial u_A'}{\partial t} + u_A' \frac{\partial u_A'}{\partial x} + v_A' \frac{\partial u_A'}{\partial y} + w_A' \frac{\partial u_A'}{\partial z} = -\frac{1}{\rho}\frac{\partial p_A'}{\partial x} + \nu\left(\frac{\partial^2 u_A'}{\partial x^2} + \frac{\partial^2 u_A'}{\partial y^2} + \frac{\partial^2 u_A'}{\partial z^2}\right) \tag{10.160}$$

To establish the correlation functions we must multiply by u_B' and then interchange the role of A and B. For example the unsteady state term becomes

$$u_B' \frac{\partial u_A'}{\partial t} + u_A' \frac{\partial u_B'}{\partial t} = \frac{\partial}{\partial t}(u_A' u_B') \tag{10.161}$$

Then, by time-averaging, we get

$$\frac{\partial}{\partial t}(\overline{u_A' u_B'}) = \frac{\partial}{\partial t}(\overline{u'^2} f(r))$$

The convective term $u_A' \frac{\partial u_A'}{\partial x} + v_A' \frac{\partial u_A'}{\partial y} + w_A' \frac{\partial u_A}{\partial z}$

will obviously give rise to triple correlations.

The pressure term will disappear after multiplying by u_B and time-averaging because $\overline{p_A' u_B'} = 0$ due to isotropy. Von Karman and Howarth [34] showed that for homogeneous, isotropic turbulence the Navier-Stokes equations become

$$\frac{\partial}{\partial t}(\overline{u'^2} f) + 2\,\overline{u'^3}\left(\frac{\partial h}{\partial r} + \frac{4h}{r}\right) = 2\nu\overline{u'^2}\left(\frac{\partial^2 f}{\partial r^2} + \frac{4}{r}\frac{\partial f}{\partial r}\right) \tag{10.162}$$

We note that we have just one equation but two unknowns f and h. Thus, if we are to determine the double correlation f we must introduce a relation connecting it to the triple correlation h. There lies the fundamental difficulty in the development of statistical theories of turbulence. Some progress, however, has been made by suggesting plausible forms of relation between f(r) and h(r).

It has been found helpful to introduce the Fourier transform of equation (10.141). [For an introduction to Fourier transform see for example reference [35]]. This approach is therefore called spectral analysis. The von Karman-Howarth equation can now be written in the form

$$\frac{\partial F}{\partial t} + W = -\ 2\nu\kappa^2 F \qquad (10.163)$$

where F and W are connected to f(r) and h(r) respectively by the appropriate relations which involve the Fourier transforms [27]. κ is the wave number which is related to the wavelength λ and frequency f by the relation

$$\kappa = \frac{2\pi}{\lambda} = \frac{2\pi f}{V} \qquad (10.164)$$

Equation (10.163) is much simpler than the original von Karman-Howarth equation (10.162). However, we cannot proceed any further without introducing relations between W and F. Considerable advances have been made in this aspect by introducing Kolmogoroff's ideas [30,36,37] into the spectral formulation.

Kolmogoroff postulated that at large Reynolds numbers the turbulence field is locally isotropic whether the large scale motions are isotropic or not. The large eddies break down into smaller eddies due to inertia forces. These in turn break down into still smaller eddies and so on. The motions of the very small eddies are governed by viscous forces and are eventually dissipated into heat. The eddy breakdown process can be simply visualized by the breakdown of drops of ink or milk that are put in water. Kolmogoroff's postulates seem to be very near the truth and became the starting point for many modern theories. In these theories the small scale motion is assumed to be governed by the dissipation rate ε per unit mass (m^2s^{-3}) and the kinematic viscosity $\nu(m^2s^{-1})$. With these two parameters one can construct characteristic length, time and velocity scales as follows:

$$\eta = \left(\frac{\nu^3}{\varepsilon}\right)^{1/4} \qquad \theta = \left(\frac{\nu}{\varepsilon}\right)^{1/2} \qquad v = (\nu\varepsilon)^{1/4} \tag{10.165}$$

We can get an estimate of ε by noting that the kinetic energy per unit mass is proportional to u'^2. The energy supplied by the large eddies should be equal to the energy dissipated by the smallest eddies. Thus, we have

$$\varepsilon \propto -\frac{du'^2}{dt} \simeq \frac{u'^2}{\frac{\ell}{u'}} = \frac{u'^3}{\ell} \tag{10.166}$$

where ℓ represents the size of the largest eddies and is of the same order of magnitude as the mixing length of Prandtl's model (Sec. 10.5.1).

Let us now use equation (10.165) and (10.166) to get an estimate of the size of the smallest eddy in a wind tunnel of 1m diameter and 100 m/s velocity. The largest fluctuations will be of the order of $u' = 0.10\times100$m/s = 10m/s. The length ℓ will be at most ℓ = 1m. Thus, $\varepsilon \simeq 10^3\ m^2/s^3$ and since $\nu \simeq 10^{-5}\ m^2/s$ we get $\eta \simeq 0.3\times10^{-4}$m = 0.03 mm. We note that the smallest eddy is much larger than the mean free path of air molecules which is of the order at 10^{-4} mm. If the same calculations were repeated for the atmospheric boundary layer $\ell \simeq 1$ km = 10^3m and a typical u' = 1 m/s we should get η = 1 mm. The frequency of the fluctuations is inversely proportional to the size of eddies. Most of the turbulent energy is associated with the large eddies, i.e., those with lower frequencies, as shown in Fig. 10.23. Detailed calculations on eddy sizes and other eddy characteristics can be found in Davies' book [4].

Despite the large number of theoretical work done on the statistical theory of turbulence we are still far from having a fully predictive theory. Perhaps, the most significant advances in recent years were made on the so-called closure problem. By this it is meant the development of approximations between the various measures of turbulence so that we are left with the same number of unknowns as the number of conservation equations. Kraichnan [38], [39] (see also Orszag [29]) has layed the foundations in this direction, however, the mathematical complexities associated with these developments are overwhelming. Some simpler and very interesting methods of calculation and experimental data for turbulent flows by various authors have been recently published in a single volume [41].

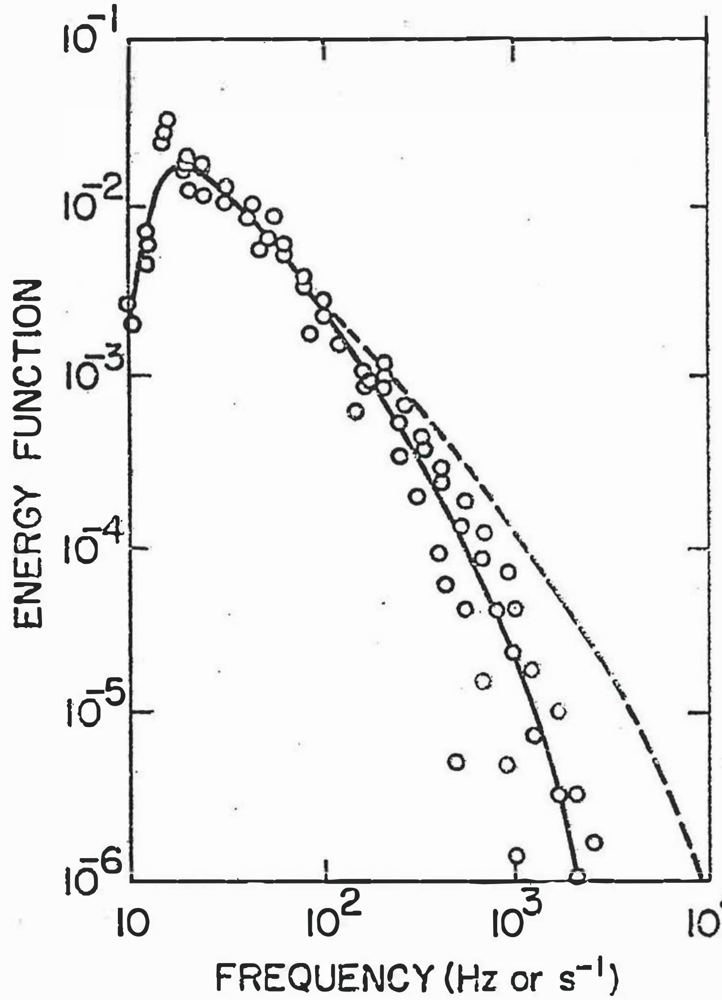

Fig. 10.23 Measured energy spectrum function F(n) where n is the frequency of the fluctuations n. F(n)dn represents the fraction of the root mean square of the fluctuations that fall within frequency range dn. The dotted line summarizes the results for a higher velocity. (From Patterson and Zakin [40] as quoted by Davies [4]).

REFERENCES

1. J.O. Hinze, "Turbulence", McGraw-Hill, 2nd ed., New York (1975)

2. J.M. Wallace, H. Eckelman, R.S. Brodkey, "The wall region in turbulent shear flow", J. Fluid Mech., 54, 39 (1972).

3. H. Reichardt, "Messungen turbulenter Schwankungen" Naturwissenschaften 404(1938); see also ZAMM, 13, 177 (1933) and ZAMM, 18, 358 (1938).

4. J.T. Davies, "Turbulence Phenomena" Academic Press, New York (1972).

5. L. Prandtl, "Über die ausgebildete Turbulenz", ZAMM, 5, 136 (1925) and Proc. 2nd. Intern. Congr. Appl. Mech., Zürich (1926).

6. H. Schlichting, :Boundary Layer Theory" McGraw-Hill, 7th. Ed., New York (1979).

7. Th. von Karman, "Mechanische Ähnlichkeit and Turbulenz" Nach. Ges. Wiss. Göttingen, Math. Phys. Klasse, 58 (1930), also NACA TM 611 (1931).

8. R.G. Deissler, NACA Report 1210 (1955). See also R.B. Bird, W.E. Stewart and E.N. Lightfoot "Transport Phenomena" J. Wiley, New York (1960).

9. J. Nikuradse, "Gesetzmässigkeiten der turbulenten Strömung in glatten Rohren" Forschungsheft 356 (1932) see also J. Nikuradse and H. Reichardt, "Heat Transfer Through Turbulent Friction Layers," NACA TM 1047 (1945).

10. J. Laufer, "The Structure of turbulence in fully developed pipe flow" NACA Tech. Report 1154 (1954).

11. P.A. Longwell, "Mechanics of Fluid Flow" McGraw-Hill, New York (1966).

12. M.M. Denn, "Process Fluid Mechanics" Prentice-Hall, Englewood Cliffs, N.J. (1980).

13. S.V. Patankar and D.B. Spalding, "Heat and Mass Transfer in Boundary Layers" International Textbook Co., London (1970).

14. T. Cebeci and P. Bradshaw, "Momentum Transfer in Boundary Layers": McGraw-Hill, New York (1977).

15. F.M. White, "Viscous Fluid Flow" McGraw-Hill, New York (1974).

16. H. Kirsten, Doctoral thesis, Leipzig (1927) as quoted by Hinze [1] and Schlichting [6].

17. S.I. Pai, "Fluid Dynamics of Jets" Van Nostrand, New York (1954).

18. G.N. Abramovich, "The Theory of Turbulent Jets" Trans. from Russian, M.I.T. Press, Cambridge, Mass. (1963).

19. N. Rajaratnam, "Turbulent Jets" Elsevier, Amsterdam (1976).

20. W. Tollmien, "Berechnung Turbulenter Ausbreitungsvorgönge" ZAMM, 6, 648 (1926) (Trans. NACA TM 1096 (1946)).

21. H. Reichardt "Gesetzmässigkeiten der freien Turbulenz" VDI-Forschungsheft, 414 91942), 2nd. ed. (1951).

22. S. Corrsin and M.S. Uberoi, "Further Experiments on the Flow and Heat Transfer in a Heated Turbulent Air Jet" NACA TN 998 (1950).

23. J.F. Tomich and E. Weger, "Some new results on momentum and heat transfer in compressible turbulent free jets" AICHE J., 13, 948 (1967).

24. G.K. Batchelor, "The Theory of Homogeneous Turbulence" Cambridge University Press, London (1959).

25. A.A. Townsend, "The Structure of Turbulent Shear Flow" Cambridge University Press, London (197).

26. S.K. Friedlander and L. Topper (Eds.), "Turbulence: Classical Papers on Statistical Theory" Interscience, New York (1962).

27. C.C. Lin, "Statistical Theories of Turbulence" Princeton University Press, Princeton, N.J. (1961).

28. A.S. Monin and A.M. Yaglom, "Statistical Fluid Mechanics" Trans. from Rusian, M.I.T. Press, Cambridge, Mass. (1971).

29. S.A. Orszag, "The Statistical Theory of Turbulence" Cambridge University Press, London (1971).

30. H. Tennekes and J.L. Lumley, "A First Course in Turbulence" M.I.T. Press, Cambridge, Mass. (1972).

31. R.S. Brodkey, "The Phenomena of Fluid Motions" Addison Wesley, Reading, Mass. (1967).

32. T. von Karman, "The Fundamentals of the statistical theory of turbulence" J. Aero. Sci., 4, 131 (1937).

33. A.L. Kistler, V.O'Brien and S. Corrsin, J. Aero, Sci, 23, 96 (1956).

34. T. von Karman and L. Howarth, "On the statistical theory of isotropic turbulence" Proc. Roy. Soc. (London), A164, 192 (1938).

35. R.V. Churchill, "Fourier Series and Boundary Value Problems" McGraw-Hill, Ed., New York (19).

36. A.N. Kolmogoroff, "The local structure of turbulence in incompressible viscous fluid for very large Reynolds numbers" Compt. Rend. (Doklady) Acad. Sci. U.R.S.S., 30, 301 (1941). Also Compt. Rend. (Doklady) Acad. Sci. U.R.S.S., 31, 538 (1941) and Compt. Rend. (Doklady) Acad. Sci. U.R.S.S., 32, 16 (1941).

37. A.N. Kolmogoroff, "A refinement of previous hypotheses concerning the local structure of turbulence in viscous incompressible fluid at high Reynolds number", J. Fluid Mech., 13, 82 (1962).

38. R.H. Kraichnan, "The closure problem of turbulence theory" Proc. Symp. Appl. Math., 13, 199 (1962).

39. R.H. Kraichnan, "Lagrangian history closure approximation for turbulence" Phys. Fluids, 8, 575 (1965).

40. G.K. Patterson and J.L. Zakin, "Hot-film anemometry measurements of turbulence in pipe flow: Organic solvents", AIChE J., 13, 513 (1967).

41. F. Durst, B.E. Launder, F.W. Schmidt and J.H. Whitelaw (Eds.), "Turbulent Shear Flows I", Springer-Verlag, Berlag (1979).

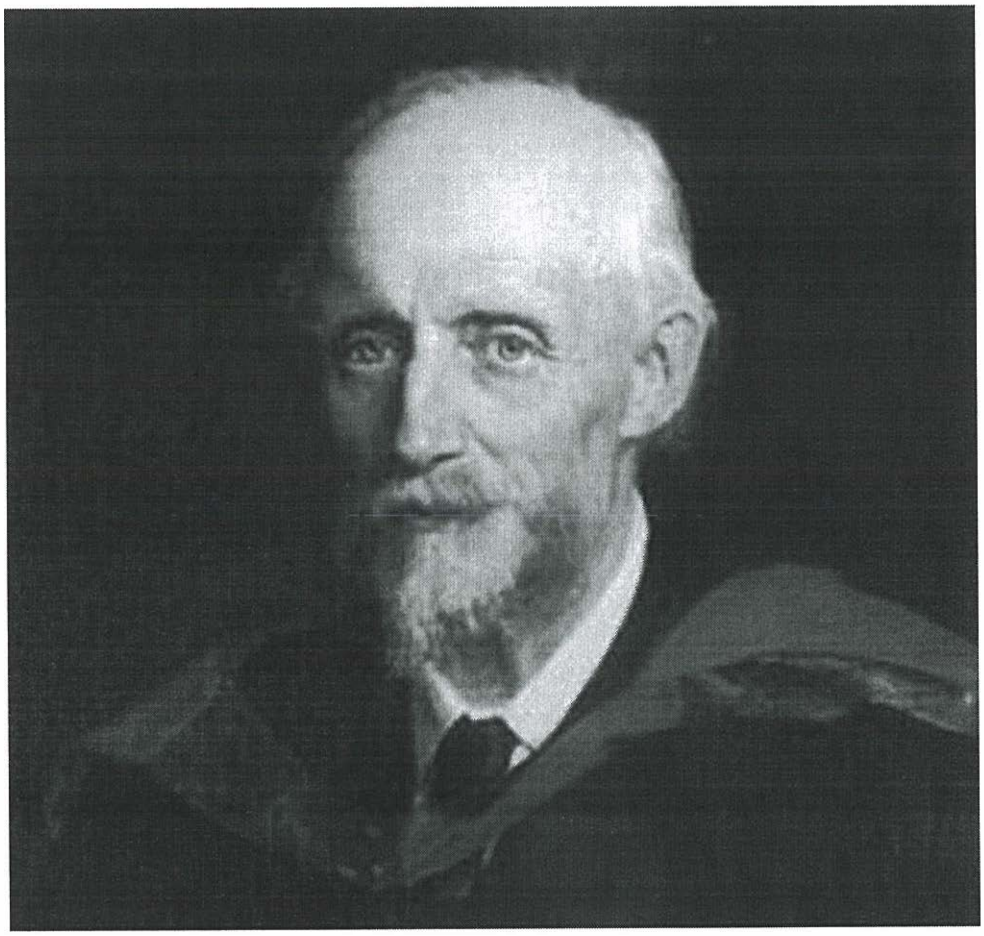

OSBORNE REYNOLDS (1842-1912)

John Vlachopoulos, *Fundamentals of Fluid Mechanics*
Chem. Eng., McMaster University, Hamilton, ON, Canada
(First Edition 1984, revised internet edition (2016), www.polydynamics.com)

CHAPTER 11

INVISCID INCOMPRESSIBLE FLOW

11.1 INTRODUCTION

The difficulties in solving the complete Navier-Stokes equations arise mainly from the non-linear inertia force term $\rho\bar{V}\cdot\nabla\bar{V}$ and from the viscous force term $\mu\nabla^2\bar{V} + \frac{1}{3}\mu\nabla(\nabla\cdot\bar{V})$. Even for incompressible flow ($\nabla\cdot\bar{V} = 0$) the remaining viscous force term $\mu\nabla^2\bar{V}$ is still the source of great complications. In Chapter 8, we examined a special class of inertialess flows (Re << 1). In Chapters 9 and 10 we examined several types of high speed flow (Re >> 1) and managed to simplify the viscous force term by invoking Prandtl's boundary layer theory. In this Chapter we introduce the assumption of inviscid flow ($\mu = 0$), so that we may eliminate the viscous force term completely from the Navier-Stokes equations.

For such an inviscid flow field the motion is governed by the Euler equation (Sec. 6.5) which is

$$\rho\left(\frac{\partial \overline{V}}{\partial t} + \overline{V} \cdot \nabla\overline{V}\right) = -\nabla p + \rho\overline{g} \tag{11.1}$$

Obviously, the equation of conservation of momentum is now greatly simplified and is more amenable to further mathematical manipulations which lead to solutions. However, great care must be taken in interpreting the various solutions, because nature does not provide us with fluids that are inviscid. This class of flows is, thus, called ideal. We noted in Chapter 9 that viscous effects are confined to a thin fluid layer adjacent to solid boundaries, outside this layer the flow field can be considered inviscid (see Fig. 9.1). Thus, inviscid flow solutions can approximate real flow fields in regions devoid of shear stresses, that is, outside wall boundary layers, jets, mixing zones and wakes.

In the absence of viscosity the flow is frictionless. No dissipation mechanism is possible and the force fields are conservative, thus, derivable from a force potential. The work done by a conservative force is a function of position and is independent of the path followed

$$W = \int_A^B \overline{F} \cdot \overline{ds} = \Phi_A - \Phi_B \tag{11.2}$$

where Φ is a scalar function called the force potential. For a closed path the work is zero

$$W = \oint \overline{F} \cdot \overline{ds} = \Phi_A - \Phi_B = 0 \tag{11.3}$$

We can now show that

$$\overline{F} = \nabla\Phi \tag{11.4}$$

because

$$W = \int (\nabla\Phi)\cdot(\overline{ds}) = \int \left(\frac{\partial\Phi}{\partial x}dx + \frac{\partial\Phi}{\partial y}dy + \frac{\partial\Phi}{\partial z}dz\right) = \int d\Phi = \Phi_A - \Phi_B \tag{11.5}$$

which also yields for a closed path

$$\oint(\nabla\Phi)\cdot(\overline{ds}) = 0 \tag{11.6}$$

In a flow field a fluid element can be rotated only under the influence of frictional (i.e. viscous) forces. In an inviscid flow field such rotations are impossible and the flow is termed <u>irrotational,</u> which means that the angular velocity or <u>vorticity</u> $\overline{\zeta}$ must be zero

$$\overline{\zeta} = 2\overline{\omega} = \nabla \times \overline{V} = 0 \tag{11.7}$$

The velocity field is, thus, derivable from a velocity potential

$$\overline{V} = \nabla\Phi \tag{11.8}$$

since

$$\overline{\zeta} = 2\overline{\omega} = \nabla \times \overline{V} = \nabla \times \nabla\Phi = 0 \tag{11.9}$$

This flow is usually called <u>potential.</u> The velocity potential is connected to the velocity components by the relations:

In rectangular coordinates x,y,z

$$v_x = \frac{\partial\Phi}{\partial x} \tag{11.10}$$

$$v_y = \frac{\partial\Phi}{\partial y} \tag{11.11}$$

$$v_z = \frac{\partial\Phi}{\partial z} \tag{11.12}$$

In cylindrical coordinates r, θ, z

$$v_r = \frac{\partial \Phi}{\partial r} \tag{11.13}$$

$$v_\theta = \frac{1}{r}\frac{\partial \Phi}{\partial \theta} \tag{11.14}$$

$$v_z = \frac{\partial \Phi}{\partial z} \tag{11.15}$$

and in spherical coordinates r, θ, ϕ

$$v_r = \frac{\partial \Phi}{\partial r} \tag{11.16}$$

$$v_\theta = \frac{1}{r}\frac{\partial \Phi}{\partial \theta} \tag{11.17}$$

$$v_\phi = \frac{1}{r\sin\theta}\frac{\partial \Phi}{\partial \phi} \tag{11.18}$$

If the fluid is incompressible, the continuity equation yields

$$\nabla \cdot \bar{V} = 0 \tag{11.19}$$

and using equation (11.8) we get

$$\nabla \cdot \nabla \Phi = \nabla^2 \Phi = 0 \tag{11.20}$$

which is the well known Laplace equation. This equation may be solved to give the velocity potential Φ and the velocity field can be determined from equation (11.8).

It is interesting to note that the equation of motion is not involved in determining the velocity field in an inviscid incompressible fluid. The velocity field is determined entirely from the kinematical equation (11.20). The dynamical equation (the Euler form of the conservation of momentum, Eq. 11.1) is needed only in the determination of the pressure from the velocity field.

Milne-Thomson's book [1] is the most authoritative reference on the subject of inviscid flow, while Lamb's [2] and Prandtl and Tietjens' [3] classics contain a wealth of information. For introductory up-to-date treatments the reader is also referred to Streeter and Wylie [4], Currie [5] and Eskinazi [6].

11.2 TWO-DIMENSIONAL POTENTIAL FLOW

The velocity potential Φ satisfies the Laplace equation, which for two-dimensional flow becomes

$$\frac{\partial^2\Phi}{\partial x^2} + \frac{\partial^2\Phi}{\partial y^2} = 0 \tag{11.21}$$

The velocity field can be obtained from Φ by making use of the relation

$$\bar{V} = v_x\bar{i} + v_y\bar{j} = \frac{\partial\Phi}{\partial x}\bar{i} + \frac{\partial\Phi}{\partial y}\bar{j} \tag{11.22}$$

where

$$v_x = \frac{\partial\Phi}{\partial x}$$

$$v_y = \frac{\partial\Phi}{\partial y} \tag{11.23}$$

In Chapter 3 the stream function was defined by the equation

$$v_x = \frac{\partial\Psi}{\partial y}$$

$$v_y = -\frac{\partial\Psi}{\partial x} \tag{11.24}$$

Using the irrotationality condition (Eq. 11.7) in two dimensions

$$\frac{\partial v_x}{\partial y} - \frac{\partial v_y}{\partial x} = 0 \tag{11.25}$$

we get the Laplace equation

$$\frac{\partial^2\Psi}{\partial x^2} + \frac{\partial^2\Psi}{\partial y^2} = 0 \tag{11.26}$$

Similarly in plane polar coordinates the stream function $\Psi(r,\theta)$ is defined by

$$v_r = \frac{1}{r}\frac{\partial\Psi}{\partial\theta}$$

$$v_\theta = -\frac{\partial\Psi}{\partial r} \tag{11.27}$$

The condition of irrotationality gives

$$0 = \frac{1}{r}\frac{\partial}{\partial r}(rv_\theta) - \frac{1}{r}\frac{\partial}{\partial\theta}(v_r)$$

$$= \frac{1}{r}\frac{\partial}{\partial r}(-\,r\,\frac{\partial\Psi}{\partial r}) - \frac{1}{r}\frac{\partial}{\partial\theta}(\frac{1}{r}\frac{\partial\Psi}{\partial\theta}) = -\,\nabla^2\Psi\,(r,\theta) \tag{11.28}$$

which is the Laplace equation in plane polar coordinates

$$\frac{1}{r}\frac{\partial}{\partial r}(r\,\frac{\partial\Psi}{\partial r}) + \frac{1}{r^2}\frac{\partial^2\Psi}{\partial\theta^2} = 0 \tag{11.29}$$

The stream function for axisymmetric flow $\Psi(r,z)$ does not satisfy the Laplace equation. For the three dimensional flow the stream function cannot be defined in the conventional sense.

Comparing equations (11.23) and (11.24), we find that

$$\frac{\partial\Phi}{\partial x} = \frac{\partial\Psi}{\partial y} \quad \text{and} \quad \frac{\partial\Phi}{\partial y} = -\,\frac{\partial\Psi}{\partial x} \tag{11.30}$$

These are the so-called Cauchy-Riemann equations. From them if either the velocity potential or the stream function is known the other may be computed. The corresponding expressions in plane polar coordinates can be obtained by direct transformation. These are

$$v_r = \frac{\partial \Phi}{\partial r} = \frac{1}{r}\frac{\partial \Psi}{\partial \theta} \qquad v_\theta = \frac{1}{r}\frac{\partial \Phi}{\partial \theta} = -\frac{\partial \Psi}{\partial r} \tag{11.31}$$

We will now show that in two dimensional potential flow the streamlines and the potential lines are orthogonal. A streamline is defined by ψ = const and a potential line by Φ = const. Thus, we have

$$d\Psi = 0 = \frac{\partial \Psi}{\partial x} dx + \frac{\partial \Psi}{\partial y} dy \tag{11.32}$$

$$d\Phi = 0 = \frac{\partial \Phi}{\partial x} dx + \frac{\partial \Phi}{\partial y} dy \tag{11.33}$$

From equation (11.32)

$$\left(\frac{dy}{dx}\right)_\Psi = -\frac{\partial \Psi/\partial x}{\partial \Psi/\partial y} = +\frac{v_y}{v_x} \tag{11.34}$$

and from equation (11.33)

$$\left(\frac{dy}{dx}\right)_\Phi = -\frac{\partial \Phi/\partial x}{\partial \Phi/\partial y} = -\frac{v_x}{v_y} \tag{11.35}$$

Thus

$$\left[\frac{dy}{dx}\right]_\Psi \left[\frac{dy}{dx}\right]_\Phi = -1 \tag{11.36}$$

Geometrically, this means that the streamlines and the potential lines are orthogonal (everywhere perpendicular to each other). The streamlines $\Psi = \Psi_i$ and the potential lines $\Phi = \Phi_i$ where Ψ_i and Φ_i have equal increments between adjacent lines form an orthogonal network as shown in Fig. 11.1.

While the velocity profile can be determined entirely from the above mentioned kinematic relations we need the equation of conservation of momentum for the determination of pressure. Euler's equation for steady flow is

$$\rho\, \overline{V}\cdot\nabla\overline{V} = -\nabla p + \rho\overline{g} \tag{11.37}$$

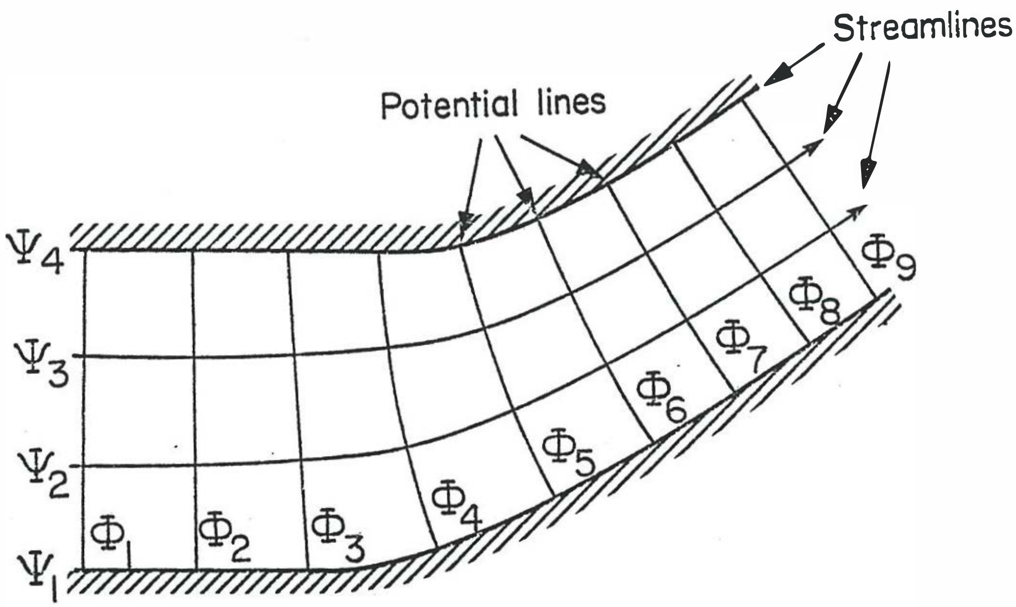

Fig. 11.1: An orthogonal flow net for two-dimensional flow.

Defining an equivalent pressure $P = p + \rho gh$, where h is pointing in a direction opposite to the direction of gravity, i.e. $g_x = -g\frac{\partial h}{\partial x}$, $g_y = -g\frac{\partial h}{\partial y}$, $g_z = -g\frac{\partial h}{\partial z}$, we have

$$\rho\overline{V}\cdot\nabla\overline{V} + \nabla P = 0 \tag{11.38}$$

Using the identity (see Appendix A)

$$\nabla(\frac{1}{2}\overline{V}^2) = \overline{V}\cdot\nabla\overline{V} + \overline{V}\times(\nabla\times\overline{V}) \tag{11.39}$$

we find that

$$\rho\nabla(\frac{1}{2}\overline{V}^2) - \rho[\overline{V}\times(\nabla\times\overline{V})] + \nabla P = 0 \tag{11.40}$$

For an irrotational flow field of an incompressible fluid $\nabla\times\overline{V} = 0$ and $\rho = \text{const}$. Thus,

$$\nabla(\frac{1}{2}\overline{V}^2) + \nabla(\frac{P}{\rho}) = 0 \tag{11.41}$$

which integrates to

$$\frac{1}{2}V^2 + \frac{P}{\rho} = \text{const} \tag{11.42}$$

or in terms of the velocity components

$$\frac{1}{2}(v_x^2 + v_y^2) + \frac{P}{\rho} = \text{const} \tag{11.43}$$

and

$$\frac{1}{2}(v_x^2 + v_y^2) + \frac{p}{\rho} + gh = \text{const} \tag{11.44}$$

Equations (11.42), (11.43) and (11.44) are different forms of the Bernoulli equation which is named after the Swiss mathematician Daniel Bernoulli (1700-82).

We now summarize the equations necessary for the description of a two-dimensional potential flow field:

$$\nabla^2 \Phi = 0 \tag{11.45}$$

$$v_x = \frac{\partial \Phi}{\partial x} = \frac{\partial \Psi}{\partial y} \qquad v_y = \frac{\partial \Phi}{\partial y} = -\frac{\partial \Psi}{\partial x} \tag{11.46}$$

and

$$\frac{1}{2}(v_x^2 + v_y^2) + \frac{P}{\rho} = \text{const} \tag{11.47}$$

A question may now be asked regarding the reasons for going through the definitions of Φ and Ψ rather than proceeding directly to the inviscid flow solution of the original equations, in terms of the primitive variables v_x, v_y and p, which are

irrotanionality ($\nabla \times \overline{V} = 0$) $$\frac{\partial v_x}{\partial y} - \frac{\partial v_y}{\partial x} = 0 \tag{11.48}$$

continuity ($\nabla \cdot \overline{V} = 0$) $$\frac{\partial v_x}{\partial x} + \frac{\partial v_y}{\partial y} = 0 \tag{11.49}$$

momentum $$\frac{1}{2}(v_x^2 + v_y^2) + \frac{P}{\rho} = 0 \tag{11.50}$$

We note that with the introduction of the velocity potential Φ the velocity field is determined by solving one differential equation (Laplace) rather than the two partial differential equations (11.48) and (11.49). There are centuries of mathematics which apply to the solution of the Laplace equation. Even with modern numerical techniques the Laplace equation route is generally simpler [see Chapter 25].

There are usually three distinct types of boundary value problems which involve the potential flow equations in two-dimensions:

TYPE I: Given the potential Φ. A velocity potential Φ is given throughout a flow field. Ψ, $\overline{V}$ and p are to be determined.

TYPE II: Given the control volume boundary conditions. The geometrical boundaries and distributions of $\overline{V}$ and p at one boundary are given.

ϕ, ψ, $\bar{V}$ and p are required throughout the control volume.

TYPE III: Given the pressure or velocity distribution for an unknown body contour. The desired p or $\bar{V}$ on an unknown body contour is given and the shape of the body (e.g. an airfoil) is to be determined.

The simplest class of potential flow problems are those of type I. The most complicated are those of type III. We will give in the next five sections some examples of type I and type II.

For some problems we make use of the principle of superposition which applies to linear equations. According to this principle if Φ_1 and Φ_2 are two different solutions of the Laplace equation (which is linear) then their sum $\Phi_3 = \Phi_1 + \Phi_2$ is also a solution. However, the corresponding pressures cannot be added because the Bernoulli equation is non-linear.

It is important to note that since there is no flow across the streamlines any streamline (Ψ = const) can represent a solid boundary.

11.3 SIMPLE POTENTIAL FLOWS

In this section we consider several simple solutions of the Laplace equation.

(a) Uniform Flow

The simple potential function $\Phi = Ax$, where A = const, obviously satisfies the Laplace equation. Thus, the velocity components for the potential flow field are

$$v_x = \frac{\partial \Phi}{\partial x} = A \qquad (11.51)$$

$$v_y = \frac{\partial \Phi}{\partial y} = 0 \qquad (11.52)$$

The streamlines can be determined from

$$A = \frac{\partial \Psi}{\partial y} \tag{11.53}$$

$$0 = -\frac{\partial \Psi}{\partial x} \tag{11.54}$$

From equations (11.53) and (11.54)

$$\Psi = Ay + C \tag{11.55}$$

where C is an arbitrary constant. By setting this constant equal to zero, we have

$$\Psi = Ay \tag{11.56}$$

Thus, the streamlines are parallel to the x-axis and the potential lines are parallel to the y-axis as shown in Fig. 11.2. The velocity is constant and equal to A (uniform flow).

In polar coordinates with the constant velocity taken along the polar z-axis, we have

$$v_r = A\cos\theta \text{ and } v_\theta = -A\sin\theta \tag{11.57}$$

Thus

$$v_r = \frac{\partial \Phi}{\partial r} = A\cos\theta \tag{11.58}$$

$$\Phi = Ar\cos\theta + C(\theta) \tag{11.59}$$

and

$$v_\theta = \frac{1}{r}\frac{\partial \Phi}{\partial \theta} = -A\sin\theta \tag{11.60}$$

$$\Phi = Ar\cos\theta + C(r) \tag{11.61}$$

Consequently, C is a constant, which is taken equal to zero to yield

$$\Phi = Ar\cos\theta \tag{11.62}$$

$$\Psi = Ar\sin\theta \tag{11.63}$$

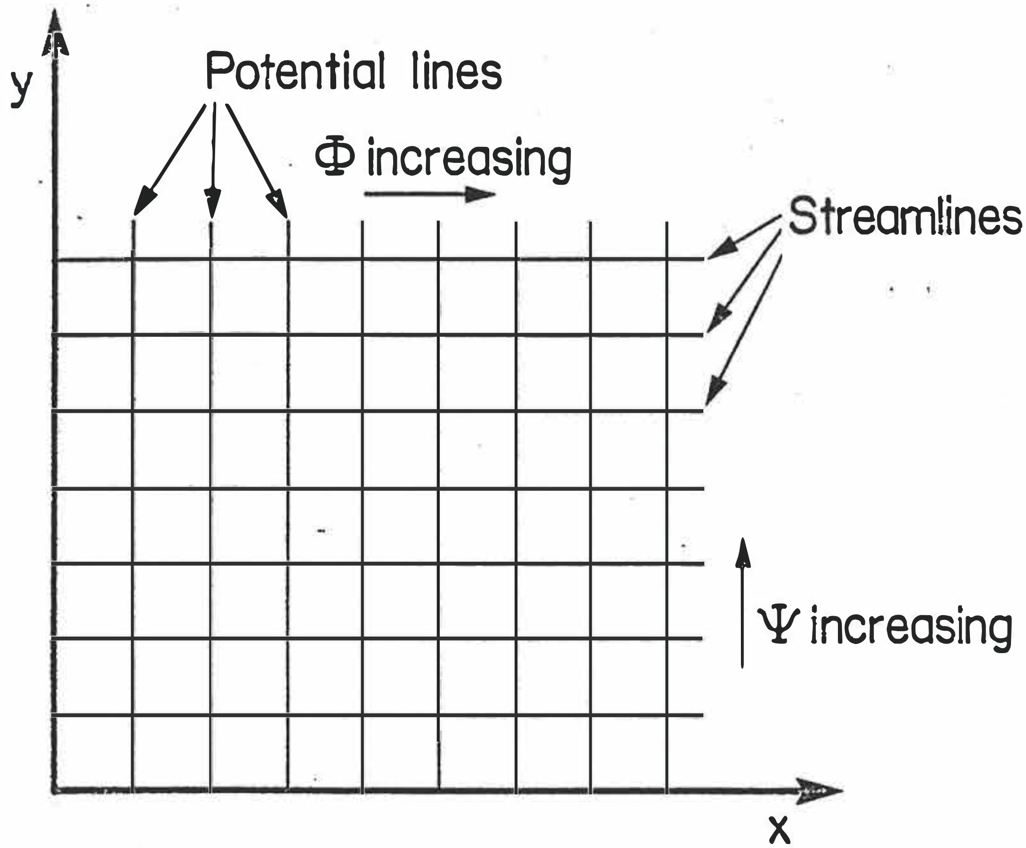

Fig. 11.2: Streamlines and potential lines for uniform flow in the x direction.

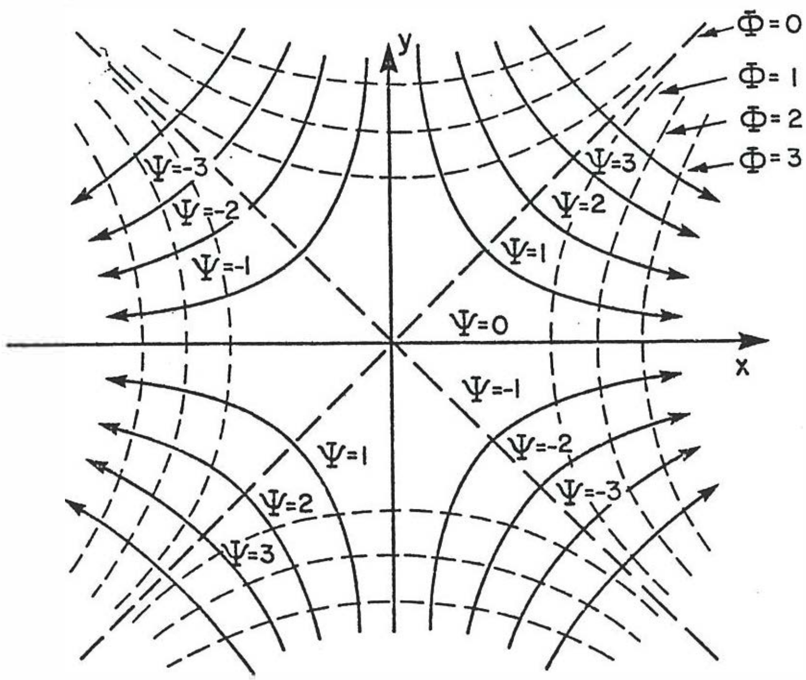

Fig. 11.3: Stagnation flow on a plate or 90° corner flow.

The plot of course is exactly the same as Fig. 11.2.

(b) Stagnation Flow

The function $\Phi = 1/2\ A(x^2 - y^2)$ satisfies the Laplace equation and therefore represents the potential of some flow field. The velocity components are

$$v_x = \frac{\partial \Phi}{\partial x} = Ax \tag{11.64}$$

$$v_y = \frac{\partial \Phi}{\partial y} = -Ay \tag{11.65}$$

The stream function Ψ can be found from Equations (11.24)

$$\Psi = \int v_x\, dy = Axy + C(x) \tag{11.66}$$

$$\Psi = -\int v_y\, dy = Axy + C(y) \tag{11.67}$$

Therefore C is a constant, which is taken equal to zero to give

$$\Psi = Axy \tag{11.68}$$

The streamlines are therefore hyperbolas and can be easily plotted as shown in Fig. 11.3. We note that the velocity is everywhere finite except at $x = y = 0$, the stagnation point. This flow net depicts flow in a corner or stagnation flow on a plane surface. Obviously, a real (viscous) fluid cannot follow this flow pattern in the immediate vicinity of the surfaces involved because even at the surface itself the velocity is assumed to be finite. The inviscid flow assumption allows slip at the wall which is unrealistic. It should be pointed out, however, that the above potential flow solutions are useful for stagnation flow regions outside the boundary layer formed near the boundaries.

(c) Line (two-dimensional) Sources or Sinks

We consider a thin pipe discharging a fluid at a uniform rate in the space between two parallel disks as shown in Fig. 11.4. Far from the origin the flow is expected to be purely radial. The amount of fluid crossing the cylindrical surface of width b and radius r, should be

$$Q = 2\pi rb\, v_r = \text{const} \tag{11.69}$$

Thus

$$v_r = \frac{Q/b}{2\pi}\,\frac{1}{r} \tag{11.70}$$

The velocity potential can be obtained from

$$v_r = \frac{\partial \Phi}{\partial r} = \frac{Q/b}{2\pi}\,\frac{1}{r} \tag{11.71}$$

$$\Phi = \frac{Q/b}{2\pi}\ln r + \text{const} \tag{11.72}$$

This function satisfies the Laplace equation because there is no flow in θ or z directions and

$$\frac{1}{r}\frac{\partial}{\partial r}\left(r\frac{\partial \Phi}{\partial r}\right) = \frac{1}{r}\frac{\partial}{\partial r}\left(r\,\frac{Q/b}{2\pi}\,\frac{1}{r}\right) = 0 \tag{11.73}$$

The stream function is obtained from

$$v_r = \frac{1}{r}\frac{\partial \Psi}{\partial \theta} = \frac{Q/b}{2\pi}\,\frac{1}{r} \tag{11.74}$$

$$\Psi = \frac{Q/b}{2\pi}\,\theta + \text{const} \tag{11.75}$$

It can be verified by direct substitution that the Laplace equation is satisfied by the stream function. Lines of constant Φ are circles distributed logarithmically with respect to radius. Lines of constant Ψ (streamlines) are straight lines through the origin as shown in

Fig. 11.5.

If Q/b is positive we have a source, if Q/b is negative we have a sink. For both sources and sinks the continuity equation is satisfied everywhere except at the origin r = 0 (singularity). Since only differences in potential and stream functions are of significance the constants are usually set equal to zero.

In rectangular coordinates the velocity potential Φ and the stream function Ψ transform to

$$\Phi = \frac{Q/b}{2\pi} \ln (x^2 + y^2)^{1/2} \quad \text{and} \quad \Psi = \frac{Q/b}{2\pi} \tan^{-1} \frac{y}{x} \tag{11.76}$$

(d) Line Vortex

Since both the velocity potential Φ and the stream function Ψ satisfy the Laplace equation in the previous example, their roles may be interchanged to give another, yet unspecified, flow field. Thus, by taking

$$\Phi = K_1 \theta \quad \text{and} \quad \Psi = K_2 \ln r \tag{11.77}$$

where K_1 and K_2 are constants, we have

$$v_r = \frac{\partial \Phi}{\partial r} = 0 \tag{11.78}$$

and

$$v_\theta = \frac{1}{r}\frac{\partial \Phi}{\partial \theta} = -\frac{\partial \Psi}{\partial r} = \frac{K_1}{r} = -\frac{K_2}{r} = \frac{K}{r} \tag{11.79}$$

This is no longer a source or sink flow field. The flow is seen to be purely circulating with tangential velocity being proportional to 1/r as shown in Fig. 11.6. Again, a singularity appears at the origin r = 0 where the velocity v_θ becomes infinite.

This flow is irrotational everywhere except at the origin, because

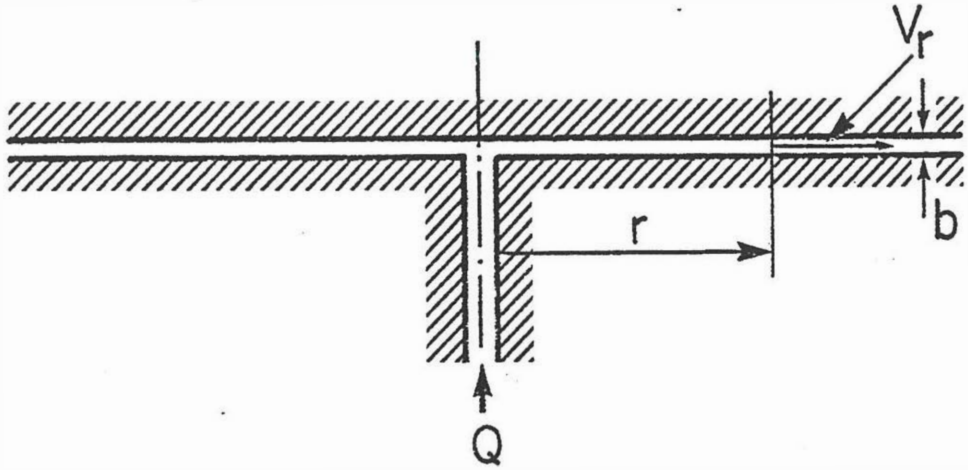

Fig. 11.4: A simple demonstration of how a line source (two dimensional) can be approximated. The fluid flows radially in the gap between the two parallel disks.

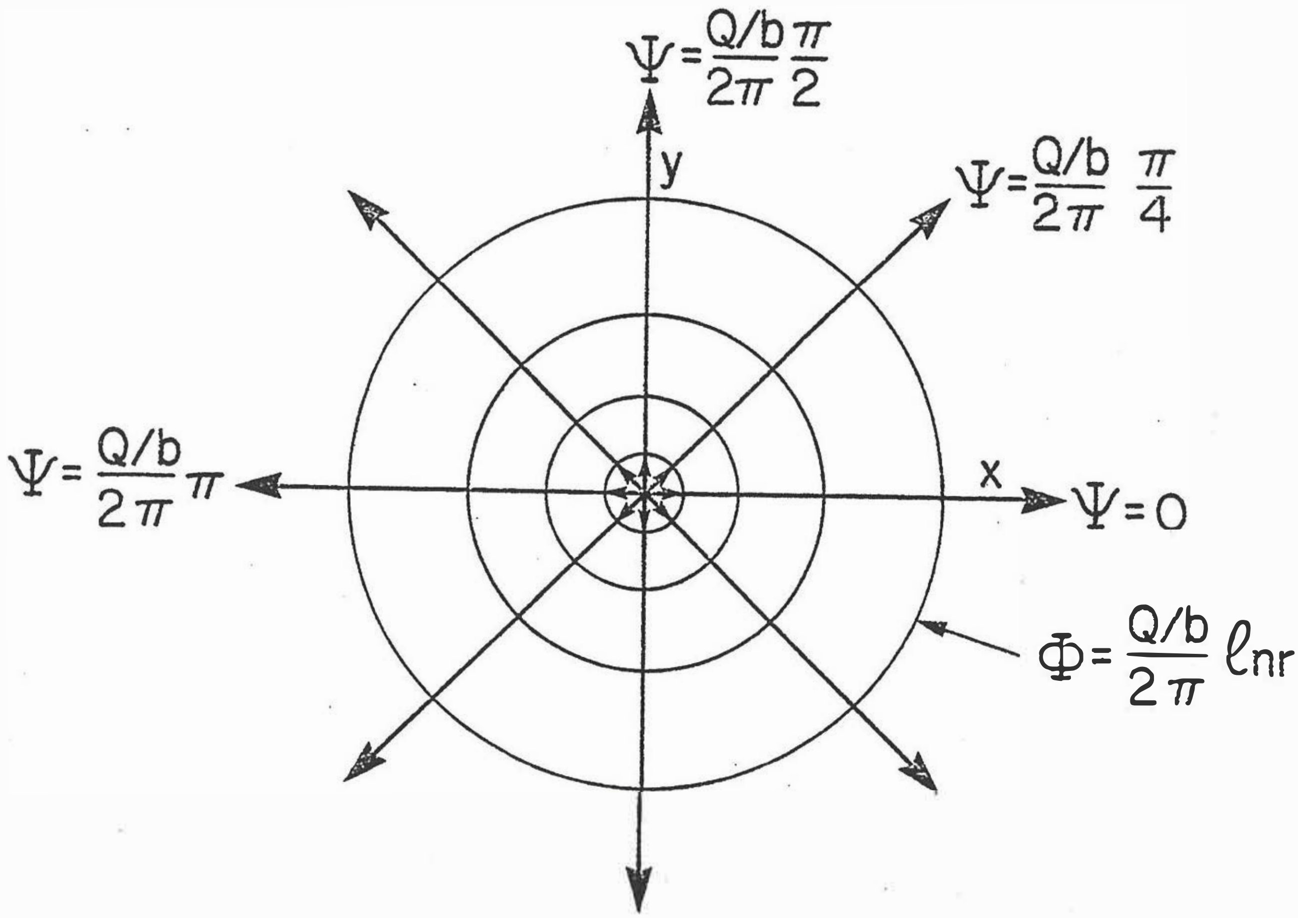

Fig. 11.5: Streamlines and potential lines for a line source.

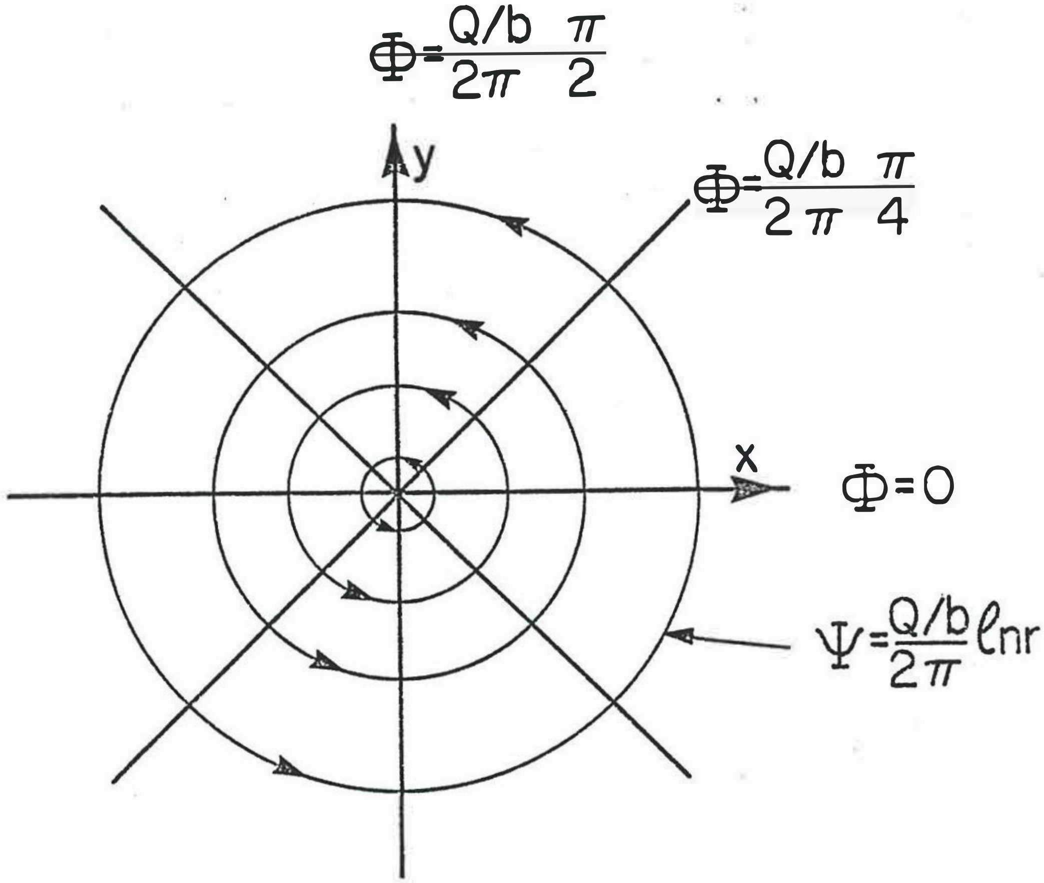

Fig. 11.6: Streamlines and potential lines for a line vortex.

$$\nabla \times \overline{V} = \overline{k}\left(\frac{1}{r}\frac{\partial(rv_\theta)}{\partial r} - \frac{1}{r}\frac{\partial v_r}{\partial \theta}\right) = 0 \quad \text{for } r > 0 \tag{11.80}$$

This flow is called a vortex.

Circulation of the velocity field $\overline{V}$ is defined as the line integral around a closed path

$$\Gamma = \int \overline{V} \cdot \overline{ds} \tag{11.81}$$

From Stokes' theorem (see Appendix) it is seen that the circulation is related to the vorticity

$$\Gamma = \int_C \overline{V} \cdot \overline{ds} = \iint_A (\nabla \times \overline{V}) \cdot \overline{dA} \tag{11.82}$$

where surface A is bounded by contour C. For a potential flow field the circulation is seen to be zero around any closed path. However, in the present case if we take a path enclosing the origin the circulation has a finite value:

$$\Gamma = \int_C \overline{V} \cdot \overline{ds} = \int_C v_\theta \, r d\theta = \int_o^{2\pi} \frac{K}{r} \, r d\theta = 2\pi K \tag{11.83}$$

Thus the constant K, which is called the vortex strength is given in terms of Γ by

$$K = \frac{\Gamma}{2\pi} \tag{11.84}$$

The tangential velocity is

$$v_\theta = \frac{\Gamma}{2\pi}\frac{1}{r} \tag{11.85}$$

The velocity potential

$$\Phi = \frac{\Gamma}{2\pi}\theta \tag{11.86}$$

The stream function

$$\Psi = -\frac{\Gamma}{2\pi} \ln r \tag{11.87}$$

A comprehensive treatment of vortex motion can be found in Eskinazi's book [6].

11.4 COMBINATION OF SIMPLE FLOWS

It was noted in Sec. 11.2 that because of the linearity of the Laplace equation, solutions can be added to form a new solution (principle of superposition). Thus, any linear combination of velocity potentials or stream functions of given flow fields will produce a new potential flow field. Here are some examples:

(a) Two Sources of Equal Strength

We consider two sources of equal strength separated by a distance 2a. The velocity potential and stream function are

$$\Phi = \frac{Q/b}{2\pi} (\ln r_1 + \ln r_2) \qquad \Psi = \frac{Q/b}{2\pi} (\theta_1 + \theta_2) \tag{11.88}$$

or in rectangular coordinates

$$\Phi = \frac{1}{2} \frac{Q/b}{2\pi} \ln [y^2 + (a-x)^2][y^2 + (a+x)^2] \tag{11.89}$$

and

$$\Psi = \frac{Q/b}{2\pi} (\tan^{-1} \frac{-y}{a-x} + \tan^{-1} \frac{y}{a+x}) = \frac{Q/b}{2\pi} \tan^{-1} \frac{2yx}{x^2 - y^2 - a^2} \tag{11.90}$$

because $\tan(\theta_1 + \theta_2) = (\tan\theta_1 + \tan\theta_2)/(1 - \tan\theta_1 \tan\theta_2)$. The potential lines and streamlines are shown in Fig. 11.7. This flow pattern may also be considered to represent a flow field near a wall (i.e. source and mirror image).

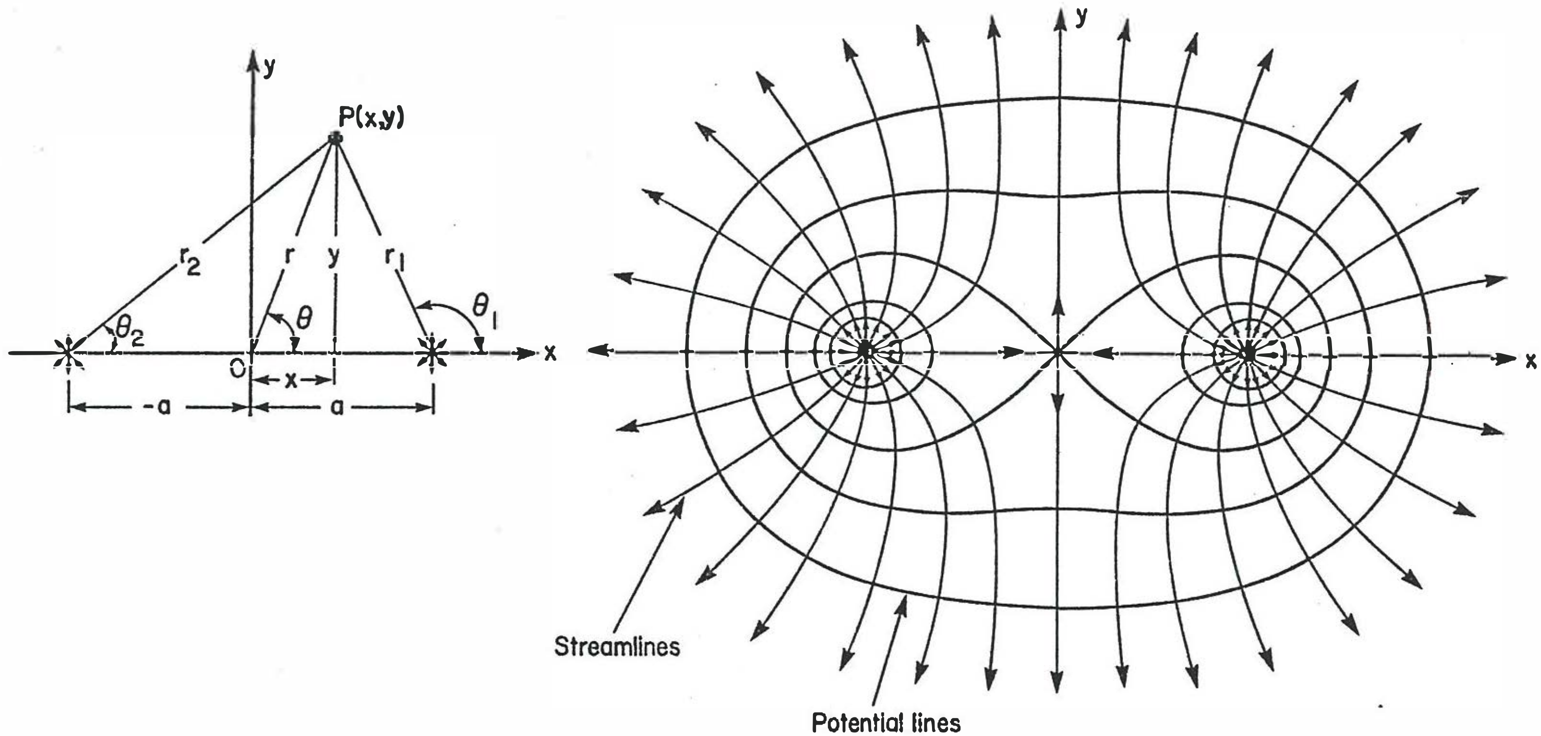

Fig. 11.7: Streamlines and potential lines for a pair of sources of equal strength.

(b) Source and Sink of Equal Strength

The streamlines of the flow field formed by the combination of a source and an equal sink are shown in Fig. 11.8. Here, the stream function is

$$\Psi = \frac{Q/b}{2\pi}\theta_1 - \frac{Q/b}{2\pi}\theta_2 = \frac{Q/b}{2\pi}(\theta_1 - \theta_2) \qquad (11.91)$$

or in rectangular coordinates

$$\Psi = \frac{Q/b}{2\pi}\left(\tan^{-1}\frac{-y}{a-x} - \tan^{-1}\frac{y}{a+x}\right) = \frac{Q/b}{2\pi}\tan^{-1}\frac{2ya}{x^2+y^2-a^2} \qquad (11.92)$$

because $\tan(\theta_1 - \theta_2) = (\tan\theta_1 - \tan\theta_2)/(1 + \tan\theta_1 \tan\theta_2)$

The velocity potential is

$$\Phi = \frac{Q/b}{2\pi}\ln r_1 - \frac{Q/b}{2\pi}\ln r_2 = \frac{1}{2}\frac{Q/b}{2\pi}\ln\frac{(a-x)^2+y^2}{(a+x)^2+y^2}$$

$$= -\frac{1}{2}\frac{Q/b}{2\pi}\ln\frac{(a+x)^2+y^2}{(a-x)^2+y^2} \qquad (11.93)$$

(c) Doublet

As the distance 2a in a source-sink pair becomes smaller the flow pattern resembles more and more a family of circles tangent to the origin. In the limit $2a \to 0$ the streamlines are circles tangent to the x axis and the potential lines are circles tangent to the y-axis at the origin as shown in Fig. 11.9. This type of flow field is called a doublet.

The stream function is

$$\Psi = \lim_{a\to 0}\left(\frac{Q/b}{2\pi}\tan^{-1}\frac{2ya}{x^2+y^2-a^2}\right) = \frac{Q/b}{2\pi}\frac{2ay}{x^2+y^2} = \frac{Q/b}{2\pi}\frac{2a\sin\theta}{r} \qquad (11.94)$$

Since $\tan\alpha \underset{\alpha\to 0}{\simeq} \alpha$

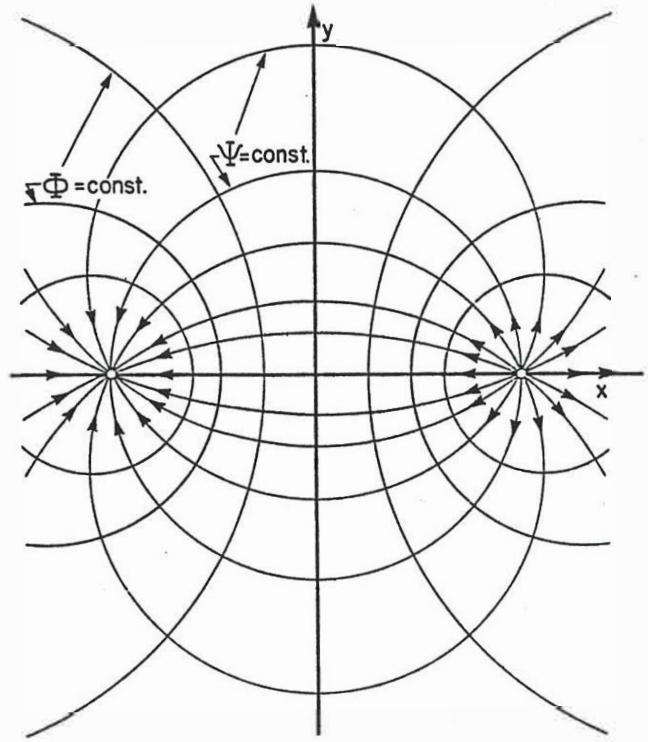

Fig. 11.8: Streamlines and potential lines for a source-sink pair.

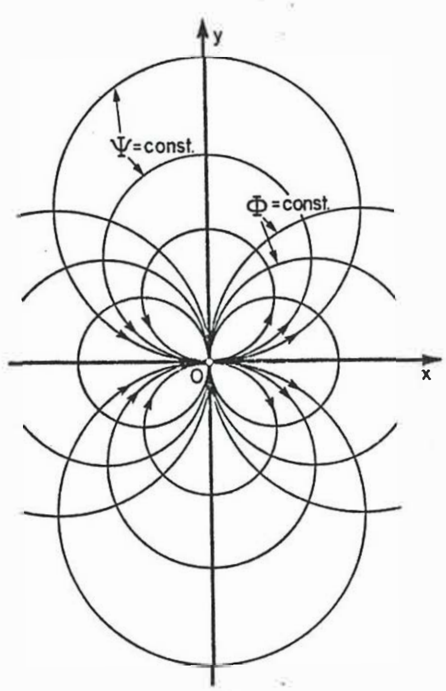

Fig. 11.9: Streamlines and potential lines for a doublet.

The velocity potential can be determined with the help of a series expansion for $\ln[(1+x)/(1-x)] = 2x + O(x^3)$. Thus

$$\Phi = \lim_{a\to 0}\left[-\frac{1}{2}\frac{Q/b}{2\pi}\ln\frac{(a+x)^2+y^2}{(a-x)^2+y^2}\right] = -\frac{Q/b}{2\pi}\frac{2ax}{x^2+y^2} = -\frac{Q/b}{2\pi}\frac{2a\cos\theta}{r} \qquad (11.95)$$

(d) Uniform Flow and a Source-Sink Pair

We consider a source and a sink of equal strength and a uniform stream parallel to the line joining the source and sink. The velocity potential is

$$\Phi = V_\infty r\cos\theta + \frac{Q/b}{2\pi}\ln r_1 - \frac{Q/b}{2\pi}\ln r_2$$

$$= V_\infty r\cos\theta + \frac{Q/b}{2\pi}\ln\frac{r_1}{r_2}$$

$$= V_\infty x + \frac{1}{2}\frac{Q/b}{2\pi}\ln\frac{(a+x)^2+y^2}{(a-x)^2+y^2} \qquad (11.96)$$

The stream function is

$$\Psi = V_\infty r\sin\theta + \frac{Q/b}{2\pi}\theta_1 - \frac{Q/b}{2\pi}\theta_2$$

$$= V_\infty r\sin\theta + \frac{Q/b}{2\pi}(\theta_1 - \theta_2)$$

$$= V_\infty y + \frac{Q/b}{2\pi}\left(\tan^{-1}\frac{y}{x+a} - \tan^{-1}\frac{y}{x-a}\right)$$

$$= V_\infty y + \frac{Q/b}{2\pi}\tan^{-1}\frac{-2ya}{x^2+y^2-a^2} \qquad (11.97)$$

because $\tan(\theta_1 - \theta_2) = (\tan\theta_1 - \tan\theta_2)/(1 + \tan\theta_1\tan\theta_2)$. The streamlines are shown in Fig. 11.10. The oval streamline can be considered an oval shaped body called the Rankine oval. By varying the distances between the hypothetical sources and sinks and varying the

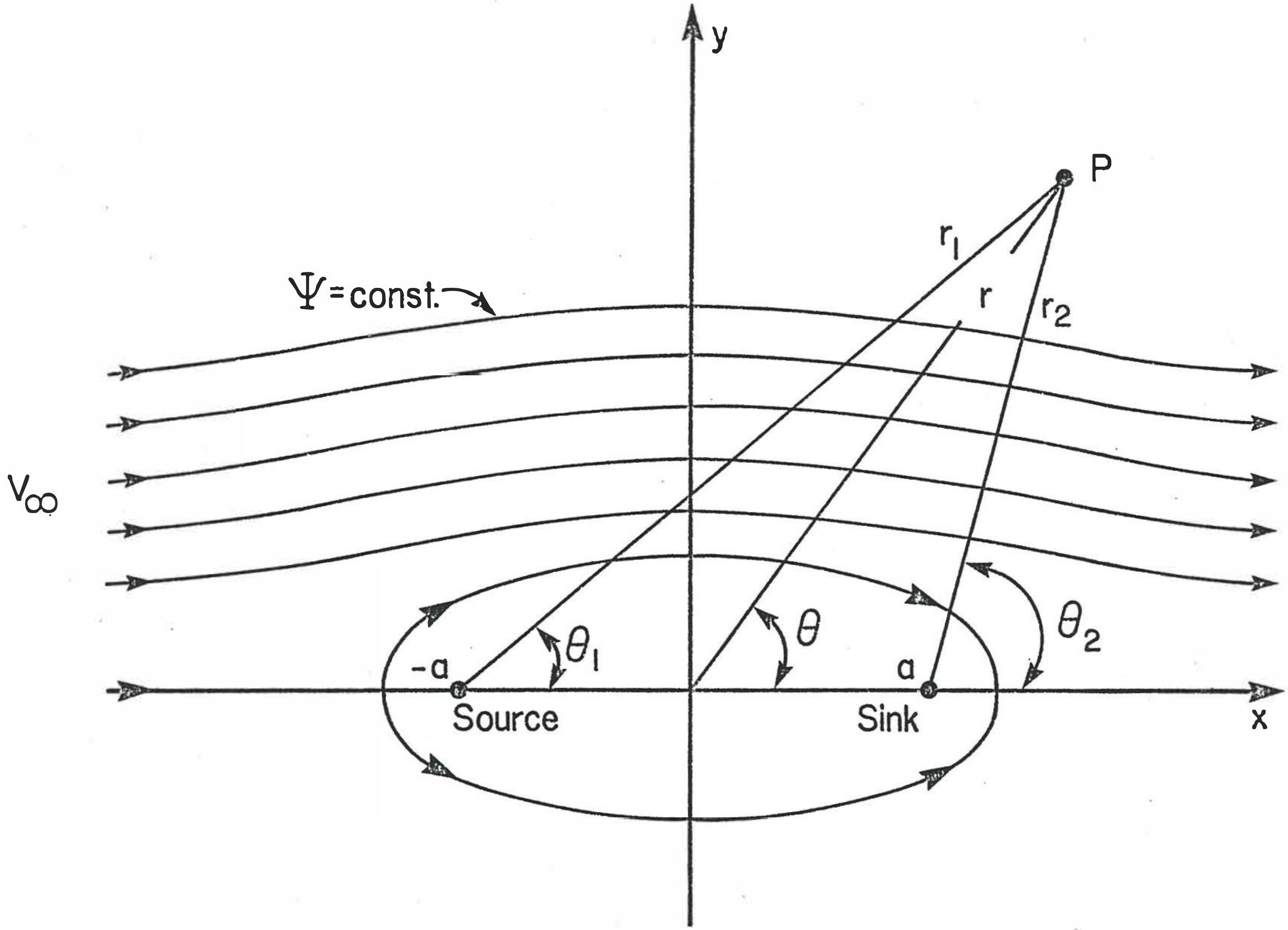

Fig. 11.10: Streamlines for flow around a Rankine oval.

strengths Q/b more complicated body shapes can be generated in order to approximate the flow around ships, airfoils, bridge piers, etc.

11.5 POTENTIAL FLOW AROUND A CYLINDER

As the spacing 2a in the uniform stream, source and sink combination (Sec. 11.4(d)) becomes smaller the Rankine oval looks more and more like a circle. In the limit $2a \to 0$, this is equivalent to a uniform stream plus a doublet. Thus, we have

$$\Phi = V_\infty r\cos\theta + \frac{Q/b}{2\pi}(2a)\frac{\cos\theta}{r} \tag{11.98}$$

The plus sign is needed rather than the minus given in Sec. 11.4 (c), because the source is located on the negative x-axis (compare Figs. 11.8 and 11.10)

$$\Psi = V_\infty r\sin\theta - \frac{Q/b}{2\pi}(2a)\frac{\sin\theta}{r} \tag{11.99}$$

Again, the sign is opposite to that given in Sec. 11.4(c) for Ψ (doublet) because the source is on the negative axis. In order for the cylinder surface of radius R to be a streamline

$$\Psi_o = 0 \quad \text{and} \quad V_\infty R^2 = \frac{Q/b}{2\pi}(2a) \tag{11.100}$$

Thus, the velocity potential and the stream function for uniform flow around a cylinder of radius R are

$$\Phi = V_\infty \left(r + \frac{R^2}{r}\right)\cos\theta \tag{11.101}$$

$$\Psi = V_\infty \left(r - \frac{R^2}{r}\right)\sin\theta \tag{11.102}$$

Using equation (11.31) we obtain the velocity components

$$v_r = V_\infty \left(1 - \frac{R^2}{r^2}\right) \cos\theta \tag{11.103}$$

$$v_\theta = - V_\infty \left(1 + \frac{R^2}{r^2}\right) \sin\theta \tag{11.104}$$

At the cylinder surface $r = R$

$$v_r = 0 \quad \text{and} \quad v_\theta = - 2\, V_\infty \sin\theta \tag{11.105}$$

Using the Bernoulli equation (11.44) without the gravitational term, we have

$$p_\infty + \frac{1}{2} \rho\, V_\infty^2 = p_s + \frac{1}{2} \rho\, (- 2\, V_\infty \sin\theta)^2 \tag{11.106}$$

or

$$p_s - p_\infty = \frac{1}{2} \rho\, V_\infty^2\, (1 - 4 \sin^2\theta) \tag{1.107}$$

where p_s is the surface pressure and p_∞ the free stream pressure.

The streamlines for potential flow around a cylinder are shown in Fig. 11.11 and the pressure distribution in Fig. 11.12. The deviation from the experimental results is due to boundary layer separation (see Chapter 12). Integrating the horizontal pressure force components for a cylinder of length W (perpendicular to the plane of the paper in Fig. 11.11), we find the surprising result that the drag force is zero:

$$F_p = - W \int_0^{2\pi} (p_s - p_\infty)\, R \cos\theta\, d\theta = 0 \tag{11.108}$$

This is known as d'Alembert's paradox, after J.R. d'Alembert who concluded in 1752 that an inviscid incompressible fluid exerts no drag on a body of any shape immersed in it, in contradiction with practical experience. This contradiction cast doubt to the inviscid flow theory and impeded greatly the progress of hydrodynamics during the eighteen

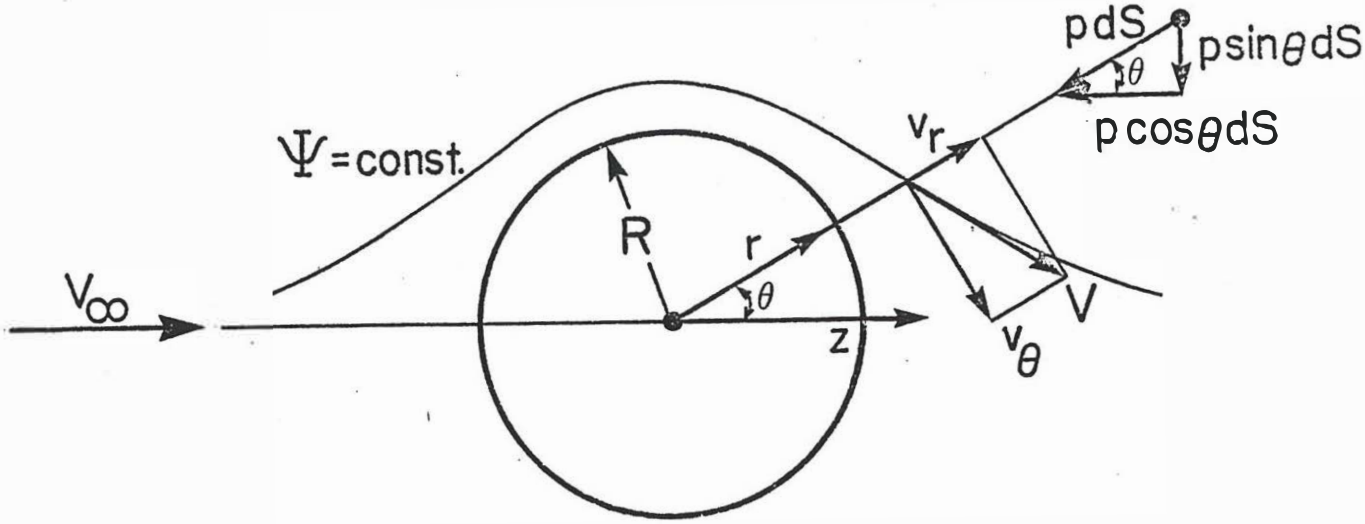

(a)

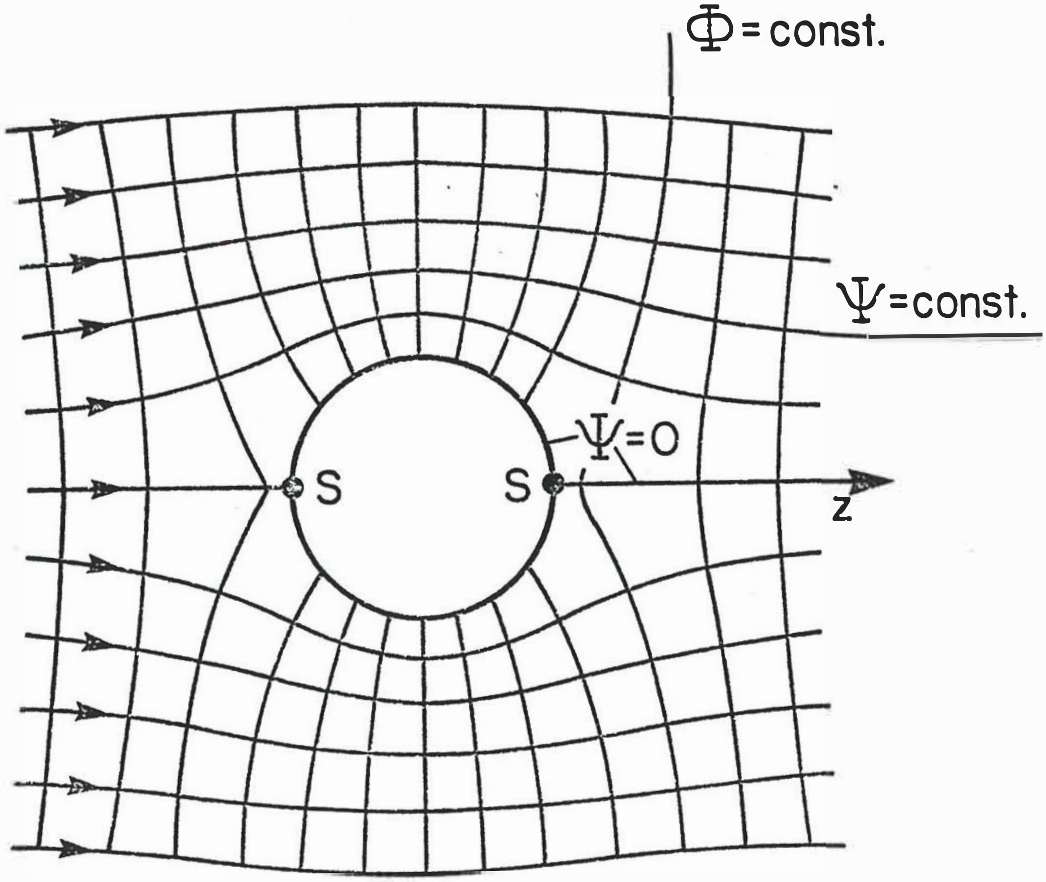

(b)

Fig. 11.11: (a) Velocity components and pressure force components for flow around a cylinder.
(b) Streamlines and potential lines for flow around a cylinder. S denotes stagnation points.

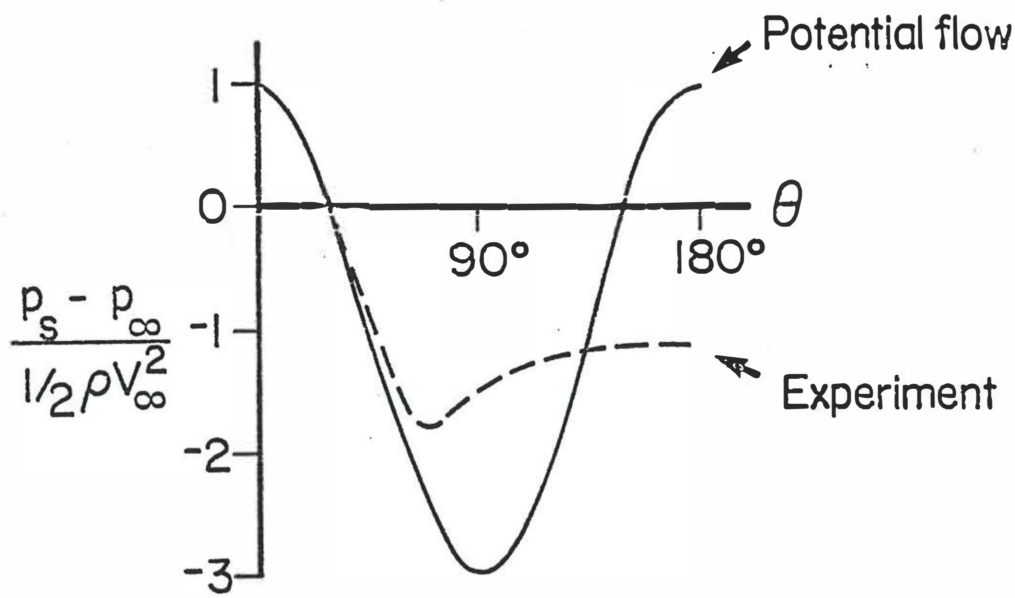

Fig. 11.12: Surface pressure variation for flow around a cylinder.

and nineteen centuries. The paradoxical results were explained after the introduction of Prandtl's boundary layer theory in 1904.

11.6 POTENTIAL FLOW AROUND A CYLINDER WITH CIRCULATION

If we superimpose a potential vortex at the doublet center of the previous problem, we have the velocity potential and stream function at a flow field composed of a uniform stream plus a doublet plus a vortex:

$$\Phi = V_\infty \left(r + \frac{R^2}{r}\right) \cos\theta + \frac{\Gamma}{2\pi}\,\theta \tag{11.109}$$

$$\Psi = V_\infty \left(r - \frac{R^2}{r}\right) \sin\theta - \frac{\Gamma}{2\pi} \ln r \tag{11.110}$$

The flow field is physically realized by a rotating cylinder in a uniform stream.

The velocity components are obtained with the help of equations (11.31)

$$v_r = V_\infty \left(1 - \frac{R^2}{r^2}\right) \cos\theta \tag{11.111}$$

$$v_\theta = - V_\infty \left(1 + \frac{R^2}{r^2}\right) \sin\theta + \frac{\Gamma}{2\pi}\,\frac{1}{r} \tag{11.112}$$

At the cylinder surface $r = R$

$$v_r = 0 \quad \text{and} \quad v_\theta = - 2\, V_\infty \sin\theta + \frac{\Gamma}{2\pi R} \tag{11.113}$$

The streamlines are shown in Fig. 11.13 for different $\Gamma/4\pi R V_\infty$ values.

The pressure distribution at the surface p_s is obtained from the Bernoulli equation (11.44), without the gravitational term

$$p_\infty + \frac{1}{2}\,\rho\, V_\infty^2 = p_s + \frac{1}{2}\,\rho \left(- 2\, V_\infty \sin\theta + \frac{\Gamma}{2\pi R}\right)^2 \tag{11.114}$$

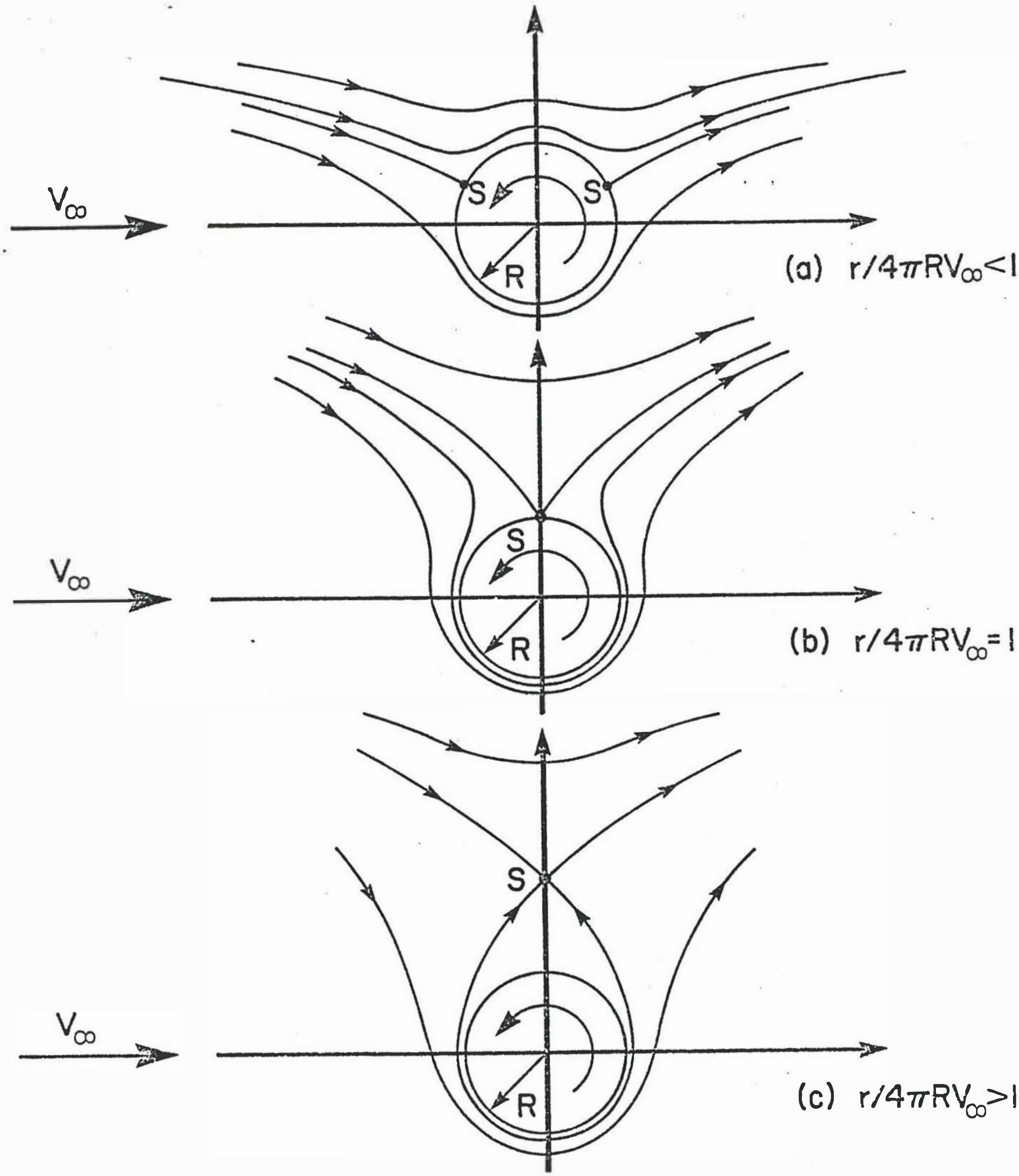

Fig. 11.13: Streamlines for flow around a cylinder with circulation for different values of the quantity $\Gamma/4\pi RV_\infty$. S denotes stagnation points.

or

$$(p_s - p_\infty) = \frac{1}{2}\rho V_\infty^2 \left(1 - 4\sin^2\theta + \frac{4\Gamma}{2\pi R V_\infty}\sin\theta - \left(\frac{\Gamma}{2\pi R V_\infty}\right)^2\right) \qquad (11.115)$$

Again the horizontal pressure force (drag) is found to be equal to zero from

$$F_D = -\int_0^{2\pi} (p_s - p_\infty)\, R\cos\theta\, d\theta = 0 \qquad (11.116)$$

The vertical pressure force is called lift and is calculated from

$$F_L = -W\int_0^{2\pi} (p_s - p_\infty)\, R\sin\theta\, d\theta \qquad (11.117)$$

We note that only the third term in the parenthesis of equation (11.115) gives a non-zero integral:

$$F_L = -\frac{1}{2}\rho V_\infty^2 \frac{4\Gamma}{2\pi R V_\infty} WR \int_0^{2\pi} \sin^2\theta\, d\theta = -\rho V_\infty \Gamma W \qquad (11.118)$$

or the lift per unit cylinder length is

$$\frac{F_L}{W} = -\rho V_\infty \Gamma \qquad (11.119)$$

The minus sign is included because Γ positive is in the counter-clockwise direction and the lift force should be downwards. Actually it is easier to determine the direction of the lift force on a rotating cylinder by noting that Bernoulli's equation states that the minimum pressure is where the velocity is maximum. This location is obviously on the vertical axis of Fig. 11.13 where the velocity is $(V_\infty + V_{surface})$. The existence of such a transverse force is known as the Magnus effect after the nineteenth century German physicist H.G. Magnus. The peculiarly curved trajectory of a rotating baseball, golf, tennis or soccer ball etc. is due to this effect. In the 1920's rotor ships were designed and built in Germany with large vertical cylinders on the deck [7]. The rotating cylinders were replacing the sails. These were able to cross the Atlantic ocean but practical problems relating to maneuverability, speed and other mechanical complications made them uneconomical. A detailed account of the investigations on the Magnus effect was presented by Swanson [8].

Equation 11.119 is known as the Kutta-Joukowski theorem, after the German Wilhelm Kutta and the Russian Nicolai Joukowski, who showed independently that for two-dimensional flow around a body the lift force per unit length is equal to $-\rho V_\infty \Gamma$.

11.7 POTENTIAL FLOW AROUND A SPHERE

Potential flow around a sphere is an axisymmetric flow problem and must be examined in spherical coordinates with ϕ-symmetry. The velocity potential is found to be [4,6]:

$$\Phi = V_\infty r\cos\theta + \frac{V_\infty R^3}{2r^2}\cos\theta \qquad (11.120)$$

The corresponding stream function is

$$\Psi = \frac{V_\infty r^2}{2}\sin^2\theta - \frac{V_\infty R^3}{2r}\sin^2\theta \qquad (11.121)$$

With the help of equations

$$v_r = \frac{\partial\Phi}{\partial r} = \frac{1}{r^2\sin\theta}\frac{\partial\Psi}{\partial\theta} \qquad (11.122)$$

$$v_\theta = \frac{1}{r}\frac{\partial\Phi}{\partial\theta} = -\frac{1}{r\sin\theta}\frac{\partial\Psi}{\partial r} \qquad (11.123)$$

we find

$$v_r = V_\infty \cos\theta \left(1 - \frac{R^3}{r^3}\right) \tag{11.124}$$

$$v_\theta = -\frac{1}{2} V_\infty \sin\theta \left(2 + \frac{R^3}{r^3}\right) \tag{11.125}$$

The velocity at the surface, $r = R$, is

$$(v_\theta)_{r=R} = -\frac{3}{2} V_\infty \sin\theta \tag{11.126}$$

and the pressure distribution is obtained from the Bernoulli equation

$$p_s - p_\infty = \frac{\rho V_\infty^2}{2} \left(1 - \frac{9}{4} \sin^2\theta\right) \tag{11.127}$$

The streamlines and potential lines for this flow are shown in Fig. 11.14(a).

The velocity potential and the stream function for a sphere moving through a fluid at rest can be easily obtained from equations (11.120) and (11.121) by subtracting the contribution of the uniform stream. Thus, we have

$$\Phi = \frac{V_\infty R^3}{2R^2} \cos\theta \qquad \Psi = -\frac{V_\infty R^3}{2r} \sin^2\theta \tag{11.128}$$

Now, V_∞ represents the velocity of translation of the sphere. The streamlines and potential lines are sketched in Fig. 11.14(b).

11.8 COMPLEX VARIABLES AND CONFORMAL MAPPING METHODS FOR POTENTIAL FLOW PROBLEMS

In the previous sections we considered the velocity potential Φ and stream function Ψ as functions of the independent real variables x and y. We now consider a new variable combination $z = x + iy$, where

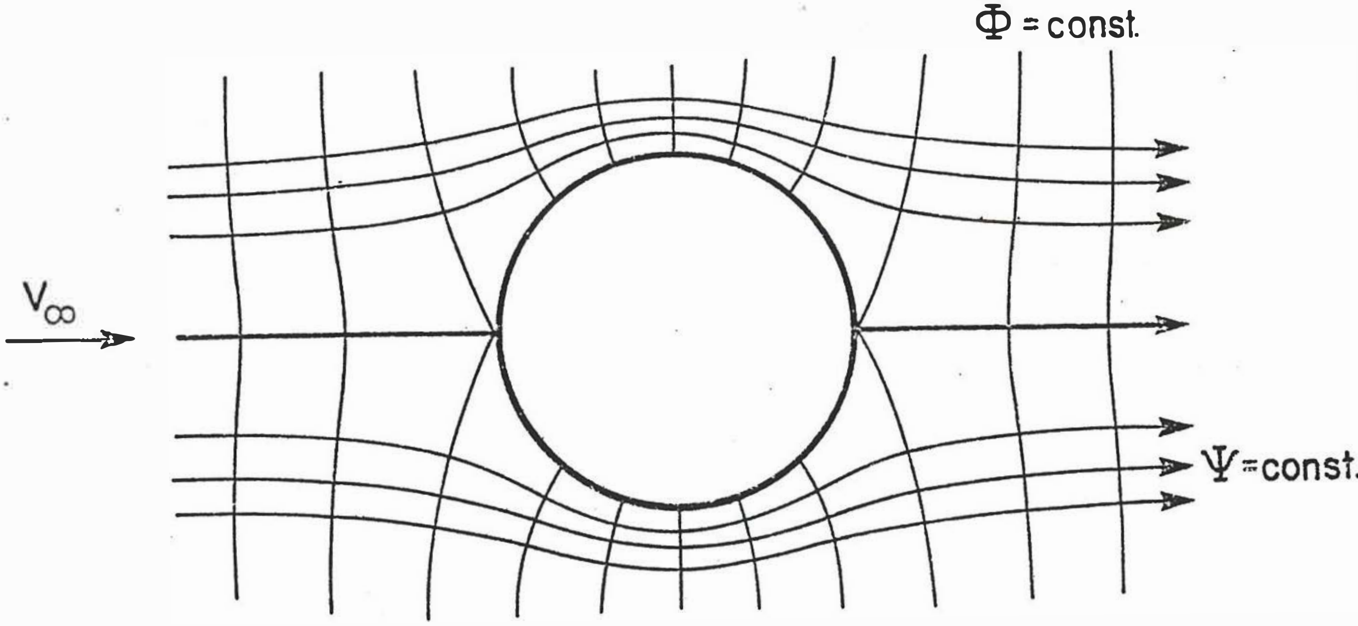

(a)

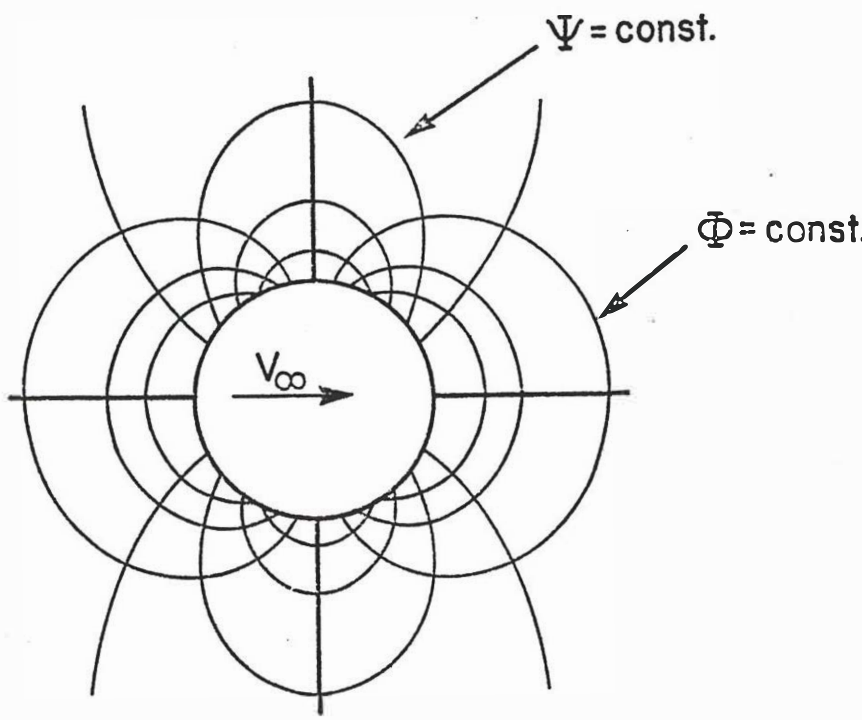

(b)

Fig. 11.14 (a) Streamlines and potential lines for uniform flow past a stationary sphere.
(b) Streamlines and potential lines due to the motion of sphere at a constant velocity.

$i = \sqrt{-1}$ with x and y representing the real and imaginary parts of the complex variable z. It can be shown [9] that because Φ and Ψ satisfy the Cauchy-Riemann equations (11.30) they represent the real and imaginary parts of an analytic function F(z), which is called the complex potential:

$$F(z) = \Phi(x,y) + i\,\Psi(x,y) \tag{11.129}$$

Thus, any analytic function F(z) represents a solution to the two-dimensional Laplace equation. Whether $\Phi(x,y)$ and $\Psi(x,y)$ represent a flow field of interest is not a priori known but must be determined in the course of flow analysis. All of the examples in the previous sections are special cases of the complex potential

$$F(z) = \frac{1}{2\pi}(Q/b + i\Gamma)\ln z + \sum_{-\infty}^{\infty}(A_n + iB_n)\, z^n \tag{11.130}$$

where A_n, B_n are constants and n is an index.

In polar coordinates (r,θ) we have

$$z = x + iy = re^{i\theta} = r(\cos\theta + i\sin\theta) \tag{11.131}$$

Since $\ln(re^{i\theta}) = \ln r + i\theta$, we can express the velocity potential Φ and the stream function Ψ as

$$\Phi = \frac{Q/b}{2\pi}\ln r - \frac{Q/b}{2\pi}\theta + \sum_{-\infty}^{\infty} r^n (A_n \cos n\theta + B_n \sin n\theta) \tag{11.132}$$

$$\Psi = \frac{Q/b}{2\pi}\theta + \frac{\Gamma}{2\pi}\ln r + \sum_{-\infty}^{\infty} r^n (A_n \sin\theta + B_n \cos n\theta) \tag{11.133}$$

As mentioned earlier any other analytic function F(z) will represent a solution to some potential flow problem which may or may not be of any practical significance.

Working in terms of complex variable z greatly simplifies the mathematical manipulations involved and expands the horizon of solution of potential flow problems. However, a good knowledge of conformal mapping [9] is required in order to determine the complex potential for given flow fields.

In the physical plane z or (x,y), Ψ = const and Φ = const represent streamlines and potential lines which are orthogonal. It is possible to introduce a transform $\zeta = f(z)$ from the z plane to another plane $\zeta = \eta + i\xi$. Such that the orthogonality at Ψ and Φ is preserved. For an illustration let us examine the transform

$$\begin{aligned} \zeta = F(z) &= z^2 \\ &= r^2 e^{i2\theta} \\ &= (x^2 - y^2) + 2xyi \\ &= \Phi + i\Psi \end{aligned} \tag{11.134}$$

Because of the first one of the above expressions, a point making an angle θ with the real axis in the z-plane transforms into a point making an angle 2θ with the real axis and is located at a distance r^2 from the origin in the ζ-plane as shown in Fig. 11.15. Lines of Φ = const and Ψ = const are parallel to the axes in the ζ-plane and form a uniform flow network. In the z-plane

$$\Phi = x^2 - y^2 = \text{const} \tag{11.135}$$

$$\Psi = 2xy = \text{const} \tag{11.136}$$

These are hyperbolas as shown in Fig. 11.15. Thus, the uniform flow field in the ζ-plane is mapped into a flow field around a 90° corner in the z-plane.

This example indicates that it is possible to construct flow patterns about complex shapes if we know the flow pattern F(z) about a simple shape. Conformal transformation tables can be found in

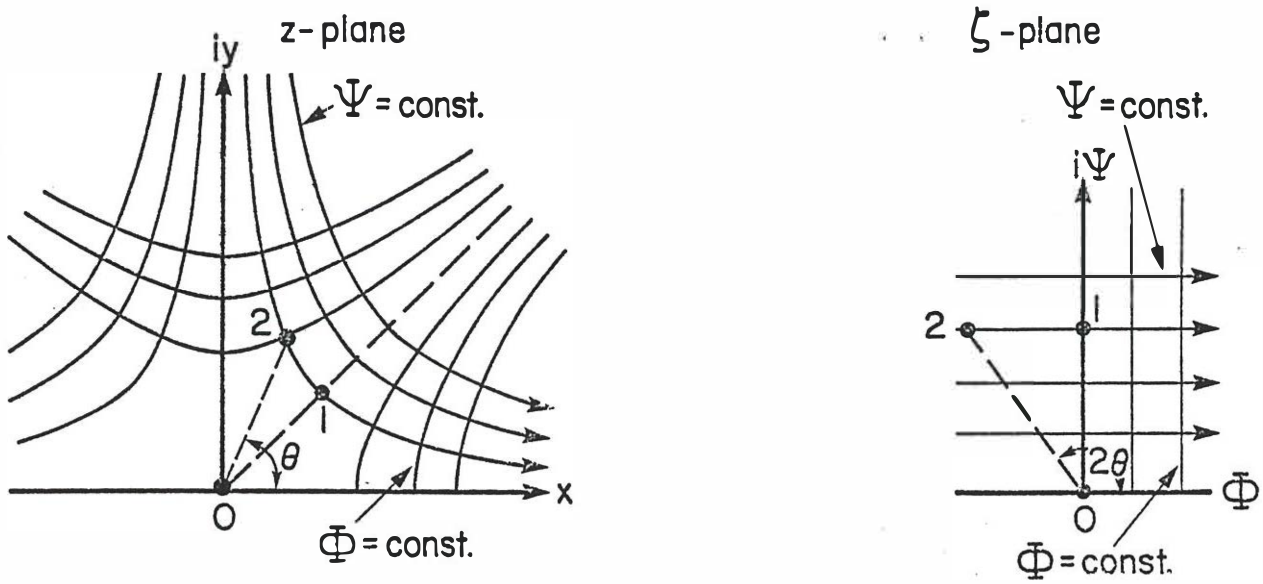

Fig. 11.15: Flow field mapping with the transformation $\zeta = z^2$.

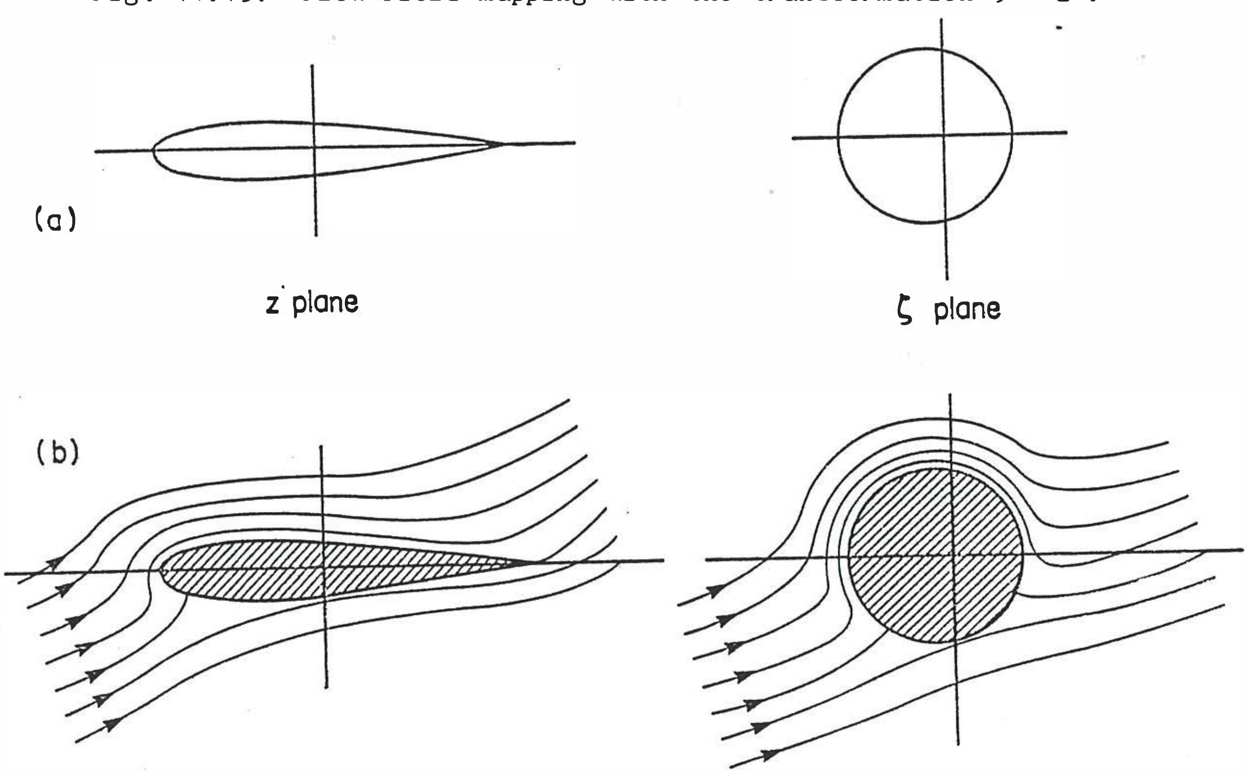

Fig. 11.16: The symmetrical Joukowski airfoil (a) mapping planes, (b) uniform flow past the airfoil.

specialized books [eg, refs. [9], [10]). Several transformations for some important flow problems can be found in books dealing extensively with potential flow theory [1,2,3,5,6]. The most famous of these transformations is the Joukowski transformation for airfoils

$$\zeta = (z + \frac{C^2}{z}) \tag{11.137}$$

where C^2 is real. The mapping planes and the flow patterns are shown in Fig. 11.16. It is interesting to note that the potential flow results for airfoils are much closer to reality than those for the cylinders. The reason is that an airfoil is much more streamlined than a cylinder and thus the boundary layer separation effects (see Chapter 12) are less pronounced.

Although comformal mapping methods are indeed very powerful tools for potential flow analysis, they have been largely displaced in modern applications because of the increasing use of numerical techniques (see Chapter 25). The Laplace equation can be easily solved by either finite difference or finite element methods. The latter method is particularly well suited for problems having irregular boundaries as discussed in Chapter 25.

11.9 SOME WORKED OUT EXAMPLES

Example 11.9.1

The stream function for a two-dimensional incompressible flow field is $\Psi = 3x^2y - y^3$. Show that the flow field is irrotational, determine the velocity magnitude $|\bar{V}|$ and the velocity potential Φ.

Solution

The irrotationality condition is $\nabla \times \bar{V} = 0$ or in two-dimensions

$$\frac{\partial v_x}{\partial y} - \frac{\partial v_y}{\partial x} = 0$$

Since

$$v_x = \frac{\partial \Psi}{\partial y} \quad \text{and} \quad v_y = -\frac{\partial \Psi}{\partial x}$$

$$\frac{\partial v_x}{\partial y} - \frac{\partial v_y}{\partial x} = \frac{\partial^2 \Psi}{\partial y^2} + \frac{\partial^2 \Psi}{\partial x^2} = 0$$

i.e. the stream function must satisfy the Laplace equation.

We have

$$\frac{\partial^2 \Psi}{\partial y^2} + \frac{\partial^2 \Psi}{\partial x^2} = \frac{\partial}{\partial y^2}(3x^2y - y^3) + \frac{\partial}{\partial x^2}(3x^2y - y^3) =$$

$$= -6y + 6y = 0$$

Therefore, the flow is irrotational. The velocity magnitude at a point (x,y) is given by

$$V = |\bar{V}| = (v_x^2 + v_y^2)^{1/2}$$

where

$$v_x = \frac{\partial \Psi}{\partial y} = \frac{\partial}{\partial y}(3x^2y - y^3) = 3x^2 - 3y^2 = 3(x^2 - y^2)$$

$$v_y = -\frac{\partial \Psi}{\partial x} = -\frac{\partial}{\partial x}(3x^2y - y^3) = -6xy$$

and

$$V = |\bar{V}| = (3^2(x^2 - y^2)^2 + (-6xy)^2)^{1/2} = (9(x^4 - 2x^2y^2 + y^4) + 36x^2y^2)^{1/2}$$

$$= 3((x^2 - y^2)^2)^{1/2}$$

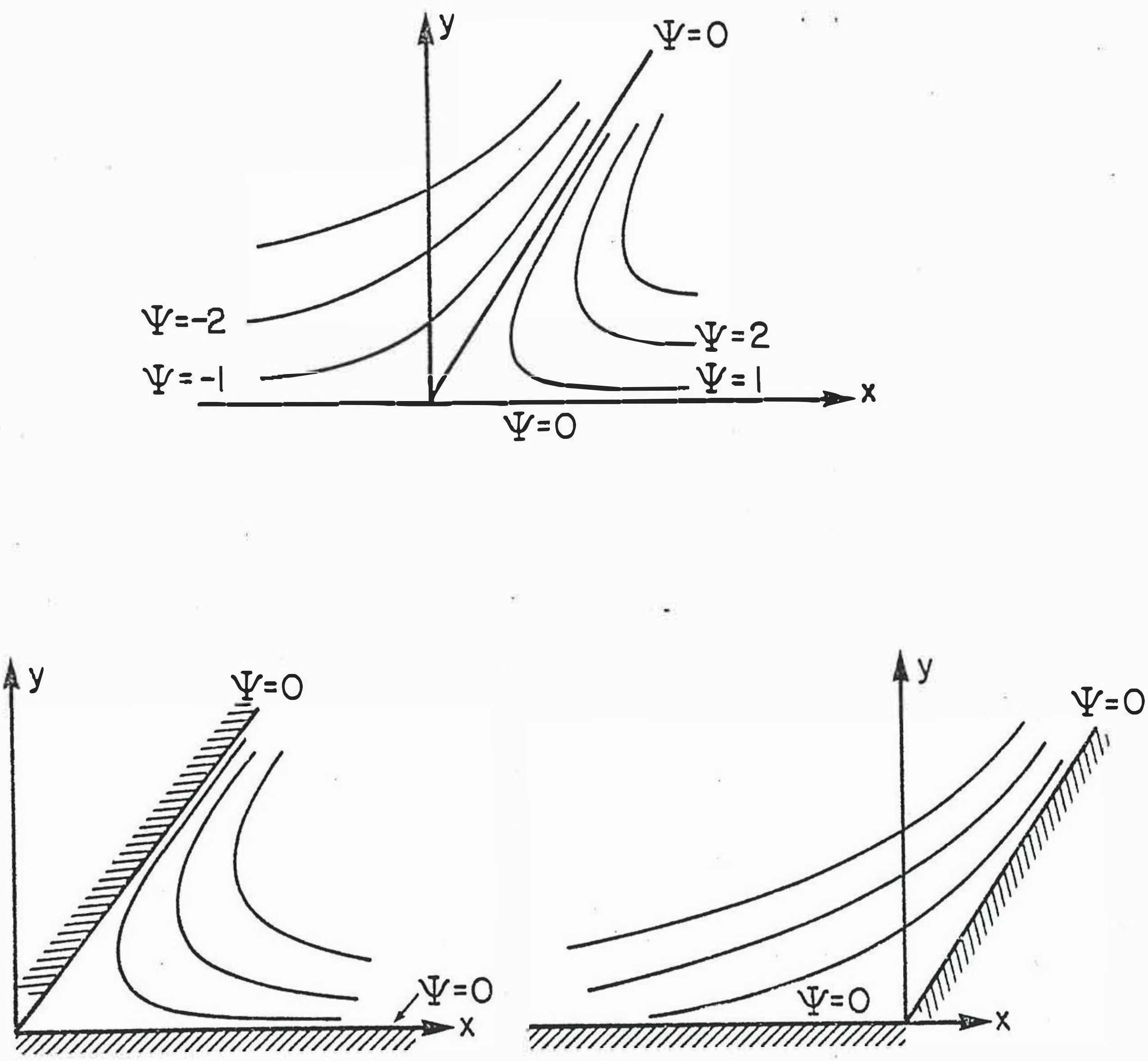

E.11.9.1

The quantity $(x^2 + y^2)^{1/2} = r$ is the distance from the origin $x = 0$, $y = 0$. Thus, $V = 3r^2$.

The velocity potential can be determined from

$$v_x = \frac{\partial\Phi}{\partial x} \quad \text{and} \quad v_y = \frac{\partial\Phi}{\partial y}$$

or

$$\frac{\partial\Phi}{\partial x} = 3(x^2 - y^2) \qquad \frac{\partial\Phi}{\partial y} = -6xy$$

$$\Phi = x^3 - 3y^2x + C(y) \quad \Phi = -3xy^2 + C(x)$$

and

$$\Phi = x^3 - 3y^2x + \text{const}$$

In Fig. E.11.9.1(a) we sketched the streamlines. The potential lines will be orthogonal. Since there is no flow across the streamlines any streamline may represent a solid boundary. If we take $\Psi = 0$ as a solid boundary, we have the flow in either one of the corners shown in Figure E.11.9.1(b) and E.11.9.1(c).

Example 11.9.2

A line source is located at a distance a from a wall. Determine the velocity distribution along the wall and the total pressure force on the wall. (Assume $Q/b = 0.5\ m^2/s$, $a = 30$ cm, $\rho = 1000\ kg/m^3$).

Solution

We noted in Sec. 11.4(a) that the flow field for a line source at a distance a from a wall is described by the same equations as the flow field for two sources placed a distance 2a apart. The stream function was given as

$$\Psi = \frac{Q/b}{2\pi}(\theta_1 + \theta_2)$$

or in rectangular coordinates (see Fig. 11.7)

$$\Psi = \frac{Q/b}{2\pi}\left(\tan^{-1}\frac{y}{x-a} + \tan^{-1}\frac{y}{x+a}\right)$$

which can be written as

$$\Psi = \frac{Q/b}{2\pi}\tan^{-1}\frac{2yx}{x^2-y^2-a^2}$$

At the wall x=0 the velocity component $v_x = 0$. The velocity component in the y-direction can be calculated from

$$v_y = \left[-\frac{\partial\Psi}{\partial x}\right]_{x=0} = -\frac{Q/b}{2\pi}\left[\frac{1}{1+\left(\frac{2xy}{x^2-y^2-a^2}\right)^2}\;\frac{(x^2-y^2-a^2)2y-4yx^2}{(x^2-y^2-a^2)^2}\right]_{x=0}$$

$$= \frac{Q/b}{2\pi}\,\frac{2y}{y^2+a^2}$$

This has a maximum which is obtained from

$$\frac{dv_y}{dy} = 0 = \frac{(y^2+a^2)-2y^2}{(y^2+a^2)^2}\;\frac{Q/b}{\pi}$$

We find that the maximum velocity v_y is located at $y = \pm a$.

We now assume that the presure in the back of the wall is the same as that of the fluid at a large distance, p_∞ where $v_y \simeq 0$. The Bernoulli equation gives

$$p + \frac{1}{2}\rho\, v_y^2 = p_\infty + 0$$

or

$$p - p_\infty = -\frac{1}{2}\rho\, v_y^2$$

Thus the total force on the wall is

$$F = -\int_{-\infty}^{+\infty} (p - p_\infty)_{x=0}\, dy = -\frac{1}{2}\rho \int_{-\infty}^{+\infty} v_y^2\, dy =$$

$$= \frac{(Q/b)^2 \rho}{8\pi^2} \int_{-\infty}^{+\infty} \frac{4y^2}{(y^2+a^2)^2}\, dy = \frac{(Q/b)^2 \rho}{4a\pi}$$

$$F = \frac{(0.5\ m^2/s)^2 (1000\ kg/m^3)}{4(0.3\ m)\ \pi} = 66.35\ N$$

Example 11.9.3

A tornado can be idealized as a line vortex formed by the interaction of wind-currents. It can be assumed that the flow field is irrotational and the tangential velocity is given by (Sec. 11.3(d)) $v_\theta = \Gamma/2\pi r = K/r$. The irrotationality property, however, cannot hold all the way to the axis, because v_θ tends to infinity. In a central core region (say $r_1 = 30$ m) viscous effects will be of importance. In such a tornado the tangential wind velocity at a radius of 250 m has been measured by a meteorological station as 45 km/hr (12.5 m/s) and the pressure as 97 kPa. Determine the pressure and the tangential velocity at the edge of the central core. Discuss the consequences of the pressure force on a house at a distance of 70 m from the path of the center of the eye of the tornado. (Assume density of air $\rho = 1.2$ kg/m^3).

Solution

Let

$r_1 = 30$ m

$r_2 = 70$ m

$r_3 = 250$ m

We have $(v_\theta)_1 = K/r_1$, $(v_\theta)_2 = K/r_2$, $(v_\theta)_3 = K/r_3$

$$(v_\theta)_1 = (v_\theta)_3 \frac{r_1}{r_3} = (12.5 \text{ m/s}) \frac{250}{30} = 104.17 \text{ m/s (375 km/hr)}$$

$$(v_\theta)_2 = (v_\theta)_3 \frac{r_2}{r_3} = (12.5 \text{ m/s}) \frac{250}{70} = 44.64 \text{ (161 km/hr)}$$

For an irrotational flow field the Bernoulli equation is applicable, thus

$$\frac{p_3}{\rho} + \frac{v_3^2}{2} = \frac{p_1}{\rho} + \frac{v_1^2}{2}$$

$$p_1 = p_3 - \frac{\rho}{2}(v_1^2 - v_3^2) =$$

$$= 97{,}000 \text{ N/m}^2 - \frac{1.2}{2}(\text{kg/m}^3)(104.17^2 - 12.5^2)(\text{m}^2/\text{s}^2)$$

$$= 97{,}000 \text{ N/m}^2 - 6{,}417 \text{ N/m}^2 = 90{,}583 \text{ N/m}^2 = 90{,}583 \text{ Pa}$$

$$p_2 = p_3 - \frac{\rho}{2}(v_2^2 - v_3^2) =$$

$$= 97{,}000 \text{ N/m}^2 - \frac{1.2}{2}(\text{kg/m}^3)(44.64^2 - 12.5^2)(\text{m}^2/\text{s}^2)$$

$$= 97{,}000 \text{ N/m}^2 - 1102 \text{ N/m}^2 = 95{,}898 \text{ Pa}$$

The house is originally at ambient pressure probably close to 97 kPa (97,000 N/m^2). As the tornado passes at a distance of 70 m the pressure on the outside drops suddenly by 1102 N/m^2. This exerts a force of about 22 KN on a 4m x 5m wall. The house will literally explode. There will also be very large drag forces, because of the very high velocities, which will increase the overall destructive force of the tornado.

The strength of the tornado is usually expressed in terms of $K = v_\theta r$. Here, we have K = 3125 m^2/s. For very strong tornados K may

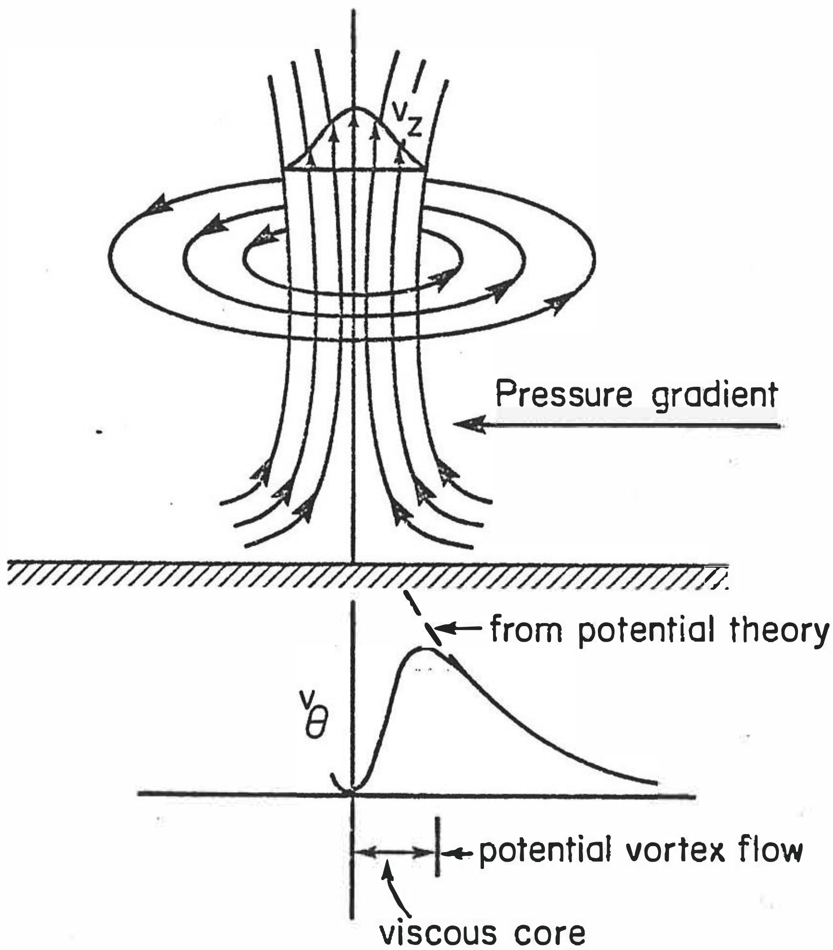

v_z
Pressure gradient
from potential theory
v_θ
potential vortex flow
viscous core

be as large as 10,000 m^2/s.

The interaction of the potential vortex flow with the ground where the velocity becomes zero results in inward directed flow near the ground and inverted funneling in the viscous core region as shown in Fig. E11.9.3. The velocity distribution v_θ throughout the tornado flow field and v_z in the central core is also sketched.

Example 11.9.4

A Quonset hut (having the shape of half cylinder) is subjected to winds of up to 100 km/hr. Determine the lift force if the hut has a hole at A as shown in Figure E.11.9.4. If hole at A is closed what should be the angle θ for a new hole that would result in zero lift?

Solution

From Sec. 11.5 for uniform flow around a cylinder, we have

$$p_s - p_\infty = \frac{1}{2}\rho V_\infty^2 (1 - 4\sin^2\theta)$$

where p_s is the pressure at the cylinder surface and p_∞ the pressure far from the cylinder. Thus,

$$p_s = p_\infty + \frac{1}{2}\rho V_\infty^2 - 2\rho V_\infty^2 \sin^2\theta$$

If p_1 is the pressure in the inside of the hut, then the net lift (upward) is

$$F = W\int_0^\pi (p_i - p_s)\, R\sin\theta\, d\theta$$

where W is the length perpendicular to the plane of the paper. Thus

$$F = WR\int_0^\pi (p_i - p_\infty - \frac{1}{2}\rho V_\infty^2 + 2\rho V_\infty^2 \sin^2\theta)\sin\theta\, d\theta$$

$$= 2(p_i - p_\infty - \frac{1}{2}\rho V_\infty^2)\, WR + \frac{8}{3}\rho V_\infty^2\, WR$$

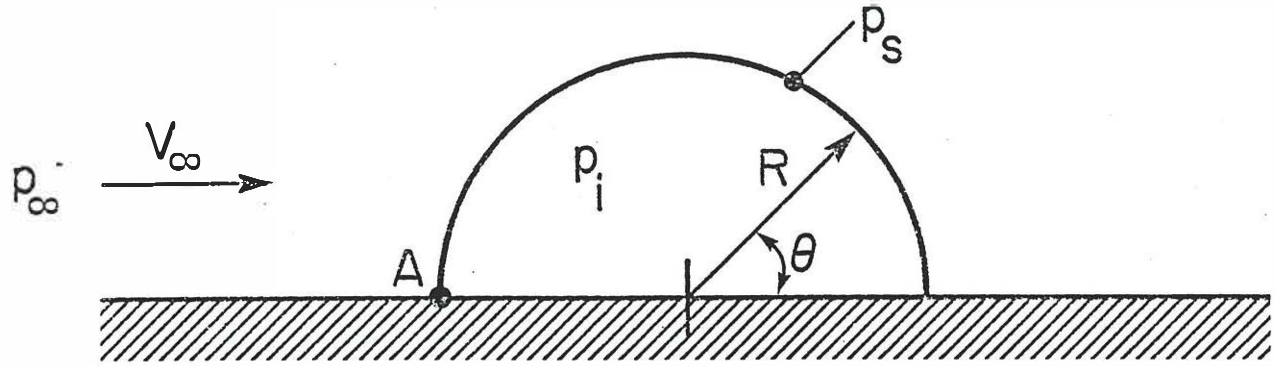

E.11.9.4

If there is a hole at A, p_i is equal to the stagnation pressure ($V_A = 0$)

$$p_i = p_\infty + \frac{1}{2} \rho V_\infty^2$$

Thus

$$F = \frac{8}{3} \rho V_\infty^2 WR = \frac{8}{3} (1.2 \text{ kg/m}^3)(27.78 \text{ m/s})^2 \times 1\text{m} \times 2\text{m}$$

$$= 4939 \text{ N}$$

In order for the lift to be zero

$$2(p_i - p_\infty - \frac{1}{2} \rho V_\infty^2) + \frac{8}{3} \rho V_\infty^2 = 0 \qquad \text{(E.1)}$$

In Sec. 11.5, we found that at the cylinder surface

$$(v_\theta)_{r=R} = - 2V_\infty \sin\theta$$

Applying the Bernoulli equation, we get

$$p_i + \frac{1}{2} \rho (- 2V_\infty \sin\theta)^2 = p_\infty + \frac{1}{2} \rho V_\infty^2$$

Introducing p_i into equation (E.1), we obtain

$$4 \rho V_\infty \sin^2\theta + \frac{8}{3} \rho V_\infty^2 = 0$$

$$\sin^2\theta = \frac{2}{3}$$

Therefore

$$\theta = 54.6^\circ$$

or

$$\theta = 90 + 54.6 = 144.6^\circ$$

REFERENCES

1. L.M. Milne-Thomson, "Theoretical Hydrodynamics", 4th Edition, MacMillan, New York (1960).
2. H. Lamb, "Hydrodynamics", 6th Edition, Dover Publications, New York (1945).
3. L. Prandtl and O.G. Tietjens, "Fundamentals of Hydro- and Aeromechanics", Dover Publications, New York (1957).
4. V.L. Streeter and E.B. Wylie, "Fluid Mechanics", 6th Edition, McGraw-Hill, New York (1975).
5. I.G. Currie, "Fundamental Mechanics of Fluids", McGraw-Hill, New York (1974).
6. S. Eskinazi, "Vector Mechanics of Fluids and Magnetofluids", Academic Press, New York (1967).
7. A. Flettner, "The Story of the Rotor", Willhoft, New York (1926).
8. W.M. Swanson, "The Magnus Effect: A Summary of Investigations to Date", Trans. ASME, D83, 3 (1961).
9. R.V. Churchill, "Complex Variables and Applications", 2nd Edition, McGraw-Hill, New York (1960).
10. L. Bieberbach, "Conformal Mapping", Chelsea Publishing Company, New York (1953).

John Vlachopoulos, *Fundamentals of Fluid Mechanics*
Chem. Eng., McMaster University, Hamilton, ON, Canada
(First Edition 1984, revised internet edition (2016), www.polydynamics.com)

CHAPTER 12

LIFT AND DRAG

12.1 INTRODUCTION

A body immersed in a flowing fluid will experience pressure and viscous forces from the flow. The sum of forces perpendicular to the direction of the flow is called lift and is responsible for the ability of birds, insects and aircraft to fly. Buoyancy may also contribute to an upward directed force, however, this has nothing to do with the term lift as it is used in this chapter. The sum of forces acting in the direction of the flow is called drag and must be overcome by all bodies moving in a fluid. In this chapter we describe how these forces are generated and how they can be calculated.

12.2 THE MOMENTUM EQUATION ALONG A STREAMLINE OUTSIDE THE BOUNDARY LAYER

Let us consider the flow of an otherwise undisturbed fluid around an airfoil as shown in Figure 12.1. As it was explained in Chapter 9, the influence of fluid viscosity dominates the momentum transfer

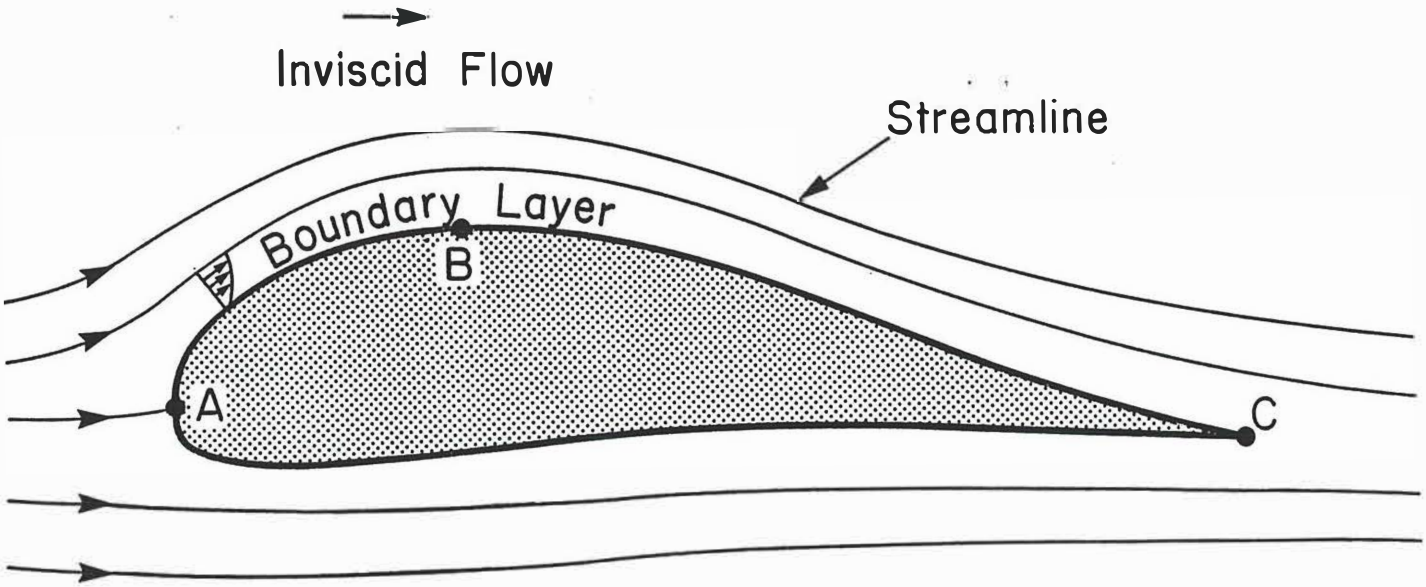

Fig. 12.1 Boundary layer flow around an airfoil.

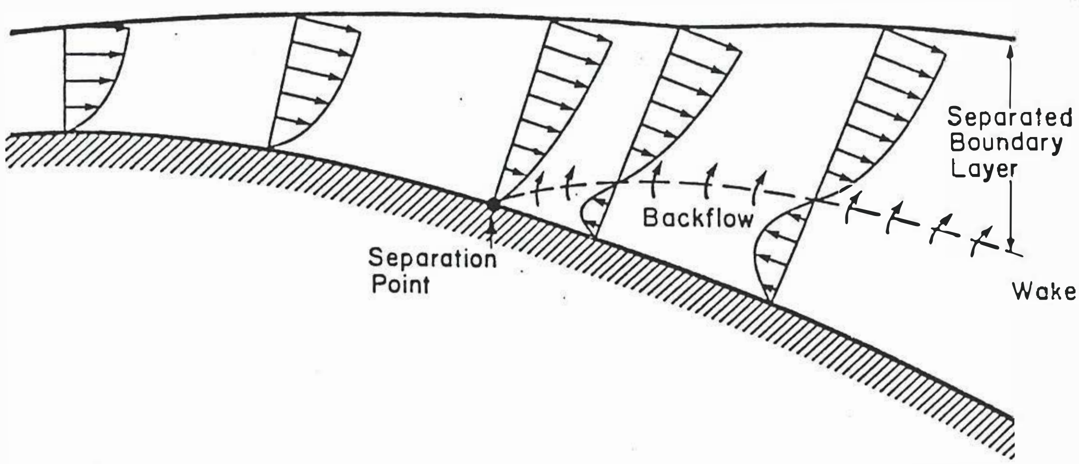

Fig. 12.2 Boundary layer separation.

mechanism only inside the boundary layer. The boundary layer can be either laminar or turbulent. Outside the boundary layer, however, the fluid can be considered as inviscid ($\mu = 0$). The momentum equation (6.94) for an inviscid, incompressible, two-dimensional, steady flow with negligible gravitational effects reduces to

$$v_x \frac{\partial v_x}{\partial x} + v_y \frac{\partial v_x}{\partial y} = -\frac{1}{\rho}\frac{\partial p}{\partial x} \tag{12.1}$$

$$v_x \frac{\partial v_y}{\partial x} + v_y \frac{\partial v_y}{\partial y} = -\frac{1}{\rho}\frac{\partial p}{\partial y} \tag{12.2}$$

In Section 3.5 a streamline $s(x,y)$ was defined as a curve drawn tangent to the velocity gradient, i.e. the velocity vector $\overline{V}(v_x, v_y)$ is parallel to $\overline{ds}(dx,dy)$ which means that

$$\frac{dx}{v_x} = \frac{dy}{v_y} \tag{12.3}$$

Thus we have

$$v_x = v_y \frac{dx}{dy} \tag{12.4}$$

$$v_y = v_x \frac{dy}{dx} \tag{12.5}$$

By substituting the above expressions into equations (12.1) and (12.2), we get

$$v_x \frac{\partial v_x}{\partial x} + v_x \frac{dy}{dx}\frac{\partial v_x}{\partial y} = -\frac{1}{\rho}\frac{\partial p}{\partial x} \tag{12.6}$$

$$v_x \frac{dx}{dy}\frac{\partial v_y}{\partial x} + v_y \frac{\partial v_y}{\partial y} = -\frac{1}{\rho}\frac{\partial p}{\partial y} \tag{12.7}$$

These equations can be rewritten as

$$\frac{1}{2}\frac{\partial}{\partial x}(v_x^2) + \frac{1}{2}\frac{\partial}{\partial y}(v_x^2)\frac{dy}{dx} = -\frac{1}{\rho}\frac{\partial p}{\partial x} \tag{12.8}$$

$$\frac{1}{2}\frac{\partial}{\partial x}(v_y^2)\frac{dx}{dy} + \frac{\partial}{\partial y}(v_y^2) = -\frac{1}{\rho}\frac{\partial p}{\partial y} \tag{12.9}$$

Multiplying through equation (12.8) by dx and equation (12.9) by dy, we get

$$\frac{1}{2}\frac{\partial}{\partial x}(v_x^2)\ dx + \frac{1}{2}\frac{\partial}{\partial y}(v_x^2)\ dy = -\frac{1}{\rho}\frac{\partial p}{\partial x}\ dx \tag{12.10}$$

$$\frac{1}{2}\frac{\partial}{\partial x}(v_y^2)\ dx + \frac{1}{2}\frac{\partial}{\partial y}(v_y^2)\ dy = -\frac{1}{\rho}\frac{\partial p}{\partial y}\ dy \tag{12.11}$$

and by summing up (12.10) and (12.11)

$$\frac{1}{2}\frac{\partial}{\partial x}(v_x^2 + v_y^2)\ dx + \frac{1}{2}\frac{\partial}{\partial y}(v_x^2 + v_y^2)\ dy = -\frac{1}{\rho}\left(\frac{\partial p}{\partial x}\ dx + \frac{\partial p}{\partial y}\ dy\right) \tag{12.12}$$

Since the square of the magnitude of the velocity vector is

$$V^2 = v_x^2 + v_y^2 \tag{12.13}$$

we may write equation (12.12) as

$$\frac{1}{2}\frac{\partial}{\partial x}(V^2)\ dx + \frac{1}{2}\frac{\partial}{\partial y}(V^2)\ dy = -\frac{1}{\rho}\left(\frac{\partial p}{\partial x}\ dx + \frac{\partial p}{\partial y}\ dy\right) \tag{12.14}$$

Both sides of the above equation represent total differentials and may be put in the form

$$d\left(\frac{V^2}{2}\right) = -\frac{1}{\rho}\ dp \tag{12.15}$$

$$d\left(\frac{V^2}{2} + \frac{p}{\rho}\right) = 0 \tag{12.16}$$

Consequently, we have

$$\frac{V^2}{2} + \frac{p}{\rho} = \text{const} \tag{12.17}$$

This is the simple form of the Bernoulli equation, which was derived by a somewhat different method in Section 11.2. It is important to note that the Bernoulli equation is an algebraic relation between pressure and velocity along a streamline. It implies that the velocity is greatest where the pressure is least.

12.3 PRESSURE DISTRIBUTION AROUND AN AIRFOIL

The boundary layer formed around an airfoil has a very small thickness as compared to the airfoil dimensions (much smaller than what is shown in Fig. 12.1). Thus, we may apply the Bernoulli equation along the "edge" of the boundary and get roughly the same qualitative results as if the application were made on the airfoil surface. For the streamline patern of Fig. 12.1, the flow velocity over the top is larger than the velocity along the bottom because of the longer fluid particle trajectories over the top. The Bernoulli equation would then give a larger pressure on the bottom than on the top. Consequently, a force perpendicular to the flow direction is produced, which is called lift. To calculate this force we must integrate the normal pressure force on the body over its surface, as it was done in Section 11.6.

Let us now examine the pressure gradient along the curved surface ABC in Fig. 12.1. From A to B, the velocity is increasing, therefore the pressure is decreasing. This means that the outside inviscid flow produces a pressure gradient in the direction of motion. From B to C, the velocity is decreasing, therefore the pressure is increasing. This means that the outside inviscid flow produces a pressure gradient against the direction of motion (usually called adverse pressure gradient).

In the boundary layer from B to C the fluid flows from left to right and it is opposed by the externally imposed (adverse) pressure gradient. Thus, the flow in the boundary layer decelerates, may be brought to a halt and gradually reverse in direction as shown (in an exaggerated way) in Fig. 12.2. This phenomenon is known as boundary layer separation. The region of reverse eddying flow is called the wake.

It is interesting to compare the boundary layer separation between laminar and turbulent flow conditions. As shown schematically in Fig. 12.3 the velocity profiles are more "flat" for turbulent flow. Thus for turbulent flow, a longer distance from the leading edge would be required for the flow to be reversed and for the boundary layer to separate than for laminar flow conditions. The wake would be larger for laminar separated boundary layer than for a turbulent one as shown in Fig. 12.3.

It should be pointed out that if the flow is slow the boundary layer may not separate at all. Separation occurs in relatively high speed flow and with surface curvatures such that a large enough adverse pressure gradient can be generated.

12.4 FRICTION AND FORM DRAG

The total resistance to steady rectilinear motion of a body immersed in a fluid will consist of two parts: The resistance due to the friction at the wall (friction drag) and the loss of momentum due to the disturbance of the streamline pattern, called form or shape drag (because of its dependence on the shape of the body).

The frictional drag can be calculated from

$$F = \tau_w A_w = \mu \left(\frac{\partial v_x}{\partial y}\right)_{y=0} A_w \tag{12.18}$$

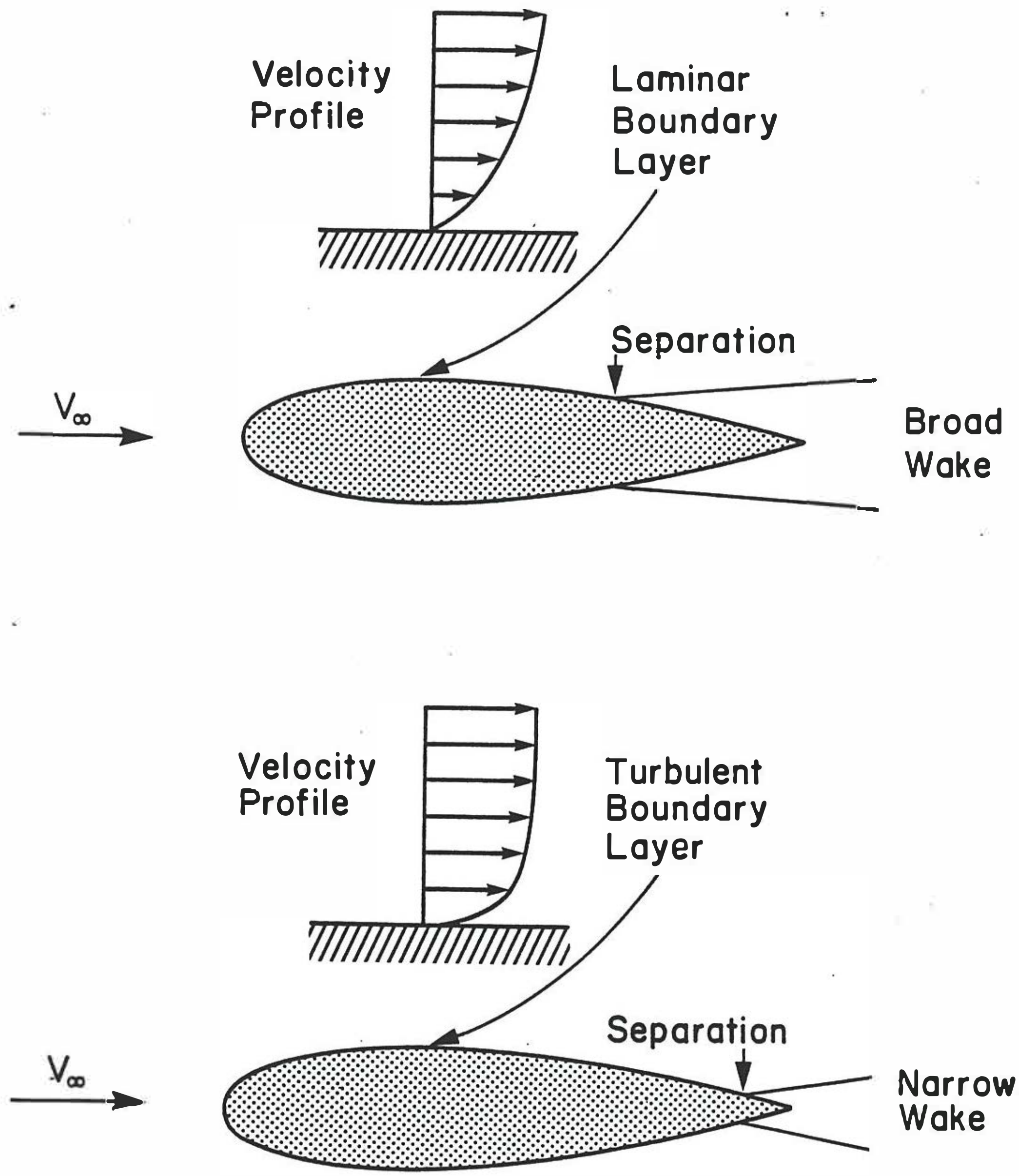

Fig. 12.3 Comparison of laminar and turbulent boundary layer separation.

where τ_w is the shear stress at the wall, μ the viscosity of the fluid $(\partial v_x/\partial y)_{y=0}$ the velocity gradient at the wall and A_w the wall area in contact with the fluid.

The form drag for slow viscous flow can be determined by integrating the component of pressure force in the main flow direction as it was done in Section 8.4. However, for high speed flow separation occurs and the form drag increases with the size of the wake, which is difficult to describe mathematically. For very high speed flow the total resistance is mainly due to form drag, the friction drag being negligible. The opposite is true for very slow flow, which can occur without boundary layer separation.

The streamlining of a body has a great influence on drag. The streamlined body and the wire shown in Fig. 12.4 are sketched to scale and both exhibit approximately the same drag (!) in high speed cross flow, despite the great difference in surface and cross sectional areas. The cylinder and the streamlined body of Fig. 12.5 have the same cross-sectional areas perpendicular to the flow direction. In high speed flow the streamlined body exhibits much lower drag than the cylinder because the wake formed behind it is smaller. The opposite is true for very low speed flow. At very low speeds there is no boundary layer separation and the total resistance is mainly due to friction drag which is proportional to the surface area of the body.

Fig. 12.6 shows the wakes formed behind two equal diameter spheres in high speed flow (same Re_D). One of the spheres has a smooth surface while the other a rough one. Separation of a laminar boundary layer occurs at about 82° from the horizontal for the smooth sphere. However, the enhanced turbulence created by the surface irregularities forces the

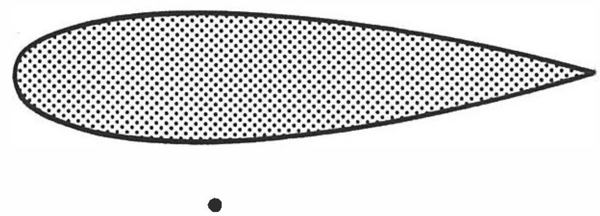

Fig. 12.4 Relative size of a streamlined body and a wire having the same drag in cross flow at high speed.

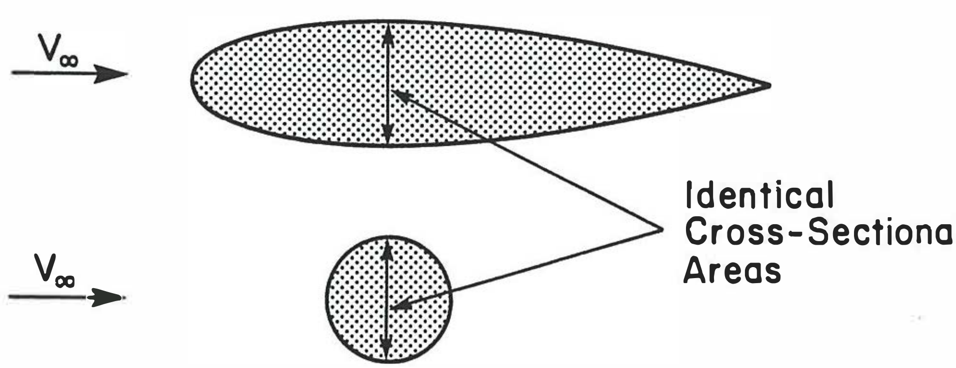

Fig. 12.5 A streamlined body and a cylinder having the same frontal areas in cross flow.

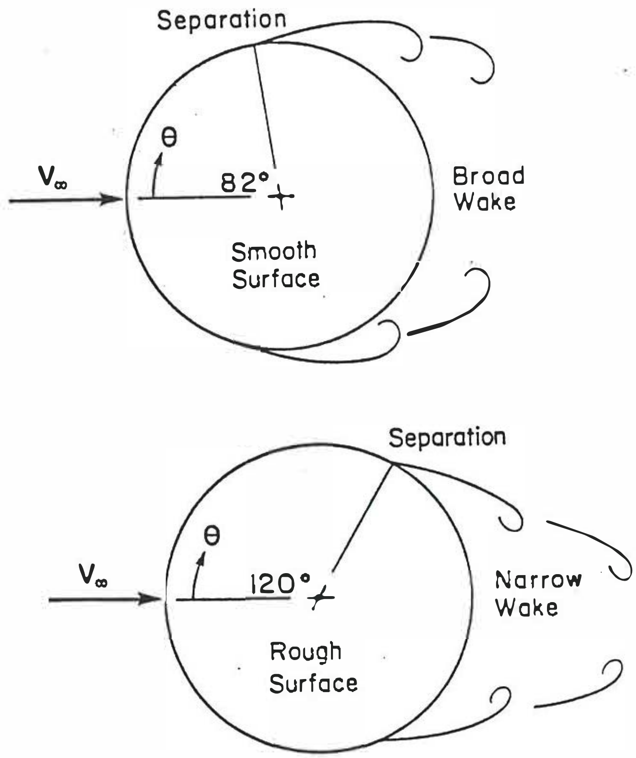

Fig. 12.6 Wake formation behind spheres in high speed flow.

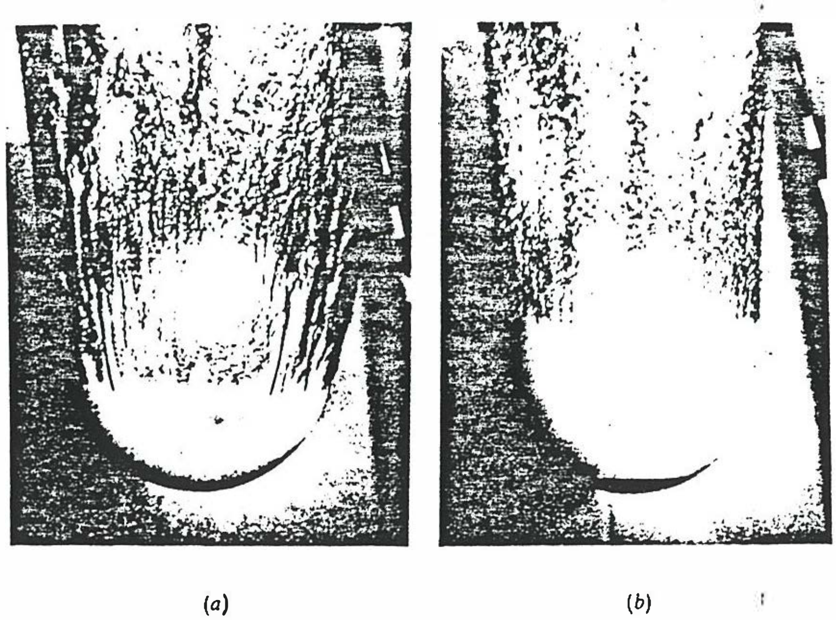

Fig. 12.7 Photographs showing the wakes formed behind (a) a smooth bowling ball, and (b) a bowling ball with a roughened nose patch (U.S. Navy photgraphs, Ordnance Test Station, Pasadena annex).

separation point to move back to something like 120° (see also Fig. 12.7). The rough sphere, therefore, exhibits much smaller (about four times) resistance to flow than the smooth one. This explains why golf balls are manufactured with various designs of dimples on the surface.

The total drag on immersed bodies usually expressed in terms of the drag coefficient C_D as follows

$$F_D = C_D \rho \frac{V^2}{2} A \tag{12.19}$$

where ρ is the density of the fluid, V the flow velocity and A the projected area of the body normal to the flow (i.e. the frontal area). The drag coefficient can be determined from the solution of the Navier-Stokes equations for certain simple geometrical shapes like spheres and cylinders at relatively low Reynolds numbers Re_D (see Section 8.4 and references [1] and [2]). For most shapes, however, the drag coefficient is determined experimentally by placing the object in a wind or water tunnel and measuring the resistance as a function of Re_D. Fig. 12.8 gives C_D for two-dimensional and Fig. 12.9 for three-dimensional bodies. Some additional C_D values are given in Table 12.1.

In recent years a considerable effort has been made by the world's major automakers to reduce the drag of automobiles by streamlining the body (see Fig. 12.10) and consequently to reduce the fuel consumption. Some modern car designs exhibit drag coefficients which might be as low as 0.3. Fuel savings are significant at higher speeds because the drag increases with the square of the speed while the rolling resistance increases linearly with speed. According to White [3] when a typical tractor-trailer travels at a speed of 90 Km/hr the total power is

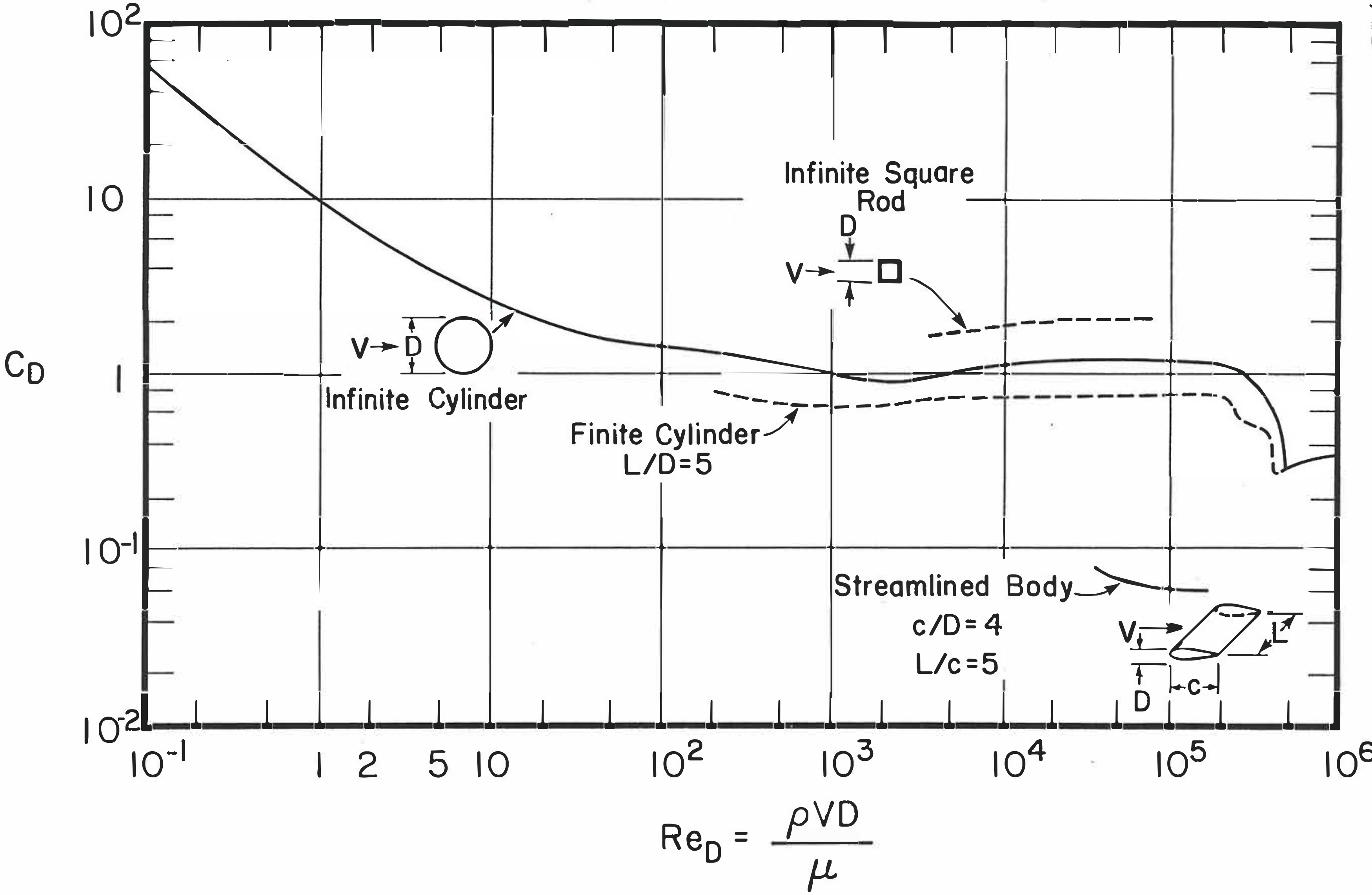

Fig. 12.8 The drag coefficient for two-dimensional bodies.

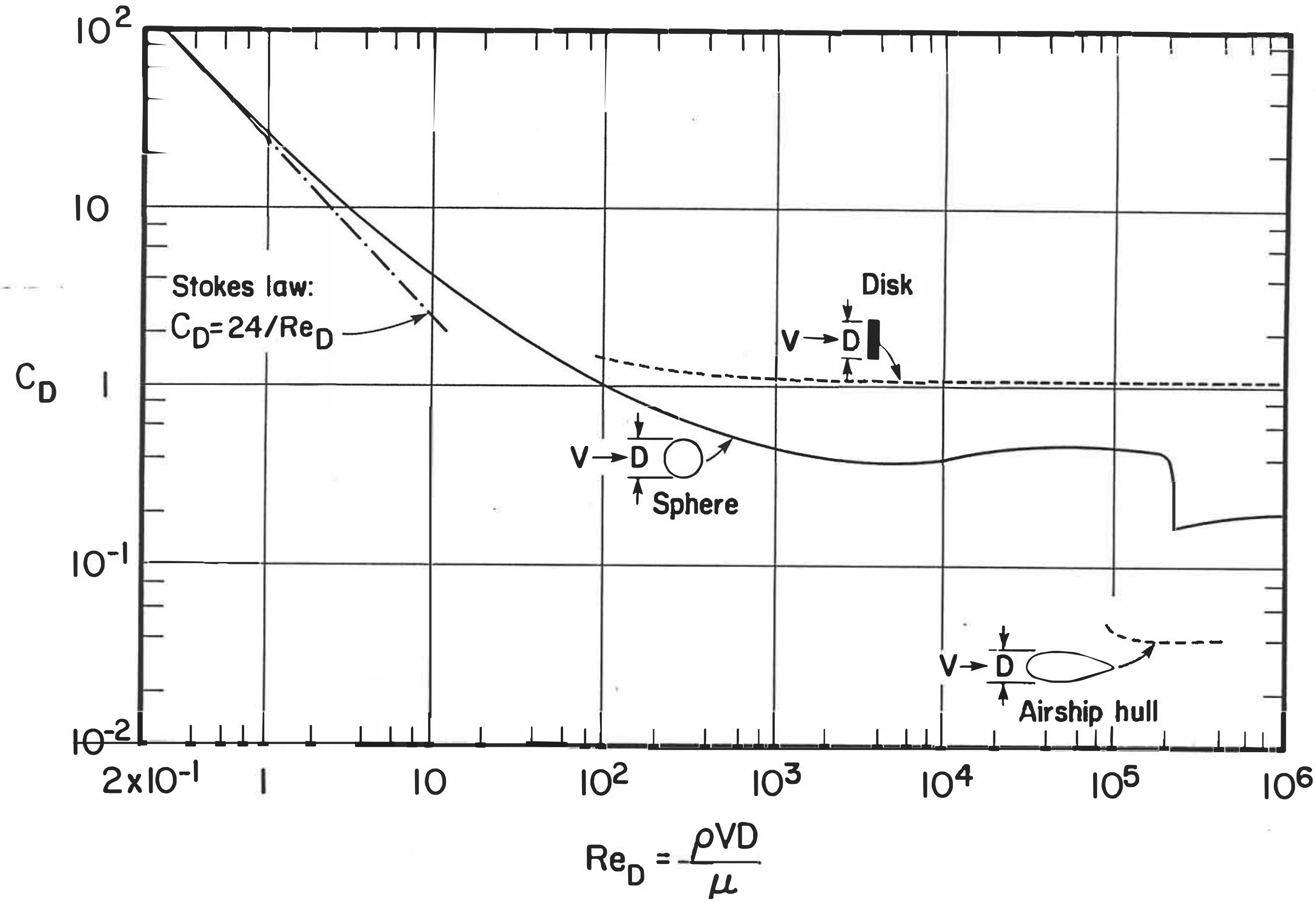

Fig. 12.9 The drag coefficient for three-dimensional bodies (For Stokes law, see Section 8.4).

Table 12.1 Approximate Drag Coefficients for Re > 10^4

Shape	C_D Based on Frontal Area
square rod	2.00
square rod	1.50
60° triangular rod	1.40
60° triangular rod	2.00
Semicircular shell	1.20
Semicircular shell	2.30
Infinite flat plate	2.0
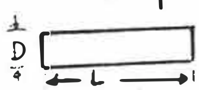 Flat plate L/D = 5	1.20
Cube	1.10
Cube	0.81
60° Cone	0.50
Ellipsoid L/D	
2	0.13
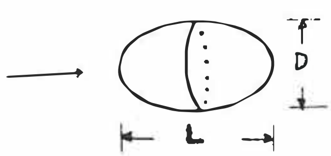 4	0.10
8	0.08
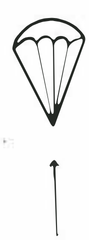 Parachute	1.2

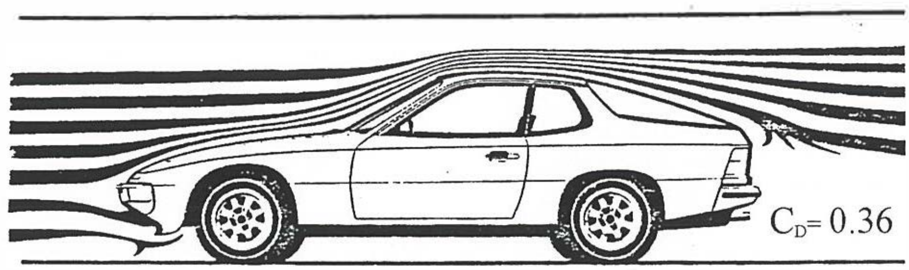

Fig. 12.10 An advertisement that appeared in a number of magazines, showing the streamlined features of a Porsche sportscar.

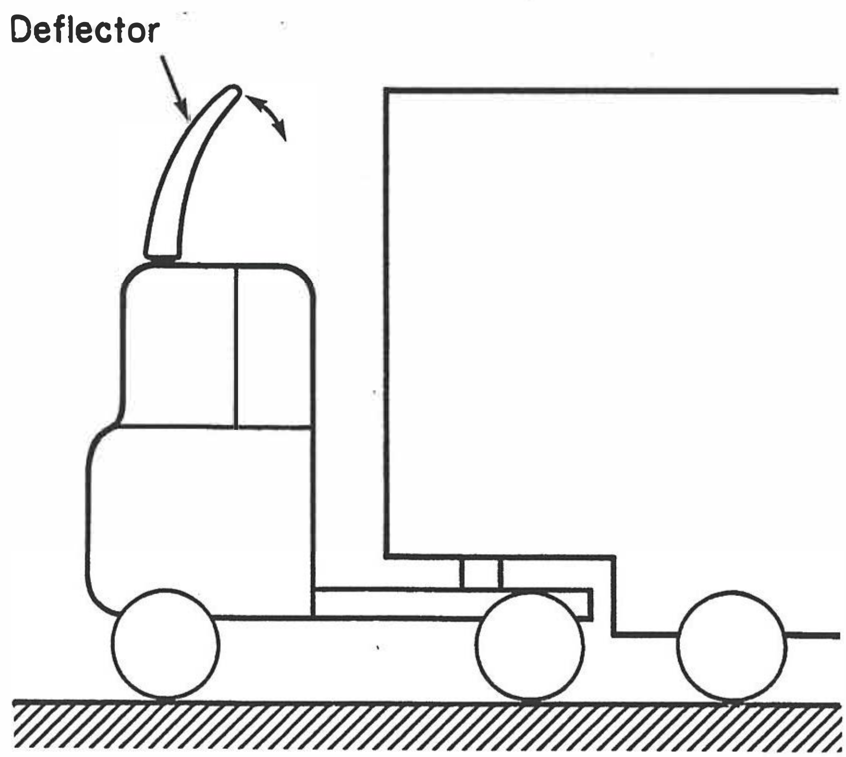

Fig. 12.11 A tractor-trailer with a deflector to reduce the air drag.

consumed about evenly by air drag and rolling resistance. Addition of a deflector (see Fig. 12.11) may reduce the air drag by up to 20% which results in reduction of total power consumption by about 10%. Additional information on drag may be found in references [3-5].

Example 12.1

An automobile with $C_D = 0.31$, $A = 2.1\ m^2$ travels at 100 km/hr. Determine the power required to overcome the air resistance (assume air density $\rho = 1.2\ kg/m^3$).

Solution

The total drag force is

$$F_D = C_D\ \rho\ \frac{V^2}{2}\ A = 0.3 \times 1.2 \times \frac{(\frac{1000}{36})^2}{2} \times 2.1 = 291.67\ N$$

Thus, the power required to overcome the air resistance can be calculated by multiplying the drag force by the velocity

$$Po = F_D \bullet V = 291.67\ \frac{1000}{36} = 8101.94\ W$$

Example 12.2

A man jumps out of an airplane at high altitude. Determine the velocity of fall at 3000 m above see level (assume $\rho = 0.909\ kg/m^3$)

(a) without having opened his parachute

(b) with a parachute open having a diameter of 6m.

Determine also the percentage of change of the speed of fall at sea level ($\rho = 1.225\ kg/m^3$). The mass of man and parachute is 90 kg.

Solution

An object falling in air, or in any other fluid, will attain its terminal velocity after an initial period of acceleration. At terminal velocity the sum of forces exerted on the object must be zero. Here we have:

$$F_{Weight} - F_{Drag} - F_{Buoyancy} = 0$$

Because the density of air is small as compared to the density of the human body, the buoyancy term is negligible and we can write

$$F_{Weight} = F_{Drag} = C_D \rho \frac{V^2}{2} A$$

$$V = \left(\frac{2\, F_{Weight}}{C_D\ \rho\ A}\right)^{1/2}$$

For the man falling without having opened his parachute we may guess a drag coefficient of $C_D \simeq 1.1$ and assume an area $A = 0.5\ m^2$. Hence

$$V = \left(\frac{2 \times 90 \times 9.81}{1.1 \times 0.909 \times 0.5}\right)^{1/2} = 59.43\ m/s\ (\text{or } 213.9\ km/hr)$$

When the parachute is open $C_D \simeq 1.2$ (from Table 12.1)

$$A = \pi \frac{D^2}{4} = \pi \frac{6^2}{4} = 28.26\ m^2$$

Thus

$$V = \left(\frac{2 \times 90 \times 9.81}{1.2 \times 0.909 \times 28.26}\right)^{1/2} = 7.57\ m/s\ (\text{or } 27.25\ km/hr)$$

This is equal to the velocity of free fall of an object from a height

$$H = \frac{V^2}{2g} = \frac{7.57^2}{2 \times 9.81} = 2.92\ m$$

At sea level the above velocities will be reduced approximately to

$(\rho/\rho_o)^{1/2} = (0.909/1.225)^{1/2} = 0.86 = 86\%$. It should be noted that in both cases the Reynolds number is sufficiently high and that validates the choice of the drag coefficients.

12.5 VORTEX SHEDDING FROM A CYLINDER IN CROSS-FLOW

The flow pattern around a cylinder in crossflow depends on the Reynolds number $Re_D = \rho VD/\mu$. At low Reynolds numbers, say $Re \leq 5$, there is no flow separation. The drag is mainly due to friction at the cylinder surface. The streamlines are regularly spaced around the cylinder as shown in Fig. 12.12 and the entire flow field is dominated by the viscous forces. As the Reynolds number increases the inertia forces become appreciable and flow separation occurs. This gives rise to the formation of a vortex pair immediately behind the cylinder and a laminar wake further downstream. At about $Re \simeq 40$, the wake develops a waviness and eventually a periodic pattern known as the Karman vortex street, after Theodore Von Karman, who presented a theoretical explanation in 1912. This pattern consists of vortices shed alternately on either side of the cylinder as shown in Fig. 12.12. The shedding frequency increases as the flow velocity increases. In the range Re_D = 150 - 300 the frequency becomes irregular because of the turbulent fluctuations which accompany the shedding of vortices. The vortex street is fully turbulent in the range $Re = 300 - 3 \times 10^5$. A substantial rearrangement of the wake and a re-establishment of a turbulent vortex street occurs at higher Reynold's numbers, as shown in Fig. 12.12.

The phenomenon of vortex shedding is not restricted to flows over cylinders, but is observed in flows over all types of blunt bodies. It

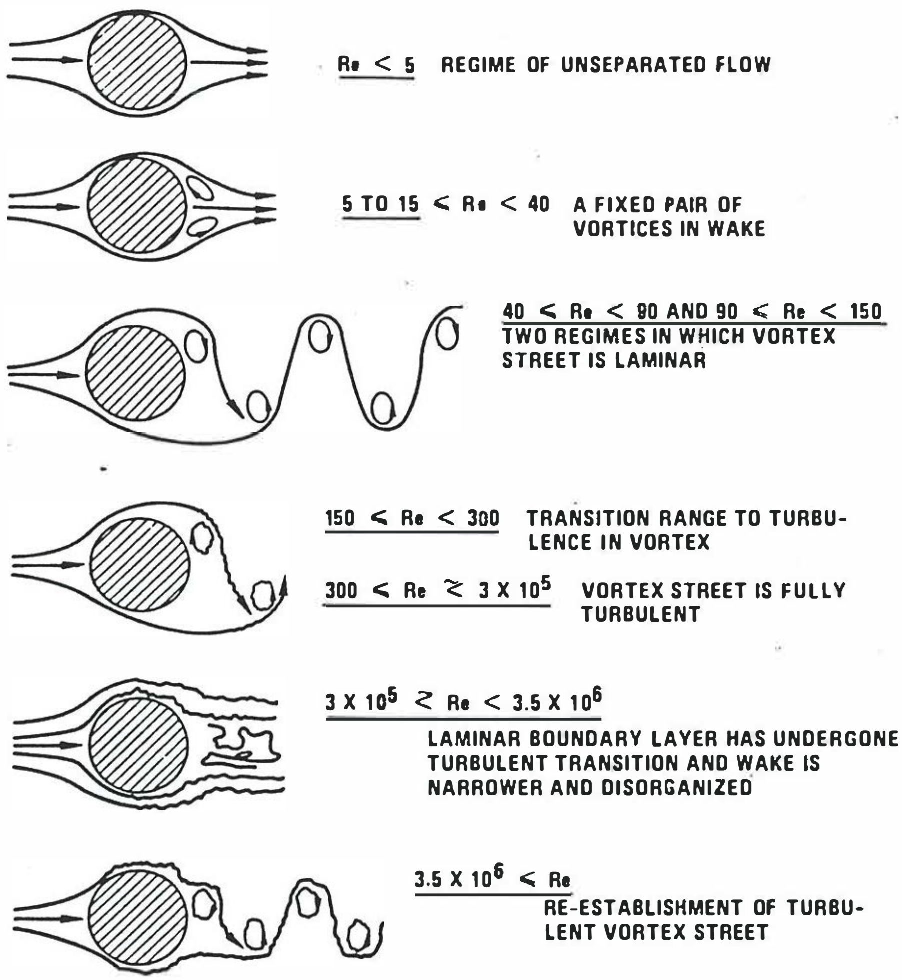

Fig. 12.12 Flow patterns around a cylinder in cross-flow according to Blevins [6].

is of major importance in engineering design because the periodic, alternate shedding of vortices produces large periodic lift forces (and smaller drag force variations). If the Reynolds number is such that the vortex shedding frequency is at the natural frequency of the body, a resonant condition will occur. This phenomenon was the primary cause of the disastrous failure of the Tacoma Narrows suspension bridge in Washington State in 1940. In addition, many failures of smokestacks and heat exchanger tubes in crossflow have been attributed to the periodicity due to vortex shedding. This phenomenon is also responsible for the "singing" of wires in the wind.

The frequency of vortex shedding is given in terms of the Strouhal number which is a dimensionless quantity defined as

$$S = \frac{fD}{V} \tag{12.20}$$

where f = frequency (cycles/second = Hz)

D = diameter of cylinder

V = free stream velocity

A plot of the Strouhal number versus the Reynolds number is given in Fig. 12.13 on the basis of a large number of literature data.

More information on flow induced variations can be found in reference [6].

12.6 APPARENT OR VIRTUAL MASS OF ACCELERATING BODIES

The force required to sustain a body in steady motion in a fluid is equal and opposite in direction to the drag force. However, to bring a body from a state of rest to a state of steady motion, the propelling force must overcome not only the fluid drag but also the inertia of the

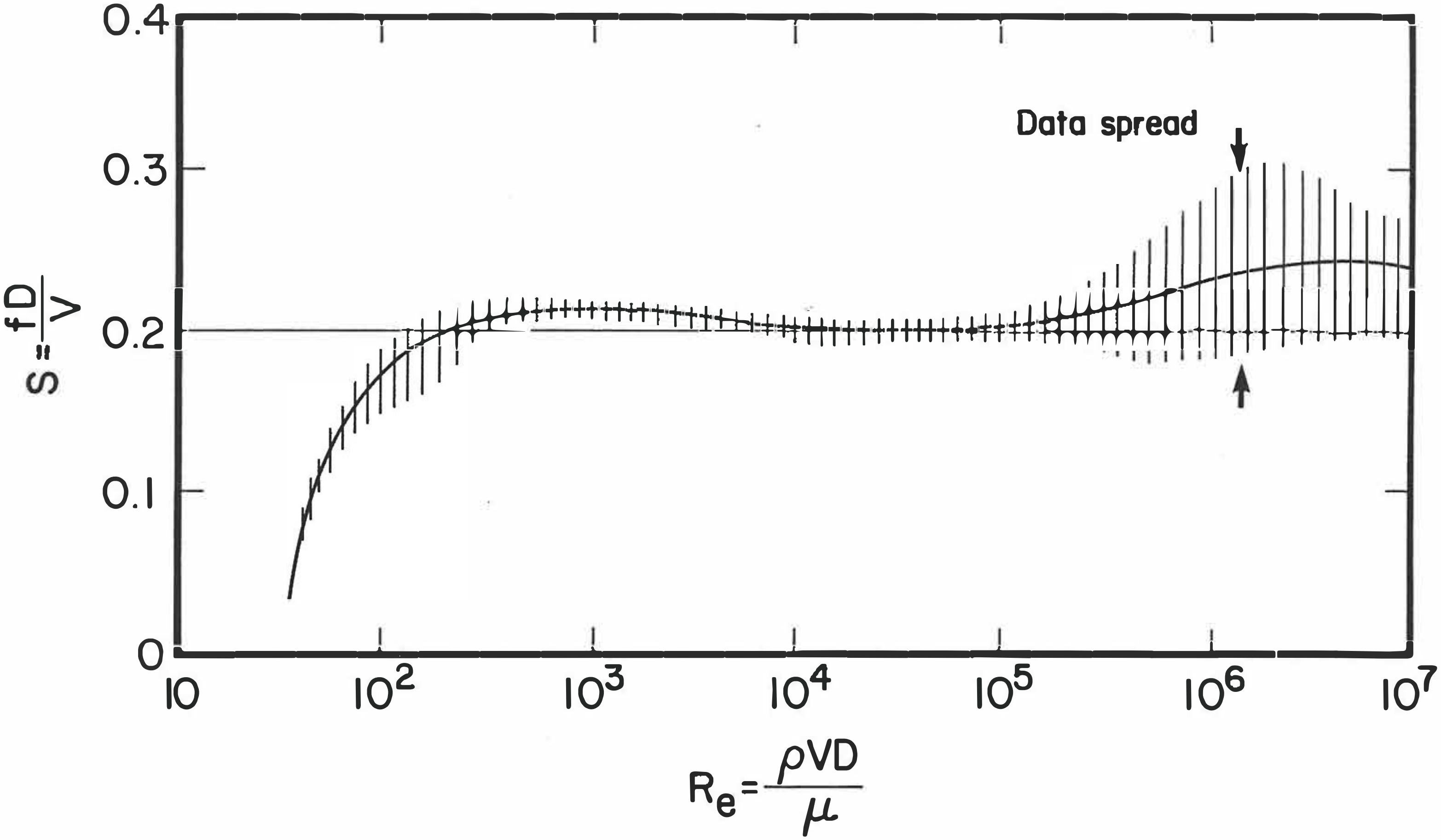

Fig. 12.13 The Strouhal number as a function of the Reynolds number for cylinders in cross-flow.

body and the inertia of any fluid set in motion. In general, the additional resistance due to an accelerating fluid can be considered as the inertia of an <u>added fluid mass</u> m_f. Thus, in accelerating motion a body of mass m_b behaves as having an <u>apparent</u> or <u>virtual mass</u> $m_b + m_f$, and Newton's second law of motion can be stated as

$$F = (m_b + m_f)\frac{d\bar{V}}{dt} \tag{12.21}$$

The added fluid mass depends only on the shape of the body, because the shape determines the quantity of fluid which can be set in motion. Obviously, a cylinder moving in the axial direction would have a different added fluid mass than when it moves in a transverse direction.

The total kinetic energy required to set a body in motion should be equal to the kinetic energy of the body plus the kinetic energy of the added fluid mass:

$$\begin{aligned} E_{total} &= E_{body} + E_{fluid} \\ &= \frac{1}{2} m_b V_\infty^2 + \frac{1}{2} m_f V_\infty^2 \end{aligned} \tag{12.22}$$

where V_∞ is the steady velocity of the body moving in an otherwise undisturbed fluid. If $\bar{V}(v_x, v_y, v_z)$ is the local fluid velocity and p the fluid density, we may write

$$E_{fluid} = \frac{1}{2} m_f V_\infty^2 = \frac{1}{2} \iiint \rho V^2 \, d\forall = \frac{1}{2} \iiint \rho(v_x^2 + v_y^2 + v_z^2)\, d\forall \tag{12.23}$$

where the integration is carried out over all the fluid affected by the motion.

For simple geometrical shapes moving in inviscid irrotational fluids the flow field is usually known. For example, for a sphere of radius R we can easily determine the velocity components from equations

(11.124) and (11.125) by subtracting the contribution of the uniform fluid stream. Thus we have

$$V^2 = v_r^2 + v_\theta^2 = V_\infty^2 \cos^2\theta \left(\frac{R}{r}\right)^6 + \frac{1}{4} V_\infty^2 \sin^2\theta \left(\frac{R}{r}\right)^6$$

$$= V_\infty^2 \left(\frac{R}{r}\right)^6 \left(\cos^2\theta + \frac{1}{4}\sin^2\theta\right) \tag{12.24}$$

An infinitesimal volume element in spherical coordinates is given by $d\forall = r^2 \sin\theta d\phi d\theta dr$, thus, we may write equation (12.23) as

$$E_{fluid} = \frac{1}{2} m_f V_\infty^2 = \frac{1}{2} \rho V_\infty^2 R^6 \int_0^{2\pi} \int_0^{\pi} \int_0^{\infty} \frac{1}{r^4} \left(\cos^2\theta \sin\theta + \frac{1}{4}\sin^3\theta\right) d\phi d\theta dr \tag{12.25}$$

Since $\cos^2\theta = 1-\sin^2\theta$, we can easily perform the integrations indicated, to get

$$E_{fluid} = \frac{1}{2} m_f V_\infty^2 = \frac{1}{2} \left(\frac{2}{3}\pi\rho R^3\right) V_\infty^2 \tag{12.26}$$

Thus, the added fluid mass of a sphere moving in an infinite fluid of density ρ is

$$m_f = \frac{2}{3}\pi\rho R^3 \tag{12.27}$$

and the apparent or virtual mass of a sphere of density ρ_b is given by

$$m_b + m_f = \frac{4}{3}\pi\rho_b R^3 + \frac{2}{3}\pi\rho R^3 \tag{12.28}$$

With a similar treatment, it can be shown that the added fluid mass of a cylinder of radius R (moving in a direction perpendicular to its axis in an infinite fluid) is

$$m_f = \pi\rho R^2 \text{ per unit length} \tag{12.29}$$

The determination of added fluid mass of bodies having sharp corners or other irregular shapes requires direct experimentation.

Mironer [6] gives an added fluid mass of $8/3\ \rho\ R^3$ of a disk of radius R moving perpendicular to its surface and $2.32\ \rho a^3$ for a cube of side a moving perpendicular to one of its surfaces. The existence of a free surface or a wall near an accelerating body has an influence on the value of the added fluid mass. The reader is referred to Mironer [6] for further details.

Example 12.3

An aluminum sphere (ρ_s = 2700 kg/m^3) of 10 cm diameter is dropped in a large water tank. Determine the terminal velocity V_T and the time required to attain it.

Solution

When the aluminum sphere moves with a constant (terminal) velocity we will have the balance of forces

$$F_{Weight} - F_{Drag} - F_{Buoyancy} = 0$$

or

$$\frac{4}{3}\rho_s g \pi R^3 - C_D \frac{1}{2}\rho_w V_t^2 A - \frac{4}{3}\rho_w g \pi R^3 = 0$$

where $A = \pi R^2$, $D = 2R$

and $$\frac{4}{3}\rho_s\ \pi R^3 - C_D \frac{1}{2}\rho_w V_t^2\ \pi R^2 - \frac{4}{3}\rho_w\ \pi R^3 = 0$$

or $$V_t = \left[\frac{g(\rho_s - \rho_w)(\frac{4}{3}D)}{C_D \rho_w}\right]^{1/2}$$

Since the drag coefficient is a function of velocity (see Fig. 12.9), we must start the calculations by making a guess, say C_D = 1.0. We have

$$V_T = \left[\frac{9.81(2700-1000)(\frac{4}{3} \times 0.1)}{1 \times 1000}\right]^{1/2} = 1.49 \text{ m/s}$$

which gives a Reynolds number

$$Re_D = \frac{\rho V D}{\mu} = \frac{1000 \times 1.49 \times 0.1}{10^{-3}} = 149,000$$

For such a Reynolds number we get, from Fig. 12.9, $C_D \simeq 0.48$. We can recalculate

$$V_T = \left[\frac{9.81(2700-1000)(\frac{4}{3} \times 0.1)}{0.48 \times 1000}\right]^{1/2} = 2.15 \text{ m/s}$$

which gives

$$Re_D = \frac{1000 \times 2.15 \times 0.1}{10^{-3}} = 215,000$$

and C_D about the same as before. Thus, no further iterations are needed.

For the initial period of acceleration we must write Newton's second law of motion, which states that the sum of forces acting on a body is equal to the mass times the acceleration, i.e.

$$F_{Weight} - F_{Drag} - F_{Buoyancy} = m \frac{dV}{dt}$$

In this case, since there is a considerable mass of water set in motion with the falling sphere, we must take into account the added mass as well. Thus, we have

$$F_{Weight} - F_{Drag} - F_{Buoyancy} = (m_s + m_f) \frac{dV}{dt}$$

where $$F_{Drag} = C_D \frac{1}{2} \rho V^2 A$$

when the sphere attains the terminal velocity $V = V_T$, $dV/dt = 0$, hence, we may rewrite the above equation as

$$C_D \frac{1}{2} \rho A (V_T^2 - V^2) = (m_s + m_f) \frac{dV}{dt}$$

Assuming that C_D is constant we may integrate with V=0 at t=0 and then rearrange to the form

$$\frac{V_T - V}{V_T + V} = \exp\left(-\frac{C_D \rho V_T A}{m_s + m_h} t\right)$$

This equation represents a familiar exponential decay, with V_T being the limiting velocity.

For $V = 0.99V_T$, we have

$$\frac{V_T - 0.99\ V_T}{V_T + 0.99\ V} = \exp\left(-\frac{C_D \rho V_T A}{m_s + m_f} t\right)$$

$$0.005 = \exp\left(-\frac{C_D \rho V_T A}{m_s + m_f} t\right)$$

and

$$t = -\frac{m_s + m_f}{C_D \rho V_T A} \ln 0.05$$

$$t = 5.29 \frac{m_s + m_f}{C_D \rho_w V_T A}$$

For a sphere, we have

$$m_s = \frac{4}{3} \pi \rho_s R^3, \quad m_f = \frac{2}{3} \pi \rho_w R^3, \quad A = \pi R^2 \text{ and } R = 2D$$

thus

$$t = 5.29 \frac{2D}{3C_D V_T} \left[\frac{\rho_s}{\rho_w} + \frac{1}{2} \right]$$

with $D = 0.1\text{m}$, $C_D \simeq 0.48$, $\rho_s = 2700\ \text{kg/m}^3$ and $\rho_w = 1000\ \text{kg/m}^3$, we get

$$t = 5.29 \frac{2 \times 0.1}{3 \times 0.48 \times 0.687} [\ 2.7 + \frac{1}{2}\ ] = 3.42\ \text{s}$$

Note that the relative contribution of the added mass is significant in this case, 1/2 versus $\rho_s/\rho_w = 2.7$.

12.7 LIFT OF AIRFOILS

From Chapter 11 it is apparent that the inviscid fluid theory does not predict a force in the main direction of the flow. This means that the drag force on an object moving in an inviscid incompressible fluid is zero (see for example Section 11.5, d'Alembert's paradox). However, the Kutta-Joukowski theorem (see Section 11.6) gives reasonably accurate values of lift by using the inviscid flow theory.

For an airfoil section like the one shown in Fig. 12.14 we define a lift coefficient C_L as

$$C_L = \frac{F_L}{\frac{1}{2}\rho V_\infty^2 A_p} \tag{12.30}$$

where F_L is the lift force (perpendicular to the main flow direction), ρ the density, V_∞ the free stream velocity and A_p the platform area, that is the area seen in plain view (equal to the product of the chord length and the span). The potential airfoil theory (see for example references [3], [7-9]) gives for an infinitely long airfoil and small angles of attack α

$$C_L = 2\pi\alpha \tag{12.31}$$

For high angles of attack, separation of flow will occur near the leading edge and that will produce deviations from this theory. Experi-

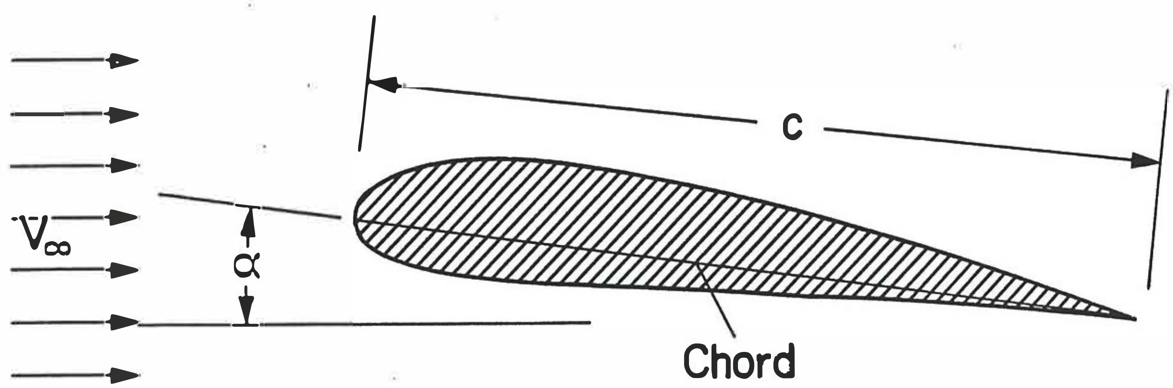

Fig. 12.14 Airfoil at an angle of attack α.

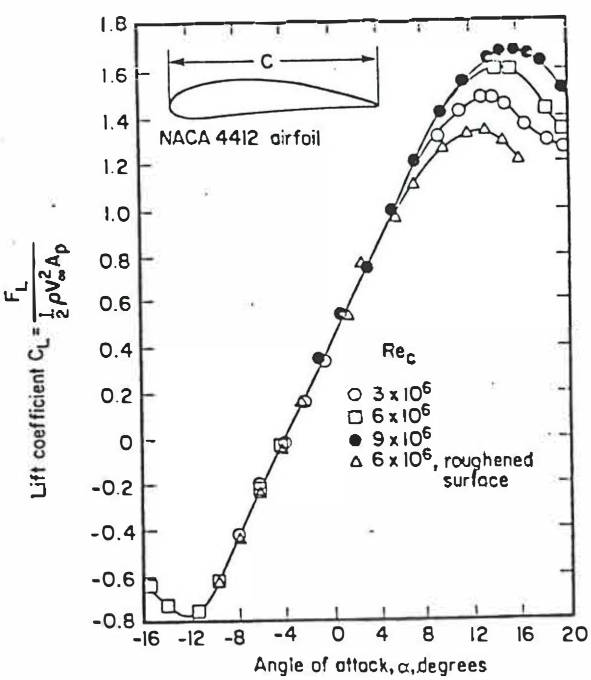

Fig. 12.15 Lift coefficient as a function of the angle of attack. (Adapted from reference [10].)

ments in a wind-tunnel are necessary to evaluate the performance of an airfoil of a given shape. For example, Fig. 12.15 shows the lift coefficient C_L as a function of the angle of attack α for various values of the Reynolds number $Re_c = \rho V_\infty c/\mu$. As the angle of attack increases the separation point moves forward towards the leading edge. At a certain angle of attack (usually between 15^o and 20^o) the flow is separated completely from the upper surface, as shown in Fig. 12.16. The lift drops off dramatically while the drag increases significantly. The airfoil is said to be stalled. The existence of a maximum in the C_L vs α curve implies the existence of a minimum speed, below which an airfoil cannot support its weight. This is the stall speed V_s and can be calculated from

$$W(\text{weight}) = F_L = C_{L,max}\left(\frac{1}{2}\rho V_s^2 A_p\right) \qquad (12.32)$$

The stall speed of aircraft usually varies between 20 and 60 m/s. Pilots are usually required to maintain a speed at least 20% greater than the stall speed to avoid the possibility of stall under any conditions.

Airfoils of finite span exhibit a reduced lift and an increased drag as a result of vortices formed at the airfoil tips. These wing-tip vortices are formed because the pressure is higher at the lower surface than at the upper one and the fluid is forced to circulate, as shown in Fig. 12.17. The lift and drag characteristics of three wing sections with aspect ratios (ℓ(span)/c(cord)) 3, 5 and 7 are shown in Fig. 12.18, according to Prandtl [12]. Using this figure we may calculate the lift with the help of equation (12.30) the drag from

$$F_D = C_D \frac{1}{2}\rho V_\infty^2 A_p \qquad (12.33)$$

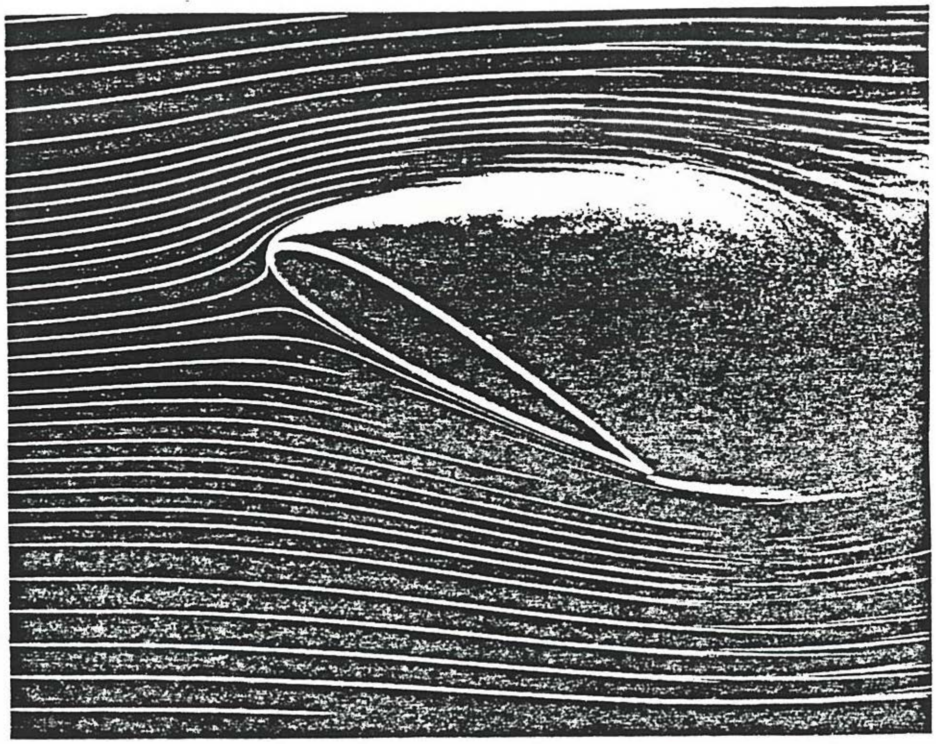

Fig. 12.16 Flow separation over the entire upper surface. The airfoil is said to be stalled. (From reference [11].)

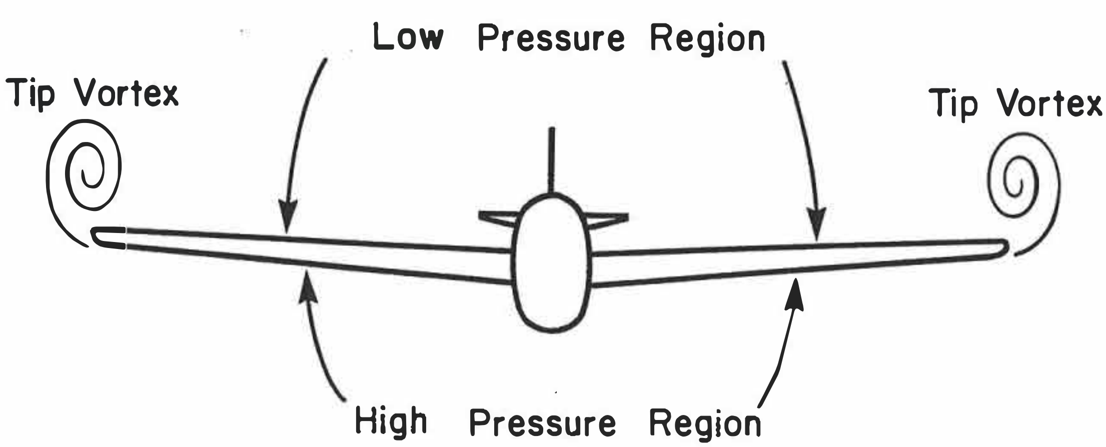

Fig. 12.17 Wing tip vortex formation.

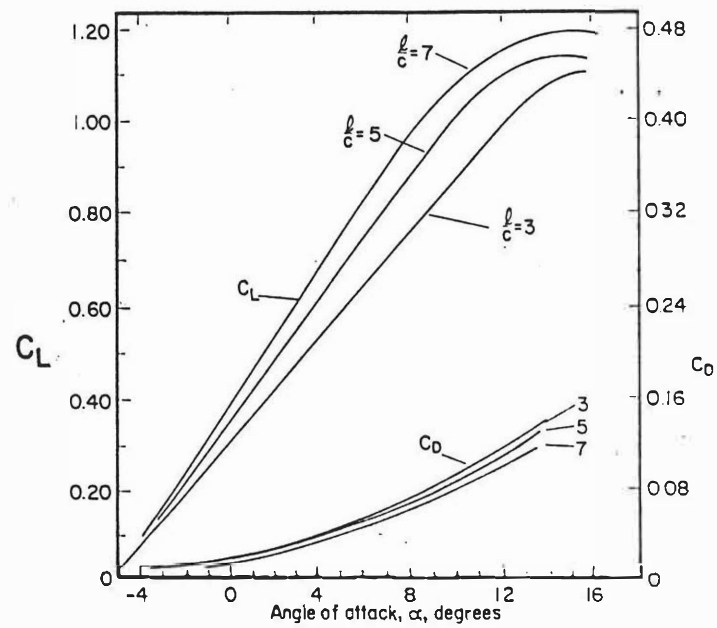

Fig. 12.18 Lift and drag coefficients for three wing sections (ℓ = span, c = cord) according to reference [12].

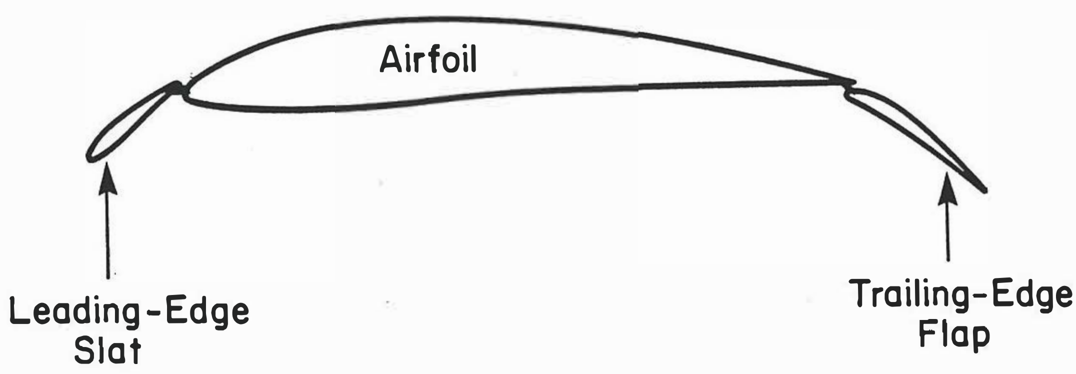

Fig. 12.19 Modern aifoil design with a leading edge slat and a trailing edge flap.

Modern airfoil designs include deflecting flaps at the trailing edge and slats at the leading edge in order to increase the lift coefficient at low speeds (see Fig. 12.19). Some modern aircraft types are equipped with wings having $C_{L,max}$ of about 3.5.

Example 12.4

A small plane weighs 2000 kg, including passengers and fuel, has a wingspan of 14 m and a chord length of 2 m. Determine the angle of attack at take-off if the take-off speed is 1.2 times the stall speed and ρ = 1.225 kg/m^3. Assume that the lift characteristics of the wing are given by Fig. 12.17.

Solution

We first calculate the stall speed, by noting that $\frac{\ell}{c} = \frac{14}{2} = 7$ and $C_{L,max} = 1.2$. We have, from equation (12.32),

$$V_s = \left(\frac{2W}{C_{L,max}\ \rho\ A_p}\right) = \left(\frac{2 \times 2000 \times 9.81}{1.2 \times 1.225 \times 28}\right)^{1/2} = 30.88 \text{ m/s}$$

According to the statement of the problem the take-off speed should be

$$V_o = 1.2\ V_s = 1.2 \times 30.88 = 37.05 \text{ m/s} = 133.4 \text{ km/hr}$$

The corresponding lift coefficient is

$$C_L = \frac{F_L}{\frac{1}{2}\rho V_o^2 A_p} = \frac{2000 \times 9.81}{\frac{1}{2} \times 1.225 \times (37.05)^2 \times 28} \simeq 0.833$$

From Fig. 12.17 we can determine the required angle of attack, about 7°.

REFERENCES

1. J. Happel and H. Brenner, "Low Reynolds Number Hydrodynamics", Noordhoff International Publishing, Leyden, The Netherlands (1973).

2. R. Cliff, J.R. Grace and W.E. Weber, "Bubbles, Drops and Particles", Academic Press, New York (1978).

3. F.M. White "Fluid Mechanics", McGraw-Hill, New York (1979).

4. J.A. Robertson and C.T. Crowe, "Engineering Fluid Mechanics", Houghton Mifflin Company, Boston (1975).

5. A. Mironer, "Engineering Fluid Mechanics", McGraw-Hill, New York (1979).

6. R.D. Blevins, "Flow-Induced Vibrations", Van Nostrand Reinhold Co., New York (1977).

7. L. Prandtl and O.G. Tietjens, "Fundamentals of Hydro- and Aero-mechanics", Dover Publications, New York (1957).

8. S. Eskinazi, "Vector Mechanics of Fluids and Magneto-Fluids", Academic Press, New York (1967).

9. I.G. Currie, "Fundamental Mechanics of Fluids, McGraw-Hill, New York (1974).

10. J. Abbot and A. van Doenhoff, "Theory of Wing Sections", Dove Publications, New York (1959).

11. National Committee for Fluid Mechanics Films, "Illustrated Experiments in Fluid Mechanics", The MIT Press, Cambridge, Mass. (1972).

12. L. Prandtl, "Applications of Modern Hydrodynamics to Aeronautics", NACA Rept. 116 (1921).

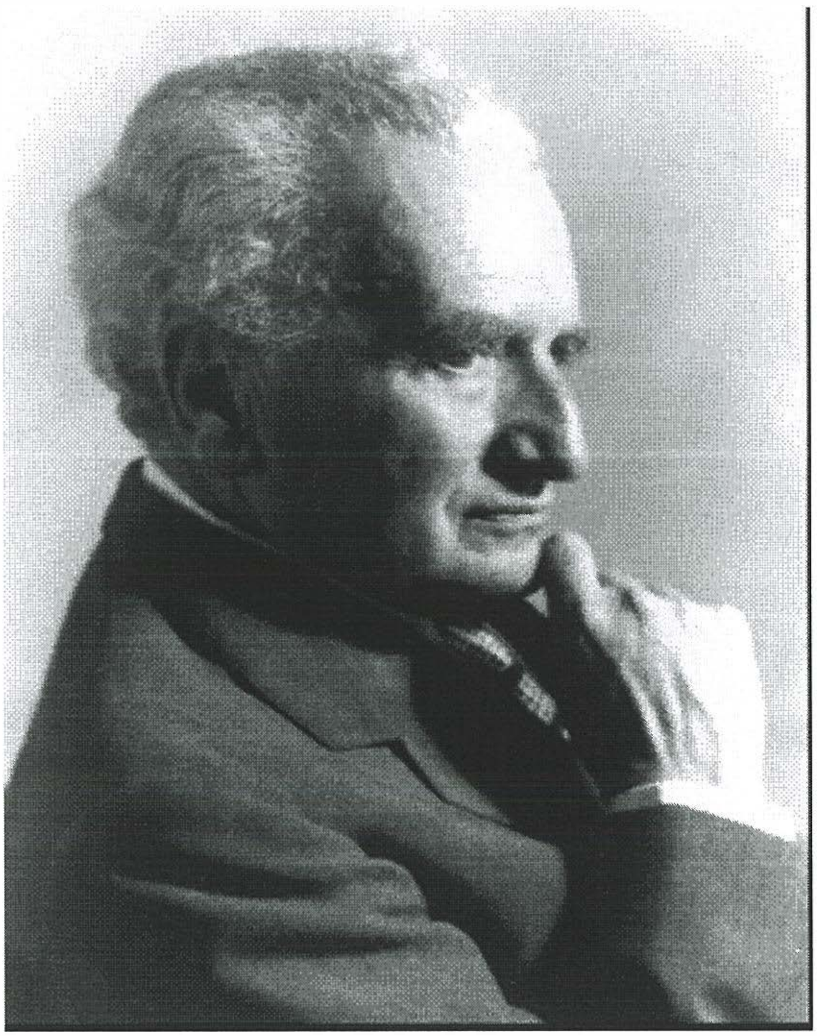

THEODORE VON KARMAN (1881-1963)

John Vlachopoulos, *Fundamentals of Fluid Mechanics*
Chem. Eng., McMaster University, Hamilton, ON, Canada
(First Edition 1984, revised internet edition (2016), www.polydynamics.com)

CHAPTER 13

CONSERVATION OF ENERGY

13.1 THE TOTAL ENERGY EQUATION

The first law of thermodynamics for a system (i.e. a material volume across whose boundaries no mass is exchanged) is usually stated as

$$\Delta E = Q - W \tag{13.1}$$

where E is the internal energy of the system, Q the heat transferred to the system and W the work done by the system to the surroundings. In some textbooks the plus sign rather than minus appears in front of W. Here, we adopted the convention that energy transfer to the body is a positive quantity.

The dynamic form of the first law of thermodynamics involves the rate of change of energy (i.e. power) and may be stated as

$$\frac{d}{dt}[\Delta E] = \frac{d}{dt}[Q] - \frac{d}{dt}[W] \tag{13.2}$$

The work is done by forces which have been identified previously as inertia forces, body forces and surface (or stress) forces. Thus, we may write

$$\frac{d}{dt}[\Delta E] = \frac{d}{dt}[Q] - \frac{d}{dt}[W_{stress}] - \frac{d}{dt}[W_{body}] - \frac{d}{dt}[W_{inertia}] \tag{13.3}$$

For a system of volume $\forall$ surrounded by a surface S, we have

$$\frac{d}{dt}[\Delta E] = \frac{d}{dt} \iiint_{\forall} \rho e d\forall \tag{13.4}$$

where ρ is the density and e the internal energy per unit mass

$$\frac{d}{dt}[W_{inertia}] = \frac{d}{dt} \iiint_{\forall} (\frac{1}{2} \rho V^2) \, d\forall \tag{13.5}$$

where $V^2 = V_1^2 + V_2^2 + V_3^2$ the velocity of the system

$$\frac{d}{dt}[W_{body}] = - \iiint_{\forall} \bar{V} \cdot (\rho \bar{g}) \, d\forall \tag{13.6}$$

where the minus sign was introduced because work is done by the external body force $\bar{g}$ <u>on</u> the system

$$\frac{d}{dt}[W_{stress}] = - \iint_{S} \bar{V} \cdot (\bar{\bar{\sigma}} \cdot \bar{n}) dS \tag{13.7}$$

again with the minus sign in front of the integral because the work is done by the surface (stress) force $\bar{\bar{\sigma}} \cdot \bar{n}$ <u>on</u> the system

$$\frac{d}{dt}[Q] = -\iint_S \bar{q}\cdot\bar{n}\, dS \tag{13.8}$$

where $\bar{q}$ is the heat flux vector given by the Fourier law of heat conduction $\bar{q} = -k\nabla T$ (k = thermal conductivity coefficient and T = temperature).

Finally, after putting the internal energy and the energy due to inertia forces under the same integral sign, the rate form of the first law of thermodynamics becomes

$$\frac{d}{dt}\iiint_{\forall} \rho(e+\frac{1}{2}V^2)\, d\forall = -\iint_S \bar{q}\cdot\bar{n}\, dS + \iint_S \bar{V}\cdot\bar{\bar{\sigma}}\cdot\bar{n}\, dS + \iiint_{\forall} \bar{V}\cdot\rho\bar{g}\, d\forall \tag{13.9}$$

Using Gauss' divergence theorem

$$\iint_S \bar{q}\cdot\bar{n}\, dS = \iiint_{\forall} (\nabla\cdot\bar{q})\, d\forall \tag{13.10}$$

$$\iint_S \bar{V}\cdot\bar{\bar{\sigma}}\cdot\bar{n}\, dS = \iiint_{\forall} \nabla\cdot(\bar{V}\cdot\bar{\bar{\sigma}})\, d\forall \tag{13.11}$$

Thus, equation (13.9) takes the form

$$\frac{d}{dt}\iiint_{\forall} \rho(e + \frac{1}{2}V^2)\, d\forall = -\iiint_{\forall}(\nabla\cdot\bar{q})\, d\forall + \iiint_{\forall} \nabla\cdot(\bar{V}\cdot\bar{\bar{\sigma}})\, d\forall + \iiint_{\forall} \bar{V}\cdot\rho\bar{g}\, d\forall \tag{13.12}$$

The total rate of change on the left hand side can be written for a control volume by using the special case of Reynolds transport theorem of example 3.1, we have

$$\frac{D}{Dt}\iiint_{\forall} \rho(e + \frac{1}{2}V^2)\, d\forall = \iiint_{\forall} \rho \frac{D}{Dt}(e + \frac{1}{2}V^2)\, d\forall \tag{13.13}$$

where D/Dt is the material derivative

$$\frac{d(\ )}{dt} = \frac{D(\ )}{Dt} = \frac{\partial(\ )}{\partial t} + \bar{V}\cdot\nabla(\ ) \qquad (13.14)$$

Equation (13.12) becomes

$$\iiint_{V} \rho \frac{D}{Dt}(e + \frac{1}{2}V^2)dV = - \iiint_{V} (\nabla\cdot\bar{q})dV + \iiint_{V} \nabla\cdot(\bar{V}\cdot\bar{\bar{\sigma}})dV + \iiint_{V} \bar{V}\cdot\rho\bar{g}\ dV \qquad (13.15)$$

Therefore

$$\rho \frac{D}{Dt}(e + \frac{1}{2}V^2) = - \nabla\cdot\bar{q} + \nabla\cdot(\bar{V}\cdot\bar{\bar{\sigma}}) + \bar{V}\cdot\rho\bar{g} \qquad (13.16)$$

The body force is usually derivable from a potential (e.g. gravity from the geopotential), therefore we may let

$$\bar{g} = - \nabla\Omega \qquad (13.17)$$

and

$$\bar{V}\cdot\rho\bar{g} = - \rho\bar{V}\cdot\nabla\Omega \qquad (13.18)$$

We note that

$$\frac{D\Omega}{Dt} = \frac{\partial\Omega}{\partial t} + \bar{V}\cdot\nabla\Omega \qquad (13.19)$$

Since the geopotential at a fixed point is independent of time

$$\rho\frac{D\Omega}{Dt} = \rho\bar{V}\cdot\nabla\Omega \qquad (13.20)$$

and equation (13.16) becomes

$$\rho \frac{D}{Dt}(e + \frac{1}{2}V^2 + \Omega) = - \nabla\cdot\bar{q} + \nabla\cdot(\bar{V}\cdot\bar{\bar{\sigma}}) \qquad (13.21)$$

The total stress tensor $\bar{\bar{\sigma}}$ is usually written as the sum of pressure and the viscous stress tensor

$$\bar{\bar{\sigma}} = - p\bar{\bar{\delta}} + \bar{\bar{\tau}} \qquad (13.22)$$

Thus, the term $\nabla\cdot(\bar{V}\cdot\bar{\bar{\sigma}})$ becomes

$$\nabla\cdot(\bar{V}\cdot\bar{\bar{\sigma}}) \Rightarrow \partial_j(V_i\ \sigma_{ij}) = V_i\ \partial_j\ \sigma_{ij} + \sigma_{ij}\ \partial_j\ V_i$$

$$= V_i\ \partial_j\ \sigma_{ji} + \sigma_{ij}\ \partial_j\ V_i$$

$$\Rightarrow \bar{V}\cdot\nabla\cdot\bar{\bar{\sigma}} + \bar{\bar{\sigma}}:\nabla\bar{V}$$

$$\Rightarrow V_i\ \partial_j\ (-p\ \delta_{ji} + \tau_{ji}) + (-p\ \delta_{ij} + \tau_{ij})\ \partial_j V_i$$

$$= -V_i\ \partial_i\ p + V_i\ \partial_j\ \tau_{ji} - p\ \partial_i\ V_i + \tau_{ij}\ \partial_j\ V_i$$

$$\Rightarrow -\bar{V}\cdot\nabla p + \bar{V}\cdot\nabla\cdot\bar{\bar{\tau}} - p\nabla\cdot\bar{V} + \bar{\bar{\tau}}:\nabla\bar{V} \qquad (13.23)$$

Equation (13.21) may now be written as

$$\rho\,\frac{D}{Dt}\,(e + \frac{1}{2}\,V^2 + \Omega) = -\nabla\cdot\bar{q} - \bar{V}\cdot\nabla p - p\nabla\cdot\bar{V} + \bar{V}\cdot\nabla\cdot\bar{\bar{\tau}} + \bar{\bar{\tau}}:\nabla\bar{V} \qquad (13.24)$$

This equation is usually known as the total energy equation. It should be noted, however, that chemical, nuclear, radiative or electromagnetic energy terms have not been included in the derivation. Such terms can be easily added in the final equation if the rate of these forms of energy generation or absorption is known.

13.2 THE MECHANICAL ENERGY EQUATION

Each term of the equation of conservation of momentum represents a force acting on a fluid particle at a point in a flow field. If we take the dot product of each term of this equation with the velocity of motion $\bar{V}$, we should get the balance of the rates of the various forms of mechanical energy (i.e. the mechanical power).

Thus, starting from the stress form of the equation of conservation of momentum, we have

$$\rho \frac{D\overline{V}}{Dt} = \nabla \cdot \overline{\overline{\sigma}} + \rho\overline{g} \tag{13.25}$$

$$\rho\overline{V} \cdot \frac{D\overline{V}}{Dt} = \overline{V} \cdot (\nabla \cdot \overline{\overline{\sigma}}) + \overline{V} \cdot \rho\overline{g} \tag{13.26}$$

$$\rho \frac{D}{Dt} (\frac{1}{2} V^2) = \overline{V} \cdot \nabla \cdot \overline{\overline{\sigma}} + \overline{V} \cdot \rho\overline{g} \tag{13.27}$$

Introducing a potential Ω ($\overline{g} = -\nabla\Omega$), as in Section 13.1 (see eq. 13.19), we get

$$\rho \frac{D}{Dt} (\frac{1}{2} V^2 + \Omega) = \overline{V} \cdot \nabla \cdot \overline{\overline{\sigma}} \tag{13.28}$$

The total stress tensor $\overline{\overline{\sigma}}$ is now written as the sum of the pressure and the viscous stress tensor $\overline{\overline{\tau}}$, i.e.

$$\overline{\overline{\sigma}} = - p\overline{\overline{\delta}} + \overline{\overline{\tau}} \tag{13.29}$$

By converting to index notation the term $\overline{V} \cdot \nabla \cdot \overline{\overline{\sigma}}$ becomes

$$\begin{aligned} \overline{V} \cdot \nabla \cdot \overline{\overline{\sigma}} &\Rightarrow V_j\, \partial_i\, \sigma_{ij} = V_j\, \partial_i\, (- p\delta_{ij} + \tau_{ij}) \\ &= - V_j\, \partial_i\, p\delta_{ij} + V_j\, \partial_i\, \tau_{ij} \\ &= - V_j\, \partial_j\, p + V_j\, \partial_i\, \tau_{ij} \\ &\Rightarrow - \overline{V} \cdot \nabla p + \overline{V} \cdot \nabla \cdot \overline{\overline{\tau}} \end{aligned} \tag{13.30}$$

Thus, equation (13.28) may be rewritten as

$$\rho \frac{D}{Dt} (\frac{1}{2} V^2 + \Omega) = - \overline{V} \cdot \nabla p + \overline{V} \cdot \nabla \cdot \overline{\overline{\tau}} \tag{13.31}$$

This is the <u>mechanical energy equation.</u>

Using the definition of material derivative and noting that $\partial\Omega/\partial t=0$, we get

$$\rho \frac{\partial}{\partial t}\left(\frac{1}{2} V^2\right) + \rho\, \bar{V}\cdot\nabla \left(\frac{1}{2} V^2 + \Omega\right) = -\, \bar{V}\cdot\nabla p + \bar{V}\cdot\nabla\cdot\bar{\bar{\tau}} \tag{13.32}$$

For steady flow and ρ = const equation (13.32) becomes

$$\bar{V}\cdot\nabla \left(\frac{1}{2}\rho V^2 + p + \rho\Omega\right) = \bar{V}\cdot\nabla\cdot\bar{\bar{\tau}} \tag{13.33}$$

If the flow is frictionless, $\bar{\bar{\tau}}=0$. Thus, equation (13.33) yields the <u>Bernoulli</u> equation

$$\frac{1}{2}\rho V^2 + p + \rho\Omega = 0 \tag{13.34}$$

which is usually written with $\Omega=gz$, where z is the height above some datum plane as

$$\frac{V^2}{2} + \frac{p}{\rho} + gz = 0 \tag{13.35}$$

13.3 THE THERMAL ENERGY EQUATION

The total energy equation was derived from the first law of thermodynamics. The mechanical energy equation was derived from Newton's second law of motion. These are, therefore, two distinct equations. By subtracting (13.31) from (13.24) we obtain the <u>thermal energy equation.</u>

$$\rho \frac{De}{Dt} = -\,\nabla\cdot\bar{q} - p\nabla\cdot\bar{V} + \bar{\bar{\tau}}:\nabla\bar{V} \tag{13.36}$$

The left-hand side $\rho De/Dt$ represents the rate of change of the internal energy, $\nabla\cdot\bar{q}$ is the rate of heat transferred by conduction, $p\nabla\cdot\bar{V}$ is the rate of compression work ($\nabla\cdot\bar{V}=0$ for incompressible fluids) and $\bar{\bar{\tau}}:\nabla\bar{V}$ is the rate of work done by the viscous stresses, usually called viscous dissipation.

Introducing the Fourier law of heat conduction

$$\bar{q} = -k\nabla T \tag{13.37}$$

we get

$$\rho \frac{De}{Dt} = k\nabla^2 T - p\nabla\cdot\bar{V} + \bar{\bar{\tau}}:\nabla\bar{V} \tag{13.38}$$

or equivalently

$$\rho \left(\frac{\partial e}{\partial t} + \bar{V}\cdot\nabla e\right) = k\nabla^2 T - p\nabla\cdot\bar{V} + \bar{\bar{\tau}}:\nabla\bar{V} \tag{13.39}$$

The last term $\bar{\bar{\tau}}:\nabla\bar{V}$ is usually written as Φ_v, where Φ_v is the viscous dissipation function. From the relation

$$\bar{\bar{\tau}}:\nabla\bar{V} = \Phi_v \tag{13.40}$$

it is easy to calculate Φ_v in terms of the components of the velocity gradient. Φ_v in rectangular, cylindrical and spherical coordinates is tabulated in Table 13.1.

Equation (13.39) can be further simplified by introducing the appropriate expressions for the internal energy e for various classes of fluids, using well-known thermodynamic relations.

For a perfect gas we have $de = C_v dT$, assuming C_v = const equation (13.39) takes the form

$$\rho C_v\left(\frac{\partial T}{\partial t} + \bar{V}\cdot\nabla T\right) = k\nabla^2 T - p\nabla\cdot\bar{V} + \Phi_v \tag{13.41}$$

For a perfect gas the specific heat under constant volume C_v and the specific heat under constant pressure are related by the expression

$$C_p - C_v = R \tag{13.42}$$

Table 13.1

THE DISSIPATION FUNCTION Φ_v FOR NEWTONIAN FLUIDS

Rectangular coordinates x, y, z

$$\Phi_v = 2\mu\left[\left(\frac{\partial v_x}{\partial x}\right)^2 + \left(\frac{\partial v_y}{\partial y}\right)^2 + \left(\frac{\partial v_z}{\partial z}\right)^2\right] + \mu\left[\left(\frac{\partial v_y}{\partial x} + \frac{\partial v_x}{\partial y}\right)^2 + \left(\frac{\partial v_z}{\partial y} + \frac{\partial v_y}{\partial z}\right)^2 + \left(\frac{\partial v_z}{\partial x} + \frac{\partial v_x}{\partial z}\right)^2\right]$$

Cylindrical Coordinates r, θ, z

$$\Phi_v = 2\mu\left[\left(\frac{\partial v_r}{\partial r}\right)^2 + \left(\frac{1}{r}\frac{\partial v_\theta}{\partial \theta} + \frac{v_r}{r}\right)^2 + \left(\frac{\partial v_z}{\partial z}\right)^2\right] + \mu\left[r\frac{\partial}{\partial r}\left(\frac{v_\theta}{r}\right) + \frac{1}{r}\left(\frac{\partial v_r}{\partial \theta}\right)\right]^2 + \mu\left[\frac{1}{r}\left(\frac{\partial v_z}{\partial \theta}\right) + \left(\frac{\partial v_\theta}{\partial z}\right)\right]^2 + \mu\left(\frac{\partial v_r}{\partial z} + \frac{\partial v_z}{\partial r}\right)^2$$

Spherical Coordinates r, θ, ϕ

$$\Phi_v = 2\mu\left[\left(\frac{\partial v_r}{\partial r}\right)^2 + \left(\frac{1}{r}\frac{\partial v_\theta}{\partial \theta} + \frac{v_r}{r}\right)^2 + \left(\frac{1}{r\sin\theta}\frac{\partial v_\phi}{\partial \phi} + \frac{v_r}{r} + \frac{v_\theta\cot\theta}{r}\right)^2\right] + \mu\left[r\frac{\partial}{\partial r}\left(\frac{v_\theta}{r}\right) + \frac{1}{r}\frac{\partial v_r}{\partial \theta}\right]^2 + \mu\left[\frac{1}{r\sin\theta}\frac{\partial v_r}{\partial \phi} + r\frac{\partial}{\partial r}\left(\frac{v_\phi}{r}\right)\right]^2 + \mu\left[\frac{\sin\theta}{r}\frac{\partial}{\partial \theta}\left(\frac{v_\phi}{\sin\theta}\right) + \frac{1}{r\sin\theta}\frac{\partial v_\theta}{\partial \phi}\right]^2$$

Multiplying through by $\rho(\frac{\partial T}{\partial t} + \bar{V}\cdot\nabla T) = \rho\,\frac{DT}{Dt}$, we get

$$\rho C_p \frac{DT}{Dt} - \rho R \frac{DT}{Dt} = \rho C_v \frac{DT}{Dt} \tag{13.43}$$

Differentiating the equation of state for a perfect gas $p = \rho RT$, we have

$$\rho R \frac{DT}{Dt} = \frac{Dp}{Dt} - \frac{p}{\rho}\frac{D\rho}{Dt} \tag{13.44}$$

With the help of the continuity equation

$$\frac{D\rho}{Dt} + \rho\nabla\cdot\bar{V} = 0 \tag{13.45}$$

we can write equation (13.44) as

$$\rho R \frac{DT}{Dt} = \frac{Dp}{Dt} + p\nabla\cdot\bar{V} \tag{13.46}$$

Then equation (13.43) becomes

$$\rho C_p \frac{DT}{Dt} - \frac{Dp}{Dt} - p\nabla\cdot\bar{V} = \rho C_v \frac{DT}{Dt} \tag{13.47}$$

Introducing the above expression in equation (13.41) we get

$$\rho C_p \left(\frac{\partial T}{\partial t} + \bar{V}\cdot\nabla T\right) = k\nabla^2 T + \left(\frac{\partial p}{\partial t} + \bar{V}\cdot\nabla p\right) + \mu\Phi_v \tag{13.48}$$

or equivalently

$$\rho C_p \frac{DT}{Dt} = k\nabla^2 T + \frac{Dp}{Dt} + \mu\Phi_v \tag{13.49}$$

for steady state

$$\rho C_p\, \bar{V}\cdot\nabla T = k\nabla^2 T + \bar{V}\cdot\nabla p + \mu\Phi_v \tag{13.50}$$

For <u>any fluid at constant pressure</u>

$$de = -\,p d\forall + C_p dT \tag{13.51}$$

and

$$\rho \frac{De}{Dt} = - p\rho \frac{D\forall}{Dt} + \rho C_p \frac{DT}{Dt}$$

$$= - p\rho \frac{D}{Dt} (\frac{1}{\rho}) + \rho C_p \frac{DT}{Dt}$$

$$= p \frac{1}{\rho} \frac{D\rho}{Dt} + \rho C_p \frac{DT}{Dt} \tag{13.52}$$

Using the continuity equation (13.45), we have

$$\rho \frac{De}{Dt} = - p\nabla \cdot \overline{V} + \rho C_p \frac{DT}{Dt} \tag{13.53}$$

Thus, equation (13.38) becomes

$$\rho C_p \frac{DT}{Dt} = k\nabla^2 T + \mu\Phi_v \tag{13.54}$$

For liquids, which are practically incompressible, we have ρ = const, $\nabla \cdot \overline{V}=0$, $C_v=C_p$ and $de = C_p dT$. Therefore, equation (13.38) can be simplified to

$$\rho C_p \frac{DT}{Dt} = k\nabla^2 T + \mu\Phi_v \tag{13.55}$$

or equivalently,

$$\rho C_p (\frac{\partial T}{\partial t} + \overline{V} \cdot \nabla T) = k\nabla^2 T + \mu\Phi_v \tag{13.56}$$

13.4 A SIMPLIFIED DERIVATION OF THE THERMAL ENERGY EQUATION FOR AN INCOMPRESSIBLE FLUID

In this section we present a derivation of the thermal energy equation by referring to a volume element $\Delta x \Delta y \Delta z$ as shown in Fig. 13.1. This derivation is in many respects similar to those presented for the conservation of mass (Section 4.1) and the conservation of momentum (Section 6.4). We first state verbally the principle of conservation of

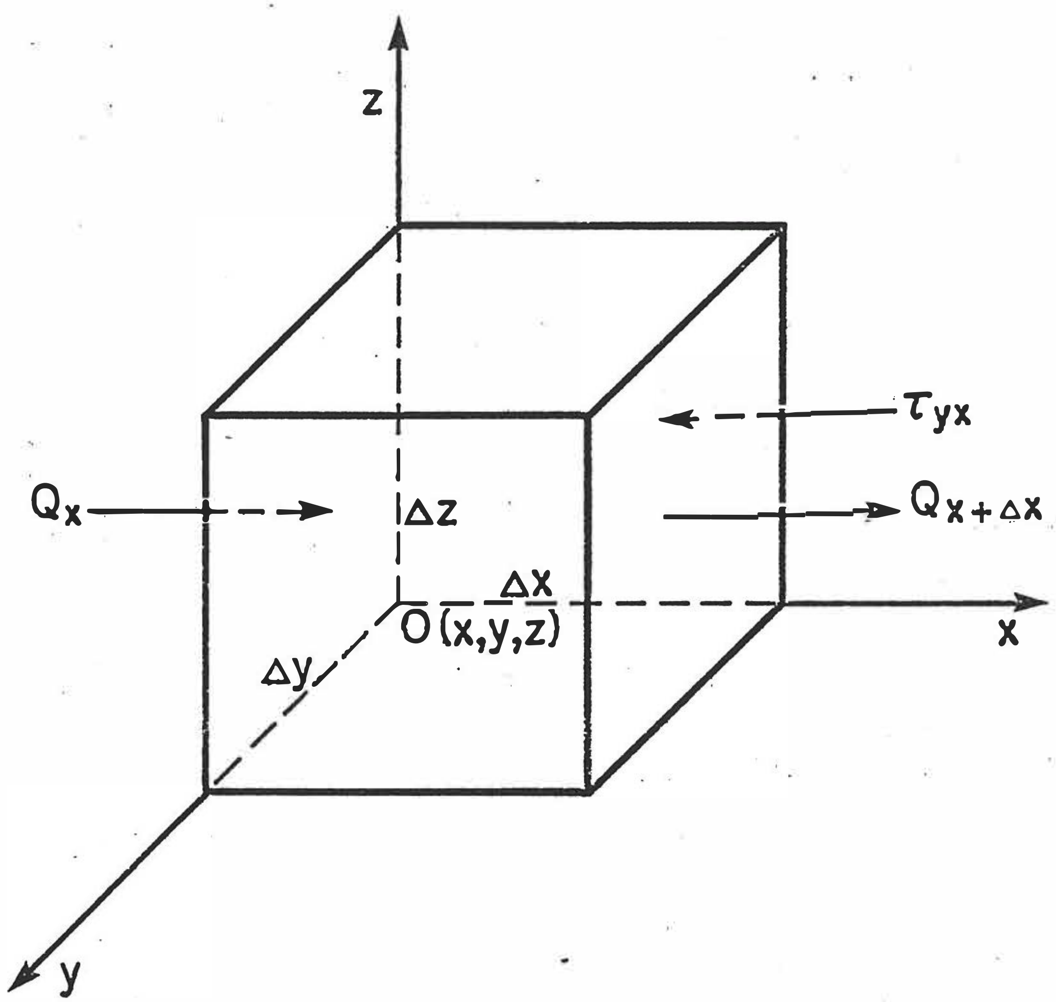

Fig. 13.1: Infinitesimal volume element in a flow field with heat transfer.

thermal energy for a control volume in a flow field as

$$\begin{matrix}\text{RATE OF} \\ \text{THERMAL ENERGY} \\ \text{ACCUMULATION}\end{matrix} = \begin{matrix}\text{RATE OF} \\ \text{THERMAL ENERGY} \\ \text{IN}\end{matrix} - \begin{matrix}\text{RATE OF} \\ \text{THERMAL ENERGY} \\ \text{OUT}\end{matrix} + \begin{matrix}\text{RATE OF} \\ \text{FRICTIONAL} \\ \text{ENERGY} \\ \text{PRODUCTION}\end{matrix} \tag{13.57}$$

The rate of energy accumulation within the volume element is

$$\frac{\partial}{\partial t}(\rho e \Delta x \Delta y \Delta z)$$

where e is the internal energy per unit mass of the fluid. Since the element has a constant volume and ρ = const, we have

$$\begin{matrix}\text{RATE OF} \\ \text{THERMAL ENERGY} \\ \text{ACCUMULATION}\end{matrix} = \Delta x \Delta y \Delta z \rho \frac{\partial e}{\partial t}$$

The energy is transferred to the volume by heat conduction (Q) and convection (Q'). With the help of the Taylor series we may write for the x direction

$$Q_{x+\Delta x} = Q_x + \frac{\partial}{\partial x}(Q_x)\ \Delta x \tag{13.58}$$

$$Q'_{x+\Delta x} = Q'_x + \frac{\partial}{\partial x}(Q_x)\ \Delta x \tag{13.59}$$

where Q_x and Q_x' represent the rates of energy in and $Q_{x+\Delta x}$, $Q'_{x+\Delta x}$ the rates of energy out of the control volume.

Using Fourier's law of heat conduction

$$Q_x = -kA\frac{\partial T}{\partial x} = -k\Delta y \Delta z\left(\frac{\partial T}{\partial x}\right) \tag{13.60}$$

the minus sign is needed because heat is conducted from higher to lower temperatures i.e. in the direction of negative temperature gradients.

The convected energy in the x direction is

$$Q_x' = \rho e v_x \Delta y \Delta z \tag{13.61}$$

Thus, we have

$$Q_x - Q_{x+\Delta x} = k \left(\frac{\partial^2 T}{\partial x^2}\right) \Delta x \Delta y \Delta z \tag{13.62}$$

$$Q_x' - Q_{x+\Delta x}' = - \rho \frac{\partial (e v_x)}{\partial x} \Delta x \Delta y \Delta z \tag{13.63}$$

Similar expressions may be derived for the energy transferred in the y and z directions, so that

$$\begin{matrix} \text{RATE OF} \\ \text{THERMAL ENERGY} \\ \text{IN} \end{matrix} - \begin{matrix} \text{RATE OF} \\ \text{THERMAL ENERGY} \\ \text{OUT} \end{matrix} =$$

$$= \left[k \left(\frac{\partial^2 T}{\partial x^2} + \frac{\partial^2 T}{\partial y^2} + \frac{\partial^2 T}{\partial z^2}\right) - \rho \left(\frac{\partial (e v_x)}{\partial x} + \frac{\partial (e v_y)}{\partial y} + \frac{\partial (e v_z)}{\partial z}\right)\right] \Delta x \Delta y \Delta z$$

$$= \left[k \left(\frac{\partial^2 T}{\partial x^2} + \frac{\partial^2 T}{\partial y^2} + \frac{\partial^2 T}{\partial z^2}\right) - \rho \left[v_x \frac{\partial e}{\partial x} + v_y \frac{\partial e}{\partial y} + v_z \frac{\partial e}{\partial z}\right.\right.$$

$$\left.\left. + e \left(\frac{\partial v_x}{\partial x} + \frac{\partial v_y}{\partial y} + \frac{\partial v_z}{\partial z}\right)\right]\right] \Delta x \Delta y \Delta z$$

$$= \left[k \left(\frac{\partial^2 T}{\partial x^2} + \frac{\partial^2 T}{\partial y^2} + \frac{\partial^2 T}{\partial z^2}\right) - \rho \left(v_x \frac{\partial e}{\partial x} + v_y \frac{\partial e}{\partial y} + v_z \frac{\partial e}{\partial z}\right)\right] \Delta x \Delta y \Delta z$$

$$= \left[k \nabla^2 T - \rho \bar{V} \cdot \nabla e\right] \Delta x \Delta y \Delta z \tag{13.64}$$

because for incompressible fluids

$$\frac{\partial v_x}{\partial x} + \frac{\partial v_y}{\partial y} + \frac{\partial v_z}{\partial z} = 0 \tag{13.65}$$

The frictional energy production is due to the stresses and is usually referred to as viscous dissipation. The rate of energy (power) is the dot product between force and velocity of a particle, i.e. $\bar{F}\cdot\bar{V}$. Thus, the rate of energy generated by a stress in the control volume of Fig. 13.1 should be given by

(STRESS)(AREA)(DIFFERENCE OF VELOCITY IN THE DIRECTION OF STRESS).

For example the rate of energy produced by the stress component τ_{yx}, should be

$$(\tau_{yx})\ \Delta x\Delta z\ (\Delta v_x) = \tau_{yx}\ \Delta x\Delta y\Delta z\ (\frac{\Delta v_x}{\Delta y}) = \tau_{yx}\ \Delta x\Delta y\Delta z\ \frac{\partial v_x}{\partial y}$$

$$= (\tau_{yx}\frac{\partial v_x}{\partial y})\ \Delta x\Delta y\Delta z = (\tau_{xy}\frac{\partial v_x}{\partial y})\ \Delta x\Delta y\Delta z \tag{13.66}$$

Thus, the rate of energy produced by all nine stresses can be written as

$$(\tau_{xx}\frac{\partial v_x}{\partial x} + \tau_{xy}\frac{\partial v_x}{\partial y} + \tau_{xz}\frac{\partial v_x}{\partial z}$$

$$+ \tau_{yx}\frac{\partial v_y}{\partial x} + \tau_{yy}\frac{\partial v_y}{\partial y} + \tau_{yz}\frac{\partial v_y}{\partial z}$$

$$+ \tau_{zx}\frac{\partial v_z}{\partial x} + \tau_{zy}\frac{\partial v_z}{\partial y} + \tau_{zz}\frac{\partial v_z}{\partial z})\ \Delta x\Delta y\Delta z$$

or in index notation as

$$\tau_{ji}\frac{\partial v_j}{\partial x_i} = \tau_{ji}\ \partial_i\ v_j \Rightarrow \bar{\bar{\tau}}:\nabla\bar{V} \tag{13.67}$$

By substituting the various expressions into the verbal statement of the principle of conservation of thermal energy, we obtain

$$\rho \left(\frac{\partial e}{\partial t} + \rho\bar{V}\cdot\nabla e\right) = k\nabla^2 T + \bar{\bar{\tau}}:\nabla\bar{V} \tag{13.68}$$

or

$$\rho \frac{De}{Dt} = k^2\nabla T + \bar{\bar{\tau}}:\nabla\bar{V} \tag{13.69}$$

This equation can also be obtained from the more general equation (13.38) by using the incompressibility condition $\nabla\cdot\bar{V} = 0$.

13.5 PROBLEM SOLVING IN NON-ISOTHERMAL NEWTONIAN FLOW

The equations of conservation of mass (continuity), momentum (Navier-Stokes) and energy (thermal) for viscous flow have been derived in Sections 4.1, 6.3 and 13.3 respectively. For a perfect gas, we may group them together as

$$\frac{\partial \rho}{\partial t} + \nabla\cdot(\rho\bar{V}) = 0 \tag{13.70}$$

$$\rho \left(\frac{\partial \bar{V}}{\partial t} + \bar{V}\cdot\nabla\bar{V}\right) = -\nabla p + \nabla\cdot\bar{\bar{\tau}} + \rho\bar{g} \tag{13.71}$$

$$\rho\, C_v\left(\frac{\partial T}{\partial t} + \bar{V}\cdot\nabla T\right) = k\nabla^2 T - p\nabla\cdot\bar{V} + \bar{\bar{\tau}}:\nabla\bar{V} \tag{13.72}$$

In rectangular coordinates with the Newtonian constitutive equation (see Section 6.5 and Chapter 17), these equations yield

$$\frac{\partial \rho}{\partial t} + \frac{\partial(\rho v_x)}{\partial x} + \frac{\partial(\rho v_y)}{\partial y} + \frac{\partial(\rho v_z)}{\partial z} = 0 \tag{13.73}$$

$$\rho \left(\frac{\partial v_x}{\partial t} + v_x \frac{\partial v_x}{\partial x} + v_y \frac{\partial v_x}{\partial y} + v_z \frac{\partial v_x}{\partial z}\right) = -\frac{\partial p}{\partial x} + \mu \left(\frac{\partial^2 v_x}{\partial x^2} + \frac{\partial^2 v_x}{\partial y^2} + \frac{\partial^2 v_x}{\partial z^2}\right)$$

$$+ \frac{1}{3}\mu \frac{\partial}{\partial x}(\nabla\cdot\bar{V}) + \rho g_x \tag{13.74}$$

$$\rho \left(\frac{\partial v_y}{\partial t} + v_x \frac{\partial v_y}{\partial x} + v_y \frac{\partial v_y}{\partial y} + v_z \frac{\partial v_y}{\partial z}\right) = - \frac{\partial p}{\partial y} + \mu \left(\frac{\partial^2 v_y}{\partial x^2} + \frac{\partial^2 v_y}{\partial y^2} + \frac{\partial^2 v_y}{\partial z^2}\right)$$

$$+ \frac{1}{3} \mu \frac{\partial}{\partial y} (\nabla \cdot \bar{V}) + \rho g_y \tag{13.75}$$

$$\rho \left(\frac{\partial v_z}{\partial t} + v_x \frac{\partial v_z}{\partial x} + v_y \frac{\partial v_z}{\partial y} + v_z \frac{\partial v_z}{\partial z}\right) = - \frac{\partial p}{\partial z} + \mu \left(\frac{\partial^2 v_z}{\partial x^2} + \frac{\partial^2 v_z}{\partial y^2} + \frac{\partial^2 v_z}{\partial z^2}\right)$$

$$+ \frac{1}{3} \mu \frac{\partial}{\partial z} (\nabla \cdot \bar{V}) + \rho g_z \tag{13.76}$$

$$\rho C_v \left(\frac{\partial T}{\partial t} + v_x \frac{\partial T}{\partial x} + v_y \frac{\partial T}{\partial y} + v_z \frac{\partial T}{\partial z}\right) = k \left(\frac{\partial^2 T}{\partial x^2} + \frac{\partial^2 T}{\partial y^2} + \frac{\partial^2 T}{\partial z^2}\right)$$

$$- p \left(\frac{\partial v_x}{\partial x} + \frac{\partial v_y}{\partial y} + \frac{\partial v_z}{\partial z}\right)$$

$$+ 2\mu \left[\left(\frac{\partial v_x}{\partial x}\right)^2 + \left(\frac{\partial v_y}{\partial y}\right)^2 + \left(\frac{\partial v_z}{\partial z}\right)^2\right] + \mu \left[\left(\frac{\partial v_y}{\partial x} + \frac{\partial v_x}{\partial y}\right)^2 + \left(\frac{\partial v_z}{\partial y} + \frac{\partial v_y}{\partial z}\right)^2\right.$$

$$\left. + \left(\frac{\partial v_z}{\partial x} + \frac{\partial v_x}{\partial z}\right)^2 \right] \tag{13.77}$$

Thus, we have five equations and five unknowns (v_x, v_y, v_z, p and T). The density ρ might also be considered as an unknown. Then the equation of state $\rho=\rho(p,T)$ is necessary as the sixth equation.

For steady, incompressible (ρ=const, $C_p=C_v$), two-dimensional boundary layer flow, we may apply the order of magnitude approximations of Chapter 9 to reduce the equations to

$$\frac{\partial v_x}{\partial x} + \frac{\partial v_y}{\partial y} = 0 \tag{13.78}$$

$$\rho \left(v_x \frac{\partial v_x}{\partial x} + v_y \frac{\partial v_x}{\partial y}\right) = - \frac{\partial p}{\partial x} + \mu \frac{\partial^2 v_x}{\partial y^2} + \rho g_x \tag{13.79}$$

$$\rho\, C_p(v_x \frac{\partial T}{\partial x} + v_y \frac{\partial T}{\partial y}) = k \frac{\partial^2 T}{\partial x^2} + \mu\, (\frac{\partial v_x}{\partial y})^2 \qquad (13.80)$$

More details on the above approximation may be found in Schlichting's standard reference [1], as well as in textbooks on heat transfer [2-5]. It should be noted, however, that the viscous dissipation term reduces to just the one term involving the main velocity gradient squared ($\mu\,(\partial v_x/\partial y)^2$), for many types of two-dimensional flow problems.

Temperature gradients may be large enough to cause significant density differences which induce fluid flow due to buoyancy forces (natural or free convection). For such problems the incompressible continuity equation is usually a valid approximation even though the density is not constant. The gravity term ρg_x must now include the buoyancy forces caused by the temperature difference and is thus replaced by $\rho g_x \beta(T-T_o)$. β is the volume expansion coefficient of the fluid ($\beta=1/T$ for a perfect gas) and T_o a reference temperature usually taken at the edge of the boundary layer. Thus, we have

$$\frac{\partial v_x}{\partial x} + \frac{\partial v_y}{\partial y} = 0 \qquad (13.81)$$

$$\rho\,(v_x \frac{\partial v_x}{\partial x} + v_y \frac{\partial v_x}{\partial y}) = -\frac{\partial p}{\partial x} + \mu \frac{\partial^2 v_x}{\partial y^2} + \rho g_x \beta(T-T_o) \qquad (13.82)$$

$$\rho\, C_p\,(v_x \frac{\partial T}{\partial x} + v_y \frac{\partial T}{\partial y}) = k \frac{\partial^2 T}{\partial y^2} + \mu\, (\frac{\partial v_x}{\partial y})^2 \qquad (13.83)$$

Example 13.1

Determine the temperature distribution due to viscous dissipation in a highly viscous liquid occupying the gap between two flat plates one of which is stationary while the other moves at a constant velocity as shown in Fig. E13.1(a).

Solution

The isothermal drag flow problem was examined in Section 7.5. The continuity and momentum equations (13.78) and (13.79) reduce to

$$\frac{d^2 v_x}{dy^2} = 0$$

which gives the linear velocity profile (see Fig. E13.1(a)).

$$v_x = \frac{V}{b} y$$

The equation of energy (13.80) can be easily simplified to the form

$$\rho \, C_p \, v_x \frac{\partial T}{\partial x} = k \frac{\partial^2 T}{\partial y^2} + \mu \left(\frac{\partial v_x}{\partial y}\right)^2$$

If the temperature does not vary in the direction of flow, we have

$$0 = k \frac{\partial^2 T}{\partial y^2} + \mu \left(\frac{\partial v_x}{\partial y}\right)^2$$

From the velocity profile we get the velocity gradient

$$\frac{\partial v_x}{\partial y} = \frac{V}{b}$$

and

$$0 = k \frac{\partial^2 T}{\partial y^2} + \mu \left(\frac{V}{b}\right)^2$$

The temperature boundary conditions are

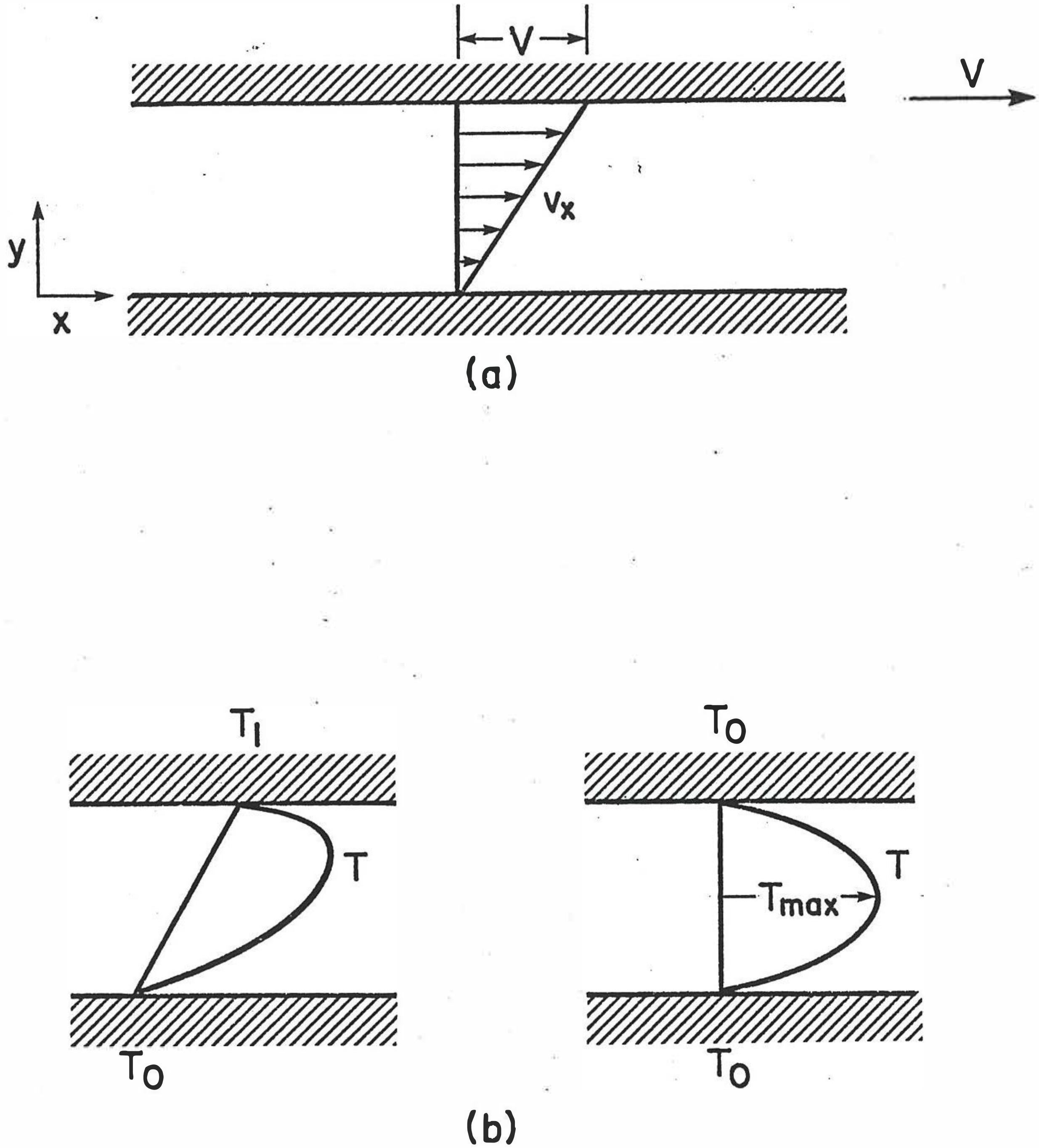

Fig. E13.1 Drag flow between two flat plates (a) velocity profile and (b) temperature profiles.

$$\text{B.C.1} \quad y=0 \quad T=T_0$$

$$\text{B.C.2} \quad y=b \quad T=T_1$$

After integrating twice and determining the integration constants we get

$$T = T_0 + \frac{T_1 - T_0}{b} y + \frac{\mu}{2k} \left(\frac{V}{b}\right)^2 y(b-y)$$

Some typical temperature profiles are sketched in Fig. 13.2(b). For the case $T_0 = T_1$ the maximum temperature occurs at $y = b/2$

$$T_{max} = T_0 + \frac{\mu}{8k} V^2$$

Assuming that the liquid is a molten plastic with $\mu = 2500$ Pa•s, $k = 0.18$ W/m•K, and $V = 10$ cm/s, we calculate the maximum temperature rise due to viscous dissipation as

$$\Delta T_{max} = T_{max} - T_0 = \frac{\mu}{8k} V^2$$

$$= \frac{2500 \text{ N} \cdot \text{s m}^{-2}}{8(0.18 \text{ N} \cdot \text{s}^{-1} \text{K}^{-1})} (0.1 \text{ m} \cdot \text{s}^{-1})^2 = 17.4^{\circ}\text{C}$$

13.6 THE DIMENSIONLESS GROUPS OF HEAT TRANSFER

Many nonisothermal laminar flow problems can be analyzed by starting from equations (13.81), (13.82) and (13.83) which are rewritten here for convenience

$$\frac{\partial v_x}{\partial x} + \frac{\partial v_y}{\partial y} = 0 \qquad (13.84)$$

$$\rho \left(v_x \frac{\partial v_x}{\partial x} + v_y \frac{\partial v_x}{\partial y}\right) = -\frac{\partial p}{\partial x} + \mu \frac{\partial^2 v_x}{\partial y^2} + \rho\, g_x\, \beta(T - T_o) \qquad (13.85)$$

$$\rho\, C_p \left(v_x \frac{\partial T}{\partial x} + v_y \frac{\partial T}{\partial y}\right) = k \frac{\partial^2 T}{\partial y^2} + \mu \left(\frac{\partial v_x}{\partial y}\right)^2 \qquad (13.86)$$

We introduce the following dimensionless variables

$$x^* = x/L$$

$$y^* = y/L$$

$$v^* = v/V$$

$$p^* = p/\rho V^2 \tag{13.87}$$

$$T^* = \frac{T - T_o}{T_w - T_o} = \frac{T - T_o}{\Delta T}$$

where L, V, T_o and T_w are characteristic flow parameters.

The dimensionless equations are

$$\frac{\partial v_x^*}{\partial x^*} + \frac{\partial v_y^*}{\partial y^*} = 0 \tag{13.88}$$

$$v_x^* \frac{\partial v_x^*}{\partial x^*} + v_y^* \frac{\partial v_x^*}{\partial y^*} = - \frac{\partial p^*}{\partial x^*} + \frac{1}{Re} \frac{\partial^2 v_x^*}{\partial y^{*2}} + \frac{Gr}{Re^2} \tag{13.89}$$

$$v_x^* \frac{\partial T^*}{\partial x^*} + v_y^* \frac{\partial T^*}{\partial y^*} = \frac{1}{Pr\ Re} \frac{\partial^2 T^*}{\partial y^{*2}} + E_c \frac{1}{Re} \left(\frac{\partial v_x^*}{\partial y^*}\right)^2 \tag{13.90}$$

where

$$Re = \frac{\rho VL}{\mu} \qquad \text{(REYNOLDS NUMBER)} \tag{13.91}$$

$$Pr = \frac{\mu C_p}{k} \qquad \text{(PRANDTL NUMBER)} \tag{13.92}$$

$$Gr = \frac{g\beta L^3 \Delta T}{\nu^2} \qquad \text{(GRASHOF NUMBER)} \tag{13.93}$$

$$Ec = \frac{V^2}{C_p \Delta T} \qquad \text{(ECKERT NUMBER)} \tag{13.94}$$

$$Pr\ Re = Pe = \frac{\rho\ C_p\ VL}{k} \qquad \text{(PECLET NUMBER)} \tag{13.95}$$

In Section 6.8 we showed that the Reynolds number represents the ratio of inertia over viscous forces. With similar arguments it is easy to show that

$$\frac{Gr}{Re^2} = \frac{\text{BUOYANCY FORCES}}{\text{INERTIA FORCES}} \tag{13.96}$$

$$Pe = Pr\ Re = \frac{\text{HEAT TRANSFERRED BY CONVECTION}}{\text{HEAT TRANSFERRED BY CONDUCTION}} \tag{13.97}$$

$$Pr\ Ec = \frac{\text{HEAT PRODUCTION BY VISCOUS DISSIPATION}}{\text{HEAT TRANSFERRED BY CONDUCTION}} \tag{13.98}$$

This last grouping is called the BRINKMAN NUMBER [6]

$$Br = Pr\ Ec = \frac{\mu V^2}{gk(\Delta T)} \tag{13.99}$$

The Prandtl number is often written as the ratio of kinematic viscosity ($\nu = \mu/\rho$) over thermal diffusivity ($\alpha = k/\rho C_p$)

$$Pr = \frac{C_p \mu}{k} = \frac{\nu}{\alpha} \tag{13.100}$$

In heat transfer calculations between fluids and solids a heat transfer coefficient h is used, which is defined by the equation

$$h\Delta T = -k\left(\frac{\partial T}{\partial y}\right)_{y=0} \tag{13.101}$$

where $(\partial T/\partial y)_{y=0}$ is the temperature gradient in the fluid evaluated at the fluid-solid interface. The heat transferred to (or from) the fluid is calculated from

$$Q = hA(\Delta T) \tag{13.102}$$

where A is the area of contact and ΔT a suitable temperature difference between solid and fluid. The heat transfer coefficient is often expressed in dimensionless form as

$$Nu = \frac{hL}{k} \qquad \text{(NUSSELT NUMBER)} \qquad (13.103)$$

or combined with the Reynolds and Prandtl numbers as

$$St = \frac{Nu}{Re\ Pr} = \frac{h}{V\rho\ C_p} \qquad \text{(STANTON NUMBER)} \qquad (13.104)$$

Without actually solving equations (13.88), (13.89) and (13.90) we would anticipate that

$$\frac{v_x}{V_\infty} = f_1\ (x, y,\ Re,\ Pr,\ Gr,\ Ec) \qquad (13.105)$$

$$\frac{T - T_0}{\Delta T} = f_2\ (x,\ y,\ Re,\ Pr,\ Gr,\ Ec) \qquad (13.106)$$

$$Nu = f_3(x,\ Re,\ Pr,\ Gr,\ Ec) \qquad (13.107)$$

Then the Nusselt number averaged over the length L should be expressed as

$$\overline{Nu} = \frac{\bar{h}L}{k} = \frac{-\int \left(\frac{\partial T}{\partial y}\right)_{y=0} L dx}{(\Delta T)} = F\ (Re,\ Pr,\ Gr,\ Ec) \qquad (13.108)$$

Such dimensionless expressions are very common in heat transfer. For laminar flows these relations can be obtained by solving the appropriate form of the conservation equations. For turbulent flows similar expressions are determined, usually, by correlating experimental data. Here are two examples:

For laminar flow inside long tubes

$$\overline{Nu} = 1.86(Re\,Pr)^{1/3} \left(\frac{D}{L}\right)^{1/3} \left(\frac{\mu}{\mu_W}\right)^{0.14} \qquad (13.109)$$

where D is the tube diameter, L the tube length, μ is the fluid viscosity and μ_W the fluid viscosity evaluated at the temperature of the wall.

For <u>turbulent</u> flow inside long smooth tubes (Re > 6000, Pr > 0.7)

$$\overline{Nu} = 0.023\, Re^{0.8}\, Pr^{1/3} \qquad (13.110)$$

More correlations can be found in textbooks on heat transfer (see references [2-5]).

With the help of the dimensionless equations (13.88), (13.89) and (13.90), we may determine the conditions under which certain dimensionless groups are important. For example, let us examine the equation of conservation of momentum

$$v_x^* \frac{\partial v_x^*}{\partial x^*} + v_y^* \frac{\partial v_x^*}{\partial y^*} = - \frac{\partial p^*}{\partial x^*} + \frac{1}{Re} \frac{\partial^2 v_x^*}{\partial y^{*2}} + \frac{Gr}{Re^2} \qquad (13.111)$$

In Section 9.1, it was shown that both the fluid inertia term $v_x^*(\partial v_x^*/\partial x^*) + v_y^*(\partial v_x^*/\partial y^*)$ and the viscous term $(1/Re)(\partial^2 v_x^*/\partial y^{*2})$ are of order of magnitude 1 for boundary layer flow. Thus, in order for the buoyancy effects to be of importance we should have

$$\frac{Gr}{Re^2} \simeq 1 \qquad (13.112)$$

Consequently, whenever the above condition is satisfied, the Nusselt number correlations must also involve the Grashof number Gr. With similar arguments we can determine the relative magnitude of other terms appearing in the general conservation equations and thus assess the importance of the physical mechanisms that they represent.

REFERENCES

1. H. Schlichting, Boundary Layer Theory, McGraw-Hill, 6th edition, New York (1968).

2. E.R.G. Eckert and R.M. Drake, Jr., Analysis of Heat and Mass Transfer, McGraw-Hill, New York (1972).

3. W.M. Kays, Convective Heat and Mass Transfer, McGraw-Hill, New York (1966).

4. M.N. Özisik, Basic Heat Transfer, McGraw-Hill, New York (1977).

5. J.P. Hollman, Heat Transfer, McGraw-Hill, 4th edition, New York (19--).

6. R.B. Bird, W.E. Stewart and E.N. Lightfoot, Transport Phenomena, Wiley, New York (1960).

John Vlachopoulos, *Fundamentals of Fluid Mechanics*
Chem. Eng., McMaster University, Hamilton, ON, Canada
(First Edition 1984, revised internet edition (2016), www.polydynamics.com)

CHAPTER 14

THE BERNOULLI EQUATION FOR DUCT FLOWS

14.1 INTRODUCTION

The Bernoulli equation was named after Daniel Bernoulli (1700-1782), who presented a form of the energy equation for steady one-dimensional, incompressible, frictionless flow without heat transfer or shear work, in his book on hydrodynamics published in 1738. This equation in its present forms is a very valuable tool (as we shall see) in solving many problems involving flow in ducts. In these problems it will often be reasonable to assume that the flow is "one-dimensional" (see Section 3.7), i.e. that the velocity profile is flat and has a magnitude equal to the average velocity over any given cross-section. We have shown that the Bernoulli equation is valid along a streamline (see Section 12.2). However, with the above assumption there will not be any difference between the various streamlines in a conduit, so that the Bernoulli equation written for one such streamline will automatically apply to the entire flow (i.e. along a streamtube). Obviously, this type of analysis will not provide any information on the velocity profiles or other details on the flow pattern. Even without this information, the results obtained by using the Bernoulli equation are often of great engineering value.

14.2 DERIVATION OF THE BERNOULLI EQUATION

Various forms of the Bernoulli equation were derived in Sections 11.2, 12.2 and 13.2. Here, we present yet another, more general, derivation by starting from the equation of conservation of momentum (6.57), which is

$$\rho \frac{\partial \bar{V}}{\partial t} + \rho \bar{V} \cdot \nabla \bar{V} = \nabla \cdot \bar{\bar{\sigma}} + \rho \bar{g} \tag{14.1}$$

We will now integrate this equation by making use of the following assumptions:

(1) The fluid is frictionless (i.e. $\mu = 0$ and $\sigma_{ij} = -p\,\delta_{ij}$)

(2) The fluid is barotropic, which means that the density is a function of pressure only, $\rho = \rho(p)$

(3) The body forces are derivable from a potential, i.e. $\bar{g} = -\nabla\Omega$

(4) The flow field is irrotational, which means $\nabla \times \bar{V} = 0$

The first assumption reduces equation (14.1) to the Euler equation (6.95), which is written here as

$$\frac{\partial \bar{V}}{\partial t} + \bar{V} \cdot \nabla \bar{V} = -\frac{\nabla p}{\rho} + \bar{g} \tag{14.2}$$

From Appendix A, we note the identity

$$\nabla(\bar{A} \cdot \bar{B}) = \bar{A} \cdot \nabla \bar{B} + \bar{B} \cdot \nabla \bar{A} + \bar{A} \times (\nabla \times \bar{B}) + \bar{B} \times (\nabla \times \bar{A}) \tag{14.3}$$

Letting $\bar{A} = \bar{B} = \bar{V}$ and $\nabla \times \bar{V} = 0$, we have

$$\nabla(V^2) = \bar{V} \cdot \nabla \bar{V} + \bar{V} \cdot \nabla \bar{V} \tag{14.4}$$

or

$$\bar{V} \cdot \nabla \bar{V} = \nabla(\frac{V^2}{2}) \tag{14.5}$$

Thus equation (14.2) becomes

$$\frac{\partial \bar{V}}{\partial t} + \nabla(\frac{V^2}{2}) = -\frac{\nabla p}{\rho} + \bar{g} \tag{14.6}$$

Since the flow field is irrotational the velocity is derivable from a potential, say Φ (see Section 11.1). Let

$$\bar{V} = \nabla\Phi \tag{14.7}$$

therefore

$$\frac{\partial \bar{V}}{\partial t} = \nabla \frac{\partial \Phi}{\partial t} \tag{14.8}$$

We may also write

$$\frac{\nabla p}{\rho} = \nabla \int \frac{dp}{\rho(p)} \tag{14.9}$$

With the help of equations (14.8) and (14.9) and with $\bar{g} = -\nabla\Omega$ (where Ω is the body force potential), we may rewrite equation (14.6) as

$$\nabla(\frac{\partial \Phi}{\partial t} + \frac{V^2}{2} + \Omega + \int \frac{dp}{\rho(p)}) = 0 \tag{14.10}$$

where $\psi(t)$ indicates a function of time only. We now introduce three more assumptions

(5) Steady state, i.e. $\frac{\partial \Phi}{\partial t} = 0$, $\Phi(t) = \text{const}$

(6) The fluid is incompressible, $\rho = \text{const}$

Thus $\int \frac{dp}{\rho} = \frac{1}{\rho} \int dp = \frac{p}{\rho}$

(7) The body force potential is just the gravitational potential, which may be expressed as the elevation z above some datum plane multiplied by the gravitational constant

$$\Omega = gz$$

Consequently, equation (14.10) becomes

$$\frac{V^2}{2} + \frac{p}{\rho} + gz = \text{const} \qquad (14.12)$$

which is the well-known Bernoulli equation.

14.3 FRICTIONAL LOSSES IN TUBES

By dividing equation (14.12) by g, we get

$$\frac{V^2}{2g} + \frac{p}{\rho g} + z = \text{const} \qquad (14.13)$$

It is easy to show that each term in the above equation has dimensions of length. These lengths are, at least conceptually, convertible into elevations above some datum plane. The elevations are commonly referred to as "heads". Thus, the Bernoulli equation states that

VELOCITY HEAD + PRESSURE HEAD + GRAVITY HEAD = CONST

All the terms of the original equation of conservation of momentum (Navier-Stokes) are accounted for, one by one, in the present "head" form of the Bernoulli equation, except for the viscous term. The velocity head represents the inertia forces, the pressure head stands for the pressure forces and the gravity head for the gravitational forces. The viscous term is not amenable to any general form of integration (since the irrotationality assumption does not hold for viscous fluids). However, just like the other terms, it should be expressible in the form of a "head". This is called the friction head and is usually denoted by h. Thus, if the friction head loss between two points in a flow field is h_{1-2}, we may write the Bernoulli equation as

$$\frac{V_1^2}{2g} + \frac{p_1}{\rho g} + z_1 = \frac{V_2^2}{2g} + \frac{p_2}{\rho g} + z_2 + h_{1-2} \tag{14.14}$$

where point 1 is upstream and point 2 downstream. In this form the Bernoulli equation can be applied to the solution of problems involving viscous flow in ducts. For a typical case, like the one shown in Fig. 14.1, equation (14.14) can be applied directly. However, since a tube rather than just a streamline is involved the velocities V_1 and V_2 represent the average velocities over the cross-sectional areas at points 1 and 2 respectively. z_1 and z_2 are the corresponding elevations. h_{1-2} is the friction head loss between the two points. p_1 and p_2 are the pressures at points 1 and 2 respectively.

Let us now apply equation (14.14) for a horizontal tube of constant diameter D=2R and length L through which a fluid is flowing under influence of a pressure difference $p_1 - p_2 = p_0 - p_L = \Delta p$. Since the tube has a constant diameter, $V_1 = V_2$. There is no difference in elevation, i.e. $z_1 = z_2$. Thus, equation (14.14) reduces to

$$\frac{p_1}{\rho g} = \frac{p_2}{\rho g} + h_{1-2} \tag{14.15}$$

and the friction head loss is

$$h_f = h_{1-2} = \frac{p_1 - p_2}{\rho g} = \frac{p_0 - p_L}{\rho g} = \frac{\Delta p}{\rho g} \tag{14.16}$$

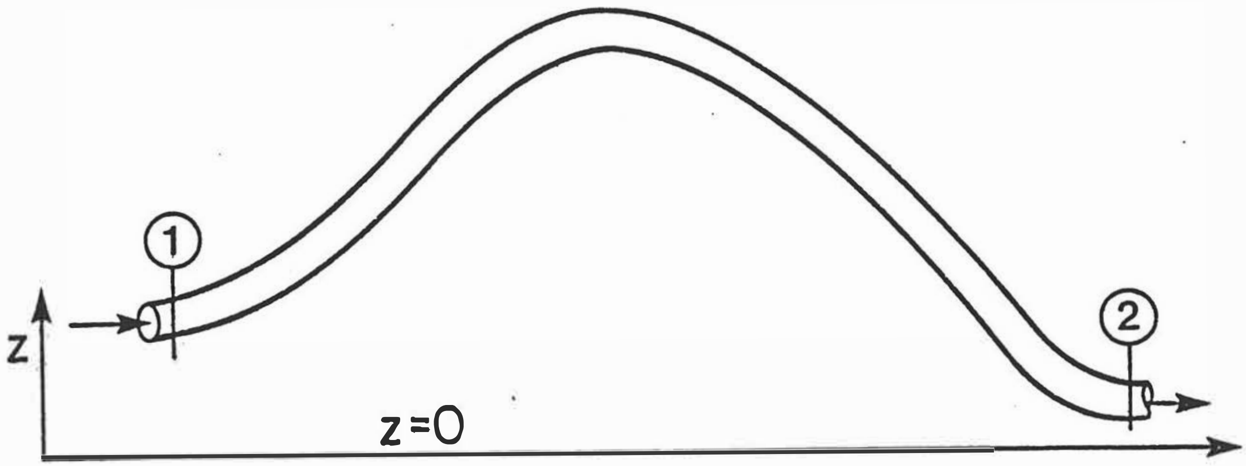

Fig. 14.1 Pipeline section.

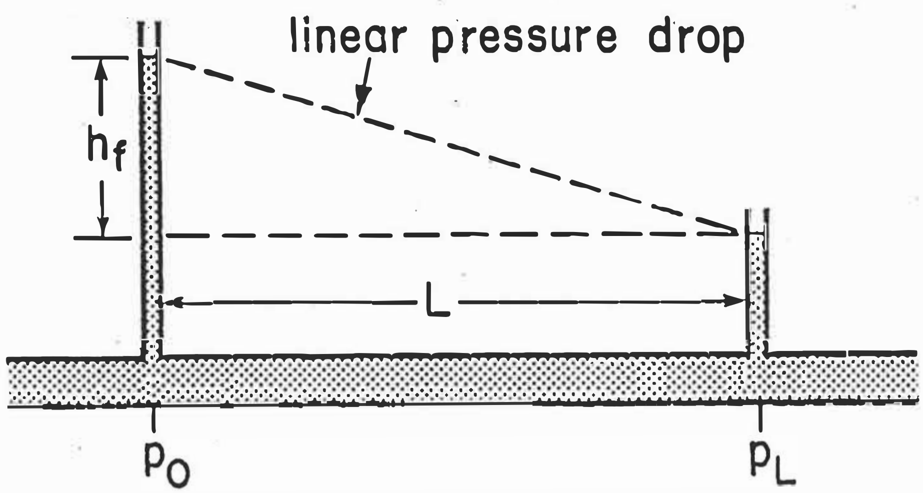

Fig. 14.2 Pressure drop in a straight horizontal tube.

We can now get an expression for h_f in terms of the average velocity in the tube V_{avg}. For laminar flow inside a tube (Section 7.3) we had

$$V_{avg} = \frac{p_0 - p_L}{8\mu L} R^2 = \frac{\Delta p}{8\mu L} R^2 \tag{14.17}$$

Thus,

$$h_f = \frac{\Delta p}{\rho g} = \frac{8\mu L\, V_{avg}}{\rho g R^2} \tag{14.18}$$

The head form $h_f = h_{1-2}$ of the pressure drop is pictorially explained in Fig. 14.2.

The frictional losses are usually expressed in the form of the Darcy-Weisbach friction factor (after Henry Darcy and Julius Weisbach, both 19th century engineers) which is defined as

$$f = \frac{h_f}{\frac{L}{D}\ \frac{V_{avg}^2}{2g}} \qquad \text{(Dimenionless)} \tag{14.19}$$

Introducing in the above expression h_f from equation (14.18), we get

$$f = \frac{32\mu}{\rho\, V_{avg}\, R} = \frac{64\mu}{\rho\, V_{avg}\, D} \tag{14.20}$$

or

$$f = \frac{64}{Re_D} \qquad \text{(for laminar flow)} \tag{14.21}$$

It was explained in Chapter 10 that turbulent flow problems are not amenable to rigorous mathematical treatment. Most results are obtained by direct experimentation. By correlating experimental data for very smooth tubes, Blasius [1] obtained a formula, which is valid up to $Re_D = 10^5$ (see also Section 10.6)

$$f = \frac{0.316}{Re_D^{1/4}} \tag{14.22}$$

Generally, the friction factor for turbulent flow is a function of the surface roughness as well as the Reynolds number

$$f = f\ (Re_D,\ \text{surface roughness}) \qquad (14.23)$$

The surface roughness of various types of commercial pipes is expressed in terms of a relative roughness factor ε/D (see also Section 10.7), where ε is the equivalent sand roughness and D the pipe diameter. Table 14.1 gives the equivalent resistances in high-speed flow to those of sand-roughened pipes.

The friction factors are given in the form of a plot known as the Moody chart [2], as shown in Fig. 14.3. In this chart, the variation in f for smooth pipes is probably around ± 5 per cent. A variation in f of about ± 10 per cent is usually expected for commercial steel pipe. Pipelines which have been in operation for extended periods of time exhibit large variation in f due to corrosion and fouling i.e. the formation of a solid substrate on the inside pipe surface. It should be always remembered that the results given in the Moody diagram are valid for new, corrosion-free pipes.

14.4 PROBLEM SOLVING WITH THE HELP OF THE MOODY FRICTION CHART

Problems dealing with uniform flow through a single pipe are usually of three different types. These are:

Type 1. Determination of the pressure drop, given the flow rate, the diameter, the kind of pipe and the fluid properties.

Type II. Determination of the flow rate, given the pressure drop, the diameter, the kind of pipe and the fluid properties.

Type III. Determination of the pipe diameter, given the kind of pipe, pressure drop, flow rate and fluid properties.

Table 14.1

Equivalent Sand Roughness of Commercial Pipes

Material (new)	ε (mm)
Glass	smooth
Drawn tubing	0.0015
Commercial steel or wrought iron	0.046
Asphalted cast iron	0.12
Galvanized iron	0.15
Cast iron	0.26
Wood stove	0.18-0.9
Concrete	0.3 to 3.0
Riveted steel	0.9-9.0

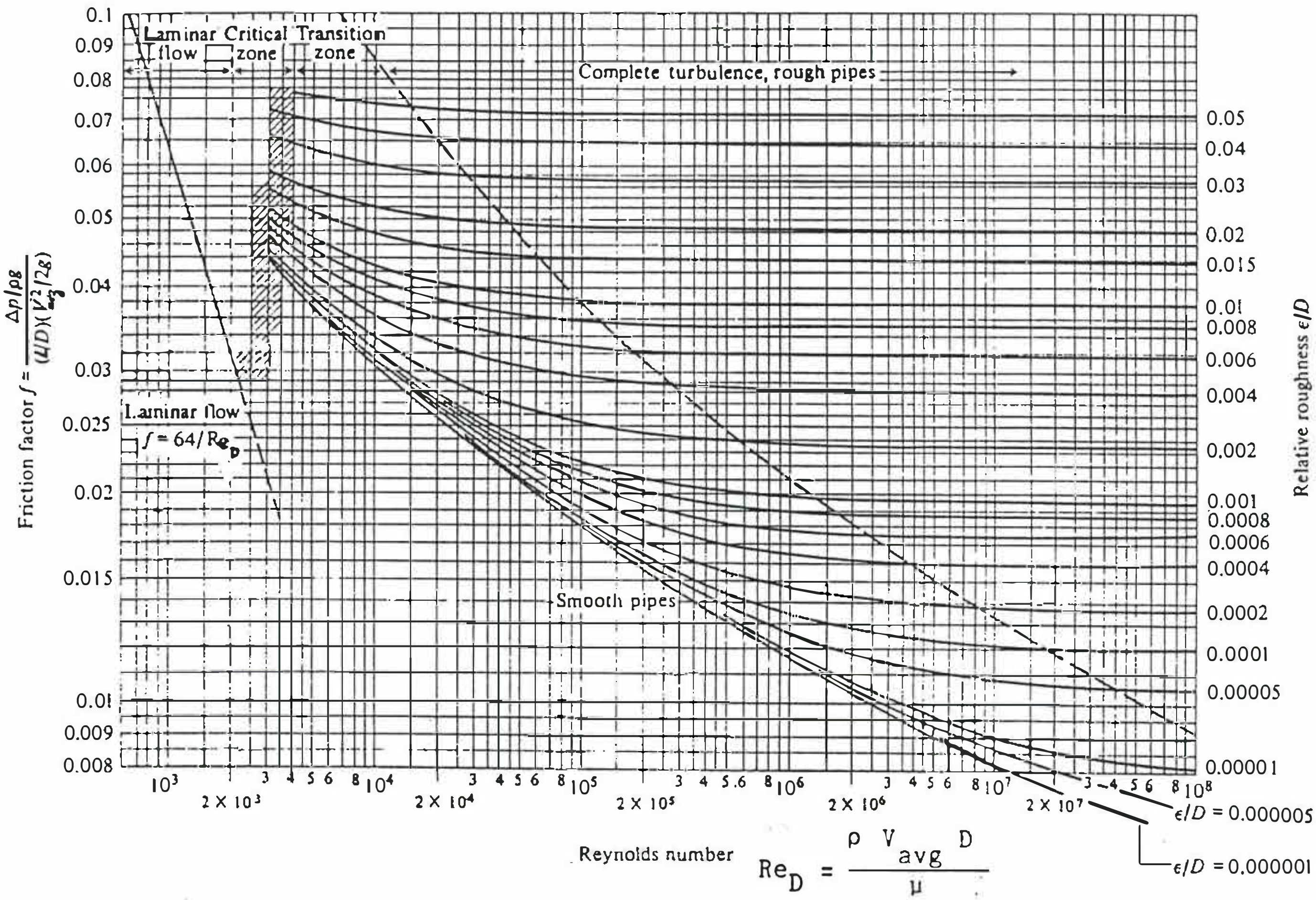

Fig. 14.3 The friction factor as a function of the Reynolds number, reproduced from L.F. Moody, "Friction Factors for Pipe Flow", Trans. ASME, 66, 671 (1944).

Type I problems are straightforward, because from the information given the Reynolds number can be calculated directly and the friction factor can be determined from the Moody chart (Fig. 14.3). The pressure drop is then determined by using the definitions of Section 14.3, i.e.

$$h_f = \frac{\Delta p}{\rho g} \tag{14.24}$$

$$f = \frac{h_f}{\frac{L}{D}\frac{V_{avg}^2}{2g}} \tag{14.25}$$

Type II problems are usually tackled by first making a guess for f, which allows the calculation of an average velocity from equations (14.24) and (14.25) and hence the flowrate. The Reynolds number Re_D is then determined and the accuracy of the initial guess is checked by determining a new f value from the Moody chart. The trial and error procedure can be continued until two consecutive values of f do not differ significantly.

Type III problems are again tackled by first making a guess for f which allows the determination of a pipe diameter from equations (14.24) and (14.25). If Q is the volume rate of flow and A the cross-sectional area, we have

$$h_f = f\,\frac{L}{D}\,\frac{V_{avg}^2}{2g} = f\,\frac{L}{D}\,\frac{Q^2/A^2}{2g} = f\,\frac{L}{D}\,\frac{Q^2}{2g\,(\frac{\pi}{4})^2\,D^4} \tag{14.26}$$

Thus

$$D^5 = \frac{fLQ^2}{(\frac{\pi}{4})^2\,2gh_f} = \frac{fLQ^2}{(\frac{\pi}{4})^2\,2g(\frac{\Delta p}{\rho g})} \tag{14.27}$$

From the above expression we can obtain a value of D which allows the determination of Re_D and with the help of the Moody chart a new value of f. Again, this trial-and-error procedure can be continued till two consecutive values of f do not differ significantly.

The Moody charts and the related definitions and formulae can be used for calculations involving non-circular conduits. The Reynolds number is

$$Re_D = \frac{\rho \, V_{avg} \, D_H}{\mu} \tag{14.28}$$

where D_H is the so-called hydraulic diameter defined as

$$D_H = \frac{4 \times (\text{cross sectional area})}{\text{wetted perimeter}} \tag{14.29}$$

Here are some examples:

(a) Pipe of circular cross-section

$$D_H = \frac{4 \times \frac{\pi D^2}{4}}{\pi D} = D \tag{14.30}$$

(b) annulus (inside diameter D_1, outside D_2)

$$D_H = \frac{4 \times [\frac{\pi D_2^2}{4} - \frac{\pi D_1^2}{4}]}{\pi D_2 + \pi D_1} = D_2 - D_1 \tag{14.31}$$

(c) rectangular conduit (area ab)

$$D_H = \frac{4 \times (ab)}{2a + 2b} = \frac{2ab}{a+b} \tag{14.32}$$

Thus, all calculations involving non-circular conduits are to be made with the Reynolds number defined in terms of the appropriate hydraulic diameter.

Example 14.1

Water (ρ = 1000 kg/m^3, μ = 10^{-3} Pa·s) flows at a rate of 0.025 m^3/s through a 1000 m long, 12.5 cm diameter cast iron pipe. Determine the pressure drop.

Solution

First calculate the Reynolds number. The average velocity is

$$V = V_{avg} = \frac{Q}{A} = \frac{0.025}{(\pi/4)(0.125)^2} = 2.04 \text{ m/s}$$

Then

$$Re = \frac{\rho VD}{\mu} = \frac{(10)^3(2.04)(0.125)}{10^{-3}} = 2.55 \times 10^5$$

For cast iron pipe $\varepsilon = 0.26$ mm (from Table 14.1), thus

$$\frac{\varepsilon}{D} = \frac{0.26 \text{ mm}}{125 \text{ mm}} = 0.0021$$

With the help of the Moody chart (Fig. 14.3) for $\varepsilon/D = 0.0021$ and $Re = 2.55 \times 10^5$ we find

$$f \simeq 0.024$$

Now, we can determine the pressure drop from equations (14.24) and (14.25)

$$\Delta p = h_f \rho g = f \frac{L}{D} \frac{V^2}{2} \rho = 0.024 \frac{1000 \text{ m}}{.125 \text{ m}} \frac{(2.04 \text{ m/s})^2}{2} (1000 \text{ kg/m}^3)$$

$$= 399{,}513 \text{ kg}\cdot\text{m}\cdot\text{s}^{-2}/\text{m}^2 = 399.51 \text{ kPa}$$

Example 14.2

Water ($\rho = 10^3$ kg/m^3, $\mu = 10^{-3}$ Pa·s) flows through a 150 m long, 20 cm diameter, asphalted cast iron pipe. Determine the flow rate if the pressure drop is 2000 Pa.

Solution

We do not know whether the flow is laminar or turbulent. Let us assume the flow is laminar, so that we may use equation (14.17) to calculate the average velocity.

We have

$$V = V_{avg} = \frac{\Delta p}{8\,\mu L} R^2 = \frac{\Delta p}{32\,\mu L} D^2 = \frac{2000}{32\,(10^{-3})\,150}(0.20)^2 = 16.66 \text{ m/s}$$

The Reynolds number is

$$Re = \frac{\rho V d}{\mu} = \frac{(1000)(16.66)(0.20)}{10^{-3}} = 3{,}332{,}000$$

This is a Reynolds number for turbulent flow. Therefore our assumption was wrong.

Since the flow is turbulent we will tackle this problem by making a guess for f. For asphalted cast-iron pipe we have $\varepsilon = 0.12$ (from Table 14.1), thus $\varepsilon/D = 0.12/200 = 0.0006$. In Fig. 14.3 we note that for $\varepsilon/D = 0.0006$ the value of f remains constant after a certain Re. We will use this value, $f \simeq 0.0175$, as our initial guess.

Combining equations (14.24) and (14.25) we get

$$V = \left(\frac{2}{f}\frac{\Delta p}{\rho}\frac{D}{L}\right)^{1/2} = \left(\frac{2}{0.0175} \times \frac{2000}{1000} \times \frac{0.20}{150}\right)^{1/2} = 0.55 \text{ m/s}$$

This velocity gives a Reynolds number

$$Re = \frac{\rho V D}{\mu} = \frac{(1000)(0.55)(0.20)}{10^{-3}} = 110{,}000$$

From Fig. 14.3, for $\varepsilon/D = 0.0006$ and $Re = 110{,}000$ we get a value of $f \simeq 0.021$. We re-calculate the average velocity

$$V = \left(\frac{2}{f}\frac{\Delta p}{\rho}\frac{D}{L}\right)^{1/2} = \left(\frac{2}{0.021} \times \frac{2000}{1000} \times \frac{0.20}{150}\right)^{1/2} = 0.50 \text{ m/s}$$

Thus the new Reynolds number is

$$Re = \frac{\rho VD}{\mu} = \frac{(1000)(0.50)(0.20)}{10^{-3}} = 100{,}000$$

In Fig. 14.3 it is virtually impossible to differentiate f values for Re = 100,000 and Re = 110,000. Thus we will accept f = 0.021 as our final estimate. The flow rate is then calculated as

$$Q = VA = (0.50)(\frac{\pi}{4}\ 0.20^2) = 0.0157 \text{ m}^3/\text{s}$$

Example 14.3

Determine the pipe diameter necessary to carry gasoline (S.G.=0.68 $\mu = 0.5 \times 10^{-3}$ Pa·s) at a flow rate of 0.15 m^3/s with a pressure drop of 175 kPa per kilometer. The pipe material is cast iron.

Solution

We will make use of equation (14.24)

$$D^5 = \frac{fLQ^2}{(\frac{\pi}{4})^2\ 2g(\frac{\Delta P}{\rho g})} = \frac{fLQ^2}{1.232\ \frac{\Delta P}{\rho}}$$

Since we do not know D we cannot calculate ε/D. However from the previous two examples a value of f = 0.017 would seem reasonable. Thus

$$D = \left(\frac{0.017 \times 1000 \times 0.15^2}{1.232 \times \frac{175 \times 1000}{0.68 \times 1000}}\right)^{1/5} = 0.26 \text{ m}$$

We can now calculate

$$\frac{\varepsilon}{D} = \frac{0.26 \text{ mm}}{260 \text{ mm}} = 0.001$$

$$V = \frac{Q}{A} = \frac{Q}{\frac{\pi}{4}D^2} = \frac{0.15}{\frac{\pi}{4}(0.260)^2} = 2.83 \text{ m/s}$$

$$Re = \frac{\rho VD}{\mu} = \frac{(0.68 \times 1000)(2.83)(0.26)}{0.5 \times 10^{-3}} \simeq 10^6$$

A new value of friction factor can be obtained from the Moody chart (Fig. 14.3) for $\varepsilon/D = 0.001$ and $Re = 10^6$

$$f \simeq 0.02$$

With this value of f we can re-calculate

$$D = 0.269 \text{ m}$$

$$\frac{\varepsilon}{D} = 0.00097$$

$$V = 2.64 \text{ m/s}$$

$$Re = 9.66 \times 10^5$$

These values give again $f \simeq 0.02$. Therefore, no more iterations are needed. Thus, a pipe of about 27 cm in diameter is capable of carrying the volume flow rate specified in the statement of problem for the given pressure drop.

Example 14.4

Rework example 14.1 if the water flows through a channel of square cross-section having the same area as the 12.5 cm pipe.

Solution

The cross-sectional area is

$$a^2 = \frac{\pi D^2}{4} = \left(\frac{\pi}{4}\right)(0.125)^2$$

$$a = 0.1108 \text{ m}$$

From equation (14.32) the hydraulic diameter is

$$D_H = \frac{2a^2}{2a} = a = 0.1108 \text{ m}$$

Therefore we may calculate

$$V = \frac{Q}{A} = 2.04 \text{ m/s}$$

$$Re = \frac{\rho V D_H}{\mu} = \frac{(10^3)\ 2.04 \times 0.1108}{10^{-3}} = 2.26 \times 10^5$$

$$\frac{\varepsilon}{D_H} = \frac{0.26 \text{ mm}}{110.8 \text{ mm}} = 0.0023$$

$$f \simeq 0.0245$$

$$\Delta p = f \frac{L}{D} \frac{V^2}{2} \rho = 0.0245 \frac{1000}{0.1108} \frac{2.04}{2} (1000) = 460 \text{ kPa}$$

The pressure drop is larger than that of example 14.1 because the wetted perimeter, and therefore the area of contact between fluid and solid, is larger.

14.5 FITTING LOSSES

Most of the problems examined in detail in previous sections of this book involved laminar flow through straight tubes and channels. Most of the semiempirical expressions given in the chapter on turbulent flow are also applicable to straight tubes and channels. The Moody chart discussed in Section 14.4 provides a means for rapid calculations in problems involving straight tubes and channels. In many practical problems, however, several types of flow irregularities may be encountered as a result of sudden contractions, sudden expansions, elbows, valves etc. The streamline pattern exhibits certain

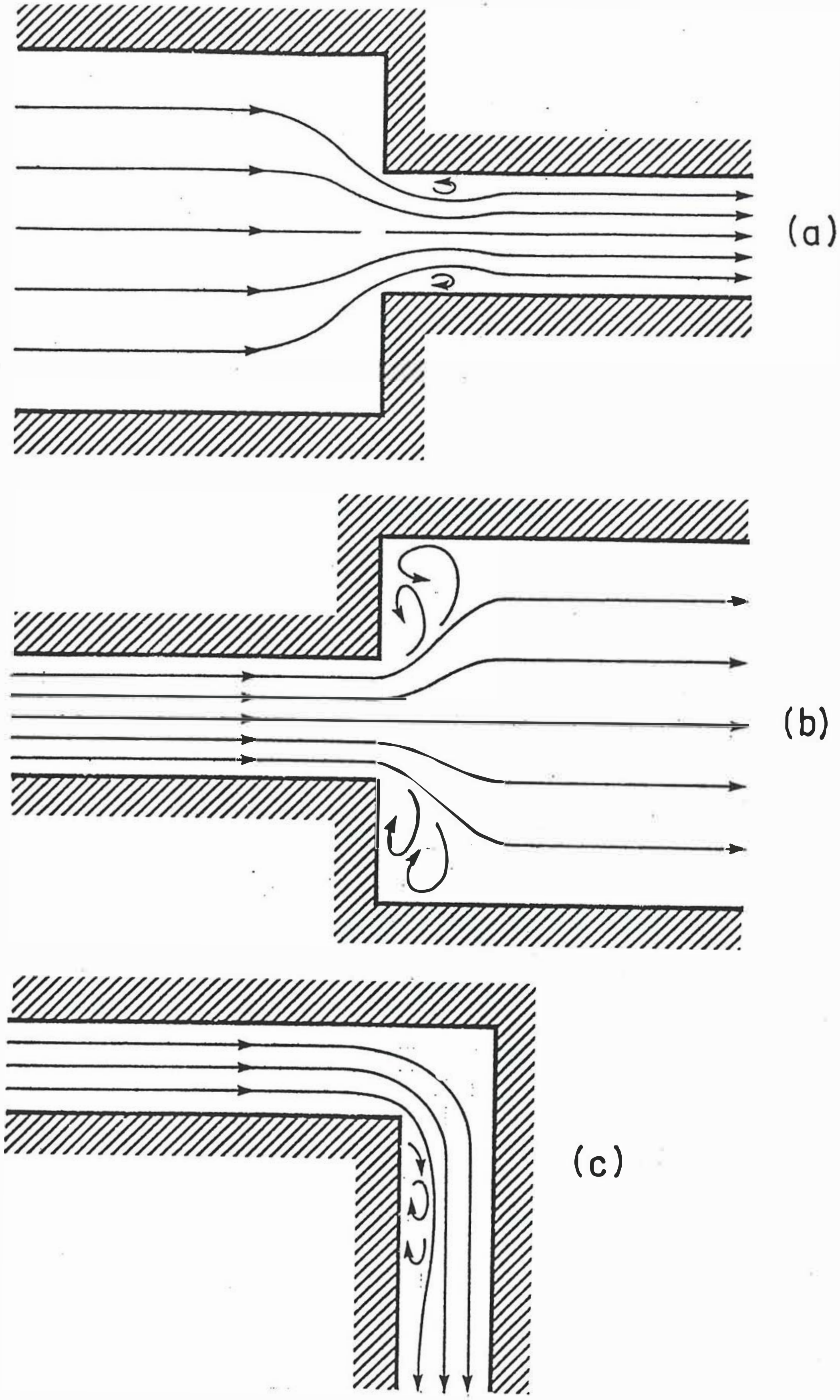

Fig. 14.4 Streamline pattern in (a) contraction, (b) expansion, (c) elbow.

peculiarities as shown schematically in Fig. 14.4. The existense of flow recirculation regions is the primary cause of the difficulties in dealing with these problems.

Flow through all these pipe fittings is usually accompanied by large pressure drops, because the fluid is forced to go through sharp edges and non-streamlined passages. These pressure drops are often referred to as "minor" losses (as opposed to major losses in straight pipe sections). The word "minor" is unfortunately a misnomer, because these losses are not minor at all. The expression "fitting losses" seems more appropriate.

The head form of the pressure drop due to flow through a pipe fitting is defined by

$$\frac{\Delta p}{\rho g} = h_L = K_L \frac{V^2}{2g} \tag{14.33}$$

where K_L is the <u>loss coefficient</u> for the particular fitting. Loss coefficients are determined experimentally by measuring directly the pressure drop and the average velocity, which is equal to the flow rate divided by the cross-sectional area. For the most common types of fittings loss coefficients are available in handbooks (e.g. references 3-6) and in company manuals. Some typical values of K_L for sufficiently large Re are given in Table 14.2.

In a typical pipeline problem there will be several fittings between the reference points 1 and 2. The Bernoulli equation may be written as

$$\frac{V_1^2}{2g} + \frac{p_1}{\rho g} + z_1 = \frac{V_2^2}{2g} + \frac{p_2}{\rho g} + z_2 + h_{1-2} \tag{14.34}$$

where h_{1-2} is equal to the sum of the head loss due to the straight pipe

Table 14.2

Loss Coefficients for Various Pipe Fittings

Description	Sketch	Additional Data	K_L	
Pipe entrances		Square-edged	0.50	
	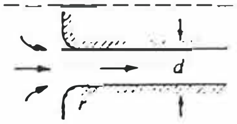	Rounded: $r/d > 0.12$	0.10	
Contractions and expansions	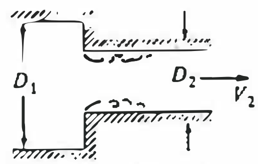 $h_L = K_c V_2^2/2g$	D_2/D_1 for K_c or D_1/D_2 for K_E:	K_c	K_E
		0.0	0.50	1.00
		0.1	0.49	0.98
		0.2	0.48	0.94
	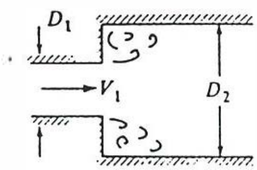 $h_L = K_E V_1^2/2g$	0.4	0.44	0.71
		0.6	0.32	0.41
		0.7	0.23	0.22
		0.8	0.15	0.13
		0.9	0.06	0.04
90° miter bend	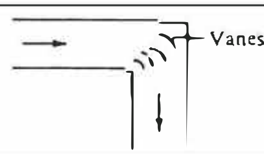	Without vanes	1.1	
		With vanes	0.2	
90° smooth bend	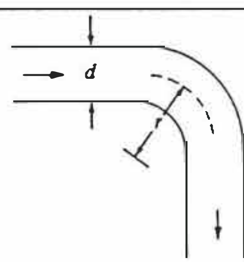	r/d		
		1	0.35	
		2	0.19	
		4	0.16	
		6	0.21	
		8	0.28	
		10	0.32	
Threaded pipe fittings	Globe valve—wide open		10.0	
	Angle valve—wide open		5.0	
	Gate valve—wide open		0.2	
	Gate valve—half open		5.6	
	Return bend		2.2	
	Tee		1.8	
	90° elbow		0.9	
	45° elbow		0.4	

(tube) sections and the fitting losses (h_L). We have

$$h_{1-2} = h_T + h_L \tag{14.35}$$

$$h_T = f\,\frac{L}{D}\,\frac{V_2^{\,2}}{2g} \tag{14.36}$$

$$h_L = \sum K_L\,\frac{V_2^{\,2}}{2g} \tag{14.37}$$

and

$$h_{1-2} = f\,\frac{L}{D}\,\frac{V_2^{\,2}}{2g} + \sum K_L\,\frac{V_2^{\,2}}{2g}$$

$$= \left(f\,\frac{L}{D} + \sum K_L\right)\frac{V_2^{\,2}}{2g} \tag{14.38}$$

The Bernoulli equation can thus be written as

$$\frac{V_1^{\,2}}{2g} + \frac{p_1}{\rho g} + z_1 = \frac{p_2}{\rho g} + z_1 + \left(1 + f\,\frac{L}{D} + \sum K_L\right)\frac{V_2^{\,2}}{2g} \tag{14.39}$$

14.6 THE BERNOULLI EQUATION FOR A PIPELINE WITH A PUMP (OR TURBINE).

When a pump is included between the reference points 1 and 2 in a pipeline as shown in Fig. 14.5, the Bernoulli equation must be modified to include a pump head h_P. The pump increases the pressure of the fluid, thus the pump head should have a sign opposite of that of the frictional loss head h_{1-2}. Equation (14.14) can therefore be modified to the form

$$\frac{V_1^{\,2}}{2g} + \frac{p_1}{\rho g} + z_1 + h_P = \frac{V_2^{\,2}}{2g} + \frac{p_2}{\rho g} + z_2 + h_{1-2} \tag{14.40}$$

If the hydraulic pump power, which is supplied to the pipeline, is P_o, we will have

$$P_o = \bar{F}\cdot\bar{V} = (\Delta p)AV = \Delta p Q = h_P\,\rho g\,Q \tag{14.41}$$

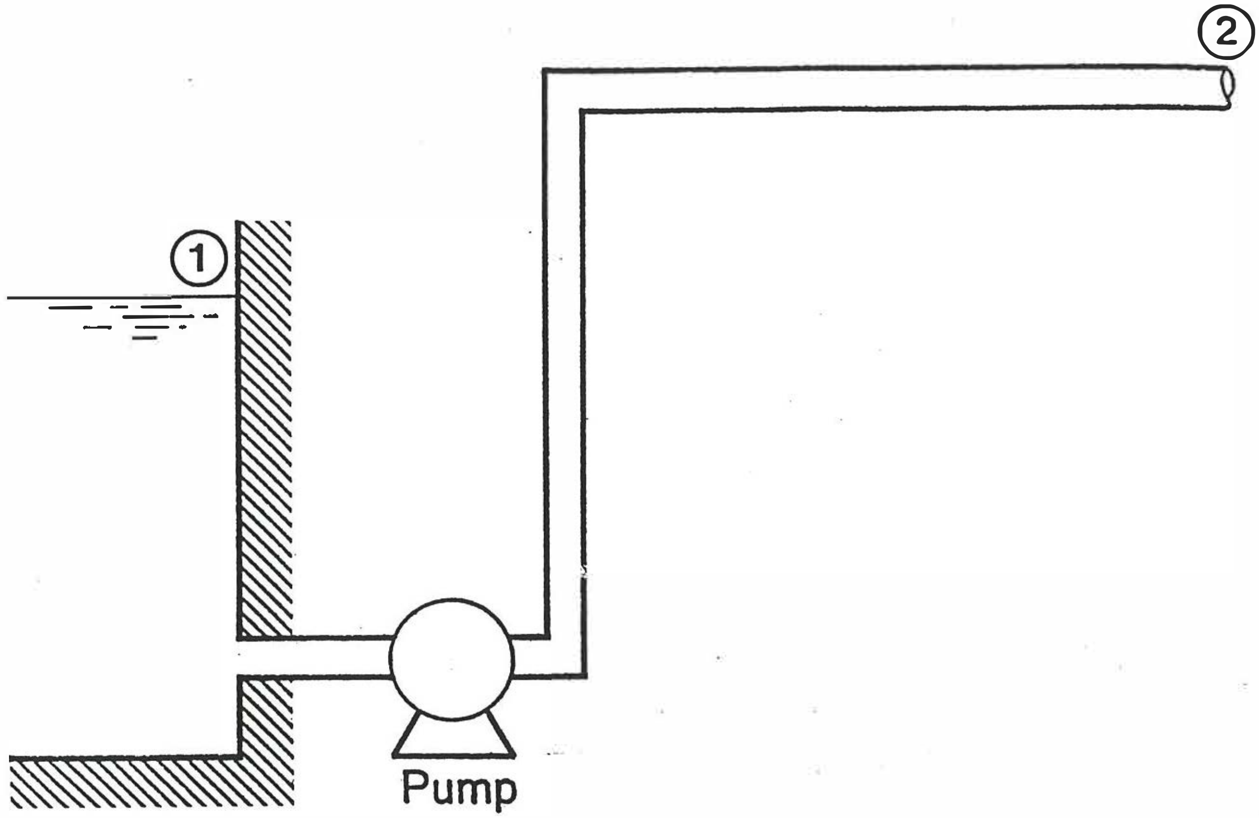

Fig. 14.5 Pipeline with a pump.

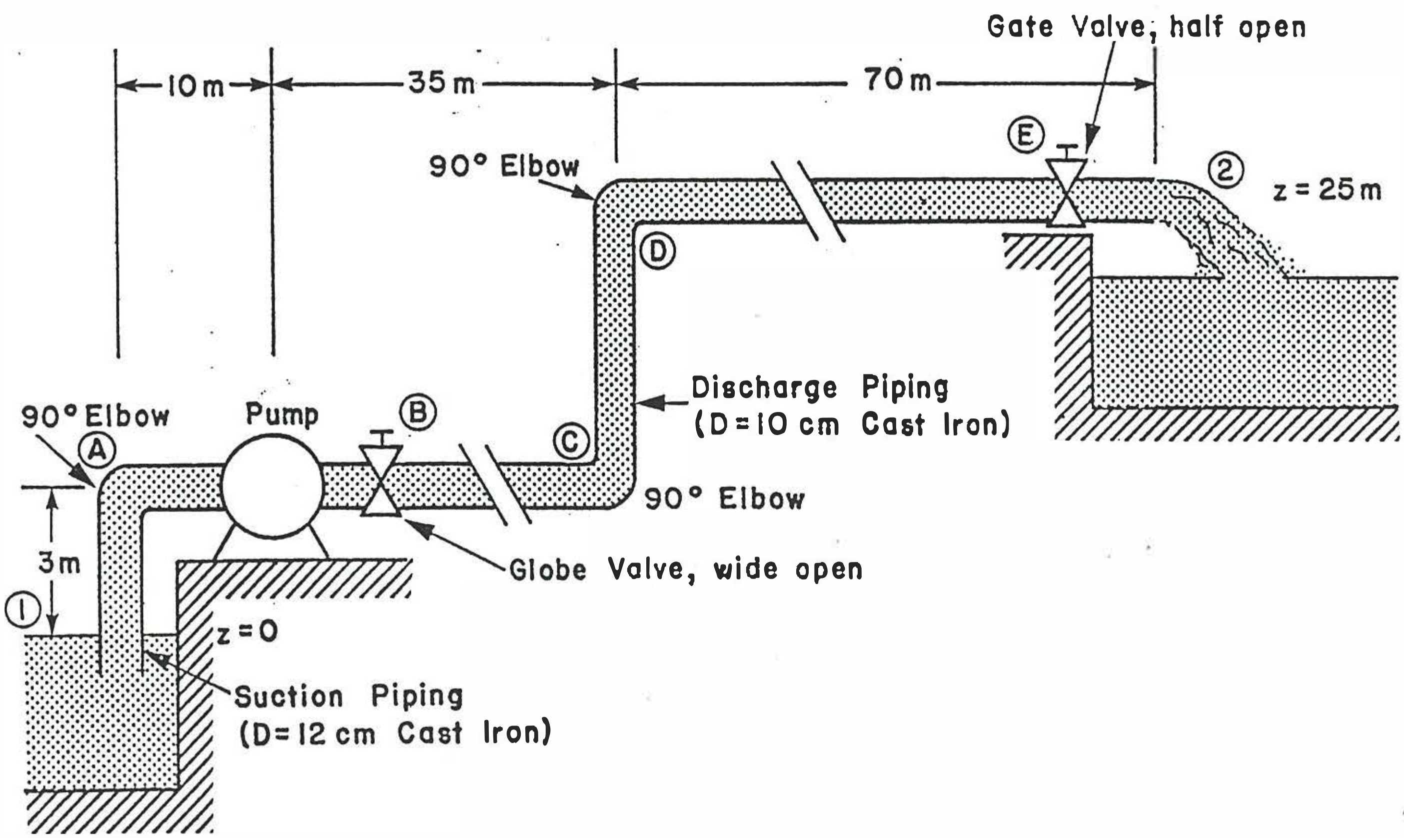

Fig. E.14.5

where Δp is the pressure rise due to the pump, A the cross-sectional area and Q the volume rate of flow. The power required to drive the pump is always larger than the hydraulic power which is supplied to the pipeline. We may thus define a pump efficiency η_P as follows

$$\eta_P = \frac{\text{Po (hydraulic)}}{\text{Po (supplied by the motor driving the pump)}} \tag{14.42}$$

More about pump efficiencies can be found in Chapter 24, Fluid Machinery.

If between the two reference points 1 and 2 a turbine rather than a pump is present, the turbine head (loss) h_{Tb} should have an opposite sign to that of the pump, i.e.

$$\frac{V_1^2}{2g} + \frac{p_1}{\rho g} + z_1 - h_{Tb} = \frac{V_2^2}{2g} + \frac{p_2}{\rho g} + z_2 + h_{1-2} \tag{14.43}$$

In textbooks on thermodynamics the Bernoulli equation (14.40 or 14.43) is usually derived from the energy balance for a control volume, which yields (for steady, one-dimensional, isothermal flow)

$$\frac{1}{2} (V_2^2 - V_1^2) + g (z_2 - z_1) + \int_{p_1}^{p_2} \frac{dp}{\rho} + W_f + W_s = 0 \tag{14.44}$$

where W_f (= g h_f) is the loss of energy per unit mass due to friction between sections 1 and 2 and W_s (= g h_s) is the shaft work per unit mass done by the fluid (positive for a turbine, negative for a pump). Introduction of the incompressibility assumption in equation (14.44) leads easily to the forms of the Bernoulli equation presented above.

Example 14.5

Determine the hydraulic power which is supplied to the pipeline of Fig. E.14.5 by the pump, for a water flow rate of 0.02 m^3/s (ρ = 1000 kg/m^3,

$\mu = 10^{-3}$ Pa.s).

Solution

We will apply equation (14.40) which is

$$\frac{V_1^2}{2g} + \frac{p_1}{\rho g} + z_1 + h_P = \frac{V_2^2}{2g} + \frac{p_2}{\rho g} + z_2 + h_{1-2}$$

Here we have

$$p_1 \simeq p_2 \simeq p_{atm}$$

$$z_1 = 0$$

$$z_2 = 25 \text{ m}$$

$$V_1 = \frac{Q}{\frac{\pi}{4} D_1^2} = \frac{0.02}{\frac{\pi}{4} (0.12)^2} = 1.76 \text{ m/s}$$

$$V_2 = \frac{Q}{\frac{\pi}{4} D_2^2} = \frac{0.02}{\frac{\pi}{4} (0.1)^2} = 2.55 \text{ m/s}$$

There are: 3 + 10 = 13 m of D=12 cm piping (suction)

35 + 22 + 70 = 127 m of D=10 cm piping (discharge)

Three 90° elbows (A,C,D)

One globe valve, wide open (B)

One gate valve, half open (E)

Thus

$$h_{1-2} = (f_1 \frac{L_1}{D_1} + K_{LA}) \frac{V_1^2}{2g} + (f_2 \frac{L_2}{D_2} + K_{LB} + K_{LC} + K_{LD} + K_{LE}) \frac{V_2^2}{2g}$$

The Reynold's number in the D = 12 cm pipe is

$$Re = \frac{\rho V D}{\mu} = \frac{(10^3)(1.76)(0.12)}{10^{-3}} = 2.11\times10^5$$

$$\frac{\varepsilon}{D} = \frac{0.26\ \text{mn}}{120} = 0.0022$$

From Fig. 14.3, we get

$$f_1 \simeq 0.0245$$

The Reynolds number in the D = 10 cm pipe is

$$Re = \frac{\rho V D}{\mu} = \frac{(10^3)(2.55)(0.10)}{10^{-3}} = 2.55\times10^5$$

$$\frac{\varepsilon}{D} = \frac{0.26}{120} = 0.0025$$

From Fig. 14.3, we get

$$f_2 = 0.025$$

Thus,

$$h_{1-2} = (0.0245\ \frac{13}{0.12} + 0.90)\ \frac{1.76^2}{2x9.81}$$

$$+ (0.025\ \frac{127}{0.10} + 10 + 0.90 + 0.90 + 5.6)\ \frac{(2.55)^2}{2x9.81}$$

$$= 0.56 + 15.99 = 16.55\ \text{m}$$

and equation (14.40) gives

$$\frac{(1.76)^2}{2x9.81} + 0 + 0 + h_p = \frac{(2.55)^2}{2x9.81} + 0 + 25 + 16.55$$

$$h_p = 25 + 16.55 + 0.33 + 0.16 = 42.04\ \text{m}$$

Thus, the hydraulic power is

$$Po = h_p \rho g\, Q = (42.04)(10^3)(9.81)(0.02) = 8248\ W$$

14.7 SOME COMMENTS REGARDING THE APPLICATION OF THE BERNOULLI EQUATION

Although the application of the Bernoulli equation to flow problems is fairly straightforward, students occasionally face difficulties. Some of the difficulties might be avoided by taking into account the following comments.

1. The choice of the reference points, say 1 and 2 can be made arbitrarily. The Bernoulli equation is applicable between any two points along a single pipeline. However, the calculations might be greatly simplified by a suitable choice of the locations of these points. The general rule is that the reference points should be chosen at locations where the velocity and/or pressure are known or can be easily calculated. Note, also, that in this textbook we use the convention that location 1 is always upstream while location 2 always downstream (good practice to follow).

2. There is often confusion regarding the pressure term $(p/\rho g)$. It must be, however, remembered that when choosing the locations of the reference points we select the boundaries of the control volume. Consequently, the pressures at these points might be determined by the conditions outside the control volume. For example in Fig. 14.6 we have $p_1 = p_{atm}$, $p_2 = \rho g H + p_{atm}$, $p_4 = p_{atm}$, while p_3 is some pressure (probably unknown) inside the pipeline. If the reservoir is large enough it might be reasonable to assume $V_1 \simeq 0$, however, in general V_2 has a finite value which is related to V_3 and V_4 by the continuity relation $V_2A_2 = V_3A_3 = V_4A_4$.

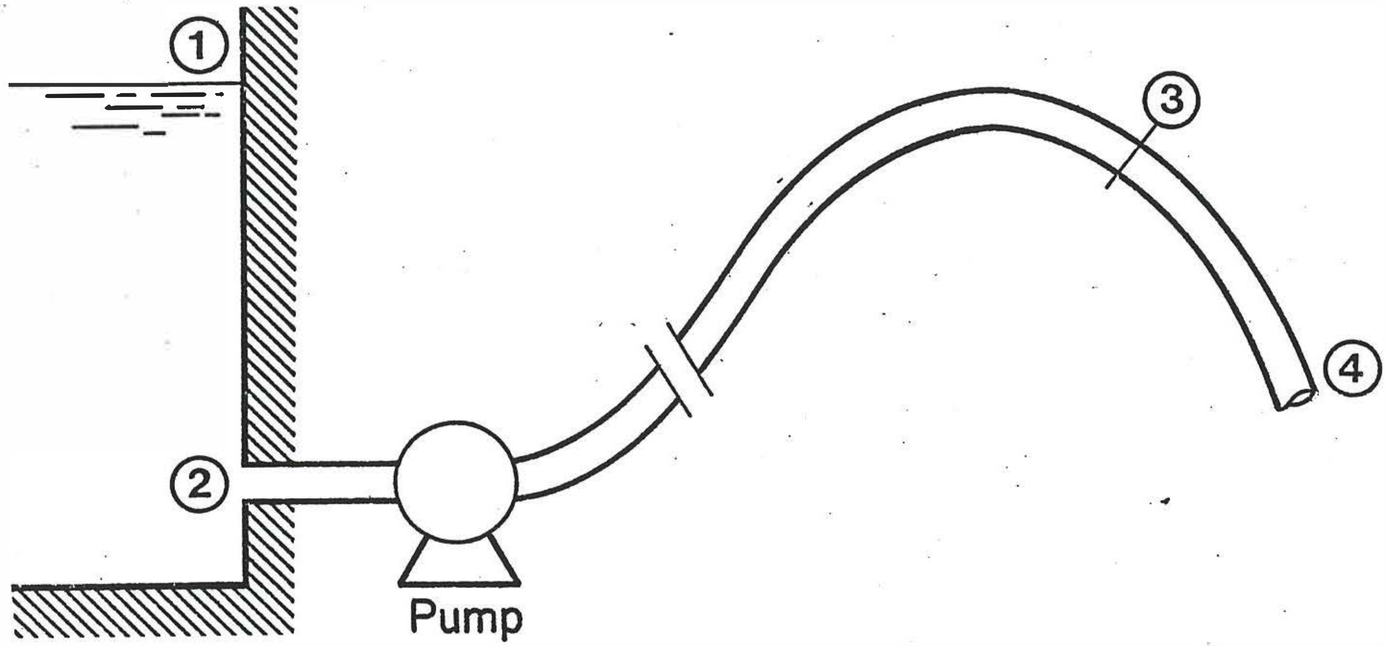

Fig. 14.6 A sketch of a pipeline with a pump with arbitrarily chosen reference points 1, 2, 3 and 4.

14.8 MULTIPLE-PIPE SYSTEMS

The methods and techniques developed for single pipes are also applicable to multiple-pipe systems. There are some basic rules, however, which can be used in order to simplify the computational procedures. We will describe them by referring to three typical examples:

(a) pipes in series (b) pipes in parallel and (c) the three-reservoir pipe junction.

Fig. 14.7(a) shows three pipes in series. Obviously the flow rate will be the same, i.e.

$$Q_A = Q_B = Q_C \tag{14.45}$$

or $$V_A D_A^2 = V_B D_B^2 = V_C D_C^2 \tag{14.46}$$

The total head loss is equal to the sum of the head losses in each pipe

$$h_{1-2} = h_A + h_B + h_C \tag{14.47}$$

Using equation (14.46), we can express the head loss in terms of one of the velocities and treat this problem like those involving a single pipe.

Pipes in parallel are shown in Fig. 14.7(b). The head loss will be the same in each pipe because the pressure difference is the same. The total flow rate will obviously be equal to the sum of the individual flow rates. Thus we have

$$h_{1-2} = h_A = h_B = h_C \tag{14.48}$$

$$Q = Q_A + Q_B + Q_C \tag{14.49}$$

If the head loss is known we can easily calculate the individual flow rates and add them up. If the total flow rate is known, we must use a

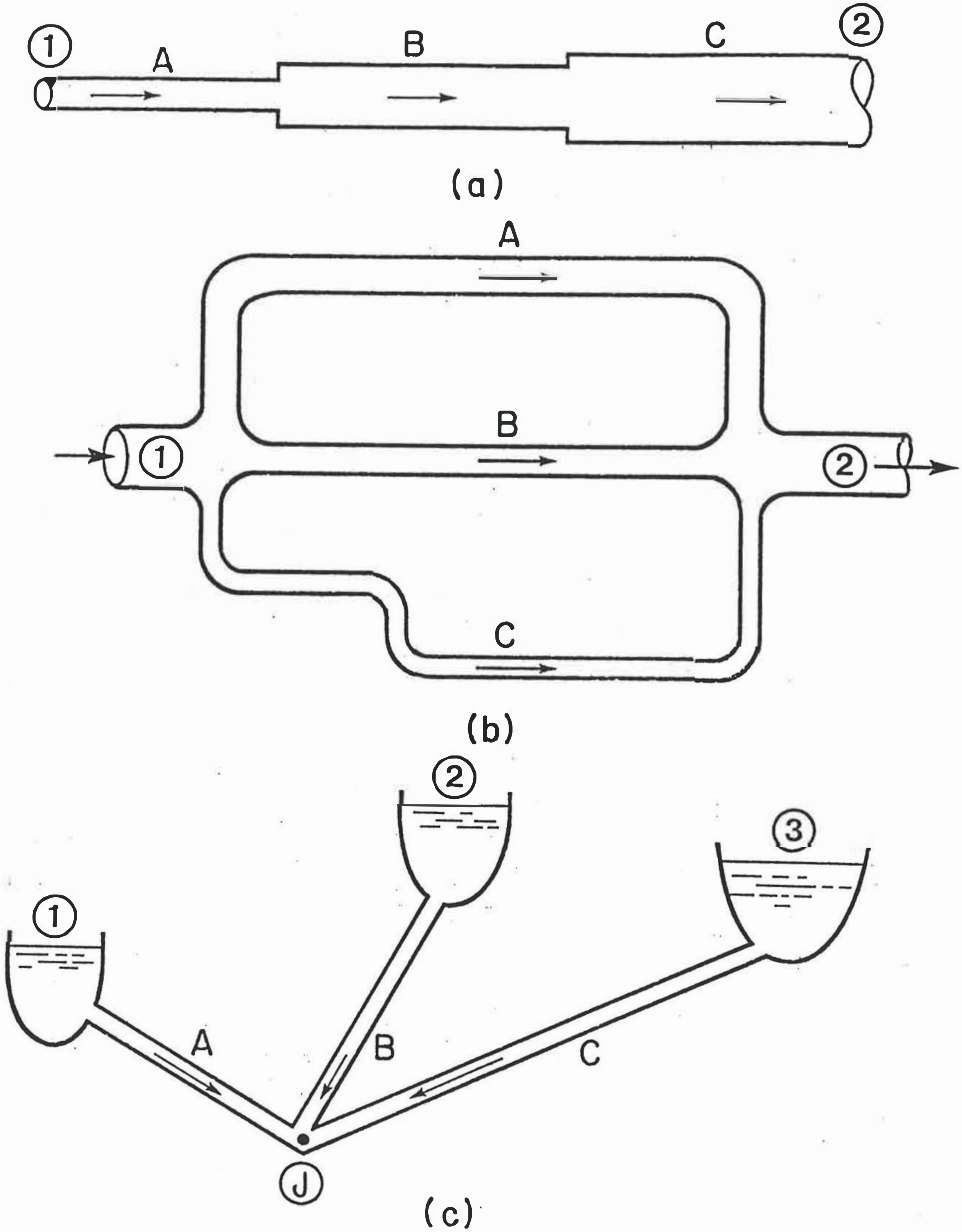

Fig. 14.7 Multiple pipe systems (a) pipes in series, (b) pipes in parallel, (c) three-reservoir pipe junction.

trial-and-error solution to determine how the flow is apportioned among the pipes. Typically we may guess, say, $Q_A = Q/3$, compute the head loss and hence Q_A and Q_B. If the sum $Q_A + Q_B + Q_C$ is not equal to Q we may scale up or down our initial guess, recalculate Q_A, Q_B and check the sum $Q_A + Q_B + Q_C$ again. Further iterations may be needed till the calculations converge within a certain tolerance.

We will now consider the three-reservoir pipe junction of Fig. 14.7(c). The net flow into the junction will obviously be zero. By taking the positive direction towards the pipe junction, we may write

$$Q_A + Q_B + Q_C = 0 \tag{14.50}$$

This means that one or two of the flow rates must be negative i.e. away from the junction. The pressure at the junction must have the same value no matter which one of the pipes is used for its calculation. Thus we have

$$\frac{p_1}{\rho g} + z_1 = z_J + \frac{p_J}{\rho g} + f_A \frac{L_A}{D_A} \frac{V_A^2}{2g} \tag{14.51}$$

$$\frac{p_1}{\rho g} + z_2 = z_J + \frac{p_J}{\rho g} + f_B \frac{L_B}{D_B} \frac{V_B^2}{2g} \tag{14.52}$$

$$\frac{p_3}{\rho g} + z_3 = z_J + \frac{p_J}{\rho g} + f_C \frac{L_C}{D_C} \frac{V_C^2}{2g} \tag{14.53}$$

Again a trial-and-error procedure is necessary. Typically we may start by guessing the quantity $z_J + \frac{p_J}{\rho g}$ and then compute, check and recompute the rest of the quantities till a satisfactory approximation is achieved [8].

We may apply the above basic rules and procedures to highly complicated piping networks like those for water-supply of cities. Such problems can be found in textbooks on hydraulics [9,10]. The final step is always the iterative solution of a large number of non-linear simultaneous algebraic equations [11]. Recently, efficient computer methods and programs have been developed.

14.9 THE BERNOULLI EQUATION FOR GASES

In deriving the usual form of the Bernoulli equation (14.12) we made the assumption that the fluid is incompressible. This is true for nearly all liquid flows. For gases the pressure term must be included in its original form i.e. before the integration. We have

$$\frac{V^2}{2} + \int \frac{dp}{\rho} + gz = \text{cost} \tag{14.54}$$

The value of the integral in equation (14.54) depends on the equation of state and the path of the process. However, the assumption of incompressibility is also valid for low velocity gas flows. Thus, the Bernoulli equation in the usual form (equation 14.12) can be applied. To show the upper limits of applicability we use a numerical example. The tank shown in Fig. 14.8 is full of air at 20°C and has a rounded nozzle through which the air is flowing to the atmosphere. It is assumed that the tank is large enough so that the flow is practically steady. We choose point 1 inside the tank where the velocity is practically zero and point 2 just at the nozzle exit where $p = p_{atm}$. The Bernoulli equation for frictionless incompressible flow is

$$\frac{V_1^{\,2}}{2g} + \frac{p_1}{\rho g} = \frac{V_2^{\,2}}{2g} + \frac{p_2}{\rho g} \tag{14.55}$$

Since $V_1 = 0$ and $p_2 = p_{atm}$, we have

$$V_2 = \left[\frac{2\,(p_1 - p_{atm})}{\rho}\right]^{1/2} \tag{14.56}$$

Using the density of air at P_{atm} and $T = 20^{\circ}C$ ($\rho = 1.14\ kg/m^3$) and $p - p_{atm} = 3$ kPa we get $V_2 = 72.5$ m/s, which compares rather well with the compressible flow calculation (Chapter 15, Section 15.5 $V_2 = 70.2$ m/s. However, for $p_1 - p_{atm} = 30$ kPa, we calculate $V_2 = 229.4$ m/s while the compressible flow calculation yields $V_2 = 212.6$ m/s. As the velocity V_2 approaches the speed of sound the incompressibility assumption ceases to apply.

14.10 TORRICELLI'S EQUATION FOR TANK DRAINING

We now consider a tank full of liquid open at the top. There is a little hole near the bottom as shown in Fig. 14.9 through which the liquid is being drained. The tank is assumed to be large enough so that the velocity of the receding free surface can be taken equal to zero. We choose point 1 at the free liquid surface and point 2 just outside the hole. The pressure at both points 1 and 2 is equal to the local atmospheric pressure. Thus the Bernoulli equation for frictionless flow reduces to

$$z_1 = \frac{V_2^{\,2}}{2g} + z_2 \tag{14.57}$$

Since $z_1 - z_2 = H$, we have

$$V_2 = (2gH)^{1/2} \tag{14.58}$$

This is known as Torricelli's equation (after Evangelista Torricelli (1608-1647)) for tank draining. Note that equation (14.58) gives a draining velocity equal to the velocity of free fall of an object at a distance H from rest.

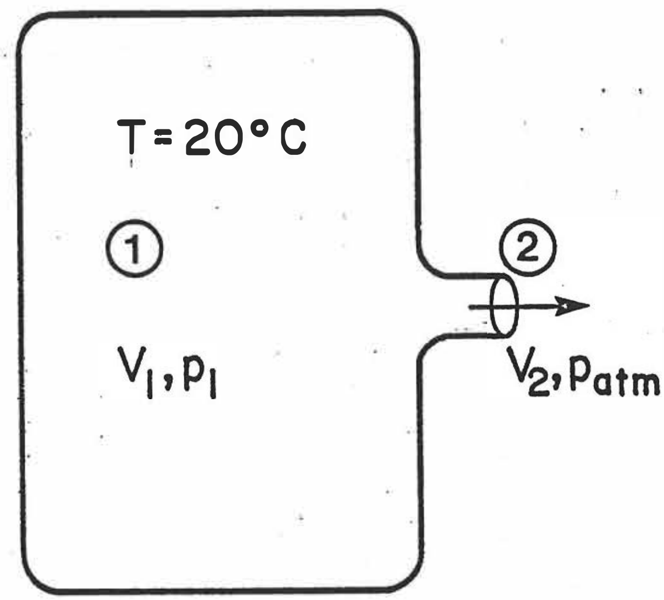

Fig. 14.8 Air tank with a smooth, rounded nozzle.

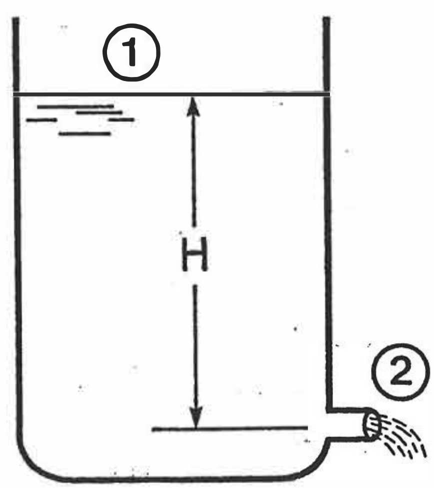

Fig. 14.9 Liquid tank draining.

14.11 THE BERNOULLI EQUATION FOR UNSTEADY FLOWS

One of the assumptions introduced in the derivation of the Bernoulli equation was that the flow is steady. This assumption permitted the elimination of the unsteady state term $\partial\bar{V}/\partial t$ from the Navier-Stokes equation. It is possible, however, to use the Bernoulli equation successfully for certain unsteady flows if the time-change in velocity is small enough to be ignored. To demonstrate such an application we will determine the time it takes a fluid level in a tank to drop from H to H_o (see Fig. 14.10).

The Bernoulli equation as applied in the previous section is useful in this problem. We have, an exit velocity

$$V_2 = (2gh)^{1/2} \tag{14.59}$$

where h is the height, a function of time. Let A_1 be the cross-sectional area of the tank and A_2 the cross-sectional area of the hole. The continuity equation gives

$$V_2 = V_1 \frac{A_1}{A_2} \tag{14.60}$$

where V_1 is the velocity of fall of the free liquid surface (much smaller than V_2). Obviously, V_1 is equal to the rate of drop of the liquid level i.e.

$$V_1 = -\frac{dh}{dt} \tag{14.61}$$

Combining equations (14.59), (14.60) and (14.61), we get

$$V_2 = -\frac{dh}{dt}\frac{A_1}{A_2} = (2gh)^{1/2} \tag{14.62}$$

or

$$-\frac{dh}{h^{1/2}} = \frac{A_2}{A_1}(2g)^{1/2}\, dt \tag{14.63}$$

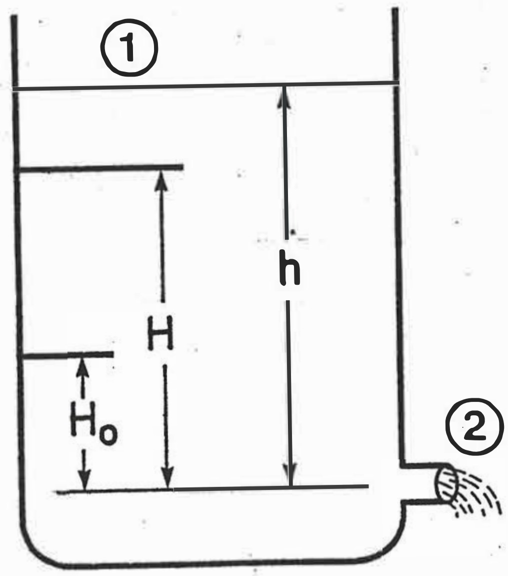

Fig. 14.10 Slow drop of liquid surface in a tank.

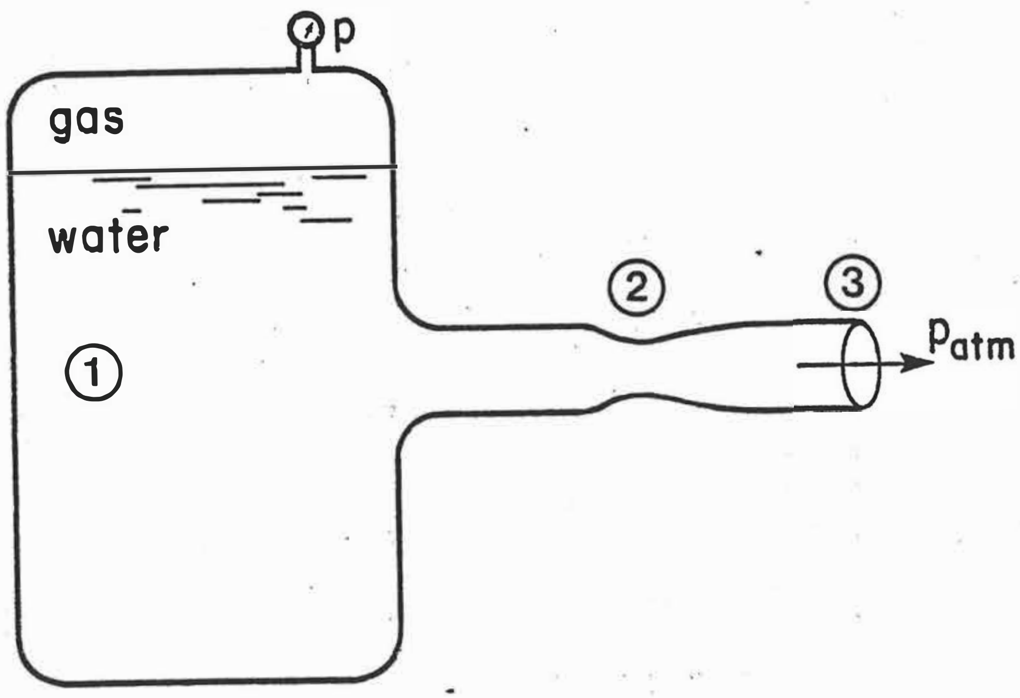

Fig. 4.11 Liquid flow from a pressurized reservoir through a constriction.

$$- \int_{H}^{H_o} \frac{dh}{h^{1/2}} = \frac{A_2}{A_1} (2g)^{1/2} \int_{t}^{t_o} dt \qquad (14.64)$$

$$\left[-2h^{1/2}\right]_{H}^{H_o} = \left[\frac{A_2}{A_1} (2g)^{1/2} t\right]_{t}^{t_o} \qquad (14.65)$$

and

$$\Delta t = t_o - t_1 = \frac{-2(H_o^{1/2} - H^{1/2})}{\frac{A_2}{A_1} (2g)^{1/2}} \qquad (14.66)$$

Letting H = 10m, H_o = 1m and A_2/A_1 = 1/100

we get

$$\Delta t = \frac{2(1^2 - 10^{1/2})\ m^{1/2}}{\frac{1}{100} (2 \times 9.81 \frac{m}{s^2})^{1/2}} = 97.6 \text{ s}$$

We note that in this example $V_2 = 100\ V_1$ and $V_2^2 = 10^4\ V_1^2$, which justifies the elimination of the $V_2^2/2g$ term from the Bernoulli equation

$$\frac{V_1^2}{2g} + z_1 = \frac{V_2^2}{2g} + z_1 \qquad (14.67)$$

that leads to Torricelli's equation $V_2 = (2gh)^{1/2}$.

14.12 PRESSURES LOWER THAN THE VAPOR PRESSURE OF LIQUIDS

We now consider liquid flow from a pressurized reservoir through a constriction, as shown in Fig. 14.11. Let us assume an absolute gas pressure of 200 kPa, and a ratio of cross-sectional areas A_2/A_3 = 0.5. We can apply the Bernoulli equation between locations 1 and 3. We have

$$\frac{V_1^2}{2} + \frac{p_1}{\rho} = \frac{V_3^2}{2} + \frac{p_3}{\rho} \qquad (14.68)$$

Inside the reservoir $V_1 \simeq 0$. Thus

$$V_3 = [\frac{2(p_1 - p_3)}{\rho}]^{1/2} \tag{14.69}$$

Where p_1 = 200 kPa (neglecting the hydrostatic pressure at 1),

$$p_3 = p_{atm} = 101.33$$

Thus

$$V_3 = 14.05 \text{ m/s}$$

and $V_2 = \frac{A_3}{A_2} V_3 = 28.1$ m/s

may now write the Bernoulli equation for points 1 and 2

$$\frac{V_1^2}{2} + \frac{p_1}{\rho} = \frac{V_2^2}{2} + \frac{p_2}{\rho} \tag{14.70}$$

where $V_1 \simeq 0$

Thus

$$p_2 = p_1 - \rho \frac{V_2^2}{2} \tag{14.71}$$

For p_1 = 200 kPa and V_2 = 28.1 m/s, we get

$$p_2 = - 194.9 \text{ kPa}$$

Negative pressure is physically meaningless. Our calculations are in error because we neglected frictional losses at these high rates of flow. It is possible, however, to reach at the constriction pressures lower than the vapor pressure p_v of liquids (for water at 20°C p_v = 2.34 while for gasoline at 20°C p_v = 55 kPa). Under such conditions bubbles of vapor will be formed. The bubbles will be moved downstream and may collapse as they enter regions of higher pressure. Implosion of bubbles near metal surfaces for long periods of time has a damaging effect in the form of fatigue failure and reduction of efficiency of fluid machinery. This phenomenon is known as <u>cavitation</u> and should be avoided by proper design (see Section 19/5).

14.13 OPTIMAL PIPE DIAMETER

The selection of pipe diameter is primarily based on economic considerations. Large diameter pipes would have higher capital costs but lower pumping power requirements than small-diameter pipes. We will take these costs into consideration for the simplest kind of economic data.

It is reasonable to assume that the annual cost of pipe (depreciation of pipe cost over a number of years) can be expressed as

$$C_{pipe} = K_e\ D^n\ L \tag{14.72}$$

where D is the diameter, L the length and K_e and n are suitable constants which may vary from one year to another.

For a horizontal pipe without any pressure differences between suction and discharge points, the pumping power will be used to overcome friction losses, i.e.

$$h_P = h_{1-2} = f\ \frac{L}{D}\ \frac{V^2}{2g} = f\ \frac{L}{D}\ \frac{Q^2/(\pi/4)^2 D^4}{2g} \tag{14.73}$$

or

$$Po = h_P\ \rho g\ Q = \left(\frac{4}{\pi}\right)^2\ f\ \frac{L}{D}\ \frac{\rho\ Q^3}{2\ D^5} \tag{14.74}$$

The annual cost of power can be expressed as

$$C_{power} = K_o \; Po = K_o \; (\frac{4}{\pi})^2 \; f \; \frac{\rho \; Q^3}{2 \; D^5} \; L \qquad (14.75)$$

where K_o will depend on power cost requirements to run the pump at a given year.

Thus, the total annual cost will be

$$C = C_{pipe} + C_{power} = K_e \; D^n L + K_o (\frac{4}{\pi})^2 \; f \; \frac{\rho \; Q^3}{2 \; D^5} \; L \qquad (14.76)$$

We can calculate the minimum total cost C by setting

$$\frac{dC}{dD} = 0 \qquad (14.77)$$

$$nK_e D^{n-1} L - 5K_o \; (\frac{4}{\pi})^2 \; f \; \frac{\rho Q^3}{2D^6} \; L = 0 \qquad (14.78)$$

Solving for D, we get

$$D = (\frac{5}{2} \; (\frac{4}{\pi})^2 \; \frac{K_o}{nK_e} \; f \; \rho Q^3)^{1/(5+n)} \qquad (14.79)$$

The value of index n is usually between 1 and 1.5 (see also De Nevers (15) and Denn (16)). Thus, the optimal pipe diameter will not change very much with the friction factor f because of the exponent 1/(5+n).

It is also interesting to determine the velocity when the optimal pipe diameter is used. We have

$$V = \frac{Q}{(\frac{\pi}{4}) D^2} = \frac{Q^{n-1}}{(\frac{\pi}{4}) [\frac{5}{2} \; (\frac{4}{\pi})^2 \; \frac{K_o}{nK_e}]^{\frac{1}{5+n}} \; f^{\frac{2}{5+n}} \; \rho^{\frac{2}{5+n}}} \qquad (14.80)$$

If we take n=1, we may write

$$V = \frac{const}{f^{1/3} \; \rho^{1/3}} \qquad (14.81)$$

Because of the exponent 1/3 there is very little dependance of the velocity on the friction factor f and density ρ of fluids. Velocities will vary within a very narrow range for all liquid flows. It turns out that for liquids like oil and water the economic velocity will be in the range of 1.5 - 2 m/s.

14.14 FURTHER COMMENTS ON FRICTION FACTORS AND LOSS COEFFICIENTS

The definition of the friction factor f varies from one textbook to another. In Section 14.3 we defined the Darcy-Weisbach friction factor as

$$f = \frac{h_f}{\frac{L}{D}\frac{V^2_{avg}}{2g}} \tag{14.82}$$

Some authors (especially in the areas of heat transfer and aerodynamics) prefer the so-called Fanning friction factor instead, which is

$$f = \frac{1}{4}\frac{h_f}{\frac{L}{D}\frac{V^2_{avg}}{2g}} \tag{14.83}$$

Thus, there will be a factor-of-four difference in all results. Consequently, care must be taken in the use of tables and formulae to make sure one has the right friction factor.

The loss coefficient of pipe fittings was defined in Section 14.5 as

$$K_L = \frac{h_L}{\frac{V^2}{2g}} \tag{14.84}$$

We expect that K_L should in general be a function of Re. However, in

Table 14.2 we gave constant values of K_L for various fittings making an implicit assumption that the Reynolds is sufficiently large (meaning Re over 10^5). The Reynolds number dependence can be taken into account by expressing K_L as an equivalent length of straight pipe, i.e.

$$K_L = f \left(\frac{L}{D}\right)_{equiv.} \tag{14.85}$$

For example Sabersky et al [17] give for a fully open globe valve $\left(\frac{L}{D}\right)_{equiv} = 340$ and for a 90^o standard elbow $\left(\frac{L}{D}\right)_{equiv} = 30$. Thus to get the K_L values given in Table 14.2 we need an approximate f value of 0.03.

REFERENCES

1. H. Blasius "Das Ähnlichkeitsgesetz bei Reibungsvorgängen in Flüssigkeiten" Forchungsheft 131, Berlin (1913).

2. L.F. Moody, "Friction Factors for Pipe Flow" ASME Trans., 66, 671 (1944).

3. J.H. Perry, The Chemical Engineer's Handbook, McGraw-Hill, 5th Ed., New York (19--).

4. E. Avallone et al " Mark's Standard Handbook for Mechanical Engineers" McGraw-Hill (2006)

5. S. A. Ofosu et al "Fluid Mechanics Handbook for Technicians" Lambert Publishing (2013)

6. "Flow of Fluids through Valves, Fittings, and Pipe" Crane Co. Tech. Pap. 410, 16th revised printing (1976), Chicago, Ill. (1976).

7. "Pipe Friction Manual" 3rd. ed., The Hydraulic Institute, New York (1961).

8. F.M. White "Fluid Mechanics" McGraw-Hill, New York (1979).

9. R.V. Giles "Fluid Mechanics and Hydraulics", Schaum's Publishing Co., New York (19--).

10. E. Brater et al "Handbook of Hydraulics" McGraw-Hill (1996)

11. Hardy Cross, "Analysis of Flow in Networks of Conduits or Conductors", Univ. of Illinois Bull. 286, November 1966.

12. T.A. Marlow et al. "Improved Design of Fluid Networks with Computers", ASCE J. Hydraul. Div., __, ___, (1966).

13. V.L. Streeter and E.B. Wylie "Fluid Mechanics" McGraw-Hill, 7th ed., New York (1979).

14. R. A. Houghtalen et al "Fundamentals of Hydraulic Engineering Systems" Pearson Education (2016)

15. N. De Nevers, "Fluid Mechanics", Addison-Wesley, Reading, Mass. (1970).

16. M.M. Denn, "Process Fluid Mechanics", Prentice-Hall, Englewood Cliffs, N.J. (1980).

17. R.H. Sabersky, A.J. Acosta and E.G. Hauptmann "Fluid Flow", 2nd edition, MacMillan, New York (1971).

John Vlachopoulos, *Fundamentals of Fluid Mechanics*
Chem. Eng., McMaster University, Hamilton, ON, Canada
(First Edition 1984, revised internet edition (2016), www.polydynamics.com)

CHAPTER 15

COMPRESSIBLE FLOW

15.1 INTRODUCTION

In previous chapters we have treated exclusively incompressible flows. We have only vaguely mentioned that a flowing fluid is said to be compressible when appreciable density changes are brought about by the motion. The assumption of incompressibility is well-founded for the flow of liquids because very large pressure differences are required for only small density variations. For example, for 1 percent change in the density of water we need a pressure change of 20,000 kPa. Such high pressure variations are very seldom encountered in practice. However, gas densities can change appreciably even for relatively small pressure variations.

Up to this point, we needed four scalar equations (the equation of continuity and three components of the equation of conservation of momentum) to describe fully a flow field. For compressible flow, however, the density and pressure changes are also accompanied by temperature changes. Thus, the energy equation becomes coupled with the equations of continuity and momentum, we therefore need all six scalar equations that were mentioned in Chapter 5, namely

Continuity equation	1	
Momentum equation	3	components
Energy equation	1	
Equation of state $\rho = \rho(p,T)$	1	
TOTAL	6	

The general theory of compressible flow is very complicated, not only because of the large number of the equations involved, but also because of the wave propagation phenomena that are predominant at flow speeds higher than the speed of sound. Fortunately, the above equations can be highly simplified for many problems. The most important simplification is based on the fact that the velocities are high, thus the viscous forces are much smaller than the inertia forces and can be neglected. Although viscous effects are always important near surfaces, they may influence only a small portion of the total flow region. Thus, it is reasonable to assume that the flow is one-dimensional (see definition of Section 3.7). Nearly all of the topics presented in this chapter are based on the one-dimensional, inviscid flow assumptions.

15.2 SPEED OF SOUND

The speed of sound is defined as the rate of propagation of an infinitesimal pressure disturbance (wave) through a continuous medium. Sound is the propagation of compression and expansion waves of finite but small amplitude such that the ear can detect them. Frequencies range from 20 to 20,000 Hertz while the magnitude is typically less than 10 Pa.

Consider a long tube filled with a motionless fluid and having a piston at one end, as shown in Fig. 15.1(a). By tapping the piston we may cause an infinitesimal pressure disturbance (wave) which will move down the tube at a constant speed. The fluid behind the wave is slighly compressed, while the fluid ahead of the wave remains undisturbed. This is an unsteady state problem. However, if we assume an infinitesimal control volume around the wave, travelling with the wave velocity a, we can apply a steady state analysis. The wave is thus stationary while the fluid flows with an approach velocity a, as shown in Fig. 15.1(b). Friction effects can be neglected and thus the velocity profile can be assumed flat. The continuity equation may be written as:

$$\rho A a = \text{const} \tag{15.1}$$

or

$$\rho A a = (\rho + d\rho)\,(a - dV)A \tag{15.2}$$

Neglecting infinitesimal quantities of higher order $(d\rho)\,(dV)$ gives

$$a\,d\rho - \rho\,dV = 0 \tag{15.3}$$

Applying the linear momentum balance (see Sec. 6.1) to the control volume, we get

$$0 = a(\rho A a) - (a - dV)\,\rho A a + pA - (p + dp)\,A \tag{15.4}$$

which further reduces to

$$dp = \rho a\,dV \tag{15.5}$$

By combining (15.3) and (15.5) we get

$$a^2 = \frac{dp}{d\rho} \tag{15.6}$$

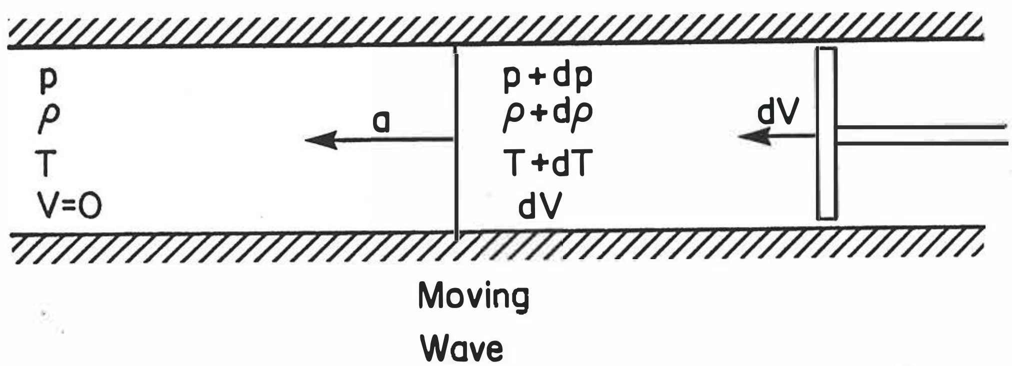

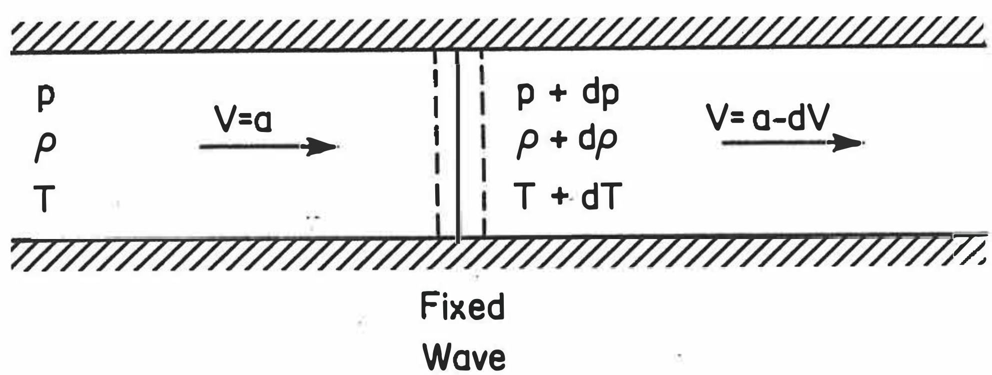

Fig. 15.1 (a) Moving pressure disturbance (wave) in a motionless fluid

(b) Fixed wave in a moving fluid

This expression gives the velocity of propagation of a compression wave. It can easily be shown to be also the velocity of propagation of an expansion wave. Since the propagation of infinitesimal expansion and compression waves is called sound, a is then the speed of sound. The above equation is equally valid for any continuum, be it a solid, a liquid, or a gas.

Since the pressure and density changes are assumed infinitesimal the process can be regarded as reversible. Because of pressure and density changes we would also expect temperature changes. However, because of the high speed of travel of the wave there is very little time for any significant heat transfer to take place, so the process is very nearly adiabatic. A reversible, adiabatic process is called isentropic. Thus, we may write

$$a^2 = \left(\frac{\partial p}{\partial \rho}\right)_s \tag{15.7}$$

For an isentropic process of perfect gas the relation between p and ρ is known from thermodynamics:

$$\frac{\rho}{\rho^k} = \text{const} \tag{15.8}$$

where $k = C_p/C_v$ is the ratio of specific heat under constant pressure to that under constant volume. k values for some common gases are given in Appendix B.

Equation (15.8) can be differentiated to give

$$\left(\frac{\partial p}{\partial \rho}\right)_s = \frac{kp}{\rho} \tag{15.9}$$

thus

$$a = \left(\frac{kp}{\rho}\right)^{1/2} \tag{15.10}$$

Then, using the equation of state for a perfect gas $p = \rho RT$, we get the speed of sound as

$$a = (kRT)^{1/2} \tag{15.11}$$

It should be noted that the constant R depends on the particular gas and it is related to the universal gas constant R by the relation R = R/molecular weight. Equation (15.11) agrees very well with experimental values for common gases at atmospheric pressure and usual temperatures. For air at 15°C, we have

$$a = [(1.4)(287)(288)]^{1/2} = 340 \text{ m/s}$$

If a continuum were incompressible equation (15.6) would give an infinite speed of sound. However, no actual liquid or solid can be perfectly incompressible. All materials have a finite speed of sound. representative values for some common materials are given in Table 15.1.

For liquids and solids it is customary to define the bulk modulus as a parameter relating the volume (or density) change to the applied pressure change:

$$E = -\frac{\Delta p}{\Delta V/V} = \frac{\Delta p}{\Delta\rho/\rho} = \rho\,\frac{dp}{d\rho} \tag{15.12}$$

Water (at 20°C and atmospheric pressure) has a bulk modulus of about 2.2×10^9 Pa while steel about 200×10^9 Pa. The bulk modulus is related to Young's modulus of elasticity K by the expression

$$\frac{E}{K} = 3\,(1 - 2\sigma) \tag{15.13}$$

where σ is Poisson's ratio. For many common metals such as steel and aluminum $\sigma \simeq 1/3$ and $E \simeq K$.

By combining equations (15.6) and (15.12) we get

$$a = \left(\frac{E}{\rho}\right)^{1/2} \tag{15.14}$$

TABLE 5.1

The speed of sound of some common materials at 15°C and pressure of 101.325 kPa.

Gases	a[m/s]
H_2	1294
He	1000
Air	340
Ar	317
CO_2	266
CH_4	185
Liquids	
Glycerin	1859
Water	1490
Mercury	1451
Ethyl Alcohol	1201
Solids	
Aluminum	5151
Steel	5059
Ice	3200

15.3 COMPRESSIBILITY AND MACH NUMBER

The definition of bulk modulus can be used in assessing the magnitude of compressibility effects. Here, we rewrite equation (15.12) as

$$\frac{\Delta\rho}{\rho} = \frac{\Delta p}{E} \tag{15.15}$$

It was stated earlier that a fluid can be considered incompressible if the density changes brought about by the motion remain small, that is, $\Delta\rho/\rho \ll 1$. For an approximate estimate of the relative magnitudes of pressure and velocity, we may use the simple (frictionless) form of the Bernoulli equation, which is

$$\frac{p}{\rho} + \frac{V^2}{2} = \text{const} \tag{15.16}$$

This indicates that the pressure change should be of the order of

$$(\Delta p) \simeq \frac{1}{2}\,\rho V^2 \tag{15.17}$$

Thus equation (15.15) becomes

$$\frac{\Delta\rho}{\rho} \simeq \frac{1}{2}\,\frac{\rho V^2}{E} \tag{15.18}$$

and with the help of equation (15.14), we have

$$\frac{\Delta\rho}{\rho} \simeq \frac{1}{2}\left(\frac{V}{a}\right)^2 \tag{15.19}$$

The ratio of the flow velocity V to the speed of sound is called the Mach number, M, after the Austrian physicist and philosopher Ernst Mach (1838-1916).

$$M = \frac{V}{a} \tag{15.20}$$

The incompressibility criterion can then be stated as

$$\frac{\Delta\rho}{\rho} \simeq \frac{1}{2} M^2 << 1 \qquad (15.21)$$

A commonly accepted limit is $\Delta\rho/\rho \leq 0.05$ which corresponds to about

$$M \leq 0.3 \qquad (15.22)$$

Air flow at standard conditions can thus be considered incompressible if the velocity is less than about 100 m/s. However, nearly all liquid flows can be considered incompressible since the flow velocities are usually small while the speed of sound very large.

Further, we may give to the dimensionless ratio called the Mach number a physical significance. We note that the numerator in Equation (15.20) represents the fluid inertia, while the denominator is related to the pressure and density change according to equation (15.6). Since the pressure change produces an elastic deformation, the Mach number represents the ratio of inertia forces to elastic forces. The critical Mach number occurs when the two forces are equal, or M = 1, that is when the flow velocity is equal to the elastic wave velocity.

Compressible flows are characterized by their Mach numbers as

$M < 1$ Subsonic

$M = 1$ Sonic

$M > 1$ Supersonic

Flows with Mach numbers over 5 are sometimes referred to as a "Hypersonic".

15.4 ONE-DIMENSIONAL FRICTIONLESS FLOW THROUGH A DUCT WITH VARYING CROSS-SECTION

For steady one-dimensional compressible flow through a duct of cross-sectional area A(x), the continuity equation (see Chapter 4) reduces the simple form

$$\rho(x)\ A(x)\ V(x) = \text{const}$$

Differentiating and then dividing by ρAV gives (15.23)

$$\frac{d\rho}{\rho} + \frac{dV}{V} + \frac{dA}{A} = 0 \tag{15.24}$$

The general form of the x component of the equation of conservation of momentum (see Chapter 6) is

$$\rho\left(\frac{\partial v_x}{\partial t} + v_x \frac{\partial v_x}{\partial x} + v_y \frac{\partial v_x}{\partial y} + v_z \frac{\partial v_x}{\partial z}\right) = -\frac{\partial p}{\partial z} + \mu\left(\frac{\partial^2 v_x}{\partial x^2} + \frac{\partial^2 v_x}{\partial y^2} + \frac{\partial^2 v_x}{\partial z^2}\right) + \rho g_x \tag{15.25}$$

Assuming steady, one-dimensional ($v_x = V$), frictionless flow and negligible gravitational effects, we may simplify the above equation to the form

$$\rho V \frac{dV}{dx} = -\frac{dp}{dx} \tag{15.26}$$

or

$$V\ dv + \frac{dp}{\rho} = 0 \tag{15.27}$$

It is interesting to note that equation (15.27) is essentially a form of the Bernoulli equation (compare to eq. 14.6) and can be written as

$$d\left(\frac{V^2}{2}\right) + \frac{dp}{\rho} = 0 \tag{15.28}$$

Equation (15.27) can also be put in the form

$$V\,dV + \frac{dp}{d\rho}\frac{d\rho}{\rho} = 0 \tag{15.29}$$

For isentropic flow, the derivative $dp/d\rho$ is equal to the speed of sound squared (eq. 15.7), thus

$$\frac{d\rho}{\rho} = -\frac{V}{a^2}\,dV \tag{15.30}$$

Then, by substituting $d\rho/\rho$ in equation (15.24), we have

$$-\frac{V}{a^2}\,dV + \frac{dV}{V} + \frac{dA}{A} = 0 \tag{15.31}$$

Introducing the definition of Mach number and rearranging gives

$$\frac{dA}{A} = (M^2 - 1)\,\frac{dV}{V} \tag{15.32}$$

This equation relates the area variation to the velocity along the duct and leads to a very important conclusion: Velocity and area changes are of opposite sign for subsonic and supersonic flow because of the factor M^2-1. There are five possibilities which are summarized in Fig. 15.2.

In the study of incompressible flow presented in previous chapters the velocity increases as the area decreases. This is also true for compressible flow at subsonic speeds. The opposite is true for supersonic flow. The velocity decreases as the cross-sectional area decreases and it increases as the cross-sectional area increases. At sonic velocity $M = 1$, since infinite acceleration is impossible we should have $dA = 0$. Thus, in order to accelerate a stagnant gas to supersonic speeds we need (a) a converging subsonic section, (b) a "sonic" throat and (c) a diverging supersonic exit. Such a device is called a converging-diverging or de Laval nozzle and is schematically shown in Fig. 15.3. It should also be noted that supersonic flow

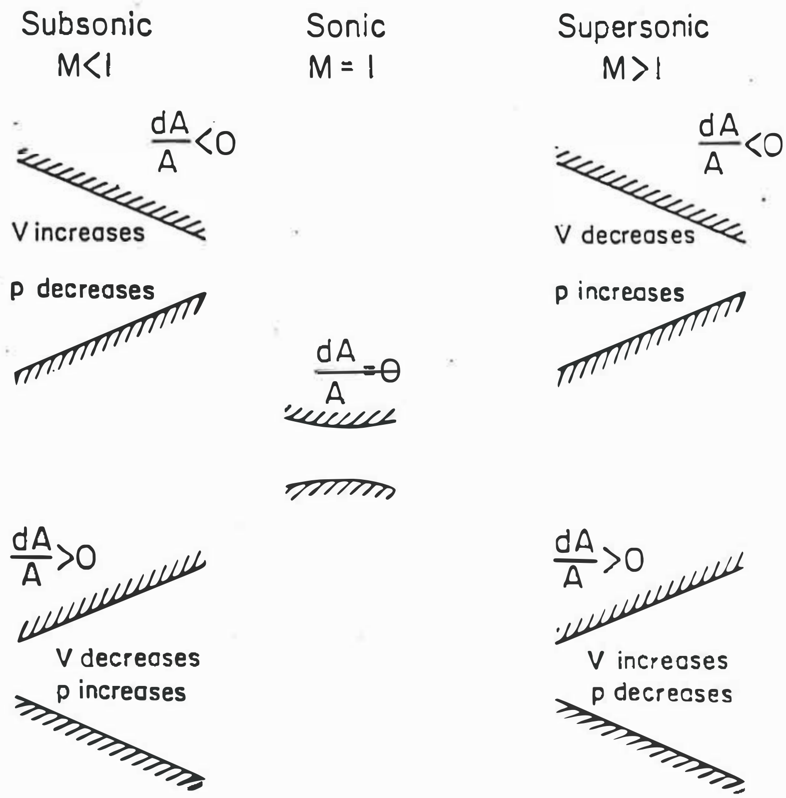

Fig. 15.2 Velocity and pressure variation in ducts with varying cross-section.

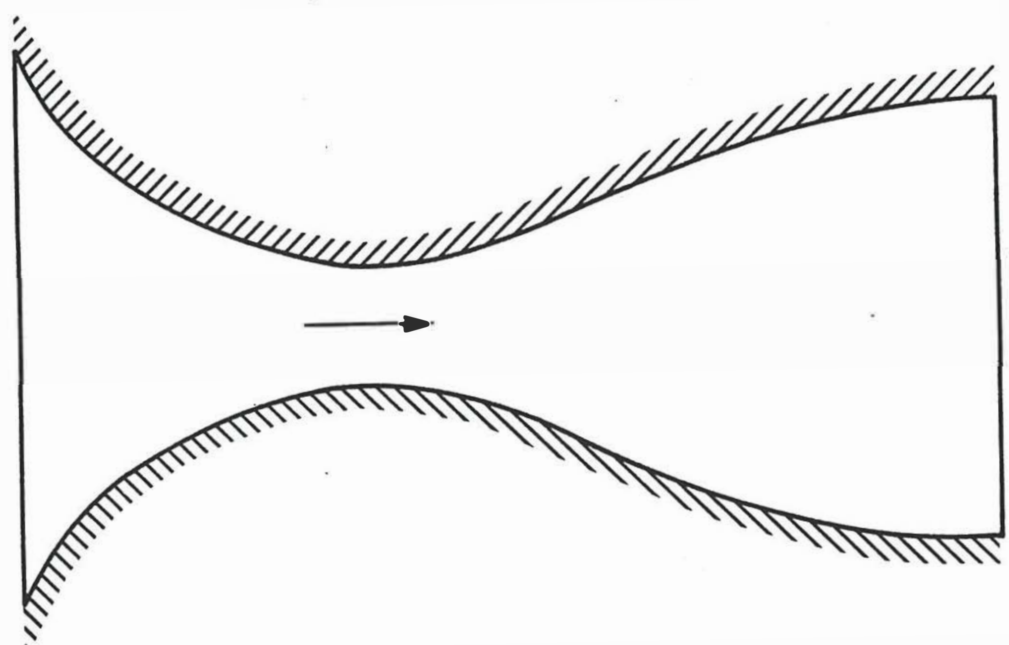

Fig. 15.3 Converging-diverging nozzle.

conditions cannot be achieved unless there is a large enough pressure differential between the reservoir of the stagnant gas and the environment at the nozzle exit.

15.5 THE BERNOULLI EQUATION FOR ISENTROPIC GAS FLOW

Although the term Bernoulli equation is usually reserved for incompressible flows, we will retain the terminology to indicate the momentum equation for one-dimensional flow. For frictionless flow and in the absence of gravitational effects we have equation (15.27), which is written here for convenience as

$$\frac{V^2}{2} + \int\frac{dp}{\rho} = \text{const} \tag{15.33}$$

or

$$\frac{V_1^2}{2} - \frac{V_2^2}{2} + \int_{p_2}^{p_1} \frac{dp}{\rho} = 0 \tag{15.34}$$

For isentropic flow

$$\frac{p}{\rho^k} = \frac{p_1}{\rho_1^k} = \frac{p_2}{\rho_2^k} = \text{const} \tag{15.35}$$

Thus

$$\int_{p_2}^{p_1} \frac{dp}{\rho} = \int_{p_2}^{p_1} \left(\frac{p_1}{p}\right)^{1/k} \frac{dp}{\rho_1} = \frac{kp_1^{1/k}}{\rho_1(k-1)} \left(p_1^{(k-1)/k} - p_2^{(k-1)/k}\right)$$

$$= \frac{k}{k-1}\frac{p_1}{\rho_1}\left[1 - \left(\frac{p_2}{\rho_1}\right)^{(k-1)/k}\right] = \frac{k}{k-1}\left(\frac{p_1}{\rho_1} - \frac{p_2}{\rho_2}\right) \tag{15.36}$$

and

$$\frac{V_1^2}{2} + \frac{k}{k-1}\frac{p_1}{\rho_1} = \frac{V_2^2}{2} + \frac{k}{k-1}\frac{p_2}{\rho_2} \tag{15.37}$$

A particularly useful form is for the case $V_1 = 0$, that is

$$\frac{V_2^2}{2} = \frac{k}{k-1}\left(\frac{p_1}{\rho_1} - \frac{p_2}{\rho_2}\right) = \frac{k}{k-1}\frac{p_2}{\rho_2}\left[\left(\frac{p_1}{p_2}\right)^{(k-1)/k} - 1\right] \tag{15.38}$$

Utilizing equation (15.10), we get

$$V_2^2 = \frac{2}{k-1} a_2^2 \left[\left(\frac{p_1}{p_2}\right)^{(k-1)/k} - 1\right] \tag{15.39}$$

or in terms of the Mach number ($M_2 = V_2/a_2$)

$$M_2^2 = \frac{2}{k-1}\left[\left(\frac{p_1}{p_2}\right)^{(k-1)/k} - 1\right] \tag{15.40}$$

This equation is also derived in somewhat different manner in the next section.

We will now use equation (15.39) to calculate the air exit velocities for the data given in Section 14.9. We have

$$a_2 = (kRT_2)^{1/2} = (1.4 \times 287 \times 293)^{1/2} = 343 \text{ m/s}$$

$$p_2 = p_{atm} = 101.325 \text{ kPa}$$

$$p_1 = p_{atm} + 3 \text{ kPa} = 104.325 \text{ kPa}$$

and

$$V_2 = 70.2 \text{ m/s}$$

while for

$$p_1 = p_{atm} + 30 \text{ kPa} = 131.325 \text{ kPa}$$

we have

$$V_2 = 212.6 \text{ m/s}$$

15.6 MACH NUMBER RELATIONS FOR ISENTROPIC FLOW

In the study of compressible flow, the concept of stagnation conditions has been found to be very helpful. These are the temperature, pressure and density at a point in a flow field where the velocity is zero. Such a stagnation point may exist in fact or it can be imagined to exist. For example, to measure the temperature we may insert a thermocouple as shown in Fig. 15.4. The moving fluid would come to rest at the thermocouple surface and the kinetic energy would be converted to heat. Thus, the thermocouple would register a temperature higher than the temperature measured by a thermometer moving with the fluid. Applying the energy equation (see Chapter 13) for steady isentropic flow between the tip of the thermocouple 0 and a point upstream gives

$$h + \frac{V^2}{2} = h_o \tag{15.41}$$

For a perfect gas with constant specific heats, the enthalpies may be replaced by C_pT and C_pT_o respectively, thus

$$C_pT + \frac{V^2}{2} = C_pT_o \tag{15.42}$$

For a perfect gas, from $C_p - C_v = R$ and $k = C_p/C_v$ we get

$$C_p = \frac{k}{k-1} R \tag{15.43}$$

and therefore

$$\frac{T_o}{T} = 1 + \frac{k-1}{2} \frac{V^2}{kRT} \tag{15.44}$$

Using equation (15.11)

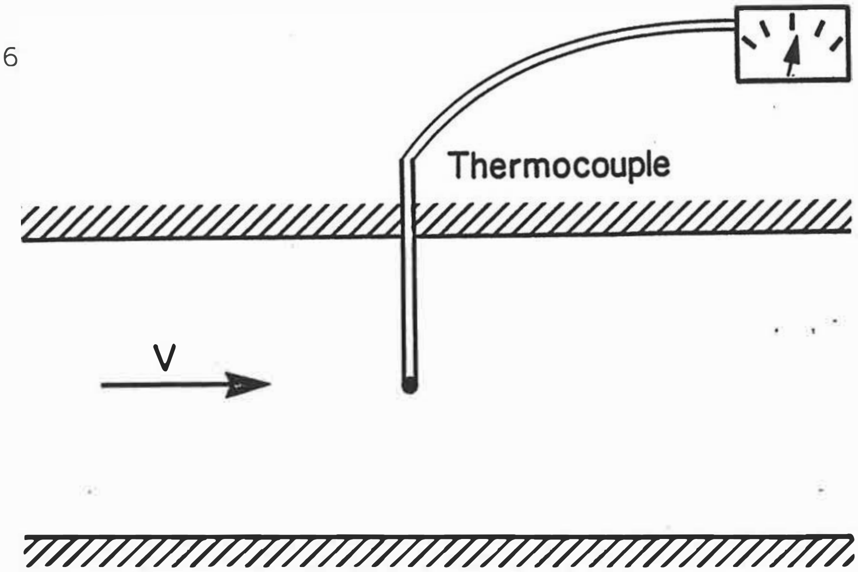

Fig. 15.4 Thermocouple for measurement of stagnation temperature.

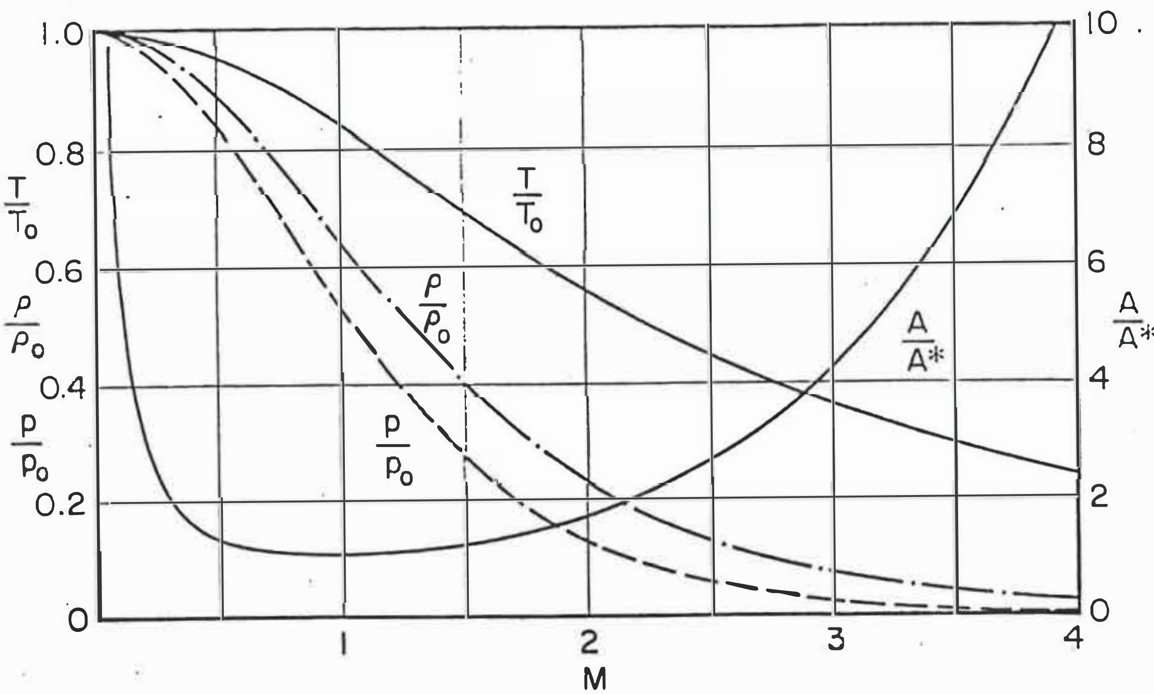

Fig. 15.5 Isentropic relations plotted as a function of Mach number M for $\kappa = 1.4$ (e.g. Air).

$$\frac{T_o}{T} = 1 + \frac{k-1}{2} M^2 \tag{15.45}$$

Further, by combining the equation of state with the isentropic process relation for a perfect gas we get

$$\frac{T_o}{T} = (\frac{p_o}{p})^{(k-1)/k} = (\frac{\rho_o}{\rho})^{k-1} \tag{15.46}$$

and

$$\frac{p_o}{p} = (1 + \frac{k-1}{2} M^2)^{k/(k-1)} \tag{15.47}$$

$$\frac{\rho_o}{\rho} = (1 + \frac{k-1}{2} M^2)^{1/(k-1)} \tag{15.48}$$

It should be noted that equation (15.47) was also derived in Section 15.5 by starting from the Bernoulli equation. Equations (15.45), (15.47) and (15.48) are plotted in Fig. 15.5 for $k = 1.4$.

The stagnation values (T_o, p_o, ρ_o) are very useful reference conditions in compressible flow calculations. Another set of useful reference values are the temperature, pressure and density for critical flow, $M = 1$. These values are denoted with an asterisk (*). We have, the critical pressure ratio

$$\frac{p^*}{p_o} = (\frac{2}{k+1})^{k/(k-1)} \tag{15.49}$$

the critical density ratio

$$\frac{\rho^*}{\rho_o} = (\frac{2}{k+1})^{1/(k-1)} \qquad (15.50)$$

and the critical temperature ratio

$$\frac{T^*}{T_o} = \frac{2}{k+1} \qquad (15.51)$$

For a diatomic gas (e.g. air), k = 1.4, we have

$$\frac{p^*}{p_o} = 0.5283 \qquad (15.52)$$

$$\frac{\rho^*}{\rho_o} = 0.6399 \qquad (15.53)$$

and

$$\frac{T^*}{T_o} = 0.8333 \qquad (15.54)$$

Further, it is easy to establish other useful ratios such as

$$\frac{p}{p^*} = \frac{p}{p_o} \; \frac{p_o}{p^*} = [\frac{(k+1)/2}{1 + \frac{k-1}{2} M^2}]^{k/(k-1)} \qquad (15.55)$$

We can also derive an area-Mach number relation for the isentropic flow of a perfect gas. The continuity equation for the steady one-dimensional flow gives

$$\rho_1 A_1 V_1 = \rho_2 A_2 V_2 \qquad (15.56)$$

The densities may be expressed as functions of the stagnation density ρ_o and Mach number M from equation (15.48). The velocities may be written, with the help of equation 15.11, as

$$V_1 = M_1 (kRT_1)^{1/2} \quad \text{and} \quad V_2 = M_2(kRT_2)^{1/2} \qquad (15.57)$$

The temperature may be expressed as a function of T_o and Mach number. Thus, equation (15.56) gives

$$\frac{\rho_o A_1 M_1 (kRT_o)^{1/2}}{(1 + \frac{k-1}{2} M_1^2)^{1/(k-1) + 1/2}} = \frac{\rho_o A_2 M_2 (kRT_o)^{1/2}}{(1 + \frac{k-1}{2} M_2^2)^{1/(k-1) + 1/2}} \qquad (15.58)$$

and

$$\frac{A_2}{A_1} = \frac{M_1}{M_2} \left(\frac{1 + \frac{k-1}{2} M_2^2}{1 + \frac{k-1}{2} M_1^2}\right)^{\frac{k+1}{2(k-1)}} \qquad (15.59)$$

Taking $M_1 = 1$ and denoting A_1 by A^*, gives in general

$$\frac{A}{A^*} = \frac{1}{M} \left(\frac{1 + \frac{k-1}{2} M^2}{1 + \frac{k-1}{2}}\right)^{\frac{k+1}{2(k-1)}} \qquad (15.60)$$

This equation is plotted in Fig. 15.5. Note the existence of a minimum for m = 1. This means that the minimum area can occur in the sonic throat section. All other duct sections must have A greater than A*.

Example 15.1

A spacecraft during re-entry into the earth's atmosphere travels at M = 5. Assuming that air is a perfect gas with $\gamma = 1.4$, determine the temperature at the frontal spacecraft surface. The air temperature is -56^oC.

Solution

We may assume nearly stagnation conditions at the frontal spacecraft surface, thus

$$T_o = T(1 + \frac{k-1}{2} M^2) = (273 - 56)\ (1 + \frac{1.4-1}{2})\ 5^2)$$

$$= 1302\ K = 1029^oC$$

Although the calculation is not very accurate because of other phenomena being also important in this case (see Reference [1]), it does however explain why meteorites and satellites burn up on entering the earth's atmosphere.

15.7 MASS FLOW RATE

The mass flow rate through any cross-section is given by

$$\dot{m} = \rho\ AV \tag{15.61}$$

By using the perfect gas law to replace ρ and by introducing the Mach number, we have

$$\dot{m} = \rho\ AaM = \frac{p}{RT}\ AM(kRT)^{1/2} = pAM\ (\frac{k}{RT})^{1/2} \tag{15.62}$$

or

$$\frac{\dot{m}}{p_oA}\ (\frac{RT_o}{k})^{1/2} = M\ \frac{p}{p_o}\ (\frac{T_o}{T})^{1/2} \tag{15.63}$$

and with the help of equation (15.46)

$$\frac{\dot{m}}{p_oA}\ (\frac{RT_o}{k})^{1/2} = M\ (\frac{p}{p_o})^{(k+1)/2k} \tag{15.64}$$

Further, we may use equation (15.47) to express the Mach number in terms of the pressure ratio, thus

$$\frac{\dot{m}}{p_oA}\ (\frac{RT_o}{k})^{1/2} = [\frac{2}{k-1}\ [(\frac{p}{p_o})^{2/k} - (\frac{p}{p_o})^{(k+1)/k}]^{1/2} \tag{15.65}$$

This equation gives the mass rate of flow in terms of reference reservoir conditions $p_o, T_o,$ the local pressure p and area A. We may also use equation (15.47) to express the mass rate of flow as a function of Mach number in the form

$$\frac{\dot{m}}{p_o A}\left(\frac{RT_o}{k}\right)^{1/2} = \frac{M}{\left[1 + \frac{k-1}{2} M^2\right]^{(k+1)/2(k-1)}} \tag{15.66}$$

Taking the derivative of $\dot{m}$ with respect to (p/p_o), in equation (15.65), and setting this derivative equal to zero for a maximum $\dot{m}$, yields

$$\frac{p}{p_o} = \left(\frac{2}{k+1}\right)^{k/(k-1)} \tag{15.67}$$

This expression gives the local pressure that will produce a maximum mass rate of flow. For a diatomic gas ($k = 1.4$)

$$\frac{p}{p_o} = 0.528 \tag{15.68}$$

Using equation (15.47) it is easy to show that this pressure ratio corresponds to Mach number $M = 1$. Thus the maximum mass rate of flow can be obtained from equation (15.66) by setting $M = 1$ and $A = A^*$ (the cross-sectional area at the throat)

$$\dot{m}_{max} = p_o\ A \frac{1}{(RT_o)^{1/2}} \frac{k^{1/2}}{\left(\frac{k+1}{2}\right)^{\frac{k+1}{2(k-1)}}} \tag{15.69}$$

For $k = 1.4$ we have

$$\dot{m}_{max} = 0.685\ p_o A^* \frac{1}{(RT_o)^{1/2}} \tag{15.70}$$

In the converging nozzle of Fig. 15.6 we can increase the flow rate by lowering the pressure of the receiver p_1 down to $p_1/p_o = 0.528$ (for air) to produce $M = 1$ at the throat. Further decrease of the receiver

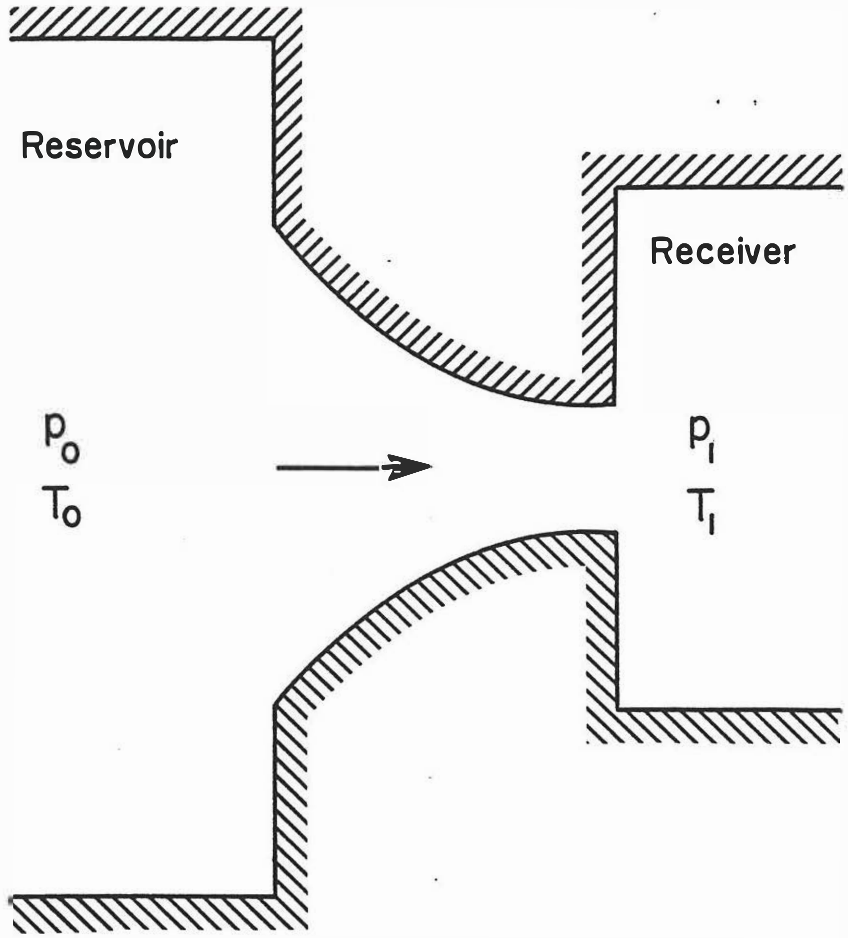

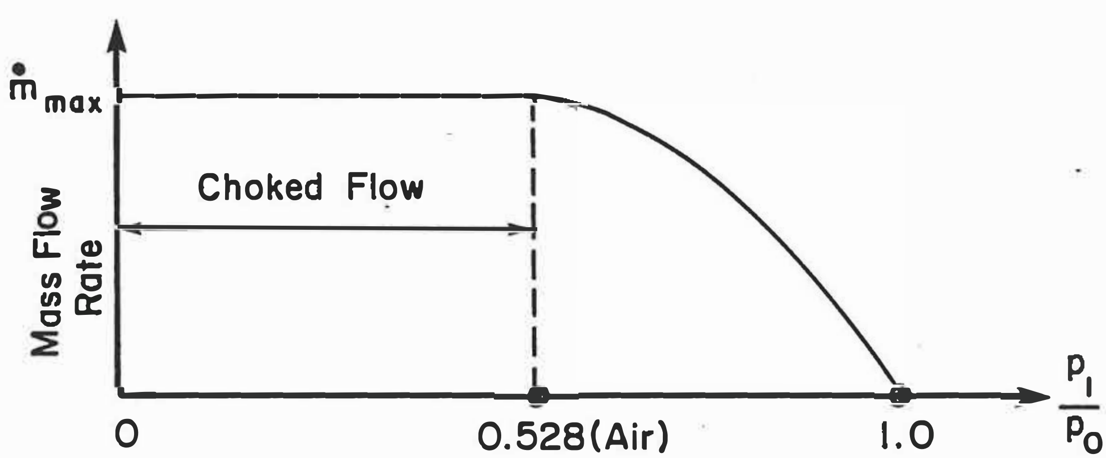

Fig. 15.6 Converging nozzle. Mass flow rate as a function of pressure ratio.

pressure p_1 will have no effect on the upstream flow, the flow rate remaining equal to $\dot{m}_{max}$ as shown in Fig. 14.6.

A simple intuitive explanation of this behavior can be given by noting that since the velocity at the exit is equal to the speed of sound there is no way to send information upstream that the exit pressure is lower than the critical pressure $p^* = 0.528\ P_o$. The flow is then fixed at the critical condition and is said to be "choked". If p_1 is less than the critical pressure p^* the gas will continue to expand. This expansion, however, occurs outside the nozzle in the form of expansion waves and shocks (see Sections 15.9 and 15.11) and dissipates the energy by friction. Under such conditions the flow is no longer one-dimensional.

15.8 OPERATION OF A CONVERGING-DIVERGING NOZZLE

We now consider the flow through a converging-diverging nozzle like the one shown in Fig. 15.7. The reservoir is at pressure p_o and the receiver at pressure p_1. We will examine what happens as p_1 is lowered.

If the receiver pressure is equal to the reservoir pressure, $p_1 = p_o$, there is no flow (Case a, in Fig. 15.7). If we lower the pressure by a small amount to P_b, a small mass flow will pass through the nozzle. The pressure will have a minimum at the throat as shown in Fig. 15.7 by curve b. By further lowering the receiver pressure to P_c we can increase the mass rate of flow to such a value as to reach critical conditions ($M = 1$) at the throat. The nozzle is passing the maximum possible flow rate for the reservoir pressure p_o and is said to be "choked". The pressure versus axial distance variation is represented by curve c.

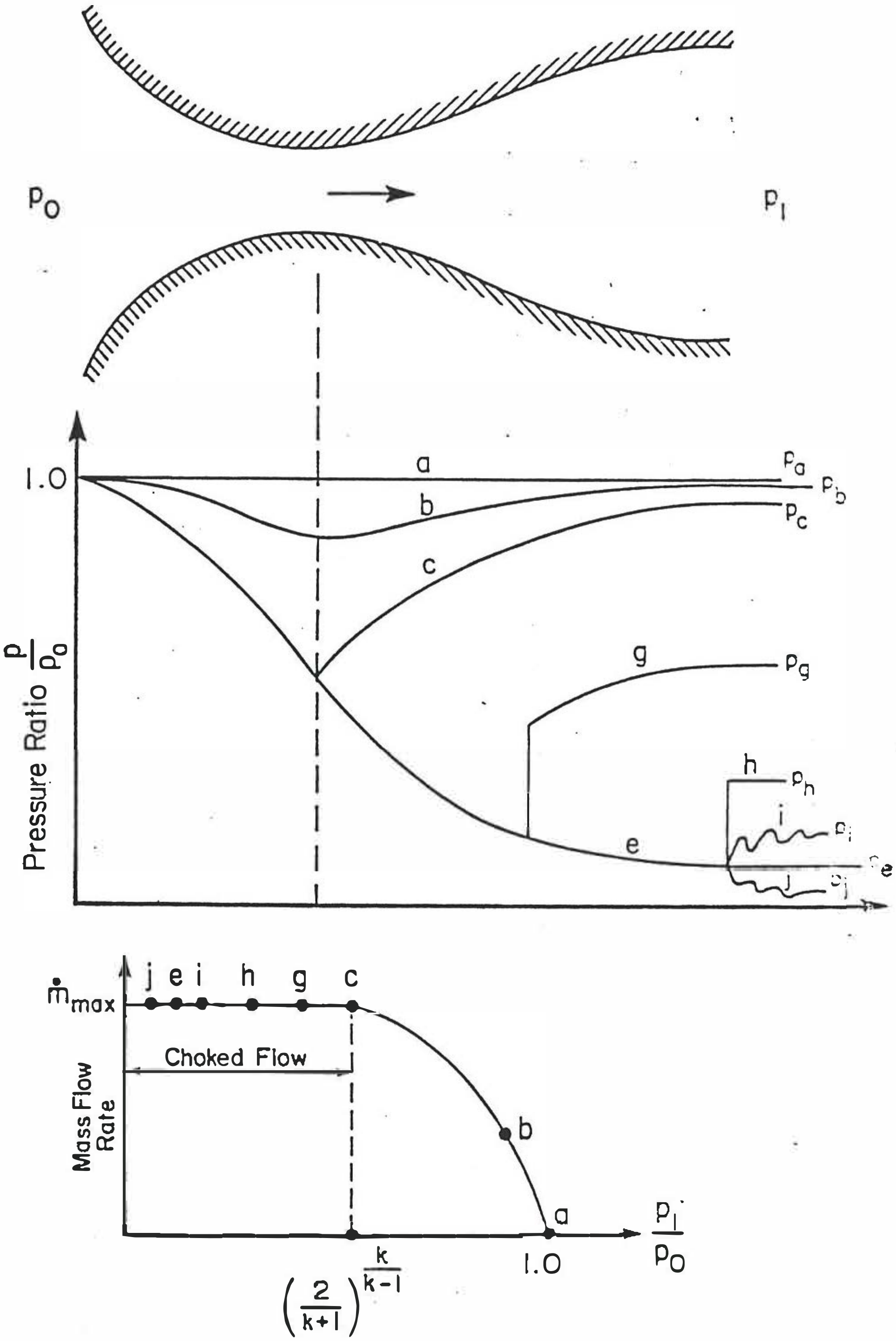

Fig. 15.7 Pressure variation and mass flow rate in a converging diverging nozzle.

The flow behavior shown by curves a, b and c in Fig. 15.7 is essentially like the flow of an incompressible fluid through a constriction. The fluid accelerates in the converging section and decelerates in the diverging section. This type of flow behavior will occur for any p_1 value between p_a and p_c. For receiver pressures lower than p_c there is some portion of the flow at supersonic speeds. In order for the flow to remain isentropic the Mach number relations of Section 15.6 must be obeyed. Using the ratio (A_e/A^*), which is the area at the exit over the area at the throat, we may calculate the exit Mach number from equation (15.60) and then the corresponding pressure p_e from equation (15.47). If the receiver pressure is equal to the value so calculated the flow remains isentropic throughout. The mass rate of flow is the same as for case c (choked flow). The Mach number will be increasing smoothly from 0 at the reservoir to 1 at the throat and further to the supersonic value calculated at the exit. The pressure will be decreasing with the axial distance from the reservoir as shown by curve e.

If the receiver pressure is between p_c and p_e the mass flow rate remains the same as in case c (or e). The flow accelerates beyond the throat to a supersonic Mach number at which a normal shock compression (see next section) occurs as shown in Fig. 15.8. Across the shock the pressure rises abruptly in a highly reversible (therefore non-isentropic) process. Downstream of the shock the flow is isentropic, subsonic and decelerating. As the receiver pressure is further lowered below p_g the normal shock moves closer to the exit. For $p_1 = p_h$ the normal shock stands right at the exit. The flow is identical to case e inside the nozzle, but it leaves the exit plane at subsonic speed. When

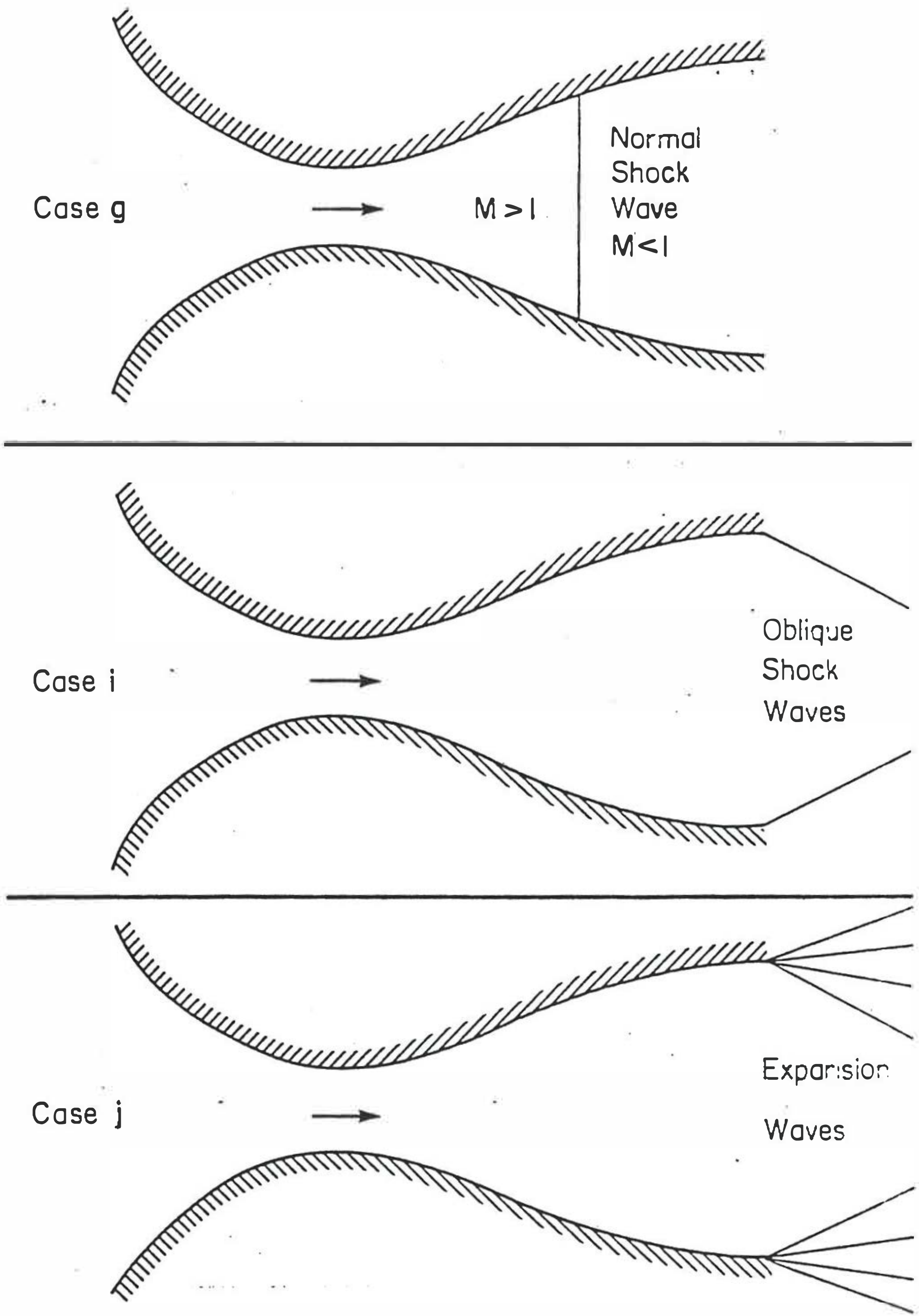

Fig. 15.8 Normal shock, oblique shocks and expansion waves in converging-diverging flow.

p_1 is between p_h and p_e the flow remains the same inside the nozzle but the normal shock is bent and extends into the flow in the form of two intersecting oblique shocks (see Fig. 15.8 and Section 15.11). The flow is said to be overexpanded because the exit-plane pressure is lower than the receiver pressure. As the receiver pressure is further lowered the shocks weaken and finally disappear for $p_1 = p_e$.

When p_1 is less than p_e an expansion wave (see Section 15.11) exists at the nozzle exit as shown in Fig. 15.8. The exit-plane pressure is higher than the receiver pressure and the flow is said to be underexpanded.

Further details on the jet flow leaving the nozzle under overexpanded or underexpanded conditions may be found in specialized books by Shapiro [9], Liepman and Roshko [3], Cambel and Jennings [4] and Thomson [5].

Example 15.2

Air flows from a reservoir where p = 500 kPa, T = 100°C through a converging-diverging nozzle to the atmosphere (assume p = 100 kPa). The area at the throat is 10 cm^2. Determine the nozzle exit area required for isentropic and shock-free flow, the mass flow rate, the Mach number and the temperature at the nozzle exit.

Solution

First we note that the pressure ratio p_1/p_o = 100/500 = 0.2 is less than the critical ratio for air (0.528). Thus the flow will be supersonic at least in some portion of the flow field.

To calculate the Mach number for isentropic flow we use equation

(15.47). We have

$$\frac{p_o}{p} = (1 + \frac{k-1}{2} M^2)^{k/(k-1)}$$

For p_o = 500 kPa, p = 100 kPa, k = 1.4 we get

$$M = 1.71$$

The exit area can be determined from equation (15.60)

$$\frac{A}{A^*} = \frac{1}{M} \left(\frac{1 + \frac{k-1}{2} M^2}{1 + \frac{k-1}{2}}\right)^{(k+1)/2(k-1)}$$

For k = 1.4 and M = 1.71 we get

$$\frac{A}{A^*} = 1.347$$

Thus

$$A_e = 1.347 \times 10 = 13.47 \text{ cm}^2$$

Next we determine the exit temperature from equation (15.45)

$$\frac{T_o}{T} = 1 + \frac{k-1}{2} M^2$$

For k = 1.4 and M = 1.71 we get

$$\frac{T_o}{T} = 1.585$$

Thus

$$T = \frac{1}{1.585} (273 + 100) = 235.4 \text{ K} = -37.6^oC$$

We note that the expansion occurring in the diverging nozzle section is accompanied by a considerable cooling of the air stream.

The mass flow rate for choked flow is calculated from equations of

Section 15.7. Since the flow is choked we may use equation (15.70)

$$\dot{m}_{max} = 0.685\ p_o A^* \frac{1}{(RT_o)^{1/2}}$$

For $R = 287$ J/kg·K, $p_o = 500{,}000$ Pa, $T_o = 373$ K and $A^* = 0.001\ m^2$ we get

$$\dot{m}_{max} = 1.047 \text{ kg/s}$$

15.9 NORMAL SHOCK WAVES

It was explained in the previous section that under certain conditions an abrupt pressure rise is necessary to accommodate the pressure imposed at the exit plane of a converging-diverging nozzle. This process is irreversible and is called a normal shock wave. Shock waves are very thin (usually of the order of 10^{-3} mm) and represent a discontinuous change of flow properties. The relations between the flow properties ahead and after the wave can be established by using the conservation principles for a thin control volume as shown in Fig. 15.9. Since the control volume is very thin we may take $A_1 \simeq A_2$, thus continuity:

$$\rho_1 V_1 = \rho_2 V_2 \tag{15.71}$$

linear momentum:

$$p_1 - p_2 = \rho_2 V_2^2 - \rho_1 V_1^2 \tag{15.72}$$

energy:

$$h_1 + \frac{V_1^2}{2} = h_2 + \frac{V_2^2}{2} \tag{15.73}$$

equation of state for a perfect gas:

$$\frac{p_1}{\rho_2 T_2} = \frac{p_2}{\rho_2 T_2} \tag{15.74}$$

and for constant C_p:

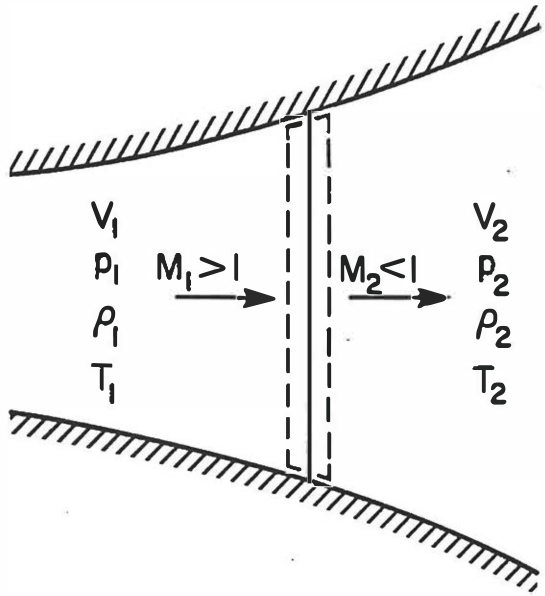

Fig. 15.9 Normal shock wave.

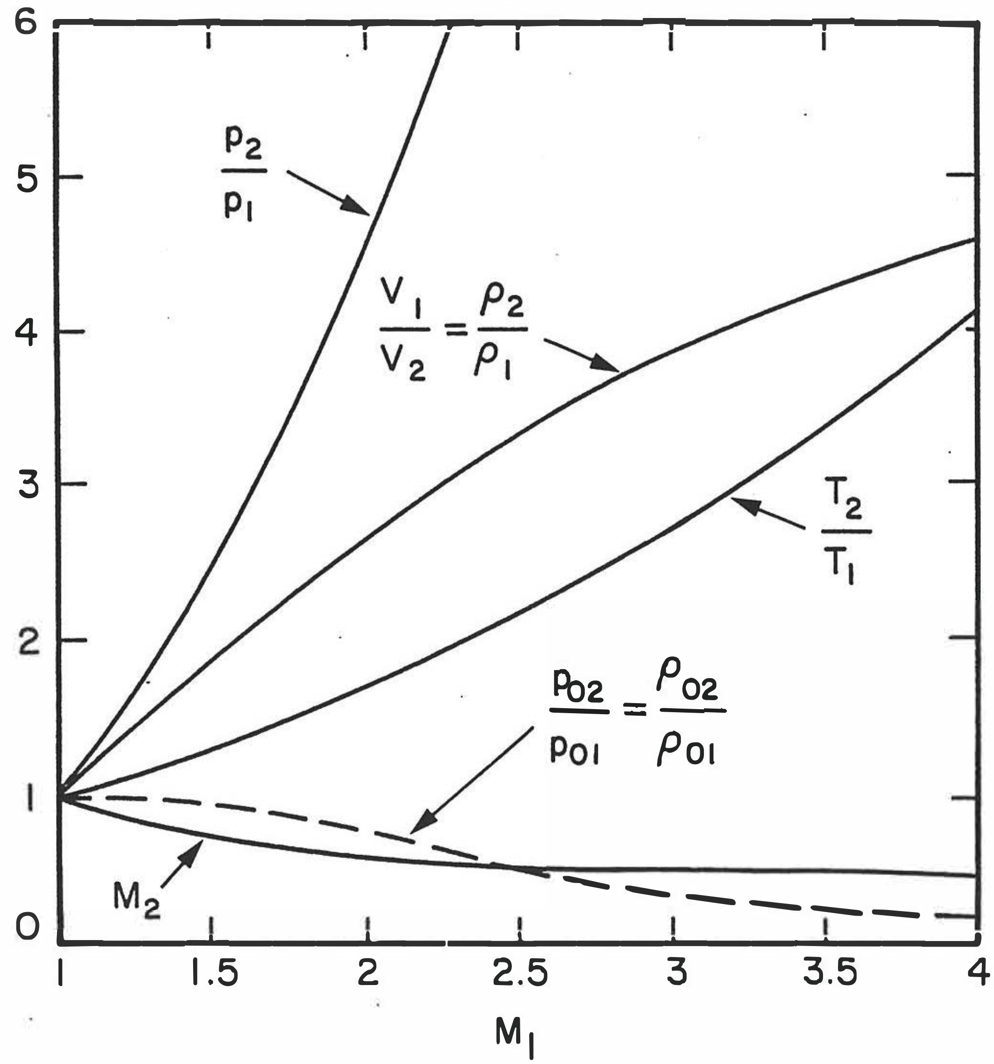

Fig. 15.10 Flow property ratios across a normal shockwave for k = 1.4.

$$h = C_p T \tag{15.75}$$

The equation of conservation of momentum (15.72) may be rewritten as

$$1 - \frac{p_2}{p_1} = \frac{\rho_2 V_2^2 - \rho_1 V_1^2}{p_1} = \frac{\rho_1 V_1^2}{p_1} \left(\frac{\rho_2 V_2^2}{\rho_1 V_1^2} - 1\right) \tag{15.76}$$

and using the continuity equation (15.71) and the speed of sound (15.10) yields

$$1 - \frac{p_2}{p_1} = k\, M_1^2 \left(\frac{V_2}{V_1} - 1\right) \tag{15.77}$$

where M_1 is the Mach number (V_1/a_1).

By manipulating the energy equation (15.73) and using (15.11) and (15.43) we get

$$1 - \frac{h_2}{h_1} = \frac{k-1}{2}\, M_1^2 \left(\frac{V_2^2}{V_1^2} - 1\right) \tag{15.78}$$

Noting that

$$\frac{h_2}{h_1} = \frac{T_2}{T_1} = \frac{p_2\, \rho_1}{p_1\, \rho_2} = \frac{p_2}{p_1} \frac{V_2}{V_1} \tag{15.79}$$

we may eliminate the enthalpy and velocity ratios from (15.77) and (15.78) to get

$$\left(1 - \frac{p_2}{p_1}\right)\left(1 - \frac{1}{kM_1^2} \frac{p_2}{p_1}\right) = \left(1 - \frac{p_2}{p_1}\right) \left[\frac{k-1}{k} + \frac{k-1}{2k^2\, M_1^2} \left(1 - \frac{p_2}{p_1}\right)\right] \tag{15.80}$$

This equation has a solution for $p_1 = p_2$, which is of no interest, because it represents the case of continuous flow with no shock wave. For $p_1 \neq p_2$ we may divide equation (15.80) by $1 - p_2/p_1$ to obtain

$$1 - \frac{1}{k\ M_1^2}\frac{p_2}{p_1} = \frac{k-1}{k} + \frac{k-1}{2k^2\ M_1^2}\ (1 - \frac{p_2}{p_1}) \tag{15.81}$$

and solving for the pressure ratio across the shock wave

$$\frac{p_2}{p_1} = \frac{2k}{k+1}\ M_1^2 - \frac{k-1}{k+1} \tag{15.82}$$

Introducing this expression into equation (15.77) and using (15.71) yields

$$\frac{\rho_1}{\rho_2} = \frac{V_2}{V_1} = \frac{k-1}{k+1} + \frac{2}{(k+1)\ M_1^2} \tag{15.83}$$

and from (15.79)

$$\frac{T_2}{T_1} = [2 + (k-1)\ M_1^2]\ \frac{2k\ M_1^2 - (k-1)}{(k+1)^2\ M_1^2} \tag{15.84}$$

Further manipulation leads to

$$M_2^2 = \frac{1 + \frac{k-1}{2}\ M_1^2}{k\ M_1^2 - \frac{k-1}{2}} \tag{15.85}$$

The stagnation properties ahead and after the wake can be obtained from the above equations by taking $V_1 = 0$ and $V_2 = 0$. We have

$$T_{01} = T_{02}$$

$$\frac{p_{02}}{p_{01}} = \frac{\rho_{02}}{\rho_{01}} = (\frac{2k}{k+1}\ M_1^2 - \frac{k-1}{k+1})^{1/(1-k)}\ (\frac{2}{(k+1)\ M_1^2} + \frac{k-1}{k+1})^{k/(1-k)} \tag{15.86}$$

The above relations are plotted as a function of the Mach number M_1 for a diatomic gas k = 1.4, in Fig. 15.10. We note that across a shock wave the pressure increases greatly while the density and temperature increase moderately. The upstream flow is supersonic while downstream the flow is subsonic.

Normal shock waves occur not only in supersonic duct flows but also in front of objects travelling at supersonic speeds. Shock waves are generated also in the laboratory in a device called shock tube by rupturing a diaphragm separating a region of high pressure from region of low pressure. When such a rupture occurs the shock wave is not stationary but it moves from the high to the low pressure region. For such a moving shock wave we can apply all the equations developed in this section by using a control volume moving with the wave. Shock tubes are used in the study of gas properties and reaction rates at very high temperatures [6,7,8].

Example 15.3

A ground level explosion creates a spherical shock wave which propagates in still air at 101.325 kPa and 15°C. The maximum registered gage pressure inside the wave is 1000 kPa. Assuming that the spherical wave can be approximated as a moving normal shock determine the wave speed and the air velocity immediately behind the wave.

Solution

We take a control volume moving with the shock wave at speed V_1. Thus

$$M_1 = \frac{V_1}{a_1}$$

where a_1 is the velocity of sound in air at 15°C

$$a_1 = (kRT)^{1/2} = (1.4 \times 287 \times 288)^{1/2} = 340 \text{ m/s}$$

M_1 can be determined from the pressure ratio across the shock with the help of equation (15.82). For

$$\frac{p_2}{p_1} = \frac{1000 + 101.325}{101.325} = 10.87$$

we have

$$10.87 = \frac{2 \times 1.4}{1.4+1} M_1^2 - \frac{1.4-1}{1.4+1}$$

$$M_1 = 3.076$$

and

$$V_1 = 3.076 \times 340 = 1045.7 \text{ m/s}$$

From equation (15.83) we calculate V_2

$$\frac{V_2}{V_1} = \frac{k-1}{k+1} + \frac{2}{(k+1)\, M_1^2}$$

$$\frac{V_2}{V_1} = \frac{1.4-1}{1.4+1} + \frac{2}{(1.4+1)(3.076)^2} = 0.2548$$

$$V_2 = 266.4 \text{ m/s}$$

Thus the air velocity immediately behind the wave will be

$$V = V_1 - V_2 = 779.3 \text{ m/s}$$

This result is in agreement with the observation that powerful explosions cause a brief flow of air at very high speeds.

15.10 COMPRESSIBLE PIPE FLOW WITH FRICTION

We now consider the adiabatic compressible flow of a perfect gas with friction, in a long pipe of constant cross-sectional area ($A = \pi D^2/4$).

For one-dimensional flow the continuity equation gives

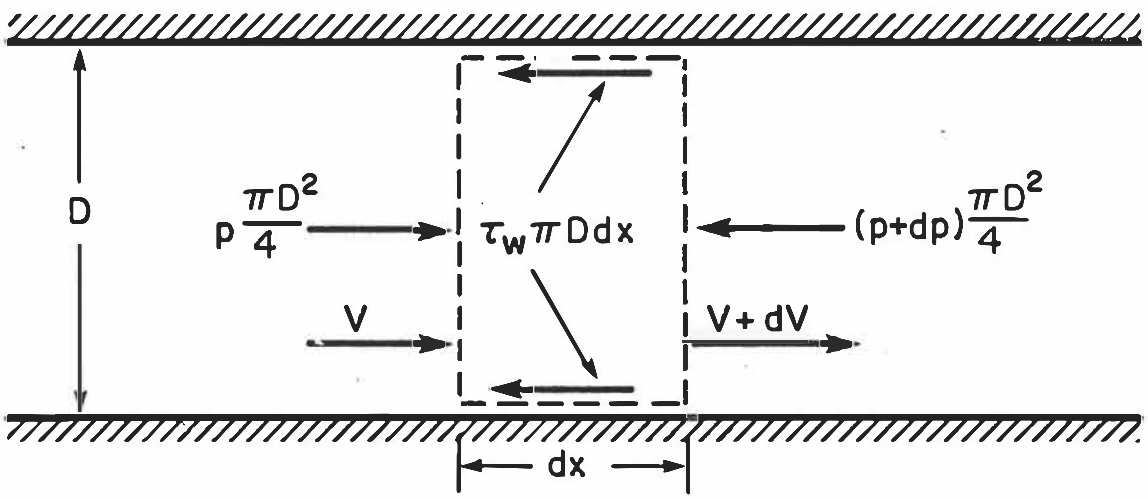

Fig. 15.11 Control volume for compressible pipe flow with friction.

$$\rho V = \frac{\dot{m}}{A} = \text{const} \qquad (15.87)$$

or

$$\frac{dV}{V} + \frac{d\rho}{\rho} = 0 \qquad (15.88)$$

The equation of conservation of linear momentum may be written as (see Fig. 15.11)

$$p\,\frac{\pi D^2}{4} - (p + dp)\,\frac{\pi D^2}{4} - \tau_w\,\pi D\,dx = \dot{m}\,(V + dV - V) \qquad (15.89)$$

or

$$\rho V\,dV + dp + \frac{4\tau_w\,dx}{D} = 0 \qquad (15.90)$$

and by introducing the Darcy-Weisbach friction factor (see Sections 10.6 and 14.3)

$$\tau_w = \frac{1}{8}\,fp\,V^2 \qquad (15.91)$$

we have

$$\rho V\,dV + dp + \frac{fp\,V^2 dx}{2D} = 0 \qquad (15.92)$$

The equation of conservation of energy is

$$h + \frac{V^2}{2} = \text{const} \qquad (15.93)$$

or

$$C_p T + \frac{V^2}{2} = \text{const} \qquad (15.94)$$

$$C_p dT + VdV = 0 \qquad (15.95)$$

The perfect gas law

$$p = \rho RT \qquad (15.96)$$

can be differentiated (after taking the logarithms) to give

$$\frac{dp}{p} = \frac{d\rho}{\rho} + \frac{dT}{T} \tag{15.97}$$

Thus we have four differential equations (15.88, 15.92, 15.95 and 15.97) and four unknowns p, ρ, T and V. It is impossible to eliminate all variables and get closed-form solutions for p(x), ρ(x), T(x) and V(x). However, it is possible to express all the variables as functions of the local Mach number M = M(x)

$$M = \frac{V}{a} \tag{15.98}$$

where

$$a = \left(\frac{kp}{\rho}\right)^{1/2} \tag{15.99}$$

or

$$M^2 = \frac{\rho V^2}{kp} \tag{15.100}$$

The momentum equation (15.92) can be rewritten as

$$kM^2 \frac{dV}{V} + \frac{dp}{p} + \frac{kf\ M^2\ dx}{2D} = 0 \tag{15.101}$$

The energy equation (15.95) for C_p = kR/(k-1) can be expressed as (see Section 15.6):

$$T = \frac{T_o}{1 + \frac{k-1}{2} M^2} \tag{15.102}$$

which gives

$$\frac{dT}{T} = - \frac{(k-1)\ MdM}{1 + \frac{k-1}{2} M^2} \tag{15.103}$$

Using (15.88) and (15.103) to replace dp/p and dT/T in equation (15.97) yields

$$\frac{dp}{p} = -\frac{dV}{V} - \frac{(k-1)\ MdM}{1 + \frac{k-1}{2} M^2} \tag{15.104}$$

The Mach number may be written as

$$M = \frac{V}{a} = \frac{V}{(KRT)^{1/2}} \tag{15.105}$$

By taking the logarithms and then differentiating, we have

$$\frac{dM}{M} = \frac{dV}{V} - \frac{1}{2}\frac{dT}{T} \tag{15.106}$$

Finally, combining equations (15.101), (15.103), (15.104) and (15.106) gives

$$\frac{(1 - M^2)\ dM}{M^3(1 + \frac{k-1}{2} M^2)} = \frac{kfdx}{2D} \tag{15.107}$$

From this equation we can easily conclude that for subsonic flow ($M < 1$), $dM/dx > 0$, which means that the Mach number increases with distance. For supersonic flow ($M > 1$) the opposite is true, $dM/dx < 0$, which means that the Mach number decreases with distance. Thus this theory predicts that the effect of friction in a constant area pipe is to cause the Mach number always to approach unity. This can occur only at the exit where for $M = 1$, $dM/dx = 0$.

Equation (15.107) can be integrated from some position in the pipe where the Mach number has a given value to a critical length where $M = 1$. We have

$$\frac{kf}{2D}\int_0^{L_{crit}} fdx = \int_M^1 \frac{(1-M^2)\ dM}{M^3(1 + \frac{k-1}{2} M^2)} \tag{15.108}$$

By assuming a constant value of the friction factor and integrating, we get

$$L_{crit} = \frac{D}{f} \left[\frac{1-M^2}{kM^2} + \frac{k+1}{2k} \ln \frac{(k+1)\ M^2}{2 + (k-1)\ M^2}\right] \tag{15.109}$$

Although f varies somewhat with the Mach number, the above equation is reasonably accurate for subsonic flow with an average f calculated from the Moody chart. For supersonic flow of air, measurements [9] give friction factors up to 50 percent less than the Moody chart. When the exit Mach number is unity the flow is said to be choked. If the actual length of a pipe L is less than the critical length L_{crit} the flow at the exit may be subsonic or supersonic depending on inlet conditions and the presence or lack of shocks (see also Section 15.8). The question may be asked as to what will happen if we increase the actual length beyond L_{crit}. We may distinguish two cases.

(a) Inlet flow subsonic.

Let L_{crit} be the critical length for an inlet Mach number M_1. By increasing the actual length $L > L_{crit}$ the inlet Mach number will be reduced so that at the exit we will always have $M = 1$. The Mach number reduction is accompanied by a reduction in flow rate and the flow is said to be choked by friction.

(b) Inlet flow supersonic.

Friction has an enormous influence on supersonic pipe flow. For example for $M = 4$ we may calculate from equation (15.109) $L_{crit} = D/f \times 0.633$. Thus if we take (see Moody chart, Fig. 14.3) an approximate value of $f \simeq 0.015$ we find that only 42 diameters of pipe length are needed to reach sonic velocity at the exit. If L is increased beyond 42 D, the flow will not choke but a normal shock will form so that the subsonic flow immediately behind the shock reaches the sonic point at the exit. By further increasing the length the shock will move back towards the inlet and eventually will produce choked flow conditions, which will be evidenced by a reduction in the mass rate of flow.

In compressible pipe flow calculations the ratios p/p^*, ρ/ρ^*, T/T^*, V/V^* are very useful. p, ρ, T and V represent the upstream conditions and p^*, ρ^*, T^* and V^* the critical conditions at the pipe exit. All these can be expressed as functions of the upstream Mach number. By manipulating the Mach number, relations of Section 15.6 and the continuity equation we get

$$\frac{p}{p^*} = \frac{1}{M} \left(\frac{\frac{k+1}{2}}{1 + \frac{k-1}{2} M^2} \right)^{1/2} \tag{15.110}$$

$$\frac{\rho}{\rho^*} = \frac{V^*}{V} = \frac{1}{M} \left(\frac{1 + \frac{k-1}{2} M^2}{\frac{k+1}{2}} \right)^{1/2} \tag{15.111}$$

$$\frac{T}{T^*} = \frac{k+1}{2 + (k-1) M^2} \tag{15.112}$$

Example 15.4

A 25 cm diameter pipe discharges air at atmospheric pressure (p = 101.325 kPa) at sonic velocity. Determine the upstream length where p = 500 kPa if the pipe is made of galvanized iron. Also, determine the velocity at this upstream location and the mass rate of flow through the pipe. The air stagnation temperature in the pipe is $T_o = 80^\circ C$.

Solution

For a pressure ratio

$$\frac{p}{p^*} = \frac{500}{101.325} = 4.9346 \text{ from equation (15.110), by}$$

trial error we get approximately

$$M = 0.242$$

It should be noted that tables of p/p^* etc. versus M are available in many textbooks (see for example reference 10). The temperature can be calculated with the help of equation (15.45)

$$T = \frac{T_o}{1 + \frac{k-1}{2} M^2}$$

$$T = \frac{273 + 80}{1 + \frac{1.4-1}{2} (0.242)^2} = 349 \text{ K}$$

The speed of sound for this temperature is

$$a = (kRT)^{1/2} = (1.4 \times 287 \times 349)^{1/2} = 374.5 \text{ m/s}$$

Thus the air velocity is

$$V = Ma = 0.242 \times 374.5 = 90.6 \text{ m/s}$$

The mass rate of flow is

$$\dot{m} = \rho AV$$

The density can be determined from the perfect gas law

$$\rho = \frac{p}{RT} = \frac{500{,}000}{287 \times 349} = 4.99 \text{ kg/m}^3$$

Thus

$$\dot{m} = 4.99 \, \pi \, \frac{0.25^2}{4} \, 90.6 = 22.18 \text{ kg/s}$$

The pipe length can be calculated from equation (15.109), we have

$$L_{crit} = \frac{D}{f}\left[\frac{1-M^2}{k\,M^2} + \frac{k+1}{2k}\,\ell n\,\frac{(k+1)\,M^2}{2+(k-1)\,M^2}\right]$$

$$L_{crit} = \frac{D}{f}\left[\frac{1-0.242^2}{1.4\times 0.242^2}\quad \frac{1.4+1}{2\times 1.4}\,\ell n\,\frac{(1.4+1)\times 0.242^2}{2+(1.4-1)\times 0.242^2}\right]$$

$$= \frac{D}{f}\,9.19$$

From the Moody chart (Fig. 14.3) for $\varepsilon/D = 0.15/250 = 0.0006$ we select a value (constant for high Re) $f \simeq 0.0175$.

Thus, $L_{crit} = \frac{0.25}{0.0175} \times 9.19 = 131.29$ m

15.11 OBLIQUE SHOCKS, EXPANSION WAVES AND THE SONIC BOOM

In one-dimensional supersonic flow only normal shocks, i.e. discontinuities normal to the flow, are possible. We now consider the two-dimensional flow over a wall with a change in direction as shown in Fig. 15.12. In subsonic flow the streamlines will adjust gradually to the change in direction (Fig. 15.12(a)). In supersonic flow no information can propagate upstream to signal the flow to adjust gradually to the change in direction. Thus the flow changes direction abruptly by passing through a discontinuity called <u>oblique shock</u> (Fig. 15.12(b).

For a change in the flow direction like the one shown in Fig. 15.13, boundary layer separation and flow reversal will take place in subsonic flow (Fig. 15.13(a)). Abrupt discontinuities cannot be formed in such an expansion turn, when the flow is supersonic, in contrast to the compression turn of Fig. 15.12(b). The change in flow direction is accomplished through a "fan" of waves usually called <u>Prandtl-Meyer expansion waves</u> (Fig. 15.13(b)).

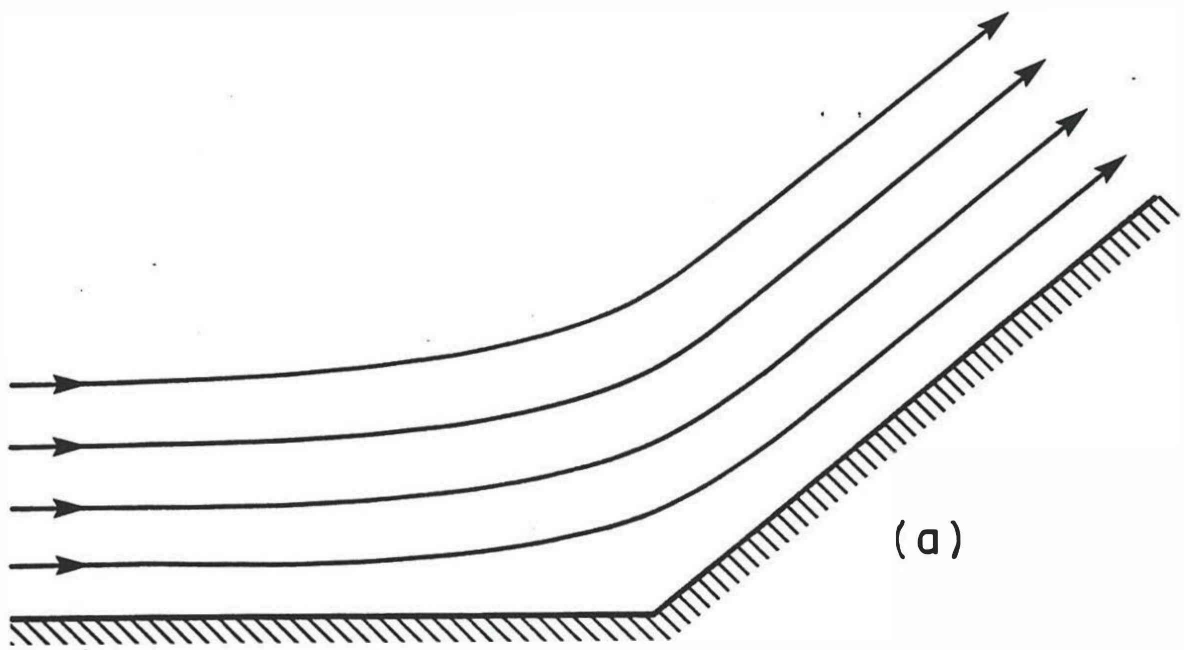

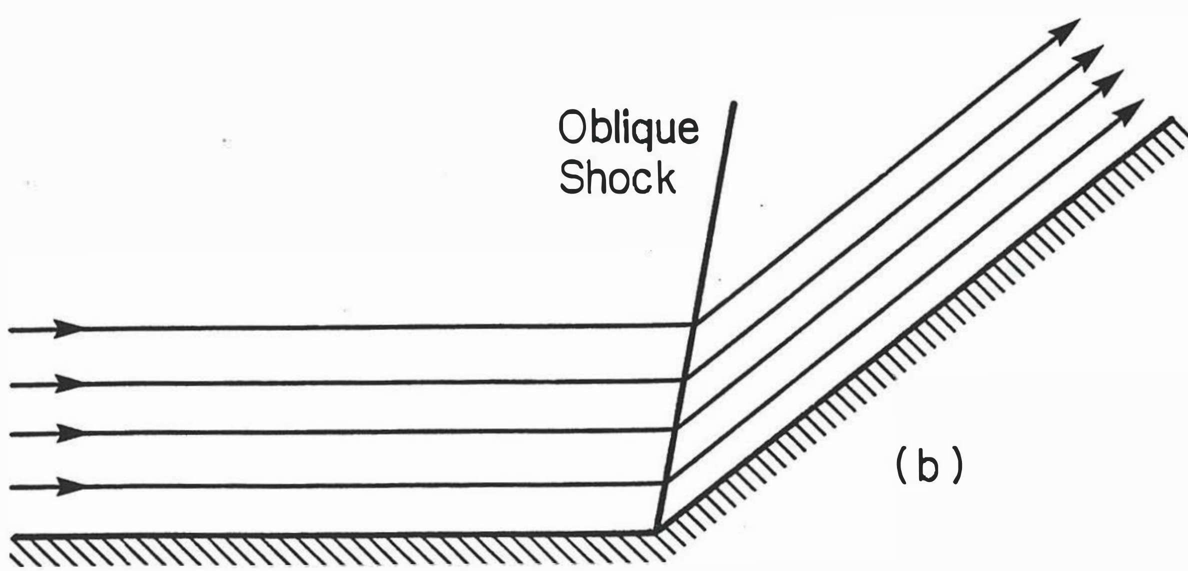

Fig. 15.12 Turning flow patterns (a) incompressible and (b) compressible.

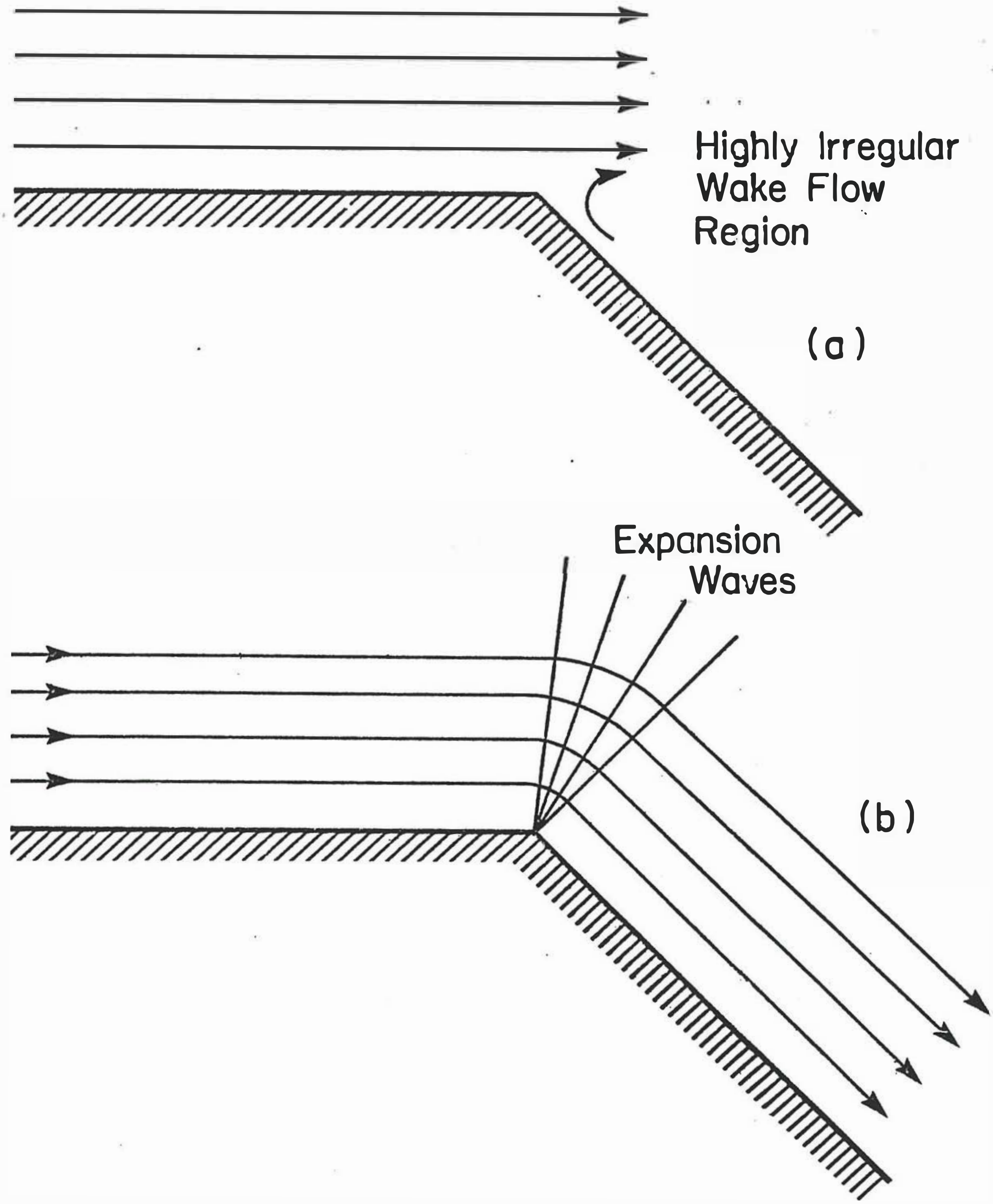

Fig. 15.13 Expanding flow patterns (a) incompressible and (b) compressible.

The flow after an oblique shock may be either subsonic or supersonic, depending on the flow deflection angle. The flow in an expansion results in an increase of the Mach number because of the flow area widens. For more details the reader is referred to introductory texts like White [10] and Sabersky et al. [11] or the specialized references [2-5].

Let us now examine the shock structure in front of a blunt body travelling at supersonic speeds in the atmosphere. There will be a normal shock, a strong oblique shock and a weaker oblique shock further out as shown qualitatively in Fig. 15.14. The weak oblique shock waves that reach ground level produce the sonic boom of supersonic aircraft. To better explain this phenomenon we refer to Fig. 15.15 where the pressure disturbances (sound waves) at times Δt equal to -1, -2, -3, -4 are shown. In Figure 15.15(a) the object is stationary and the distribution of disturbances is symmetrical about the source. When the object moves subsonically (Fig. 15.15(b)) the disturbances are no longer distributed symmetrically. When the object moves at exactly the speed of sound the disturbances pile up exactly at the position of the object to produce a line of concentrated action (i.e. a shock wave) which is usually called a Mach wave (Fig. 15.15(c)). The disturbance-free region ahead of the object is called the zone of silence. At supersonic speeds the disturbances are confined within the so-called Mach cone (Fig. 15.15(d)). An observer on the ground does not hear a plane passing overhead until the plane is well past. The piling up of disturbances on the Mach cone surface produces the familiar sonic boom. Refering to Fig. 15.15(d) we have

$$\sin\mu = \frac{a\Delta t}{V\Delta t} = \frac{a}{V} = \frac{1}{M} \qquad (15.113)$$

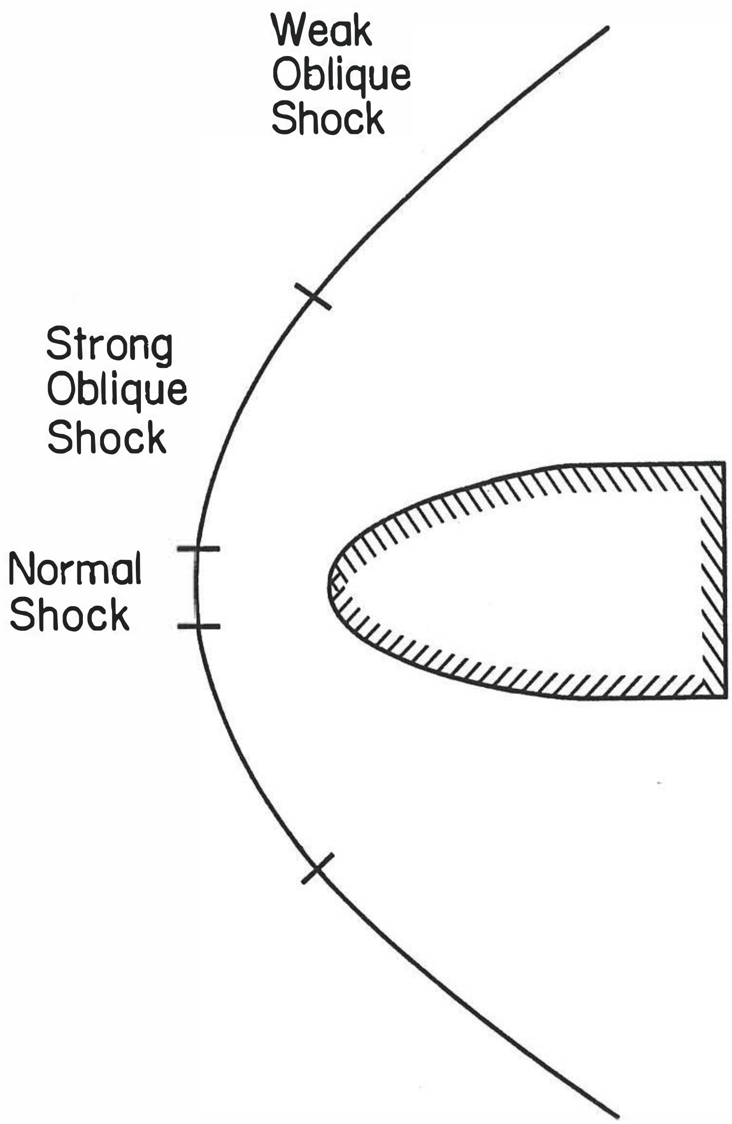

Fig. 15.14 Schematic of shock wave formation in front of a blunt body travelling at supersonic speeds.

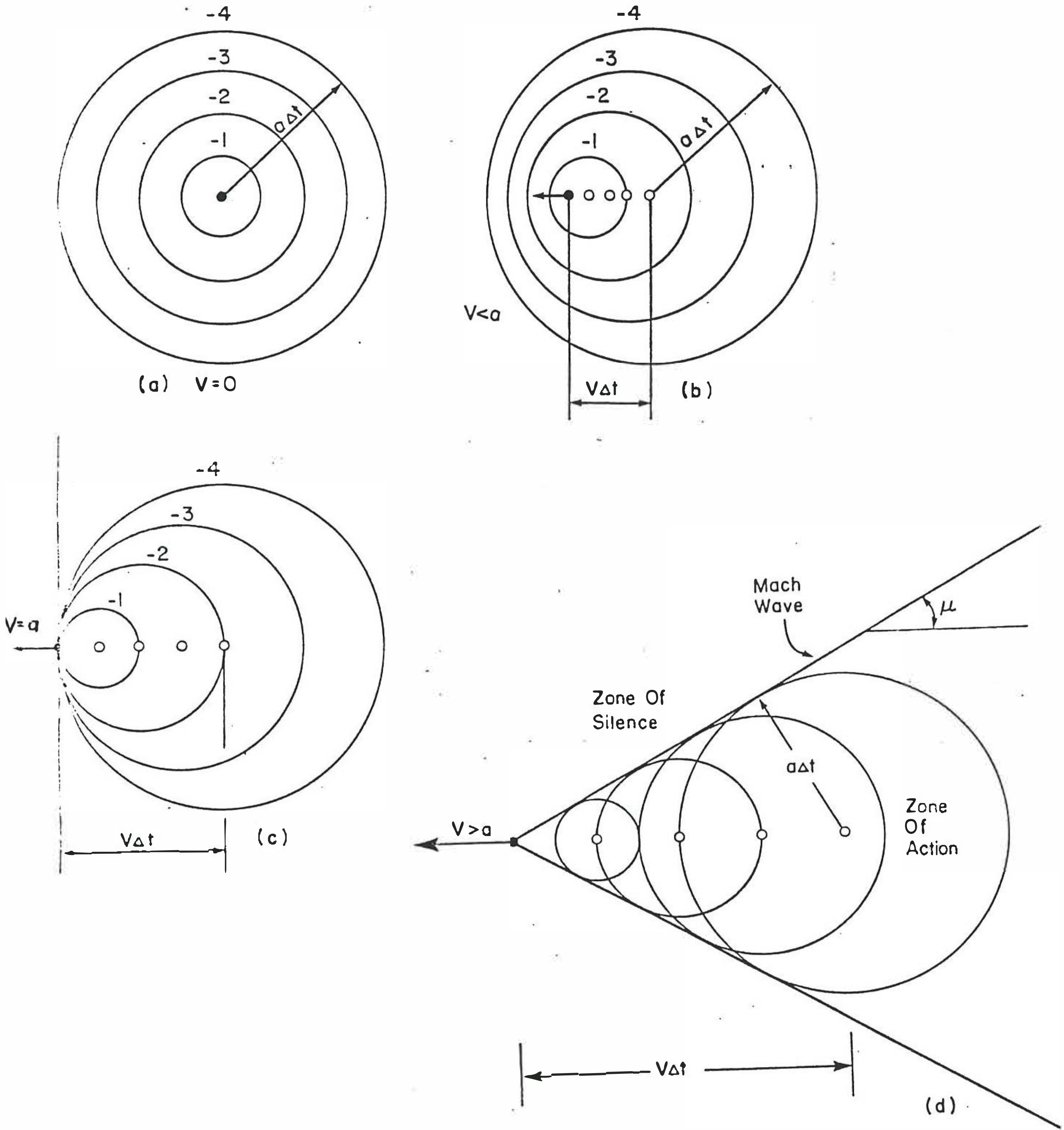

Fig. 15.15 Pressure disturbances (waves) generated by a stationary (a) and moving object (b), (c) and (d).

and the Mach angle is

$$\mu = \sin^{-1}\frac{1}{M} \tag{15.114}$$

More on sonic boom, shock waves etc. can be found in references [12,13].

Example 15.5

A supersonic aircraft travels at an altitude of 12,000 m with a Mach number M = 2. Determine the position of the aircraft when an observer on the ground hears the sonic boom. Neglect the variation of sound speed with altitude.

Solution

We refer to Fig. E15.15. We have

$$\mu = \sin^{-1}\frac{1}{M} = \sin^{-1}\frac{1}{2} = 30^{\circ}$$

Thus, the horizontal distance will be

$$L = \frac{12{,}000}{\tan 30^{\circ}} = 20{,}783 \text{ m}$$

15.12 EFFECT OF COMPRESSIBILITY ON DRAG

As it was explained in Chapter 12, the total drag in incompressible flow is due to frictional resistance and the phenomena accompanying the wake formation. In subsonic flow as the Mach number increases there is a slight increase of the drag coefficient due to the compressibility effects on pressure distribution. A sharp increase is observed as the local Mach number reaches unity at some point on the body (depending on contour) because of the generation of shock waves. The drag coefficient

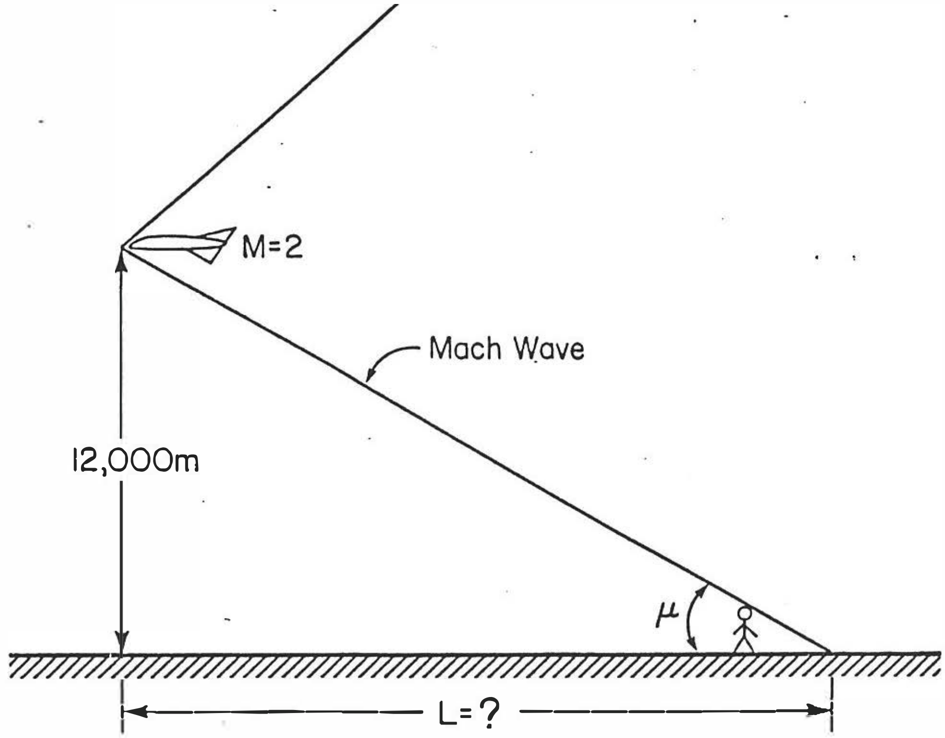

Fig. E.15.5

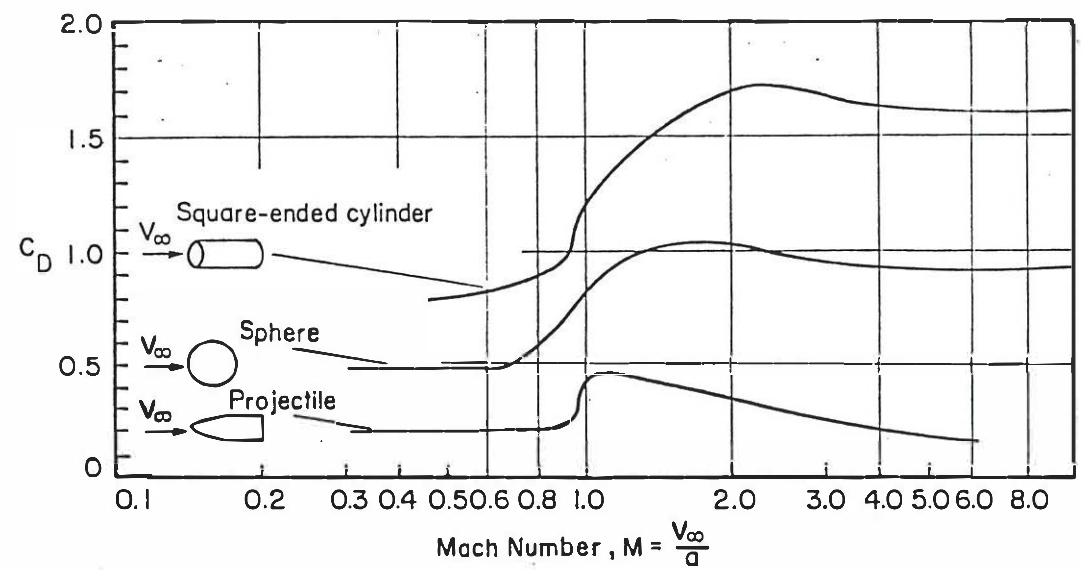

Fig. 15.16 The drag coefficient (C_D = 1/2 ρ V^2A, where A is the frontal area) as a function of Mach number at Re = 10^4, according to Rouse [14].

continues to increase as the Mach number increases, reaches a maximum and then decreases. Figure 15.16 shows the drag coefficient as a function of the Mach number $M = V_\infty/a$, for a Reynolds number of approximately 10^4, from reference [14]. It can be seen that the drag coefficient increase around M = 1 is smaller for the projectile than for the sphere or the cylinder. The reason for this is that the projectile has a sharp nose and the normal and oblique shock waves are smaller and weaker than those generated in front of the other two bodies.

When studying the effect of Mach number on the drag coefficient the Reynolds number must also be taken into account. Thus three dimensional contour plots are required [15,16] to express the relation $C_D=f(Re_D,M)$.

15.13 PRESSURE WAVES IN LIQUIDS - THE WATERHAMER

We consider the reservoir and pipeline system shown in Fig. 15.17. Whenever the valve is closed rapidly a pressure wave in the liquid is generated that travels upstream with approximately the speed of sound, which is given by equation (15.14) as

$$a = \left(\frac{E}{\rho}\right)^{1/2} \tag{15.115}$$

where E is the bulk modulus of elasticity and ρ the density of the liquid.

The wave reaches the reservoir and is reflected back towards the valve while the fluid begins to flow back from the pipe into the reservoir. When this wave reaches the valve it causes an expansion wave to move back towards the reservoir. This expansion wave reaches eventually the reservoir and results in a liquid flow from the reservoir towards the valve again. Thus a full cycle is completed at time

$$t_c = \frac{4L}{a} \tag{15.116}$$

The whole process repeats itself, but in a few cycles the available energy is reduced to zero by friction and all motions stop. Streeter and Wylie [17] note that "the sequence of events taking place in a pipe may be compared with the sudden stopping of a freight train when the engine hits an immovable object".

The setting up to pressure waves in a liquid in a pipe is known as the waterhammer phenomenon. It occurs in pipeline systems when starting or stopping pumps or turbines and when closing valves quickly. Under certain conditions extremely large pressures with destructive effects may be developed.

The maximum pressure developed by the wave formation and propagation may be determined by applying the linear momentum principle (Sec. 6.1), for a thin control volume around the wave (Fig. 15.18). For a control volume moving with constant velocity (see also Sec. 15.2) by neglecting frictional effects, we have

$$(V + a)\ \rho_2 Aa - a\rho_2 Aa + p_1 A - (p + \Delta p)\ A = 0 \tag{15.117}$$

Because of the small compressibility of liquids we may take $\rho_1 \simeq \rho_2 = \rho$, thus

$$\Delta p = \rho a V \tag{15.118}$$

Under certain conditions the pressure developed can be very high. High peak pressures can be avoided by properly timing the starting and stopping of turbomachinery, the closing of valves, and by using surge tanks [17,18,19] (see Fig. 15.19).

Fig. 15.17 Reservoir and pipeline system with a rapid closing valve.

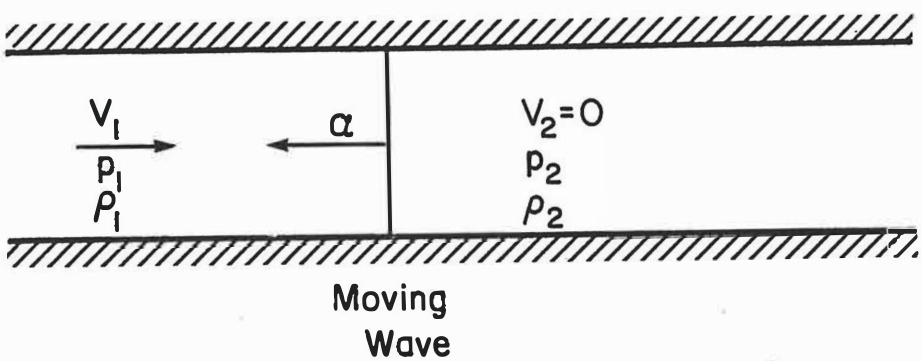

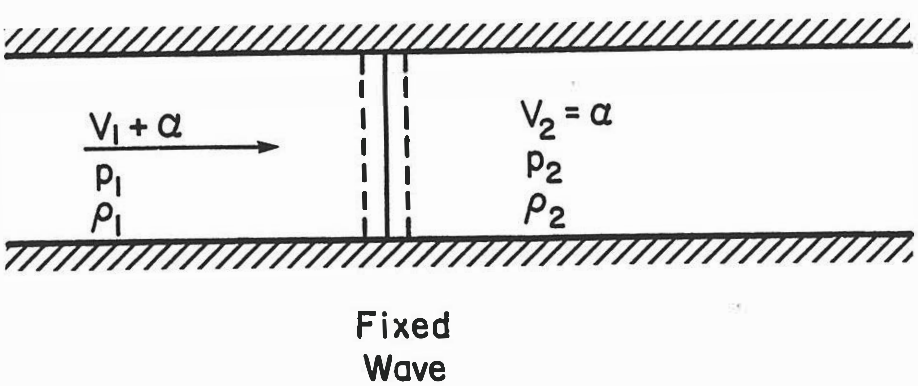

Fig. 15.18 Notation for a moving and a fixed pressure wave in a pipeline.

Example 15.6

Water flows from a reservoir through a pipeline at an average velocity of 1.80 m/s. The gage pressure in the pipeline is 300 kPa. Suddenly a valve is closed. Determine the maximum pressure developed in the pipeline (for water, take ρ = 1000 kg/m^3 and E = 2.20 × 10^6 kPa).

Solution

The velocity of sound in water is

$$a = (\frac{E}{\rho})^{1/2} = (\frac{2.20 \times 10^9}{10^3}) = 1.483 \text{ m/s}$$

Thus

$$\Delta p = \rho a V = 10^3 \times 1483 \times 1.8$$

$$= 2669 \text{ kPa}$$

and the maximum pressure is

$$p_{max} = p + \Delta p = 300 + 2669 = 2969 \text{ kPa}$$

15.14 CONCLUDING REMARKS

In this chapter we presented an analysis of one-dimensional, inviscid compressible flow. With these simplifications we were able to express many important results in the form of algebraic equations. These results are in reasonable agreement with experimental measurements for many compressible flow problems. The inviscid flow approximation is valid for even a larger class of compressible flow problems because of the high velocities involved (i.e. inertia forces are much larger than viscous forces). However, the one-dimensional flow approximation does not hold for flow around bends, corners, etc. Under such conditions we may write the continuity and momentum equations as

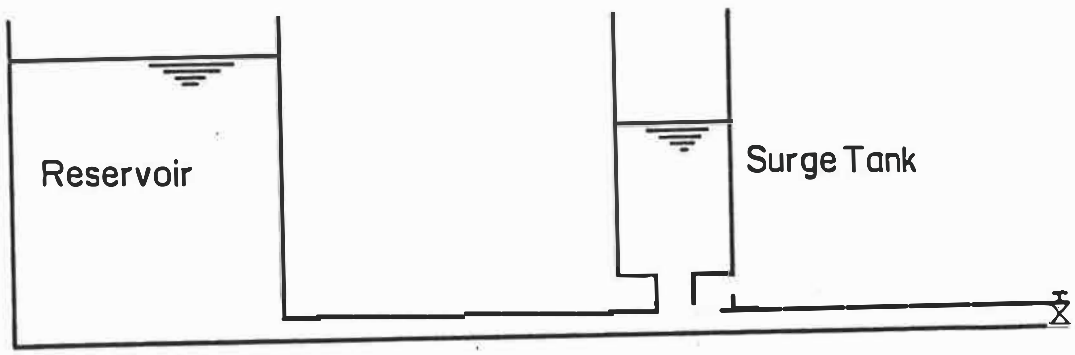

Fig. 15.19 Surge tank on a pipeline.

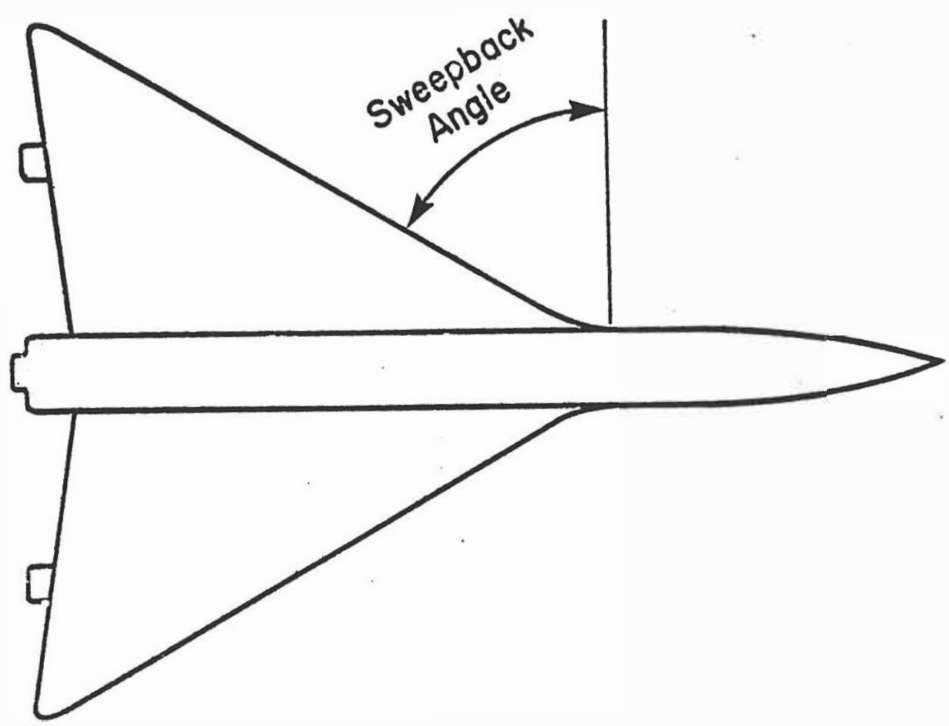

Fig. 15.20 Sketch of a modern supersonic aircraft.

$$\frac{\partial \rho}{\partial t} + \frac{\partial}{\partial x}(\rho\ v_x) + \frac{\partial}{\partial y}(\rho\ v_y) = 0$$

$$\rho\ (\frac{\partial\ v_x}{\partial t} + v_x\ \frac{\partial\ v_x}{\partial x} + v_y\ \frac{\partial\ v_x}{\partial y}) = -\ \frac{\partial p}{\partial x}$$

$$\rho\ (\frac{\partial\ v_y}{\partial t} + v_x\ \frac{\partial\ v_y}{\partial x} + v_y\ \frac{\partial\ v_y}{\partial y}) = -\ \frac{\partial p}{\partial y}$$

By further assuming an irrotational ($\nabla \times \bar{V} = 0$) and barotropic fluid ($\rho = f(p)$) and introducing the speed of sound, it is possible to obtain a single equation in terms of a velocity potential ϕ (see for example references [2,11]). This equation is non-linear and very difficult to solve in general. However, for certain flow problems this equation can be reduced to a linear hyperbolic differential equation which can be solved by the method of separation of variables or more commonly by the method of characteristics. These topics are beyond the scope of the present book and the reader is advised to consult references [2-5, 11-13].

For supersonic aircraft the designer faces up to three-dimensional problems. Because of the existence of shocks and expansion waves the drag coefficient is much larger than for the subsonic case. To minimize the drag the wings are given a large "sweepback" angle (see Fig. 15.20). Thus the component at the velocity normal to the wings is made smaller than the speed of sound and the airfoils are thus operating subsonically. The drag due to the fuselage is minimized by tapering the nose to a needle point. Wind tunnel tests are performed to determine the shape changes required for optimum performance, which are difficult to be obtained from theory alone.

REFERENCES

1. W.H. Dorrance, "Viscous Hypersonic Flow", McGraw-Hill, New York (1962).

2. A.H. Shapiro, "The Dynamics and Thermodynamics of Compressible Fluid Flow", 2 Vols., Ronald, New York (1953).

3. H.W. Liepman and A. Roshko, "Elements of Gas Dynamics", Wiley, New York (1957).

4. A.B. Cambel and B.H. Jennings, "Gas Dynamics" McGraw-Hill, New York (1958).

5. P.A. Thompson, "Compressible Fluid Dynamics", McGraw-Hill, New York (1972).

6. S.W. Churchill, "Inertial Flows", Etaner Press, Thornton, PA (1980).

7. H.N. Bradley, "Shock Waves in Chemistry and Physics", Wiley, New York (1962).

8. A.G. Gaydon and I.R. Hurle, "The Shock Tube in High Temperature Chemical Physics", Chapman and Hall, London (1963).

9. J.H. Keenan and E.P. Neumann, "Measurements of Friction in a Pipe for Subsonic and Supersonic Flow of Air", J. Appl. Mech., 13, p. A-91 (1946).

10. F.M. White, "Fluid Mechanics", McGraw-Hill, New York (1979).

11. R.H. Sabersky, A.J. Acosta and E.G. Hauptman, "Fluid FLow", The MacMillan Company, New York (1971).

12. I.I. Glass, "Shock Waves and Man", University of Toronto Press, Toronto (1974).

13. R. Courant and K.O. Friedrichs, "Supersonic Flow and Shock Waves", Interscience, New York (1948).

14. H. Rouse, "Elementary Mechanics of Fluids", Wiley, New York (1946).

15. J.A. Roberson and C.T. Crowe, "Engineering Fluid Mechanics", Houghton Mifflin Company, Boston (1975).

16. C.T. Crowe et al., "Drag Coefficient for Particles in Rarefied, Low Mach-Number Flows", in Progress in Heat and Mass Transfer, 6, 419-431, Pergamon Press, New York (1972).

17. V.L. Streeter and E.B. Wylie, "Fluid Mechanics", 6th Edition, McGraw-Hill, New York (1975).

18. W.M. Swanson, "Fluid Mechanics", Holt, Rinehart and Winston, New York (1970).

19. E.B. Wylie and V.L. Streeter, "Fluid Transients", McGraw-Hill, New York (1978).

ERNST MACH (1838-1916)

John Vlachopoulos, *Fundamentals of Fluid Mechanics*
Chem. Eng., McMaster University, Hamilton, ON, Canada
(First Edition 1984, revised internet edition (2016), www.polydynamics.com)

CHAPTER 16

OPEN-CHANNEL FLOW

16.1 INTRODUCTION

Open-channel flow is the motion of a liquid in a conduit with a free surface. The flow is partially enclosed by a solid boundary and its top (free) surface is maintained at a constant pressure (nearly always atmospheric). Open-channel flows are encountered in nature as well as in engineering. Natural examples include flow in rivers, streams and estuaries while engineering applications include flow in irrigation channels, canals, drainage ditches and sewers.

The presence of the free surface both simplifies and complicates the analysis. The simplification is due to the fact that the pressure is constant along the free surface and, thus, does not enter directly into the analysis. The complication arises from the fact that the shape of the free surface is not known a priori and thus it must be determined in the course of the analysis. Actual channels encountered in practice can be of simple geometrical shape such as aquaducts or extremely complex such as tree-lined floodplains.

In this chapter we present a highly simplified analysis of flow in open-channels. Despite the simplifications this analysis leads to many results of considerable practical importance. Some more details on this subject may be found in hydraulics textbooks [1,2] and much more in specialized books on open channel flows [3-9].

16.2 FLOW CONFIGURATION AND CLASSIFICATION

Most open-channel flows encountered in practice are turbulent. On the solid boundary the no-slip condition is satisfied while the free surface exhibits negligible resistance due to the contact with air (see Section 7.17). The velocity profiles are very complex and depend on the shape of channel. Velocity measurements show that the maximum velocity does not occur on the free surface, as one might anticipate, but at a depth approximately 20 percent below the free surface. This is apparently due to secondary flow occuring in open channels as shown schematically in Fig. 16.1. The complexity of velocity profiles increases with the complexity of channel geometry.

Very little work has been done on the theoretical determination of velocity profiles in open channels because of the complexity of the boundaries and of the physical phenomena involved. The usual approach is to use the one-dimensional flow approximation as the fluid flows in, say, the x-direction with average velocity $V(x)$ at cross-sectional area $A(x)$. However, with the recent developments on finite difiference and finite element methods (see Chapter 25) many complicated problems can be solved without the need to resort to the one-dimensional approximation.

For frictional loss calculations we may use the Moody chart (see Section 14.4) with hydraulic diameter given by the usual definition

$$D_H = \frac{4 \times \text{cross sectional area}}{\text{wetted perimeter}} \tag{16.1}$$

Thus for a rectangular channel of width W and depth h as shown in Fig. 16.2, we have

$$D_H = \frac{4\ Wh}{W+2h} \tag{16.2}$$

The more conventional way for open-channel flow, is to define a hydraulic radius which is one-fourth of the hydraulic diameter, i.e.

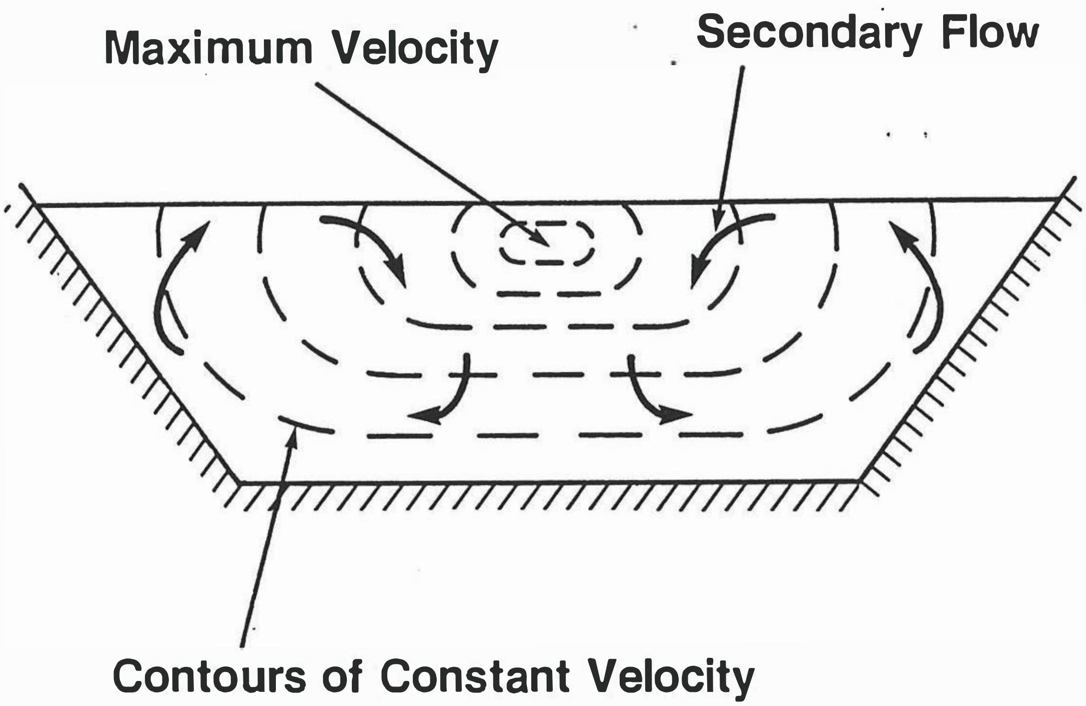

Fig. 16.1 Typical flow patterns in an open channel.

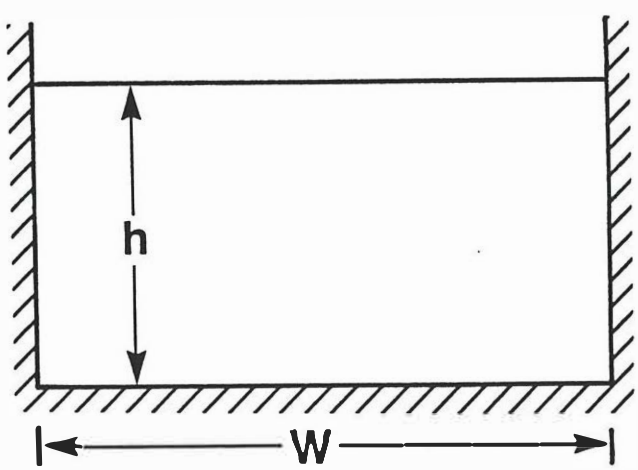

Fig. 16.2 A rectangular open channel.

$$R_H = \frac{\text{cross-sectional area}}{\text{wetted perimeter}} = \frac{1}{4} D_H \qquad (16.3)$$

This definition will be used in the Chézy and Manning formulas that are discussed in the Section 16.4.

Open-channel flows can be steady or unsteady and can be classified as uniform or varied flows depending on the depth variation. In uniform flow the fluid depth z above the channel bed remains constant. Varied flow is the flow where the depth changes and can be further classified as gradually varied or rapidly varied flow. Uniform and gradually varied flows can be analysed with the one-dimensional flow approximation while rapidly varied flows require multidimensional flow theory.

16.3 LAMINAR FLOW OVER AN INCLINED SURFACE

Laminar flow of a liquid film over a flat plate was examined in the context of fully developed unidirectional flow in Section 7.8. It was found that the velocity profile is given by

$$v_x = \frac{\rho g \delta^2 \sin\theta}{2\mu} [1 - (\frac{y}{\delta})^2] \qquad (16.4)$$

and the film thickness by

$$\delta = (\frac{3\mu Q}{\rho g W \sin\theta})^{1/3} \qquad (16.5)$$

where ρ is the density, μ is the viscosity, W the plate width, Q the volume flow rate and θ the angle with the horizontal, as shown in Fig. 16.3.

16.4 FRICTION LOSS IN UNIFORM FLOW: THE CHÉZY AND MANNING FORMULAS

Depending on the Reynolds number open channel flow can be classified as laminar or turbulent. The definition of the Reynolds number for open channel flows is usually based on the hydraulic diameter (see equation (16.3))

$$Re = \frac{\rho V_{avg} R_H}{\mu} \qquad (16.6)$$

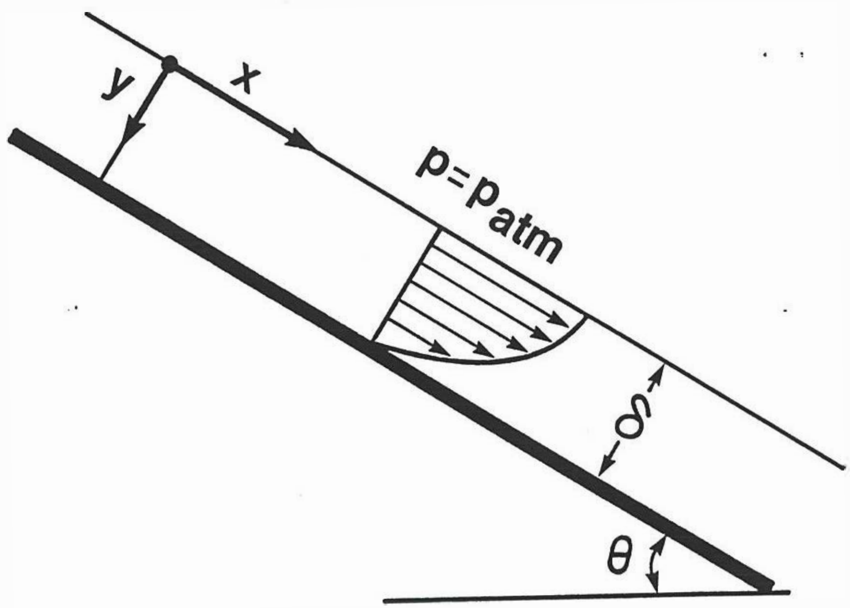

Fig. 16.3 Laminar flow over an inclined surface.

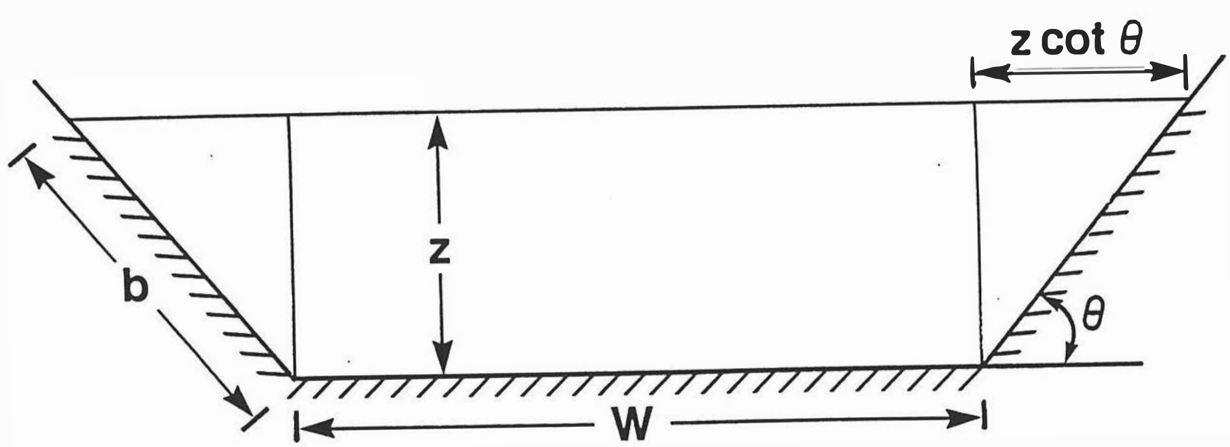

Fig. 16.4 Geometrical characteristics of an open channel of trapezoidal cross-section.

Transition from laminar to turbulent flow occurs over the Reynolds number range of 5×10^2 and 2×10^3. In this section we will assume that the flow is fully turbulent when the Reynolds number is larger than 1000.

We consider uniform flow in a long straight channel of constant slope, constant depth and constant cross-section. The Bernoulli equation with friction (Section 14.3) is

$$\frac{V_2^2}{2g} + \frac{p_1}{\rho g} + z_1 = \frac{V_2^2}{2g} + \frac{p_2}{\rho g} + z_2 + h_f \tag{16.7}$$

Since $p_1 = p_2 = p_{atm}$ and $V_1 = V_2$, we have

$$h_f = z_1 - z_2 \tag{16.8}$$

When the channel makes an angle θ with the horizontal we denote the slope as

$$S_o = \tan\theta \tag{16.9}$$

Thus

$$h_f = z_1 - z_2 = S_o L \tag{16.10}$$

For uniform open-channel flow we may use the Darcy-Weisbach definition for the friction factor (Sec. 14.14). We have

$$h_f = f \frac{L}{D_H} \frac{V_{avg}^2}{2g} \tag{16.11}$$

where f is the friction factor, L the length of the channel, V_{avg} the average velocity and D_H the hydraulic diameter which is related to the hydraulic radius R_H by

$$D_H = 4 R_H \tag{16.12}$$

Combining equations (16.9), (16.10), (16.11) and (16.12) we get

$$V_{avg} = \left(\frac{8g}{f}\right)^{1/2} (R_H S_o)^{1/2} \tag{16.13}$$

or simply

$$V_{avg} = C(R_H S_o)^{1/2} \tag{16.14}$$

where C is called the Chézy coefficient, after the 18th century French engineer who developed the above formula by correlating experimental data in 1769. Originally the coefficient $C = (8g/f)^{1/2}$ was thought to be constant. During the past century several correlations were proposed expressing the Chézy coefficient as a function of roughness, shape, and slope of various open channels. The most popular relationship was developed towards the end of the 19th century and was attributed to the Irishman R. Manning (1889):

$$C = \left(\frac{8g}{f}\right)^{1/2} = \frac{1}{n} R_H^{1/6} \qquad (R_H \text{ in meters}) \tag{16.15}$$

Thus

$$V_{avg} = \frac{1}{n} R_H^{2/3} S^{1/2} \text{ and } Q = V_{avg} A \tag{16.16}$$

where n is called the Manning roughness coefficient and is considered dimensionless. This means that n takes the same numerical values irrespective of the units of R_H. Thus the numerator must change when R_H is given in units other than meters. For example in British units equation (16.15) is given as

$$C = \frac{1.49}{n} R_H^{1/6} \qquad (R_H \text{ feet}) \tag{16.17}$$

because $1.49 = (3.28 \text{ ft/m})^{1/3}$. Some historical comments on the development of this coefficient can be found in references [5] and [6].

The Manning roughness coefficient depends on surface roughness, channel irregularities, channel alignment, vegetation in natural streams and several other factors which are detailed in textbooks on open-channel flows [3-6]. This coefficient has the same significance in open-channel flow as the coefficient ε/D in pipe flow (see Section 14.3). Some typical values are given in Table 16.1 (adapted from V.T. Chow's classical textbook on open channel hydraulics [5]).

TABLE 16.1

AVERAGE VALUE OF THE MANNING ROUGHNESS COEFFICIENT

Channel or Bed Material	n
Metals	
Brass	0.011
Steel (smooth)	0.012
Steel (polished)	0.014
Steel (riveted)	0.016
Cast iron	0.013
Wrought iron	0.015
Corrugated metal	0.024
Non-metals	
Glass	0.010
Cement (finished)	0.012
Cement (unfinished)	0.014
Wood	0.012
Clay	0.015
Brickwork	0.015
Asphalt	0.016
Rubble masonry (cemented)	0.025
Excavated earth channels	
Clean	0.022
Gravelly	0.025
Weedy	0.035
Natural channels	
Clean and straight	0.030
Rivers	0.035
Channels with weeds, brush	0.080

Example 16.1

A semicircular channel made of finished cement has a radius of 1.2m and a slope of 0.5^o. Determine the volume flow rate using the Manning formula.

Solution

(a). The flow rate is given by

$$Q = A\ V_{avg}$$

where [from equations (16.14) and (16.15)]

$$V_{avg} = \frac{1}{n} R_H^{\ 1/6} (R_H\ S_o)^{1/2} = \frac{1}{n} R_H^{\ 2/3}\ S_o^{\ 1/2}$$

The cross-sectional area is $A = \frac{1}{2}\pi R^2$. The wetted perimeter is $P = \pi R$. Hence the hydraulic radius is

$$R_H = \frac{1/2\pi R^2}{\pi R} = \frac{1}{2} R = 0.6\text{m}$$

From Table 16.1 the Manning friction factor is $n \simeq 0.012$ we have

$$V_{avg} = \frac{1}{0.012} 0.6^{2/3} (\tan 0.5)^{1/2} = \frac{1}{0.012} 0.6^{2/3} \times 0.00873^{1/2}$$

$$= 5.539 \text{ m/s}$$

and $$Q = \frac{1}{2} \pi R^2\ V_{avg} = \frac{1}{2} \pi\ 1.2^2 \times 5.539 = 12.52 \text{ m}^3/\text{s}$$

16.5 HYDRAULICALLY OPTIMUM CROSS SECTIONS

The Manning formula for flow rate in a uniform open channel flow simply gives

$$Q = AV_{avg} = \frac{A\ R_H^{\ 3/2}\ S^{1/2}}{n} \tag{16.18}$$

or using the definition of hydraulic diameter $R_H = A/P$

$$Q = \frac{A^{5/3}\ S^{1/2}}{n\ P^{2/3}} \tag{16.19}$$

To maximize Q for a given area A we must minimize the wetted perimeter

P. A channel with semicircular cross-section has the minimum wetted perimeter for a given flow area.

For the trapezoid of Fig. 16.4, we have

$$A = Wz + z^3 \cot\theta \qquad (16.20)$$

and

$$P = W + 2b = W + 2\,\frac{z}{\sin\,\theta} \qquad (16.21)$$

Solving equation (16.20) for W and introducing it into equation (16.21) we get

$$P = \frac{A}{z} - z\,\cot\,\theta + 2\,\frac{z}{\sin\,\theta} \qquad (16.22)$$

For minimum perimeter $dP/dz = 0$

Thus $$\frac{dP}{dz} = -\frac{A}{z^2} - \cot\,\theta + \frac{2}{\sin\,\theta} = 0 \qquad (16.23)$$

Solving we get

$$z^2 = \frac{A\,\sin\,\theta}{2 - \cos\,\theta} \qquad (16.24)$$

For angle $\theta = 90^\circ$ (rectangular channel)

$$z^2 = \frac{A}{2} \qquad (16.25)$$

Since $A = Wz$

$$z = \frac{W}{2} \qquad (16.26)$$

Thus the optimum rectangular channel has depth equal to one-half its width.

To minimize the perimeter with respect to θ we set $dP/d\theta = 0$ keeping A and z constant. We have

$$\frac{dP}{d\theta} = 1 - 2\,\cos\,\theta = 0 \qquad (16.27)$$

$$\cos\,\theta = \frac{1}{2} \text{ and } \theta = 60^\circ \qquad (16.28)$$

This means that the optimum trapezoid cross-section is half a hexagon.

16.6 SPEED OF GRAVITY WAVES AND FROUDE NUMBER

Consider a long shallow horizontal channel containing a motionless fluid of depth z. A surface wave in the form of small increase in elevation dz (see Fig. 16.5(a)) moves down the channel at a constant speed c. The fluid ahead of the wave remains motionless. When the wave passes it causes a fluid-particle velocity dV. To analyze this problem we consider a frame of reference moving with the wave at velocity c. This is analogous to the assumptions made for the determination of the speed of sound in Section 15.2. The wave is thus stationary while the fluid flows from left to right at velocity c (Fig. 16.5(b)). Frictional losses are neglected and the velocity profile is therefore flat. The continuity equation for a control volume of width W is

$$\rho c z W = \rho(c-dV)(z+dz)W \tag{16.29}$$

Carrying out the multiplication and neglecting the infinitesimal quantity of second order, (dV)(dz), we get

$$c\,dz - z\,dV = 0 \tag{16.30}$$

Now we apply the Bernoulli equation between two points on either side of the control volume of Fig. 16.5(b)

$$\frac{p_{atm}}{\rho g} + z + \frac{c^2}{2g} = \frac{p_{atm}}{\rho g} + (z+dz) + \frac{(c-dV)^2}{2g} \tag{16.31}$$

Expanding and rearranging, we get

$$dz - \frac{c\,dV}{g} + \frac{(dV)^2}{2g} = 0 \tag{16.32}$$

Again eliminating the infinitesimal term of second order $(dV)^2/2g$ yields

$$g\,dz = c\,dV \tag{16.33}$$

Combining equations (16.30) and (16.33) we have

$$c = \sqrt{gz} \tag{16.34}$$

This is the wave speed of a small gravity wave moving on the surface of shallow water. The Froude number was defined in Section 6.8 as the

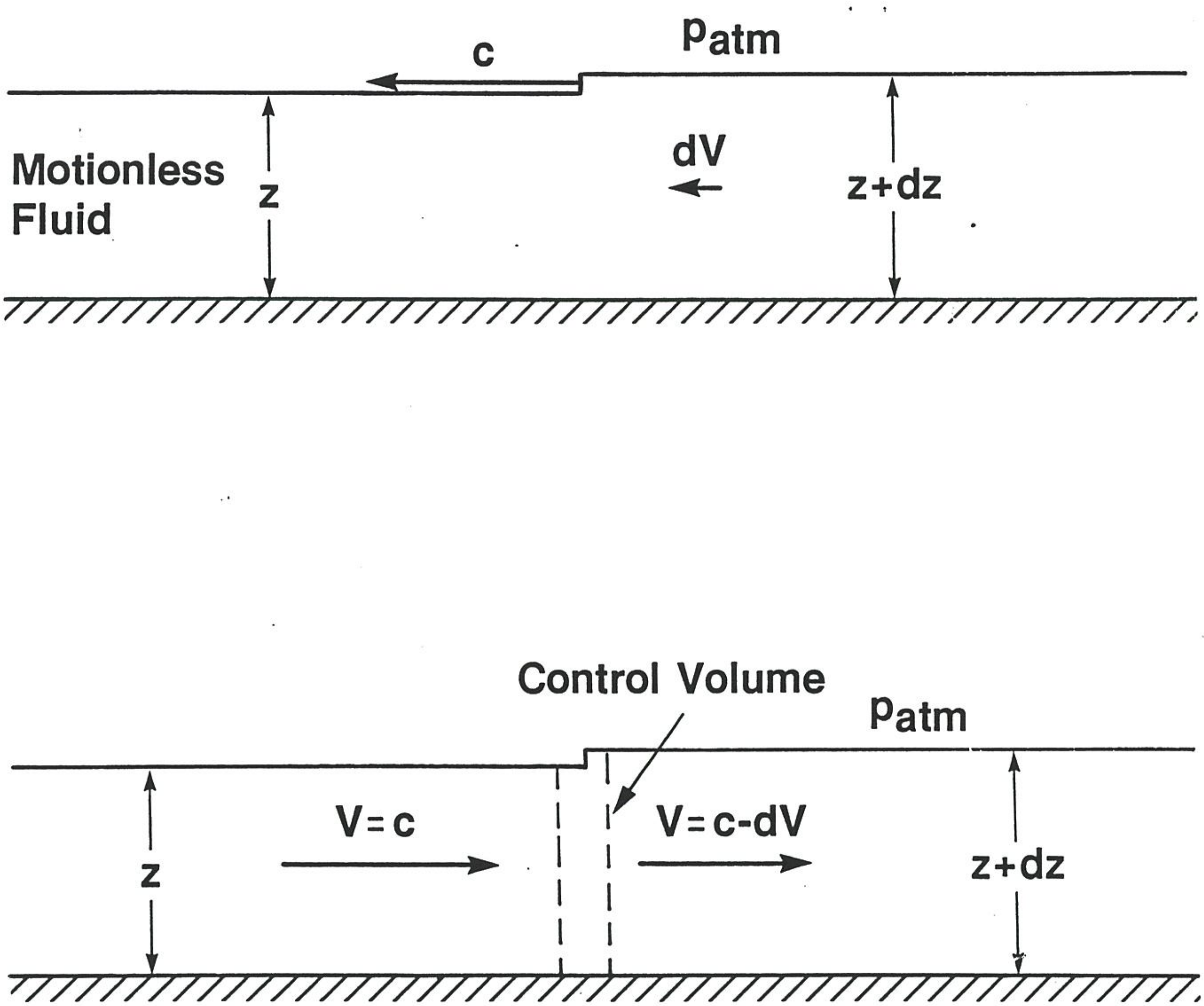

Fig. 16.5 (a) Motion of a small gravity wave in a motionless fluid.
(b) Fixed wave in a moving fluid.

ratio of inertia to gravity forces and for a channel of depth z takes the form

$$Fr = \frac{V}{\sqrt{gz}} = \frac{V}{c} \tag{16.35}$$

Thus the Froude number can be given another physical interpretation as representing the ratio of fluid-particle velocity to small amplitude wave speed. It can be thought of as being analogous to the Mach number (see Section 15.3). In fact the analogy has further physical implications and the flow can be considered subcritical ($Fr<1$), critical ($Fr=1$) or supercritical ($Fr>1$). In compressible flow for critical condition $M=1$ a shock is formed (see Section 15.9). In open channel flow we have the appearance of hydraulic jump. This is an abrupt change of flow conditions accompanied by a change of fluid depth and violent turbulent mixing. This happens when fluid-particles (travelling at velocity V) arrive at a downstream location before the arrival of "signals" about an upstream disturbance (which travel with velocity c) i.e. when $V \geq c$ (see Section 16.7).

16.7 FRICTIONLESS FLOW OVER AN OBSTACLE

The one-dimensional, frictionless flow approximation can be used for the study of open channel flow over an obstacle as shown in Fig. 16.6. The fluid is approaching the obstacle with a constant velocity V_∞ and the free surface is z_∞ above the datum plane. The velocity is $V(x)$ over the obstacle and the surface is $z(x) + h(x)$ over the datum plane. The continuity equation for a channel of uniform width W is

$$Q = \rho V z = \text{const} \tag{16.36}$$

and the Bernoulli equation

$$\frac{V^2}{2g} + z + h = \text{const} \tag{16.37}$$

Differentiating the above equations with respect to x we have

$$z\frac{dV}{dx} + V\frac{dz}{dx} = 0 \tag{16.38}$$

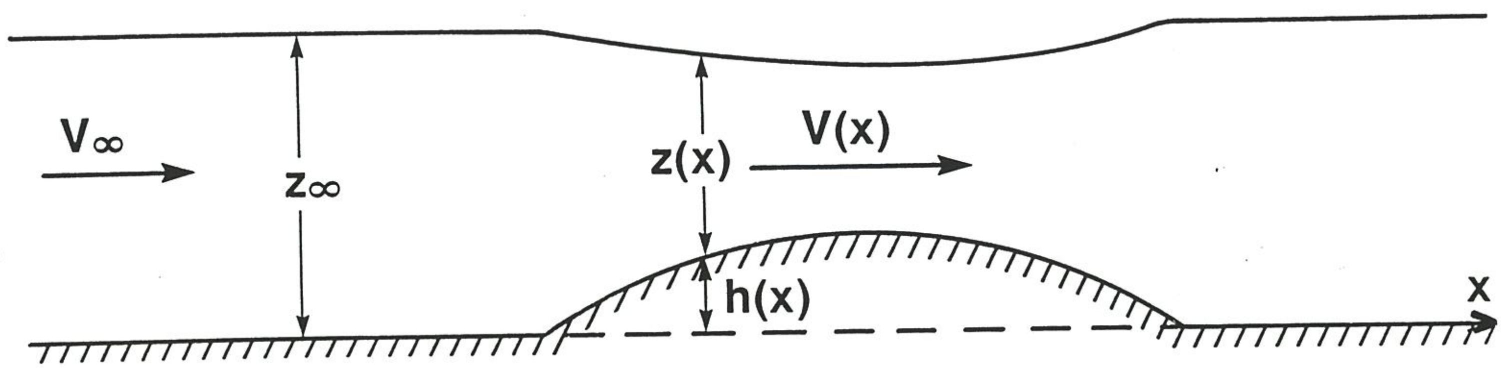

Fig. 16.6 Flow over an obstacle.

$$\frac{V}{g}\frac{dV}{dx} + \frac{dz}{dx} + \frac{dh}{dx} = 0 \qquad (16.39)$$

Eliminating dV/dx between the two equations, we obtain an expression for the slope of the free surface

$$\frac{dz}{dx} = -\frac{dh/dx}{1 - \frac{V^2}{gz}} = -\frac{dh/dx}{1 - Fr^2} \qquad (16.40)$$

where F is the Froude number, $Fr = V/\sqrt{gz}$.

This equation relates the slope of the free surface to the slope of the surface of the obstacle.

If Fr is less than 1, the quantity $1 - Fr^2$ is positive, thus dz/dx and dh/dx have opposite signs. This means that if the bed elevation h increases (dh/dx positive) the liquid depth must decrease and the flow accelerates. If the bed elevation decreases (dh/dx negative) the liquid depth must increase and the flow decelerates. Under these conditions the flow is referred to as <u>subcritical</u>. In subcritical flow, disturbances (waves) can travel upstream because V<c.

If Fr is greater than 1, the quantity $1 - Fr^2$ is negative, thus dz/dx and dh/dx have the same sign. Therefore for increasing h the liquid depth increases and the flow decelerates, while for decreasing h the liquid depth decreases and the flow accelerates. The flow is referred to as <u>supercritical</u>. In supercritical flow, disturbances (waves) cannot travel upstream.

When Fr = 1 (critical flow), the slope dh/dx must be zero since dz/dx cannot be infinite. However, the converse is not true, i.e. when dh/dx = 0, F is not necessarily equal to 1. These results are summarized in Fig. 16.7. It is important to note the analogy between the present results and those discussed in Section 15.4 on compressible flow. In compressible flow Mach number is the critical parameter while in open channel flow we have the Froude number. This analogy has been exploited for compressible gas dynamics experimentation [10].

In open channel flow the <u>specific head</u> (also called <u>specific energy</u>) is a very useful parameter. It is defined as the sum of the depth of flow and the velocity head:

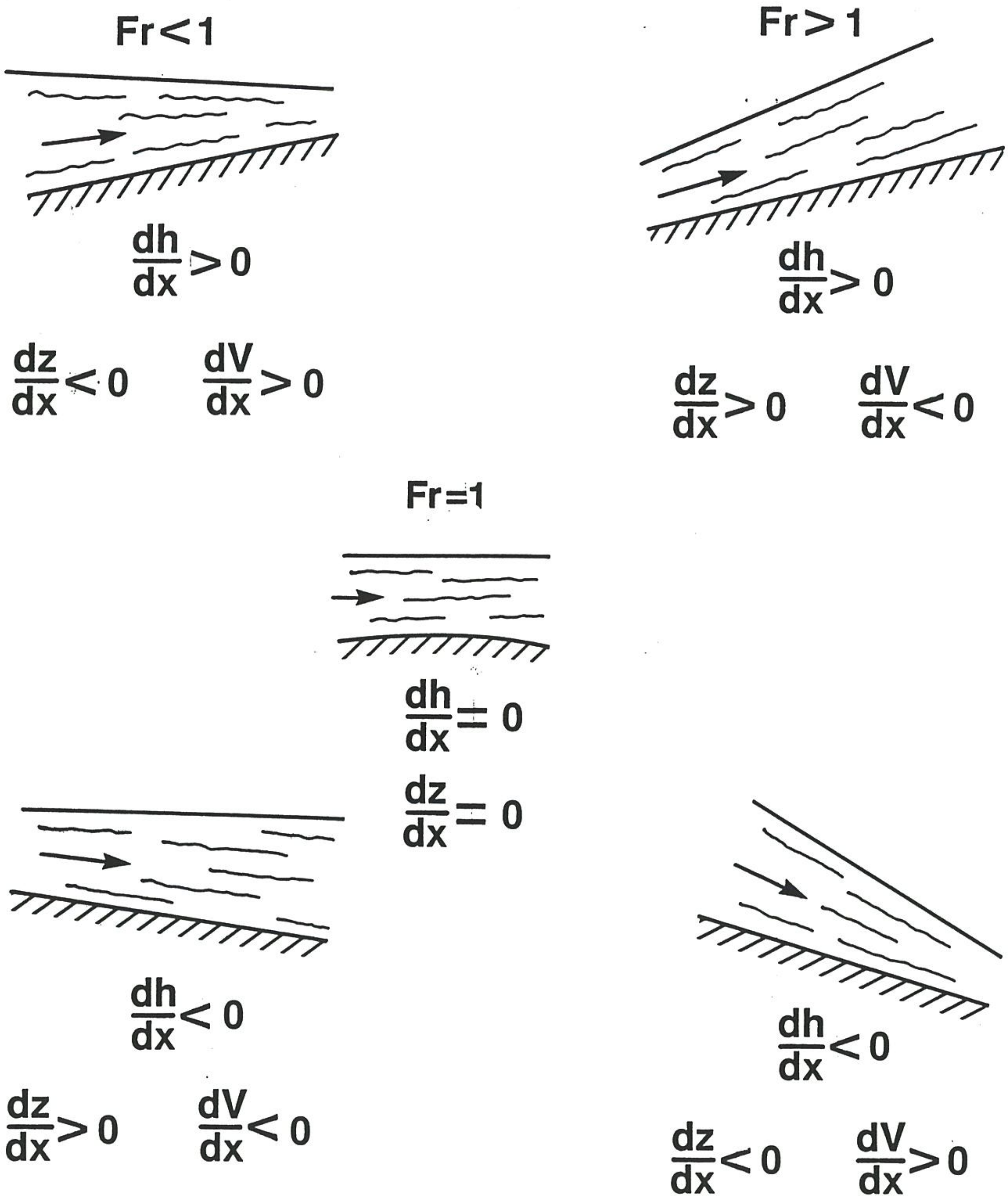

Fig. 16.7 Graphical representation of flow-depth relationships.

$$H = z + \frac{V^2}{2g} \tag{16.41}$$

For a rectangular channel of width W and depth z we may express the flow rate as

$$Q = VWz \tag{16.42}$$

Thus equation (16.41) can be written as

$$H = z + \frac{(Q/W)^2}{2gz^2} \tag{16.43}$$

A plot of specific head H as a function of depth z for different Q/W values is shown in Fig. 16.8. It is interesting to note that each Q/W curve has a minimum H. To determine the z value corresponding to minimum H for a constant Q/W we differentiate equation (14.43) and set equal to zero:

$$\frac{dH}{dz} = 1 - \frac{(Q/W)^2}{gz^3} = 0 \tag{16.44}$$

Thus
$$z = [\frac{(Q/W)^2}{g}]^{1/3} \tag{16.45}$$

and from equation (16.43)

$$H_{min} = \frac{3}{2} z \tag{16.46}$$

The continuity equation (16.42) gives

$$\frac{Q}{W} = \sqrt{gz^3} = zV \tag{16.47}$$

or using the definition of the Froude number

$$Fr = \frac{V}{\sqrt{gz}} = 1 \tag{16.48}$$

This is the condition for critical flow and the corresponding velocity V_c and depth z_c are referred to as critical velocity and critical depth respectively.

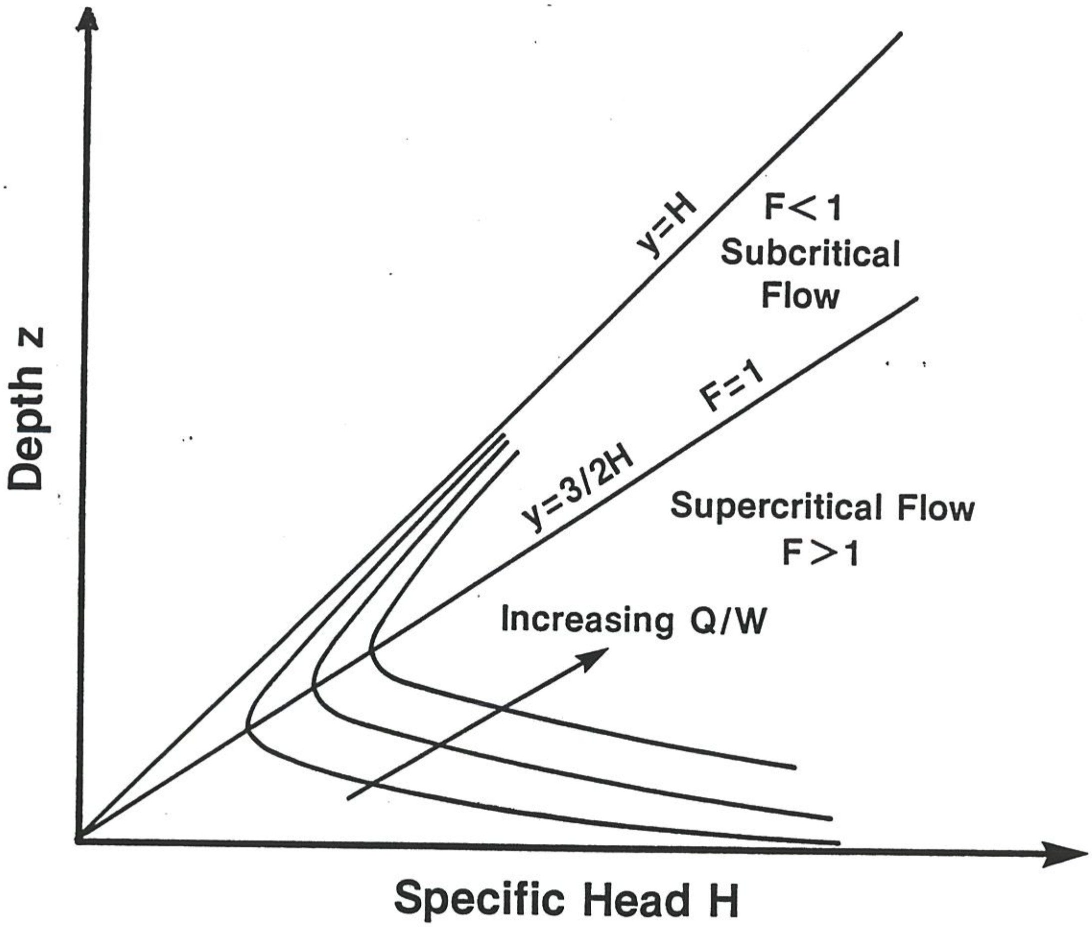

Fig. 16.8 Specific head as a function of depth.

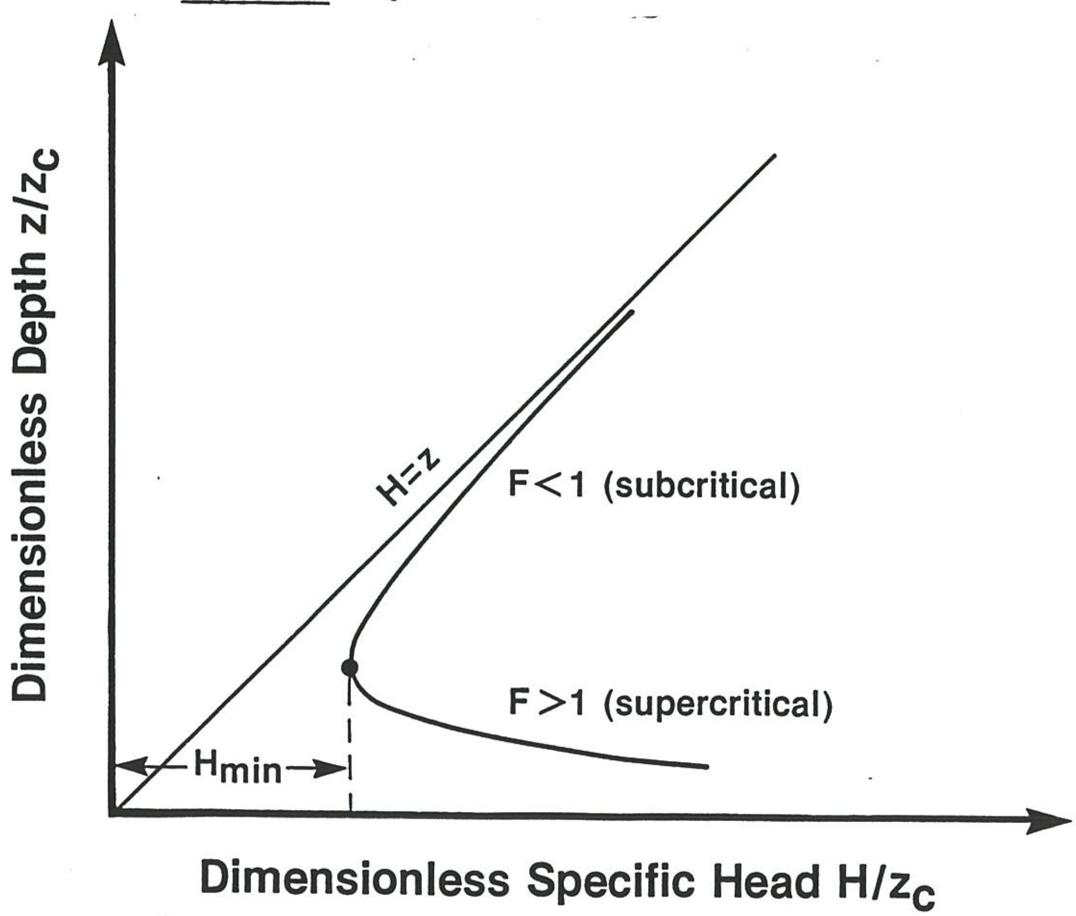

Fig. 16.9 Dimensionless specific head as function of dimensionless depth.

For $H < H_{min}$, no solution of equation (16.43) is possible and such a flow is impossible physically. For $H > H_{min}$, two solutions are possible, i.e. for each value of H, we obtain two z depths from the two branches of constant Q/W curves as shown in Fig. 16.8.

The Froude number can also be expressed in terms of the critical depth as

$$Fr = \frac{V}{\sqrt{gz}} = \frac{Q/W}{z\sqrt{gz}} = \frac{\sqrt{g\,z_c^3}}{\sqrt{gz^3}} = \left(\frac{z_c}{z}\right)^{3/2} \qquad (16.49)$$

Thus, on the upper branch $z > z_c$ and $Fr < 1$ (subcritical flow), while on the lower branch, $z < z_c$ and $F > 1$ (supercritical flow). All the curves of Fig. 16.8 can be collapsed into a single curve by dividing equation (16.43) by z_c

$$\frac{H}{z_c} = \frac{(Q/W)^2}{2gz^2 z_c} + \frac{z}{z_c} = \frac{1}{2}\left(\frac{z_c}{z}\right)^2 + \frac{z}{z_c} \qquad (16.50)$$

This is shown in Fig. 16.9. We note that for large values of H/z_c, the upper branch of the curve has slope 45^o (i.e. it approaches the line $y = H$).

For <u>non-rectangular channels</u>, $W=W(z)$ and the specific head equation (16.41) can be rewritten as

$$H = z + \frac{Q^2}{2gA^2} \qquad (16.51)$$

where $A = A(z)$. To determine the minimum H for constant Q, we differentiate equation (16.51) and set equal to zero:

$$\frac{dH}{dz} = 1 - \frac{Q^2}{gA^3}\frac{dA}{dz} = 0 \qquad (16.52)$$

or

$$\frac{dA}{dz} = \frac{gA^3}{Q^2} \qquad (16.53)$$

If the channel width at the free surface is b, we have $dA = bdz$ and equation (16.53) gives the critical area

$$A_c = \left(\frac{bQ^2}{g}\right)^{1/3} \tag{16.54}$$

The critical velocity is

$$V_c = \frac{Q}{A_c} = \left(\frac{gA_c}{b}\right)^{1/2} \tag{16.55}$$

Example 16.2

A 7.1 m wide rectangular channel has a flow rate $Q = 75\ m^3/s$. Calculate the critical depth and critical velocity. What type of flow is possible if the actual depth is 1.5 m?

Solution

(a) The critical depth is given by equation (16.45). We have

$$z_c = \left[\frac{(Q/W)^2}{g}\right]^{1/3} = \left[\frac{(75/7.1)^2}{9.81}\right]^{1/3} = 2.25\ m$$

The critical velocity is (equation 16.48)

$$V_c = \sqrt{gz_c} = \sqrt{9.81 \times 2.25} = 4.70\ m/s$$

(b) If the actual depth is 1.5 m, the flow is supercritical because $1.5 < z_c$.

Example 16.3

A triangular channel has dimensions as shown as in Fig. E16.3 and a flow rate of $22\ m^3/s$. Calculate the critical depth and the critical velocity.

Solution

From the geometrical characteristics of the channel, we have

$$A = z^2 \tan 60^\circ \qquad b = 2z \tan 60^\circ$$

Now, we use equation (16.54)

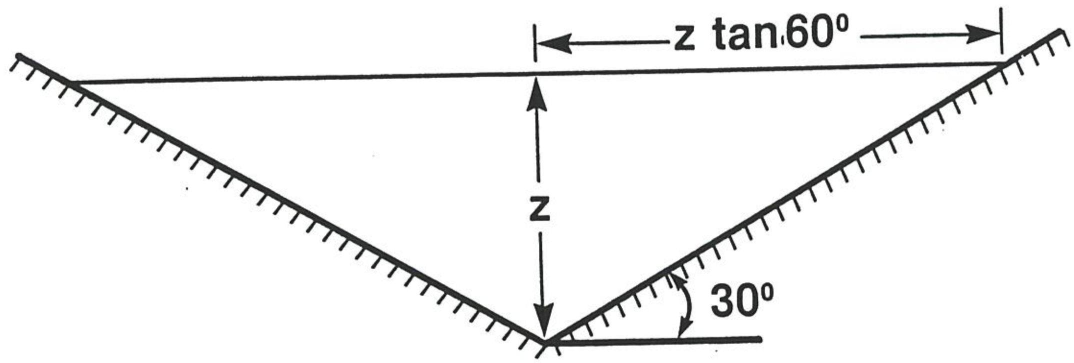

Fig. E16.3

$$A_c = \left(\frac{b\ Q^2}{g}\right)^{1/3}$$

$$z_c^2 \tan 60^\circ = \left(\frac{2z_c \tan 60^\circ \times 22^2}{9.81}\right)^{1/3}$$

$$z_c^6 \tan^3 60^\circ = \frac{2z_c \tan 60^\circ \times 22^2}{9.81}$$

$$z_c = \left(\frac{2 \times 22^2}{9.81 \tan^2 60^\circ}\right)^{1/s} = 2.01 \text{ m}$$

and

$$V_c = \frac{Q}{A_c} = \frac{22}{2.01^2 \tan 60^\circ} = 3.14 \text{ m/s}$$

16.7 HYDRAULIC JUMP

As was discussed in the previous section, in subcritical flow, disturbances in the form of waves can travel both downstream and upstream. This results in smooth and gradual changes of the flow as they might be required by the local conditions. In supercritical flow, waves cannot travel upstream to signal a gradual change. Thus, if the local conditions require a change from supercritical to subcritical flow, this cannot be signalled upstream and an abrupt change occurs which is called hydraulic jump (see Fig. 16.10). The upstream flow is fast and shallow, and the downstream flow is slow and deep. This is analogous to a normal shock wave occurring in compressible flow as discussed in Section 15.9. However, unlike shock waves that are very thin (of the order of 10^{-3} mm), hydraulic jumps are quite thick, usually 4 to 6 times larger than the downstream depth. The flow within the hydraulic jump is very turbulent and dissipates large amounts of mechanical energy. A circular hydraulic jump is observed as a water jet from a water tap strikes a flat surface. Near the center of the flow, the water flows rapidly and is supercritical. As the radius increases, the velocity decreases, and the flow becomes subcritical by passing through a circular hydraulic jump as shown in Fig. 16.11.

Fig. 16.10 Hydraulic Jump in a horizontal rectangular channel.

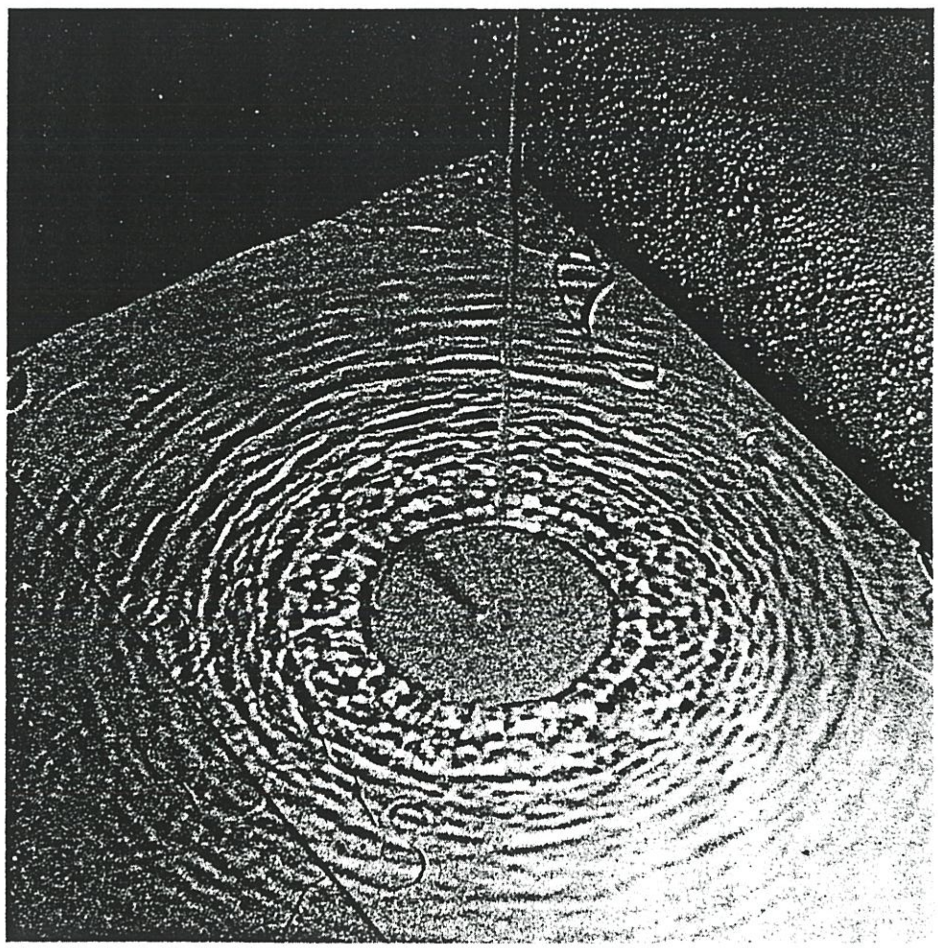

Fig. 16.11 Circular hydraulic jump.

Now, we confine our attention to a hydraulic jump occurring in a horizontal rectangular channel of width W. We apply a linear momentum balance (equations 6.3, 6.10) for the control volume of Fig. 16.12, neglecting the small frictional forces acting on the bottom surface, we have

$$0 = -p_1 A_1 + p_2 A_2 - \rho A_1 V_1^2 + \rho A_2 V_2^2 \qquad (16.56)$$

The pressures p_1 and p_2 are the hydrostatic pressures exerted at <u>half</u> the water depth (see Section 2.5), thus we may write

$$0 = -\frac{1}{2}\rho g z_1 z_1 W + \frac{1}{2}\rho g z_2 z_2 W - \rho z_1 W V_1^2 + \rho z_2 W V_2^2 \qquad (16.57)$$

or

$$\frac{g z_1^2}{2} - \frac{g z_2^2}{2} = z_2 V_2^2 - z_1 V_1^2 \qquad (16.58)$$

The continuity equation gives

$$Q = \rho z_1 W V_1 = \rho z_2 W V_2 \qquad (16.59)$$

or $$z_1 V_1 = z_2 V_2 \qquad (16.60)$$

Using equation (16.60) to eliminate V_2 from equation (16.58) and then dividing by $z_1 - z_2$, we get

$$\left(\frac{z_2}{z_1}\right)^2 + \frac{z_2}{z_1} - 2\,\frac{V_1^2}{g z_1} = 0 \qquad (16.61)$$

or using the definition of the upstream Froude number we have

$$\left(\frac{z_2}{z_1}\right)^2 + \frac{z_2}{z_1} - 2\,Fr_1 = 0 \qquad (16.62)$$

Solving this quadradic equation we obtain an expression for the depth ratio as a function of the upstream Froude number

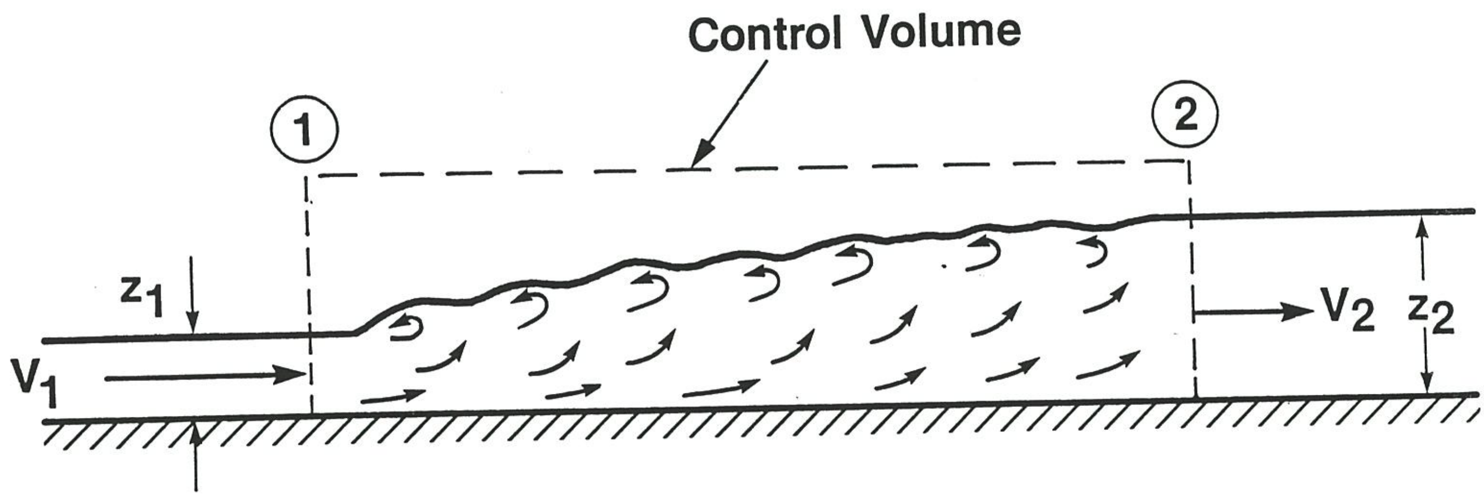

Fig. 16.12 Control volume for hydraulic jump.

$$\frac{z_2}{z_1} = \frac{1}{2}\left(-1 + \sqrt{8Fr_1^2 + 1}\right) \tag{16.63}$$

The positive root is the only one with physical significance because z_2/z_1 cannot be negative.

The mechanical energy dissipation can be determined by using the Bernoulli equation:

$$h_f = \left(z_1 + \frac{V_1^2}{2g}\right) - \left(z_2 + \frac{V_2^2}{2g}\right) \tag{16.64}$$

Introducing equations (16.60) and (16.61) and after some algebraic manipulations, we get

$$h_f = \frac{(z_2 - z_1)^3}{4z_1z_2} \tag{16.65}$$

In order for the dissipation to be positive z_2 must be larger than z_1. If the dissipation were negative we would have mechanical energy addition to the control volume. Since there is no source of mechanical energy in a hydraulic jump, $z_2 < z_1$ is physically impossible. Equation (16.63) then requires that the flow upstream be supercritical ($Fr_1 > 1$). A relation between downstream and upstream Froude numbers can be obtained by combining equations (16.60) and (16.63):

$$\frac{Fr_1}{Fr_2} = \frac{V_1}{V_2}\sqrt{\frac{z_2}{z_1}} = \left(\frac{z_2}{z_1}\right)^{3/2} = \left[\frac{1}{2}\left(\sqrt{8Fr_1 + 1} - 1\right)\right]^{3/2} \tag{16.66}$$

The above theory is for hydraulic jumps in wide horizontal channels. For the theory of prismatic or sloping channels the reader is referred to specialized texts [e.g. ref. 5].

The hydraulic jump is a very effective energy dissipator and finds practical engineering use in stilling-basins and spillways [11]. For example, spillways from dams are usually designed in such a way as to produce hydraulic jumps. Since the flow is slowed downstream of the jump the erosion of structures and river beds is reduced. While a hydraulic jump is produced for $Fr_1 > 1$ engineering applications require "good and strong" jumps which are produced for $Fr_2 \geq 4.5$ with accompanying energy dissipation of more than 50%.

Example 16.4

Water flows in a 10m wide channel at a flow rate Q = 85 m^3/s at a depth z_1 = 0.91 m. If a hydraulic jump is produced, determine (a) z_2, (b) V_2, (c) Fr_2, (d) h_f and (e) the percentage dissipation.

Solution

(a) From continuity, we have

$$V_1 = \frac{Q}{Wz_1} = \frac{85}{10\times 0.91} = 9.34 \text{ m/s}$$

The upstream Froude number is

$$Fr_1 = \frac{V}{\sqrt{gz_1}} = \frac{9.34}{\sqrt{9.81\times 0.91}} = 3.126 \text{ (supercritical)}$$

The depth z_2 is obtained from equation (16.63)

$$\frac{z_2}{z_1} = \frac{1}{2}(-1 + \sqrt{8Fr_1^2 + 1})$$

$$= \frac{1}{2}(-1 + \sqrt{8\times 3.126^2 + 1}) = 3.95$$

$$z_2 = 3.95 \times 0.91 = 3.59 \text{ m}$$

(b) From continuity

$$V_2 = \frac{z_1 V_1}{z_2} = \frac{0.91 \times 9.34}{3.59} = 2.367 \text{ m/s}$$

(c) The downstream Froude number is

$$Fr_2 = \frac{V_2}{\sqrt{gz_2}} = \frac{2.367}{\sqrt{9.81 \times 3.59}} = 0.399$$

(d) The dissipation (head) loss is

$$h_f = \frac{(z_2-z_1)^3}{4z_1z_2} = \frac{(3.59-0.91)^3}{4\times 0.91\times 3.59} = 1.473 \text{ m}$$

(e) The upstream mechanical energy is (in head form)

$$H_1 = z_1 + \frac{V_1^2}{2g} = 0.91 + \frac{9.34^2}{2\times 9.81} = 5.356 \text{ m}$$

$$\text{Percentage loss} = (100) \times \frac{1.473}{5.356} = 27.5\%$$

16.8 LAKE AND OCEAN CURRENTS

Currents in oceans and lakes are caused by a variety of physical mechanisms. One of the most important of them is the dragging action of winds on the water surface. Another mechanism is due to tidal motions which are caused by attractive forces of the moon and the sun on large water masses. Smaller currents are also caused by temperature and salinity variations. These phenomena are discussed in detail in specialized textbooks [12,13].

The general equations for the conservation of mass and momentum must be used for all such flows (see Chapter 6), but with a difference. Since we use a frame of reference fixed on the water surface and the earth rotates at angular speed of 1 revolution per 24 hours (0.726×10^{-4} rad/s) we are dealing with a rotating coordinate system. Thus, we must include the acceleration terms due to the fictitious centrifugal and Coriolis forces [14]. The introduction of such terms in the equations of conservation of momentum is discussed by Batchelor [15] and in greater detail by Proudman [16] and Greenspan [17]. Actually, the centrifugal force is completely taken into account into the pressure term (p) and requires no further separate consideration. The Coriolis acceleration (named after the French engineer and mathematician, Gustave-Gaspard Coriolis, who described it in 1835), is given by the cross-product $2\bar{\Omega}\times\bar{V}$, where $\bar{V}$ is the velocity relative to a coordinate system rotating with steady angular velocity $\bar{\Omega}$. The Coriolis force is responsible for the direction of rotation of hurricanes and the bathtub vortex, which is counterclockwise in the Northern Hemisphere and clockwise in the Southern Hemisphere [18].

The general equation for the conservation of momentum (6.61) can be written in the form

$$\rho\left(\frac{\partial\bar{V}}{\partial t} + \bar{V}\cdot\nabla\bar{V} + 2\bar{\Omega}\times\bar{V}\right) = -\nabla p + \nabla\cdot\bar{\bar{\tau}} + \rho g \qquad (16.67)$$

The relative magnitude of the inertia forces $\bar{V}\cdot\nabla\bar{V}$ (per unit mass) and Coriolis forces $2\bar{\Omega}\times\bar{V}$ (per unit mass) can be expressed in terms of the Rossby number (named in honour of the Swedish meteorologist C.G. Rossby) which is defined as

$$\mathrm{Ro} = \frac{V}{L\Omega} = \frac{\text{inertia forces}}{\text{Coriolis forces}} \tag{16.68}$$

where V is a characteristic velocity and L is a measure of the distance over which the velocity varies appreciably. When Ro<<1, the Coriolis forces dominate, while for Ro>>1, the Coriolis forces are insignificant. For example, in studying current patterns in a small lake we may have $V=1\,\mathrm{m/s}$, $L=10^4\,\mathrm{m}$ and $\Omega=0.726\times10^{-4}$ rad/s. Thus we get

$$\mathrm{Ro} = 1.377$$

Under such conditions, both inertia and Coriolis forces must be taken into account. However, for ocean currents, typical values might be $V=1\,\mathrm{m/s}$, $L=1000\,\mathrm{km}=10^6\,\mathrm{m}$ and $\Omega=0.726\times10^{-4}\,\mathrm{s}^{-1}$. Thus

$$\mathrm{Ro} = \frac{V}{L\Omega} = 1.37 \times 10^{-2}$$

Under such conditions, the inertia effects can be neglected and such flows are called geostrophic (e.g. the Gulf Stream).

It should be also be noted that in laboratory scale (e.g. for L=1m), the Rossby number is very large and Coriolis effects are negligible.

We can now write down the equations of motion of a layer of fluid on the earth's surface by referring to Fig. 16.13. Using spherical polar coordinates, we have velocity components (v_r, v_θ, v_ϕ) in a system that rotates with the earth. The components of the earth's angular velocity are $(\Omega\cos\theta, -\Omega\sin\theta, 0)$. The radial velocity can be neglected and thus the angular acceleration term appearing in equation (16.67) can be written

$$2\Omega\times\bar{V} = \begin{matrix} -2\Omega\, v_\phi \sin\theta \\ -2\Omega\, v_\phi \cos\theta \\ 2\Omega\, v_\theta \cos\theta \end{matrix}$$

This means that the Coriolis acceleration in the r-direction is $-2\Omega v_\theta \sin\theta$, in the θ-direction $-2\Omega v_\phi \cos\theta$, and in ϕ-direction $2\Omega v_\theta \cos\theta$.

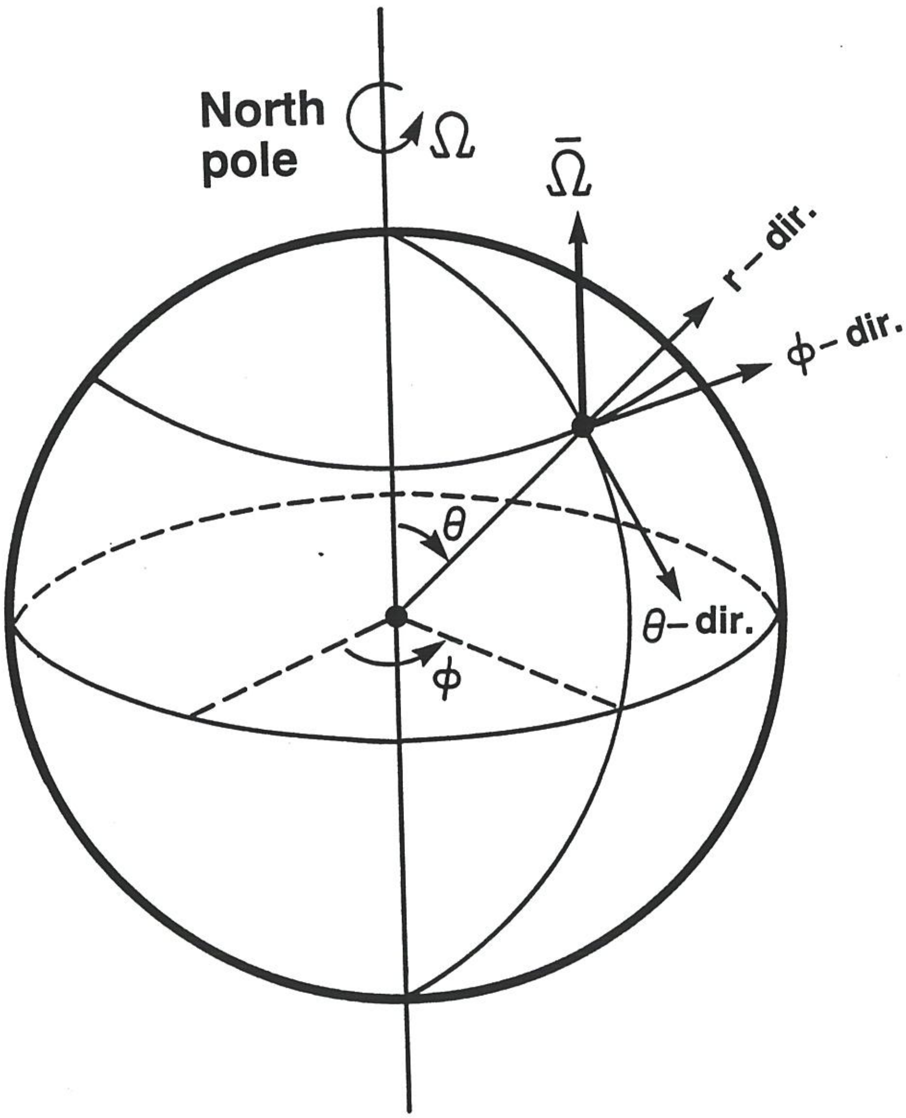

Fig. 16.13 Rotating frame of reference on the Earth's surface.

In a shallow fluid layer on the earth's surface, flow in the r-direction would be insignificant. Thus we have to deal with only two components, $-2\Omega v_\theta \cos\phi$ and $2\Omega v_\theta \cos\theta$. It is customary to define a Coriolis parameter

$$f = 2\Omega\cos\theta$$

which is approximately $10^{-4} s^{-1}$ at $\theta = 45^\circ$.

Thus, the terms $-fv_\phi$ and fv_θ must be included always in the equations of motion for the description of lake and ocean current flows.

For most problems, it is convenient to define a rectangular system of coordinates x,y,z where z represents the vertical direction (upward). The conservation equations with the inclusion of the Coriolis acceleration terms take the form

continuity $$\frac{\partial v_x}{\partial x} + \frac{\partial v_y}{\partial y} + \frac{\partial v_z}{\partial z} = 0$$

x-momentum $$\rho\left(\frac{\partial v_x}{\partial t} + v_x\frac{\partial v_x}{\partial x} + v_y\frac{\partial v_x}{\partial y} + v_z\frac{\partial v_z}{\partial z}\right) - fv_y = -\frac{\partial p}{\partial x} + \frac{\partial \tau_{xx}}{\partial x} + \frac{\partial \tau_{yx}}{\partial y} + \frac{\partial \tau_{zx}}{\partial z} + \rho g_x$$

y-momentum $$\rho\left(\frac{\partial v_y}{\partial t} + v_x\frac{\partial v_y}{\partial x} + v_y\frac{\partial v_y}{\partial y} + v_z\frac{\partial v_y}{\partial z} + fv_x\right.$$

$$= -\frac{\partial p}{\partial x} + \frac{\partial \tau_{xy}}{\partial x} + \frac{\partial \tau_{yy}}{\partial y} + \frac{\partial \tau_{zy}}{\partial z} + \rho g_y$$

z-momentum $$\rho\left(\frac{\partial v_z}{\partial t} + v_x\frac{\partial v_z}{\partial x} + v_y\frac{\partial v_z}{\partial y} + v_z\frac{\partial v_z}{\partial z}\right) = -\frac{\partial p}{\partial z} + \frac{\partial \tau_{xz}}{\partial x} + \frac{\partial \tau_{yz}}{\partial y} + \frac{\partial \tau_{zz}}{\partial z} + \rho g_z$$

For a relatively shallow lake we may assume that the motions in the vertical direction will be less important than the motions in the x and y directions and we may eliminate the z-momentum component. The stress components will normally be represented by the Reynolds stresses (see Chapter 10) i.e.

$$\tau_{yx} = \mu^{(t)}\frac{\partial v_x}{\partial y}$$

where $\mu^{(t)}$ is the eddy viscosity coefficient. Usually the eddy viscosity coefficients have different values when considered is x, y and

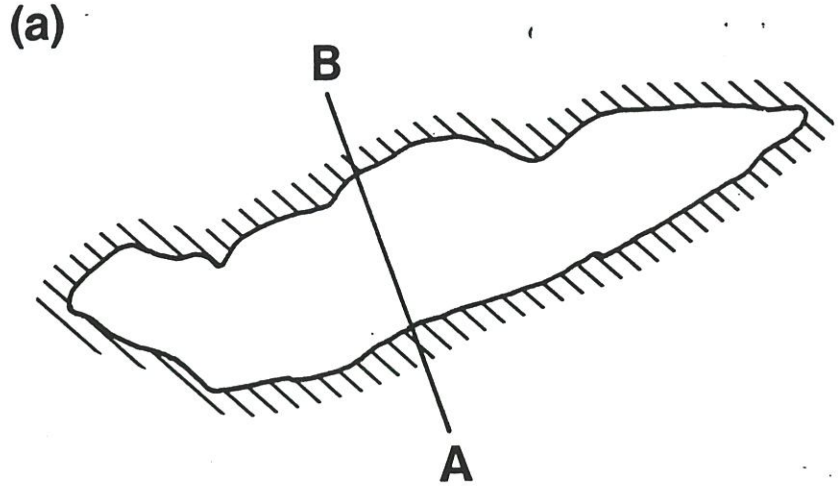

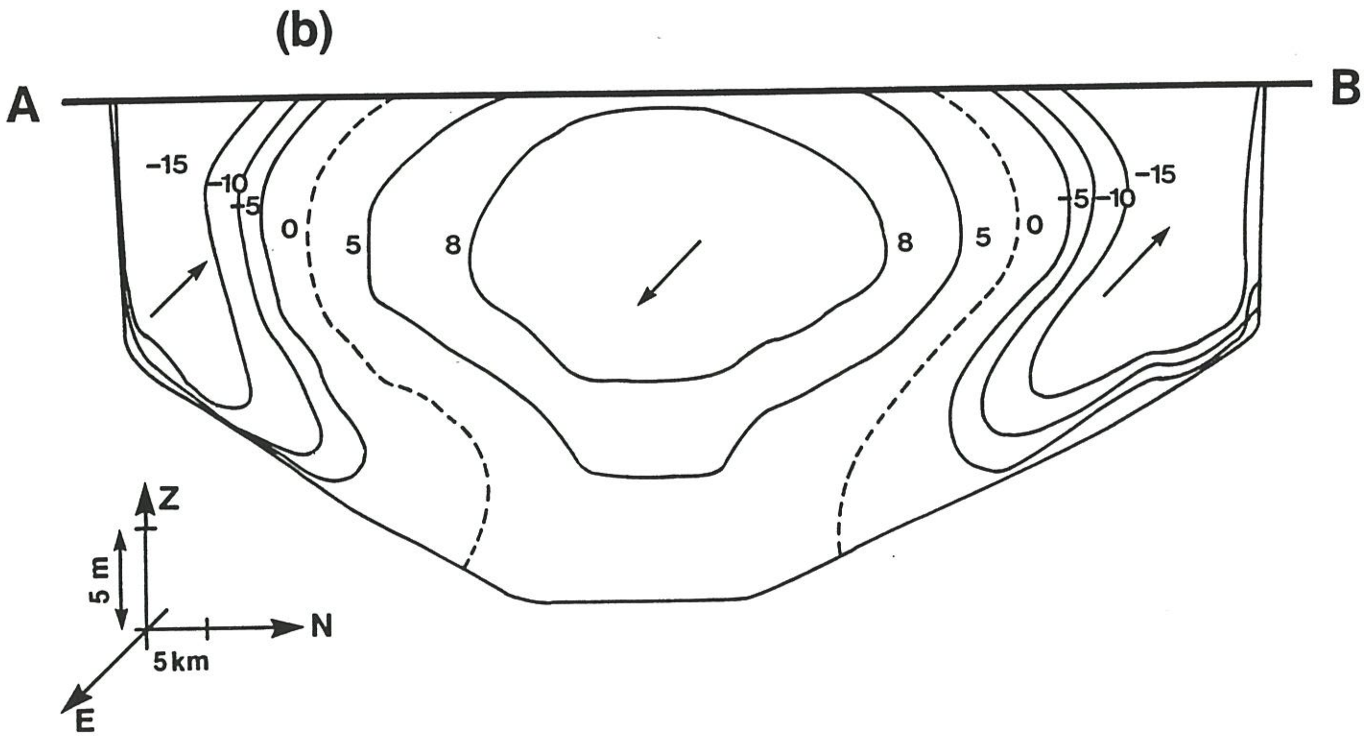

Fig. 16.14 (a) Sketch of Lake Erie.

(b) The shore-parallel component of velocity in Lake Erie for an imposed wind velocity of 10 m/s from north-east according to ref. [19].

z directions. Invariably numerical techniques are necessary for the determination of flow patterns in lakes and oceans. Some results of a numerical simulation are shown in Fig. 16.14 from reference [19]. These topics, however, are beyond the scope of this book and the reader is referred to specialized books [13, 19-21].

REFERENCES

1. H.M. Morris and J.M. Wiggert, "Applied Hydraulics in Engineering", Ronald, New York (1972).

2. J.M.K. Dake, "Essentials of Engineering Hydraulics", 2nd edition, Macmillan, New York (1983).

3. B.A. Bakhmeteff, "Hydraulics of Open Channels", McGraw-Hill, New York (1932).

4. S.M. Woodward and C.J. Posey, "Steady Flow in Open Channels", Wiley, New York (1941).

5. Ven Ten Chow, "Open Channel Hydraulics", McGraw-Hill, New York (1959).

6. F.M. Henderson, "Open Channel Flow", Macmillan, New York (1966).

7. S. Leliavsky, "An Introduction to Fluvial Hydraulics", Constable, London (1955).

8. A.T. Ippen, "Estuary and Coastline Hydrodynamics", McGraw-Hill, New York (1966).

9. A.J. Raudkivi, "Loose Boundary Hydraulics", Pergamon Press.

10. P.A. Thomson, "Compressible-Fluid Dynamics", McGraw-Hill, New York (1972).

11. E.A. Elevatorski, "Hydraulic Energy Dissipators", McGraw-Hill, New York (1959).

12. G. Neumann and W.J. Pierson, "Principles of Physical Oceanography", Prentice-Hall, Englewood Cliffs, NJ (1966).

13. K. Hutter, L.A. Mysak, N.S. Heaps, J. Sunderman, J. Kielmann, T.J. Simons and K.H. Mortimer, "Hydrodynamics of Lakes", Springer-Verlag, New York (1983).

14. H. Goldstein, "Classical Mechanics", Addison-Wesley, Cambridge, MA (19__).

15. G.K. Batchelor, "An Introduction to Fluid Dynamics", Cambridge University Press, Cambridge, U.K. (1967).

16. J. Proudman, "Dynamical Oceanography", Dover Publications, New York (19__).

17. H.P. Greenspan, "The Theory of Rotating Fluids", Cambridge University Press, Cambridge, U.K. (1968).

18. M. Sibulkin, "A Note on the Bathtub Vortex and the Earth's Rotation", Amer. Sci., 71, 352 (1983).

19. A.E. Elzawahry, "Advection, Diffusion and Settling in the Coastal Zone of Lake Erie", Ph.D. Thesis, Dept. of Civil Engineering, McMaster University, Hamilton, Ontario, Canada (1985).

20. G.T. Csanady, "Turbulent Diffusion in the Environment", D. Reidel Publishing Company, Holland (1973).

21. G.F. Pinder and W.G. Gray, "Finite Element Simulation in Surface and Subsurface Hydrology", Academic Press, New York (1977).

John Vlachopoulos, *Fundamentals of Fluid Mechanics*
Chem. Eng., McMaster University, Hamilton, ON, Canada
(First Edition 1984, revised internet edition (2016), www.polydynamics.com)

CHAPTER 17

MAGNETOHYDRODYNAMICS

17.1 INTRODUCTION

Under certain conditions charged particles, ions or electrons, might be present in a fluid. For example, gases at high temperatures can be ionized, thus becoming conductors of electricity. When the net charge of a finite volume of a gas is zero, it is called plasma. Molten metals also are electrically conducting fluids. When such fluids are flowing within magnetic or electric fields, they are subjected to electromagnetic forces. These are body forces because they act on the charges distributed throughout the fluid mass (see Chapter 5 for distinction between body and surface forces). The fluid motion is also accompanied by the generation of electric and magnetic fields by induction. These electromagnetic effects are essentially the same like those occurring in the conventional electric generators and motors, except that in the present case conducting fluids rather than solid conductors (copper windings) are involved. Man made devices using the interaction between flowing fluids and magnetic and electric fields include power generators, pumps, propulsion units, metallurgical furnaces, flow meters and many others. Such interactions also occur in nature, for example in the earth's interior, the ionosphere, the sun and the stars.

The branch of fluid mechanics that is concerned with the interaction between electromagnetic forces and flowing incompressible fluids is called Magnetohydrodynamics (MHD). For compressible fluids we use the term magnetogasdynamics, and to designate both types of flow the term magnetofluidmechanics. Certain problems are treated by statistical methods and belong to the realm at plasma dynamics. All these are relatively new branches of engineering science and are rapidly increasing in importance both for power generation and for materials processing.

17.2 CONSERVATION OF MASS AND MOMENTUM

The equation of conservation of mass (Chapter 4) remains unchanged for a conducting fluid, thus we have

$$\frac{\partial \rho}{\partial t} + \nabla \cdot (\rho \bar{V}) = 0 \qquad (17.1)$$

The equation of conservation of momentum for a conducting fluid moving in the presence of an electromagnetic field must include the electromagnetic (body) forces. In the derivation of Chapter 6, we considered only one body force, gravity. In the differential equation (6.94) the gravity force term was designated as $\rho \bar{g}$. For the more general case of a body force field $\bar{f}$ consisting of gravitational and electromagnetic (Lorentz) forces, we may write [1,2]

$$\rho\bar{f} = \rho\bar{g} + \rho_e \bar{E} + \bar{J} \times \bar{B} \qquad (17.2)$$

where ρ_e is the charge density, $\bar{E}$ the electric field strength, $\bar{J}$ the electric current density and $\bar{B}$ the magnetic flux density. Obviously, $\rho_e\bar{E}$ represents the electric force and $\bar{J} \times \bar{B}$ the magnetic force whose direction is given by the familiar right-hand rule of elementary physics [3]. In order for the equation(17.1) to be dimensionally correct, each term must be expressed in units of force per cubic meter (N/m^3). The SI units of the various quantitites appearing in equation (17.1)are: ρ (kg/m^3), ρ_e (Coulomb per cubic meter, C/m^3), $\bar{g}$ (m/s^2), $\bar{E}$ (volt per meter, V/m), $\bar{J}$ (ampere per square meter, A/m^2) and $\bar{B}$ (tesla or Weber per square meter, Wb/m^2). For conversion to base units the reader is refered to the tables of units at the end of this book. The equation of conservation of momentum for a compressible fluid (6.94), can be modified to the form

$$\rho \left(\frac{\partial\bar{V}}{\partial t} + \bar{V}\cdot\nabla\bar{V}\right) = -\nabla p + \mu\nabla^2 \bar{V} + \frac{1}{3}\mu\nabla(\nabla\cdot\bar{V}) + \rho\bar{g} + \rho_e\bar{E} + \bar{J} \times \bar{B} \qquad (17.3)$$

We note that we have introduced the quantitites ρ_e, $\bar{E}$, $\bar{J}$ and $\bar{B}$ which represent ten new scalar unknowns, while equations(17.1) and(17.3) constitute only four scalar equations. Consequently, we need ten new independent scalar equations in order to fully describe the flow, electric and magnetic fields. These additional equations are (from electromagnetism):

i) the equation of conservation of charges

ii) Ohm's law

iii) Maxwell's equations.

The equation of conservation of charges is of the same form as the equation of conservation of mass where $\rho\bar{V}$, the mass flux is replaced by the current density $\bar{J}$ (charge per unit area per unit time). We have the scalar equation

$$\frac{\partial \rho_e}{\partial t} + \nabla \cdot \bar{J} = 0 \tag{17.4}$$

Ohm's law for conducted and convected current

$$\bar{J} = \sigma(\bar{E} + \bar{V} \times \bar{B}) + \rho_e \bar{V} \tag{17.5}$$

where σ is the electric conductivity of the fluid, represents three scalar equations.

Two of Maxwell's (four) equations are needed. These are

$$\nabla \times \bar{E} = - \frac{\partial \bar{B}}{\partial t} \tag{17.6}$$

$$\nabla \times \bar{H} = \bar{J} + \frac{\partial \bar{D}}{\partial t} \tag{17.7}$$

where the electric displacement $\bar{D}$ is defined by $\bar{D} = \varepsilon \bar{E}$ (ε = electric permitivity (farad per meter, F/m)) and the magnetic field strength $\bar{H}$ by $\bar{H} = 1/\mu_m \bar{B}$ (where μ_m is the magnetic permeability (henry per meter, H/m)). Equations (17.6) and (17.7) constitute six scalar equations and thus with the definitions for $\bar{D}$ and $\bar{H}$, the description of the flow field of a conducting fluid is now complete.

Equation (17.3) can be simplified under certain conditions. For an electrically neutral fluid (plasma) the net charge is zero which means $\rho_e = 0$ and $\rho_e E = 0$. If the electric and magnetic fields are parallel $\bar{J} \times \bar{B} = 0$, thus we get the momentum equation (6.94) of conventional fluid mechanics. Several other simplifications are also possible for conducting fluids, by introducing the approximations discussed in previous sections for non-conducting fluids, such as creeping flow, boundary layer flow etc. In each case, however, the order of magnitude of the electromagnetic terms must be properly assessed.

17.3 HYDROMAGNETIC PRESSURE-DRIVEN FLOW BETWEEN TWO FLAT PLATES

We consider steady laminar flow of an incompressible conducting fluid between two horizontal parallel plates under the influence of a pressure gradient (Hartmann flow). A magnetic field B_o perpendicular to the plates is applied as shown in Fig. 17.1 (a) and (b). The induced current, as well as the magnetic and force fields are shown in Fig. 17.1(c).

This problem is similar to that of Section 7.2 except for the existense of a magnetic force which interacts with the fluid motion. The momentum equation (17.3) can be simplified to the form (compare to equation (7.34))

$$0 = -\frac{\partial p}{\partial x} + \mu \frac{\partial^2 v_x}{\partial y^2} + (\bar{J} \times \bar{B})_x \qquad (17.8)$$

Here, we have

$$\bar{V}(v_x, 0, 0), \quad \bar{B}\,(0, B_o, 0) \quad \text{and} \quad \bar{E}(0, 0, E_z)$$

thus, with the help of Ohm's law

$$\bar{J} = \sigma(\bar{E} + \bar{V} \times \bar{B})$$

for negligible convected current ($\rho_e \bar{V} = 0$), we get

$$J_z = \sigma(E_z + v_x B_o) \qquad (17.9)$$

and

$$(\bar{J} \times \bar{B})_x = -\sigma(E_z + V_x B_o) B_o \qquad (17.10)$$

Thus, equation (17.8) becomes

$$0 = -\frac{\partial p}{\partial x} + \mu \frac{\partial^2 v_x}{\partial y^2} + \sigma(E_z + V_x B_o) B_o \qquad (17.11)$$

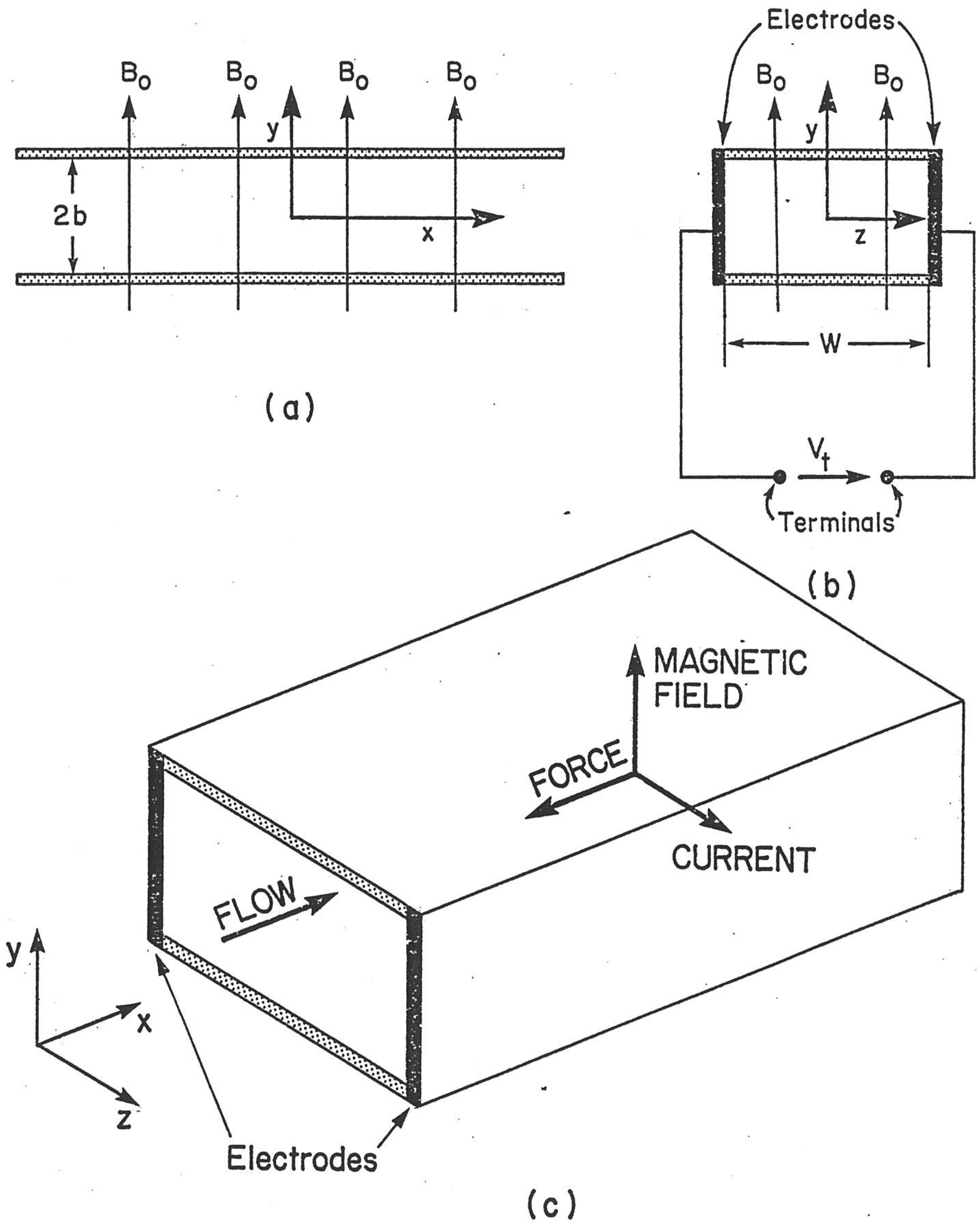

Fig. 17.1 Hydromagnetic flow between two flat plates

which can be integrated with the no-slip boundary conditions

$$v_x = 0 \quad \text{at} \quad y = b \tag{17.12}$$

$$v_x = 0 \quad \text{at} \quad y = -b$$

to give the velocity profile as

$$v_x = \frac{b^2}{Ha^2}\left(\frac{1}{\mu}\frac{\partial p}{\partial x} + \frac{Ha}{b}\sqrt{\frac{\sigma}{\mu}}\,E_z\right)\left(\frac{\cosh(Ha\ y/b)}{\cosh Ha} - 1\right) \tag{17.13}$$

where

$$Ha = B_o b\sqrt{\sigma/\mu} \tag{17.14}$$

is the Hartmann number, named after the pioneering work of the Danish physisist Hartmann. This dimensionless group can be interpreted as the ratio of magnetic to viscous forces.

A sketch of equation (17.13) is shown in Fig. 17.2 We note that as the Hartmann number increases the velocity profile flattens because the magnetic force is acting against the direction of flow.

The current density J_z can be calculated from Ohm's law with the help of equation (17.13.) We have

$$J_z = \sigma E_z \frac{\cosh(Ha\ y/b)}{\cosh Ha} + \frac{b}{Ha}\sqrt{\frac{\sigma}{\mu}}\frac{\partial p}{\partial x}\left(\frac{\cosh(Ha\ y/b)}{\cosh Ha} - 1\right) \tag{17.15}$$

The total current $\langle J\rangle$ (per unit channel length in the x direction) can be evaluated by integrating J_z along y

$$\langle J\rangle = \int_{-b}^{b} J_z dy = 2\sigma b\, E_z \frac{\tanh Ha}{Ha} + \frac{2b^2}{Ha}\sqrt{\frac{\sigma}{\mu}}\frac{\partial p}{\partial x}\left(\frac{\tanh Ha}{Ha} - 1\right) \tag{17.16}$$

The terminal voltage V_t (i.e. the potential difference between the two electrodes at the sides of the channel) can be determined by integrating $E_z = E_z(y)$ along z, i.e. (17.17)

$$V_t = \int_{o}^{W} E_z\, dz = E_z W$$

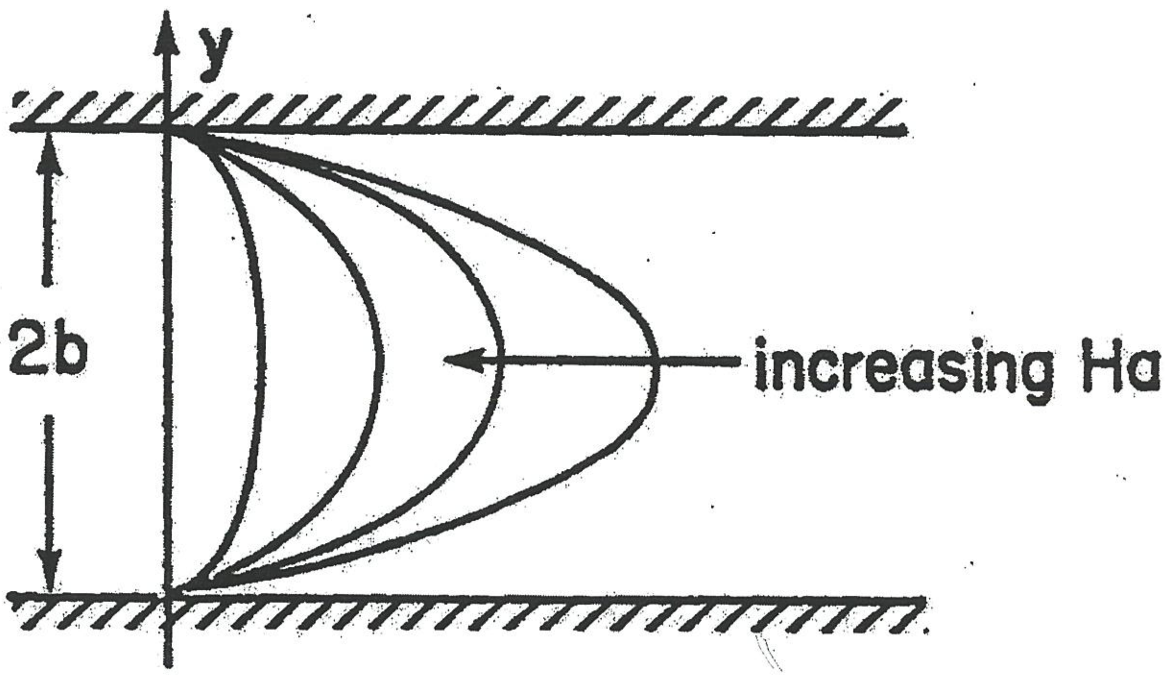

Fig.17.2 Velocity profiles for hydromagnetic pressure flow between two flat plates under the influence of a constant pressure gradient (Hartmann flow).

or, by solving equation (17.16) for E_z we get V_t in terms of $\langle J \rangle$ as

$$V_t = - \frac{W\ Ha\langle J \rangle}{2\sigma b \tanh Ha} + \frac{Wb}{Ha\sqrt{\sigma\mu}} \frac{\partial p}{\partial x} \left(1 - \frac{Ha}{\tanh Ha}\right) \qquad (17.18)$$

Further evaluations may involve the induced magnetic field H_x. From Maxwell's equation (17.7) assuming negligible displacement current ($\partial D/\partial t = 0$), we have

$$\frac{dH_x}{dy} = -J_z \qquad (17.19)$$

By introducing J_z from equation (17.15) and integrating we can get H_x.

The pressure gradient in the y direction is not constant. It can be evaluated, however, from the equation of conservation of momentum in the y direction, which is

$$0 = - \frac{\partial p}{\partial y} + J_z\ B_x \qquad (17.20)$$

where J_z is given by equation (17.15) and $B_x = \mu_m\ H_x$.

More details on the above problem, as well as many other problems of this type can be found in specialized textooks, see, for instance references [1,2,4,5]. The general analysis as presented above can also be applied to MHD devices such as generators and pumps.

Example 17.1

Liquid mercury is flowing in a channel similar to that shown in Fig. 17.1. The channel width is 2b = 4 cm. An electromagnentic field with $B_o = 0.02$ Wb/m^2 and $E_z = 0.2$ V/m is applied in the absence of an external pressure gradient. The density of mercury is $\rho = 13.6 \times 10^3$ kg/m^3, the viscosity $\mu = 1.55$ Pa•s and the electric conductivity $\sigma = 1.07 \times 10^6$ S/m (siemens/m). Determine the maximum velocity in the channel.

Solution

We first calculate the Hartmann number

$$Ha = B_o b \sqrt{\frac{\sigma}{\mu}} = 0.02 \times 0.02 \times \sqrt{\frac{1.07 \times 10^6}{1.55}} = 0.332$$

From equation (17.13) with $\partial p/\partial x = 0$, we have $v_x = V_{max}$ at $y = 0$

$$V_{max} = \frac{b}{Ha} \sqrt{\frac{\sigma}{\mu}} E_z \left(\frac{1}{\cosh Ha} - 1\right)$$

and

$$V_{max} = \frac{0.02}{0.332} \times \sqrt{\frac{1.07 \times 10^6}{1.55}} \times 0.2 \left(\frac{1}{1.055} - 1\right) = -0.52 \text{ m/s}$$

The velocity is negative because the fluid is flowing in the negative x direction. We must now calculate the Reynolds number to see whether the flow is laminar. Since the average flow velocity has not been calculated (integration of the velocity profile is required) we will use the maximum velocity and a hydraulic radius equal to 2b, for an approximate estimate

$$Re = \frac{\rho VD}{\mu} = \frac{13.6 \times 10^3 \times 0.52 \times 0.04}{1.55} \simeq 182$$

Thus, the flow is indeed laminar.

17.4 HYDROMAGNETIC LAMINAR BOUNDARY LAYER FLOW

We now consider the boundary layer approximations of Chapter 9, for steady flow of a conducting incompressible fluid in an applied transverse steady magnetic field B_o. Assuming that the induced field is negligible compared to B_o, we may simplify equations (17.1) and (17.3)

$$\frac{\partial v_x}{\partial x} + \frac{\partial v_y}{\partial y} = 0 \tag{17.21}$$

$$\rho \left(v_x \frac{\partial v_x}{\partial x} + v_y \frac{\partial v_x}{\partial y}\right) = - \frac{\partial p}{\partial x} + \mu \frac{\partial^2 v_x}{\partial y^2} + (\bar{J} \times \bar{B})_x \tag{17.22}$$

From Ohm's law (for zero impressed electric field) we have

$$(\bar{J} \times \bar{B})_x = - \sigma v_x B_o^2 \tag{17.23}$$

Thus, equation (17.22) becomes

$$v_x \frac{\partial v_x}{\partial x} + v_y \frac{\partial v_x}{\partial y} = - \frac{1}{\rho} \frac{\partial p}{\partial x} + \nu \frac{\partial^2 v_x}{\partial y^2} - \frac{\sigma v_x B_o^2}{\rho} \tag{17.24}$$

where $\nu = \mu/\rho$. Equations (17.21) and (17.24) are the boundary layer equations for steady incompressible hydromagnetic flow.

For boundary layer flow over a flat plate as shown in Fig. 17.3 in the absence of a pressure gradient, we have

$$v_x \frac{\partial v_x}{\partial x} + v_y \frac{\partial v_x}{\partial y} = \nu \frac{\partial^2 v_x}{\partial y^2} - \frac{\sigma v_x B_o^2}{\rho} \tag{17.25}$$

Applying the integral momentum approximation of Section 9.6 for a velocity profile

$$\frac{v_x}{V_\infty} = \frac{3}{2} \left(\frac{y}{b}\right) - \frac{1}{2} \left(\frac{y}{b}\right)^3 \tag{17.26}$$

we get

$$\frac{3 \nu V_\infty}{2 \delta_m} + \frac{5 \sigma V_\infty B_o^2}{8 \rho} = \frac{39}{280} V_\infty^2 \frac{d\delta_m}{dx} \tag{17.27}$$

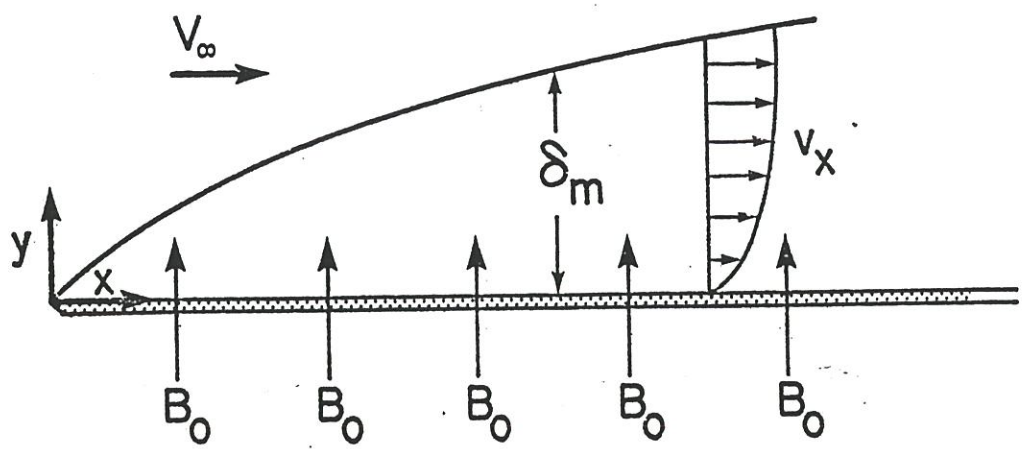

Fig.17.3 Hydromagnetic boundary layer over a flat plate.

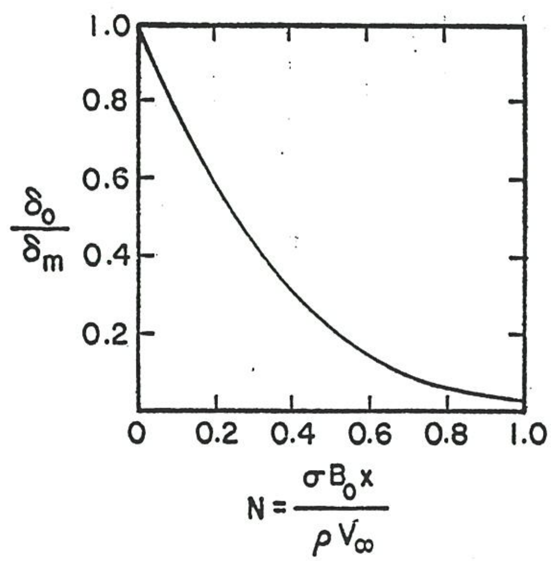

Fig.17.4 Influence of magnetic field on boundary layer thickness.

This differential equation may be solved for δ_m^2 to give

$$\left(\frac{\delta_m}{x}\right)^2 = \frac{2.40}{Re_x N}\left(e^{8.97N} - 1\right) \tag{17.28}$$

where

$$Re_x = \frac{\rho V_\infty x}{\mu} \tag{17.29}$$

is the Reynolds number and

$$N = \frac{\sigma B_o^2 x}{\rho V_\infty} \tag{17.30}$$

is the so-called magnetic influence number. In Section 9.5 we found that for laminar flow in the absence of electromagnetic interactions

$$\frac{\delta}{x} = \frac{4.64}{Re_x^{1/2}} \tag{17.31}$$

Thus the ratio of magnetic to non-magnetic boundary layer thicknesses is

$$\frac{\delta_m}{\delta} = \frac{0.334}{N^{1/2}}\left(e^{8.97N} - 1\right) \tag{17.32}$$

This equation is plotted in Fig. 17.4 We note that as the magnetic field increases the boundary layer thickness increases. This is due to the fact that the magnetic field imposes a force against the direction of the flow.

Equations (17.21) and (17.24) also describe the flow field in a two-dimensional jet of a conducting fluid in a transverse magnetic field. Similarity solutions and numerical calculations [7] show that the centerplane (maximum) velocity decreases (see Fig.17.5) while the jet thickness increases as the Hartmann number increases. This is again

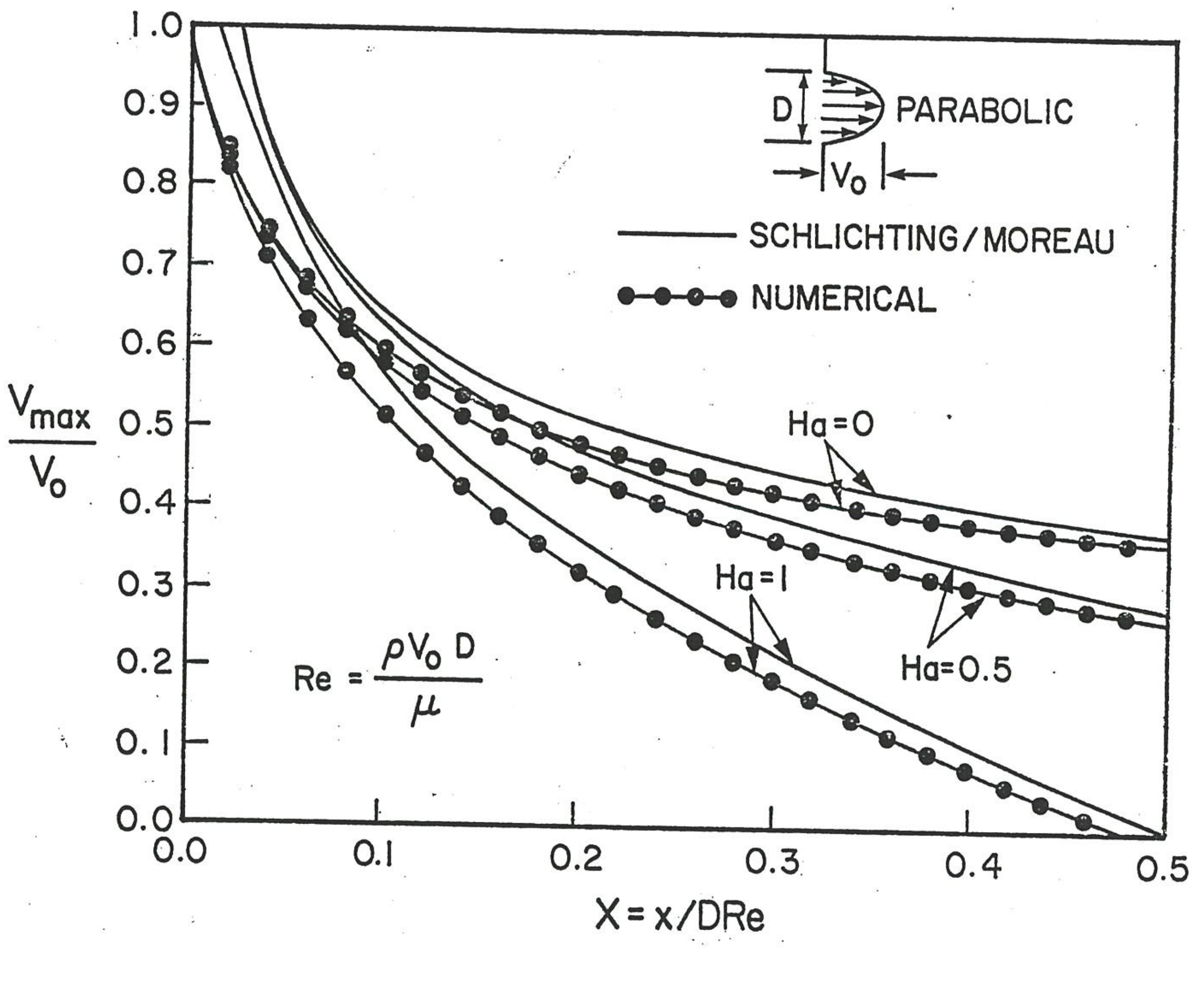

Fig. 17.5 Maximum jet velocity as a function of distance from the nozzle exit for a two-dimensional hydromagnetic jet ($Ha = B_o D \sqrt{\sigma/\mu}$)

due to the increased retarding force exerted by the magnetic field.

17.5 CONSERVATION OF ENERGY

The thermal energy equation of Section 13.3 can be modified for conducting fluids in the presence of electromagnetic interactions, by including the Joule heating J_c^2/σ. Thus, we have

$$\rho \frac{De}{Dt} = K\nabla^2 T - p\nabla\cdot\bar{V} + \bar{\bar{\tau}}:\nabla\bar{V} + \frac{J_c^2}{\sigma} \tag{17.33}$$

where J_c is the conduction current.

For an incompressible fluid equation (17.33) reduces to

$$\rho\, C_p \frac{DT}{Dt} = k\nabla^2 T + \bar{\bar{\tau}}:\nabla\bar{V} + \frac{J_c^2}{\sigma} \tag{17.34}$$

or equivalently

$$\rho\, C_p \left(\frac{\partial T}{\partial T} + \bar{V}\cdot\nabla T\right) = k\nabla^2 T + \bar{\bar{\tau}}:\nabla\bar{V} + \frac{J_c^2}{\sigma} \tag{17.35}$$

For steady two-dimensional boundary layer flow, equation (17.35) becomes

$$\rho\, C_p \left(v_x \frac{\partial T}{\partial x} + v_y \frac{\partial T}{\partial y}\right) = k \frac{\partial^2 T}{\partial y^2} + \mu \left(\frac{\partial v_x}{\partial y}\right)^2 + \frac{J_c^2}{\sigma} \tag{17.36}$$

For more details on the above equations the reader is referred to Hughes and Young [5].

17.6 FURTHER REMARKS ON MHD

In this chapter, we have given a brief introduction to the flow of conducting fluids in the presence of electromagnetic fields. We have regarded the flow problems as differing from the conventional ones only because of the presence of the additional electromagnetic (body) force, the Lorentz force. We have shown how the velocity profiles, as well as certain important electromagnetic quantities can be evaluated. There is also a large body of knowledge on turbulence, waves and shocks in MHD flows, which may be found in references [2,4-6,8]. Some interesting metallurgical applications of MHD are discussed by Szekely [9]. The whole field of magnetofluidmechanics is a rapidly growing area of engineering technology and research.

REFERENCES

1. S. Eskinazi, "Vector Mechanics of Fluids and Magnetofluids", Academic Press, New York (1967).

2. A.B. Cambel, "Plasma Physics and Magnetofluid-Mechanics", McGraw-Hill, New York (1963).

3. R. P. Feynman et al *Lectures on Physics* Addison-Wesley, New York (1965)

4. P.H. Roberts, "An Introduction to Magnetohydrodynamics", Longmans, London (1967).

5. W.F. Hughes and F.J. Young, "The Electrodynamics of Fluids", Wiley, New York (1966).

6. A. Jeffrey, "Magnetohydrodynamics", Interscience (Wiley), Oliver and Boyd (1966).

7. J. Vlachopoulos, "A Numerical Study of Laminar Magnetohydrodynamic Free Jets", Comp. Fluids, 2, 261 (1974).

8. G.W. Sutton and A. Sherman, "Engineering Magnetohydrodynamics", McGraw-Hill, New York (1965).

9. J. Szekely, "Fluid Flow Phenomena in Metals Processing" Academic Press, New York (1979)

John Vlachopoulos, *Fundamentals of Fluid Mechanics*
Chem. Eng., McMaster University, Hamilton, ON, Canada
(First Edition 1984, revised internet edition (2016), www.polydynamics.com)

CHAPTER 18

MEASUREMENTS IN FLUID MECHANICS

18.1 INTRODUCTION

Measurements in fluid mechanics include the determination of viscosity, pressure, velocity, flow rate, turbulence intensity, density gradients and shock waves. While reference to the measurement of some of these quantities was made in previous chapters, we will present here a summary of the principles behind the various measurement techniques. The design details of the various instruments will be omitted. The list of methods and instruments is certainly not complete. For a more complete listing and more detailed description of various measurement techniques the reader is referred to some specialized books [1-6].

18.2 MEASUREMENT OF VISCOSITY

Viscosity was defined in Chapter 1 of this book (see Section 1.3 and Section 20.3) as the ratio of shear stress to shear rate i.e.

$$\mu = \frac{\tau}{\frac{du}{dy}} \tag{18.1}$$

Thus, the determination of viscosity requires the independent measurement of shear stress (which is the tangential force divided by the surface area) and the shear rate (velocity gradient).

In the concentric (or co-axial) cylinder viscometer described in Section 1.3 (see also Example 7.18.4) the shear stress is obtained from the torque and the shear rate from the angular velocity and gap size.

In the capillary viscometer (see Example 7.18.2) the viscosity is obtained directly from the Hagen-Poiseuille formula (see Section 7.3) which in effect relates the shear stress to the pressure drop and the shear rate to the volume rate of flow.

In the falling sphere viscometer (see Example 8.1) the viscosity is obtained from Stokes' law (see Section 8.4) which relates implicitly the shear stress to the balance of weight, drag and buoyance forces and the shear rate to the terminal velocity.

The cone-and-plate instrument (or Weissenberg rheogoniometer) is used for viscosity measurements of some highly viscous fluids especially of polymer solutions and melts at low shear rates.

Besides the above viscosity (or more precisely shear viscosity) the elongational or extensional viscosity is defined as the ratio of the normal stress to the elongation rate, i.e.,

$$\eta_e = \frac{\sigma_{xx}}{\frac{dv_x}{dz}} \tag{18.2}$$

The elongational viscosity is important in the characterization of highly viscous materials, such as polymer solutions and melts, which are very often subjected to extensional (i.e. stretching) flows.

For details about this as well as other important measurements with polymer melts the reader is referred to a recent book [7].

18.3 MEASUREMENT OF PRESSURE

There are two types of pressure measurement: static pressure and stagnation pressure. Static pressure is measured by a device that causes no velocity change to the flow. This is usually accomplished by drilling a small hole normal to a wall along which the fluid is flowing

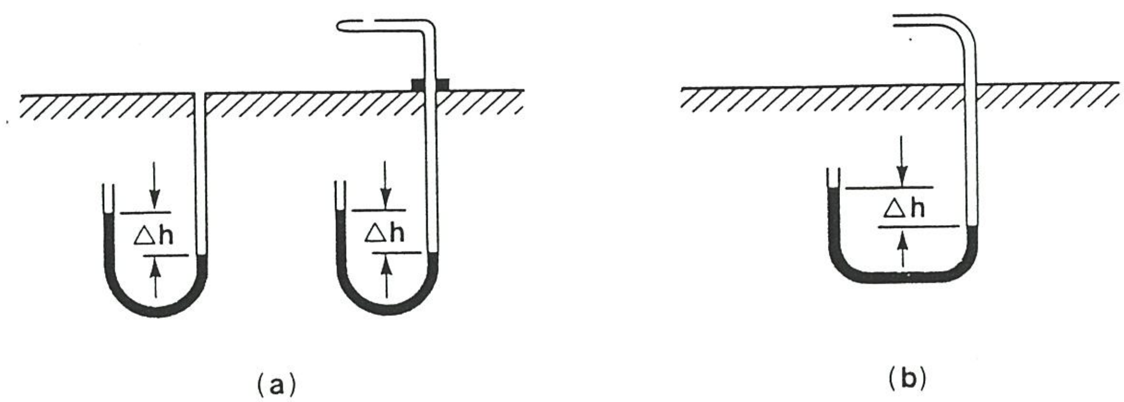

Fig. 18.1 (a) Static pressure taps.
(b) Pitot tube (stagnation pressure tap).

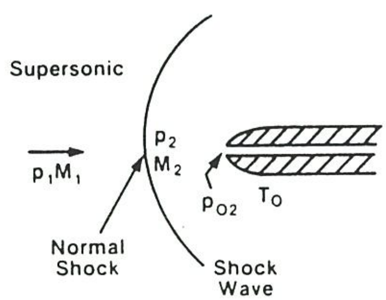

Fig. 18.2 Pitot tube in supersonic flow.

and connecting the opening to a manometer or pressure gauge as shown in Fig. 18.1(a).

Stagnation pressure is the pressure measured by an open-ended tube facing the flow direction as shown in **Fig.18.1(b)**. Such a device is called a Pitot tube. The process of bringing the flow to rest is assumed to be isentropic (i.e. without frictional loss) so that the Bernoulli equation may be used to calculate the indicated pressure. Referring to **Fig.18.1(b)** we have

$$\frac{p_1}{\rho} + \frac{V_1^2}{2} = \frac{p_2}{\rho} + \frac{V_2^2}{2} \tag{18.3}$$

where p_1 is the static pressure of the fluid (p) and V_1 the fluid velocity upstream (V). $V_2 = 0$ (stagnation) and p_2 is the recorded (stagnation) pressure (p_o). Thus

$$p_o = p + \frac{1}{2}\rho V^2$$

When a Pitot tube is used in subsonic compressible gas flow the stagnation pressure equation (15.47) must be used, thus

$$p_o = p\left(1 + \frac{k-1}{2} M^2\right)^{k/(k-1)} \tag{18.4}$$

where $k = C_p/C_v$ and M the Mach number.

When a Pitot tube is used in supersonic compressible flow a normal shock will form directly in front of the opening, as shown in Fig. 18.2 To obtain the stagnation pressure the equations derived in Section 15.9 can be used by noting that the Pitot tube will indicate the stagnation pressure behind the shock.

18.4 MEASUREMENT OF VELOCITY

Local-velocity measurements can be made with one of the following methods:

1. Rotating mechanical devices
2. Buoyant particle trajectories
3. Pitot tube or Pitot-static probe
4. Hot wire and hot film anemometer
5. Laser-Doppler anemometer

Rotating mechanical devices: Several types of rotating devices are used for velocity measurements in gases or liquids. Two popular designs are shown in Fig. 18.3. These can be attached to counters and the frequency of rotation can be directly related to the velocity of flow by appropriate calibration. Their main disadvantage is that they are relatively large and thus they give a velocity averaged over a relatively large area rather than the velocity at a "point".

Buoyant particles: In transparent fluids small particles, powders or bubbles may be introduced and their trajectories may be followed. By suitable illumination techniques pictures of the particles may be taken. If successive exposures are taken on the same film, the velocities and the accelerations of the particles can be determined. One must establish however, whether the particles really move at the same local velocity as the fluid. To insure that, the size, shape and density of the particles must be carefully chosen (see also Section 18.6. Flow Visualization).

Pitot tube: A bent, transparent, stagnation tube can be used for measuring velocity in open channel flows as shown in Fig.18.4. We note that V_1 is the stream velocity to be determined while at point 2 the flow is stopped by the tube completely (V_2=0). Writing the Bernoulli equation between points 1 and 2 we have

$$\frac{p_2}{\rho} + \frac{V_2}{2} = \frac{p_1}{\rho} + \frac{V_1^2}{2} \tag{18.5}$$

Thus $$V_1 = \left[\frac{2(p_2 - p_1)}{\rho}\right]^{1/2} \tag{18.6}$$

where $$p_1 = p_{atm} + \rho g h$$

$$p_2 = p_{atm} + \rho g(h+H)$$

$$p_1 - p_2 = \rho g H$$

and $$V_1 = (2gH)^{1/2} \tag{18.7}$$

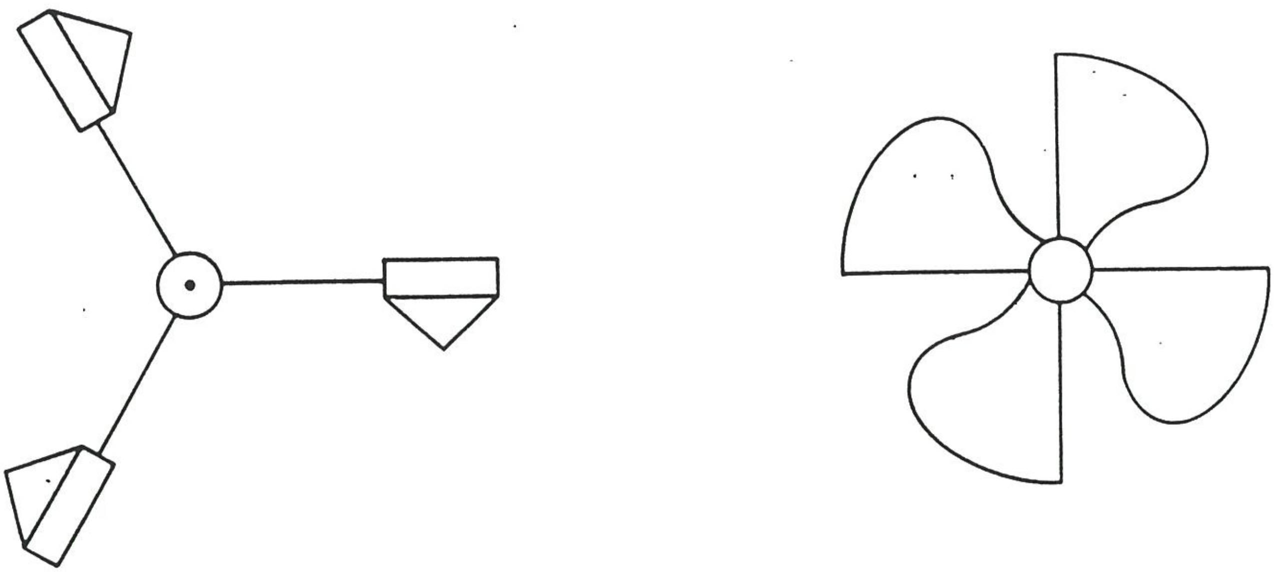

Fig. 18.3 (a) Three-cup anemometer.
(b) Propeller meter.

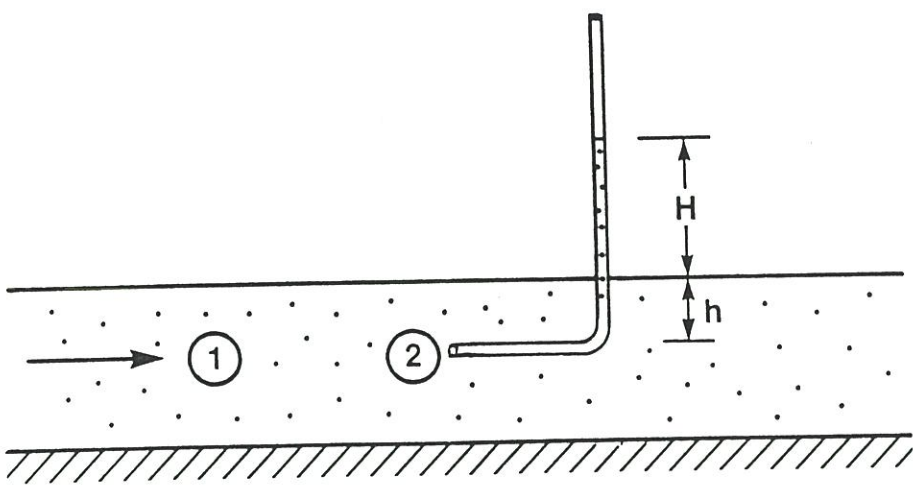

Fig. 18.4 Pitot tube in an open channel.

The Pitot tube is used for measuring the velocity of open channel flows and for determining the velocity of boats.

Pitot-Static Probe

As explained in Section 18.3 a pressure tap that causes no disturbance in the flow field measures the static pressure. The Pitot tube measures the stagnation pressure which is equal to the static pressure plus the velocity term $1/2\ \rho V^2$. The static and Pitot tube are often combined into the one-piece Pitot-static probe as shown in Fig. 18.5. The stagnation pressure is

$$p_o = p + \frac{1}{2}\rho\ V^2 \tag{18.8}$$

Thus

$$V = \left[\frac{2(p_o - p)}{\rho}\right]^{1/2} \tag{18.9}$$

The pressure difference can be recorded by a differential manometer or any other pressure measuring instrument. The Pitot-static probe is a standard device for determining velocity profiles in conduits and for measuring the speed of airplanes. A major problem in the use of an ordinary Pitot-static tube is to obtain proper alignment of the tube with the flow direction. It should also be noted that the response is slow when liquid manometers are used for unsteady flow measurements.

Hot-wire and hot-film anemometer

The hot-wire anemometer measures the instantaneous velocity at a point. This instrument consists basically of a very fine electrically heated wire (diameter 0.01 mm or less) stretched across the ends of two prongs as shown in Fig. 18.6. The principle of operation is based on the fact that the electrical resistance of the wire depends on its temperature. The temperature, in turn, depends on the heat transfer rate and the heat transfer rate depends on the local velocity. The electric power supplied to the wire can be expressed according to L.V. King's relation [8-10]

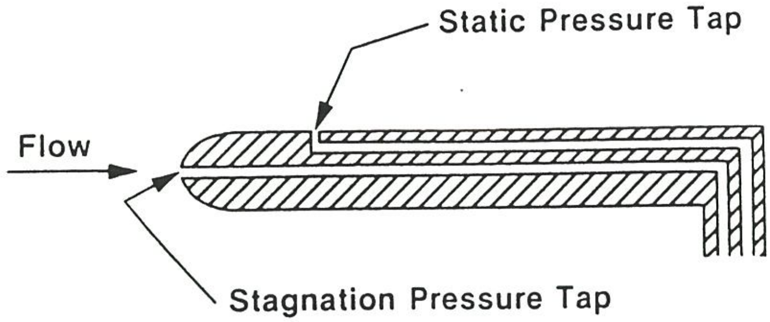

Fig. 18.5 Pitot-static probe.

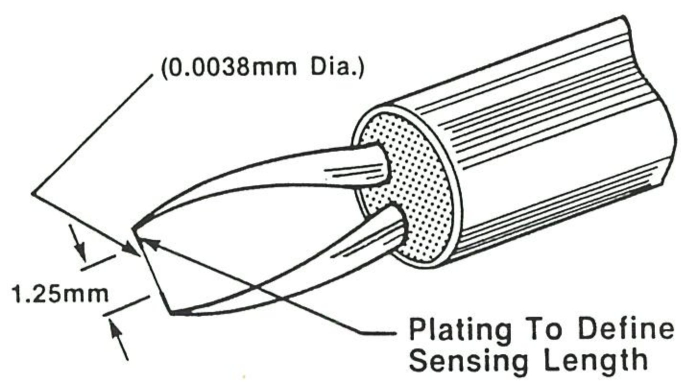

Fig. 18.6 A typical hot-wire anemometer.

$$I^2R \simeq a + b(\rho V)^n \tag{18.10}$$

The wire can be calibrated to find the best fit for a, b and n. It can be operated either at constant I, so that the resistance R is a measure of V, or at constant resistance R, with I being a measure of velocity V.

Hot-wires are not suited for liquid flows because of breakage problems. A more robust yet sensitive device for liquid flow measurements is the hot-film anemometer. This anemometer consists of a thin metallic film, usually platinum, mounted onto a relatively thick support in the shape of a wedge, a cone, or a cylinder. The hot-film operates in the same way as the hot-wire.

The hot-wire or hot-film anemometer is very useful for turbulence measurements because it can respond to very rapid changes in flow velocity. Two or more wires at one point can make simultaneous measurements of the fluctuating components.

Laser-Doppler Anemometer

Laser-Doppler anemometry is a powerful experimental technique that uses light scattering and the Doppler phenomenon to measure velocity components [11]. A laser beam provides a highly coherent, highly focused, monochromatic light which is scattered from moving particles in the flow. Because of the particle motion a stationary observer would observe a change in frequency, known as Doppler shift, of the scattered light. This shift is proportional to the velocity of the particles and can be measured by suitable electronic circuitry. For the dual-beam arrangement shown in Fig. 18.7, the particle velocity is given by

$$V = \frac{\lambda \Delta f}{2 \sin \left(\frac{\theta}{2}\right)} \tag{18.11}$$

where Δf is the frequency shift and λ is the wavelength of the laser light.

For operation of the laser-Doppler anemometer the presence of small particles in the flow is required. For liquid flows impurities serve as scattering centers. Gas flows make required "seeding" e.g. smoke. The measuring volume is very small and the particles even smaller so that detailed measurements of complex flows can be made. These include

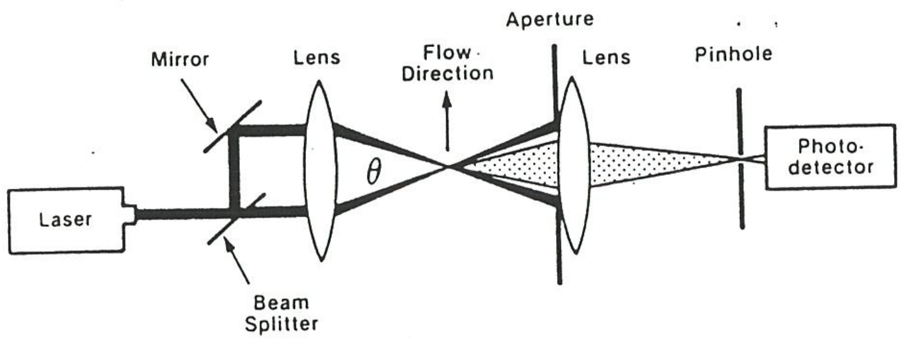

Fig. 18.7 Dual-beam laser-Doppler anemometer.

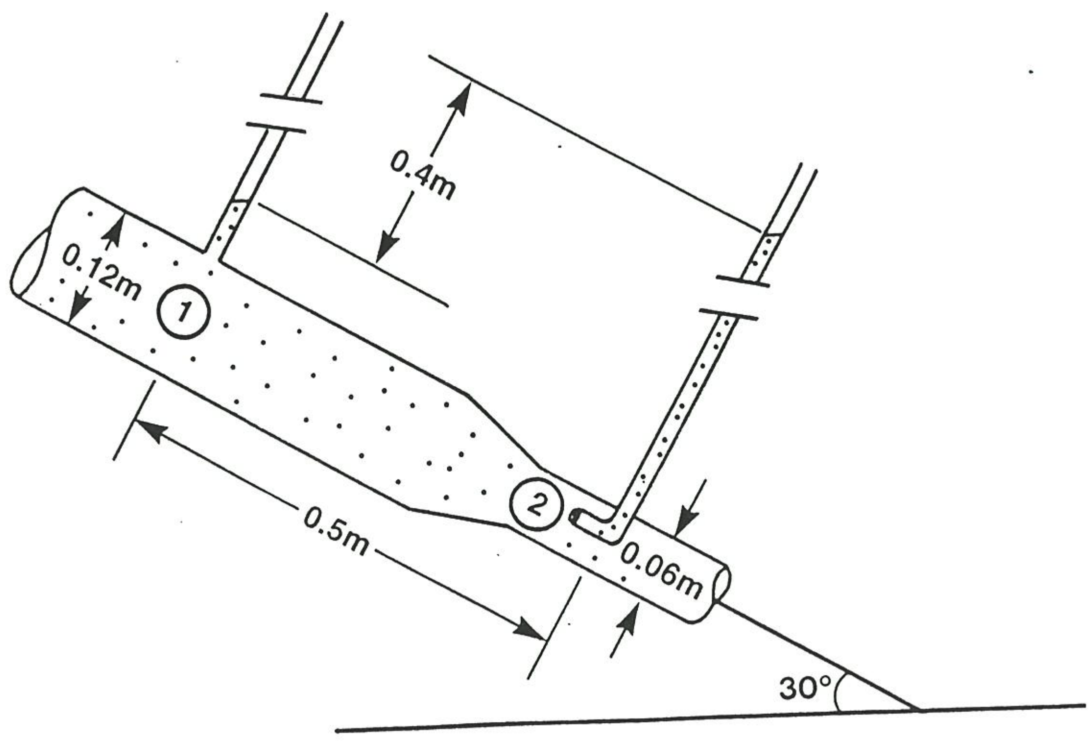

Fig. E.18.1.

turbulent boundary layers, supersonic flows, burner flames, rocket exhausts and in-vivo measurements of blood flow. Wang [12] reports that velocity measurements in blood vessels as small as 5-μm diameter can be made with a suitable arrangement.

The advantages of the laser-Doppler method are (1) no disturbance to the flow field, (2) wide velocity range from 10^{-4} to 10^{3} m/s, (3) no need for calibration, (4) high spatial resolution because the wavelength of the light is very short and can easily be focused to a very small spot, and (5) independence from density and temperature fluctuations. The disadvantages are (1) usually low signal-to-noise ratio, because scattering light intensity is very weak, (2) the need for seed particles, and (3) high cost for the optical system and the electronic circuitry.

Example 18.1

Water is flowing through the pipe shown in Fig.E.18.1. Determine the volume rate of flow.

Solution

We apply the Bernoulli equation between points 1 and 2 as shown. Point 2 is at the stagnation tube opening where $V_2 = 0$. We have

$$\frac{V_1^2}{2} + \frac{p_1}{\rho} + gz_1 = \frac{p_2}{\rho}$$

$$z_1 = 0.5 \sin 30^{\circ} = 0.25$$

$$p_1 = \rho g h_1 \cos 30^{\circ}$$

$$p_2 = \rho g h_2 \cos 30^{\circ}$$

$$p_2 - p_1 = \rho g(h_2 - h_1)\cos 30^{\circ} = 1000 \times 9.81 \times 0.8 \times 0.866$$
$$= 6797 \text{ Pa}$$

$$\frac{V_1^2}{2} = \frac{p_2 - p_1}{\rho} - gz_1$$

$$V_1 = \left[2\left(\frac{p_2 - p_1}{\rho} - gz_1\right)\right]^{1/2} = \left[2(6.796 - 2.452)\right]^{1/2} = 2.947 \text{ m/s}$$

The water volume rate of flow through the pipe is

$$Q = \frac{\pi D^2}{4} V_1 = \frac{\pi (0.12)^2}{4} 2.947 = 0.0333 \ m^3/s$$

18.5 MEASUREMENT OF FLOW RATE

Measurement of volume or mass flow rate is very important in many engineering applications. There are many mechanical devices that make such measurements by trapping a quantity of fluid and counting it. These include weighing tanks, volume tanks, reciprocating pistons and gear impellers, to name just a few. There are some special measuring devices such as electromagnetic, ultrasonic, and vortex flow meters. Among commonplace instruments is the turbine flow meter, which consists of a wheel with a set of curved vanes (blades) and is used for monitoring the flow rate in fuel-supply systems by measuring electromagnetically its rotational speed. Here, we focus our attention to <u>indirect</u> measurements of flow rate using devices that obstruct the flow field [13-15]. These are:

1. Venturi meter
2. Orifice meter
3. Rotameter
4. Weir

<u>Venturi Meter</u>: This device consists of a conical contraction, a short cylindrical throat and a conical expansion as shown schematically in Fig. 18.8. A differential manometer measures the static pressure difference between points 1 and 2 as shown. Applying the Bernoulli equation, we have

$$\frac{p_2}{\rho} + \frac{V_2^2}{2} = \frac{p_1}{\rho} + \frac{V_1^2}{2} \tag{18.12}$$

From continuity

$$\rho_1 A_1 V_1 = \rho_2 A_2 V_2 \tag{18.13}$$

or $$V_1 = V_2 \frac{A_2}{A_1}$$

Equation (18.12) is rewritten as

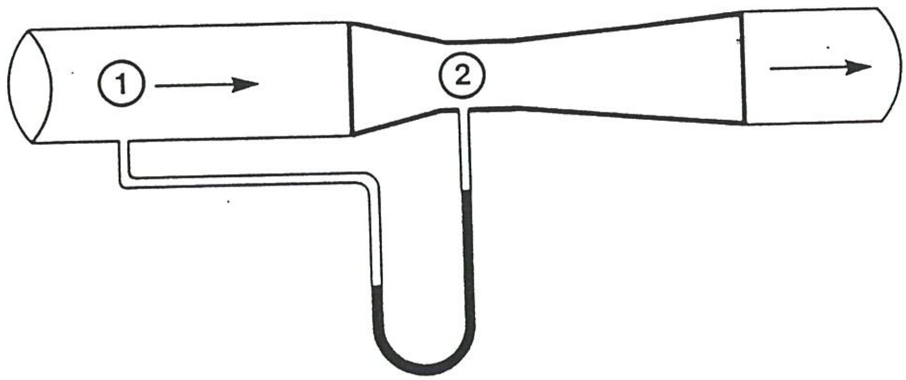

Fig. 18.8 Venturi meter.

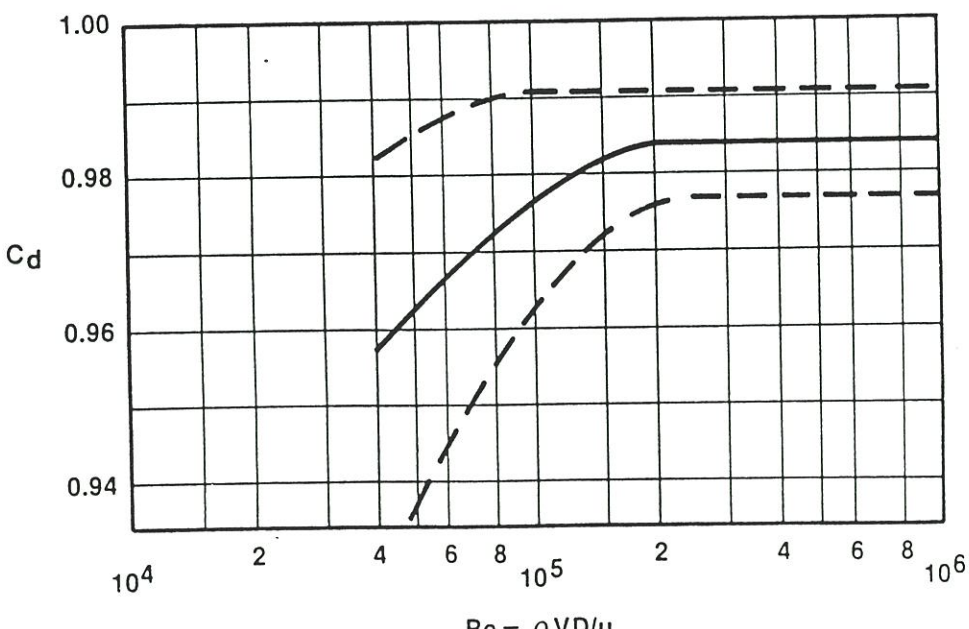

Fig. 18.9 Discharge coefficient for Venturi meters as function of pipe Reynolds number. The scatter of experimental data is indicated by dashed lines (adapted from reference [12]).

$$V_2^2 - V_1^2 = \frac{2(p_1 - p_2)}{\rho}$$

$$V_2^2 - V_1^2 \frac{A_2^2}{A_1^2} = \frac{2(p_1 - p_2)}{\rho}$$

and
$$V_2 = \left[\frac{2(p_1 - p_2)}{\rho\left(1 - \frac{A_2^2}{A_1^2}\right)}\right]^{1/2} = \left[\frac{2(p_1 - p_2)}{\rho\left(1 - \frac{D_2^4}{D_1^4}\right)}\right]^{1/2} \tag{18.14}$$

where $A_1 = \pi D_1^2/4$ and $A_2 = \pi D_2^2/4$

This is the velocity at the "throat" which is assumed to be uniform. This result has been obtained by assuming that frictional effects are negligible. In practice frictional effects can be accounted for by introducing an empirical coefficient C_d (usually known as discharge coefficient).

$$V_2 = C_d \left[\frac{2(p_1 - p_2)}{\rho\left(1 - \frac{D_2^4}{D_1^4}\right)}\right]^{1/2} \tag{18.15}$$

Large numbers of experiments have shown that C_d is a function of the pipe Reynolds number as shown in Fig. 18.9. The venturi tube is a reliable flow rate measuring device that causes little pressure drop. It is widely used particularly for large liquid and gas flows in the Reynolds number range from about 10^5 to $2x10^6$.

<u>Orifice meter</u>: This device consists of a thin flat plate with a circular hole drilled in the center of it. A differential manometer measures the static pressure difference upstream and downstream from the plate as shown in Fig. 18.10. As the fluid flows from left to right a jet forms at the orifice that constricts the flow field even more than the orifice (vena contracta). The Bernoulli equation can be applied in exactly the same manner as in the derivation of the venturi meter equation. The appropriate flow area to consider will be the minimum

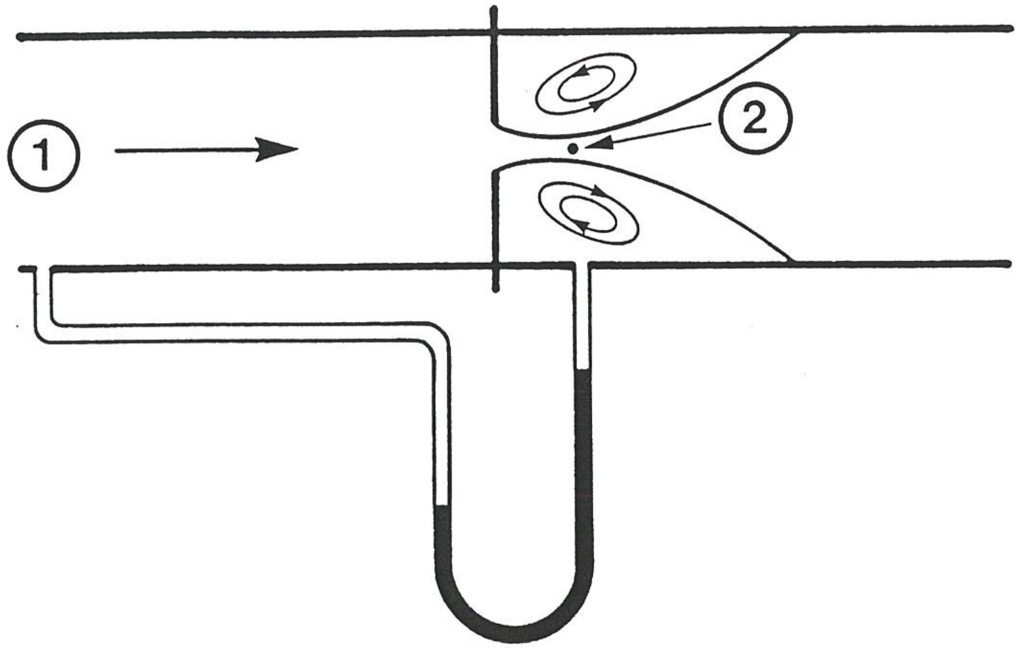

Fig. 18.10 Orifice meter.

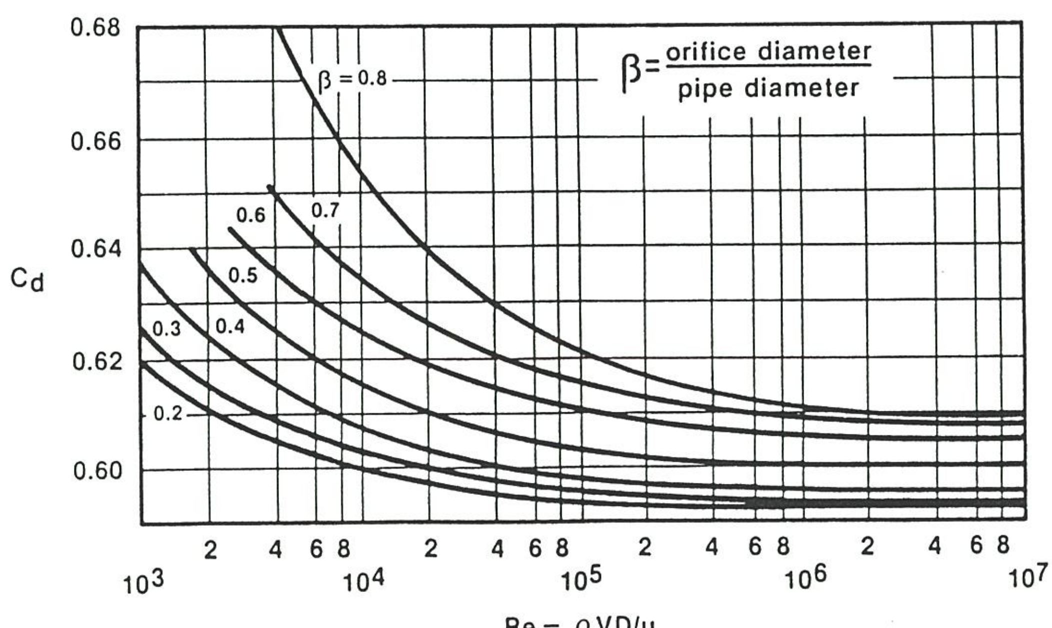

Fig. 18.11 Discharge coefficients for orifice meters as function of pipe Reynolds number (adapted from reference [12]).

flow area of the jet. This is, of course, difficult to measure. Thus we will simply use the orifice area and incorporate all non-idealities (due to vena contracta and friction) into the orifice meter discharge coefficient C_d. We have

$$V_2 = C_d \left[\frac{2(p_1 - p_2)}{\rho\left(1 - \frac{D_2^4}{D_1^4}\right)}\right]^{1/2} \tag{18.16}$$

Discharge coefficients for drilled-plate orifices are given in Fig. 18.11. Orifice meters are less expensive and easier to install than venturi meters, but they cause much larger pressure drops.

Rotameter: This is a simple and very useful device for measuring the flow rate of gases and liquids. It consists of a vertical tapered tube (see Fig. 18.12), through which the fluid flows and causes the "float" to move upward. The "float" rises to the point where the drag forces are just balanced by the weight and buoyancy forces. The tube is graduated and the flow rate can be deduced from an experimentally obtained calibration curve.

Weir: It is a simple device used for measuring the flow rate in open channels. It consists of a vertical plate with an opening that is inserted in the channel to obstruct the flow. The opening is usually rectangular or V-shaped.

Application of the Bernoulli equation between a point upstream of the weir and a point in the plain of the weir (see Fig. 18.13) yields

$$\frac{p_1}{\rho} + \frac{V_1^2}{2} + H = \frac{p_2}{\rho} + \frac{V_2^2}{2} + z \tag{18.17}$$

The pressures are both equal to atmospheric and the upstream velocity is negligible compared to V_2. Hence

$$V_2 = \sqrt{2g(H-z)} = \sqrt{2gh} \tag{18.18}$$

The volume rate of flow through a stream layer dh is

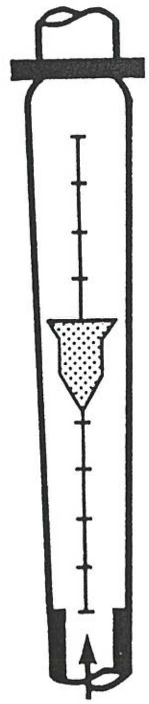

Fig. 18.12 Rotameter.

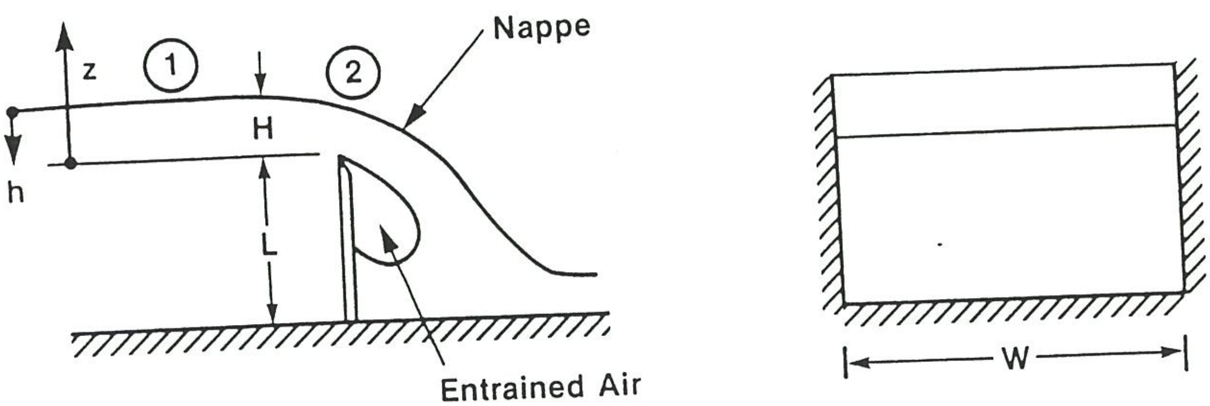

Fig. 18.13 Rectangular weir.

$$dQ = VWdh = \sqrt{2gh}\, W\, dh \tag{18.19}$$

Integrating from h=0 to h=H, we obtain

$$Q = \sqrt{2g}\, W \int_0^H \sqrt{h}\, dh = \frac{2}{3} W \sqrt{2g}\, H^{3/2} \tag{18.20}$$

We have neglected the frictional losses and the fact that the nappe will actually contract somewhat. These can be accounted for by introducing an experimentally determined discharge coefficient C_d, so that

$$Q = C_d \frac{2}{3} L \sqrt{2g}\, H^{3/2} \tag{18.21}$$

Experiments show that C_d varies according to the relation

$$C_d = 0.605 + \frac{0.08H}{L} \tag{18.22}$$

where L is the height of the weir.

Example 18.2

An orifice meter like that shown in Fig. 18.10 is used to monitor the water flow rate in a 10 cm diameter pipe. Determine the flow if the orifice has a diameter at 2 cm and the manometer shows a 30 cm difference in mercury.

Solution

We first use equation (18.16) assuming no frictional losses, i.e. $C_d = 1.0$. We have

$$V_2 = \left[\frac{2(p_2 - p_1)}{\rho\left(1 - \frac{D_2^4}{D_1^4}\right)}\right]^{1/2}$$

where $p_2 - p_1 = \rho_m gh - \rho gh = gh(\rho_m - \rho) = 9.81 \times 0.30\ (13600 - 1000)$

$= 37081.8$ Pa

Therefore

$$V_2 = \left[\frac{2 \times 37081.8}{1000\left(1 - \frac{0.02^4}{0.10^2}\right)} \right]^{1/2} = 8.61 \text{ m/s}$$

The water velocity in the pipe is

$$V_1 = V_2 \frac{D_2^2}{D_1^2} = 0.345 \text{ m/s}$$

and the pipe Reynolds number

$$Re = \frac{\rho V_1 D_1}{\mu} = \frac{1000 \times 0.345 \times 0.10}{0.001} = 34500$$

From Fig. 18.11 we have approximately $C_d \simeq 0.595$ (for $\beta = 0.2$).

We can now recalculate V_2 using equation (18.16) to get

$$V_2 = C_d \times 8.61 = 0.595 \times 8.61 = 5.123 \text{ m/s}$$

The new pipe Reynolds is simply

$$Re = 0.595 \times 34500 = 20527$$

Again from Fig. 18.11 we get approximately

$$C_d = 0.597$$

and recalculate

$$V_2 = 0.597 \times 8.61 = 5.140 \text{ m/s}$$

$$Re = 0.597 \times 34500 = 20596$$

For such a small change in the Reynolds number the discharge coefficient remains the same. Thus the flow rate is

$$Q = V_2 \frac{\pi D^2}{4} = 5.140 \times \frac{\pi 0.02^2}{4}$$

$$= 0.00161 \text{ m}^3/\text{s} = 5.796 \text{ m}^3/\text{h}$$

18.6 FLOW VISUALIZATION

Liquid or gas flows can be made visible by adding particles of foreign substances, such as dyes, powders, smoke, or gas bubbles. The techniques of observing and recording the motion of particles have been highly refined in recent years. Exact time-controlled photographic exposures are usually made that provide a wealth of information on the flow field. When making flows visible by this method it is important to examine whether the particles of the foreign substance move in exactly the same way as the surrounding fluid. Particles are subjected to drag and lift forces (as shown in the self-explanatory boundary layer example of Fig. 18.14 and may follow paths of their own. Also, in highly turbulent flow fields foreign particles cannot always follow the rapid fluid fluctuations.

Variable density flows can be visualized by optical techniques because the refractive index of fluids is a function of their density. The free-convection boundary layer forming on a horizontal electric hot plate can be seen with the naked eye and usual room lighting because of density gradients in the heated air. Photographs can be taken when light goes through the transparent walls of a transparent flow field and the regions of sharp density differences (such as shock waves) can be determined (shadowgraph method). The method depends on ray deflection which can be shown to be equal to the second derivative of density $\partial^2\rho/\partial y^2$. Fig. 18.15 is an example of the quality of pictures that can be taken with this method.

In the schlieren method a knife-edge is used to cut off part of the light after it is brought to focus by a lens. The contrast on a receiving screen can be shown to be directly proportional to the density

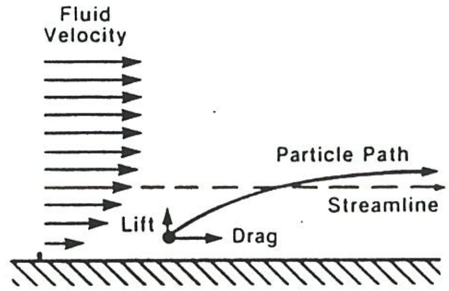

Fig. 18.14 Lift and drag forces on a small particle in a boundary layer.

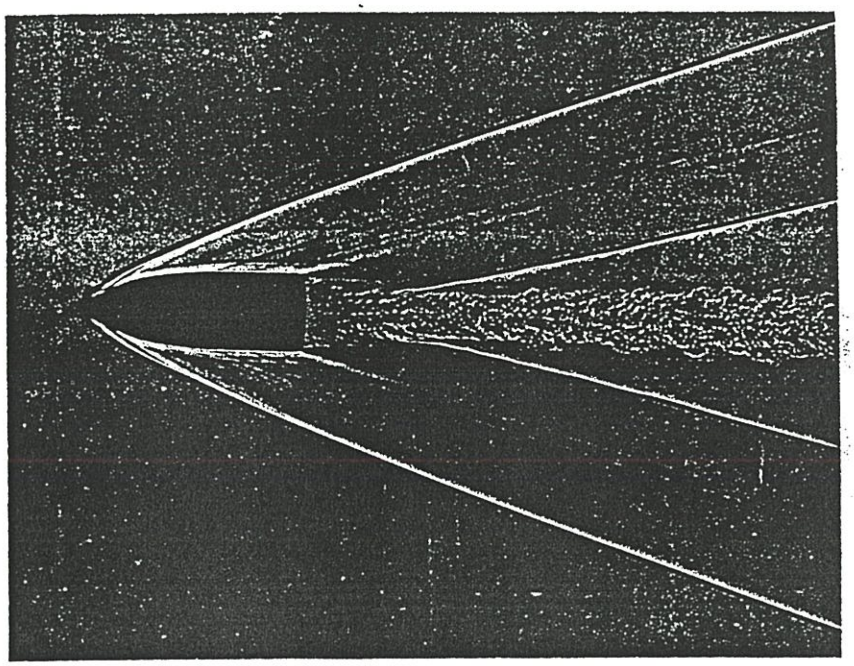

Fig.18.15 Shadowgraph of a 0.22-caliber bullet travelling at 1250 m/s. The thickness of the shock wave appears much larger than it actually is (courtesy ARO, Inc. Arnold Air Force Base, Tenn.).

gradient ($\partial\rho/\partial y$). A more precise instrument is the Mach-Zehnder interferometer, in which two light beams that follow different optical paths are joined together to produce light and dark regions called fringes. This instrument gives a direct quantitative indication of density changes in the test section. It is applicable to a wide range of flow conditions ranging from low-speed flow in free-convection boundary layers to shock-wave phenomena in supersonic flow.

Detailed discussions on the above visualization techniques are given in references [1,2,6,16-18]. A beautiful collection of photographs have been assembled by Van Dyke [19].

REFERENCES

1. J.P. Holman, "Experimental Methods for Engineers", McGraw-Hill, Second Edition, New York (1971).

2. T.G. Beckwith and N. Lewis Buck, "Mechanical Measurements", Addison-Wesley Publishing Company, Reading, Mass. (1969).

3. P. Bradshaw, "Experimental Fluid Mechanics", Pergamon Press, Oxford (1970).

4. E. Ower and R.C. Pankhurst, "The Measurement of Air Flow", Fifth Edition, Pergamon Press, Oxford (1977).

5. R.P. Benedict, "Fundamentals of Temperature, Pressure and Flow Measurement", Wiley, New York (1969).

6. R.J. Emrich (Ed.), "Fluid Dynamics", Vol. 18 of "Methods of Experimental Physics", Edited by L. Marton and C. Marton, Academic Press (1981).

7. J.M. Dealy, "Rheometers for Molten Plastics", Van Nostrand Reinhold, New York (1982).

8. L.V. King, "On the Convection of Heat from Small Cylinders in a Stream of Fluid with Applications to Hot-wire Anemometry", Phil. Trans. Roy. Soc., London, 14, 373 (1914).

9. P. Freymuth, "History of Thermal Anemometry", Chapter 4 in N.P. Cheremisinoff and R. Gupta (Eds.), "Handbook of Fluids in Motion", Ann Arbor Science Publishers, Ann Arbor, Michigan (1983).

10. A.E. Perry, "Hot-wire Anemometry", Clarendon Press, Oxford (1982).

11. F. Durst, A. Melling and J.H. Whitelaw, "Principles and Practice of Laser-Doppler-Anemometry", Academic Press, New York (1976).

12. C.P. Wang, "Laser Anemometry", Amer. Sci., 65, 289 (1977).

13. "Fluid Meters: Their Theory and Application", Sixth Edition, American Society of Mechanical Engineers, New York (1971).

14. "Measurement of Fluid Flow by Means of Orifice Plates, Nozzles, and Venturi Tubes Inserted in Circular Cross Section Conduits Running Full", Int. Organ. Stand. Rep., DIS-516, Geneva, April 1976.

15. N.P. Cheremisinoff, "Applied Fluid Flow Measurement: Fundamentals and Technology", Marcel Dekker, New York (1979).

16. W. Merzkirch, "Flow Visualization", Academic Press, New York (1974).

17. W. Merzkirch (Ed.), "Flow Visualization II", Hemisphere Publishing, Washington (1982).

18. W. Merzkirch, "Making Flows Visible", Amer. Sci., 67, 330 (1979).

19. M. Van Dyke, "An Album of Fluid Motion", The Parabolic Press, Stanford, California (1982).

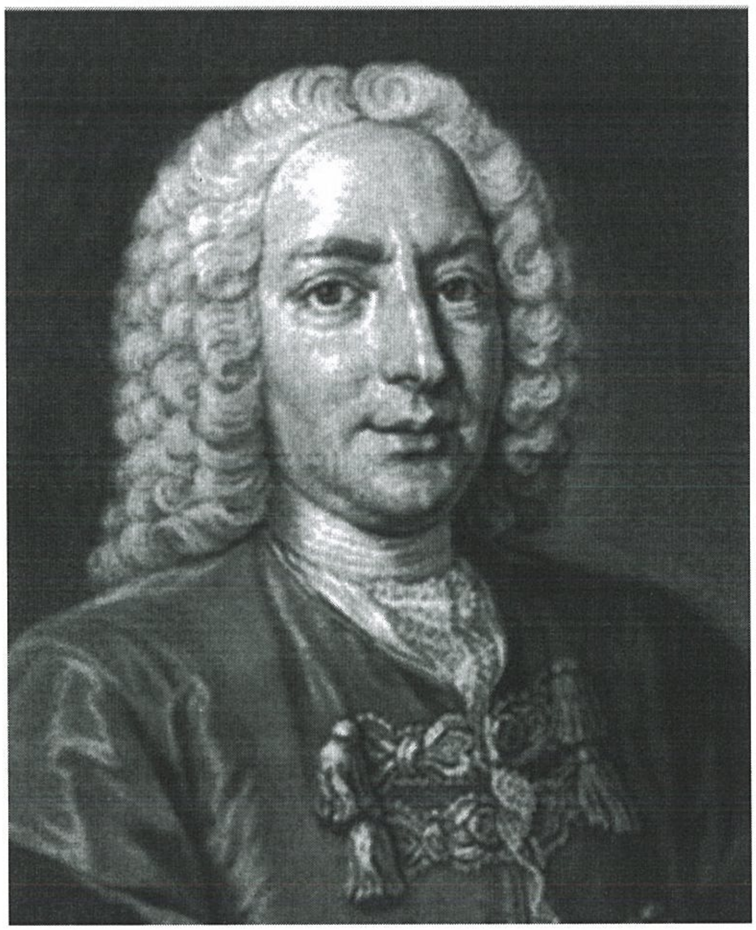

DANIEL BERNOULLI (1700-1782)

John Vlachopoulos, *Fundamentals of Fluid Mechanics*
Chem. Eng., McMaster University, Hamilton, ON, Canada
(First Edition 1984, revised internet edition (2016), www.polydynamics.com)

CHAPTER 19

PUMPS AND TURBINES

19.1 INTRODUCTION

Fluid machines are devices which either give energy to fluids or extract energy from them. If a machine gives energy to a fluid it is generally called a pump. If the fluid being pumped is a gas, the device is usually called a fan (for very low pressure rise), a blower (for intermediate pressure rise), or a compressor (for high pressure rise). If a machine extracts energy from a liquid or gas and transmits this energy by a rotating shaft, it is called a turbine (from the Latin turbo, which means spin or whirl). If the initial mechanical movement is a reciprocating one the term engine (e.g. steam engine) is used.

Pumps may be classified as positive-displacement pumps, rotodynamic pumps or special design pumps. Turbines may be classified as reaction turbines or impulse turbines.

In this chapter we give a very brief and superficial introduction into the principles of operation of pumps and turbines, using highly simplified analyses. For further information the reader is referred to specialized texts on turbomachinery in general [1-8], on pumps [9-14] and on turbines [15-22].

19.2 POSITIVE-DISPLACEMENT PUMPS

Positive-displacement (PD) pumps work by using the movement of a solid boundary to trap a certain quantity of fluid in a cavity and then to force it out. The schematic diagrams of the reciprocating pump in Fig. 19.1 (a) and the gear pump in Fig.19.2 (b) show the principle of operation of these two common types. Positive-displacement pumps are extremely common and important. Examples include the fuel and oil pumps of automobiles and the hearts of animals.

These pumps, when they operate at fixed motor speed, are practically constant volume flow rate devices and can generate very large pressures. If the outlet is blocked while pumping an incompressible fluid the pressure will rise vertically (as shown in Fig. 19.2 if there are no leaks, until something breaks. Well designed pumps are usually equipped with a safety pin to prevent serious damage. Pulsations in the flow are present both in the inlet and outlet of PD pumps. These devices are most suitable for low flow rates and particularly for high pressures. For greater flow rates and low pressures rotodynamic pumps are usually more satisfactory.

Example 19.1

A PD pump having a flow rate capacity of 0.2 m^3/min is placed above an open water tank as shown in **Fig.E.19.1** and the motor is started. Determine the maximum possible height h if the suction pipe has a diameter of 4 cm.

Solution

A PD pump can generally operate like a vacuum pump. When the pump is started with the inlet tube filled with air a vacuum will be created and the water will rise. Applying the Bernoulli equation without frictional losses we have

$$\frac{V_1^2}{2g} + \frac{p_1}{\rho g} + z_1 = \frac{V_2^2}{\rho g} + \frac{p_2}{\rho g} + z_2$$

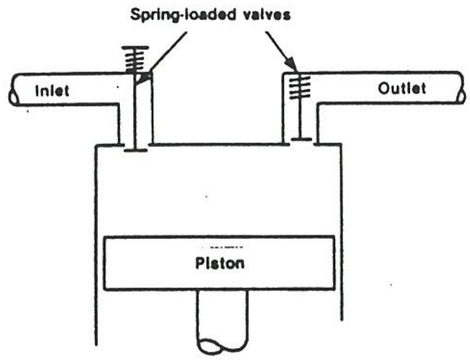

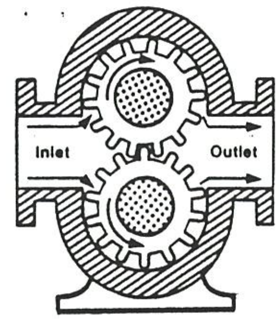

Fig. 19.1 (a) Reciprocating pump, (b) Gear pump.

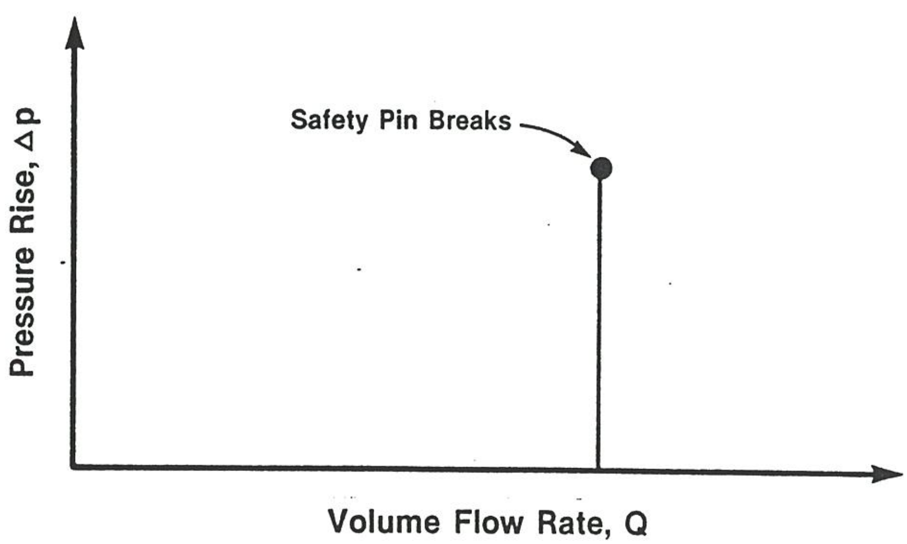

Fig. 19.2 Pressure rise in a positive displacement pump with obstructed outlet.

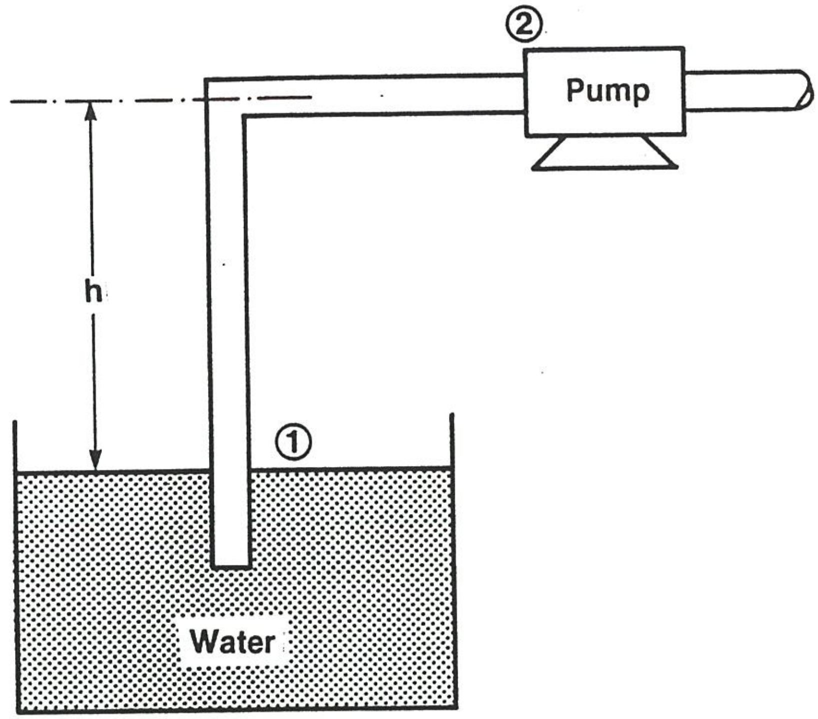

Fig.E.24.1 Suction experiment.

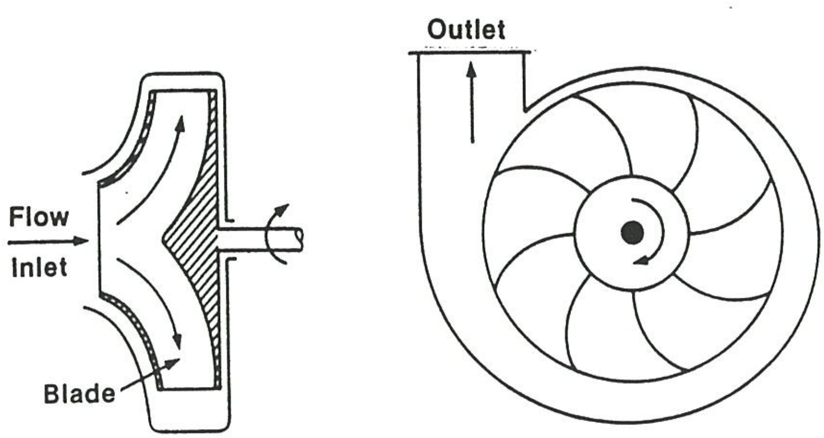

Fig. 19.3 Centrifugal pump.

or

$$h = z_2 - z_1 = \frac{p_1 - p_2}{\rho} + \frac{V_1^2 - V_2^2}{2g}$$

V_1 will be approximately equal to zero. Thus

$$h = \frac{p_1 - p_2}{\rho g} - \frac{V_2^2}{2g}$$

$p_1 = p_{atm} = 101.33$ kPa

p_2 should not be less that the vapor pressure of water (at 20^{o}C p_v = 2.34 kPa) because the water will boil.

V_2 can be calculated from the volume rate of flow

$$V_2 = \frac{Q}{\frac{\pi D^2}{4}} = \frac{0.2}{60\ \frac{\pi(0.04)^2}{4}} = 2.65 \text{ m/s}$$

Thus we have

$$h = \frac{101330 - 2340}{1000 \times 9.81} - \frac{2.65^2}{2 \times 9.51}$$

$$= 10.09 - 0.36 = 9.73 \text{ m}$$

This height is usually known as suction lift. Actually the suction lift will be smaller than that, because of frictional losses in the suction pipe, the valve and the pump itself.

19.3 CENTRIFUGAL PUMPS

Pumps that increase the momentum and pressure by means of rotating blades or vanes are called rotodynamic pumps. These are further subdivided into centrifugal (or radial flow) pumps and axial flow pumps.

In the centrifugal pump shown in Fig.19.3 the fluid enters axially through the "eye" of the casing, is forced outward by the rotating blades of the impeller, and is discharged at its periphery into the diffuser.

For a highly simplified analysis we may neglect friction losses and assume that the flow is uniform at any cross-section. Applying the Bernoulli equation (14.34) between points (1) and (2) of Fig.19.3, we have, the pump head

$$h_p = \left(\frac{V_2^2}{2g} + \frac{p_2}{\rho g} + z_2\right) - \left(\frac{V_1^2}{2g} + \frac{p_1}{\rho g} + z_1\right) \tag{19.1}$$

Usually the velocities V_1 and V_2 are about equal and the elevation $z_2 - z_1$ is small. Thus, we may write

$$h_p = \frac{p_2 - p_1}{2g} = \frac{\Delta p}{\rho g} \tag{19.2}$$

The hydraulic pump power is given by equation (14.41) as

$$P_H = h_p \rho g Q \tag{19.3}$$

The pump efficiency was defined by equation (14.42) as

$$\eta = \frac{P_H \text{ (hydraulic)}}{P_B \text{ (supplied by the motor driving the pump}} \tag{19.4}$$

The power supplied by the motor driving the pump P_B, i.e. the shaft input power, is usually called the brake power.

For the determination of the hydraulic power, we assume that the fluid enters the impeller at $r = R_1$ and exits at $r = R_2$ with a velocity component W tangent to the blade and tangential speed U, equal to the tangential impeller speed as shown in Fig. 19.4.

To determine the applied torque we use Euler's turbine equation (6.118) which is here written as

$$T_o = \rho Q(R_2 V_{t2} - R_1 V_{t1}) \tag{19.5}$$

where V_{t1} and V_{t2} are the (average) tangential velocities of the fluid

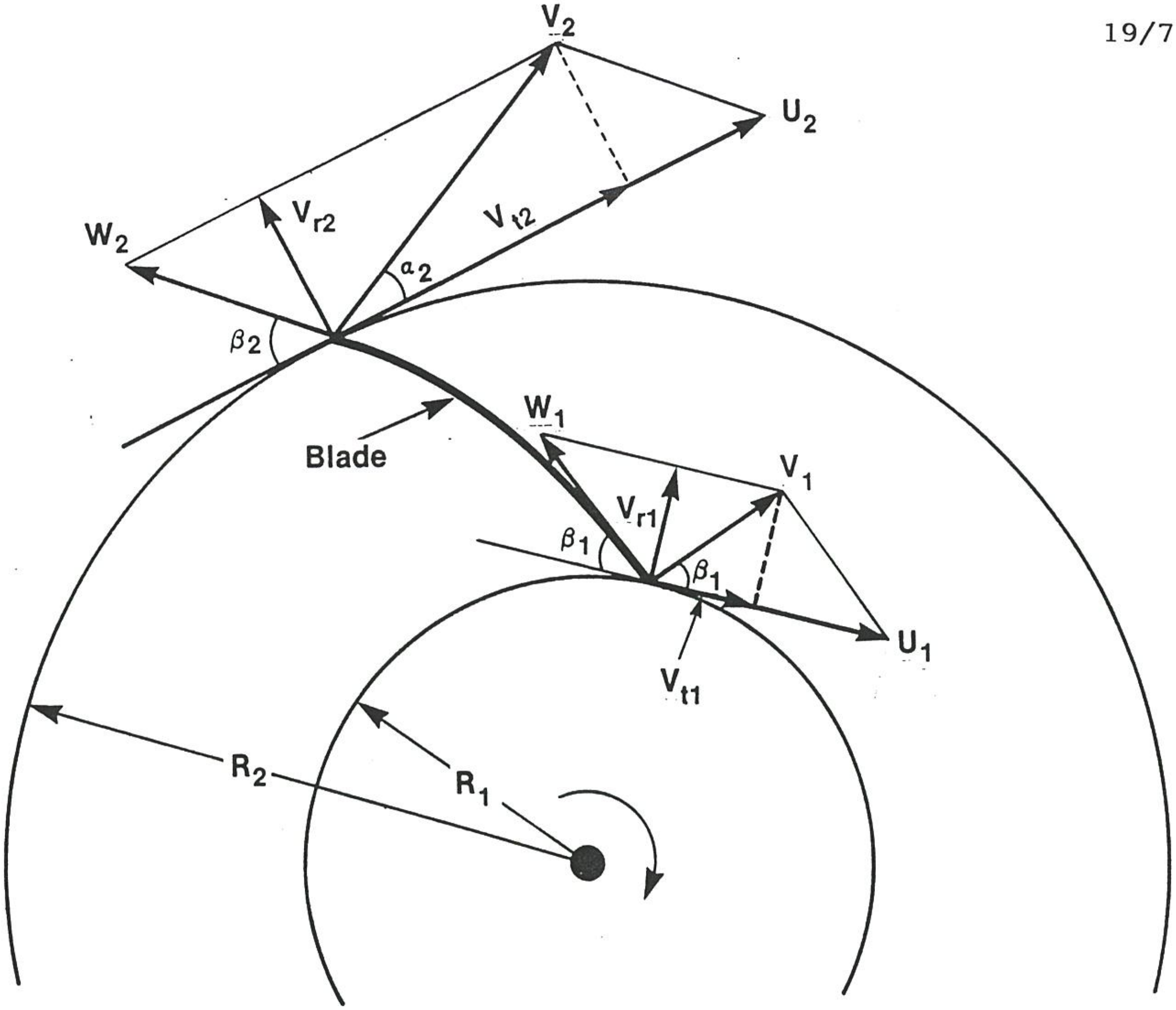

Fig. 19.4 Inlet and outlet velocity diagram for a centrifugal pump.

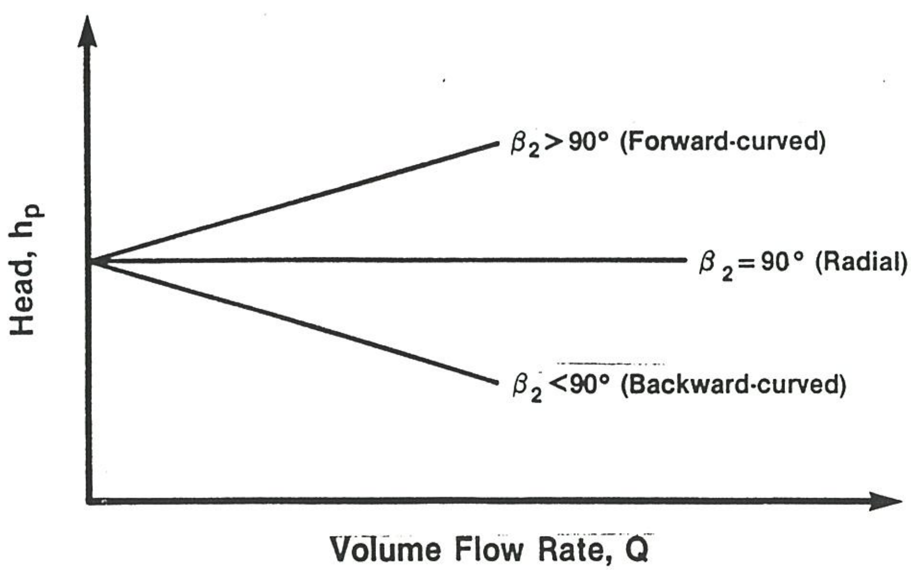

Fig. 19.5 Effect of outlet blade angle on pump head according to equation (19.13).

at inlet and outlet respectively. When we applied this equation in Example 6.6 we assumed that the tangential velocities of the fluid as it enters and leaves the pump are equal to the tangential velocities of the impeller at the corresponding radii. Here, however, for a more accurate analysis we will take into account the actual shape of the blades, by referring to Fig. 19.4, to calculate V_{t1} and V_{t2}. We have

$$V_{t1} = V_1 \cos \alpha_1 = V_{r1} \cot \alpha_1 \tag{19.6}$$

$$V_{t2} = V_2 \cos \alpha_2 = V_{r2} \cot \alpha_2$$

Consequently the applied torque is

$$T_o = \rho Q(R_2 V_{r2} \cot\alpha_2 - R_1 V_{r1} \cot\alpha_1) \tag{19.7}$$

and the power supplied (assuming $\eta = 1$)

$$P_B = P_H = \Omega T_o = \rho Q(U_2 V_{r2} \cot\alpha_2 - U_1 V_{r1} \cot\alpha_1) \tag{19.8}$$

where the tangential impeller velocities are $U_2 = R_1\Omega$ and $U_2 = R_2\Omega$. The radial velocity components V_{r1} and V_{r2} can be calculated from the equation of conservation of mass

$$Q = 2\pi R_1 b_1 V_{r1} = 2\pi R_2 b_2 V_{r2} \tag{19.9}$$

where b_1 and b_2 are the blade widths at the inlet and outlet respectively.

The blades of the impeller are usually designed such that $\alpha_1 = \pi/2$, that is $V_1 = V_{r1}$. For such a case equation (19.8) becomes

$$P_H = \rho Q U_2 V_{r2} \cot\alpha_2 = \rho Q U_2 V_{t2} \tag{19.10}$$

where

$$V_{t2} = U_2 - V_{r2} \cot \beta_2 \tag{19.11}$$

and

$$V_{r2} = \frac{Q}{2\pi R_2 b_2} \qquad (19.12)$$

The pump head can thus be written as

$$h_p = \frac{P_H}{\rho g Q} = \frac{U_2^2}{g} - \frac{U_2 \cot \beta_2}{2\pi R_2 b_2 g} Q \qquad (19.13)$$

This equation is plotted in Fig. 19.5 for $\beta_2 < 90^o$, for $\beta_2 = 90^o$ and for $b_2 > 90^o$. We note that the slope is negative for $\beta_2 < 90^o$ (backward-curved blades) and positive for $\beta_2 > 90^o$ (forward-curved blades). The various blade shapes are shown in Fig. 19.6. For $\beta_2 > 90^o$ an unstable condition known as pump surging may occur, for this reason pump impellers are nearly always designed with backward-curved blades. However, turbine impellers are usually designed with forward-curved blades.

Example 19.2

A centrifugal pump rotating at 1800 rpm is used to rerun the experiment of example 19.1. Determine the head developed when the inlet tube is filled with air. Assume an impeller radius of 20 cm and $\beta_2 = 90^o$.

Solution

Equation (24.13) may be used. Since $\beta_2 = 90^o$, $\cot \beta_2 = 0$, we have

$$h_p = \frac{U_2^2}{g}$$

This is the head in meters of the fluid inside the pump (air)
U_2 is the tangential velocity of the tip of the blades.

$$U_2 = \Omega R_1 = (2\pi N)R_2 = 2\pi \times \frac{1800}{60} \times 0.20 = 37.68 \text{ m/s}$$

Thus

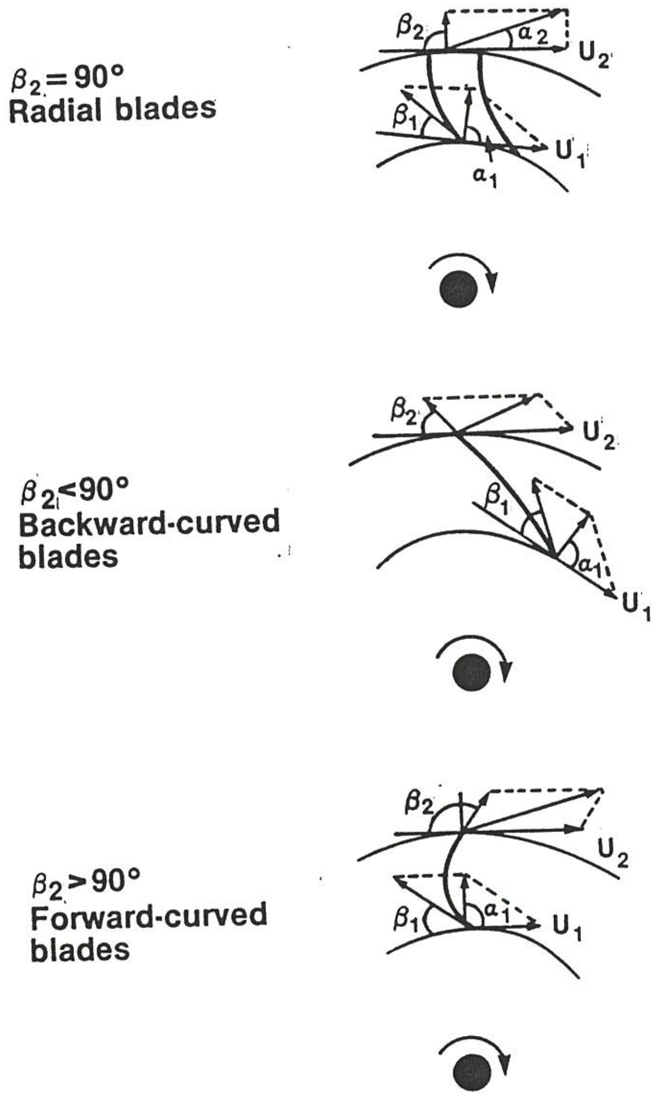

Fig. 19.6 Blade shapes for radial flow machines.

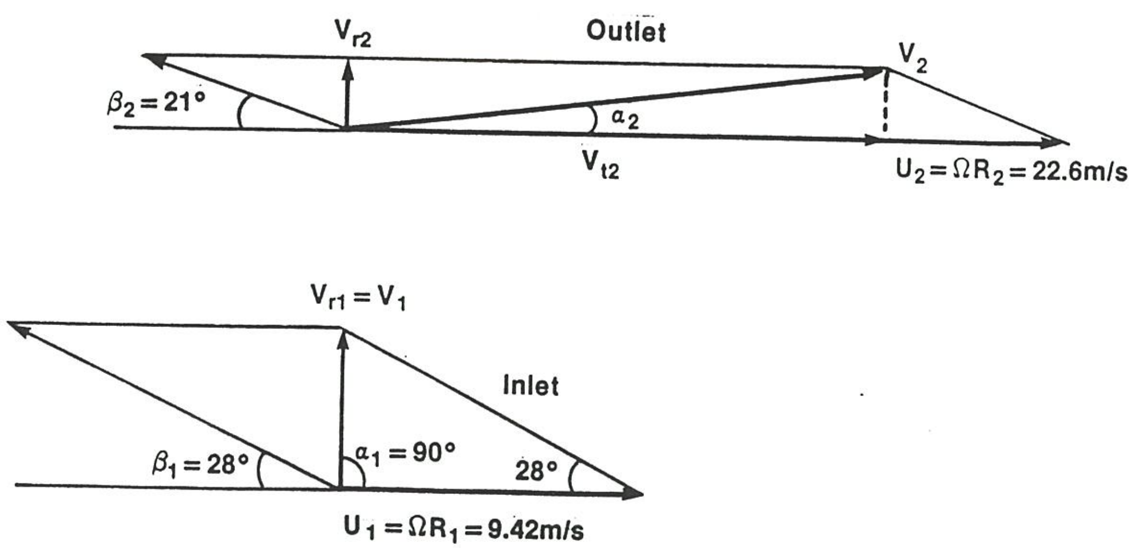

Fig.E.19.3 Inlet and outlet velocity diagram.

$$h_p = \frac{37.68^2}{9.81} = 144.72 \text{ m of Air}$$

or

$$h_p = 144.72 \frac{\rho_{Air}}{\rho_{Water}} = 144.72 \frac{1.225}{1000} = 0.17 \text{ m of water(!)}$$

The air pumped creates a very small head. Thus, to get the centrifugal pump going, it is necessary to replace the air with liquid. This process is called priming.

The present pump is capable of developing a head of 144.72 of water if the whole system is filled with water. However, the theoretical suction lift will be same as in Example 19.1 for the same flow rate through the same size of suction pipe. The problems associated with the formation of vapor bubbles through the pump are discussed in Section 19.5 (Cavitation).

Example 19.3

The impeller of a centrifugal water pump rotates at 1800 rpm. The inlet radius of the impeller is 5 cm, while its outlet radius is 18 cm. The blade width is 4 cm and the blade angles are $\beta_1 = 28^o$ and $\beta_2 = 21^o$. Assuming that the flow enters normal to the impeller ($\alpha_1 = \pi/2$) and an efficiency of 90%, determine

(a) the volume flow rate

(b) the pump head

(c) the hydraulic pump power

(d) the brake power (i.e. shaft input power)

Solution

The inlet velocity diagram is shown in Fig.E19.3(a) We have

$$U_1 = \Omega R_1 = 2\pi \frac{1800}{60} 0.05 = 9.42 \text{ m/s}$$

$$V_1 = U_1 \tan \beta_1 = 9.42 \tan 28^o = 5.009 \text{ m/s}$$

The volume rate of flow is $Q = 2\pi R_1 b_1 V_{r1}$. Here $V_{r1} = V_1$, thus $Q = 2\pi \times 0.05 \times 0.04 \times 5.009 = 0.0629\ m^3/s$. The outlet velocity diagram is shown in **Fig. E.19.3(b)**. We have

$$U_2 = \Omega R_2 = 2\pi \ \frac{1800}{60}\ 0.12 = 22.60\ m/s$$

$$V_{r2} = \frac{Q}{2\pi R_2 b} = \frac{0.0629}{2\pi \times 0.12 \times 0.04} = 2.087\ m/s$$

Then using equation (19.11) we get

$$V_{t2} = U_2 - V_{r2} \cot \beta_2 = 22.60 - 2.087 \cot 21^\circ = 17.163\ m/s$$

$$V_2 = (V_{r2}^2 + V_{t2}^2)^{1/2} = (2.087^2 + 17.163^2)^{1/2} = 17.289\ m/s$$

$$\cot \alpha_2 = \frac{V_{t2}}{V_{r2}} = \frac{17.163}{2.087} = 8.224$$

$$\alpha_2 = 6.93^\circ$$

The hydraulic pump power is

$$P_H = \rho Q U_2 V_{t2} = 1000 \times 0.0629 \times 22.60 \times 17.163$$
$$= 24{,}397\ W = 24.397\ kW$$

and the pump head

$$h_p = \frac{P_H}{\rho g Q} = \frac{24397}{1000 \times 9.81 \times 0.0629} = 39.538$$

The brake (or shaft input) power will be

$$P_B = \frac{24{,}397}{0.9} = 27{,}107\ W = 27.107\ kW$$

19.4 PERFORMANCE CHARACTERISTICS OF CENTRIFUGAL PUMPS

The theory presented in the previous section is one-dimensional and does not take into account leakage, frictional, turbulence or secondary flow phenomena that occur in centrifugal pumps. Actual performance is lower than that calculated on the basis of the idealized analysis of section 19.3.

Measured performance characteristics include the head, the input shaft power and efficiency as a function of volume flow rate. Some typical performance curves for a centrifugal pump operating at a constant speed of rotation are shown in Fig. 19.7. The head is nearly constant at low flow rates and it drops as the flow rate becomes large. The input shaft power increases almost linearly. The efficiency rises to a maximum of about 90% and then drops.

Neglecting viscous effects and other non-idealities mentioned above we can easily conclude from the analysis of Section 19.3 that the head is proportional to impeller tip velocity. Thus for an impeller of diameter D with a speed of rotation N we may write

$$h_p \propto (ND)^2 \tag{19.14}$$

The dimensionless grouping

$$C_H = \frac{gh_p}{N^2D^2} \tag{19.15}$$

is known as the head coefficient.

Using equation (19.9) we conclude that the volume flow rate is proportional to the impeller tip velocity and the flow area $2\pi Rb$, which is in turn is proportional to the reference linear dimension D^2. Thus

$$Q \propto D^2(ND) \propto ND^3 \tag{19.16}$$

The dimensionless grouping

$$C_Q = \frac{Q}{ND^3} \tag{19.17}$$

is known as the capacity (or discharge) coefficient.

The hydraulic power is

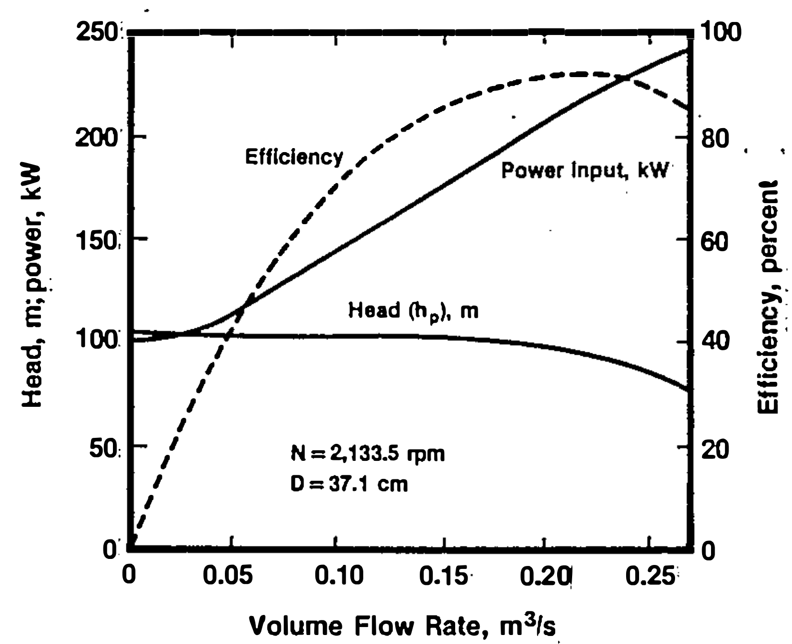

Fig. 19.7 Typical performance curves after Daugherty and Franzini [23, 6th edition].

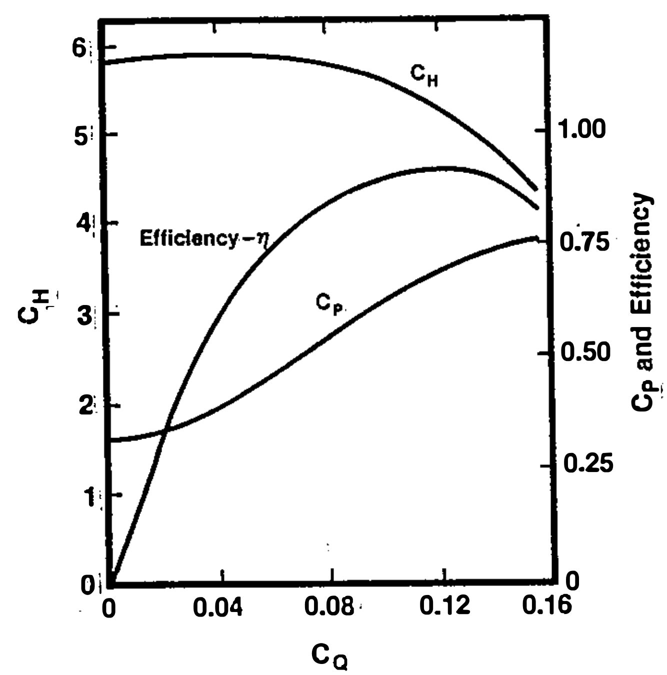

Fig. 19.8 Dimensionless representation of the performance curves of Fig.19.7.

$$P_H = \rho g Q h_p \tag{19.18}$$

thus we may write for the input shaft (brake) power

$$P_B \propto Qh_p \propto (ND^3)\ (ND)^2 \propto N^3 D^5 \tag{19.19}$$

The dimensionless grouping

$$C_p = \frac{P_B}{\rho N^3 D^5} \tag{19.20}$$

is called the power coefficient.

It is interesting to note the effect of rotational speed (N^3) and the more dramatic effect of impeller size (D^5) on input shaft power.

The above dimensionless quantities can be actually derived from formal dimensionless analysis methods like those described in Chapter 5 (see also Dixon [2], Daugherty and Franzini [23] and White [24]). The proportionality relations are very useful in comparing the performance of two pumps of the same geometrical design. The heads, flow rates and powers should obey the following relations

$$\frac{(h_p)_2}{(h_p)_1} = \frac{N_2^2 D_2^2}{N_1^2 D_1^2} \tag{19.21}$$

$$\frac{Q_2}{Q_1} = \frac{N_2 D_2^3}{N_1 D_1^3} \tag{19.22}$$

$$\frac{(P_B)_2}{(P_B)_1} = \frac{\rho_2 N_2^3 D_2^5}{\rho_1 N_1^3 D_1^5} \tag{19.23}$$

These similarity rules can be used for scaling-up purposes, i.e. from the performance of small pump we can determine the performance of a large one of the same geometrical design. Unfortunately these similarity relations do not have general applicability. They are valid for low viscosity fluids, such as water and thin oils, and pumps of reasonably large dimensions and speeds.

The performance characteristics shown in Fig. 19.7 are plotted in dimensionless form in Fig. 19.8. The efficiency has been assumed to be always the same, i.e. $\eta_1 = \eta_2$. Moody [25] has developed a formula for turbines which is also valid for pumps in the form

$$\frac{1 - \eta_2}{1 - \eta_1} \approx \left(\frac{D_1}{D_2}\right)^{1/5} \qquad (19.24)$$

Example 19.4

A pump is to be designed having similar performance characteristics to those of Fig. 19.7. This pump will have an impeller 3 times larger rotating at 600 rpm. Both pumps are assumed to operate near maximum efficiency. Determine the head, flow rate and power of this new pump for water.

Solution

We will use the dimensionless form of Fig. 19.7, that is Fig. 19.8. For maximum efficiency we have

$$C_H = 5.30$$

$$C_Q = 0.115$$

$$C_p = 0.70$$

We can now calculate the head, flow rate and power for the pump to be designed.

$$(h_p) = C_H \frac{N^2 D^2}{g} = 5.3 \frac{\left(\frac{600}{60}\right)^2 (3 \times 0.371)^2}{9.81}$$

$$= 66.9 \text{ m}$$

$$Q = C_Q N D^3 = 0.115 \times \left(\frac{600}{60}\right) (3 \times 0.371)^3$$

$$= 1.58 \text{ m}^3/\text{s}$$

$$(P_B) = C_p \ \rho \ N^3 D^5 = 0.70 \times 1000 \times \left(\frac{600}{60}\right)^3 \ (3 \times 0.371)^5$$

$$= 1195 \text{ W}$$

$$= 1195 \text{ kW}$$

This would be the power if the two pumps had the same efficiency (from Fig. 19.7 ${}_1 \simeq 0.91$). We can also use Moody's equation(19.24) to obtain the efficiency of the new pump

$$\eta_2 = 0.928$$

Thus, the power required will be

$$(P_B) = \frac{0.928}{0.91} \times 1195 = 1218 \text{ kW}$$

19.5 CAVITATION

When pumps (or turbines) are used with liquids local velocities can be very high and local pressures may drop below the vapor pressure of the liquid being pumped. Consequently local boiling occurs resulting in the formation of bubbles and regions of vapor. This phenomenon is called cavitation. The bubbles are swept downstream to regions of higher pressure where they collapse producing itermittent pressures which can be very high. The pressure waves that are generated continuously may cause damage to the blade surface and the surrounding structure. In addition, the vapor distorts the flow field and may cause significant reduction in pump efficiency. Cavitation also occurs in ship propellers and valve casings in regions of high local velocity liquid flow which, from the Bernoulli equation, are expected to have low local pressure (Section 14.12).

The appropriate dimensionless group to consider is Euler number which was defined in Section 6.8 as the ratio of pressure and inertia forces. A special form of the Euler number is the <u>cavitation number</u> which is defined as

$$C_c = \frac{p - p_v}{\rho \frac{V_{rel}^2}{2}} \qquad (19.25)$$

where p is a reference (free stream) pressure, p_v the vapor pressure and V a reference velocity (which may be a relative velocity in the case of turbomachinery). Acceptable values of C_c are found from experiments with different types of fluid machinery (pumps, turbines, propellers, etc.).

The head required at the pump inlet to avoid cavitation is called the <u>net positive suction head</u> (NPSH). This is given by

$$\text{NPSH} = \frac{p_i}{\rho g} + \frac{V_i^2}{2g} - \frac{p_v}{\rho g} \qquad (19.26)$$

where p_i and V_i are the pressure and velocity at the pump inlet and p_v is the vapor pressure of the liquid.

The Bernoulli equation between the free surface of a reservoir at pressure p_o and the pump inlet at elevation z_i above the reservoir surface is:

$$\frac{p_o}{\rho g} + \frac{V_o^2}{2g} = \frac{p_i}{\rho g} + \frac{V_i}{2g} + z_i + h_f \qquad (19.27)$$

where h_f is the frictional heat loss and $V_o \cong 0$. Thus, the expression for the net positive suction head may be written as

$$\text{NPSH} = \frac{p_o}{\rho g} - z_i - h_f - \frac{p_v}{\rho g} \qquad (19.28)$$

Pump manufacturers measure the required NPSH for their pumps and report it, as in Fig. 19.9. When a pump is used to pump a liquid at elevated temperatures or near the boiling point, the vapor pressure is high and the NPSH might be negative. This requires that the pump be installed below the reservoir level as shown in Fig. 19.10 to avoid cavitation.

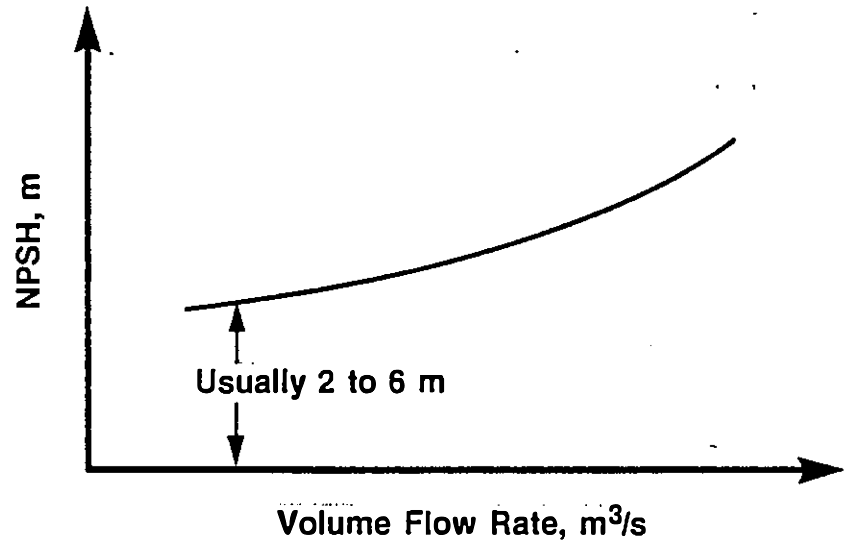

Fig. 19.9 Net positive suction head as a function of flow rate.

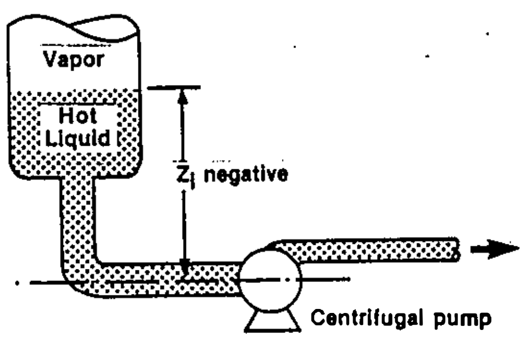

Fig.19.10 A pump placed below a liquid container to prevent cavitation.

Example19.5

Water is to be pumped at $80^{\circ}C$ ($p_v \simeq 50.66$ kPa) from an open reservoir. The pump has NPSH = 6 m at the desired flow rate and the frictional head loss is $h_f = 1.5$ m. Determine the elevation of the pump inlet to avoid cavitation.

Solution

Using equation (19.28) we have

$$NPSH \leq \frac{p_o}{\rho g} - z_i - h_f - \frac{p_v}{\rho g}$$

$$6 \leq \frac{101330}{1000 \times 9.81} - z_1 - 1.5 - \frac{50660}{1000 \times 9.81}$$

$$6 \leq 10.33 - z_1 - 1.5 - 5.16$$

$$6 \leq 3.67 - z_1$$

$$z_1 \leq - 2.33$$

This means that the pump must be placed at least 2.33 m below the reservoir surface to avoid cavitation.

19.6 AXIAL-AND MIXED-FLOW PUMPS

In axial-flow pumps the fluid enters and leaves the machine mainly in an axial direction. A schematic diagram of an axial pump is shown in Fig. 19.11. The radius of this pump remains unchanged along the direction of the flow. The stationary guide vanes on the outlet side are designed to remove the whirl component of the velocity which the fluid receives from the impeller. Sometimes guide vanes are also provided on the inlet side when appreciable tangential motion exists in the inlet pipe.

The impeller of mixed-flow pumps is designed in such a way that the fluid enters axially and leaves with a substantial radial component, i.e. these pumps represent an intermediatte design between axial and centrifugal pumps.

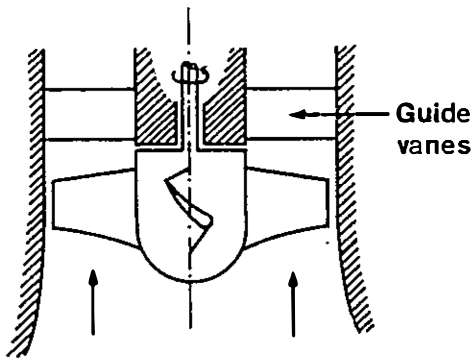

Fig. 19.11 Axial flow pump.

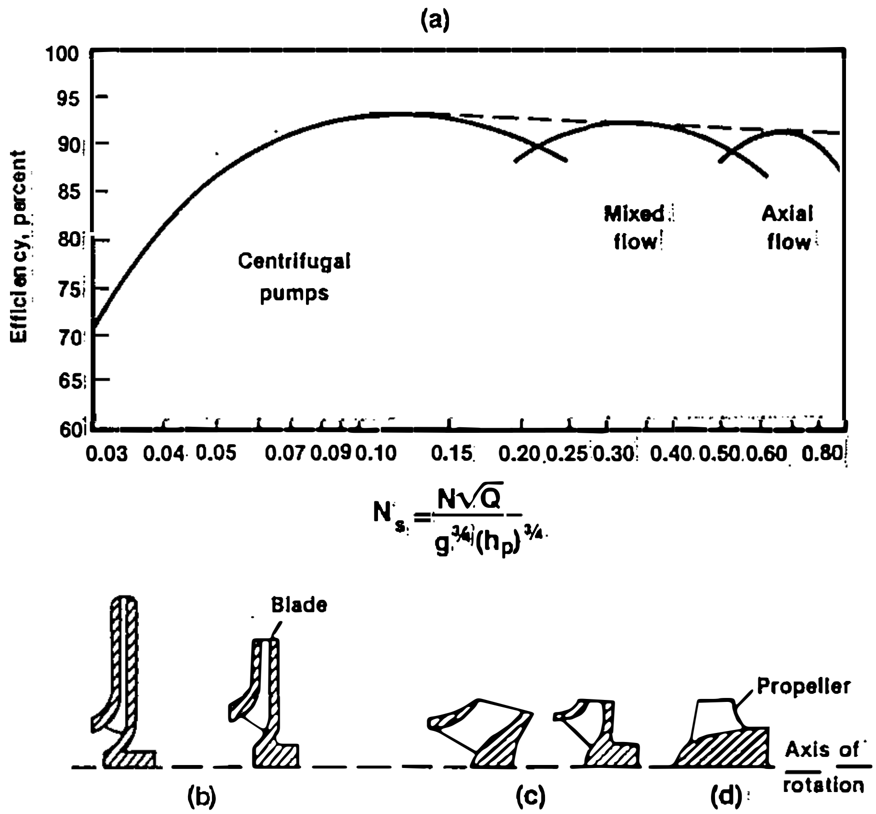

Fig. 19.12 (a) maximum pump efficiency as a function of specific speed, (b) typical pump impeller designs.

To determine the torque of these pumps we can start again from Euler's turbine equation (6.118)

$$T_o = \dot{m}\,[(rv_\theta)_{out} - (rv_\theta)_{in}] \tag{19.29}$$

For an axial-flow pump $r_{in} = r_{out} = R$, thus

$$T_o = \dot{m}\,R[(v_\theta)_{out} - (v_\theta)_{in}] \tag{19.30}$$

Using the same terminology as in the analysis of centrifugal pumps we have

$$T_o = \rho QR\ (V_{t2} - V_{t1}) \tag{19.31}$$

where V_{t1} and V_{t2} represent the average tangential fluid velocities at the inlet and outlet respectively. These velocity components can be related to the axial flow velocity by taking into account the geometrical orientation of moving and stationary vanes (see, for example John and Haberman [26]).

Axial-flow pumps have high flow rates and low heads while centrifugal pumps have high heads and low flow rates.

19.7 PUMP SELECTION

The selection of a pump for a given engineering application is not an easy task. There is a wide variety of pump types and pump designs. Whole books have been written on this subject [11,12]. The engineer must decide what type of equipment is appropriate in order to provide reliable and efficient service with a minimum of maintenance costs.

One of the parameters that is used in pump selection is the specific speed. This is a dimensionless grouping obtained by combining the definition of C_H and C_Q (Section 19.4) in such a manner that the diameter D is eliminated:

$$N_s = \frac{C_Q^{\ 1/2}}{C_H^{\ 3/4}} = \frac{(Q/ND^3)^{1/2}}{(gh_p/D^2N^2)^{3/4}} = \frac{NQ^{1/2}}{g^{3/4}h_p^{\ 3/4}} \tag{19.32}$$

This definition is used for Q and h_p corresponding to maximum efficiency. Thus a single number is obtained for an entire group of similar type pumps. When the efficiencies of different pumps are plotted as a function of specific speed the maximum efficiency will occur at different N_s for the different designs. As seen from Fig. 19.12(a) centrifugal pumps have low specific speeds and axial flow pumps have high specific speeds. The different impeller designs are shown in Fig. 19.12 (b).

Example 2.6

Determine the appropriate pump and the power required to move 0.8 m^3/s of water with a head of 4.2 m. The available motor rotates at 900 rpm.

Solution

We calculate the specific speed

$$N_s = \frac{N Q^{1/2}}{g^{3/4} h_p^{3/4}} = \frac{\frac{900}{60} \times 0.8^{1/2}}{9.81^{3/4} 4.2^{3/4}} = 0.8262$$

From Fig. 19.12 it is clear that we should use an axial flow pump. An approximate value of efficiency is $\eta = 0.84$.

The required (shaft) input power will be

$$P_B = \frac{P_H}{\eta} = \frac{\rho g Q h_p}{\eta} = \frac{1000 \times 9.81 \times 0.8 \times 4.2}{0.84}$$

$$= 39240 \text{ W} = 39.24 \text{ KW}$$

19.8 COMPRESSORS

Positive displacement compressors have been used as industrial tools for more than a century. They are complicated, heavy, expensive and low-flow rate devices. The developments in aircraft industry necessitated the design at light weight, efficient rotary compressors which are now used in many other industrial applications.

Both centrifugal and axial-flow compressors have been developed. Multistaging is used to achieve high pressure ratios. This can be demonstrated by refering to Fig. 19.13. The gas is successively accelerated by each row of rotor blades and then slowed by the corresponding stator blades. Thus the kinetic energy is converted into pressure, which becomes progressively higher at each stage. Because the density of air or gases used is much less than liquid densities, the compressor must rotate at very high speeds (e.g. 20000 rpm) for large pressure rise. More details of the mechanical arrangements can be found in specialized texts [e.g. Ref. 6,16,22]. It is interesting to note that many important results can be obtained on compressors by purely thermodynamic considerations [27,28].

19.9 TURBINES

Turbines are devices that extract energy from fluids and for analysis purposes they can be thought of as pumps run backwards. The basic theory is essentially the same, however, there are some differences in physical features as well as in terminology. Turbines are usually classified as impulse or reaction, turbines depending on how the hydrostatic head in converted to power. In impulse turbines a high velocity jet issuing from a nozzle strikes a set of blades attached to a wheel (or runner) as they pass by the nozzle exit. In reaction turbines the flow completely fills the blade passages and causes the impeller to rotate.

Impulse Turbines

Impulse turbines are suitable for relatively high heads and low power. A schematic diagram of an impulse turbine is shown in Fig. 19.14. The jet strikes the vanes and produces power as the runner rotates. The Pelton water turbine features curved buckets divided in half by a splitter edge that diverts the water into two streams. This device was patented in 1889 by an American engineer named L.A. Pelton. The force exerted by a jet on a moving blade was calculated by applying a linear momentum balance on a moving control volume in Section 6.2.3. Here, we we will compute the average torque by assuming there is an

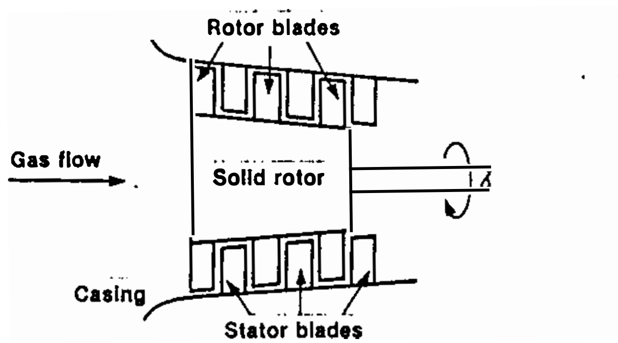

Fig. 19.13 Multistaged rotary compressor.

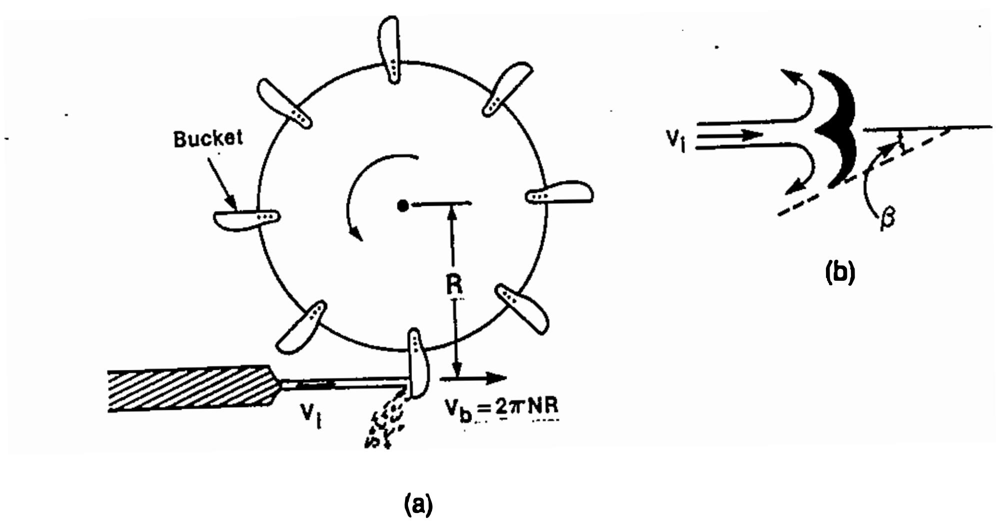

Fig. 19.14 Impulse turbine (Pelton wheel).

average steady flow of the jet and that this steady flow corresponds to the instantaneous flow of the full jet when it strikes a bucket. This means that we consider essentially a stationary control volume. Thus, we will have $\dot{m} = \rho A V_j$, however, the relative velocity remains $V_j - V_b$ as in Section 6.2.3. With these assumptions equation (6.22) can be modified to the form

$$F = -\rho A V_j \, (V_j - V_b) \, [\cos \beta + 1] \tag{19.33}$$

The minus sign is retained to indicate that F is the force exerted by the liquid on the bucket. The power extracted from the liquid is

$$P_H = F V_b = \rho A V_j V_b \, (V_j - V_b) \, [\cos \beta + 1] \tag{19.34}$$

The power will be maximum for $\cos \beta = 1$, i.e. for $\beta = 0$. This is impractical because of the interference between leaving flow and the incoming jet. In practice, β is usually about 15^o, or $\cos \beta + 1 = 1.9659$, which gives only 2% less than maximum power.

To maximize the power with respect to V_b we take $dP_H/dV_b = 0$ or

$$\rho A V_j \, (V_j - 2V_b) \, [\cos \beta + 1] = 0 \tag{19.35}$$

which gives

$$V_b = \frac{1}{2} V_j$$

Pelton wheels are usually employed for high heads, e.g. 200 m to more than 1 km. Efficiencies of the complete hydraulic installation from headwater to tailwater (see Fig. 19.15) can reach 85%. More information on Pelton wheels is given by Daugherty and Franzini [23].

Reaction Turbines

Reaction turbines are suitable for low-head, high-flow installations. In these devices rotation is achieved mainly through the reactive force created by the acceleration of water in the runner, or rotor, rather than in the nozzle as in the case of the impulse turbine.

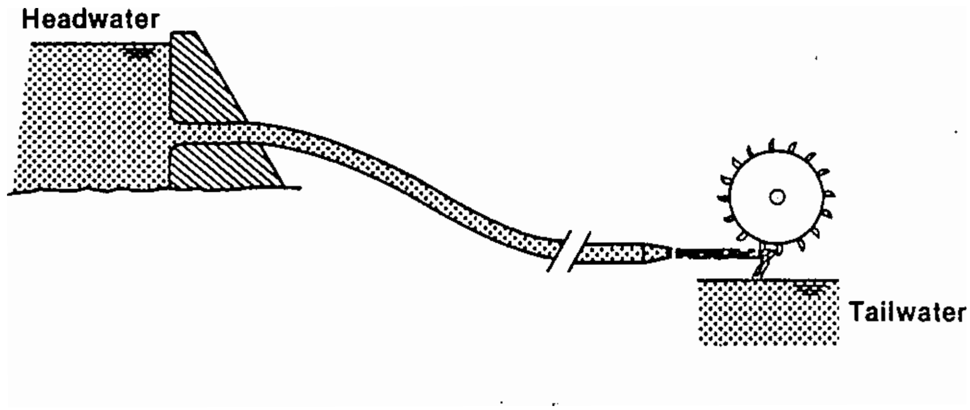

Fig. 19.15 Schematic diagram of a hydroelectric installation with a Pelton wheel.

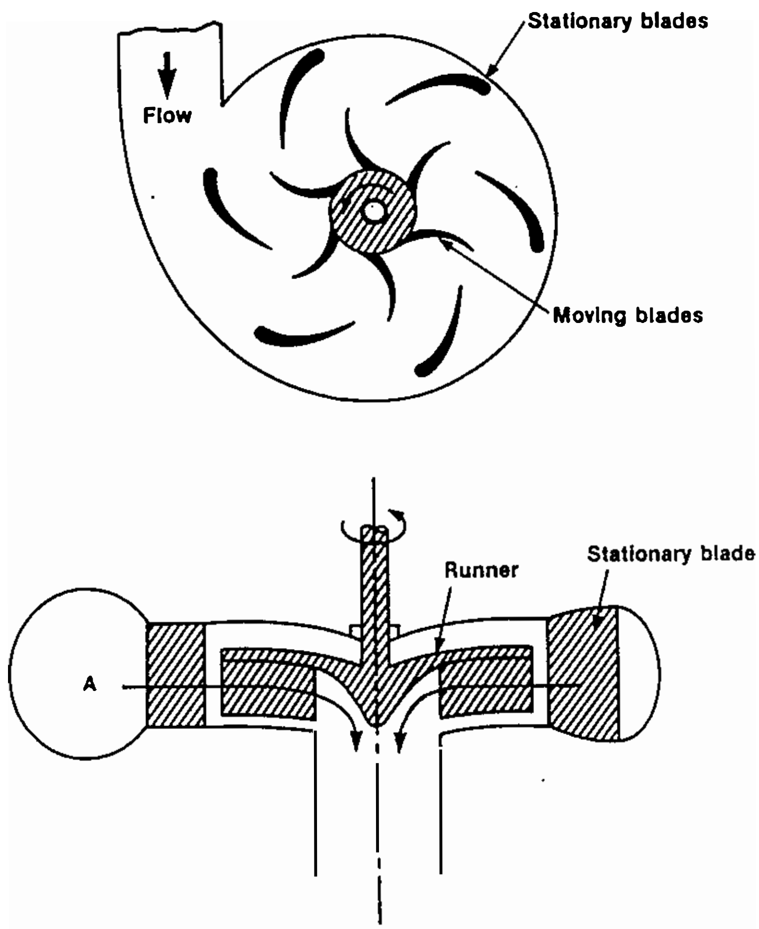

Fig. 19.16 Radial flow (Francis) turbine.

There are many different types of reaction turbines having radial-, axial- or mixed-flow configurations. The most extensively used turbines for hydroelectric installations are probably radial or mixed-flow machines called Francis turbines, after J.B. Francis an American engineer who designed the first-efficient inward-flow turbine. A schematic diagram of such a turbine is shown in Fig. 19.16. At this nominal position the stationary guide vanes deflect the incoming water onto the rotating vanes. Assuming purely radial flow we can use exactly the same equations as those developed in Section 19.3 for centrifugal (i.e. radial flow) pumps. Introducing a minus sign to indicate that the torque is done by the water on the shaft we can rewrite equation (19.8) as

$$T_o = -\rho Q \left(R_2 V_{r2} \cot \alpha_2 - R_1 V_{r1} \cot \alpha_1\right) \qquad (19.36)$$

and the power

$$P_H = \left|\Omega T_o\right| = \rho Q \left(U_2 V_{r2} \cot \alpha_2 - U_1 V_{r1} \cot \alpha_1\right) \qquad (19.37)$$

Further simplifications can be made in exactly the same manner as in Section 19.3. In fact the whole analysis could have been presented as applicable to radial flow machines, to include both centrifugal pumps and radial flow turbines. The reader, however, must be reminded that while pumps have backward curved vanes, turbines have forward curved vanes (see Fig. 19.6).

Francis turbines are used for a wide range of heads from the lowest economically useable (about three meters) to about 600 meters (see Fig. 19.17). At low-heads propeller turbines having purely axial flow are more economical than Francis turbines. One popular axial-flow design with adjustable blades is the Kaplan turbine, named after the Austrian inventor Viktor Kaplan who patented his design in 1920.

For the selection of turbines for a given application use is often made of the coefficients C_Q, C_H and C_p which have exactly the same definition for turbines and pumps (see Section 19.4). To compare the output power to the available head, independently of size, we eliminate the diameter D from C_H and C_p. We define the power specific speed as

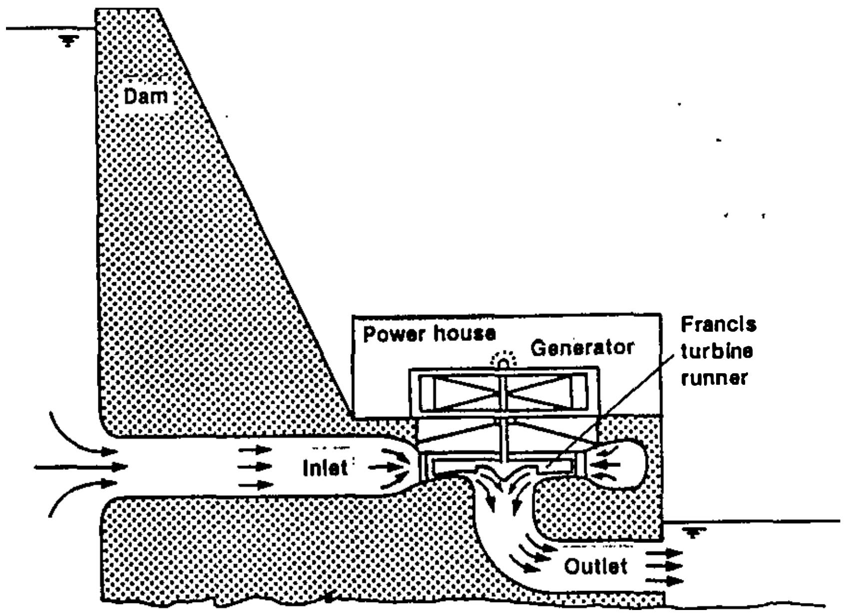

Fig. 19.17 Schematic diagram of a hydroelectric installation with a Francis turbine.

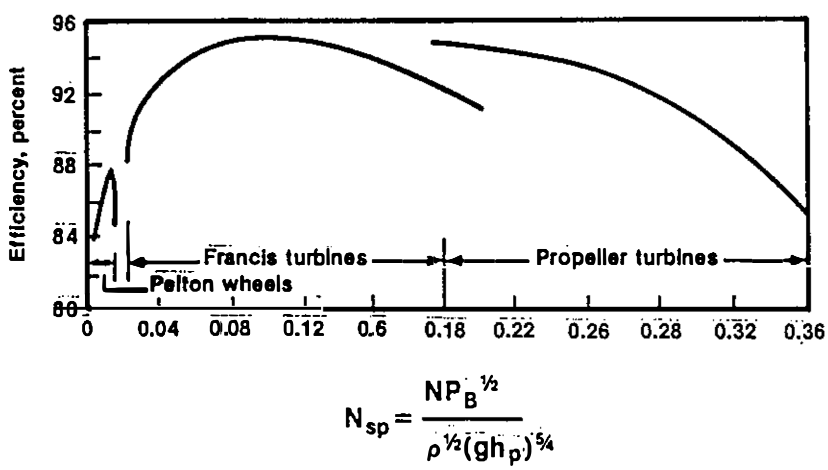

Fig. 19.18 Maximum turbine efficiency as a function of power specific speed.

$$N_{sp} = \frac{C_p^{1/2}}{C_H^{5/4}} = \frac{NP_B^{1/2}}{\rho^{1/2}(gh_p)^{5/4}} \tag{19.38}$$

Fig. 19.18 gives the optimum efficiency of the three turbine types discussed as a function of specific speed. Impulse turbines are best suited for very low specific speeds, Francis turbines for intermediate specific speeds and propeller turbines for high specific speeds.

For detailed elementary analyses of these machines the reader is referred to references [23,26,29] and for more rigorous analyses to references [2,3,6].

Example 19.7

A Pelton water turbine is used to drive a generator at 600 rpm. The water jet is 12 cm in diameter and has a velocity of 90 m/s. The bucket angle is 15° and the runner rotates at the peripheral speed for maximum power conversion.

Solution

We use equation (19.34)

$$P_H = -\rho A V_j V_b (V_j - V_b)[\cos\beta + 1]$$

For maximum power (equation (19.35))

$$V_b = \frac{1}{2} V_j = 45 \text{ m/s}$$

Thus

$$P_H = -1000 \times \frac{\pi}{4} (0.12)^2\ 90 \times 45\ (90 - 45)\ [\cos 15^{\circ} + 1]$$

$$= 4.05 \times 10^6 \text{ W} = 4050 \text{ kW}$$

19.10 WIND TURBINES

Windmills have been used for many centuries for grinding and pumping water. Wind machines that produce electricity made their first appearance about a hundred years ago. However, the use of inexpensive fossil fuels after World War I resulted in a decline of wind energy utilization. Renewed interest in wind energy started in the early seventies as oil prices rose.

Wind machines are devices that convert the kinetic energy present in the wind into rotating shaft motion. These are commonly divided into propeller-type converters and cross-wind converters. In propeller-type converters the shaft axis is parallel to the direction of the wind. In cross-wind converters the shaft axis is perpendicular to the wind direction. Most of wind energy converters are of the propeller-type having two or usually three blades, like that shown in Fig.19.19(a). Cross-wind converters of the type shown in Fig.(19.19(b) , known as Darrieus turbines, attracted considerable interest in recent years. The advantage of cross-wind machines is that their operation is independent of wind direction. For a discussion on these and other types of wind converters the reader is referred to the books by Simmons [31], Sorensen [32] and for an overview of wind energy possibilities in a comprehensive paper by Sorensen [33]. Other books on the subject were published by Cheremisinoff [34] and DeRenzo [35].

The derivation of expressions for the determination of power generated by propeller-type wind turbines is based on propeller theory [1,30]. For a simplified presentation we consider a control volume as shown by the dotted line in Fig. 19.20. Applying a linear momentum balance in the direction of the flow (see Section 6.1), we have

$$\dot{m}\, V_i - \dot{m}\, V_e + F = 0 \tag{19.39}$$

where F is the force exerted by the blade on the fluid. Considering a "thin" control volume around the blade ($V_1 = V_2 = V_a$) we get

$$p_1 A - p_2 A + F = 0 \tag{19.40}$$

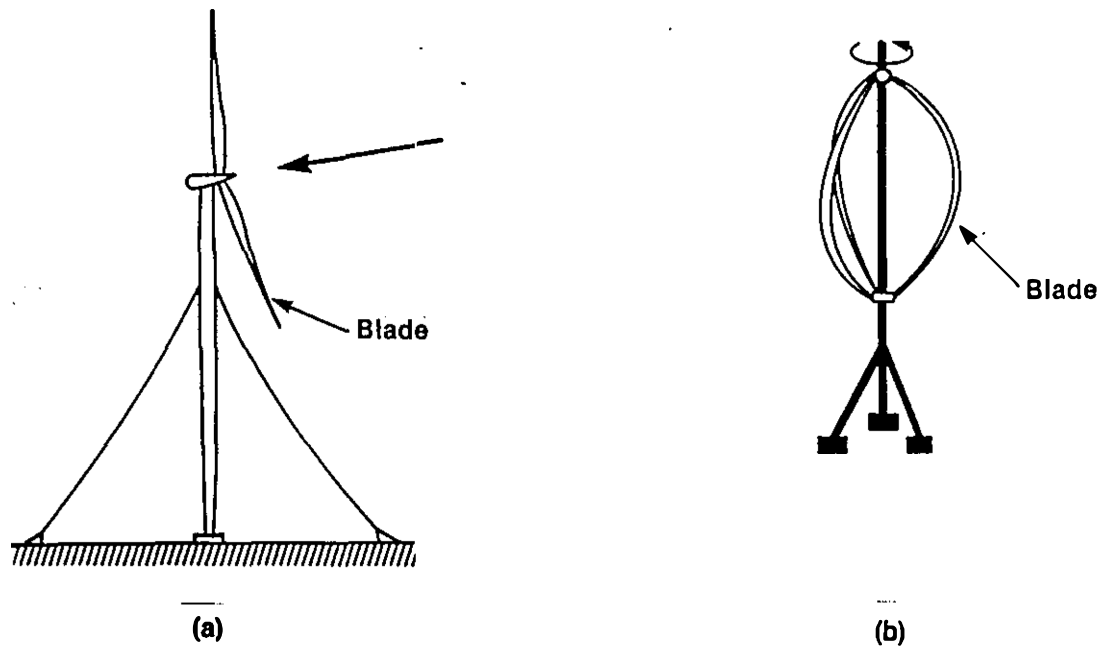

Fig. 19.19 (a) Propeller-type wind converter, (b) Darrieus turbine.

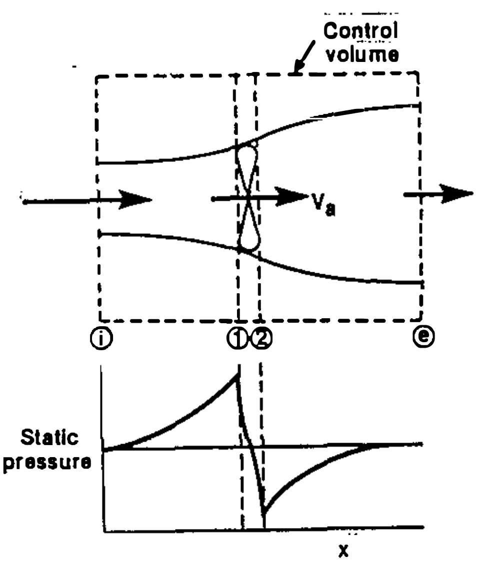

Fig. 19.20 Flow past the propeller of a wind converter.

Combining equations (19.39) and (19.40), we get

$$(p_1 - p_2)A = \dot{m}(V_i - V_e) \tag{19.41}$$

where $\dot{m} = \rho A V_a$

thus

$$(p_1 - p_2) = \rho V_a(V_i - V_e) \tag{19.42}$$

Applying the Bernoulli equation between i and 1 and then between 2 and e we get

$$\frac{p_i}{\rho} + \frac{V_i^2}{2} = \frac{p_1}{\rho} + \frac{V_1^2}{2} \tag{19.43}$$

$$\frac{p_2}{\rho} + \frac{V_2^2}{2} = \frac{p_e}{\rho} + \frac{V_e^2}{2} \tag{19.44}$$

Summing up by noting that $p_i = p_e$ and $V_1 = V_2 = V_a$ we get

$$p_1 - p_2 = \frac{\rho}{2}(V_i^2 - V_e^2) \tag{19.45}$$

Combining equations (19.42) and (19.45) we get

$$V_a = \frac{V_i + V_e}{2}$$

Now, we apply the Bernoulli equation between i and e noting that the turbine extracts power from the control volume, $P_H = h_{Tb}\rho g Q$ (see Section 14.6). We have

$$\frac{V_i^2}{2g} - h_{Tb} = \frac{V_e^2}{2g}$$

or

$$P_H = \rho Q \left(\frac{V_i^2 - V_e^2}{2}\right)$$

$$= \rho A V_a \left(\frac{V_i^2 - V_e^2}{2}\right)$$

$$= \rho A \frac{V_i + V_e}{2} \left(\frac{V_i^2 - V_e^2}{2}\right)$$

To obtain the maximum power, we set the derivitive with respect to V_e equal to zero.

$$\frac{dP_H}{dV_e} = 0$$

or

$$V_i = 3V_e$$

Therefore, the maximum power which can be extracted from the wind is

$$P_H = \frac{8}{27} \rho A V_i^3$$

The total power available in the wind is simply

$$P_o = F.V_i = (\Delta p)AV_i = \frac{1}{2} \rho A V_i^2 V_i = \frac{1}{2} \rho A V_i^3$$

Thus, the maximum wind turbine efficiency is

$$\eta = \frac{\text{Power extracted}}{\text{Power available}} = \frac{\frac{8}{27} \rho A V_i^3}{\frac{1}{2} \rho A V_i^3} = \frac{16}{27} \text{ or } 59.3\%$$

Actual efficiency will be lower due to frictional losses. There are also several other technical problems that must be solved before the wide of use of wind energy becomes reality. Among these are (1) the unpredictable wind speed variations which would necessitate some form of energy storage for continuous power supply, (2) structural problems for large wind turbines, some of them having diameters of 100 m or more, (3) environmental impact of arrays of such turbines. Despite these problems Sorensen [33] claims that it is possible to satisfy perhaps 10-20% of present world consumption of electric power. This is a very interesting area of engineering research which may lead to the dawning of the age of wind energy.

Example

Calculate the electric power that can be generated by a wind turbine having diameter of 90 m, assuming rotor and gearing efficiency of 71% and generator efficiency of 80%. The average wind speed is 25 km/hr.

Solution

$$\text{Electric Power} = 0.71 \times 0.80 \times P_H$$

$$= 0.71 \times 0.80 \times \frac{8}{27} \rho A V_i^3$$

$$= 0.71 \times 0.80 \times \frac{8}{27} \times 1.225 \times \frac{\pi\ 90^2}{4} \times \left(\frac{25000}{3600}\right)^3$$

$$= 439 \times 10^3 \text{ W} = 439 \text{ kW}$$

REFERENCES

1. A. Betz, "Introduction to the Theory of Flow Machines", Pergamon Press, New York (1966).

2. S.L. Dixon, "Fluid Mechanics, Thermodynamics of Turbomachinery", Third edition, Pergamon Press, Oxford (1978).

3. G.T. Csanady, "Theory of Turbomachines", McGraw-Hill, New York (1964).

4. G.F. Wislicenus, "Fluid Mechanics of Turbomachinery", 2nd edition, McGraw-Hill, New York (1965).

5. D.H. Norrie, "An Introduction to Incompressible flow Machines", American Elsevier, New York (1963).

6. D.G. Shepherd, "Principles of Turbomachinery", MacMillan, New York (1965).

7.. V. Kadambi and M. Prasad, "An Introduction to Energy Conversion", Vol. III, "Turbomachinery", Wiley, New York (1977).

8. E. Logan, Jr., "Turbomachinery", Marcel Dekker, New York (1981).

9. A.J. Stepanoff, "Centrifugal and Axial Flow Pumps", Wiley, New York (1957).

10. A.H. Church, "Centrifugal Pumps and Blowers", Krieger, Huntington, New York (1972).

11. "Pump Selector for Industry", Worthington Pump, Mountainside, N.J. (1977).

12. R. Walker, "Pump Selection", Ann Arbor Science Publishers, Ann Arbor, Michigan (1972).

13. I.J. Karassik et al, "Pump Handbook", McGraw-Hill, New York (1976).

14. N.P. Cheremisinoff, "Fluid Flow: Pumps, Pipes and Channels", Ann Arbor Science Publishers, Ann Arbor, Mich. (1982).

15. J.H. Horlock, "Axial Flow Turbines", Krieger, Huntington, New York (1973).

16. H. Cohen, G.F.C. Rogers and H.I.H. Saravanamuttoo, "Gas Turbine Theory" Longman, London (1974).

17. A.W. Judge, "Small Gas Turbines", Chapman and Hall, London (1960).

18. J.F. Lee, "Theory and Design of Steam and Gas Turbines", McGraw-Hill, New York (1954).

19. W.J. Kearton, "Steam Turbine Theory and Practice", 6th ed., Pitman (1951).

20. H.A. Sorensen, "Gas Turbines", Ronald, New York (1951).

21. E.T. Vincent, "The Theory and Design of Gas Turbines and Jet Engines", McGraw-Hill, New York (1950).

22. J.L. Kerrebrock, "Aircraft Engines and Gas Turbines", MIT Press, Cambridge, Mass. (1977).

23. R.L. Daugherty and J.B. Franzini, "Fluid Mechanics", 7th Edition, McGraw-Hill, New York (1977).

24. F.M. White, "Fluid Mechanics", McGraw-Hill, New York (1979).

25. L.F. Moody, "The Propeller Type Turbine", ASCE Trans., 89, 628 (1926).

26. J.E.A. John and W.L. Haberman, "Introduction to Fluid Mechanics", 2nd Edition, Prentice-Hall, Englewood Cliffs, N.J. (1980).

27. F.F. Huang, "Engineering Thermodynamics", MacMillan, New York (1976).

28. R.W. Wood, "Applications of Thermodynamics", Addison-Wesley, Reading, Mass. (1982).

29. W.S. Janna, "Introduction to Fluid Mechanics", Brooks/Cole Engineering Division, Monterey, Calif. (1983).

30. H. Glauert, "The Elements of Aerofoil and Airscrew Theory", Cambridge University Press, Cambridge, U.K. (1959).

31. D.M. Simmons, "Wind Power", Noyes Data Corporation, Park Ridge, California (1975).

32. B. Sorensen, "Renewable Energy", Academic Press, New York (1979).

33. B. Sorensen, "Turning to the Wind", Amer. Sci., 69, 501 (1981).

34. N.P. Cheremisinoff, "Fundamentals of Wind Energy", Ann Arbor Science Publishers, Ann Arbor, Michigan (1978).

35. D.J. DeRenzo, "Wind Power", Noyes Data Corporation, Park Ridge, California (1979).

John Vlachopoulos, *Fundamentals of Fluid Mechanics*
Chem. Eng., McMaster University, Hamilton, ON, Canada
(First Edition 1984, revised internet edition (2016), www.polydynamics.com)

CHAPTER 20

CONSTITUTIVE EQUATIONS

20.1 INTRODUCTION

While generalizing the linear momentum balance in Section 6.3 we ended up with the stress form of the differential equation of momentum (6.57), which is

$$\rho \frac{\partial \bar{V}}{\partial t} + \rho \bar{V} \cdot \nabla \bar{V} = \nabla \cdot \bar{\bar{\sigma}} + \rho \bar{g} \tag{20.1}$$

The stress tensor $\bar{\bar{\sigma}}$ may be written in terms of its components as

$$\sigma_{ij} \Rightarrow \begin{matrix} \sigma_{11} & \sigma_{12} & \sigma_{13} \\ \sigma_{21} & \sigma_{22} & \sigma_{23} \\ \sigma_{31} & \sigma_{32} & \sigma_{33} \end{matrix} \tag{20.2}$$

We have, thus, introduced nine quantities in addition to the three velocity components V_1, V_2, V_3 and the pressure p. Actually, the new unknowns are only six because the stress tensor is symmetric, which means that $\sigma_{32} = \sigma_{23}$, $\sigma_{13} = \sigma_{31}$ and $\sigma_{23} = \sigma_{32}$. These quantities are unknown because nothing was said about the fluid properties, that is how the fluid responds to an applied stress. In order to reduce the unknowns to the usual four (V_1, V_2, V_3 and p) we must somehow relate the stress tensor to the fluid motion.

20.2 RATE OF ROTATION AND RATE OF DEFORMATION

The instantaneous motion of a fluid is described according to the Eulerian point of view by its velocity field. Let us consider a typical position P and a neighboring one P'. If the distance PP' is infinitesimal we can apply Taylor's expansion formula

$$V_i = V_i' + \frac{\partial V_i}{\partial x_j}(x_j - x_j') + 0\,(x_j - x_j')^2 \qquad (20.3)$$

where V_i and V_i' are the velocities at points P and P' respectively. The last term $0\,(x_j - x_j')^2$ represents infinitesimals of higher order which will be neglected from now on.

We may write

$$dV_i = V_i - V_i' = \frac{\partial V_i}{\partial x_j}(x_j - x_j') \qquad (20.4)$$

$\partial V_i/\partial x_j$ is the velocity gradient tensor

$$\frac{\partial V_i}{\partial x_j} \Rightarrow \begin{matrix} \frac{\partial V_1}{\partial x_1} & \frac{\partial V_1}{\partial x_2} & \frac{\partial V_1}{\partial x_3} \\ \frac{\partial V_2}{\partial x_1} & \frac{\partial V_2}{\partial x_2} & \frac{\partial V_2}{\partial x_3} \\ \frac{\partial V_3}{\partial x_1} & \frac{\partial V_3}{\partial x_2} & \frac{\partial V_3}{\partial x_3} \end{matrix} \qquad (20.5)$$

Thus, the velocity difference can be expressed as the product of the velocity gradient tensor and the distance. This difference may be due to translational, rotational or deformational motion (see Section 3.6).

The velocity gradient tensor can be split up into symmetric and asymmetric parts

$$\frac{\partial V_i}{\partial x_j} = \frac{1}{2}\left(\frac{\partial V_i}{\partial x_j} + \frac{\partial V_j}{\partial x_i}\right) + \frac{1}{2}\left(\frac{\partial V_i}{\partial x_j} - \frac{\partial V_j}{\partial x_i}\right) \tag{20.6}$$

We define the tensors

$$e_{ij} = \frac{1}{2}\left(\frac{\partial V_i}{\partial x_j} + \frac{\partial V_j}{\partial x_i}\right) \tag{20.7}$$

$$\omega_{ij} = \frac{1}{2}\left(\frac{\partial V_i}{\partial x_j} - \frac{\partial V_j}{\partial x_i}\right) \tag{20.8}$$

Thus, we have

$$\frac{\partial V_i}{\partial x_j} = e_{ij} + \omega_{ij} \tag{20.9}$$

By multiplying both sides of the above equation by the asymmetric tensor $\frac{1}{2}\varepsilon_{mji}$ we get a vector equation

$$\frac{1}{2}\varepsilon_{mji}\frac{\partial V_i}{\partial x_j} = \frac{1}{2}\varepsilon_{mji}\, e_{ij} + \frac{1}{2}\varepsilon_{mji}\,\omega_{ij} \tag{20.10}$$

Since ε_{mji} is an asymmetric tensor and e_{ij} is a symmetric one, their product is identical to zero. Therefore we are left with the expression for the angular velocity of a rigid body

$$\frac{1}{2}\varepsilon_{mji}\frac{\partial V_i}{\partial x_j} \Rightarrow \frac{1}{2}\nabla \times \bar{V} \Rightarrow \frac{1}{2}\varepsilon_{mji}\,\omega_{ij} = -\frac{1}{2}\varepsilon_{mji}\,\omega_{ji} = \omega_m \Rightarrow \bar{\omega} \tag{20.11}$$

This means that only the asymmetric part

$$\omega_{ij} = \frac{1}{2}\left(\frac{\partial V_i}{\partial x_j} - \frac{\partial V_j}{\partial x_i}\right) \tag{20.12}$$

of the velocity gradient tensor $\partial V_i/\partial x_j$ is related to rigid body rotation (see Section 3.6). In rigid body rotation there is no deformation, while in rigid body translation the velocity gradient is identical to zero. Thus, the remaining symmetric part

$$e_{ij} = \frac{1}{2}\left(\frac{\partial V_i}{\partial x_j} + \frac{\partial V_j}{\partial x_i}\right) \tag{20.13}$$

of the velocity gradient tensor $\partial V_i/\partial x_j$ should account for the deformational motion and is called the rate of deformation or the rate of strain tensor.

To illustrate the physical meaning of the deformation tensor we refer to the shearing motion between two flat plates of Fig.20.1 The fluid is assumed to flow in the x (or 1) direction while the velocity varies in the y (or 2) direction. All components of the rate of deformation tensor vanish except for two, these are

$$e_{12} = \frac{1}{2}\frac{dV_2}{dx_2} = \frac{1}{2}\frac{dv_x}{dy} = \frac{1}{2}\frac{V}{b} \text{ and } e_{21} = \frac{1}{2}\frac{dV_1}{dx_2} = \frac{1}{2}\frac{dv_x}{dy} = \frac{1}{2}\frac{V}{b} \tag{20.14}$$

Thus, we may write

$$e_{ij} = \begin{matrix} 0 & \frac{1}{2}\frac{dv_x}{dy} & 0 \\ \frac{1}{2}\frac{dv_x}{dy} & 0 & 0 \\ 0 & 0 & 0 \end{matrix} = \begin{matrix} 0 & \frac{1}{2}\frac{V}{b} & 0 \\ \frac{1}{2}\frac{V}{b} & 0 & 0 \\ 0 & 0 & 0 \end{matrix} \tag{20.15}$$

This type of flow is called simple shear flow. It should be noted that some authors define the deformation rate tensor e_{ij} without the 1/2 factor.

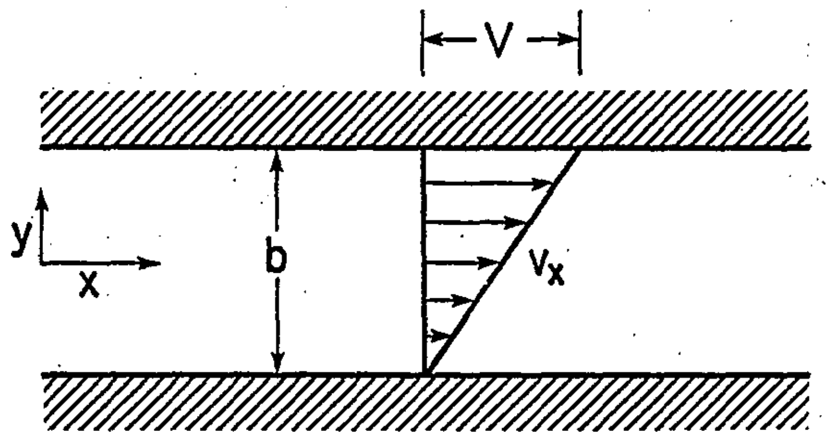

Fig. 20.1 Simple shear flow.

20.3 THE NEWTONIAN CONSTITUTIVE EQUATION

Intuitively we expect that the stress at a point in a flow field should depend on the rate of deformation. Such a relation between dynamic (stresses) and kinematic (rates of deformation) quantities is called a constitutive equation. Truesdell and Toupin [1] and Serrin [2] give excellent presentations on the theory of constitutive equations. Simplified and elegant versions of this theory can be found in the textbooks of Aris [3], Scipio [4] and Whitaker [5].

To formulate the constitutive equation of Newtonian fluids we introduce three postulates.

Postulate I: The stress tensor is a function of the rate of deformation tensor

$$\sigma_{ij} = F_{ij}(e_{mn}) \tag{20.16}$$

This expression represents a tensor function of a tensor. To explain what is meant by this, we note that

(a) a scalar function of a scalar is expressed as, say

$$p = f(T) \tag{20.17}$$

(b) a scalar function of a vector is expressed as, say

$$p = f(x_i) = f(x_1, x_2, x_3) \tag{20.18}$$

(c) a vector function of a vector is expressed as, say,

$$V_i = f_i(x_i) \tag{20.19}$$

or

$$\begin{aligned} V_1 &= f_1(x_1, x_2, x_3) \\ V_2 &= f_2(x_1, x_2, x_3) \\ V_3 &= f_3(x_1, x_2, x_3) \end{aligned} \tag{20.20}$$

and

(d) a tensor function of a tensor represents the functional relations of each component of one tensor with all the components of the other. Since the stress tensor and the rate of deformation tensor are symmetric, only six, rather than nine, components of each are necessary, i.e.

$$\sigma_{ij} = F_{ij}\,(e_{mn}) \tag{20.21}$$

represents the following six functional relations

$$\begin{aligned}
\sigma_{11} &= F_{11}\,(e_{11}, e_{22}, e_{33}, e_{12}, e_{13}, e_{23}) \\
\sigma_{22} &= F_{22}\,(e_{11}, e_{22}, e_{33}, e_{12}, e_{13}, e_{23}) \\
\sigma_{33} &= F_{33}\,(e_{11}, e_{22}, e_{33}, e_{12}, e_{13}, e_{23}) \\
\sigma_{12} &= F_{12}\,(e_{11}, e_{22}, e_{33}, e_{12}, e_{13}, e_{23}) \\
\sigma_{13} &= F_{13}\,(e_{11}, e_{22}, e_{33}, e_{12}, e_{13}, e_{23}) \\
\sigma_{23} &= F_{23}\,(e_{11}, e_{22}, e_{33}, e_{12}, e_{13}, e_{23})
\end{aligned} \tag{20.22}$$

<u>Postulate II:</u> The stress is a linear function of the rate of deformation tensor

$$\sigma_{ij} = A_{ij} + B_{ijmn}\,e_{mn} \tag{20.23}$$

where A_{ij} and B_{ijmn} are second and fourth order tensors respectively, independent of e_{mn} but may be functions at the thermodynamic state of the fluid.

<u>Postulate III:</u> The fluid is isotropic, so that there is no preferred direction.

This means that both A_{ij} and B_{ijmn} should be isotropic tensors. The isotropic tensors of second order are scalar multiples of the Kronecker delta δ_{ij} (see Appendix A).

$$A_{ij} = C_1\,\delta_{ij} \tag{20.24}$$

The most general isotropic tensor of fourth order is given by the expression (see Appendix A)

$$B_{ijmn} = C_2\ \delta_{in}\ \delta_{jm} + C_3\ \delta_{ij}\ \delta_{mn} + C_4\ \delta_{im}\ \delta_{jn} \qquad (20.25)$$

Following the usual notation in the literature we introduce the symbols

$$C_1 = -p, \quad C_2 = \beta, \quad C_3 = \lambda, \quad C_4 = \gamma \qquad (20.26)$$

The physical meaning of these parameters is still to be established.

Therefore, we have

$$\sigma_{ij} = -p\ \delta_{ij} + \beta\ \delta_{in}\ \delta_{jm}\ e_{mn} + \lambda\ \delta_{ij}\ \delta_{mn}\ e_{mn} + \gamma\ \delta_{im}\ \delta_{jn}\ e_{mn} \qquad (20.27)$$

We note that

$$\begin{aligned} \delta_{jm}\ e_{mn} &= e_{jn} \\ \delta_{in}\ e_{jn} &= e_{ji} = e_{ij} \\ \delta_{mn}\ e_{mn} &= e_{kk} \\ \delta_{jn}\ e_{mn} &= e_{mj} \\ \delta_{im}\ e_{mj} &= e_{ij} \end{aligned} \qquad (20.28)$$

Consequently

$$\sigma_{ij} = -p\ \delta_{ij} + \lambda\ \delta_{ij}\ e_{kk} + (\beta + \gamma)\ e_{ij} \qquad (20.29)$$

or by setting $\beta + \gamma = 2\ \mu$

$$\sigma_{ij} = -p\ \delta_{ij} + \lambda\ \delta_{ij}\ e_{kk} + 2\mu\ e_{ij} \qquad (20.30)$$

Introducing the definition for the rate of deformation tensor

$$e_{ij} = \frac{1}{2}\left(\frac{\partial V_i}{\partial x_j} + \frac{\partial V_j}{\partial x_i}\right) \qquad (20.31)$$

we get

$$\sigma_{ij} = -\ p\ \delta_{ij} + \lambda\ \delta_{ij}\ \frac{\partial V_k}{\partial x_k} + \mu\left(\frac{\partial V_i}{\partial x_j} + \frac{\partial V_j}{\partial x_i}\right) \qquad (20.32)$$

In the absence of fluid motion, we have

$$\sigma_{ij} = -\ p\ \delta_{ij} \qquad (20.33)$$

Since the only stress possible in a fluid at rest is the pressure, this should be represented by p.

For an incompressible fluid

$$\nabla\cdot\bar{V} \Rightarrow \partial_k V_k = \frac{\partial V_k}{\partial x_k} = \frac{\partial V_1}{\partial x_1} + \frac{\partial V_2}{\partial x_2} + \frac{\partial V_3}{\partial x_3} = 0 \tag{20.34}$$

and

$$\sigma_{ij} = -p\,\delta_{ij} + \mu\left(\frac{\partial V_i}{\partial x_j} + \frac{\partial V_j}{\partial x_i}\right) \tag{20.35}$$

For the simple shear flow of Fig. 20.1 we have only one velocity component V_1 (or v_x) which varies in the 2 (or y) direction, thus σ_{ij} reduces to

$$\sigma_{21} = \sigma_{yx} = \mu\frac{dV_1}{dx_1} = \mu\frac{dv_x}{dy} \tag{20.36}$$

Consequently, μ is the usual viscosity coefficient of the fluid (or more precisely the coefficient of <u>shear</u> viscosity of the fluid).

Taking the trace of equation (20.32) we have

$$\sigma_{ii} = -3p + (3\lambda + 2\mu)\frac{\partial V_k}{\partial x_k} \tag{20.37}$$

or

$$\frac{1}{3}\sigma_{ii} = -p + (\lambda + \frac{2}{3}\mu)\frac{\partial V_k}{\partial x_k} \tag{20.38}$$

For an incompressible fluid $\partial V_k/\partial x_k = 0$. Thus the pressure is equal to minus the mean normal stress

$$p = -\bar{p} = -\frac{1}{3}\sigma_{ii} = -\frac{1}{3}(\sigma_{11} + \sigma_{22} + \sigma_{33}) \tag{20.39}$$

For a compressible fluid, we have

$$p - \bar{p} = (\lambda + \frac{2}{3}\mu)\frac{\partial V_k}{\partial x_k} = (\lambda + \frac{2}{3}\mu)\,\nabla\cdot\bar{V} \tag{20.40}$$

In Section 3.4, it was shown that

$$\nabla \cdot \bar{V} = \frac{1}{\forall} \frac{d\forall}{dt} \tag{20.41}$$

where $\forall$ is an arbitrary control volume. Thus, we have

$$p - \bar{p} = (\lambda + \frac{2}{3} \mu) \frac{1}{\forall} \frac{d\forall}{dt} = (\lambda + \frac{2}{3} \mu) \frac{d(\ln \forall)}{dt} \tag{20.42}$$

The proportionality constant $\kappa = \lambda + 2/3\ \mu$ is called the coefficient of <u>bulk viscosity,</u> because it represents the resistance to volume deformation. The constant λ is often called the <u>second viscosity coefficient.</u> Stokes [6] assumed that equation(20.39) is also true for a compressible fluid and was led to the conclusion that

$$\kappa = \lambda + \frac{2}{3} \mu = 0 \tag{20.43}$$

This result is in agreement with the kinetic theory of gases (for monatomic gases). For polyatomic gases or liquids this is generally not true. However, very large density changes are necessary for non-zero values of κ. Further details on the relative importance of the viscosity coefficients are given in references [7-13].

Equation (17.32) is often written as

$$\sigma_{ij} = - p\ \delta_{ij} + \tau_{ij} \tag{20.44}$$

or

$$\sigma_{ij} \Rightarrow \begin{matrix} -p + \tau_{11} & \tau_{12} & \tau_{13} \\ \tau_{21} & -p + \tau_{22} & \tau_{23} \\ \tau_{31} & \tau_{32} & -p + \tau_{33} \end{matrix} \tag{20.45}$$

where

$$\tau_{ij} = \lambda \delta_{ij} \frac{\partial V_k}{\partial x_x} + \mu \left(\frac{\partial V_i}{\partial x_j} + \frac{\partial V_j}{\partial x_i}\right) \tag{20.46}$$

is called the deviatoric or viscous stress tensor. If Stokes relation (eq.20.43) is valid, $\lambda = 2/3\ \mu$ (not bad for nearly incompressible fluids), we have

$$\tau_{ij} = \mu \left(\frac{\partial V_i}{\partial x_j} + \frac{\partial V_j}{\partial x_i}\right) - \frac{2}{3} \mu \left(\frac{\partial V_k}{\partial x_x}\right) \delta_{ij} \tag{20.47}$$

This can be written in vector notation as

$$\bar{\bar{\tau}} = \mu \left[(\nabla \bar{V}) + (\nabla \bar{V})^T\right] - \frac{2}{3} \mu (\nabla \cdot \bar{V})\ \bar{\bar{\delta}} \tag{20.48}$$

The components of the viscous stress tensor in rectangular, cylindrical and spherical coordinates are tabulated in Appendix C.

The development of constitutive equations for non-Newtonian fluids is much more difficult. The pressure cannot be defined in the conventional sense for fluids possessing elasticity. The postulate regarding the linearity of the functional relation between stress and the rate of strain tensor is not applicable. These matters are the objective of a branch of engineering science called rheology. To introduce the basic ideas involved, we present some very simplified constitutive equations for non-Newtonian fluids in the next chapter.

REFERENCES

1. C. Truesdell and R.A. Toupin, "The Classical Fluid Theories", S. Flügge (Ed.) in Handbuch der Physik, Bd. VIII/1, Springer Verlag, Berlin (1960).

2. J. Serrin, "Mathematical Principles of Classical Fluid Mechanics", in S. Flügge (Ed.) Handbuch der Physik, Bd. III/1, Springer Verlag, Berlin (1959).

3. R. Aris, "Vectors, Tensors, and the Basic Equations of Fluid Mechanics", Prentice-Hall, Englewood Cliffs, N.J. (1962).

4. L.A. Scipio, "Principles of Continua", Wiley, New York (1967).

5. S. Whitaker, "Introduction to Fluid Mechanics", Prentice-Hall, Englewood Cliffs, N.J. (1968).

6. G.G. Stokes, "On the Theory of the Internal Friction of Fluids in Motion", Trans. Camb. Phil. Soc. No. 8 (1845).

7. C. Truesdell, "The Mechanical Foundations of Elasticity and Fluid Dynamics", J. Ratl. Mech. and Anal. 1, 228-231 (1952).

8. L. Rosenhead, "The Second Coefficient of Viscosity: A Brief Review of Fundamentals", Proc. Roy. Soc. London, A226 1 (1954).

9. G.I. Taylor, "The Two Coefficients of Viscosity for an Incompressible Fluid Containing Air Bubbles", Proc. Roy. Soc., London, A226, 34 (1954).

10. R.O. Davies, "A Note on Sir Geoffrey Taylor's Paper", Proc. Roy. Soc. London, A226, 39 (1954).

11. J. Meixner, "On the Thermodynamic Theory of the Second Viscosity", Proc. Roy. Soc. London, A226, 51 (1954).

12. L.D. Landau and E.M. Lifshitz, "Fluid Mechanics", Pergamon Press, Oxford (1959).

13. S. Eskinazi, "Vector Mechanics of Fluids and Magnetofluids", Academic Press, New York (1967).

John Vlachopoulos, *Fundamentals of Fluid Mechanics*
Chem. Eng., McMaster University, Hamilton, ON, Canada
(First Edition 1984, revised internet edition (2016), www.polydynamics.com)

CHAPTER 21

NON – NEWTONIAN FLOW

21.1 INTRODUCTION

In Chapter 1 we defined Newtonian fluids as those obeying a linear relationship between shear stress and shear rate: $\tau = \mu(du/dy)$. In this chapter, we follow the terminology of most books on rheology [1-16] and we use the Greek letter η instead of μ, $\tau = \eta(du/dy)$, for viscosity. This simple expression was generalized in Chapter 20 to the Newtonian constitutive equation (20.35), for three-dimensional flow fields.

In Section 1.4 we defined as non-Newtonian fluids those that exhibit non-linear stress versus shear rate relationships such as Bingham, pseudoplastic (shear thinning) or dilatant fluids (shear thickening) as shown in Figure 21.1. Actually the term non-Newtonian is broader and the flow phenomena exhibited by non-Newtonian fluids are much more interesting and complex than just the departure from the linearity between stress and shear rate. Liquids with complex structure, such as polymer solutions, polymer melts, suspensions of particles, soap solutions, whole human blood, slurries, pastes etc. behave in unusual ways. The flow behavior of these liquids is the object of the science of rheology [1,16]. Macromolecular (polymeric) solutions and melts exhibit many unexpected flow phenomena and are the most interesting from the rheological point of view. Some of these are explained pictorially in Figs. 21.2(a) to 21.2(f).

Figure 21.2(a) shows the rod-climbing or Weissenberg effect (after the Austrian born physicist Karl Weissenberg 1883-1976). While a Newtonian fluid would have a parabolic depressed surface near a rotating rod (see Section 7.11), polymeric liquids would climb up the rod. Fig.21.2(b) shows the phenomenon of extrudate swell exhibited by polymeric liquids. The diameter of the jet emerging from a tube can increase up to 400% while for Newtonian fluids, like water, it remains approximately the same as the diameter of the tube (actually 13% larger, see Middleman[4]). Fig.21.2(c) shows a siphon experiment. For Newtonian fluids, the siphon works as long as one end of the tube is beneath the surface of the liquid. For polymeric liquids the siphon can work even if the tube end is several centimeters above the liquid surface! Fig.21.2(d) compares the flow pattern for very slow viscous (creeping) flow from a large reservoir into a smaller diameter tube. The polymeric liquid forms a large vortex. Fluid particles trapped in this vortex will circulate continuously and will not move into the small diameter tube. Fig.21.2(e) shows the behavior as the fluids are pumped through tubes. We follow the motion by inserting a streak of dye. Before the motion starts the streak is flat and after starting up the pump, progressively looks like an elongated parabola. When the motion stops (by turning off the pump) the Newtonian fluid comes to rest while the polymeric liquid "recoils". Fig.21.2(f) shows a pressure difference between the inner and the outer tube for annular flow of a

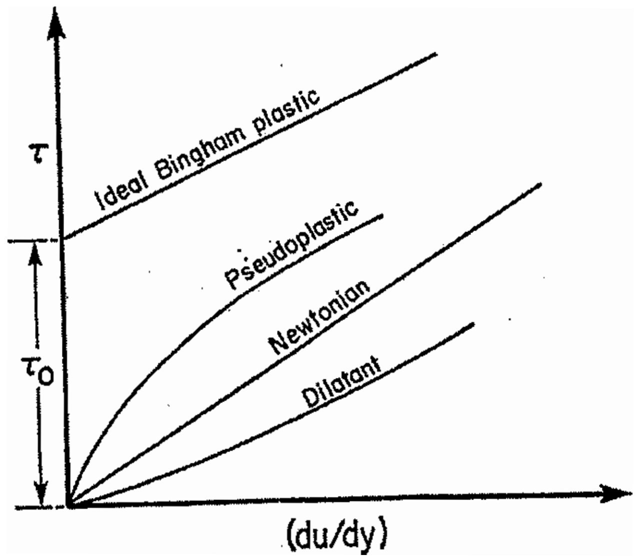

Fig. 21.1 Shear stress (τ) versus shear rate (du/dy) for Newtonian and non-Newtonian fluids

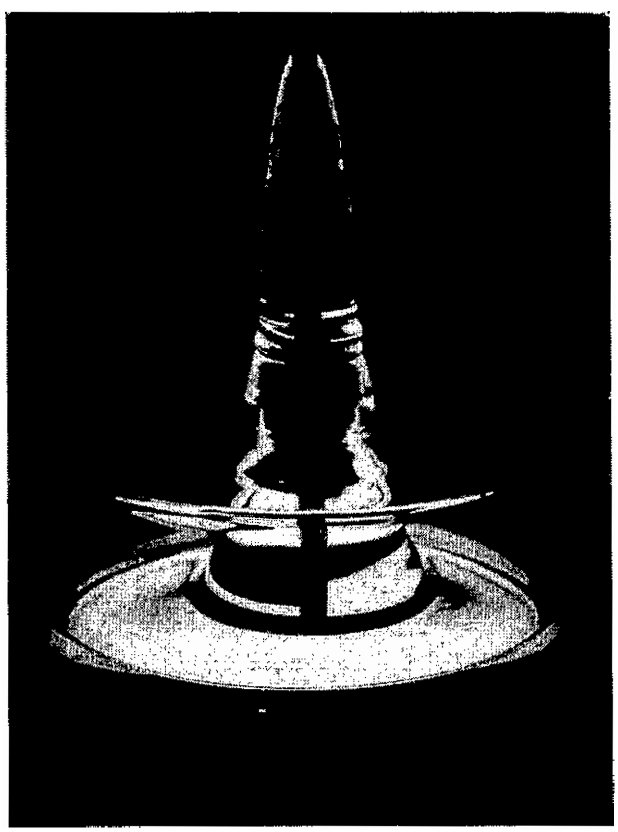

Fig. 21.2(a) Polymeric liquid climbing up a rotating rod (Weissenberg effect) (from reference [11])

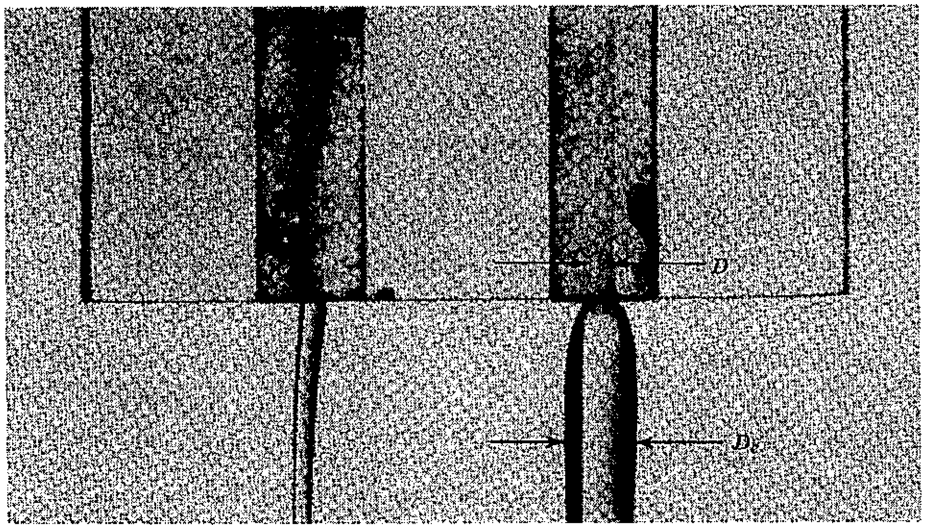

Fig. 21.2(b) Extrudate swell of polymeric liquid emerging from a long tube (from Reference [1]).

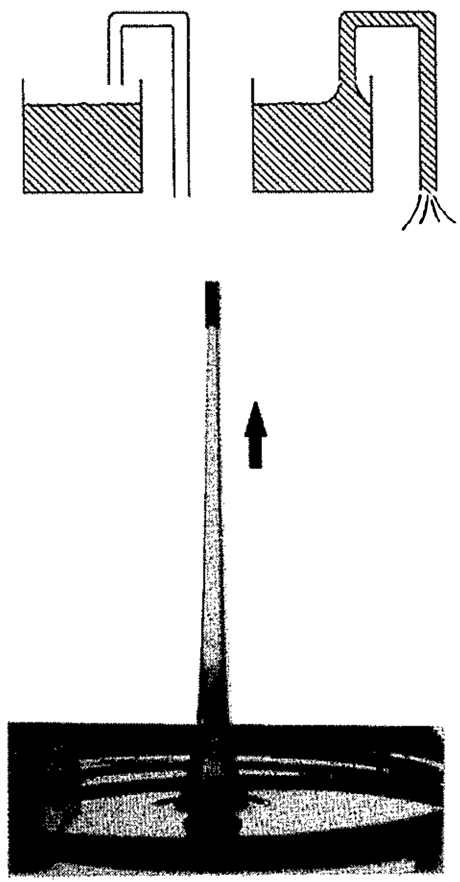

Fig. 21.2(c) Siphon experiment with a polymeric liquid (from Reference [1])

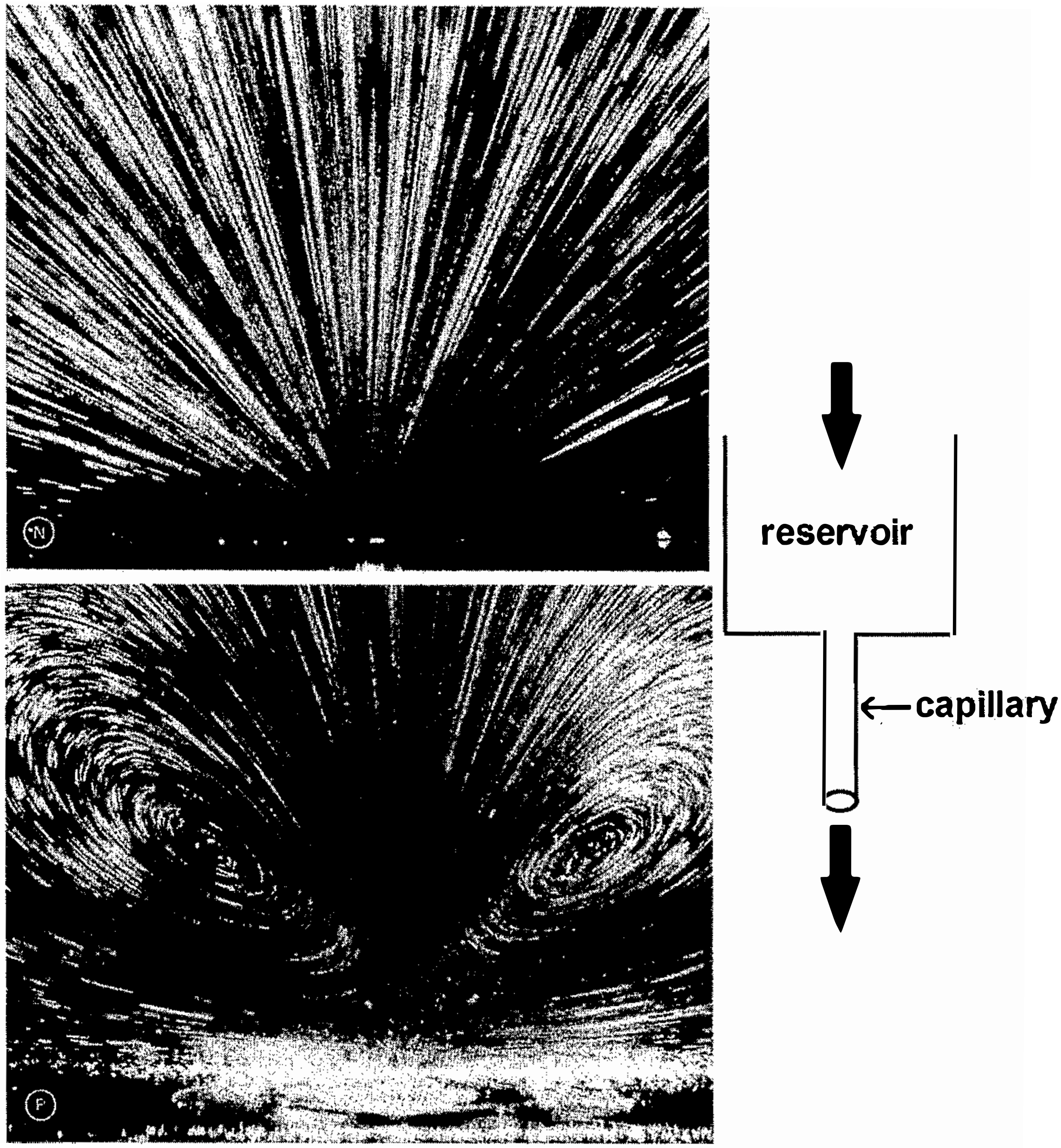

Fig. 21.2(d) Entry from a reservoir into a small diameter (capillary).
Ⓝ Newtonian and Ⓟ Polymeric (from reference [1])

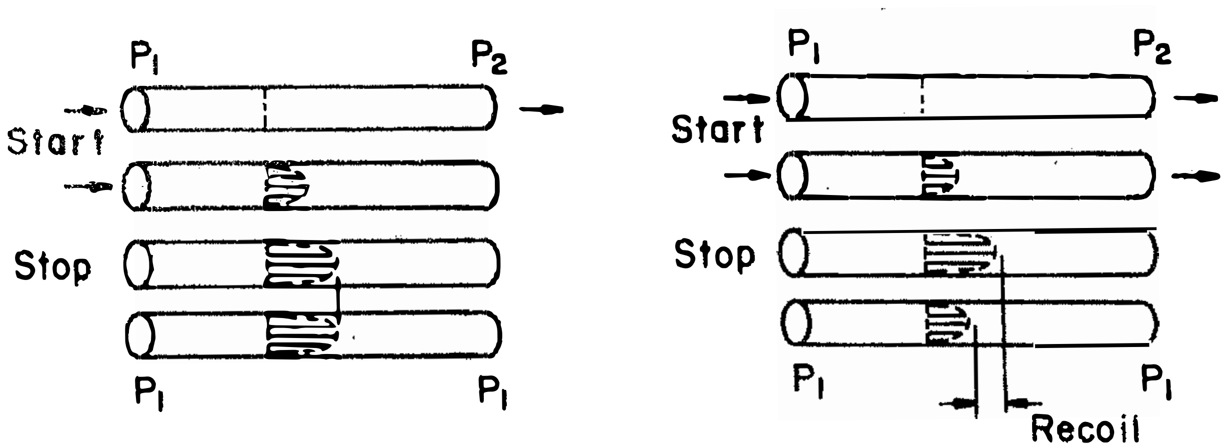

Fig. 21.2(e) Recoil of a polymeric liquid and lack thereof of Newtonian liquid when pumping is stopped (from Reference [10])

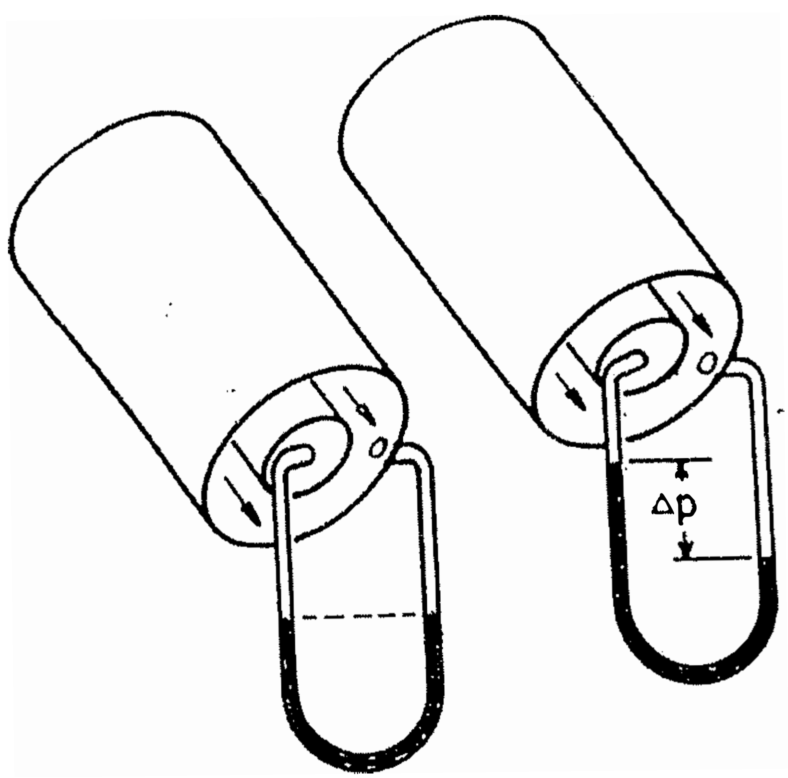

Fig. 21.2(f) Pressure differences during annular flow of Newtonian (left) and polymeric (right) liquids (from Reference [10])

polymeric liquid, while for the same flow field there is no pressure difference for Newtonian flow. For explanations regarding the unusual flow behavior of polymeric liquids the reader is directed to Section 21.12 Viscoelasticity.

To describe mathematically the various effects, we can start from the equations of mass, momentum (and energy, if temperature differences are present). However, it is necessary to introduce complex constitutive equations that relate stresses to the rates of strain.

21.2 VISCOSITY OF SUSPENSIONS

The unexpected non-Newtonian phenomena are due to very complex fluid structure. It is important to point out that even the behavior of a dilute suspension of solid spheres is imperfectly understood. Einstein (see Batchelor [17]) formulated and solved the problem for the determination of resistance to shearing caused by the presence of a single sphere of neutral density. By extending the applicability of the single sphere calculations to a dilute suspension of spheres, Einstein showed that the response remained Newtonian and the viscosity of the suspension is given by

$$\eta = \eta_o\left(1 + 2.5\phi\right) \tag{21.1a}$$

where η_o is the viscosity of the suspending fluid and ϕ the volume fraction occupied by the spheres. This is valid for ϕ up to 1%. For larger values of ϕ, interactions between spheres (or particles in general) become important and non-linearities appear. For higher concentrations the particle-particle interactions are important and Batchelor's equation [17] is valid up to perhaps ϕ=0.2

$$\eta = \eta_o\left(1 + 2.5\phi + 6.2\phi^2\right) \tag{21.1b}$$

In very dilute solutions, particles will rotate due to the action of the shear field. As the concentration is increased, hydrodynamic interactions between the particles become important. Particles come close to particles on nearby streamlines and the fluid is disturbed in their vicinity. As the concentration is further increased, colloidal interactions (of attraction or repulsion) involve three, four or more particles and the rigorous analyses of Einstein and Batchelor no longer apply.

Since the behavior of dilute suspensions of particles is so complex, it can be easily concluded that the description of behavior of concentrated suspensions having different size and shape of particles (e.g. human blood, cement slurries, printing inks) and macromolecular solutions or melts would be a very challenging task.

21.3 SHEAR-THINNING BEHAVIOR OF POLYMERS

In Chapter 1, pseudoplastic fluids were defined those which exhibit decrease in viscosity as the shear rate increases. This property is frequently called shear- thinning. It should not be confused with the term thixotropy, which is the reduction of viscosity with time, due to structural changes. Dilatant fluids were defined those which exhibit increase in viscosity as the shear rate increases. This shear thickening effect should not be confused with rheopexy, which refers to increase of viscosity with time, due to structural changes. Time-dependent fluid effects are beyond the scope of this book.

In Chapter 1, it was pointed out that polymer chains tend to align in the direction of flow and disentangle and they exhibit less resistance to flow as the rate of shearing increases (pseudoplastic or shear-thinning behavior). The apparent viscosity (usually called simply viscosity) was defined as the ratio of shear stress to shear rate

$$\eta = \frac{\tau}{(du/dy)} \tag{21.2}$$

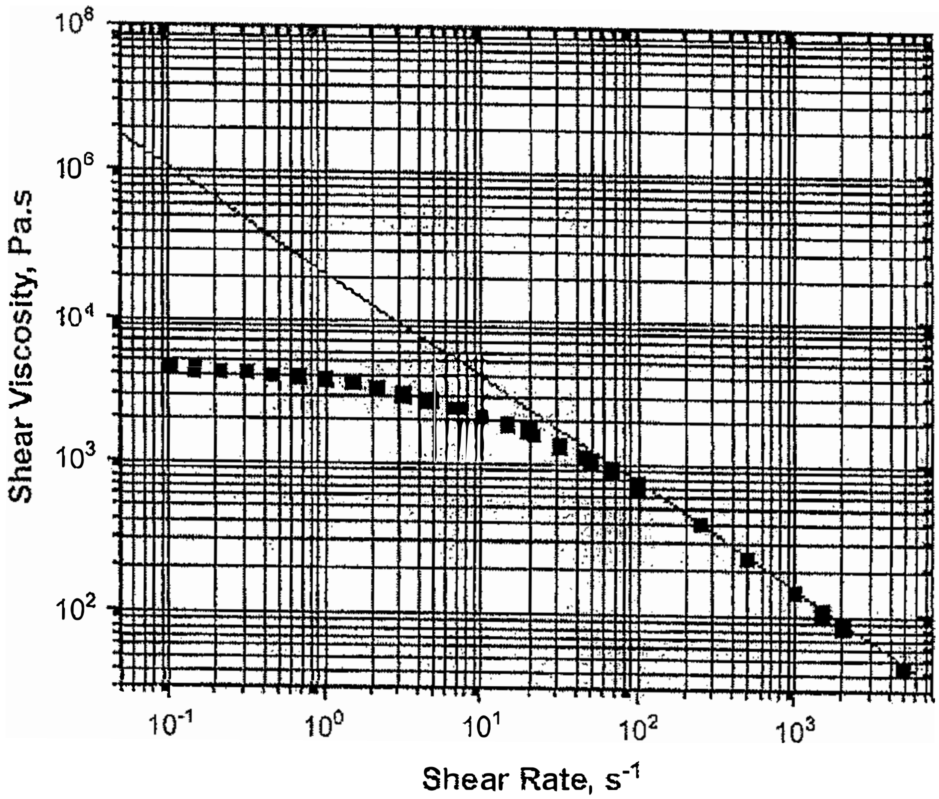

Fig. 21.3 Viscosity as a function of shear rate of a polymer melt. The straight line represents a power-law fit with $m \approx 20{,}000$ Pa·s^n and $n \approx 0.3$

For non-Newtonian fluids the Greek letter η rather than μ is used to designate the viscosity. Fig.21.3 shows a typical polymer melt viscosity curve. We note a Newtonian region at zero shear rate and it is possible to have another Newtonian region at very high shear rates in polymer solutions. The power-law expression (also called Ostwald-de Waele model) gives

$$\tau = m\left(\frac{du}{dy}\right)^n \quad \text{or} \quad \eta = \frac{\tau}{(du/dy)} \Rightarrow \eta = m\left(\frac{du}{dy}\right)^{n-1} = m\dot{\gamma}^{n-1} \tag{21.3}$$

The shear rate is frequently designated with the Greek letter $\dot{\gamma}$, m is a measure of the consistency of the fluid, the larger the m the more viscous the fluid and n (always n<1 for polymer solutions and melts) indicates the degree of non-Newtonian behavior. For n=1 the fluid is Newtonian and the viscosity is constant. As n becomes smaller than unity the shear-thinning behavior is more pronounced.

The power-law relation gives

$$\log\eta = \log m + (n-1)\log\dot{\gamma} \tag{21.4}$$

where $\dot{\gamma}$ is the shear rate. Note that the consistency index m is the viscosity at $\dot{\gamma}=1s^{-1}$ and n-1 is the slope on a log-log graph, as shown in Fig.21.3.

Typical values of the power-law exponent n for some common polymer melts are: Polyethylene 0.3-0.6, Polyvinyl chloride 0.2-0.5, and nylon 0.6-0.9. The consistency index can be in the range m=1,000-100,000 $Pa\cdot s^n$ and it is sensitive to changes in temperature. For the range from 150°C to 250°C, usual in the processing of most polymers, a common representation is

$$m = m_o \exp[-b(T - T_o)] \tag{21.5}$$

where m_o is the consistency index at the reference temperature T_o and b is the temperature coefficient. Typically, b is of the order of 0.01-0.04 K^{-1} for many common polymers implying a reduction of viscosity of roughly between 10% and

35% for a 10°C rise in temperature. Some polymer melts have more temperature sensitive viscosity and b can be as high as 0.1 K^{-1}.

The power-law equation is very useful for many engineering problems involving non-Newtonian fluids, but it has the drawback that it cannot capture the upper or lower Newtonian regions of viscosity. Several other empirical equations have been used that bear the names of their inventors, such as

Ellis: $$\dot{\gamma} = A\tau + B\tau^n \tag{21.6}$$

Powell-Eyring: $$\tau = A\dot{\gamma} + B\sinh^{-1}(C\dot{\gamma}) \tag{21.7}$$

Casson: $$(\tau)^{0.5} = (A)^{0.5} + K\dot{\gamma}^{0.5} \tag{21.8}$$

More recently the Carreau-Yasuda model

$$\frac{\eta - \eta_\infty}{\eta_o - \eta_\infty} = \left[1 + (\lambda\dot{\gamma})^a\right]^{\frac{n-1}{a}} \tag{21.9}$$

and the Cross model

$$\frac{\eta - \eta_\infty}{\eta_o - \eta_\infty} = \frac{1}{\left(1 + \lambda\dot{\gamma}^{n-1}\right)} \tag{21.10}$$

have become very popular for computer simulations of polymeric fluid flows. For a 5% polystyrene solution in Aroclor (see Bird et al [1]), the Carreau-Yasuda model is fitted with

$$\eta_o = 101\,\mathrm{Pa\cdot s} \qquad \eta_\infty = 0.059\,\mathrm{Pa\cdot s} \qquad \lambda = 0.84\,\mathrm{s} \qquad n = 0.380 \qquad a = 2$$

For a polystyrene melt at 180°C

$$\eta_o = 14800\,\mathrm{Pa\cdot s} \qquad \eta_\infty = 0 \qquad \lambda = 1.04\,\mathrm{s} \qquad n = 0.398 \qquad a = 2$$

21.4 POWER-LAW FLUID IN THREE-DIMENSIONAL FLOW

The power-law equation as given above is valid for simple shear flow between two flat plates one of which is moving and the other stationary. The viscosity is simply function of the shear rate

$$\eta = m\left(\frac{du}{dy}\right)^{n-1} = m\dot{\gamma}^{n-1} \tag{21.11}$$

For general three-dimensional flow we can expect that the viscosity would be a function of the strain rate tensor (see Chapter 20)

$$e_{ij} = \frac{1}{2}\left(\frac{\partial V_i}{\partial x_j} + \frac{\partial V_j}{\partial x_i}\right) \tag{21.12}$$

Actually, from the theory of constitutive equations [1-5], it turns out that the viscosity is a function of the so-called second invariant $\left(\frac{1}{2}II\right)$ of the rate of strain tensor.

$$\eta = m\left|\frac{1}{2}II\right|^{\frac{n-1}{2}} \tag{21.13}$$

The function $\frac{1}{2}II$ is given in Table 21.1 in rectangular, cylindrical and spherical coordinates. It can be easily shown (by eliminating all terms equal to zero) that for the case $V_x=V_x(y)$ and $V_y=V_z=0$ we have $\eta = m\left|\frac{dV_x}{dy}\right|^{n-1}$.

To solve problems, we must use the equation of conservation of momentum in terms of stresses and then eliminate any stress terms that are zero. Admittedly, it is harder to work with stresses than with velocity components. A good practice is to check whether the simplified equations for the corresponding Newtonian problem can be obtained after the necessary substitutions and assuming that the viscosity is constant. The solution procedure will become more clear by carefully studying the examples that follow, for unidirectional flow.

21.5 PRESSURE DRIVEN FLOW OF A POWER-LAW FLUID BETWEEN TWO FLAT PLATES

The Newtonian problem was studied in section 7.2. We will solve this problem by starting from the general conservation equations. Again the

Table 21.1

The second invariant of the strain rate tensor $\left(\frac{1}{2}\mathrm{II}\right)$ in rectangular, cylindrical and spherical coordinates.

Rectangular:
$$\frac{1}{2}\mathrm{II} = 2\left[\left(\frac{\partial v_x}{\partial x}\right)^2 + \left(\frac{\partial v_y}{\partial y}\right)^2 + \left(\frac{\partial v_z}{\partial z}\right)^2\right] + \left[\frac{\partial v_y}{\partial x} + \frac{\partial v_x}{\partial y}\right]^2 + \left[\frac{\partial v_z}{\partial y} + \frac{\partial v_y}{\partial z}\right]^2 + \left[\frac{\partial v_x}{\partial z} + \frac{\partial v_z}{\partial x}\right]^2$$

Cylindrical:
$$\frac{1}{2}\mathrm{II} = 2\left[\left(\frac{\partial v_r}{\partial r}\right)^2 + \left(\frac{1}{r}\frac{\partial v_\vartheta}{\partial \vartheta} + \frac{v_r}{r}\right)^2 + \left(\frac{\partial v_z}{\partial z}\right)^2\right] + \left[r\frac{\partial}{\partial r}\left(\frac{v_\vartheta}{r}\right) + \frac{1}{r}\frac{\partial v_r}{\partial \vartheta}\right]^2 + \left[\frac{1}{r}\frac{\partial v_z}{\partial \vartheta} + \frac{\partial v_\vartheta}{\partial z}\right]^2 + \left[\frac{\partial v_r}{\partial z} + \frac{\partial v_z}{\partial r}\right]^2$$

Spherical:
$$\frac{1}{2}\mathrm{II} = 2\left[\left(\frac{\partial v_r}{\partial r}\right)^2 + \left(\frac{1}{r}\frac{\partial v_\vartheta}{\partial \vartheta} + \frac{v_r}{r}\right)^2 + \left(\frac{1}{r\sin\vartheta}\frac{\partial v_\varphi}{\partial \varphi} + \frac{v_r}{r} + \frac{v_\vartheta \cot\vartheta}{r}\right)^2\right] + \left[r\frac{\partial}{\partial r}\left(\frac{v_\vartheta}{r}\right) + \frac{1}{r}\frac{\partial v_r}{\partial \vartheta}\right]^2 + \left[\frac{\sin\vartheta}{r}\frac{\partial}{\partial \vartheta}\left(\frac{v_\varphi}{\sin\vartheta}\right) + \frac{1}{r\sin\vartheta}\frac{\partial v_\vartheta}{\partial \varphi}\right]^2 + \left[\frac{1}{r\sin\vartheta}\frac{\partial \upsilon_r}{\partial \varphi} + r\frac{\partial}{\partial r}\left(\frac{\upsilon_\varphi}{r}\right)\right]^2$$

simplified continuity equation (7.32) is valid

$$\frac{\partial V_x}{\partial x} = 0 \tag{21.14}$$

The x component of the stress form of the equation of conservation of momentum (See Appendix D) simplifies to

$$0 = -\frac{\partial p}{\partial x} + \frac{\partial \tau_{yx}}{\partial y} \tag{21.15}$$

Although $\tau_{xy}=\tau_{yx}$ (stress is a symmetric tensor) we write τ_{yx} in the above equation because the usual convention is that the second index indicates the direction of the stress component and the first index is the direction perpendicular to the plane where the stress component acts. The y component gives again

$$0 = -\frac{\partial p}{\partial y} - \rho g \tag{21.16}$$

and the z component again

$$0 = -\frac{\partial p}{\partial z} \tag{21.17}$$

As in Section 7.2 the pressure gradient is

$$\frac{\partial p}{\partial x} = -\frac{\Delta p}{L} \tag{21.18}$$

Thus equation 21.15 becomes

$$\frac{\partial \tau_{yx}}{\partial y} = -\frac{\Delta p}{L} \tag{21.19}$$

Integration gives

$$\tau_{yx} = -\frac{\Delta p}{L} y + C_1 \tag{21.20}$$

We now introduce the power-law equation in the form

$$\tau_{yx} = m\left|\frac{\partial V_x}{\partial y}\right|^{n-1}\left(\frac{dV_x}{dy}\right) \tag{21.21}$$

The absolute value is necessary for avoiding problems with negative velocity gradient

$$m\left|\frac{\partial V_x}{\partial y}\right|^{n-1}\left(\frac{\partial V_x}{\partial y}\right)=-\frac{\Delta p}{L}y+C_1 \qquad (21.22)$$

Since $\frac{\partial V_x}{\partial y}=0$ at y=0 (symmetry)

$$C_1=0 \qquad (21.23)$$

and by replacing the partial differentiation by an ordinary one, we get

$$m\left|\frac{dV_x}{dy}\right|^{n-1}\left(\frac{dV_x}{dy}\right)=-\frac{\Delta p}{L}y \qquad (21.24)$$

The right hand side is negative and the absolute value of the velocity gradient is raised to the power n-1, therefore $\frac{dV_x}{dy}$ must be negative and may be written as

$$\frac{dV_x}{dy}=-\left(\frac{1}{m}\frac{\Delta p}{L}\right)^{1/n}y^{1/n} \qquad (21.25)$$

This is integrated to give

$$V_x=-\frac{n}{n+1}\left(\frac{1}{m}\frac{\Delta p}{L}\right)^{1/n}y^{(n+1)/n}+C_2 \qquad (21.26)$$

The no-slip condition $V_x=0$ at y=0 gives

$$C_2=-\frac{n}{n+1}\left[\frac{1}{m}\left(\frac{\Delta p}{L}\right)\right]^{1/n}b^{(n+1)/n}$$

Hence the velocity profile is

$$V_x=\left(\frac{n}{n+1}\right)\left[\frac{b^{n+1}}{m}\left(\frac{\Delta p}{L}\right)\right]^{1/n}\left[1-\left(\frac{y}{b}\right)^{\frac{n+1}{n}}\right] \qquad (21.27)$$

The maximum velocity is at y=0

$$V_{max} = \left(\frac{n}{n+1}\right)\left[\frac{b^{n+1}}{m}\left(\frac{\Delta p}{L}\right)\right]^{1/n} \tag{21.28}$$

and the velocity profile can be expressed as

$$V_x = V_{max}\left[1-\left(\frac{y}{b}\right)^{\frac{n+1}{n}}\right] \tag{21.29}$$

The average velocity is

$$V_{avg} = \frac{\iint V_x dzdy}{\iint dzdy} \Rightarrow V_{avg} = \frac{\int_{-b}^{b} V_x dy}{\int_{-b}^{b} dy} \Rightarrow V_{avg} = \frac{n+1}{2n+1}V_{max} \tag{21.30}$$

The volume rate of flow per unit width is

$$\frac{Q}{W} = V_{avg}2b \Rightarrow \frac{Q}{W} = \frac{2n}{2n+1}\left[\frac{1}{m}\frac{\Delta p}{L}\right]^{1/n} b^{\frac{1}{n}+2} \tag{21.31}$$

and the pressure drop

$$\Delta p = mL\left[\frac{2n+1}{2n}\frac{Q}{W}\right]^{n} b^{-(2n+1)} \tag{21.32}$$

where L is the channel length and b the half gap. By setting n=1 we obtain the corresponding results for the Newtonian problem which was treated in Section 7.2. The velocity profile is exactly parabolic for n=1, more flat for n<1 and more elongated for n>1, as shown in Fig.21.4.

21.6 PRESSURE-DRIVEN FLOW OF A POWER-LAW FLUID IN A TUBE

The Newtonian problem was examined in Section 7.3. Again we will solve this problem by starting from the conservation equations which are given in Appendix D.

The continuity equation reduces to

$$\frac{\partial v_z}{\partial z} = 0 \tag{21.33}$$

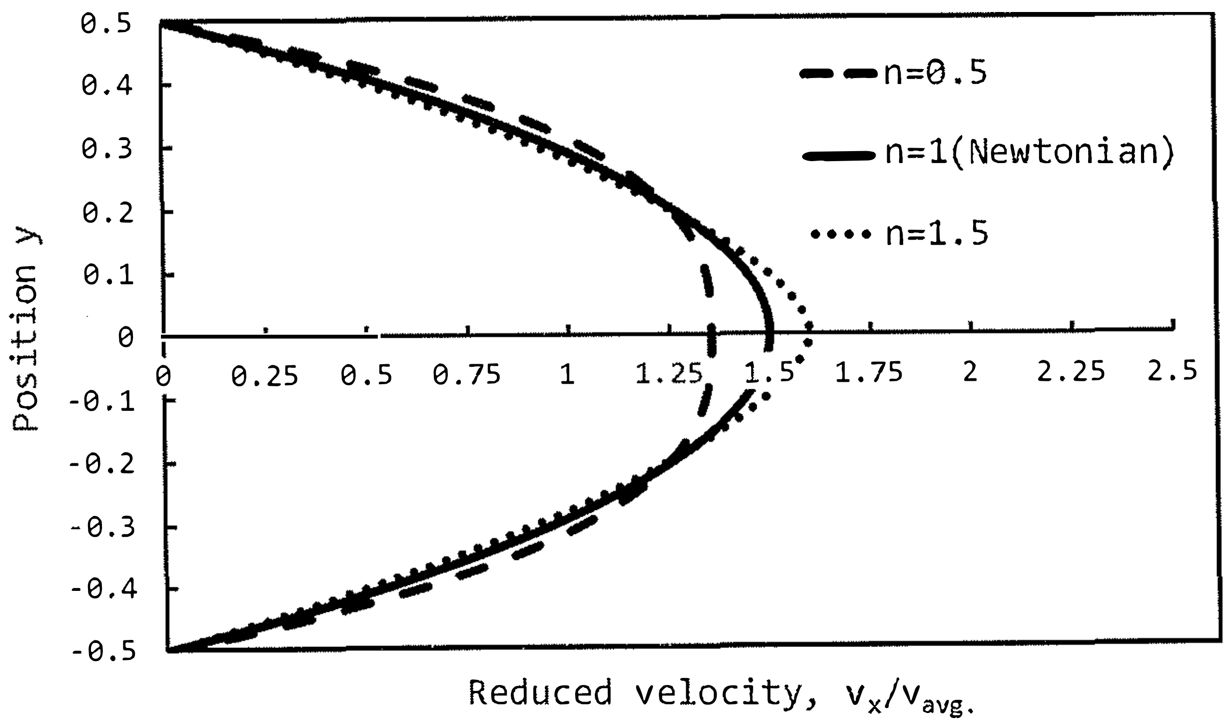

Fig. 21.4 Velocity profiles for power-law fluids flowing under a pressure gradient between two flat plates with n=0.5 (shear thinning), n=1 (Newtonian) and n=1.5 (shear thickening).

The stress form of the equation of conservation of momentum simplifies to

r component $$0=-\frac{\partial p}{\partial r}+\rho g_r \tag{21.34}$$

θ component $$0=-\frac{1}{r}\frac{\partial p}{\partial \theta}+\rho g_\theta \tag{21.35}$$

z component $$0=-\frac{\partial p}{\partial z}+\frac{1}{r}\frac{\partial}{\partial z}\left(r\tau_{rz}\right) \tag{21.36}$$

The r- and θ- components are identical to those for the Newtonian problem (equations 7.74 and 7.75). The z component contains the shear stress term which will be replaced by the power-law equation

$$\tau_{rz}=m\left|\frac{\partial V_z}{\partial r}\right|^{n-1}\frac{\partial V_z}{\partial r} \tag{21.37}$$

We have

$$-\frac{\Delta p}{L}=\frac{1}{r}\frac{\partial}{\partial z}\left(r\tau_{rz}\right) \tag{21.38}$$

Integration gives

$$r\tau_{rz}=-\frac{\Delta p}{2L}r^2+C_1 \tag{21.39}$$

and dividing by r we have

$$\tau_{rz}=-\frac{\Delta p}{2L}r+\frac{C_1}{r} \tag{21.40}$$

C_1 must be zero in order for the shear stress τ_{rz} to remain finite at r=0. Thus

$$\tau_{rz}=-\frac{\Delta p}{2L}r \tag{21.41}$$

Introducing the power-law equation (21.37) we have

$$m\left|\frac{\partial V_z}{\partial r}\right|^{n-1}\frac{\partial V_z}{\partial r}=-\frac{\Delta p}{2L}r \tag{21.42}$$

The right hand side is negative and the absolute value of the velocity gradient is raised to the power n-1, therefore $\frac{\partial V_z}{\partial r}$ must be negative and may be written as

$$\frac{dV_z}{dr} = -\left(\frac{\Delta p}{2mL}\right)^{1/n} r^{1/n} \tag{21.43}$$

By integrating we have

$$V_z = -\frac{n}{n+1}\left(\frac{\Delta p}{2mL}\right)^{1/n} r^{(n+1)/n} + C_2 \tag{21.44}$$

With the help of the no-slip boundary condition $V_z=0$ at $r=R$ we determine the integration constant

$$C_2 = \frac{n}{n+1}\left(\frac{\Delta p}{2mL}\right)^{1/n} R^{(n+1)/n} \tag{21.45}$$

and the velocity profile is

$$V_z = \frac{n}{n+1}\left[\frac{R^{(n+1)}}{2m}\left(\frac{\Delta p}{L}\right)\right]^{1/n}\left[1-\left(\frac{r}{R}\right)^{(n+1)/n}\right] \tag{21.46}$$

The maximum velocity is at $y=0$

$$V_{max} = \frac{n}{n+1}\left[\frac{R^{(n+1)}}{2m}\left(\frac{\Delta p}{L}\right)\right]^{1/n} \tag{21.47}$$

and the velocity profile can be expressed as

$$V_z = V_{max}\left[1-\left(\frac{r}{R}\right)^{(n+1)/n}\right] \tag{21.48}$$

The average velocity is obtained by integrating over the cross-sectional area and then dividing by the cross-sectional area

$$V_{avg} = \frac{\int_0^{2\pi}\int_0^{R} V_z r\,dr\,d\theta}{\int_0^{2\pi}\int_0^{R} r\,dr\,d\theta} \Rightarrow V_{avg} = \frac{n}{(3n+1)}\left[\frac{R^{n+1}}{2m}\left(\frac{\Delta p}{L}\right)^{1/n}\right] \tag{21.49}$$

The volume rate of flow is

$$Q = V_{avg}\pi R^2 = \pi\frac{n}{3n+1}\left[\frac{1}{2m}\left(\frac{\Delta p}{L}\right)\right]^{1/n} R^{\frac{1}{n}+3} \tag{21.50}$$

and the pressure drop

$$\Delta p = 2mLR^{-(3n+1)}\left[\frac{Q}{\pi}\left(\frac{1}{n}+3\right)\right]^n \qquad (21.51)$$

Again, by setting n=1 we obtain the corresponding expressions for Newtonian fluid (Section 7.3). The velocity profiles are similar to those of Figure 21.4. For n=1 we get the parabolic (Newtonian) profile, for n<1 the profile is more blunt and for n>1 more pointed.

21.7 CAPILLARY VISCOMETER ANALYSIS

The most frequently used instrument for the determination of viscosity of polymer melts is the capillary viscometer (schematically shown) in Fig. 21.5. The diameter is typically D=1~2 mm and the length to diameter ratio L/D=16~32.

For Newtonian fluids the relation between pressure drop Δp and flow rate Q is used for measurement of viscosity. For non-Newtonian fluids like polymer melts the viscosity is not constant but a function of the shear rate therefore, in order to use the pressure drop and flow rate measurements, we must be able to express the shear stress and the shear rate in terms of these quantities and then

$$\eta = \frac{\tau}{(du/dy)}$$

From the previous section we can see that the shear stress at the wall can be obtained from

$$\tau_w = -\frac{\Delta p}{2L}R \qquad (21.52)$$

This holds for both Newtonian and non-Newtonian fluids. The shear rate at the wall for Newtonian fluids can be obtained by differentiating equation (7.58) for the velocity profile

$$\dot{\gamma}_w = \left(\frac{dV_z}{dr}\right)_w = \frac{1}{2\mu}\left(\frac{\Delta p}{L}\right)R \qquad (21.53)$$

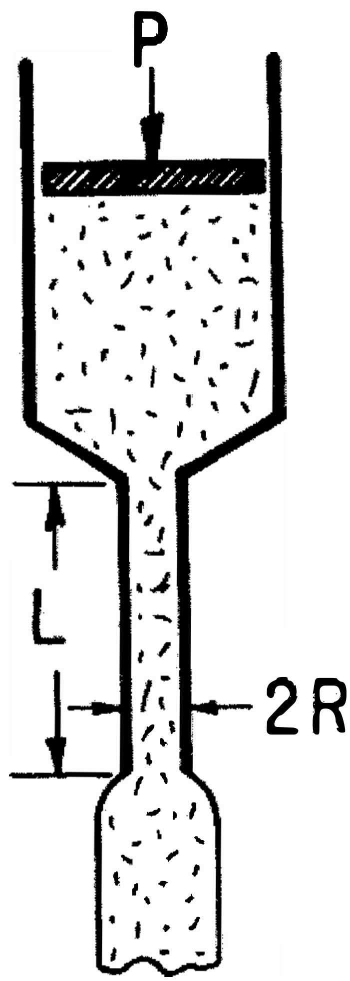

Fig. 21.5 Schematic of a capillary viscometer of diameter D=2R and length L. The polymer is heated and melted in the reservoir and then pushed by the piston through the capillary die, swelling at the exit (from Reference [9])

By using the Hagen-Poiseuille formula (7.61) we have

$$\dot{\gamma}_w = \frac{4Q}{\pi R^3} \tag{21.54}$$

For non-Newtonian fluids we will develop a general expression for the shear rate at the wall by starting from the definition of the volume rate of flow

$$Q = 2\pi \int_0^R r v_z dr \tag{21.55}$$

An integration by parts yields

$$Q = \pi r^2 v_z \Big|_0^R - \int_0^R \pi r^2 \left(\frac{dV_z}{dr}\right) dr \tag{21.56}$$

Applying the "no-slip" boundary condition at R i.e. $V_z=0$ at r=R we have

$$Q = -\pi \int_0^R r^2 \left(\frac{dV_z}{dr}\right) dr \tag{21.57}$$

Since $r/R = \tau_{rz}/\tau_w$ (τ_w is the shear stress at the wall), we can eliminate r from the above expression to get

$$\frac{\tau_w{}^3 Q}{\pi R^3} = \int_0^{\tau_w} \tau_{rz}{}^2 \left(\frac{dV_z}{dr}\right) d\tau_{rz} \tag{21.58}$$

Differentiating both sides with respect to τ_w and using the Leibnitz rule we obtain

$$\left(\frac{dV_z}{dr}\right)_w = \frac{1}{\pi R^3}\left(\tau_w \frac{dQ}{d\tau_w} + 3Q\right) \tag{21.59}$$

Or

$$\dot{\gamma}_w = \frac{4Q}{\pi R^3}\left(\frac{3}{4} + \frac{1}{4}\frac{d\ln Q}{d\ln \tau_w}\right) \tag{21.60}$$

This equation is usually referred to as the Rabinowitsch equation. It gives the shear rate at the wall of a capillary in terms of Q, R and τ_w. The term in brackets may be considered as a "correction" to Newtonian expression which is simply $4Q/\pi R^3$. To obtain $\dot{\gamma}_w$ we must plot Q versus τ_w on logarithmic coordinates to evaluate the derivative $d\ln Q/d\ln\tau_w$

For non-Newtonian fluids that obey the power-law equation

$$\tau = m\dot{\gamma}^{n-1} \tag{21.61}$$

We may write an empirical expression

$$\tau_w = m'\left(\frac{4Q}{\pi R^3}\right)^n \tag{21.62}$$

in which n is the slope of the $\log\tau_w$ versus $\log(4Q/\pi R^3)$ plot, that is

$$n = \frac{d\log\tau_w}{d\log\left(4Q/\pi R^3\right)} \tag{21.63}$$

So, Equation (21.60) may be written as

$$\dot{\gamma}_w = \frac{4Q}{\pi R^3}\left(\frac{3}{4} + \frac{1}{4n}\right) \tag{21.64}$$

Combining equations (21.62) and (21.64) we obtain

$$m = m'\left(\frac{4n}{3n+1}\right)^n \tag{21.65}$$

This means that for a typical polymer melt having n=0.4 the consistency index will be $m = m'\left(\frac{4\times 0.4}{3\times 0.4+1}\right)^{0.4} = 0.88m'$. In other words, the consistency index will be 88% of its value obtained by plotting the shear stress τ_w against the apparent shear rate $(4Q/\pi R^3)$

<u>Example 21.1</u>

(a) What should the load be in kg, in order that a power-law polymer melt with $m=7909\ Pa\cdot s^n$ and n=0.46 flow out of a D_T=3 mm diameter tube (see Fig. E.21.1) so that the wall shear stress is τ_w=0.14 MPa?

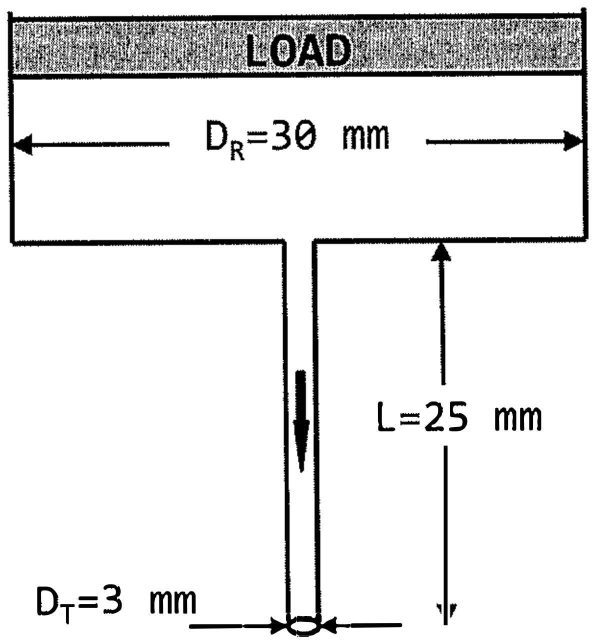

Fig. E.21.1

(b) What is the flow rate (kg/h) and the wall shear rate (s^{-1}) under such conditions? The density of the molten polymer is ρ=766 kg/m^3.

Solution

(a) First, we need to calculate the pressure exerted by the load, using the following equation (Eq. 21.52)

$$\tau_w = -\frac{\Delta p}{2L} R_T$$

As the sign in the above equation is a matter of convention, we use the positive sign which represents stress exerted from the fluid to the wall, so solving with respect to Δp and introducing the numerical values

$$\Delta p = \frac{\tau_w 4L}{D_T} = \frac{\left(0.14 \times 10^6 \mathrm{Pa}\right) \times 4 \times \left(25 \times 10^{-3} \mathrm{m}\right)}{3 \times 10^{-3} \mathrm{m}} = 4.66 \times 10^6 \mathrm{Pa}$$

By neglecting the pressure in the reservoir (because the diameter is very large), the weight m_L of the load can be calculated from

$$\Delta p = \frac{F}{A_R} = \frac{m_L g}{\pi D_R^2 / 4}$$

$$m_L = \frac{\Delta p \cdot \pi D_R^2}{4g}$$

where F is the force the load exerts on the fluid, m_L the load weight, g the gravitational acceleration (g=9.8 m/s^2) and A_R the load cross-sectional area. Introducing the numerical values in the above equation gives

$$m_L = \frac{\left(4.66 \times 10^6 \mathrm{Pa}\right) \times 3.1415 \times \left(30 \times 10^{-3} \mathrm{m}\right)^2}{4 \times 9.8 \mathrm{m/s^2}} = 336 \mathrm{kg}$$

(b) The flow rate can be calculated from Eq. 21.51

$$\Delta p = 2mLR^{-(3n+1)} \left[\frac{Q}{\pi}\left(\frac{1}{n} + 3\right)\right]^n$$

or

$$Q=\left(\frac{\pi}{1/n+3}\right)\left(\frac{R^{3n+1}\Delta p}{2mL}\right)^{\frac{1}{n}}$$

Introducing the numerical values in the above equation gives

$$Q=\left(\frac{3.1414}{1/0.46+3}\right)\left[\frac{\left(1.5\times10^{-3}m\right)^{3\times0.46+1}\times4.66\times10^{6}Pa}{2\times7908Pa\cdot s^{n}\times25\times10^{-3}m}\right]^{\frac{1}{0.46}}$$
$$=1.06\times10^{-6}\frac{m^3}{s}$$

and the mass flow rate will be: $766\frac{kg}{m^3}\times1.06\times10^{-6}\frac{m^3}{s}=2.92\frac{kg}{h}$

The wall shear can be calculated from Eq. 21.64

$$\dot{\gamma}_w=\frac{4Q}{\pi R^3}\left(\frac{3}{4}+\frac{1}{4n}\right)$$

Substituting the numerical values, we obtain

$$\dot{\gamma}_w=\frac{4\times1.06\times10^{-6}\frac{m^3}{s}}{3.1415\times\left(1.5\times10^{-3}m\right)^3}\left(\frac{3}{4}+\frac{1}{4\times0.46}\right)$$
$$=519.72\ s^{-1}$$

21.8 PRESSURE DROP FOR FLOW OF A POWER-LAW FLUID THROUGH A TAPERED TUBE

Truncated conical dies (i.e. tapered tubes like that shown in Fig.21.5) are used very often in processing of molten polymers which, as we have said earlier, are described by the power-law equation satisfactorily. The determination of pressure drop is of primary importance in process equipment design. Here, we will use the results of Section 21.6 to calculate the pressure drop for flow in a slightly tapered tube.

We start from equation (21.51) which is

$$\Delta p=2mLR^{-(3n+1)}\left[\frac{Q}{\pi}\left(\frac{1}{n}+3\right)\right]^{n} \tag{21.66}$$

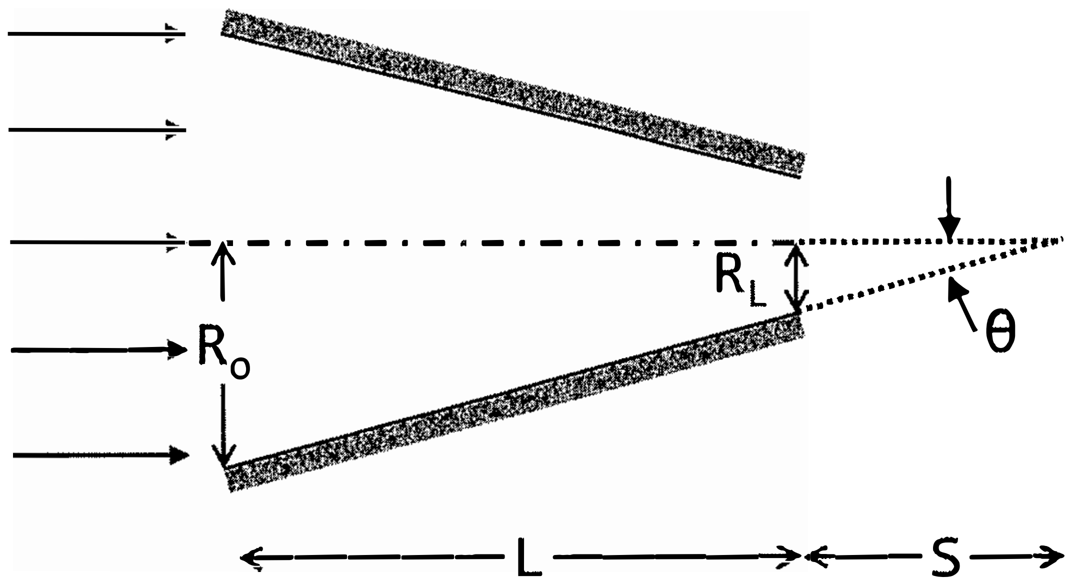

Fig. 21.6 Geometry of a tapered tube of radius R and length L.

Thus, for an infinitesimal tube of length dz we may write

$$dp = 2mR^{-(3n+1)}\left[\frac{Q}{\pi}\left(\frac{1}{n}+3\right)\right]^n dz \tag{21.67}$$

For a tapered tube we may neglect the velocity in the r-direction (small if the taper angle is small) and simply integrate between z=0 and z=L, noting that

$$R = R_o - (R_o - R_L)\frac{z}{L} \tag{21.68}$$

We get

$$\Delta p = p_o - p_L = \frac{2mL}{3n}\left[\frac{Q}{\pi}\left(\frac{1}{n}+3\right)\right]^n\left(\frac{R_L^{-3n} - R_o^{-3n}}{R_o - R_L}\right) \tag{21.69}$$

Further noting that

$$R_o = \frac{(L+S)}{\cot\theta} \qquad \text{and} \qquad R_L = \frac{S}{\cot\theta} \tag{21.70}$$

we may write

$$\Delta p = \frac{2m\cot\theta}{3n}\left[\frac{Q}{\pi}\left(\frac{1}{n}+3\right)\right]^n R_L^{-3n}\left[1-\left(\frac{R_L}{R_o}\right)^{3n}\right] \tag{21.71}$$

This equation gives good results up to half cone angles of 15° (see reference [18]).

21.9 PRESSURE DRIVEN FLOW OF A BINGHAM FLUID IN A TUBE

A Bingham plastic (or more precisely ideal Bingham plastic) which was defined in Chapter 1 will not flow unless the shear stress exceeds a certain value τ_o called yield stress. This behavior is mathematically expressed by

$$\tau_{rz} = \tau_o + \mu_o\frac{dV_z}{dr} \qquad \text{if} \quad \tau > \tau_o \tag{21.72}$$

$$\frac{dV_z}{dy} = 0 \qquad \text{if} \quad \tau \le \tau_o$$

as shown in Fig.21.1. A Bingham plastic is not a “pure” fluid because it does not flow below the yield stress τ_o.

In pressure driven flow in a tube the shear stress is <u>zero along the axis and increases linearly with r</u> as shown in Section 7. Thus the Bingham plastic will behave like a fluid near the tube wall and will move like a solid plug in the center region $r<r_o$ where $\tau \le \tau_o$ as shown schematically in Fig.21.7 The mathematical manipulations of equation 21.6 up to equation (21.41) apply here also. We have

$$\tau_{rz} = -\frac{\Delta p}{2L} r \tag{21.73}$$

Thus, for the wall region $r_o<r<R$

$$\tau_o + \mu_o \frac{dV_z}{dr} = -\frac{\Delta p}{2L} r \tag{21.74}$$

This may be integrated with the no-slip condition at the wall ($V_z=0$ at $r=R$), to give the velocity distribution

$$V_z = \frac{\Delta p}{4\mu L} R^2 \left[1-\left(\frac{r}{R}\right)^2\right] - \frac{\tau_o R}{\mu_o}\left[1-\left(\frac{r}{R}\right)\right] \qquad r_o<r<R \tag{21.75}$$

At $r=r_o$ this will be equal to the plug velocity

$$V_{plug} = \frac{\Delta p}{4\mu L} R^2 \left[1-\left(\frac{r_o}{R}\right)^2\right] - \frac{\tau_o R}{\mu_o}\left[1-\left(\frac{r_o}{R}\right)\right] \tag{21.76}$$

Also, from equation 21.73 we have

$$\text{at } r=r_o, \qquad \tau_o = -\frac{\Delta p}{2L} r_o \qquad \text{and at } r=R, \qquad \tau_w = -\frac{\Delta p}{2L} R \tag{21.77}$$

Eliminating r_o and $(\Delta P/2L)R$, we get

$$V_{plug} = \frac{\tau_w}{2\mu_o} R \left[1 - \frac{\tau_o}{\tau_w}\right]^2 \tag{21.78}$$

The total volume rate of flow is equal to the sum of the “plug” and the “fluid” regions

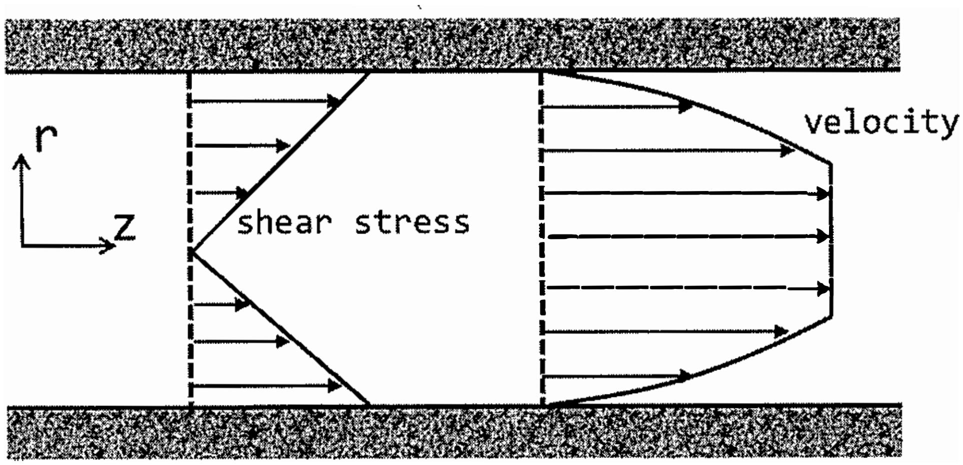

Fig. 21.7 Shear stress and velocity profile for a Bingham fluid flowing between two flat parallel plates under the influence of a pressure gradient. In the central portion the fluid moves like a solid plug.

$$Q = Q_{plug} + Q_{fluid} = \pi r_o^2 V_{plug} + 2\pi \int_{r_o}^{R} V_z r dr \tag{21.79}$$

Inserting equation (21.75) into the integral, integrating and using the expressions for τ_o, τ_w and V_{plug} we have

$$Q = \frac{\pi R^3 \tau_w}{4\mu_o L}\left[1 - \frac{4}{3}\left(\frac{\tau_o}{\tau_w}\right) + \frac{1}{3}\left(\frac{\tau_o}{\tau_w}\right)^4\right] \tag{21.80}$$

21.10 EXTENSIONAL (or ELONGATIONAL) VISCOSITY

We consider the uniaxial stretching of a cylinder of fluid as shown in Fig. 21.8. Of course, stretching of a liquid like water is difficult to visualize. However, molten polymers have considerable melt strength and can be stretched a lot without breaking. In fact, this property enables the production of synthetic fibers for fabrics, clothing, ropes, and other products.

As the cylinder is elongated in the x-direction it will contract in the y- and z-directions. If the stretch rate is

$$\frac{\partial V_x}{\partial x} = \dot{\varepsilon} \tag{21.81}$$

then the contraction in the other two directions will be

$$\frac{\partial V_y}{\partial y} = \frac{\partial V_z}{\partial z} = -\frac{1}{2}\dot{\varepsilon} \tag{21.82}$$

So that the equation of continuity will be satisfied ($\nabla \cdot \overline{V} = 0$)

$$\frac{\partial V_x}{\partial x} + \frac{\partial V_y}{\partial y} + \frac{\partial V_z}{\partial z} = 0 \tag{21.83}$$

$$\dot{\varepsilon} - \frac{1}{2}\dot{\varepsilon} - \frac{1}{2}\dot{\varepsilon} = 0 \tag{21.84}$$

The stretch (or elongation or extension) rate for a rod of length L that is stretched at a velocity V is

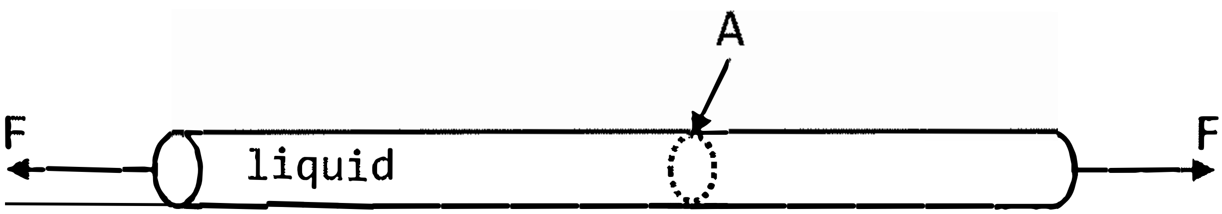

Fig. 21.8 Stretching of a liquid cylinder

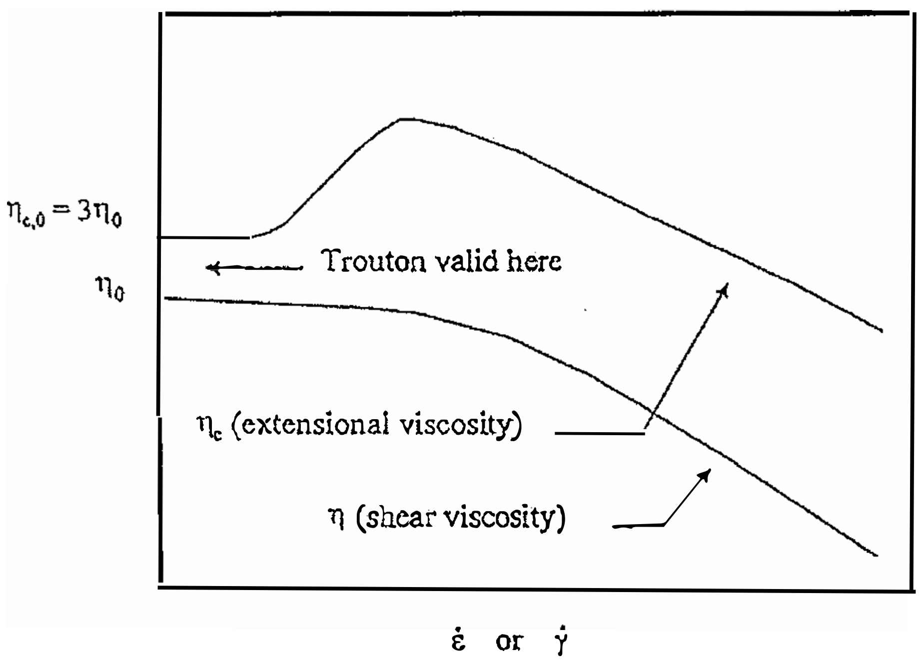

Fig. 21.9 Extensional (elongational) viscosity η_e as a function of stretch rate and shear viscosity η as a function of shear rate.

$$\dot{\varepsilon} = \frac{\partial V_x}{\partial x} = \frac{V}{L} = \frac{1}{L}\frac{dL}{dt} \tag{21.85}$$

In a manner analogous to the definition of shear viscosity we define the extensional (elongational) viscosity as the ratio of the stretching stress to the stretch rate i.e.

$$\eta_e = \frac{\sigma_{11}}{\dot{\varepsilon}} = \frac{F/A}{\dot{\varepsilon}} \tag{21.86}$$

where F is the force and A is the cross-sectional area of the cylinder. As explained in Chapter 1, the ordinary (shear) viscosity μ (η in this chapter) represents the resistance to shearing. The elongational viscosity represents resistance to extension (stretching). Since both quantities represent resistance to flow (shearing in one case and stretching in the other) the question might be asked how η and η_e are related.

Starting from the Newtonian constitutive equation (see chapter 20) we have for the total stress tensor

$$\sigma_{ij} = -p\delta_{ij} + \tau_{ij} \tag{21.87}$$

where p is the pressure, δ_{ij} the Kronecker delta and τ_{ij} the viscous stress tensor. Alternatively

$$\sigma_{ij} = -p\delta_{ij} + 2\eta e_{ij} \tag{21.88}$$

where $e_{ij} = \frac{1}{2}\left(\frac{\partial V_i}{\partial x_j} + \frac{\partial V_j}{\partial x_i}\right)$, which gives

$$\sigma_{11} = -p + 2\eta\frac{\partial V_x}{\partial x} \tag{21.89}$$

$$\sigma_{22} = -p + 2\eta\frac{\partial V_y}{\partial y} \tag{21.90}$$

$$\sigma_{33} = -p + 2\eta\frac{\partial V_z}{\partial z} \tag{21.91}$$

Summing up we get

$$\sigma_{11} + \sigma_{22} + \sigma_{33} = -3p + 2\eta\left(\frac{\partial v_x}{\partial x} + \frac{\partial v_y}{\partial y} + \frac{\partial v_z}{\partial z}\right) \tag{21.92}$$

The quantity in the parenthesis is equal to zero (continuity equation $\nabla \cdot \overline{V} = 0$ for incompressible fluids). Thus

$$p = -\frac{\sigma_{11} + \sigma_{22} + \sigma_{33}}{3} = -\frac{\sigma_{ii}}{3} \tag{21.93}$$

For the uniaxial stretching experiment of Fig.21.7 we have $\sigma_{22}=0$, $\sigma_{33}=0$ and from equations 21.89 and 21.93

$$p = -\frac{\sigma_{11}}{3} \tag{21.94}$$

$$\frac{2}{3}\sigma_{11} = 2\eta\frac{\partial v_x}{\partial x} = 2\eta\dot{\varepsilon} \tag{21.95}$$

Thus

$$\eta_e = \frac{\sigma_{11}}{\dot{\varepsilon}} = 3\eta \tag{21.96}$$

Therefore the elongational viscosity is equal to three times the shear viscosity for Newtonian fluids. This is known as the Trouton relation [2,7].

The (shear) viscosity of polymeric liquids is a function of shear rate and usually obeys a power-law relation in the form

$$\eta = m\dot{\gamma}^{n-1} \tag{21.96}$$

where usually 0.2<n<0.8 except a Newtonian plateau at very low-shear rates. The elongational viscosity for very low stretch rates $\left(\dot{\varepsilon} < 10^{-3}\right)$ obeys the Trouton relation, exhibits a maximum and drops as a power-law function as shown in Fig.21.9

$$\eta_e = L\dot{\varepsilon}^q \tag{21.97}$$

Usually n<q<1.0 which means that stretch "weakening" is less prominent than shear thinning.

The elongational viscosity of polymeric liquids at high stretch rates is many times larger than the corresponding shear viscosity. It is a material property in its own sake and should be measured independently (see for example reference [7]).

21.11 FLOW IN A SUDDEN CONTRACTION

Flow from a large reservoir into a small diameter tube is encountered in practice very frequently and it is perhaps the most extensively studied problem in rheology. We consider the axisymmetric sudden contraction problem as shown in Fig.21.10 The Reynolds number is assumed to be very small (creeping flow). Fluid inertia is negligible and the flow is determined by the balance of viscous and pressure forces. Under these conditions Newtonian fluids exhibit a very small and weak vortex at the corner as shown in Fig.21.10. In fact the corner vortex is weak and the fluid within the vortex is so slow that led some people in the past, to believe that it was a region of stagnant fluid. On the other hand, polymeric liquids for the same low Reynolds number (e.g. Re = 10^{-3}–10^{-4}) as shown in Fig.21.2d exhibit very large and strong vortices. The vortex size and strength depends on the elongational viscosity of polymeric liquids.

Another difference between Newtonian and polymeric fluids is in the pressure drop. Within the reservoir or the small diameter outlet tube of Fig.21.11 the pressure drop is linear. At the tube entry there is an additional pressure drop which is small for Newtonian fluids and large for polymer solutions or melts. The vortex, the entrance and the (relatively small) exit pressure at can be determined [2, 12] by solving numerically the creeping flow equations

$$\nabla \cdot \overline{V} = 0 \tag{21.99}$$

$$0 = -\nabla p + \nabla \cdot \overline{\overline{\tau}} \tag{21.100}$$

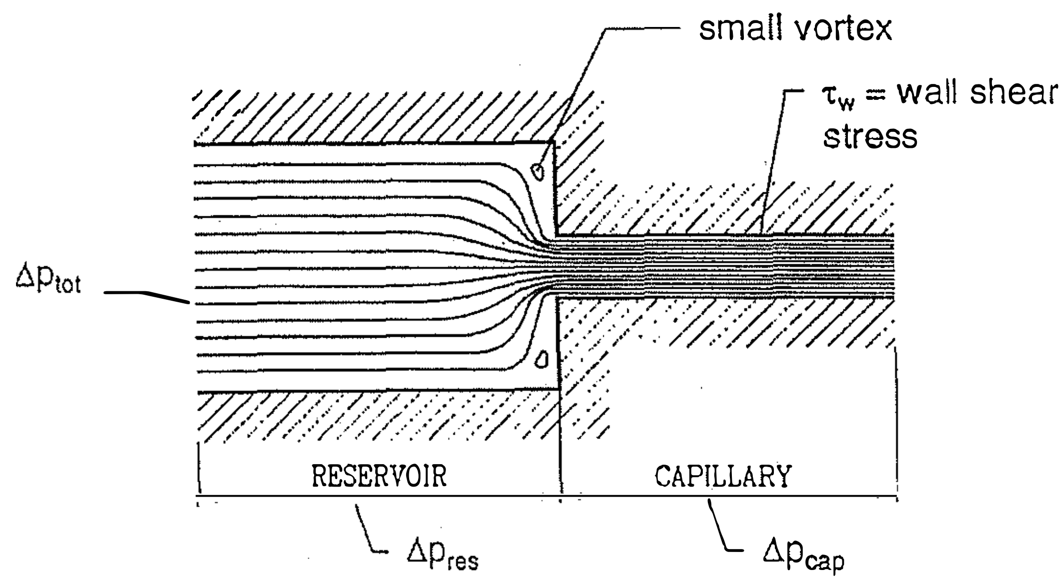

Fig. 21.10. Newtonian entrance flow into a capillary

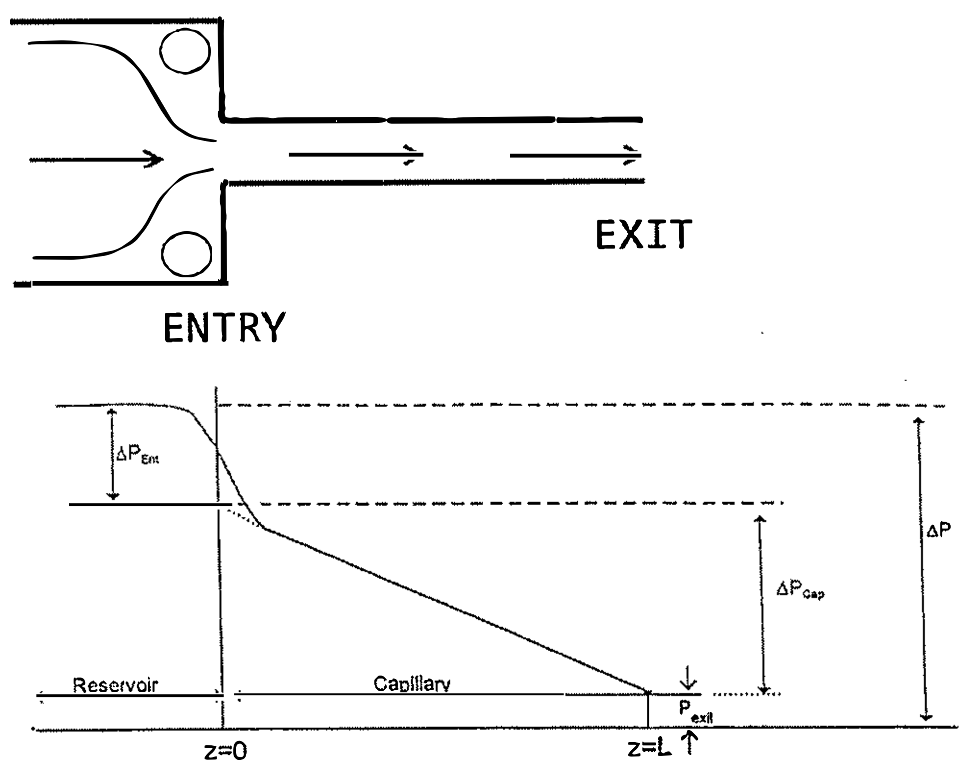

Fig. 21.11 Polymeric liquid entrance vortex and pressure drops at entry and exit

The calculated excess pressure drop is equal to the total pressure drop minus the (linear) pressure drop in the reservoir for Poiseuille flow minus the same for the small diameter (capillary) tube i.e.

$$\Delta p_e = (\Delta p)_{tot.} - (\Delta p)_{res.} - (\Delta p)_{cap.} \tag{21.101}$$

$(\Delta p)_{tot.}$ is determined from the numerical solution of the conservation equations (21.99) and (21.100). $(\Delta p)_{res.}$ and $(\Delta p)_{cap.}$ are determined from the Poiseuille flow equations (see Section 21.6).

The large excess pressure drop at the entrance for polymeric liquids is apparently due to large elongational viscosities exhibited by these substances. Entry flow is mainly elongational in character. Fluid elements are stretched as they enter from a large reservoir into a small diameter tube. Obviously, this stretching is resisted by the fluid elongational viscosity, which is relatively small for Newtonian fluids (3η) and large for polymers (from 3η to more than 100η at very high stretch rates). When the elognational viscosity is very large a portion of the fluid is obstructed from entering and a flow recirculation region (vortex) is formed.

The excess pressure drop at the entry, which is also called entrance loss, is usually expressed in dimensionless form as

$$\eta_B = \frac{\Delta p_e}{2\tau_w} \tag{21.102}$$

(where τ_w is the shear stress at the wall of the outlet tube) and is known as the Bagley correction in capillary viscometry [7,12].

For Newtonian fluids accurate finite element simulations [2] give

$$\eta_B = \frac{\Delta p_e}{2\tau_w} = 0.587 \tag{21.103}$$

For polymer melts measurements range from the Newtonian value at low shear rates to about n_B=20. Finite element simulations of polymer melt flow in abrupt contraction is a challenging task and the reader is referred to specialized textbooks [2,12] and publications [19].

21.12 VISCOELASTICITY

The response of polymeric liquids to an imposed stress may, under certain conditions, resemble behavior of a solid, in addition to the non-linear dependence of stress on shear rate. These liquids are composed of very long molecular chains of molecular weight usually in the range of 10,000 to 10,000,000 with many commercial products being in the range of 50,000 to 500,000.

When these liquids are at rest, the molecular chains are randomly distributed. When an external stress is applied, the intermolecular bonds are stretched, the chains commence to flow past another, to disentangle and to align in the direction of the flow. However, for these processes to occur certain time is required. On the other hand, the response of small molecular weight liquids, like water, can be instantaneous. From molecular arguments it can be estimated that steady shearing can be established in water in about 10^{-12} seconds and, of course mechanical instruments would have a much larger response time, so it is impossible to measure directly that constant. With polymeric liquids we can measure characteristic response times usually in the range of 10^{-2} to 10^{2} s (the lower values for solutions and the higher for melts).

It is apparent that time constants are necessary to describe the behavior of polymer melts and solutions. Reiner [20] used the biblical expression that "mountains flowed in front of the God" to name as the <u>Deborah Number</u> the ratio of a characteristic material time (λ) to a characteristic experiment or process time (θ)

$$De=\frac{\lambda}{\theta}=\frac{\text{material time}}{\text{process time}} \tag{21.104}$$

Let us choose a typical polymer melt with a characteristic time λ=1s. If the process time is very large ($\theta \to \infty$ and $De \to 0$) the material will behave like a fluid. However, when the process time is very short $\theta \to 0$ and $De \to \infty$ the polymer melt will behave like a solid. Many polymer processing operations require times comparable to the characteristic material times. For example, in polymer shaping and forming operations, the passage through a die or filling of a mold may take place in 0.1 to 10 seconds and De might be in the range of 1-10. Consequently, the polymer melt behavior will have both fluid (viscous) and solid (elastic) characteristics and it is said to be viscoelastic.

To study the behavior of viscoelastic materials, we must develop mathematical models (called constitutive equations, which are much more complicated than the Newtonian version of Chapter 20) that describe such behavior. The simplest of them involves a simple combination of a Newtonian fluid and an elastic (Hookean) solid.

For the Newtonian fluid we have a linear relation between stress (τ) and rate of strain ($\dot{\gamma}_f$)

$$\tau=\eta\dot{\gamma}_f \tag{21.105}$$

where η is the viscosity.

For the elastic (Hookean) solid we have a linear relation between stress (τ) and the strain (γ_s)

$$\tau=G\gamma_s \tag{21.106}$$

where G is the modulus of elasticity.

We assume that the combined material will have a shear rate equal to the sum of the two shear rates

$$\dot{\gamma}=\dot{\gamma}_f+\dot{\gamma}_s \tag{21.107}$$

or

$$\dot{\gamma}=\frac{\tau}{\eta}+\frac{\dot{\tau}}{G} \tag{21.108}$$

$$\tau+\frac{\eta}{G}\dot{\tau}=\eta\dot{\gamma} \tag{21.109}$$

The ratio η/G has dimensions of time and is usually denoted by λ

$$\tau+\lambda\dot{\tau}=\eta\dot{\gamma} \tag{21.110}$$

This mathematical model is referred to as a Maxwell fluid.

Actually, it is easier to understand the behavior of this mathematical model by referring to the mechanical analogue of Fig.21.12. The spring represents the Hookean solid $\left(\tau=G\gamma_s\right)$ and the dashpot the Newtonian liquid $\left(\tau=\eta\dot{\gamma}_f\right)$.

Let us assume that the mechanical model of Fig.21.11 is suddenly extended to a position and held there. This means that we impose a constant extension (strain γ=const) and therefore $\dot{\gamma}=0$

Equation (21.110) becomes

$$\tau+\lambda\dot{\tau}=0 \tag{21.111}$$

or

$$\tau+\lambda\frac{d\tau}{dt}=0 \tag{21.112}$$

$$\frac{d\tau}{\tau}=-\frac{dt}{\lambda} \tag{21.113}$$

$$\tau=C_1e^{-t/\lambda} \tag{21.114}$$

Let τ=S at t=0

$$\frac{\tau}{S}=e^{-t/\lambda} \tag{21.115}$$

We see that for t=λ

$$\frac{\tau}{S}=e^{-1}=\frac{1}{e}=0.37 \tag{21.116}$$

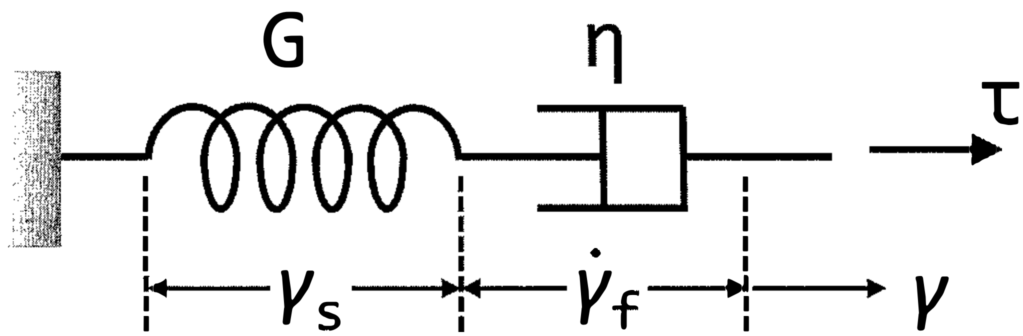

Fig. 21.12. A mechanical contraption representing the Maxwell fluid model.

Thus, λ represents the time for the stress to decay by a factor 1/e=0.37 and is called the relaxation time. The physical meaning of this quantity can be better understood by referring to the mechanical analogue of Fig.21.12. If we impose a sudden extension and stop the spring will respond instantaneously. However, the stress will be relaxed gradually (exponentially) as the dashpot will start moving. Given enough time the stress will become zero.

This model is too crude to represent quantitatively the stress relaxation behavior of polymeric liquids, but it gives a good qualitative picture. The sudden stop of extension and subsequent relaxation of the mechanical model corresponds to the following fluid flow experiment: Assume that a polymeric liquid is sheared in a concentric cylinder viscometer, like that of Fig.21.13. If the rotation is suddenly stopped i.e. $\dot{\gamma} = 0$ the measured stress will not become instantaneously zero (as for Newtonian fluids) but will decay in an exponential-like manner as shown in Fig.21.14.

The relaxation behavior is not the only unusual time response for polymeric liquids. If we start suddenly shearing from rest a Newtonian fluid will respond instantaneously, while a polymer solution or melt will exhibit an overshoot as shown in Fig.21.15.

Under shearing the long molecular chains can be thought of as acting as springs or rubber bands. By shearing, the springs are stretched around a rotating shaft in Fig.21.2a and exert a contraction force toward the axis of the rotation like a "strangulation" [10] which forces the fluid towards the axis. This results in the rod climbing, or Weissenberg effect. Similarly, when a polymeric liquid exits from a tube (Fig.21.2b) the "springs" which are extended inside the tube, contract and this causes the phenomenon of extrudate swell. The contraction of fluid elements which is responsible for the characteristic "puff up", can also be thought of as originating from the relaxation of the viscoelastic forces at the exit.

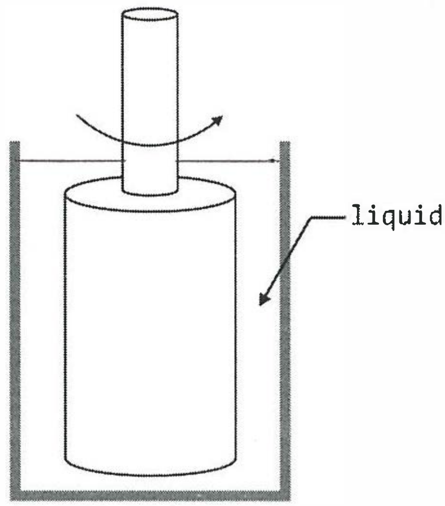

Fig. 21.13. Coaxial cylinder viscometer

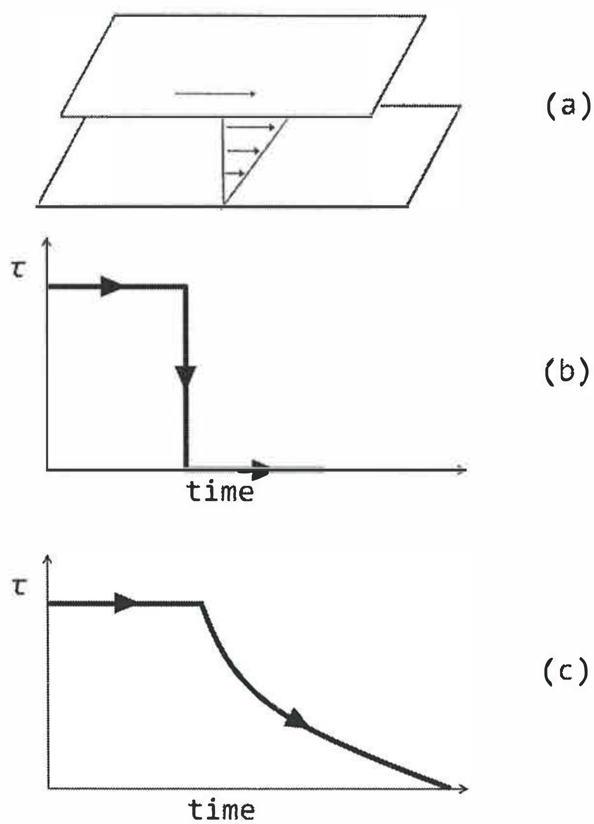

Fig. 21.14. Stress relaxation after (a) shear flow cessation (b) Newtonian and (c) polymeric liquid (viscoelastic).

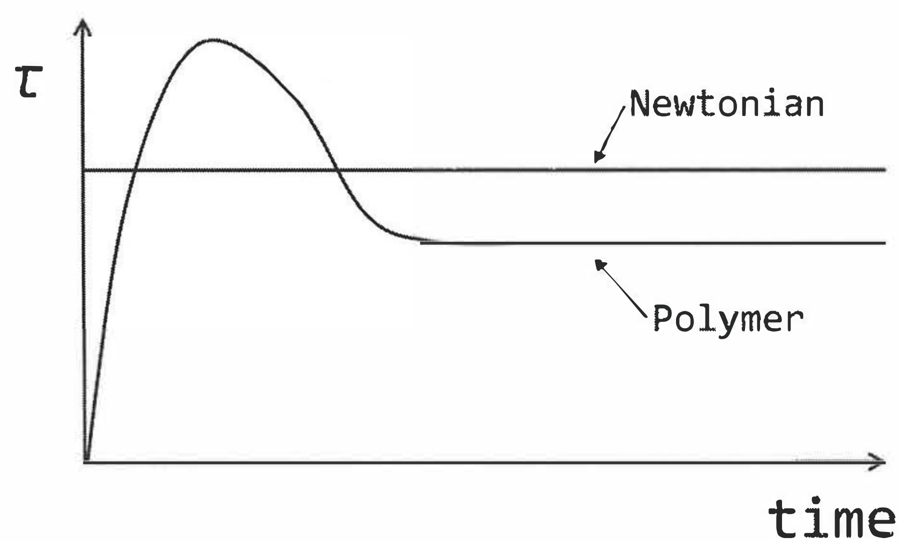

Fig. 21.15. Stress “overshoot” at flow start-up.

The pressure difference between the inner and outer cylinder in steady axial flow in an annulus (Fig.21.2f) is due to development of stresses that do not exist in Newtonian fluids. These stresses which are developed in viscoelastic fluids under shear in directions normal to the direction of flow are called normal stresses. They increase with shear rate and disappear when the fluid is at rest. The simple molecular picture given earlier, that of stretched springs or rubber bands, is too crude to present reality. There is, of course, some stretching of the macromolecular chains during shear, but also disentaglements and other interactions. There is a great variety of polymer types some of them of equal size chains (monodisperse), other of different size (polydisperse), yet others with branches (short or long) and molecular weights ranging from a few thousand to several million. The development of an accurate description of the various processes at the molecular level during shear or other deformation is an extremely daunting task. We will adopt the continuum mechanics approach and will consider only the stresses developed and the balance of the corresponding forces.

Whenever a polymeric liquid is sheared as shown in Fig.21.16, normal stresses are developed because shearing results also in extension in the x-direction and compression in the y- and z-directions. A measuring device would record the total normal stresses i.e. there will be contributions from both the static pressure in the fluid and the normal stresses developed due to shear. Following the convention adopted in Section 6.3 that pressure forces are compressive and therefore negative, we may write the total stresses as

$$\sigma_{11} = -p + \tau_{11} \tag{21.117}$$

$$\sigma_{22} = -p + \tau_{22} \tag{21.118}$$

$$\sigma_{33} = -p + \tau_{33} \tag{21.119}$$

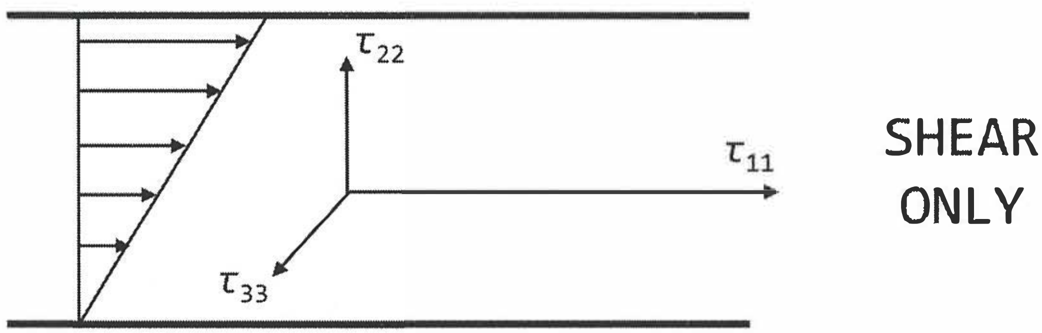

τ_{11}-τ_{22}=N_1 (first NORMAL stress Diff.)

τ_{22}-τ_{33}=N_2 (second NORMAL stress Diff.)

Fig. 21.16. Simple shear flow of a polymeric liquid between two flat parallel plates.

Measurements of σ_{11}, σ_{22} and σ_{33} will not be useful in assessing the elasticity level of the fluid because the pressure p can be set arbitrarily from anexternal source (e.g. pump). To eliminate the contribution of pressure we take the differences

$$N_1 = \sigma_{11} - \sigma_{22} = (-p + \tau_{11}) - (-p + \tau_{22}) = \tau_{11} - \tau_{22} \quad \text{First normal stress difference} \tag{21.120}$$

$$N_1 = \sigma_{22} - \sigma_{33} = (-p + \tau_{22}) - (-p + \tau_{33}) = \tau_{22} - \tau_{33} \quad \text{Second normal stress difference} \tag{21.121}$$

The first normal stress difference can be measured directly with a cone-and-plate instrument, which is also known as the Weissenberg rheogoniometer (see sketch in Fig.21.17). As the cone turns the tendency to climb up the rotating shaft is converted in a normal force N_F which can be measured by a suitable mechanical or electronic device.

From flow analysis of the cone-and-plate instrument, it turns out that the first normal stress difference is

$$N_1 = \tau_{11} - \tau_{22} = \frac{2N_F}{\pi R^2} \tag{21.122}$$

The second normal stress difference is much more difficult to measure. For different measurement methods the reader is refereed to Tanner [2] and Macosko [7]. Up to the mid 1960's it was thought that N_2=0. More recent measurements showed that N_2 is negative and approximately 10-20% of the magnitude of N_1.

The normal stress differences are functions of the shear rate and there are sometimes expressed in terms of the so-called normal stress coefficients which are defined as follows

$$\Psi_{12}(\dot{\gamma}) = \frac{N_1}{\dot{\gamma}^2} = \frac{\tau_{11} - \tau_{22}}{\dot{\gamma}^2} \tag{21.123}$$

$$\Psi_{23}(\dot{\gamma}) = \frac{N_2}{\dot{\gamma}^2} = \frac{\tau_{22} - \tau_{33}}{\dot{\gamma}^2} \tag{21.124}$$

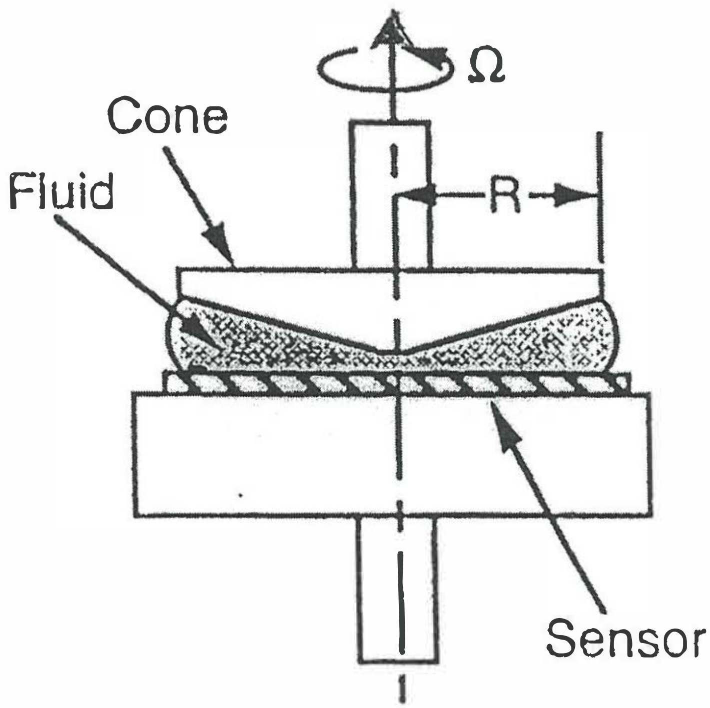

Fig. 21.17. Cone-and-plate instrument (also known as Weissenberg rheogoniometer)

These definitions are equivalent to the definition of apparent viscosity coefficient

$$\eta = \frac{\tau_{12}}{\dot{\gamma}} \tag{21.125}$$

The square of the shear rate in equations (21.123) and (21.124) is due to experimental evidence that at very low values of $\dot{\gamma}$ the normal stress differences are proportional to $\dot{\gamma}^2$.

For molten polymers the first normal stress difference obeys expressions in the form

$$N_1 = A\tau_{12}{}^{b} \tag{21.126}$$

For molten polystyrenes a rough approximation might be [21] A = 0.00347 and b = 1.66.

Under usual processing conditions for the fabrication of plastic parts by extruding a molten polymer through a die the shear stress is likely to be τ_{12} = 10^5 Pa. Using the above equation, we get approximately $N_1 \approx 7\times10^5$ i.e. under customary processing conditions the first normal stress difference is much larger than the shear stress.

To describe the flow behavior of polymer solutions and melts it is necessary to develop constitutive equations (see also Chapter 20), capable of representing not only the departure of viscosity from linearity (e.g. power-law) but also stress relaxation, stress overshoot, normal stresses and elongational viscosity that does not obey the Trouton relation of section 21.10. This is a very challenging task beyond the scope of this book and the reader is referred to specialized books dedicated to the rheology of polymers [1-16, 22].

21.13 HELE-SHAW FLOW APPROXIMATION

For slow viscous flow (creeping, Re<<1) spreading in a narrow gap between two nearly parallel plates as shown in Fig. 21.18, the pressure is expected to have negligible variation in the z-direction and the flow can be described (Hele-Shaw approximation) [23, 24] by the simplified form of the equations of mass and momentum (in x and y directions)

$$\frac{\partial}{\partial x}\left(HV_{x,avg}\right)+\frac{\partial}{\partial y}\left(HV_{y,avg}\right)=0 \tag{21.127}$$

$$0=\frac{\partial}{\partial z}\left(\eta\frac{\partial V_x}{\partial z}\right)-\frac{\partial p}{\partial x} \tag{21.128}$$

$$0=\frac{\partial}{\partial z}\left(\eta\frac{\partial V_y}{\partial z}\right)-\frac{\partial p}{\partial y} \tag{21.129}$$

where $V_{x,avg}$ and $V_{y,avg}$ denote average values across the gap. For a generalized Newtonian fluid the viscosity is

$$\eta=\eta(x,y,z) \tag{21.130}$$

Applying the no-slip condition at the wall and symmetry at the centerplane, Equations (21.131) and (21.132) give

$$V_x=-\frac{\partial p}{\partial x}\int_z^{H/2}\frac{z'}{\eta}dz' \tag{21.131}$$

$$V_y=-\frac{\partial p}{\partial y}\int_z^{H/2}\frac{z'}{\eta}dz' \tag{21.132}$$

and the average values are

$$V_{x,avg}=\frac{1}{H/2}\int_0^{H/2}V_x dz=-\frac{\partial p}{\partial x}\frac{S}{H/2} \tag{21.133}$$

$$V_{y,avg}=\frac{1}{H/2}\int_0^{H/2}V_y dz=-\frac{\partial p}{\partial y}\frac{S}{H/2} \tag{21.134}$$

where

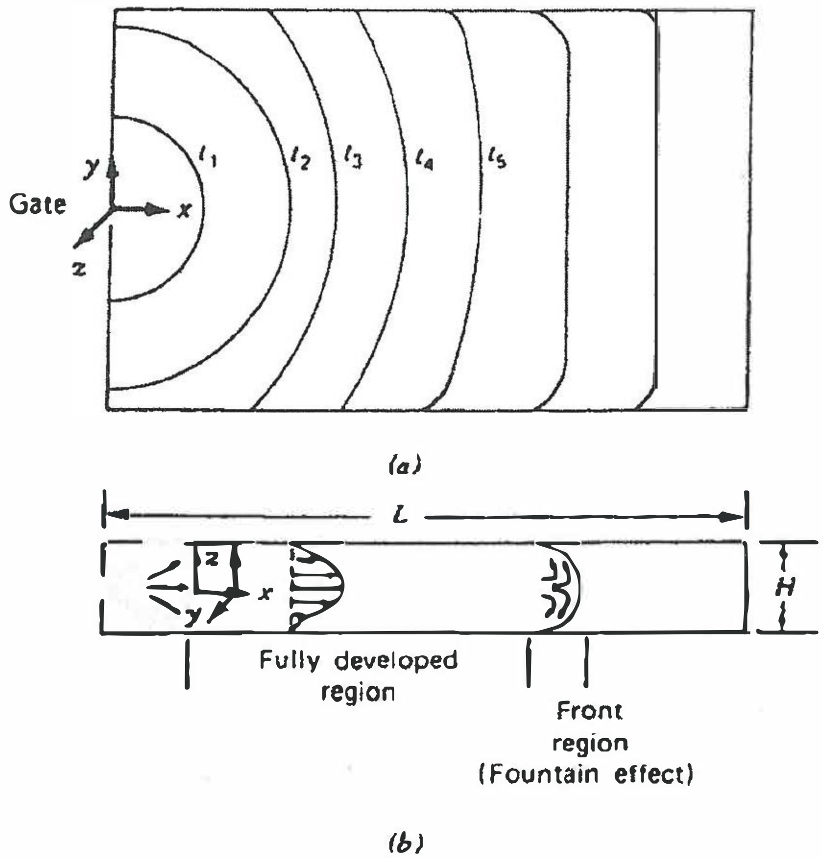

Fig. 21.18. Schematic representation of single-gated rectangular cavity: (a) top-view (spreading plane), (b) side view (transverse plane) from Reference[24].

$$S = \int_0^{H/2} \frac{z^2}{\eta} dz \tag{21.135}$$

Substituting Equations (21.136) and (21.137) into (21.130)

$$\frac{\partial}{\partial x}\left(S\frac{\partial p}{\partial x}\right) + \frac{\partial}{\partial y}\left(S\frac{\partial p}{\partial y}\right) = 0 \tag{21.136}$$

This approximation is used extensively for determining spreading of flow in injection molding of molten polymers into "thin" and "wide" cavities, as shown on top of Fig. 21.18.Of course, it is easier to solve equation (21.139), get the pressure and then V_x and V_y, than the Stokes equation (see Chapter 8), for Non-Newtonian flow. It should be noted that there is a transverse velocity component which drives the fluid elements towards the walls. This motion, when viewed from a frame of reference moving with the flow front, gives a fountain like picture. The implication of fountain flow in injection molding [24] is beyond the scope of this book.

REFERENCES

1. R.B. Bird, R.C. Armstrong and O. Hassager, "Dynamics of Polymeric Liquids: Volume 1 Fluid Mechanics", 2nd Ed., Wiley, New York (1987).
2. R.I. Tanner, "Engineering Rheology", Oxford University Press, New York (1985).
3. M.M. Denn, "Process Fluid Mechanics", Prentice-Hall, Englewood Clffs,NJ (1980).
4. S. Middleman, "Fundamentals of Polymer Processing", McGraw-Hill, New York (1977).
5. M.M. Denn, "Polymer Melt Processing: Foundations in Fluid Mechanics and Heat Transfer", Cambridge University Press, New York (2008).
6. N. Midoux, "Mécanique et Rhéologie des Fluides en Génie Chimique", Lavoisier, Paris (1985).

7. C.W. Macosko, "Rheology: Principles, Measurements and Applications", VCH Publishers, New York (1994).

8. F.A. Morrison, "Understanding Rheology", Oxford University Press, New York (2001).

9. L. E. Nielsen, "Polymer Rheology", Marcel Dekker, New York (1977).

10. R. Darby, "Viscoelastic Fluids: An Introduction to their Properties and Behavior", Marcel Dekker, New York (1976).

11. H.A. Barnes, J.F. Hutton and K. Walters, "An Introduction to Rheology", Elsevier, New York (1989).

12. C.D. Han, "Rheology and Processing of Polymeric Materials: Volumes 1 and 2 P", Oxford University Press, New York (2007).

13. M.J. Crochet, A.R. Davies and K. Walters, "Numerical Simulation of Non-Newtonian Flow", Elsevier, Amsterdam (1984).

14. M. Pahl, W. Gleißle and H.-M. Laun, "Praktische Rheologie der Kunststoffe und Elastomere", VDI-Verlag, Düsseldorf (1995).

15. W.R. Schowalter, "Mechanics of Non-Newtonian Fluids", Pergamon Press, Oxford (1978).

16. J.F. Steffe, "Rheological Methods in Food Process Engineering", 2nd Ed., Freeman Press, East Lansing,MI (1996).

17. G.K. Batchelor, "The Effect of Brownian Motion on the Bulk stress in a Suspension of Spherical Particles", J. Fluid Mech., 83(part 1), 97 (1977).

18. J. Vlachopoulos and P.S. Scott, "Pressure Drop for Molten Polymer Flow through Tapered Dies", Adv. Polym. Techn., 5, 81 (1985).

19. E. Mitsoulis, M. Schwetz and H. Münstedt, "Entry Flow of LDPE Melts in a Planar Contraction", J. Non-Newt. Fluid Mech., 111, 41 (2003).

20. M.M. Denn, "Just What Did Deborah Say?", Rheology Bulletin, 80 (1), 12 (2011).

21. K. Oda, J.L. White and E.S. Clark, "Correlations of Normal Stresses in Polystyrene Melts and its Implications", Polym. Eng. Sci., 18, 25 (1978).

22. J. Vlachopoulos and N. Polychronopoulos, Basic Concepts in Polymer Melt Rheology and their Importance in Processing, Chapter 1, pages 1-27 in M. Kontopoulou (Ed.), "Applied Polymer Rheology Polymeric Fluids with Industrial Applications", Wiley (2012).

23. J.A. Dantzig and C.L. Tucker III, "Modeling in Materials Processing", Cambridge University Press, UK (2001).

24. H. Mavridis, A.N. Hrymak and J. Vlachopoulos, "Mathematical Modeling of Injection Mold Filling: A Review", Adv. Polym. Techn., 6, 457 (1986).

John Vlachopoulos, *Fundamentals of Fluid Mechanics*
Chem. Eng., McMaster University, Hamilton, ON, Canada
(First Edition 1984, revised internet edition (2016), www.polydynamics.com)

APPENDIX A
VECTORS AND TENSORS

Vector is an entity that has magnitude and direction. To denote vectors we use alphabetic symbols with a bar on top, i.e. $\bar{A}$, $\bar{B}$, $\bar{a}$, $\bar{r}$, etc. are vectors. If A_1, A_2, A_3 are the Cartesian components of vector $\bar{A}$ we have

$$\bar{A} = A_1 \bar{i} + A_2 \bar{j} + A_3 \bar{k}$$

where $\bar{i}$, $\bar{j}$, $\bar{k}$ are the unit vectors in the x,y and z directions respectively. Instead of (x, y, z) we often write (x_1, x_2, x_3) to indicate the coordinate axes. The magnitude of vector A is

$$A = |\bar{A}| = \sqrt{A_1^2 + A_2^2 + A_3^2}$$

To indicate vector $\bar{A}$ we may write the three Cartesian components (A_1, A_2, A_3) or in the so-called index notation, we may simply write A_i where $i = 1, 2, 3$.

Range Convention:

Whenever a small subscript appears unrepeated in a term, it is understood to take on the values 1, 2, 3 (the number of physical dimensions).

A_i stands for (A_1, A_2, A_3)

A_{ij} stands for the array of nine quantities

$$\begin{matrix} A_{11} & A_{12} & A_{13} \\ A_{21} & A_{22} & A_{33} \\ A_{31} & A_{32} & A_{33} \end{matrix}$$

when such an array obeys a linear transformation law it is called a tensor.

Mnemonic rule for tensors: $\text{rows} \nearrow A_{ij} \nwarrow \text{columns}$

Order of Tensor:

A = tensor of zero order (scalar)

A_i = tensor of first order (vector)

A_{ij} = tensor of second order (usually called simply tensor)

A_{ijk} = tensor of third order

etc.

In 3-dimensional space a tensor of order N has 3^N Cartesian components.

Summation (or Einstein) Convention:

Whenever a small subscript appears repeated in a term, it is understood to represent a summation over the range 1, 2, 3.

Examples:

(a) $$A_{ii} = \sum_{i=1}^{i=1} A_{ii} = A_{11} + A_{22} + A_{33}$$

(b) $a_{ij}\ A_j$ we note j is repeated and i unrepeated

$$a_{ij}\ A_j = \sum_{j=1}^{j=3} a_{ij}\ A_j = a_{i1}\ A_1 + a_{i2}\ A_2 + a_{i3}\ A_3$$

$$= \begin{pmatrix} a_{11}\ A_1 + a_{12}\ A_2 + a_{13}\ A_3 \\ a_{21}\ A_1 + a_{22}\ A_2 + a_{23}\ A_3 \\ a_{31}\ A_1 + a_{32}\ A_2 \quad a_{33}\ A_3 \end{pmatrix}$$

This means that $a_{ij}\ A_j$ represents an array of three quantities (each one of them is a sum of three terms) and is a vector.

Kronecker Delta δ_{ij}

We define

$$\delta_{ij} = \begin{cases} 1 & \text{if} \quad i = j \\ 0 & \text{if} \quad i \neq j \end{cases}$$

or

$$\delta_{ij} \rightarrow \begin{pmatrix} 1 & 0 & 0 \\ 0 & 1 & 0 \\ 0 & 0 & 1 \end{pmatrix}$$

Alternating Tensor ε_{ijk}

We define

$\varepsilon_{ijk} = 1$ for even permutations 123123...

$\varepsilon_{ijk} = -1$ for odd permutations 321321...

$\varepsilon_{ijk} = 0$ for all other

e.g.

$$\varepsilon_{123} = 1 \quad \varepsilon_{231} = 1 \quad \varepsilon_{213} = -1 \quad \varepsilon_{112} = 0$$

Dot Product Between Two Vectors

$$\bar{A} \cdot \bar{B} = A_i\ B_i = \sum_{i=1}^{i=3} A_i\ B_i = A_1\ B_1 + A_2\ B_2 + A_3\ B_3 \text{ (scalar)}$$

Cross Product Between Two Vectors

Is a vector $\bar{C} = \bar{A} \times \bar{B}$

$$\bar{C} = \begin{vmatrix} i & j & k \\ A_1 & A_2 & A_3 \\ B_1 & B_2 & B_3 \end{vmatrix} = \begin{vmatrix} A_2 B_3 - A_3 B_2 \\ A_3 B_1 - A_1 B_3 \\ A_1 B_2 - A_2 B_1 \end{vmatrix} = \varepsilon_{ijk} A_j B_k$$

Mnemonic rule for the <u>cross</u> product: $\varepsilon_{ijk} A_j B_k$ (they...... cross)

<u>Dyad</u> is the outer product at two vectors.

$$\bar{A}\,\bar{B} = A_i\, B_j \text{ is a tensor} \rightarrow \begin{pmatrix} A_1 B_1 & A_1 B_2 & A_1 B_3 \\ A_2 B_1 & A_2 B_2 & A_2 B_3 \\ A_3 B_1 & A_3 B_2 & A_3 B_3 \end{pmatrix}$$

Note that if we place a dot between the two vectors $\bar{A}$ and $\bar{B}$ we get the dot product:

$$\bar{A} \cdot \bar{B} = A_i\, B_i$$

which is a scalar.

<u>TENSOR PRODUCTS</u>

In general, if we place two tensors side by side we have the <u>outer</u> product which is a tensor of order equal to the sum of the orders of the two tensors.

<u>Neighboring Index Convention:</u>

A dot between two tensors is equivalent to identifying two <u>neighboring</u> subscripts with the same symbol and then applying the summation convention.

<u>Examples</u>

(a) $\bar{A} \cdot \bar{B}$ means $A_i\, B_i = \sum_{i=1}^{i=3} A_i\, B_i = A_1 B_1 + A_2 B_2 + A_3 B_3$

(b) $\bar{A}\cdot\bar{\bar{B}}$ means $A_i \, B_{ij} = \sum_{i=1}^{i=3} A_i \, B_{ij}$

This, in general, is <u>not</u> equal to $A_i \, B_{ji}$

(c) $\bar{\bar{B}}\cdot\bar{A}$ means $B_{ij} \, A_j = \sum_{j=1}^{j=3} B_{ij} \, A_j$

(d) $\bar{\bar{A}} \, \bar{\bar{B}}$ is the fourth order tensor $A_{ij} \, B_{mn}$ which has $3^4 = 144$ components

$\bar{\bar{A}}\cdot\bar{\bar{B}}$ means $A_{ij} \, B_{jn} = \sum_{j=1}^{j=3} A_{ij} \, B_{jn}$

Since we have two free subscripts, this quantity is a tensor of order two. The quantity

$\bar{\bar{A}}:\bar{\bar{B}}$ is the scalar $A_{ij} \, B_{ji} = \sum_{i=1}^{i=3} \sum_{j=1}^{j=3} A_{ij} \, B_{ji}$ (sum of 9 terms)

(i) Note that each dot represents a reduction from the sum of the orders by two.

(ii) The subscripts i, j, k etc. are dummy variables standing for 1, 2, 3. Thus, it does not make any difference whether we identify two subscripts with i, j or any other letter, i.e.

$$\bar{\bar{A}}\cdot\bar{\bar{B}} = A_{ij} \, B_{jn} = A_{ir} \, B_{rn}$$

(iii) Remember that each dot means identification of <u>neighboring</u> indices with the same symbol i.e.

$\bar{\bar{A}}\cdot\bar{\bar{B}}$ means $A_{ir} \, B_{rn}$ and <u>not</u> $\cancel{A_{io} \, B_{jn}}$

VECTOR OPERATOR ∇

The vector differential operator ∇ (del) is defined by

$$\nabla = \frac{\partial}{\partial x}\bar{\imath} + \frac{\partial}{\partial y}\bar{\jmath} + \frac{\partial}{\partial z}\bar{k}$$

in index notation we may simply write

∂_i or $\frac{\partial}{\partial x_i}$ which is equivalent to $(\frac{\partial}{\partial x}, \frac{\partial}{\partial y}, \frac{\partial}{\partial z})$ or $(\frac{\partial}{\partial x_1}, \frac{\partial}{\partial x_2}, \frac{\partial}{\partial x_3})$

If $\phi(x,y,z)$ is a scalar field we define the gradient of ϕ as

$$\text{grad } \phi = \nabla\phi = \frac{\partial\phi}{\partial x}\bar{\jmath} + \frac{\partial\phi}{\partial y}\bar{\jmath} + \frac{\partial\phi}{\partial z}\bar{k} \quad \text{(vector)}$$

or in index notation

$$\partial_i\phi \quad \text{or} \quad \frac{\partial\phi}{\partial x_i} \rightarrow (\frac{\partial\phi}{\partial x_1}, \frac{\partial\phi}{\partial x_2}, \frac{\partial\phi}{\partial x_3}) \rightarrow (\frac{\partial\phi}{\partial x}, \frac{\partial\phi}{\partial y}, \frac{\partial\phi}{\partial z})$$

If $\bar{A}$ is vector field, we define the divergence of $\bar{A}$ as

$$\text{div } \bar{A} = \nabla\cdot\bar{A} = \frac{\partial A_1}{\partial x} + \frac{\partial A_2}{\partial y} + \frac{\partial A_3}{\partial z} \text{ (scalar)}$$

which is written in index notation as

$$\partial_i A_i \quad \text{or} \quad \frac{\partial A_i}{\partial x_i} = \frac{\partial A_1}{\partial x_1} + \frac{\partial A_2}{\partial x_2} + \frac{\partial A_3}{\partial x_3} = \frac{\partial A_1}{\partial x} + \frac{\partial A_2}{\partial y} + \frac{\partial A_3}{\partial z}$$

The curl or rotation of $\bar{V}$ is written as

$$\nabla \times \bar{V} = \begin{vmatrix} \bar{\imath} & \bar{\jmath} & \bar{k} \\ \frac{\partial}{\partial x} & \frac{\partial}{\partial y} & \frac{\partial}{\partial z} \\ V_1 & V_2 & V_3 \end{vmatrix}$$

$$= (\frac{\partial V_3}{\partial y} - \frac{\partial V_2}{\partial z})\bar{\imath} + (\frac{\partial V_1}{\partial z} - \frac{\partial V_3}{\partial x})\bar{\jmath} + (\frac{\partial V_2}{\partial x} - \frac{\partial V_1}{\partial y})\bar{k}$$

$$= \epsilon_{ijk}\,\partial_j\,V_k = \epsilon_{ijk}\frac{\partial V_k}{\partial x_j}$$

The Laplacian ∇^2 is defined as

$$\nabla^2 = \nabla \cdot \nabla = \frac{\partial^2}{\partial x^2} + \frac{\partial^2}{\partial y^2} + \frac{\partial^2}{\partial z^2}$$

$$= \partial_i \, \partial_i = \frac{\partial}{\partial x_i} \frac{\partial}{\partial x_i} = \sum_{i=1}^{i=3} \frac{\partial}{\partial x_i^2}$$

DIFFERENTIATION FORMULAE

Let $\bar{A}$ and $\bar{B}$ be arbitrary vectors and f a scalar, we have:

1. $\nabla \cdot (f\bar{A}) = f\nabla \cdot \bar{A} + \bar{A} \cdot \nabla f$
2. $\nabla \times f\bar{A} = f\nabla \times \bar{A} + \nabla f \times \bar{A}$
3. $\nabla \cdot (\bar{A} \times \bar{B}) = \bar{B} \cdot \nabla \times \bar{A} - \bar{A} \cdot \nabla \times \bar{B}$
4. $\nabla \times (\bar{A} \times \bar{B}) = \bar{B} \cdot \nabla \bar{A} - \bar{A} \cdot \nabla \bar{B} + \bar{A}(\nabla \cdot \bar{B}) - \bar{B}(\nabla \cdot \bar{A})$
5. $\nabla(\bar{A} \cdot \bar{B}) = \bar{A} \cdot \nabla \bar{B} + \bar{B} \cdot \nabla \bar{A} + \bar{A} \times (\nabla \times \bar{B}) + \bar{B} \times (\nabla \times \bar{A})$
6. $\nabla \times (\nabla f) = \text{curl grad } f = 0$
7. $\nabla \cdot (\nabla \times \bar{A}) = \text{div curl } \bar{A} = 0$
8. $\nabla \times (\nabla \times \bar{A}) = \text{curl curl } \bar{A} = \nabla(\nabla \cdot \bar{A}) - \nabla \cdot \nabla \bar{A}$

$$= \text{grad div } \bar{A} - \nabla^2 \bar{A}$$

- The quantity $\nabla \bar{A}$ is a dyad and may be written as

$$\nabla \bar{A} = \partial_i \, A_j = \frac{\partial A_j}{\partial x_i} \rightarrow \begin{pmatrix} \frac{\partial A_1}{\partial x_1} & \frac{\partial A_2}{\partial x_1} & \frac{\partial A_3}{\partial x_1} \\ \frac{\partial A_1}{\partial x_2} & \frac{\partial A_2}{\partial x_2} & \frac{\partial A_3}{\partial x_2} \\ \frac{\partial A_1}{\partial x_3} & \frac{\partial A_2}{\partial x_3} & \frac{\partial A_3}{\partial x_3} \end{pmatrix}$$

- The quantity $\nabla \cdot \bar{\bar{\tau}}$ is written as

$$\nabla \cdot \bar{\bar{\tau}} = \partial_i \; \tau_{ij} = \frac{\partial}{\partial x_i} \tau_{ij} = \sum_{i=1}^{i=3} \frac{\partial}{\partial x_i} \tau_{ij} \rightarrow \begin{pmatrix} \frac{\partial \tau_{11}}{\partial x_1} + \frac{\partial \tau_{21}}{\partial x_2} + \frac{\partial \tau_{31}}{\partial x_3} \\ \frac{\partial \tau_{12}}{\partial x_1} + \frac{\partial \tau_{22}}{\partial x_2} + \frac{\partial \tau_{32}}{\partial x_3} \\ \frac{\partial \tau_{13}}{\partial x_1} + \frac{\partial \tau_{23}}{\partial x_2} + \frac{\partial \tau_{33}}{\partial x_3} \end{pmatrix}$$

and it is a vector.

- The quantity $\bar{\bar{\tau}}:\nabla\bar{V}$ represents the scalar

$$\bar{\bar{\tau}}:\nabla\bar{V} = \tau_{ij} \; \partial_j \; V_i = \sum_{i=1}^{i=3} \sum_{j=1}^{j=3} \tau_{ij} \frac{\partial V_i}{\partial x_j} =$$

$$\tau_{11} \frac{\partial V_1}{\partial x_1} + \tau_{12} \frac{\partial V_1}{\partial x_2} + \tau_{13} \frac{\partial V_1}{\partial x_3} + \tau_{21} \frac{\partial V_2}{\partial x_1} + \tau_{22} \frac{\partial V_2}{\partial x_2} + \tau_{23} \frac{\partial V_2}{\partial x_3}$$

$$+ \tau_{31} \frac{\partial V_3}{\partial x_1} + \tau_{32} \frac{\partial V_3}{\partial x_2} + \tau_{33} \frac{\partial V_3}{\partial x_3} \qquad \text{(scalar)}$$

The quantity $\bar{V}\cdot\nabla\bar{V}$ is a vector $V_i \; \partial_i \; V_j = V_i \frac{\partial}{\partial x_i} V_j = \sum_{i=1}^{i=3} V_i \frac{\partial}{\partial x_i} V_j$

INTEGRAL THEOREMS

1. Gauss' Divergence Theorem:

$$\iiint_{\forall} (\nabla\cdot\bar{A}) \, d\forall = \oiint_S (\bar{A}\cdot\bar{n}) \, dS$$

2. Stokes' Theorem:

$$\int \bar{A}\cdot d\bar{r} = \iint_S (\nabla \times \bar{A})\cdot\bar{n} \, dS$$

3. Differentiation of an Integral (Leibnitz formula)

$$\frac{d}{du} \left(\int_{a(u)}^{b(u)} F(x,u) \, dx \right) = \int_a^b \frac{\partial F}{\partial u} dx + F(b,u) \left(\frac{db}{du}\right) - F(a,u) \left(\frac{da}{du}\right)$$

John Vlachopoulos, *Fundamentals of Fluid Mechanics*
Chem. Eng., McMaster University, Hamilton, ON, Canada
(First Edition 1984, revised internet edition (2016), www.polydynamics.com)

APPENDIX **B**

FINITE DIFFERENCE AND FINITE ELEMENT METHODS

B.1 INTRODUCTION

We have seen some simple analytical solutions for certain well defined problems in previous chapters of this book. It is true that an awful lot of engineering problems can be solved using simple equations and formulas. However, for many other problems simplifications that render the problems amenable to analytical solutions are not possible. We must resort to numerical methods and powerful computers.

The basic idea is to discretize our problem. Instead of having a continuous problem we will solve the differential equations for a discrete one. There are two basic ways to achieve this. One way is to choose a finite number of points, and to replace the derivatives by differences. This is the finite difference method (FDM). The other way is to choose functions, preferably polynomials, and to approximate the exact solution by a combination of these functions over small interconnected regions (elements). This is the basic idea behind the finite element method (FEM). Under special circumstances finite differences and finite elements may lead to exactly the same sets of algebraic difference equations.

In setting up a finite difference scheme a regular grid is necessary over the domain of integration. In the finite elment method elements of different sizes can be easily interconnected. Either method can be used to solve the partial differential equations (PDEs) of fluid mechanics. Finite differences are easier to program. Finite elements are more difficult to program but can handle much better irregular geometrical boundaries and unusual boundary conditions. The question whether finite differences or finite elements should be used for a given problem is difficult to answer. Both methods have advantages and disadvantages and the controversy is still going on. At the moment it appears that most researchers in the field of turbulence prefer finite difference methods while for creeping flow problems they prefer finite element methods. In other areas neither method seems to have the edge and the decision to go with FDM or FEM may simply depend on the experience and background of the problem solver.

For an interesting overview of various methods of solution of partial differential equations the reader is referred to a textbook by Strang (1). Roache (2) gives an extensive review of FD techniques applicable to various kinds of fluid flow problems. The application of finite elements to fluid mechanics is described in great detail by Huebner and Thornton (3) and Baker (4).

B.2 FINITE DIFFERENCE APPROXIMATIONS AND SOLUTIONS

The finite difference method is a very powerful tool for the solution of partial differential equations (PDEs). In this method the differential equation is approximated at a finite number of locations (nodes) of the domain of integration. The solution can be accomplished by following the four-step procedure outlined below:

1. Discretize the domain of the integration using a one- two- or three-dimensional grid depending on the problem.
2. Write the appropriate finite difference approximations of the derivatives.

3. Approximate the PDE with its finite difference approximation at each node of the discretized domain.

4. Solve the resulting difference equations to obtain approximate values of the unknown variables at each node.

Finite difference approximations of the derivatives can be obtained by using the expansion of a function in Taylor series.

If f(x) is a continuous differentiable function we may write

$$f(x_0 + \Delta x) = f(x_0) + \Delta x \frac{df(x_0)}{dx} + \frac{(\Delta x)^2}{2!} \frac{d^2 f(x_0)}{dx} + \ldots \tag{B.1}$$

or

$$f(x_0 - \Delta x) = f(x_0) - \Delta x \frac{df(x_0)}{dx} + \frac{(\Delta x)^2}{2!} \frac{d^2 f(x_0)}{dx} - \ldots \tag{B.2}$$

Thus, the first order derivative can be approximated by a forward difference

$$\frac{df(x_0)}{dx} = \frac{f(x_0 + \Delta x) - f(x_0)}{\Delta x} + 0(\Delta x) \tag{B.3}$$

or a backward difference

$$\frac{df(x_0)}{dx} = \frac{f(x_0) - f(x_0 + \Delta x)}{\Delta x} + 0(\Delta x) \tag{B.4}$$

The error in both cases is of order Δx.

Subtracting equation (B.2) from equation (B.1) we obtain a central difference approximation

$$\frac{df(x_0)}{dx} = \frac{f(x_0 + \Delta x) - f(x - \Delta x)}{2\Delta x} + 0(\Delta x)^2 \tag{B.5}$$

The error is of order $(\Delta x)^2$.

Adding equations (B.1) and (B.2) we obtain an approximation of the second order derivative

$$\frac{d^2 f(x_0)}{dx} = \frac{f(x_0 + \Delta x) - 2f(x_0) + f(x_0 - \Delta x)}{(\Delta x)^2} + 0(\Delta x)^2 \tag{B.6}$$

This procedure can be used for the determination of finite difference approximations of derivatives of any order. These expressions are further used to approximate the PDE at each node of the finite difference grid as explained in the example below.

Example

The equation for pressure driven flow between two flat plates is

$$\mu \frac{\partial^2 v_x}{\partial y^2} = \frac{dp}{dx}$$

The boundary conditions are $v_x=0$ at $y=b$ and $v_x=0$ at $y=-b$. Solve this problem using the method of finite differences and compare to the analytical solution of Section 7.2.

Solution

To simplify the solution procedure we use a one-dimensional grid of only five points as shown in Fig. B.1(a) let us define $v_x=V$ and $(1/\mu)\ dp/dx = -A$ (Minus because the pressure gradient is negative in the direction of flow). We have

$$\frac{d^2V}{dy^2} = -A$$

The finite difference approximation is

$$\frac{d^2V}{dy^2} = \frac{V(y+\Delta y) - 2V(y) + V(y-\Delta y)}{(\Delta y)^2}$$

The differential equations can be approximated as

node 2:

$$\frac{V_3 - 2V_2 + V_1}{(\Delta y)^2} = -A$$

node 3:

$$\frac{V_4 - 2V_3 + V_2}{(\Delta y)^2} = -A$$

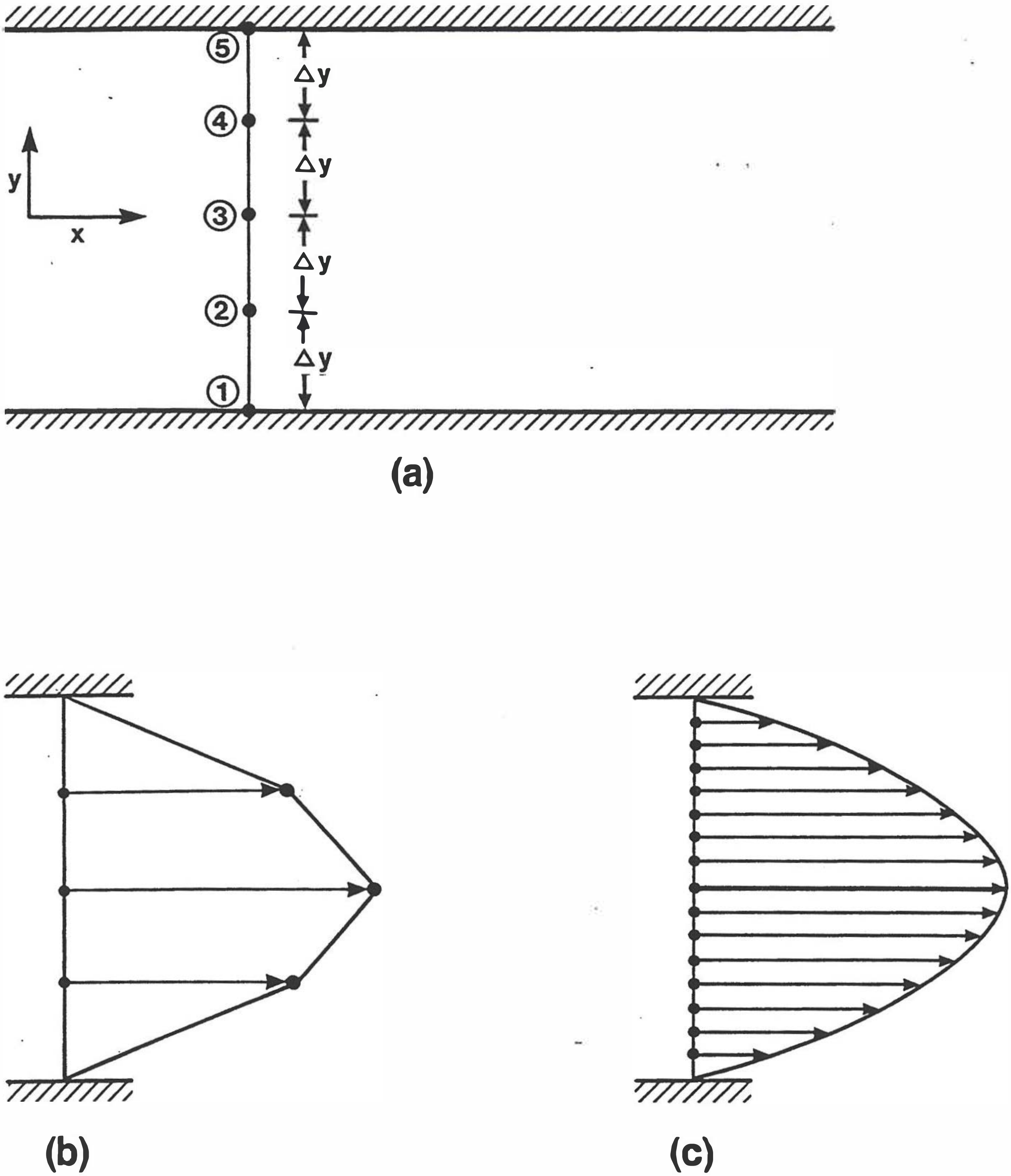

Fig. .B.1

node 4:

$$\frac{V_5-2V_4+V_3}{(\Delta y)^2} = -A$$

Noting that $V_1 = V_5 = 0$ and redefining $V/A(\Delta y)^2 = V^*$

we have

$$V_3^* - 2V_2^* = -1$$

$$V_4^* - 2V_3^* + V_2^* = -1$$

$$V_5^* - 2V_4^* = -1$$

Solving these algebraic equations we get

$$V_2^* = 1.5$$

$$V_3^* = 2$$

$$V_4^* = 1.5$$

This velocity profile leaves much to be desired as shown in Fig. B.1(b) Obviously if more nodes were used the profile could be made virtually identical to a parabola (shown in Fig.B.1(c)).

It is interesting to note that the system of algebraic equations is of the tridiagonal form

$$A_1F_1 + B_1F_2 = D$$

$$C_m F_{m-1} + A_m F_m + B_m F_{m+1} = D_m \text{ for } m = 2, 3, \ldots, k-1$$

$$C_kF_{k-1} + A_kF_k = D_k$$

where F_m are the unknown nodal values and A_m, B_m and C_m are constants.

The solution of such a system of linear algebraic equations can be easily carried out in a digital computer using well known methods [5].

Example

Use the method of the above example to solve the equation for pressure driven flow in a tube

$$\mu \frac{1}{r}\frac{\partial}{\partial r}\left(r\frac{\partial v_z}{\partial r}\right) = \frac{dp}{dz}$$

with boundary conditions at $r=0$ $\partial v_z/\partial r = 0$ and at $r=R$ $v_z=0$

Solution

We rewrite the differential equation as

$$\frac{1}{r}\frac{d}{dr}\left(r\frac{dV}{dr}\right) = -A$$

and carry out the differentiation

$$\frac{1}{r}\frac{dV}{dr} + \frac{d^2V}{dr^2} = -A$$

We will use the following finite difference approximations

$$\frac{dV}{dr} = \frac{V(r+\Delta r) - V(r)}{\Delta r}$$

and

$$\frac{d^2V}{dr^2} = \frac{V(r+\Delta r) - 2V(r) + V(r-\Delta r)}{(\Delta r)^2}$$

For simplicity we choose a four-node grid as shown in Fig. B.2(a). The finite difference approximations of the differential equations are:

node 2:

$$\frac{1}{\Delta r}\frac{V_1 - V_2}{\Delta r} + \frac{V_3 - 2V_2 + V_1}{(\Delta r)^2} = -A$$

node 3:

$$\frac{1}{2\Delta r}\frac{V_2 - V_3}{\Delta r} + \frac{V_4 - 2V_3 + V_2}{(\Delta r)^2} = -A$$

The velocity V_1 at the centerline is unknown and thus, we must write another equation for node 1. We note, however, that at the centerline the differential equation has one indefinite term i.e.

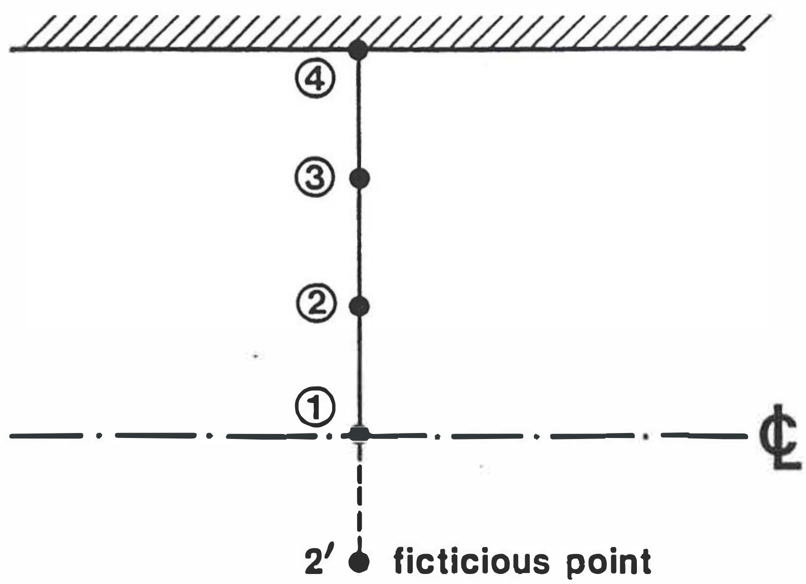

(a)

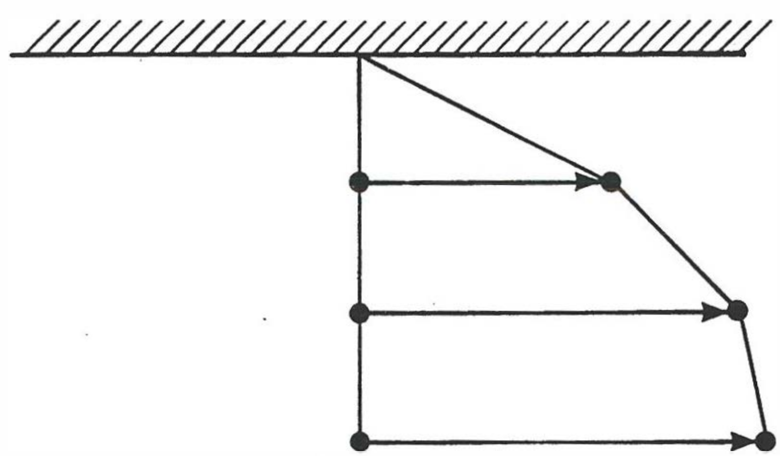

(b)

Fig. B.2

$$\frac{0}{0} + \frac{d^2V}{dr^2} = -A$$

Using L'Hopital's rule, we get

$$\frac{d^2V}{dr^2} + \frac{d^2V}{dr^2} = -A$$

or

$$2\,\frac{d^2V}{dr^2} = -A$$

Thus, for node 1, we have:

$$2\,\frac{V_2' - 2V_1 + V_2}{(\Delta r)^2} = -A$$

Due to symmetry the velocity at fictitious point (V_2') should be equal to velocity V_2 i.e $V_2' = V_2$ or

$$\frac{4V_2 - 4V_1}{(\Delta r)^2} = -A$$

After some minor rearrangements the difference equations become

node 1

$$-4V_1 + 4V_2 = -A(\Delta r)^2$$

node 2

$$2V_1 - 3V_2 + V_3 = -A(\Delta r)^2$$

node 3

$$\frac{3}{2}V_2 - \frac{5}{2}V_3 + V_4 = -2A(\Delta r)^2$$

Noting that $V_4 = 0$ and dividing by $A(\Delta r)^2$ we have

$$-4V_1^* + 4V_2^* = -1$$

$$2V_1^* - 3V_2^* + V_3^* = -1$$

$$\frac{3}{2}V_2^* - \frac{5}{2}V_3^* = -1$$

Again this system of equations is of the tridiagonal form as in Example EB.1. Solving, we get

$$V_1^* = \frac{20}{4} = 5.00$$

$$V_2^* = \frac{19}{4} = 4.75$$

$$V_3^* = \frac{13}{4} = 3.25$$

The velocity profile is sketched in Fig. B.2(b). More nodes will yield a profile virtually identical to a parabola.

B.3 UNSTEADY FLOW ANALYSIS BY THE EXPLICIT METHOD

We will now use a finite difference method to solve the parabolic differential equation that describes the flow field near a plate suddenly set in motion (see Section 7.15). We have

$$\frac{\partial v_x}{\partial t} = \nu \frac{\partial^2 v_x}{\partial y^2} \tag{B.7}$$

$$\begin{aligned} v_x &= 0 \quad \text{at} \quad t = 0 \\ v_x &= V \quad \text{at} \quad y = 0 \\ v_x &= 0 \quad \text{at} \quad y \rightarrow \infty \end{aligned} \tag{B.8}$$

To simplify the notation let $v_x = U$. We will solve the differential equation

$$\frac{\partial U}{\partial t} = \nu \frac{\partial^2 U}{\partial y^2} \tag{B.9}$$

using the following finite difference approximations

$$\frac{\partial^2 U}{\partial y^2} = \frac{U_{i+1}^j - 2U_i^j + U_{i-1}^j}{(\Delta y)^2} \tag{B.10}$$

$$\frac{\partial U}{\partial t} = \frac{U_i^{j+1} - U_i^j}{\Delta t} \tag{B.11}$$

The subscripts denote position and superscripts denote time.

Substituting equations (B.10) and (B.11) into (B.9) and solving for U_i^{j+1}, we get

$$U_i^{j+1} = \nu \frac{\Delta t}{(\Delta y)^2}\left(U_{i+1}^j - U_{i-1}^j\right) + \left(1 - 2\nu \frac{\Delta t}{(\Delta y)^2}\right) U_i^j \qquad (B.12)$$

This equation gives the velocity at time t_{j+1} if the velocity at time t_j is known. Since the unknown velocity is a function of known quantities and can be determined directly, this method is called explicit.

Stability of this numerical scheme (see ref. 5) requires that

$$1 - 2\nu \frac{\Delta t}{(\Delta y)^2} \geq 0 \qquad (B.13)$$

or

$$\nu \frac{\Delta t}{(\Delta y)^2} \geq \frac{1}{2} \qquad (B.14)$$

An obvious choice is

$$\nu \frac{\Delta t}{(\Delta y)^2} = \frac{1}{2} \qquad (B.15)$$

so that equation (B.12) becomes

$$U_i^{j+1} = \frac{1}{2}(U_{i+1}^j + U_{i-1}^j) \qquad (B.16)$$

Example

Use the explicit finite difference method to determine the development of the velocity profile near a plate suddenly set in motion with an arbitrary velocity 1.

Solution

At time zero, we have

$$U_1 = 0 \quad U_2 = 0 \quad U_3 = 0 \quad U_4 = 0 \quad U_5 = 0 \; .... \; U_n = 0$$

Using equation (B.16) we get

First time step

$$U_1 = 1 \quad U_2 = 0.5 \quad U_3 = 0 \quad U_4 = 0 \quad U_5 = 0 \; .... \; U_n = 0$$

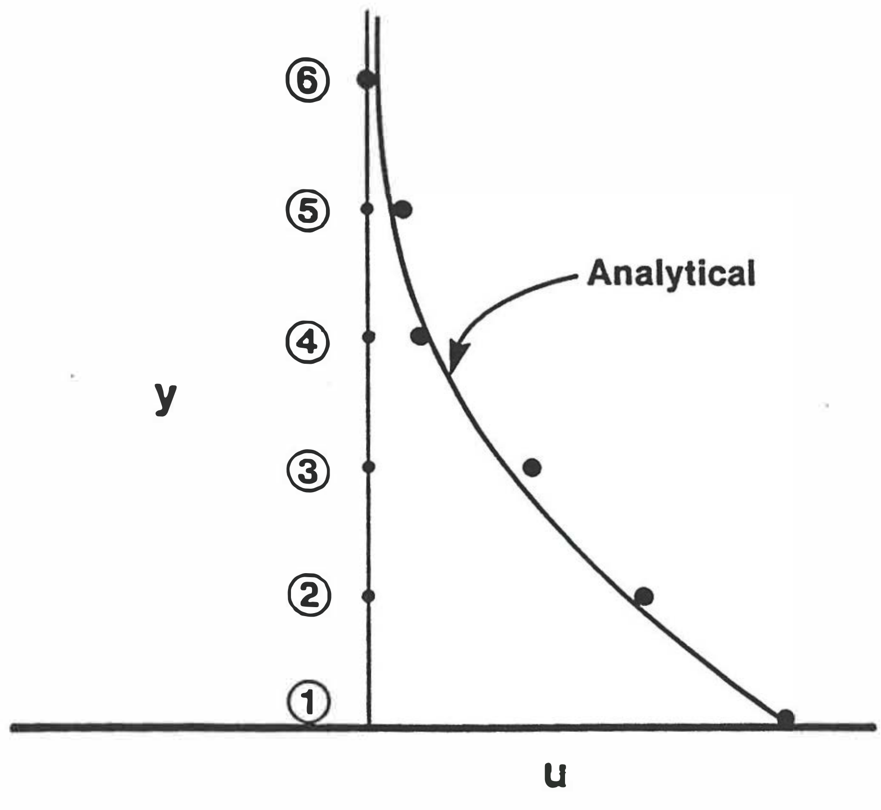

Fig. B.3

Second time step

$$U_1 = 1 \quad U_2 = 0.5 \quad U_3 = 0.25 \quad U_4 = 0.0 \quad U_5 = 0 \ldots U_n = 0$$

Third time step

$$U_1 = 1 \quad U_2 = 0.625 \quad U_3 = 0.25 \quad U_4 = 0.125 \quad U_5 = 0 \ldots U_n = 0$$

Fourth Time Step

$$U_1 = 1 \quad U_2 = 0.625 \quad U_3 = 0.375 \quad U_4 = 0.125 \quad U_5 = 0.0625 \quad U_4 = 0 \quad U_5 = 0 \ldots U_n = 0$$

A plot of the velocity profile after four time steps is shown in Fig. B.3. The agreement between these numerical results and the analytical solution

$$\frac{v_x}{V} = 1 - \operatorname{erf}\left(\frac{y}{\sqrt{4\nu t}}\right)$$

is relatively good. However, it should be pointed out that not all problems give such good results. Depending on the form of the equation to be solved and the boundary conditions, the solution might contain considerable errors.

B.4 UNSTEADY FLOW ANALYSIS BY THE IMPLICIT METHOD

Again we solve the partial differential equation of the previous section

$$\frac{\partial U}{\partial t} = \nu \frac{\partial^2 U}{\partial y^2} \tag{B.17}$$

with the boundary conditions

$$\begin{aligned} U &= 0 \quad \text{at} \quad t = 0 \\ U &= 1 \quad \text{at} \quad y = 0 \\ U &= 0 \quad \text{at} \quad y \to \infty \end{aligned} \tag{B.18}$$

For the time instant $j+1$ we approximate the equation by

$$\frac{U_i^{j+1} - U_i^j}{\Delta t} = \nu \frac{U_{i+1}^{j+1} - 2U_i^{j+1} U_{i-1}^{j+1}}{(\Delta y)^2} \tag{B.19}$$

Letting

$$r = \nu \frac{\Delta t}{(\Delta y)^2} \tag{B.20}$$

and rearranging, we get

$$- r U_{i-1}^{j+1} + (2r+1) U_i^{j+1} - r U_{i-1}^{j+1} = U_i^j \tag{B.21}$$

Let us now choose as in the previous section

$$r = \nu \frac{\Delta t}{(\Delta y)^2} = \frac{1}{2} \tag{B.22}$$

Thus we have

$$-\frac{1}{2} U_{i-1}^{j+1} + 2U_i^{j+1} - \frac{1}{2} U_{i-1}^{j+1} = U_i^j \tag{B.23}$$

We now use a 6 node grid and we assume that node 6 is far enough so that always $U_6 = 0$. We can write for the first time step:

node 2

$$-\frac{1}{2} U_1 + 2U_2 - \frac{1}{2} U_3 = 0$$

node 3

$$-\frac{1}{2} U_2 + 2U_3 - \frac{1}{2} U_4 = 0$$

node 4

$$-\frac{1}{2} U_3 + 2U_4 - \frac{1}{2} U_4 = 0$$

node 5

$$-\frac{1}{2} U_4 + 2U_5 - \frac{1}{2} U_6 = 0$$

Since $U = 1$ and $U_6 = 0$, we get

$$2 U_2 - \frac{1}{2} U_3 = \frac{1}{2}$$

$$-\frac{1}{2} U_2 + 2U_3 - \frac{1}{2} U_4 = 0$$

$$-\frac{1}{2} U_3 + 2U_4 - \frac{1}{2} U_5 = 0$$

$$-\frac{1}{2} U_4 + 2U_5 = 0$$

Solving these equations we obtain

$U_2 = 0.26794 \quad U_3 = 0.07177 \quad U_4 = 0.01910 \quad U_5 = 0.00477$

Since the nodal velocities are known at the first time step we can move to the second time step using equation (B.23) and so forth. At each step we must solve a system of algebraic equations that is why the method is referred to as an implicit method.

A very popular implicit method is the so-called Crank-Nicolson method [5,6]. This is a numerical scheme in which the second order derivative $\partial^2 u/\partial y^2$ is replaced by the mean of its finite-difference approximations on the (j + 1)th and jth time steps giving a representation of equation (B.17) in the form

$$\frac{U_i^{j+1}-U_i^j}{\Delta t} = \nu\frac{1}{2}\left(\frac{U_{i+1}^j-2U_i^j+U_{i-1}^j}{(\Delta y)^2}+\frac{U_{i+1}^{j+1}-2U_i^{j+1}+U_{i-1}^{j+1}}{(\Delta y)^2}\right)$$

While implicit methods are more complicated they exhibit much better stability (and convergence) characteristics than the explicit ones. The vast majority of scientific articles on finite difference solution of fluid mechanics problems are based on implicit methods.

By Convergence we mean that the results of the numerical method approach the analytical values as Δt and Δy approach zero. By Stability we mean that errors introduced by the numerical method remain bounded.

B.5 FINITE DIFFERENCE ANALYSIS OF A LAMINAR FREE JET

The steady laminar flow of a two-dimensional free jet is described by the boundary layer equations which are (see Section 9.4):

continuity
$$\frac{\partial v_y}{\partial y} + \frac{\partial v_z}{\partial z} = 0 \tag{B.25}$$

momentum
$$v_y\frac{\partial v_z}{\partial y} + v_z\frac{\partial v_z}{\partial z} = \nu\frac{\partial^2 v_z}{\partial y^2} \tag{B.26}$$

Note that the left-hand side of the momentum equations is non-linear.

The boundary conditions are:

$$z = 0 \qquad v_z = v_o(y)$$

$$y = 0 \qquad \frac{\partial v_z}{\partial z} = 0 \qquad v_y = 0$$

$$y \rightarrow \infty \qquad v_z = 0$$

To simplify the notation, let $v_z = U$ and $v_y = V$.

The finite difference grid is shown in Fig. B.4. We use the following expressions to approximate the derivatives at an arbitrary node $(z+\Delta z, y)$:

$$\frac{\partial U}{\partial z} = \frac{U(z+\Delta z,y) - U(z,y)}{\Delta z} \tag{B.27}$$

$$\frac{\partial U}{\partial y} = \frac{U(z+\Delta z,y+\Delta y) - U(z+\Delta z,y-\Delta y)}{2\Delta y} \tag{B.28}$$

$$\frac{\partial^2 U}{\partial y^2} = \frac{U(z+\Delta z,y+\Delta y) - 2U(z+\Delta z,y) + U(z+\Delta z,y-\Delta y)}{(\Delta y)^2} \tag{B.29}$$

$$\frac{\partial V}{\partial y} = \frac{V(z+\Delta z,y) - V(z+\Delta z,y-\Delta y)}{\Delta y} \tag{B.30}$$

Now, with the help of the above expressions, we approximate the momentum equation at an arbitrary node $(z+\Delta z, y)$. We have

$$V(z+\Delta z,y)\frac{U(z+\Delta z,y+\Delta y) - U(z+\Delta z,y-\Delta y)}{2\Delta y}$$

$$+ U(z+\Delta z,y) - \frac{U(z+\Delta z,y) - U(z,y)}{\Delta z}$$

$$= \nu \frac{U(z+\Delta z,y+\Delta y) - 2U(z+\Delta z,y) + U(z+\Delta z,y-\Delta y)}{(\Delta y)^2} \tag{B.31}$$

This equation may be written in the form

$$A\,U(z+\Delta z,y-\Delta y) + B\,U(z+\Delta z,y) + C\,U(z+\Delta z,y+\Delta y) = D \tag{B.32}$$

where

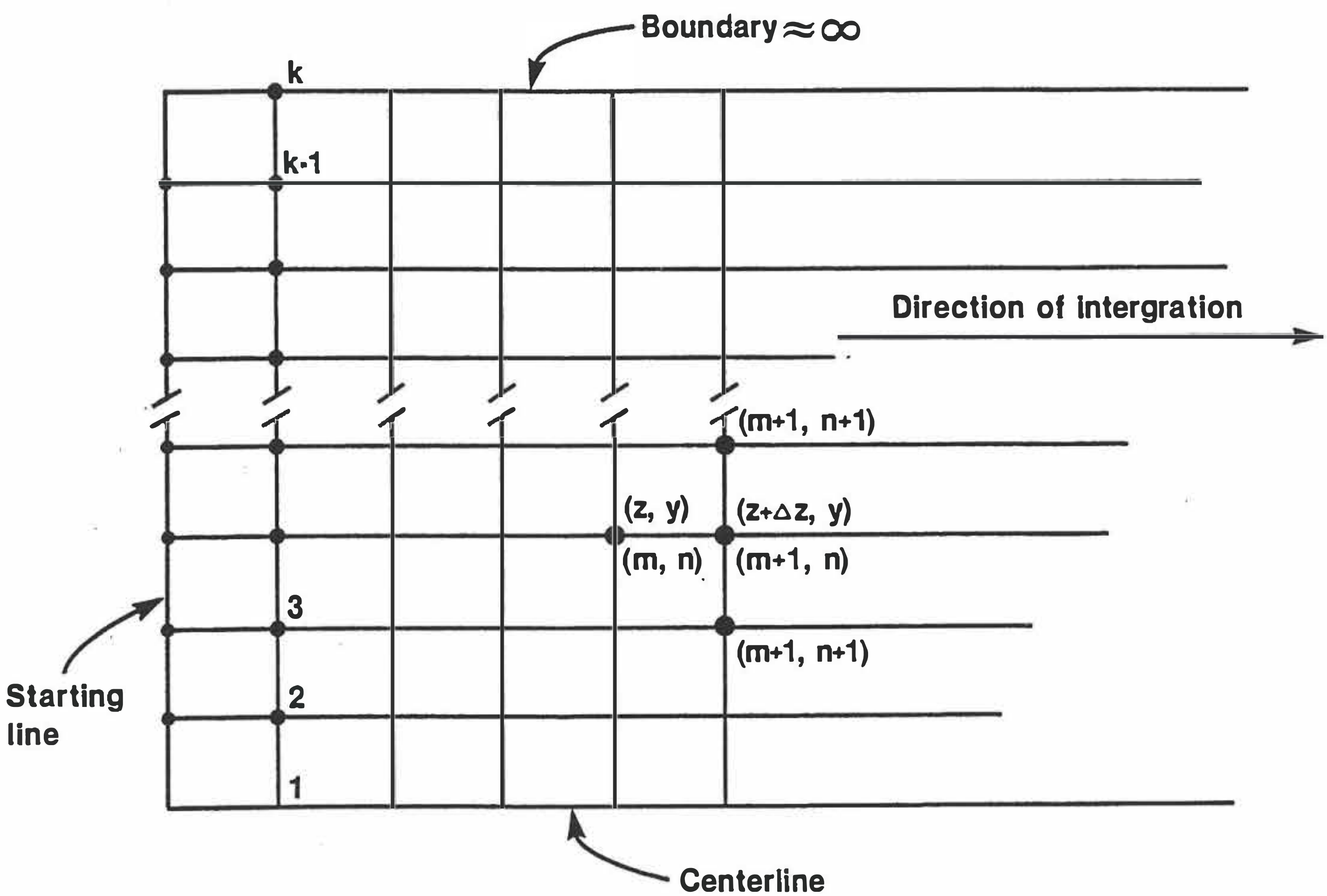

Fig. B.4 Finite difference grid for a laminar free jet.

$$A = -\frac{V(z+\Delta z,y)}{2\Delta y} - \frac{\nu}{(\Delta y)^2}$$

$$B = \frac{U(z+\Delta z,y)}{\Delta z} + \frac{2\nu}{(\Delta y)^2}$$

$$C = \frac{V(z+\Delta z,y)}{2\Delta y} - \frac{\nu}{(\Delta y)^2}$$

$$D = U(z+\Delta z,y)\frac{U(z,y)}{\Delta z}$$

Now, in order to write the finite difference equation for each interior point of the grid at Fig. B.4, we start from the axis of symmetry along which the points are labelled with the subscript 1. We have (along any m+1 line)

$$B_1 U_1 + 2C_1 U_2 = D_1 \tag{B.33}$$

$$A_n U_{n-1} + B_n U_n + C_n U_{n+1} = D_1 \qquad \text{for } n = 2, 3, \ldots, k-1 \tag{B.34}$$

$$A_k U_{k-1} + B_k U_k = D_k \tag{B.35}$$

This a nonlinear system of algebraic equations which can be linearized iteratively. At the starting line of Fig. B.4, all quantites are known and can be used to calculate A_n, B_n and C_n and then the triagonal system of equations above is solved to yield the unknown velocities U_n at the first vertical line after the starting line. These velocities are then introduced to the expression for A_n, B_n and C_n and the solutions repeated until the results of two successive iterations do not change more than a predetermined tolerance. The velocity V is also required for these calculations and it is determined explicitly from the continuity equation (B.25) which is written as

$$\frac{V(z+\Delta z,y) - V(z+\Delta z,y-\Delta y)}{\Delta y} + \frac{U(z+\Delta z,y) - U(z,y)}{\Delta z} = 0 \tag{B.36}$$

or

$$V(z+\Delta z,y) = V(z+\Delta z,y-\Delta y) - \frac{\Delta y}{\Delta z}(U(z+\Delta z,y) - U(z,y)) \tag{B.37}$$

After the calculations are completed for the first line, the solution is carried out to the next line (m+2) and so forth <u>(marching procedure).</u> If the iterative scheme exhibits poor convergence characteristics, it is advisable to use weighted averages between consecutive iterations. It is important to note that the speed of convergence depends greatly on the relative magnitude of the step sizes Δz and Δy. Usually a well-posed and well-behaved numerical scheme should not require more than a dozen iterations to converge [7]

More details about finite difference solutions of the boundary layer equations can be found in specialized texts [8--10] and literally many thousands of research papers.

B.6 FINITE ELEMENT FORMULATION

The finite element method (FEM) evolved gradually from physical arguments for problems in structural mechanics. It was later recognized that the approximations can be obtained from more general principles which are applicable to all types of problems involving partial differential equations. The major advances in the field of structural mechanics were done in the 1960's. Serious applications of finite element methods in fluid mechanics started in the early 1970's.

In the finite element method, again, the objective is to obtain difference equations. In the finite difference method we started from the <u>strong form</u> of the differential equations and approximated the derivatives directly by differences. In the finite element method the proper framework is the <u>weak form</u> where instead of asking for an equation that holds at each point we need an equation that holds for each function. This is the basis of the Galerkin method {named after the Russian engineer and mathematician B. Galerkin (1871-1945)}.

Consider the differential equation

$$L(u) - f = 0 \tag{B.38}$$

where L is some differential operator which may include $\partial/\partial x$, $\partial^2/\partial x^2$, $\partial/\partial t$ etc. and u is the unknown variable. The equation is valid in a domain D.

Approximate u by û where

$$\hat{u} = \sum_{i=1}^{n_i} N_i u_i \qquad (B.39)$$

N_i are assumed functions and u_i are unknown parameters and n the number of unknowns.

In general, there will be an approximation error, so that

$$L(\hat{u}) - f = R \neq 0 \qquad (B.40)$$

where R is called the residual error.

A weighted residual method (11) method determines the n unknowns by creating n equations which specify that the weighted average residual is zero, over some domain. For example,

$$\int_D W_i [L(u) - f] \, dD = \int_D W_i R \, dD = 0 \qquad i = 1,2,3,\ldots,n \qquad (B.41)$$

There are many choices for the weights W_i. In the Garlerkin method we simply choose $W_i = N_i$, i.e.

$$\int_D N_i [L(u) - f] \, dD = 0 \qquad i = 1,2,3,\ldots,n \qquad (B.42)$$

This relation can be applied over a local element and then by summing up the local Galerkin integrals we obtain an approximation for the entire domain. This will become more clear by applying this method to a simple problem in the next section.

B.7 FINITE ELEMENT SOLUTION FOR PRESSURE DRIVEN FLOW BETWEEN FLAT PLATES (Courtesy of H. Mavridis)

We have dealt with this problem by analytical methods (Sec. 7.2) and by finite differences (Fig. B.1). Here, we will solve the differential equation

$$\frac{d^2u}{dy^2} + 1 = 0 \qquad (B.43)$$

subject to the boundary conditions (see Fig. B.5 (a))

$$\frac{du}{dy} = 0 \quad \text{at } y=0 \qquad (B.44)$$

$$u = 0 \quad \text{at } y=1$$

We follow the five step procedure outlined below:

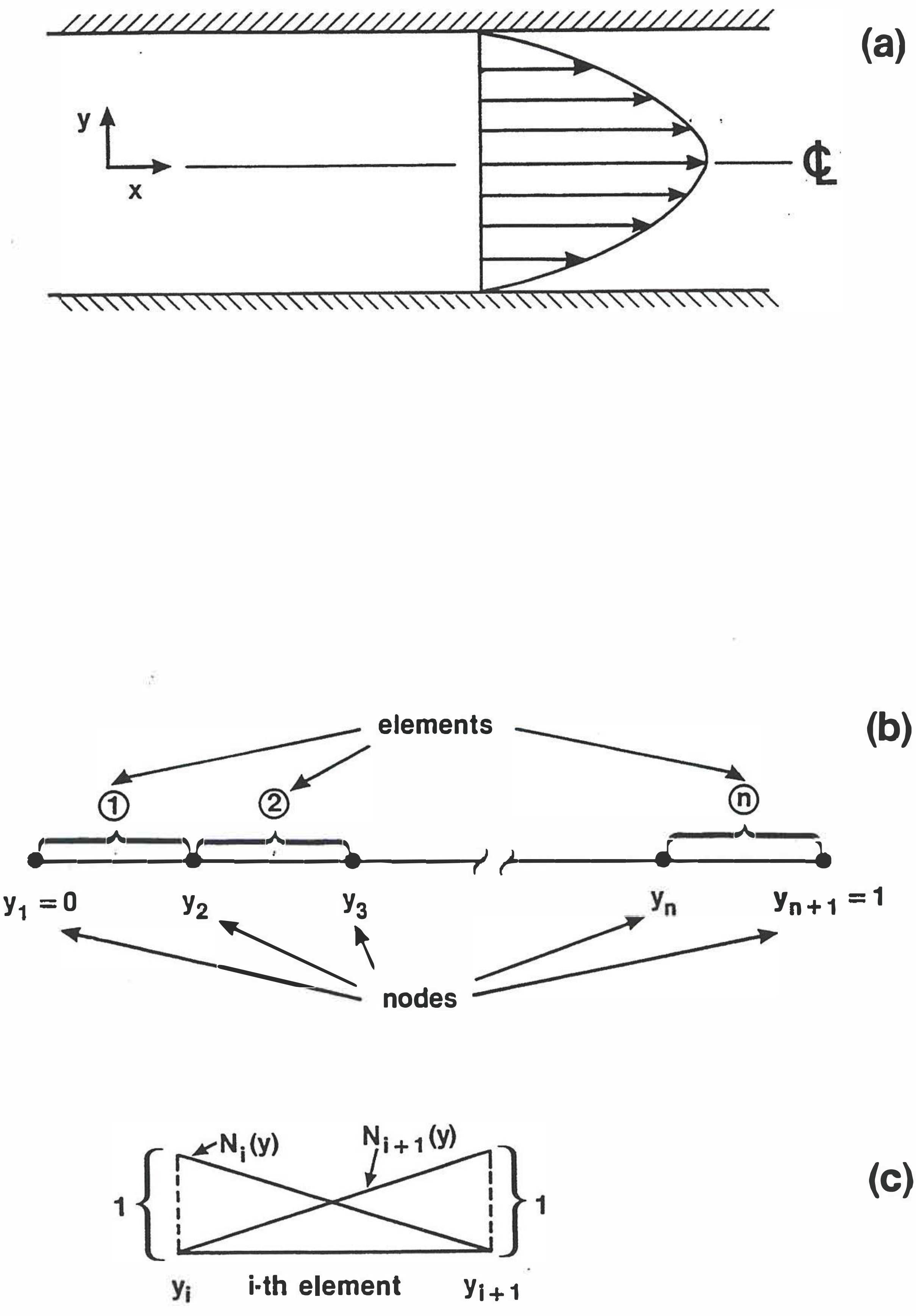

Fig. B.5 Problem definition and finite element discretization for pressure driven flow between flat plates.

(a) Discretize the solution domain as shown in Fig. B.5(b) . n+1 nodes define n elements (linear in this case). The discretization need not be equidistant (but it is used later on for the sake of simplicity).

(b) Define the approximating function as

$$u(y) = \sum_{i=1}^{n} N_i(y)\, u_i \tag{B.45}$$

where u_i is the u-value at node y_i (nodal variable) and $N_i(y)$ an appropriate interpolation function defined over the elements that share the i-th node. In our case $N_i(y)$ can be linear, so that at the element level

$$N_{i+1}(y) = \frac{y - y_{i+1}}{y_i - y_{i+1}} \tag{B.46}$$

We note that (see also Fig. B.3(c))

$$N_i(y_j) = 1 \qquad \text{if } i=j$$

$$= 0 \qquad \text{if } i \neq j$$

(c) Insert the approximation

$$\hat{u}(y) = \sum_{i=1}^{n} N_i(y)\, u_i \tag{B.47}$$

into the differential equation. Generally, there will be a residual i.e. an approximation error, so that

$$\frac{d^2}{dy^2}(\hat{u}(y)) + 1 \neq 0 \tag{B.48}$$

The Galerkin method requires this error to vanish in an average sense: the integral of residual over the domain weighted by the interpolation function to be zero, i.e.

$$R_i = \int \left\{ \frac{d^2}{dy^2}(u) + 1 \right\} N_i \, dy = 0 \tag{B.49}$$

and the u_i's are determined as the values that result in a zero average (=weighted) error (=residual).

There is a weighted residual R_i for every interior node, thus giving $(n-1)$ equations. Two more equations are provided from the end points by incorporating the boundary conditions. Therefore, we have $(n+1)$ equations for the $(n+1)$ unknowns $u_1, u_2, u_3, \ldots, u_{n+1}$.

(d) Simplify the expression for the residual by integrating by parts the highest derivative under the integral. The advantage of this approach is lower order differentiability requirements for the interpolation functions and most important the boundary terms that arise from the partial integration make easier the incorporation of boundary conditions. We have

$$R_i = \int_a^b \left\{ \frac{d^2}{dy^2}(\hat{u}) + 1 \right\} N_i \, dy \tag{B.50}$$

$$= \int_a^b \left\{ N_i \frac{d^2}{dy^2}(\hat{u}) + N_i \right\} dy$$

Integration by parts gives

$$\int_a^b N_i \frac{d}{dy}\left(\frac{d\hat{u}}{dy}\right) dy = N_i \frac{d\hat{u}}{dy}\bigg|_a^b - \int_a^b \frac{dN_i}{dy}\frac{d\hat{u}}{dy} \cancel{dy} \tag{B.51}$$

Thus

$$R_i = \int_a^b \left\{ \frac{dN_i}{dy}\frac{d\hat{u}}{dy} - N_i \right\} dy - N_i \frac{d\hat{u}}{dy}\bigg|_a^b = 0 \tag{B.52}$$

(e) Proceed to the solution by assembling the expressions for the residuals at each node which are determined from equation (B.52). The interpolation function should be such as to ensure the integrability of the expression under the integral sign. In this case we will use the simplest form which is a first order polynomial. Integrability also allows the evaluation at the element level. We note, however, that the second term is not under an integral and can simply be determined at the two ends of the solution domain. Thus, in assembling the contributions at the element level we must only evaluate the expressions under the integral sign.

To illustrate the above five step procedure we choose the four linear elements shown in Fig. (B.6).

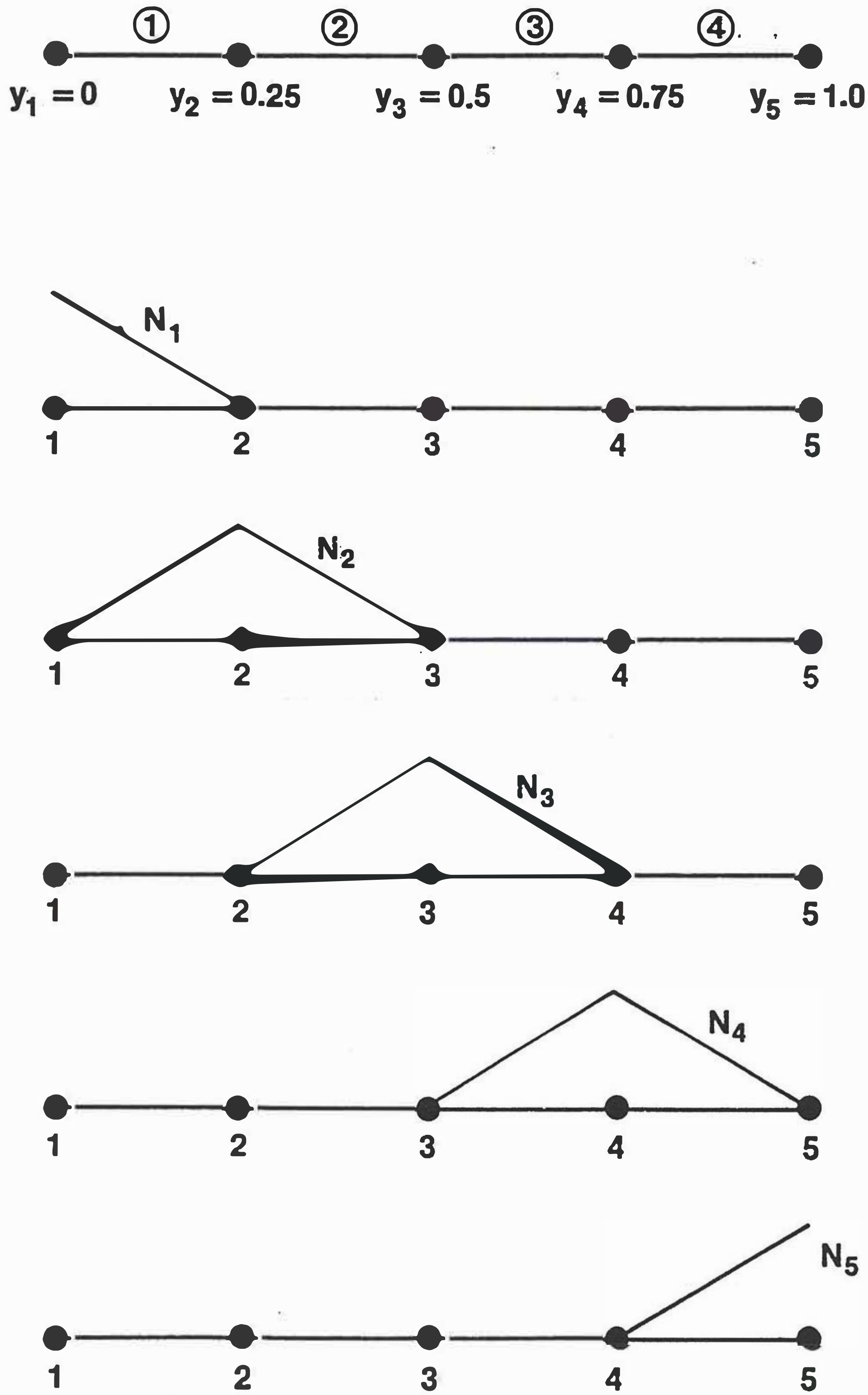

Fig. B.6 The F.E. grid and the corresponding values of the interpolation functions N.

For every element there are two residuals associated with it. $R_i^{\,j}$ indicates the contribution of the j-th element to the i-th residual. The residual at each interior node will be the sum of the residuals from the elements to the left and to the right of it.

First we note that

$$N_j = \frac{y - y_{j+1}}{y_j - y_{j+1}}$$

$$N_{j+1} = \frac{y - y_j}{y_j - y_{j+1}}$$

All other N_i's are zero in the interval $[y_j, y_{j+1}]$ (see also Fig. B.6). We have

$$R_j^{\,j} = \int_{y_j}^{y_{j+1}} \left\{ \frac{dN_j}{dy}\left(\frac{dN_j}{dy} u_j + \frac{d\,N_{j+1}}{dy} u_{j+1} \right) - N_j \right\} dy$$

$$= \left\{ \int_{y_j}^{y_{j+1}} \left(\frac{dN_j}{dy} \right)^2 dy \right\} u_j + \left\{ \int_{y_j}^{y_{j+1}} \frac{dN_j}{dy} \frac{d\,N_{j+1}}{dy}\, dy \right\} u_{j+1} - \int_{y_j}^{y_{j+1}} N_j dy$$

Since

$$\frac{dN_j}{dy} = - \frac{1}{y_{j+1} - y_i} \qquad \frac{dN_{j+1}}{dy} = \frac{1}{y_{j+1} - y_i}$$

we get

$$R_i^{\,j} = \left(- \frac{1}{y_{j+1} - y_j} \right)^2 (y_{j+1} - y_j) u_j - \frac{1}{(y_{j+1} - y_j)^2} (y_{j+1} - y_j) u_{j+1} - \frac{y_{j+1} - y_i}{2}$$

$$R_i^j = \frac{1}{y_{j+1} - y_j} u_j - \frac{1}{y_{j+1} - y_j} u_{j+1} - \frac{y_{j+1} - y_j}{2}$$

Similarly

$$R^j_{j+1} = \int_{y_j}^{y_{j+1}} \left\{ \frac{dN_{j+1}}{dy} \left(\frac{dN_j}{dy} u_j + \frac{dN_{j+1}}{dy} u_{j+1} \right) - N_{j+1} \right\} dy$$

$$= \int_{y_j}^{y_{j+1}} \frac{dN_{j+1}}{dy} \frac{dN_j}{dy} u_j dy + \int_{y_j}^{y_{j+1}} \left(\frac{dN_{j+1}}{dy} \right)^2 u_{j+1} dy - \int_{y_j}^{y_{j+1}} N_{j+1} dy$$

$$= \left(\frac{1}{y_{j+1} - y_j} \right) \left(- \frac{1}{y_{j+1} - y_j} \right) (y_{j+1} - y_j) u_j$$

$$+ \frac{1}{(y_{j+1} - y_j)^2} (y_{j+1} - y_i) u_{j+1} - \frac{y_{j+1} - y_j}{2}$$

$$R^j_{j+1} = - \frac{1}{y_{j+1} - y_j} u_j + \frac{1}{y_{j+1} - y_j} u_{j+1} - \frac{y_{j+1} - y_j}{2}$$

we have,

$$y_{j+1} - y_j = 0.25$$

Element ①

$$R_1^{①} = 4 u_1 - 4 u_2 - 0.125 = 0$$

$$R_2^{①} = -4 u_1 + 4 u_2 - 0.125 = 0$$

Element ②

$$R_2^{②} = 4 u_2 - 4 u_3 - 0.125 = 0$$

$$R_3^{②} = -4 u_2 + 4 u_3 - 0.125 = 0$$

Element ③

$$R_3^{③} = 4u_3 - 4u_4 - 0.125 = 0$$

$$R_4^{③} = -4u_3 + 4u_4 - 0.125 = 0$$

Element ④

$$R_4^{④} = 4u_4 - 4u_5 - 0.125 = 0$$

$$R_5^{④} = -4u_4 + 4u_5 - 0.125 = 0$$

We can now assemble the residual for each node noting also that the second term of equation (B.52) gives

$$N_i \frac{du}{dy}\bigg|_{y=0} = N_1 \frac{du}{dy}\bigg|_{y=0} = \frac{du}{dy}\bigg|_{y=0} \text{ and } N_i \frac{du}{dy}\bigg|_{y=1} = N_5 \frac{du}{dy}\bigg|_{y=1} = \frac{du}{dy}\bigg|_{y=1}$$

we have

$$R_1^{①} = R_1 = 4u_1 - 4u_2 - 0.125 - du/dy\bigg|_{y=0} = 0$$

$$R_2^{①} + R_2^{②} = R_2 = -4u_1 + 8u_2 - 4u_3 - 0.25 = 0$$

$$R_3^{②} + R_3^{③} = R_3 = -4u_2 + 8u_3 - 4u_4 - 0.25 = 0$$

$$R_4^{③} + R_4^{④} = R_4 - 4u_3 + 8u_4 - 4u_5 - 0.25 = 0$$

$$R_5^{④} = R_5 = -4u_4 + 4u_5 - 0.125 - \frac{du}{dy}\bigg|_{y=1}$$

or

$$4u_1 - 4u_2 = 0.125 + du/dy \Big|_{y=0}$$

$$-4u_1 + 8u_2 - 4u_3 = 0.25$$

$$-4u_2 + 8u_3 - 4u_4 = 0.25$$

$$-4u_3 + 8u_4 - 4u_5 = 0.25$$

$$-4u_4 + 4u_5 = 0.125 + \frac{du}{dy}\Big|_{y=1}$$

and after applying the boundary conditions ($du/dy|_{y=0} = 0$ $u_5 = 0$) and discarding R_5 (since we know the velocity $u_5 = 0$ we do not need an approximation at this point) we get

$$4u_1 - 4u_2 = 0.125$$

$$-4u_1 + 8u_2 - 4u_3 = 0.25$$

$$-4u_2 + 8u_3 - 4u_4 = 0.25$$

$$-4u_3 + 8u_4 = 0.25$$

The solution is

$u_1 = 0.5$	$y_1 = 0$
$u_2 = 0.46875$	$y_2 = 0.25$
$u_3 = 0.375$	$y_3 = 0.5$
$u_4 = 0.21875$	$y_4 = 0.75$
$u_5 = 0$	$y_5 = 1.0$

This is actually the exact solution! In Fig. B.7 we interpolate by drawing straight lines between the calculated points. Obviously with a few more linear elements the numerical solution could be indistinguishable from the analytical (parabolic) velocity profile.

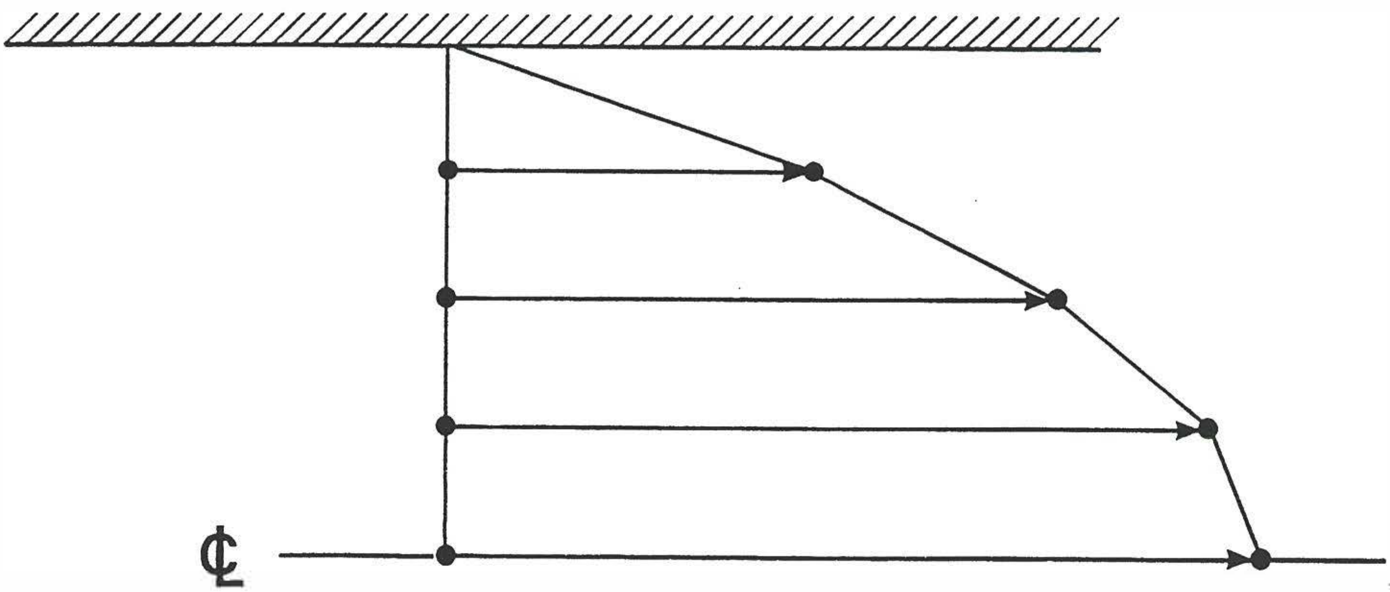

Fig. B.7 Velocity profile as determined by the finite element method.

REFERENCES

1. G. Strang, "Introduction to Applied Mathematics", Wellesley-Cambridge Press, Wellesley, Mass.

2. P.J. Roache, "Computational Fluid Dynamics", 2nd Edition, Hermosa Publishers, Albuquerque, NM (1976).

3. K.H. Huebner and E.A. Thornton, "The Finite Element Method for Engineers", 2nd Edition, Wiley, New York (1982).

4. A.J. Baker, "Finite Element Computational Fluid Mechanics", McGraw-Hill, New York (1983).

5. C.F. Gerald, "Applied Numerical Analysis", Edition, Addison-Wesley, Reading, Mass (198__).

6. G.D. Smith, "Numerical Solution of Partial Differential Equations: Finite Difference Methods", 2nd Edition, Clarendon Press, Oxford (1978).

7. J. Vlachopoulos, "A Numerical Study of Laminar Magnetohydrodynamic Free Jets", Computers and Fluids, 2, 261 (1974).

8. S.V. Patankar and D.B. Spalding "Heat and Mass Transfer in Boundary Layers" 2nd Edition, Intertext Books, London, (1970).

9. S.V. Patankar "Numerical Heat Transfer and Fluid Flow" Hemisphere Publishing Corp. Washington (1980).

10. C-Y Chow "An Introduction to Computational Fluid Mechanics" J. Wiley, New York (1979).

11. B.A. Finlayson, "The Method of Weighted Residuals and Variational Principles" Academic Press, New York, (1972).

The achievements of one of the pioneers of the Finite Element Method (FEM) are described in a special presentation:

JOHN H. ARGYRIS ENGINEERING PIONEER, INNOVATOR AND VISIONARY (1913-2004). Presented at 5th GRACM INTERN. CONGRESS COMP. MECH. Limassol, Cyprus, June 29-July 1, 2005, by John Vlachopoulos. Available at www.polydynamics.com

APPENDIX C

Fluid Property Data

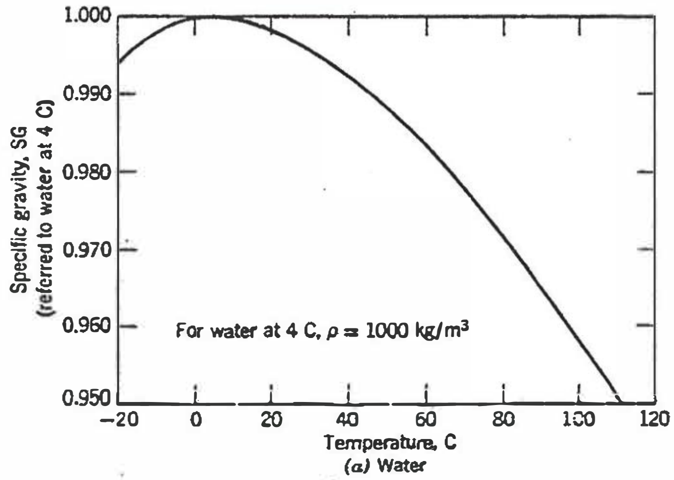

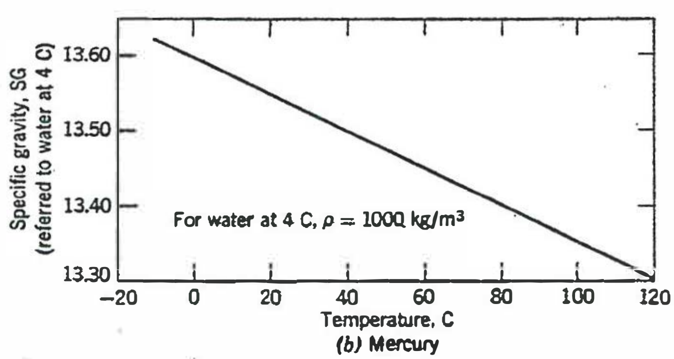

Specific gravity of water and mercury as functions of temperature (data from Ref. 1).

Specific Gravities of Several Common Manometer Fluids at 20 C

Fluid	Specific Gravity*
E. V. Hill blue oil	0.797
Meriam red oil	0.827
Benzene	0.879
Dibutyl phthalate	1.04
Monochloronaphthalene	1.20
Carbon tetrachloride	1.595
Bromoethylbenzene (Meriam blue)	1.75
Tetrabromoethane	2.95
Mercury	13.55

Specific gravity, $SG \equiv \rho/\rho_{H_2O}$ (at 4 C); ρ_{H_2O} (at 4 C) = 1000 kg/m^3 (1.94 slug/ft^3)

Physical Properties of Common Liquids at 20 C

Liquid	Isentropic Bulk Modulus* (GN/m^2)	Specific Gravity (−)
Benzene	1.48	0.879
Carbon tetrachloride	1.36	1.595
Castor oil	2.11	0.969
Gasoline	—	0.72
Glycerin	4.59	1.26
Heptane	0.886	0.684
Kerosine	1.43	0.82
Lubricating oil	1.44	0.88
Mercury	28.5	13.55
Octane	0.963	0.702
Sea water	2.42	1.025
Water	2.24	0.998

* Calculated from speed of sound; 1 GN/m^2 = 10^9 N/m^2 (1 N/m^2 = 1.45×10^{-4} lbf/in.^{2})

Surface Tension of Common Liquids at 20 C

Liquid	Surface Tension, σ (mN/m)*	Contact Angle, θ (degrees)
(a) In contact with air		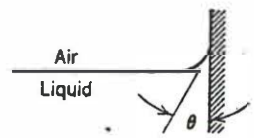
Benzene	28.9	
Carbon tetrachloride	27.0	
Glycerin	63.0	
Hexane	18.4	
Kerosine	26.8	
Lube oil	25–35	
Mercury	484	140
Methanol	22.6	
Octane	21.8	
Water	72.8	~ 0
(b) In contact with water		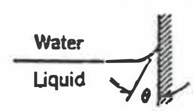
Benzene	35.0	
Carbon tetrachloride	45.0	
Hexane	51.1	
Mercury	375	140
Methanol	22.7	
Octane	50.8	

* 1 mN/m = 10^{-3} N/m

Properties of the U.S. Standard Atmosphere

Geometric Altitude (meters)	Temperature (K)	p/p_0 (—)	ρ/ρ_0 (—)
−500	291.4	1.061	1.049
0	288.2	1.000*	1.000†
500	284.9	0.9421	0.9529
1,000	281.7	0.8870	0.9075
1,500	278.4	0.8345	0.8638
2,000	275.2	0.7846	0.8217
2,500	271.9	0.7372	0.7812
3,000	268.7	0.6920	0.7423
3,500	265.4	0.6492	0.7048
4,000	262.2	0.6085	0.6689
4,500	258.9	0.5700	0.6343
5,000	255.7	0.5334	0.6012
6,000	249.2	0.4660	0.5389
7,000	242.7	0.4057	0.4817
8,000	236.2	0.3519	0.4292
9,000	229.7	0.3040	0.3813
10,000	223.3	0.2615	0.3376
11,000	216.8	0.2240	0.2978
12,000	216.7	0.1915	0.2546
13,000	216.7	0.1636	0.2176
14,000	216.7	0.1399	0.1860
15,000	216.7	0.1195	0.1590
16,000	216.7	0.1022	0.1359
17,000	216.7	0.08734	0.1162
18,000	216.7	0.07466	0.09930
19,000	216.7	0.06383	0.08489
20,000	216.7	0.05457	0.07258
22,000	218.6	0.03995	0.05266
24,000	220.6	0.02933	0.03832
26,000	222.5	0.02160	0.02797
28,000	224.5	0.01595	0.02047
30,000	226.5	0.01181	0.01503
40,000	250.4	0.002834	0.003262
50,000	270.7	0.0007874	0.0008383
60,000	255.8	0.0002217	0.0002497
70,000	219.7	0.00005448	0.00007146
80,000	180.7	0.00001023	0.00001632
90,000	180.7	0.000001622	0.000002588

* $p_0 = 1.01325 \times 10^5$ N/m² absolute (= 14.696 psia)
† $\rho_0 = 1.2250$ kg/m³ (= 0.002377 slug/ft³)

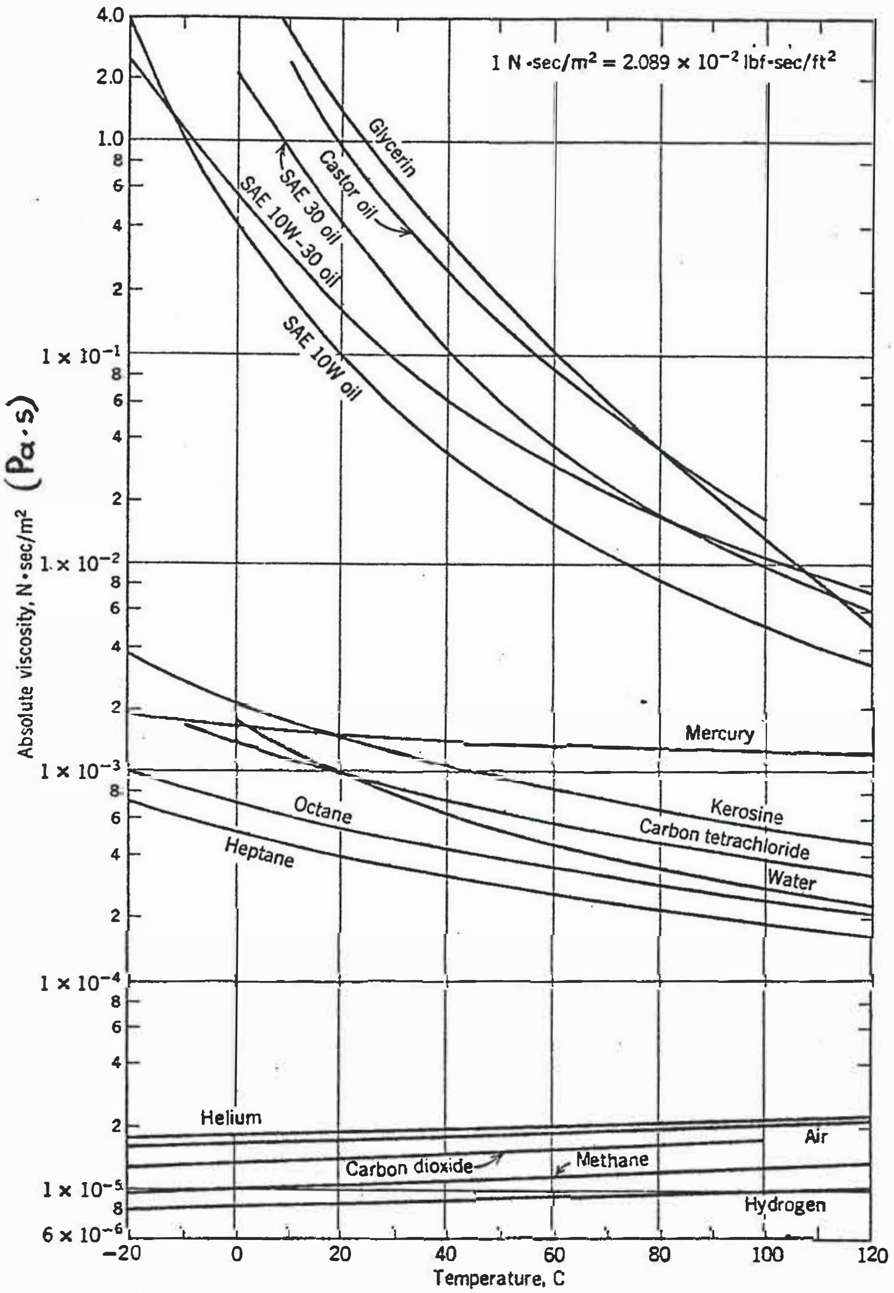

Dynamic (absolute) viscosity of common fluids as a function of temperature

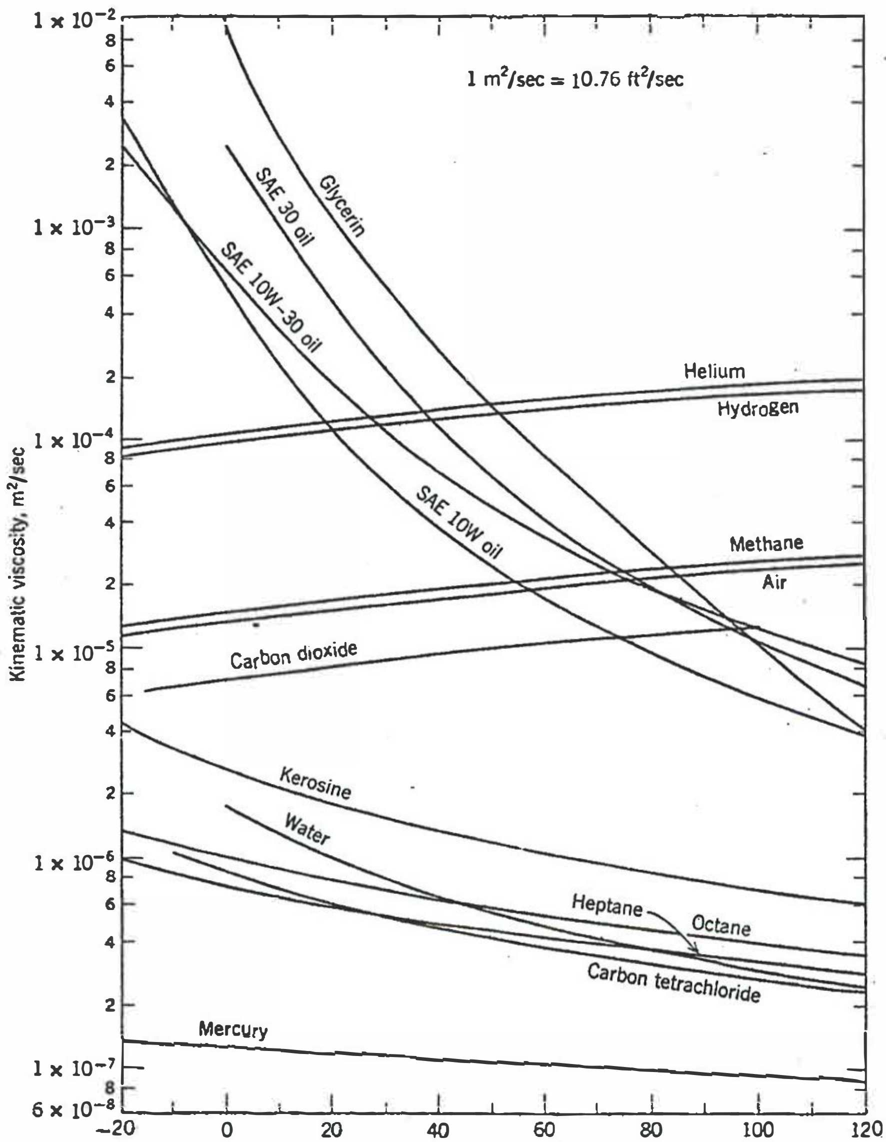

Kinematic viscosity of common fluids (at atmospheric pressure) as a function of temperature

Allowable Viscosity Ranges for SAE Lubricant Classifications

Lubricant Type	SAE Viscosity Number	Viscosity Range (centistokes)* At 0 F Minimum	At 0 F Maximum	At 210 F Minimum	At 210 F Maximum
Crankcase	5 *W*		1,200	3.9	
	10 *W*	1,200	2,400	3.9	
	20 *W*	2,400	9,600	3.9	
	20			5.7	9.6
	30			9.6	12.9
	40			12.9	16.8
	50			16.8	22.7
Transmission and axle	75		15,000		
	80	15,000	100,000		
	90			75	120
	140			120	200
	250			200	
Automatic transmission fluid	Type *A*	39†	43†	7	8.5

* 1 centistoke = 1 cSt = 10^{-6} m^2/sec (= 1.08 × 10^{-5} ft^2/sec)
† At 100 F.

Thermodynamic Properties of Common Gases at STP*

Gas	Chemical Symbol	Molecular Mass, M_m	$R^\dagger$ $\left(\frac{J}{kg \cdot K}\right)$	c_p $\left(\frac{J}{kg \cdot K}\right)$	c_v $\left(\frac{J}{kg \cdot K}\right)$	$k = \frac{c_p}{c_v}$ (—)	$R^\dagger$ $\left(\frac{ft \cdot lbf}{lbm \cdot R}\right)$	c_p $\left(\frac{Btu}{lbm \cdot R}\right)$	c_v $\left(\frac{Btu}{lbm \cdot R}\right)$
Air	—	28.98	286.9	1,004	717.4	1.40	53.33	0.2399	0.1713
Carbon dioxide	CO_2	44.01	188.9	840.4	651.4	1.29	35.11	0.2007	0.1556
Carbon monoxide	CO	28.01	296.8	1,039	742.1	1.40	55.17	0.2481	0.1772
Helium	He	4.003	2,077	5,225	3,147	1.66	386.1	1.248	0.7517
Hydrogen	H_2	2.016	4,124	14,180	10,060	1.41	766.5	3.388	2.402
Methane	CH_4	16.04	518.3	2,190	1,672	1.31	96.32	0.5231	0.3993
Nitrogen	N_2	28.01	296.8	1,039	742.0	1.40	55.16	0.2481	0.1772
Oxygen	O_2	32.00	259.8	909.4	649.6	1.40	48.29	0.2172	0.1551
Steam‡	H_2O	18.02	461.4	~2,000	~1,540	~1.30	85.78	~0.478	~0.368

* STP = standard temperature and pressure, T = 15 C (59 F) and p = 101.325 kPa absolute (14.696 psia).

† $R \equiv R_u/M_m$; R_u = 8314.3 J/kgmol · K (1545.3 ft · lbf/lbmol · R); 1 Btu = 778.2 ft · lbf.

‡ Water vapor behaves as an ideal gas when superheated by 55 C (100 F) or more.

APPENDIX D

THE CONSERVATION EQUATIONS IN VARIOUS COORDINATES

CURVILINEAR COORDINATES

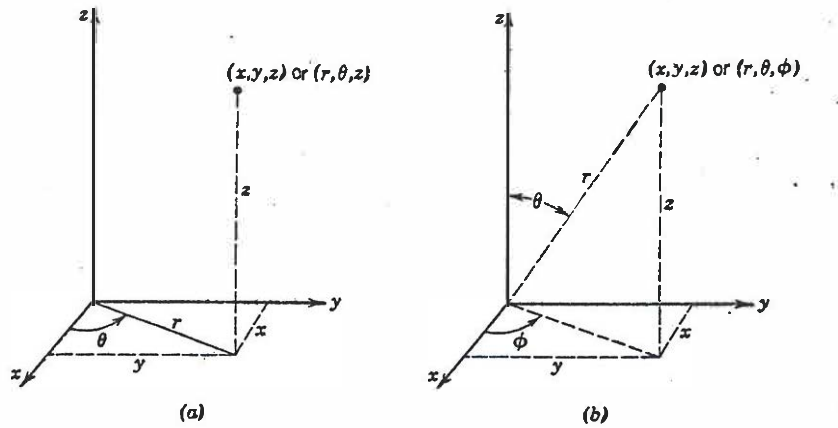

(a) Cylindrical coordinates. The ranges of the variables are $0<r<\infty$, $0<\theta<2\pi$, $-\infty<z<\infty$. (b) Spherical coordinates. The ranges of the variables are $0<r<\infty$, $0<\theta<\pi$, and $0<\phi<2\pi$.

Cylindrical Coordinates

$$\begin{cases} x = r\cos\theta \\ y = r\sin\theta \\ z = z \end{cases} \qquad \begin{cases} r = +\sqrt{x^2+y^2} \\ \theta = \arctan(y/x) \\ z = z \end{cases}$$

Spherical Coordinates

$$\begin{cases} x = r\sin\theta\cos\phi \\ y = r\sin\theta\sin\phi \\ z = r\cos\theta \end{cases} \qquad \begin{cases} r = +\sqrt{x^2+y^2+z^2} \\ \theta = \arctan\left(\sqrt{x^2+y^2}/z\right) \\ \phi = \arctan(y/x) \end{cases}$$

THE EQUATION OF CONTINUITY IN SEVERAL COORDINATE SYSTEMS

Rectangular coordinates (x, y, z):

$$\frac{\partial \rho}{\partial t} + \frac{\partial}{\partial x}(\rho v_x) + \frac{\partial}{\partial y}(\rho v_y) + \frac{\partial}{\partial z}(\rho v_z) = 0 \qquad (A)$$

Cylindrical coordinates (r, θ, z):

$$\frac{\partial \rho}{\partial t} + \frac{1}{r}\frac{\partial}{\partial r}(\rho r v_r) + \frac{1}{r}\frac{\partial}{\partial \theta}(\rho v_\theta) + \frac{\partial}{\partial z}(\rho v_z) = 0 \qquad (B)$$

Spherical coordinates (r, θ, ϕ):

$$\frac{\partial \rho}{\partial t} + \frac{1}{r^2}\frac{\partial}{\partial r}(\rho r^2 v_r) + \frac{1}{r \sin\theta}\frac{\partial}{\partial \theta}(\rho v_\theta \sin\theta) + \frac{1}{r \sin\theta}\frac{\partial}{\partial \phi}(\rho v_\phi) = 0 \qquad (C)$$

MOMENTUM EQUATION IN RECTANGULAR CARTESIAN (x, y, z) COORDINATES

x component: $$\rho\left(\frac{\partial v_x}{\partial t} + v_x\frac{\partial v_x}{\partial x} + v_y\frac{\partial v_x}{\partial y} + v_z\frac{\partial v_x}{\partial z}\right) = -\frac{\partial p}{\partial x} + \frac{\partial \tau_{xx}}{\partial x} + \frac{\partial \tau_{yx}}{\partial y} + \frac{\partial \tau_{zx}}{\partial z} + \rho g_x$$

y component: $$\rho\left(\frac{\partial v_y}{\partial t} + v_x\frac{\partial v_y}{\partial x} + v_y\frac{\partial v_y}{\partial y} + v_z\frac{\partial v_y}{\partial z}\right) = -\frac{\partial p}{\partial y} + \frac{\partial \tau_{xy}}{\partial x} + \frac{\partial \tau_{yy}}{\partial y} + \frac{\partial \tau_{zy}}{\partial z} + \rho g_y$$

z component: $$\rho\left(\frac{\partial v_z}{\partial t} + v_x\frac{\partial v_z}{\partial x} + v_y\frac{\partial v_z}{\partial y} + v_z\frac{\partial v_z}{\partial z}\right) = -\frac{\partial p}{\partial z} + \frac{\partial \tau_{xz}}{\partial x} + \frac{\partial \tau_{yz}}{\partial y} + \frac{\partial \tau_{zz}}{\partial z} + \rho g_z$$

STRESS CONSTITUTIVE EQUATION FOR A NEWTONIAN FLUID IN RECTANGULAR CARTESIAN (x, y, z) COORDINATES

$$\tau_{xx} = \eta\left[2\frac{\partial v_x}{\partial x} - \tfrac{2}{3}(\nabla \cdot \mathbf{v})\right]$$

$$\tau_{yy} = \eta\left[2\frac{\partial v_y}{\partial y} - \tfrac{2}{3}(\nabla \cdot \mathbf{v})\right]$$

$$\tau_{zz} = \eta\left[2\frac{\partial v_z}{\partial z} - \tfrac{2}{3}(\nabla \cdot \mathbf{v})\right]$$

$$\tau_{xy} = \tau_{yx} = \eta\left[\frac{\partial v_x}{\partial y} + \frac{\partial v_y}{\partial x}\right]$$

$$\tau_{yz} = \tau_{zy} = \eta\left[\frac{\partial v_y}{\partial z} + \frac{\partial v_z}{\partial y}\right]$$

$$\tau_{zx} = \tau_{xz} = \eta\left[\frac{\partial v_z}{\partial x} + \frac{\partial v_x}{\partial z}\right]$$

$$(\nabla \cdot v) = \frac{\partial v_x}{\partial x} + \frac{\partial v_y}{\partial y} + \frac{\partial v_z}{\partial z}$$

The viscosity is usually denoted by

the Greek letter μ (for Newtonian fluids)

or η (for Non-Newtonian fluids)

MOMENTUM EQUATION IN CYLINDRICAL (r, θ, z) COORDINATES

r component:

$$\rho\left(\frac{\partial v_r}{\partial t} + v_r \frac{\partial v_r}{\partial r} + \frac{v_\theta}{r}\frac{\partial v_r}{\partial \theta} - \frac{v_\theta^2}{r} + v_z \frac{\partial v_r}{\partial z}\right) = -\frac{\partial p}{\partial r} + \frac{1}{r}\frac{\partial}{\partial r}(r\tau_{rr}) + \frac{1}{r}\frac{\partial \tau_{r\theta}}{\partial \theta} - \frac{\tau_{\theta\theta}}{r} + \frac{\partial \tau_{rz}}{\partial z} + \rho g_r$$

θ component:

$$\rho\left(\frac{\partial v_\theta}{\partial t} + v_r \frac{\partial v_\theta}{\partial r} + \frac{v_\theta}{r}\frac{\partial v_\theta}{\partial \theta} + \frac{v_r v_\theta}{r} + v_z \frac{\partial v_\theta}{\partial z}\right) = -\frac{1}{r}\frac{\partial p}{\partial \theta} + \frac{1}{r^2}\frac{\partial}{\partial r}(r^2\tau_{r\theta}) + \frac{1}{r}\frac{\partial \tau_{\theta\theta}}{\partial \theta} + \frac{\partial \tau_{\theta z}}{\partial z} + \rho g_\theta$$

z component:

$$\rho\left(\frac{\partial v_z}{\partial t} + v_r \frac{\partial v_z}{\partial r} + \frac{v_\theta}{r}\frac{\partial v_z}{\partial \theta} + v_z \frac{\partial v_z}{\partial z}\right) = -\frac{\partial p}{\partial z} + \frac{1}{r}\frac{\partial}{\partial r}(r\tau_{rz}) + \frac{1}{r}\frac{\partial \tau_{\theta z}}{\partial \theta} + \frac{\partial \tau_{zz}}{\partial z} + \rho g_z$$

STRESS CONSTITUTIVE EQUATION FOR A NEWTONIAN FLUID IN CYLINDRICAL (r, θ, z) COORDINATES

$$\tau_{rr} = \eta\left[2\frac{\partial v_r}{\partial r} - \tfrac{2}{3}(\nabla \cdot \mathbf{v})\right]$$

$$\tau_{\theta\theta} = \eta\left[2\left(\frac{1}{r}\frac{\partial v_\theta}{\partial \theta} + \frac{v_r}{r}\right) - \tfrac{2}{3}(\nabla \cdot \mathbf{v})\right]$$

$$\tau_{zz} = \eta\left[2\frac{\partial v_z}{\partial z} - \tfrac{2}{3}(\nabla \cdot \mathbf{v})\right]$$

$$\tau_{r\theta} = \tau_{\theta r} = \eta\left[r\frac{\partial}{\partial r}\left(\frac{v_\theta}{r}\right) + \frac{1}{r}\frac{\partial v_r}{\partial \theta}\right]$$

$$\tau_{\theta z} = \tau_{z\theta} = \eta\left[\frac{\partial v_\theta}{\partial z} + \frac{1}{r}\frac{\partial v_z}{\partial \theta}\right]$$

$$\tau_{zr} = \tau_{rz} = \eta\left[\frac{\partial v_z}{\partial r} + \frac{\partial v_r}{\partial z}\right]$$

$$(\nabla \cdot \mathbf{v}) = \frac{1}{r}\frac{\partial}{\partial r}(r v_r) + \frac{1}{r}\frac{\partial v_\theta}{\partial \theta} + \frac{\partial v_z}{\partial z}$$

The viscosity is usually denoted by the Greek letter μ (for Newtonian fluids) or η (for Non-Newtonian fluids)

MOMENTUM EQUATION IN SPHERICAL (r, θ, ϕ) COORDINATES

r component:
$$\rho\left(\frac{\partial v_r}{\partial t} + v_r\frac{\partial v_r}{\partial r} + \frac{v_\theta}{r}\frac{\partial v_r}{\partial \theta} + \frac{v_\phi}{r\sin\theta}\frac{\partial v_r}{\partial \phi} - \frac{v_\theta^2 + v_\phi^2}{r}\right)$$
$$= -\frac{\partial p}{\partial r} + \frac{1}{r^2}\frac{\partial}{\partial r}(r^2\tau_{rr}) + \frac{1}{r\sin\theta}\frac{\partial}{\partial \theta}(\tau_{r\theta}\sin\theta) + \frac{1}{r\sin\theta}\frac{\partial \tau_{r\phi}}{\partial \phi} - \frac{\tau_{\theta\theta} + \tau_{\phi\phi}}{r} + \rho g_r$$

θ component:
$$\rho\left(\frac{\partial v_\theta}{\partial t} + v_r\frac{\partial v_\theta}{\partial r} + \frac{v_\theta}{r}\frac{\partial v_\theta}{\partial \theta} + \frac{v_\phi}{r\sin\theta}\frac{\partial v_\theta}{\partial \phi} + \frac{v_r v_\theta}{r} - \frac{v_\phi^2\cot\theta}{r}\right)$$
$$= -\frac{1}{r}\frac{\partial p}{\partial \theta} + \frac{1}{r^2}\frac{\partial}{\partial r}(r^2\tau_{r\theta}) + \frac{1}{r\sin\theta}\frac{\partial}{\partial \theta}(\tau_{\theta\theta}\sin\theta) + \frac{1}{r\sin\theta}\frac{\partial \tau_{\theta\phi}}{\partial \phi} + \frac{\tau_{r\theta}}{r} - \frac{\cot\theta}{r}\tau_{\phi\phi} + \rho g_\theta$$

ϕ component:
$$\rho\left(\frac{\partial v_\phi}{\partial t} + v_r\frac{\partial v_\phi}{\partial r} + \frac{v_\theta}{r}\frac{\partial v_\phi}{\partial \theta} + \frac{v_\phi}{r\sin\theta}\frac{\partial v_\phi}{\partial \phi} + \frac{v_\phi v_r}{r} + \frac{v_\theta v_\phi}{r}\cot\theta\right)$$
$$= -\frac{1}{r\sin\theta}\frac{\partial p}{\partial \phi} + \frac{1}{r^2}\frac{\partial}{\partial r}(r^2\tau_{r\phi}) + \frac{1}{r}\frac{\partial \tau_{\theta\phi}}{\partial \theta} + \frac{1}{r\sin\theta}\frac{\partial \tau_{\phi\phi}}{\partial \phi} + \frac{\tau_{r\phi}}{r} + \frac{2\cot\theta}{r}\tau_{\theta\phi} + \rho g_\phi$$

STRESS CONSTITUTIVE EQUATION FOR A NEWTONIAN FLUID IN SPHERICAL (r, θ, ϕ) COORDINATES

$$\tau_{rr} = \eta\left[2\frac{\partial v_r}{\partial r} - \tfrac{2}{3}(\nabla\cdot\mathbf{v})\right]$$
$$\tau_{\theta\theta} = \eta\left[2\left(\frac{1}{r}\frac{\partial v_\theta}{\partial \theta} + \frac{v_r}{r}\right) - \tfrac{2}{3}(\nabla\cdot\mathbf{v})\right]$$
$$\tau_{\phi\phi} = \eta\left[2\left(\frac{1}{r\sin\theta}\frac{\partial v_\phi}{\partial \phi} + \frac{v_r}{r} + \frac{v_\theta\cot\theta}{r}\right) - \tfrac{2}{3}(\nabla\cdot\mathbf{v})\right]$$
$$\tau_{r\theta} = \tau_{\theta r} = \eta\left[r\frac{\partial}{\partial r}\left(\frac{v_\theta}{r}\right) + \frac{1}{r}\frac{\partial v_r}{\partial \theta}\right]$$
$$\tau_{\theta\phi} = \tau_{\phi\theta} = \eta\left[\frac{\sin\theta}{r}\frac{\partial}{\partial \theta}\left(\frac{v_\phi}{\sin\theta}\right) + \frac{1}{r\sin\theta}\frac{\partial v_\theta}{\partial \phi}\right]$$
$$\tau_{\phi r} = \tau_{r\phi} = \eta\left[\frac{1}{r\sin\theta}\frac{\partial v_r}{\partial \phi} + r\frac{\partial}{\partial r}\left(\frac{v_\phi}{r}\right)\right]$$
$$(\nabla\cdot\mathbf{v}) = \frac{1}{r^2}\frac{\partial}{\partial r}(r^2 v_r) + \frac{1}{r\sin\theta}\frac{\partial}{\partial \theta}(v_\theta\sin\theta) + \frac{1}{r\sin\theta}\frac{\partial v_\phi}{\partial \phi}$$

The viscosity is usually denoted by

the Greek letter μ (for Newtonian fluids)

or η (for Non-Newtonian fluids)

THE EQUATIONS OF MOTION FOR CONSTANT μ AND ρ IN RECTANGULAR COORDINATES (x, y, z)

x-Direction

$$\rho\left(\frac{\partial v_x}{\partial t} + v_x\frac{\partial v_x}{\partial x} + v_y\frac{\partial v_x}{\partial y} + v_z\frac{\partial v_x}{\partial z}\right) = -\frac{\partial p}{\partial x} + \rho g_x + \mu\left(\frac{\partial^2 v_x}{\partial x^2} + \frac{\partial^2 v_x}{\partial y^2} + \frac{\partial^2 v_x}{\partial z^2}\right) \quad \text{(a)}$$

y-Direction

$$\rho\left(\frac{\partial v_y}{\partial t} + v_x\frac{\partial v_y}{\partial x} + v_y\frac{\partial v_y}{\partial y} + v_z\frac{\partial v_y}{\partial z}\right) = -\frac{\partial p}{\partial y} + \rho g_y + \mu\left(\frac{\partial^2 v_y}{\partial x^2} + \frac{\partial^2 v_y}{\partial y^2} + \frac{\partial^2 v_y}{\partial z^2}\right) \quad \text{(b)}$$

z-Direction

$$\rho\left(\frac{\partial v_z}{\partial t} + v_x\frac{\partial v_z}{\partial x} + v_y\frac{\partial v_z}{\partial y} + v_z\frac{\partial v_z}{\partial z}\right) = -\frac{\partial p}{\partial z} + \rho g_z + \mu\left(\frac{\partial^2 v_z}{\partial x^2} + \frac{\partial^2 v_z}{\partial y^2} + \frac{\partial^2 v_z}{\partial z^2}\right) \quad \text{(c)}$$

THE EQUATIONS OF MOTION FOR CONSTANT μ AND ρ IN CYLINDRICAL COORDINATES (r, θ, z)

r-Direction

$$\rho\left(\frac{\partial v_r}{\partial t} + v_r\frac{\partial v_r}{\partial r} + \frac{v_\theta}{r}\frac{\partial v_r}{\partial \theta} - \frac{v_\theta^2}{r} + v_z\frac{\partial v_r}{\partial z}\right)$$

$$= -\frac{\partial p}{\partial r} + \rho g_r + \mu\left[\frac{\partial}{\partial r}\left(\frac{1}{r}\frac{\partial}{\partial r}(r v_r)\right) + \frac{1}{r^2}\frac{\partial^2 v_r}{\partial \theta^2} - \frac{2}{r^2}\frac{\partial v_\theta}{\partial \theta} + \frac{\partial^2 v_r}{\partial z^2}\right] \quad \text{(a)}$$

θ-Direction

$$\rho\left(\frac{\partial v_\theta}{\partial t} + v_r\frac{\partial v_\theta}{\partial r} + \frac{v_\theta}{r}\frac{\partial v_\theta}{\partial \theta} + \frac{v_r v_\theta}{r} + v_z\frac{\partial v_\theta}{\partial z}\right)$$

$$= -\frac{1}{r}\frac{\partial p}{\partial \theta} + \rho g_\theta + \mu\left[\frac{\partial}{\partial r}\left(\frac{1}{r}\frac{\partial}{\partial r}(r v_\theta)\right) + \frac{1}{r^2}\frac{\partial^2 v_\theta}{\partial \theta^2} + \frac{2}{r^2}\frac{\partial v_r}{\partial \theta} + \frac{\partial^2 v_\theta}{\partial z^2}\right] \quad \text{(b)}$$

z-Direction

$$\rho\left(\frac{\partial v_z}{\partial t} + v_r\frac{\partial v_z}{\partial r} + \frac{v_\theta}{r}\frac{\partial v_z}{\partial \theta} + v_z\frac{\partial v_z}{\partial z}\right)$$

$$= -\frac{\partial p}{\partial z} + \rho g_z + \mu\left[\frac{1}{r}\frac{\partial}{\partial r}\left(r\frac{\partial v_z}{\partial r}\right) + \frac{1}{r^2}\frac{\partial^2 v_z}{\partial \theta^2} + \frac{\partial^2 v_z}{\partial z^2}\right] \quad \text{(c)}$$

THE EQUATIONS OF MOTION CONSTANT μ AND ρ IN SPHERICAL COORDINATES (r, θ, ϕ)†

r-Direction

$$\rho\left(\frac{\partial v_r}{\partial t} + v_r\frac{\partial v_r}{\partial r} + \frac{v_\theta}{r}\frac{\partial v_r}{\partial \theta} + \frac{v_\phi}{r\sin\theta}\frac{\partial v_r}{\partial \phi} - \frac{v_\theta^2 + v_\phi^2}{r}\right)$$

$$= -\frac{\partial p}{\partial r} + \rho g_r + \mu\left(\nabla^2 v_r - \frac{2v_r}{r^2} - \frac{2}{r^2}\frac{\partial v_\theta}{\partial \theta} - \frac{2\,v_\theta\cot\theta}{r^2} - \frac{2}{r^2\sin\theta}\frac{\partial v_\phi}{\partial \phi}\right) \quad \text{(a)}$$

θ-Direction

$$\rho\left(\frac{\partial v_\theta}{\partial t} + v_r\frac{\partial v_\theta}{\partial r} + \frac{v_\theta}{r}\frac{\partial v_\theta}{\partial \theta} + \frac{v_\phi}{r\sin\theta}\frac{\partial v_\theta}{\partial \phi} + \frac{v_r v_\theta}{r} - \frac{v_\phi^2\cot\theta}{r}\right)$$

$$= -\frac{1}{r}\frac{\partial p}{\partial \theta} + \rho g_\theta + \mu\left(\nabla^2 v_\theta + \frac{2}{r^2}\frac{\partial v_r}{\partial \theta} - \frac{v_\theta}{r^2\sin^2\theta} - \frac{2\cos\theta}{r^2\sin^2\theta}\frac{\partial v_\phi}{\partial \phi}\right) \quad \text{(b)}$$

ϕ-Direction

$$\rho\left(\frac{\partial v_\phi}{\partial t} + v_r\frac{\partial v_\phi}{\partial r} + \frac{v_\theta}{r}\frac{\partial v_\phi}{\partial \theta} + \frac{v_\phi}{r\sin\theta}\frac{\partial v_\phi}{\partial \phi} + \frac{v_\phi v_r}{r} + \frac{v_\theta v_\phi}{r}\cot\theta\right)$$

$$= -\frac{1}{r\sin\theta}\frac{\partial p}{\partial \phi} + \rho g_\phi + \mu\left(\nabla^2 v_\phi - \frac{v_\phi}{r^2\sin^2\theta} + \frac{2}{r^2\sin\theta}\frac{\partial v_r}{\partial \phi} + \frac{2\cos\theta}{r^2\sin^2\theta}\frac{\partial v_\theta}{\partial \phi}\right) \quad \text{(c)}$$

† For spherical coordinates the Laplacian is,

$$\nabla^2 = \frac{1}{r^2}\frac{\partial}{\partial r}\left(r^2\frac{\partial}{\partial r}\right) + \frac{1}{r^2\sin\theta}\frac{\partial}{\partial \theta}\left(\sin\theta\frac{\partial}{\partial \theta}\right) + \frac{1}{r^2\sin^2\theta}\left(\frac{\partial^2}{\partial \phi^2}\right)$$

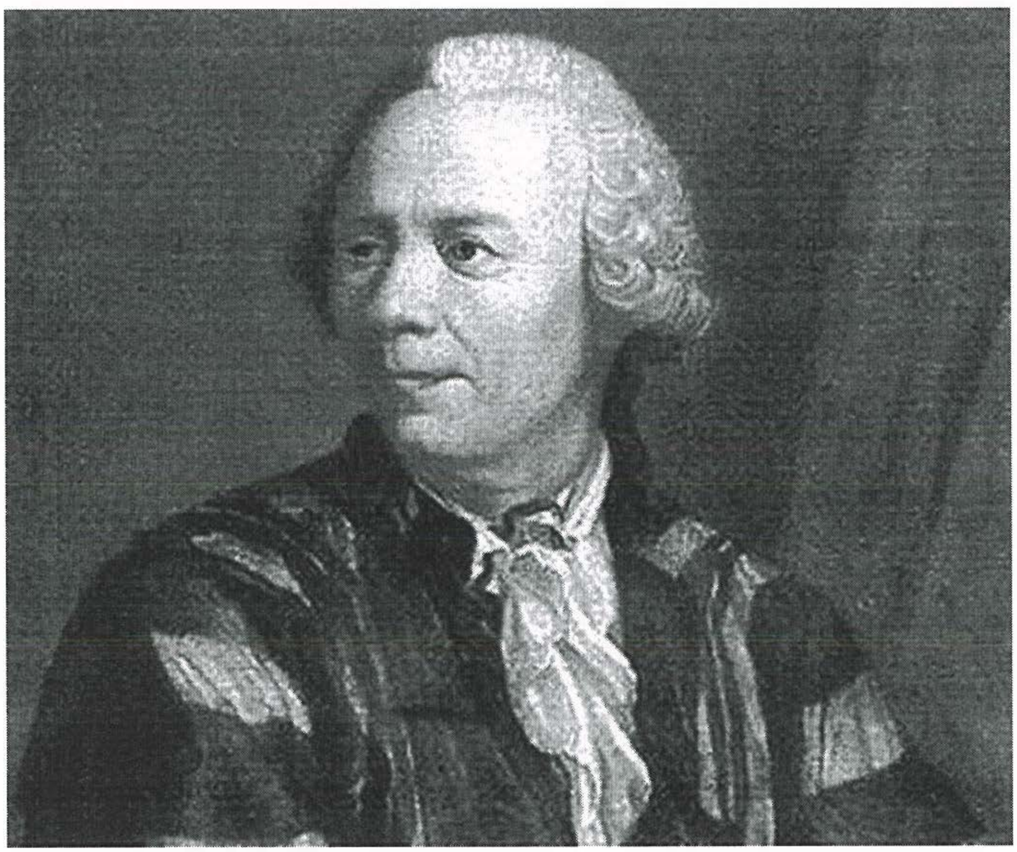

LEONARD EULER (1707-1783)

APPENDIX E

GEOMETRICAL RELATIONS

Properties of areas

	Sketch	Area or volume	Location of centroid	I or I_c
Rectangle	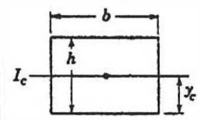	bh	$y_c = \frac{h}{2}$	$I_c = \frac{bh^3}{12}$
Triangle	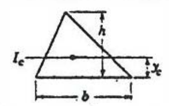	$\frac{bh}{2}$	$y_c = \frac{h}{3}$	$I_c = \frac{bh^3}{36}$
Circle	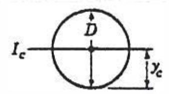	$\frac{\pi D^2}{4}$	$y_c = \frac{D}{2}$	$I_c = \frac{\pi D^4}{64}$
Semicircle	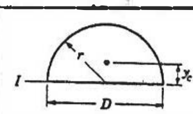	$\frac{\pi D^2}{8}$	$y_c = \frac{4r}{3\pi}$	$I = \frac{\pi D^4}{128}$
Ellipse	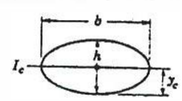	$\frac{\pi bh}{4}$	$y_c = \frac{h}{2}$	$I_c = \frac{\pi bh^3}{64}$
Semiellipse	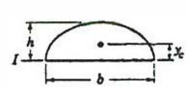	$\frac{\pi bh}{4}$	$y_c = \frac{4h}{3\pi}$	$I = \frac{\pi bh^3}{16}$

SOLIDS

The surface of a sphere of radius r and diameter $d (= 2r)$

$$= 4\pi r^2 = \pi d^2 = 12.57 r^2.$$

The volume of a sphere

$$= \tfrac{4}{3}\pi r^3 = \tfrac{1}{6}\pi d^3 = 4.189 r^3.$$

The curved surface of a right cylinder where r = the radius of the base and h, the altitude,

$$= 2\pi r h.$$

The volume of a cylinder, data as above,

$$= \pi r^2 h.$$

The curved surface of a right cone whose altitude is h and radius of base r

$$= \pi r \sqrt{r^2 + h^2}.$$

The volume of a cone, data as above,

$$= \frac{\pi}{3} r^2 h = 1.047 r^2 h.$$

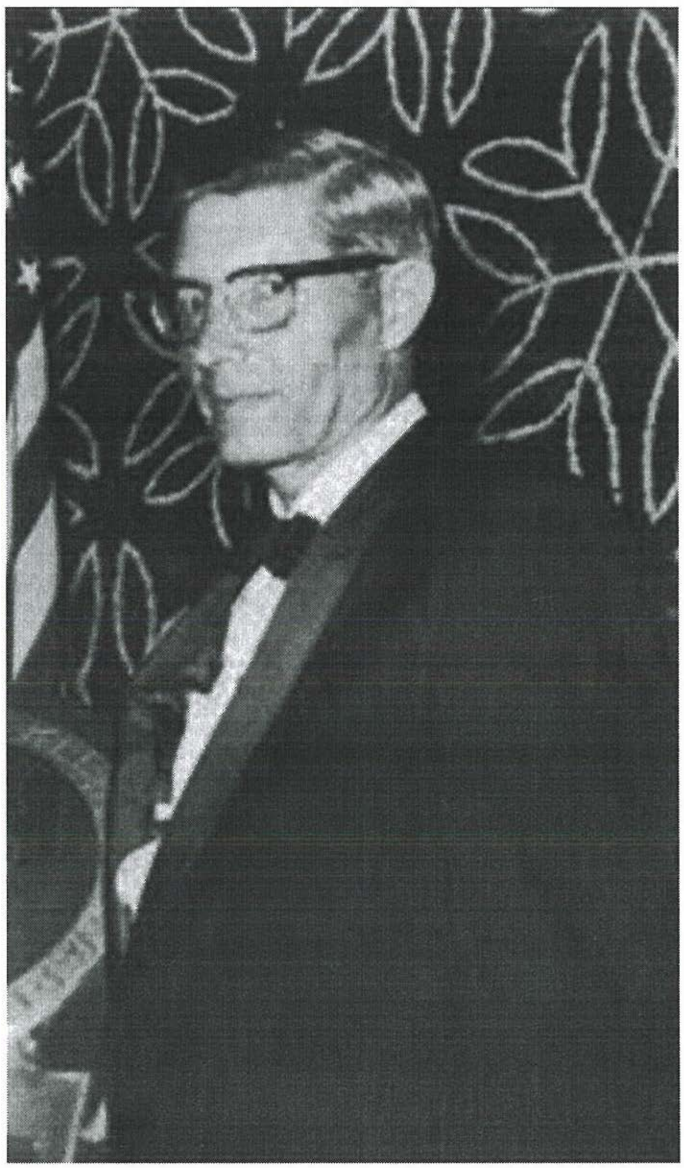

KURT H. HOHENEMSER (1906-2001), one of my distinguished professors at Washington University, St. Louis (WUSTL), student of Ludwig Prandtl, co-worker of Anton Flettner and colleague of William Prager

APPENDIX E
Unit Conversion Factors

The following table was compiled after consulting several books including Progelhof and Throne (1) and Wildi (2).

References

1. R. C. Progelhof and J. L. Throne, *Polymer Engineering Principles*, Hanser Gardner, Cincinnati, Ohio (1993).
2. T. Wildi, *Metric Units and Conversion Charts*, 2nd Ed., IEEE Press (1995).

Length		Multiplied by		Gives		Multiplied by		Gives
m	×	3.28	=	ft	×	0.3048	=	m
m	×	39.37	=	in	×	0.02540	=	m
yd	×	3	=	ft	×	3^{-1}	=	yd
ft	×	12	=	in	×	12^{-1}	=	ft
μm	×	1×10^{-6}	=	m	×	1×10^{6}	=	μm
km	×	0.621	=	mile	×	1.609	=	km
Å	×	1×10^{-10}	=	m	×	1×10^{10}	=	Å
Å	×	0.0001	=	μm	×	1×10^{4}	=	Å
mm	×	39.37	=	mils (0.001 in)	×	0.02540	=	mm
μm	×	0.0394	=	mils (0.001 in)	×	25.40	=	μm
Area								
m^2	×	1.196	=	yd^2	×	0.8361	=	m^2
m^2	×	10.76	=	ft^2	×	0.0929	=	m^2
m^2	×	1550.	=	in^2	×	0.00064516	=	m^2
cm^2	×	0.155	=	in^2	×	6.452	=	cm^2
mm^2	×	0.00155	=	in^2	×	645.2	=	mm^2
Volume								
m^3	×	264.17	=	gallon (US)	×	0.003785	=	m^3
m^3	×	35.31	=	ft^3	×	0.02832	=	m^3
m^3	×	61024.	=	in^3	×	0.000016387	=	m^3
liter	×	1000.	=	cm^3	×	0.001	=	liter
cm^3	×	0.0338	=	fluid oz (US)	×	29.57	=	cm^3
mm^3	×	6.102×10^{-5}	=	in^3	×	1.639×10^{4}	=	mm^3
gal	×	231.	=	in^3	×	0.004329	=	gal

Mass								
g	×	0.0022046	=	lb_m	×	453.6	=	g
kg	×	2.2046	=	lb_m	×	0.4536	=	kg
kg	×	0.0011	=	ton (short)	×	907.	=	kg
kg	×	0.001	=	ton (metric)	×	1000	=	kg
lb_m	×	0.0005	=	ton (short)	×	2000	=	lb_m
Density								
g/cm^3	×	62.43	=	lb_m/ft^3	×	0.01602	=	g/cm^3
g/cm^3	×	0.03613	=	lb_m/in^3	×	27.68	=	g/cm^3
kg/m^3	×	0.06243	=	lb_m/ft^3	×	16.02	=	kg/m^3
g/cm^3	×	0.5780	=	oz_m/in^3	×	1.730	=	g/cm^3
kg/m^3	×	0.0005780	=	oz_m/in^3	×	1730.	=	kg/m^3
Force								
N	×	0.2248	=	lb_f	×	4.448	=	N
N	×	1.0×10^5	=	dyne	×	1.0×10^{-5}	=	N
dyne	×	2.248×10^{-6}	=	lb_f	×	4.448×10^5	=	dyne
N	×	1.0×10^{-6}	=	meganewton (MN)	×	1.0×10^6	=	N
MN	×	100.4	=	ton-force (UK)	×	0.009964	=	MN
MN	×	112.4	=	ton-force	×	0.008897	=	MN
Pressure and Stress								
Pa	×	1.450×10^{-4}	=	lb_f/in^2	×	6895.	=	Pa
kPa	×	0.1450	=	lb_f/in^2	×	6.895	=	kPa
MPa	×	145.0	=	lb_f/in^2	×	0.006895	=	MPa
kgf/cm^2	×	14.22	=	lb_f/in^2	×	0.07031	=	kgf/cm^2
N/mm^2	×	1.0	=	MPa	×	1.0	=	N/mm^2
Pa	×	10	=	$dyne/cm^2$	×	0.1	=	Pa
Pa	×	0.007501	=	mm Hg	×	133.3	=	Pa
Pa	×	0.004019	=	in H_2O	×	248.8	=	Pa
kPa	×	7.501	=	torr	×	0.1333	=	kPa
torr	×	1.0	=	mm Hg	×	1.0	=	torr
MPa	×	9.869	=	atm	×	0.1013	=	MPa
MPa	×	10	=	bar	×	0.1	=	MPa

Fluid Flow Rate								
liter/min	×	0.2642	=	gal/min (GPM)	×	3.785	=	liter/min
liter/min	×	2.119	=	ft^3/h	×	0.4719	=	liter/min
m^3/h	×	4.403	=	gal/min (GPM)	×	0.2271	=	m^3/h
m^3/min	×	264.2	=	gal/min (GPM)	×	0.003785	=	m^3/min
Mass Flow Rate								
kg/s	×	7937.	=	lb_m/h (PPH)	×	0.0001260	=	kg/s
kg/h	×	2.205	=	lb_m/h (PPH)	×	0.4536	=	kg/h
Viscosity								
Pa·s	×	10.	=	poise	×	0.1	=	Pa·s
Pa·s	×	1000.	=	centipoise	×	0.001	=	Pa·s
m^2/s	×	10.76	=	ft^2/s	×	0.0929	=	m^2/s
Pa·s	×	0.672	=	lb_m/s ft	×	1.488	=	Pa·s
centipose	×	0.000672	=	lb_m/s ft	×	1488.	=	centipose
m^2/s	×	1.0×10^6	=	centistokes	×	1.0×10^{-6}	=	m^2/s
Pa·s	×	0.000145	=	$lb_f\ s/in^2$	×	6895.	=	Pa·s
Pa·s	×	0.02088	=	$lb_f\ s/ft^2$	×	47.88	=	Pa·s
poise	×	1.45×10^{-5}	=	$lb_f\ s/in^2$	×	6.895×10^4	=	poise

The following table relates length from angstroms to meters.

# of Å	= One
1	Å
10	Nm
100	
1,000	
10,000	µm
100,000	
1,000,000	
10,000,000	mm
100,000,000	cm
1,000,000,000	
10,000,000,000	m

J. Vlachopoulos and J.R. Wagner *The SPE Guide on Extrusion Technology and Troubleshooting*

The Society of Plastics Engineers (SPE), Brookfield, CT, USA (2001)

TABLE G.1 SI Units and Prefixes[a]

SI Units	Quantity	Unit	SI Symbol	Formula
SI base units:	Length	meter	m	—
	Mass	kilogram	kg	—
	Time	second	s	—
	Temperature	kelvin	K	—
SI supplementary unit:	Plane angle	radian	rad	—
SI derived units:	Energy	joule	J	N • m
	Force	newton	N	kg • m/s^2
	Power	watt	W	J/s
	Pressure	pascal	Pa	N/m^2
	Work	joule	J	N • m

SI prefixes	Multiplication Factor	Prefix	SI Symbol
	1 000 000 000 000 = 10^{12}	tera	T
	1 000 000 000 = 10^9	giga	G
	1 000 000 = 10^6	mega	M
	1 000 = 10^3	kilo	k
	0.01 = 10^{-2}	centi	c
	0.001 = 10^{-3}	milli	m
	0.000 001 = 10^{-6}	micro	μ
	0.000 000 001 = 10^{-9}	nano	n
	0.000 000 000 001 = 10^{-12}	pico	p

[a] Source: ASTM Standard for Metric Practice E 380–97, 1997.

Constant	Symbol	Value	Application
Natural base	e	2.7183	Science, mathematics
Natural log	ln 10	2.3026	Science, mathematics
Radian unit	π	3.1416	Science, mathematics, angular kinematics
Speed of light in air	c_l	2.998×10^8 m/s	Optics, relativity theory
Speed of sound in air	c	340m/s	Acoustics, compressible flow
Ideal gas constant	R	$1.987 \frac{\text{cal g}}{\text{mol K}}$	Ideal gas law
		$82.05 \frac{\text{cm}^3\text{ atm}}{\text{mol K}}$	Thermodynamics
		$8.314 \frac{\text{N m}}{\text{mol K}} = \frac{\text{J}}{\text{mol K}}$	Gas mechanics
		$1.544 \frac{\text{ft lb}_f}{\text{lbmol °R}}$	Heat-work machines
Gravity acceleration	g	981 cm/s^2 32.17 ft/s^2	Mechanics Kinematics
Joule's constant	α	$788 \frac{\text{ft lb}_f}{\text{Btu}}$	Thermodynamics
		4.184 J/cal	Heat–work machines
Planck's constant	h	$6.62 \times 10^{-27} \frac{\text{erg}}{\text{s}}$	Quantum mechanics
Avogadro's number	N_A	$6.02 \times 10^{23} \frac{\text{molecules}}{\text{mol}}$	Chemistry, thermodynamics
Boltzmann's constant	k	R/N_A	Statistical mechanics

John Vlachopoulos, *Fundamentals of Fluid Mechanics*
Chem. Eng., McMaster University, Hamilton, ON, Canada
(First Edition 1984, revised internet edition (2016), www.polydynamics.com)

SUBJECT INDEX

A

B

INDEX 2

C

E

F

M

N

O

P

R

S

INDEX 14

KARL WEISSENBERG (1893-1976)

and

JOHN VLACHOPOULOS

at the University of Stuttgart, Germany

in February 1975

NIAGARA FALLS, ONTARIO, CANADA